Salmonella Paratyphi A: an insight into mechanisms of typhoidal *Salmonella* pathogenesis

Elli Effrosyni Mylona

April 2020

Thesis submitted to the
Department of Life Sciences, Imperial College London

For the degree of Doctor of Philosophy

Abstract

The human-restricted, typhoidal *Salmonella* Paratyphi A (*S.* Paratyphi A) and *S.* Typhi are the major causes of enteric (typhoid) fever and are endemic in regions with poor sanitation. Despite the recent increased rate of *S.* Paratyphi A isolation from patients in Asia, its pathogenesis remains largely unknown. Asymptomatic chronic carriage in the gallbladder is encountered in about 5% of patients and is facilitated by efficient immune evasion. In this study, we have shown that bile changes the expression of > 5% of genes in *S.* Paratyphi A, including both bile tolerance and virulence-associated genes. *S.* Paratyphi A and *S.* Typhi may differentially regulate certain metabolic pathways in response to bile. Furthermore, a clinical *S.* Paratyphi A isolate appears to exhibit distinct regulatory mechanisms. As inflammasomes have been shown to play a key role in *Salmonella* infection, we also investigated their role following infection of macrophages with *S.* Paratyphi A, using *S.* Typhi and *S.* Typhimurium as controls. This work demonstrates that *S.* Paratyphi A and *S.* Typhi induce pyroptosis, which is lower than that triggered by *S.* Typhimurium. While the pathway activated during *S.* Typhi infection remains unclear, *S.* Paratyphi A-triggered pyroptosis occurs via activation of caspase-1, caspase-4, caspase-8 and NLRP3. Both *S.* Paratyphi A and *S.* Typhi require their SPI-1 injectisome to enable inflammasome activation. However, while the Vi antigen of *S.* Typhi is dispensable for limiting pyroptosis, the *S.* Paratyphi A FepE-mediated synthesis of very long O-antigen chains impairs macrophage cell death and a Δ*fepE* mutant elicited enhanced inflammasome activation. Very long O-antigen chains can also act as an inflammasome dampening mechanism in *S.* Typhimurium, but reduced *fepE* expression indicates that this strategy is not exploited by this pathogen. Therefore, this work points towards distinct mechanisms of virulence by *S.* Paratyphi A, highlighting the need for a systematic characterisation of its molecular pathogenesis.

Declaration of originality

I confirm thattheworkpresentedinthisthesisismyown . Any contributionstothisstudybyothers are acknowledged in text (see Materials & Methods and Figure legends) and any sources of information orsoftware/tools areappropriately referenced.

ElliMylona
April2020

Copyright declaration

Thecopyright ofthisthesisrestswiththeauthorandismade availableunderaCreativeCommons Attribution Non -Commercial No Derivatives licence. Researchers are free to copy, distribute or transmitthethesisontheconditionthattheyattributeit,thattheydonot useitforcommercial purposes and that they do not alter, transform or build upon it. For any reuse or redistribution, researchersmustmakeclear toothersthelicensetermsofthiswork.

Acknowledgments

This work was funded by the MRC, through a DTP Studentship. I would like to further thank MRC for awarding me a grant through the MRC supplement scheme to cover my visit to Vietnam.

I would like to thank my supervisor Gad Frankel for his academic support, as well as for being understanding and patient with everything that arose during my time in his lab. Many thanks to Avinash Shenoy for his endless knowledge on inflammasomes and his constructive feedback. I am particularly thankful to Stephen Baker not only for hosting me in his lab in Vietnam, but also for reigniting my enthusiasm about research and of course for introducing us to Paratyphi.

I wish to thank all Frankel lab members, past and present, without exceptions. You've been there for me through tough times. I am particularly grateful to Dani Carson for always being there for a hug and some sisterly love, and Sabrina Slater for putting up with my insecurities and providing excellent language skills. I am glad I was in this with you two and thanks for all your support in both academic and personal matters. Julia Sanchez-Garrido, I just wish you had joined the lab earlier – a massive thank you for your patience, your immense help with finishing my paper, and your support in any way you could. Many thanks to Josh Wong for being the calm voice I needed to hear when I most needed it. Jayne Watson, thanks for being an amazing office buddy. Becky Johnson, thanks for teaching me all the CL3 procedures and helping me get a hang of Typhi. Alex Byrne, your supervision at the early stages of my time in the lab was invaluable for me to continue. Special thanks to Pippa Goddard, for helping me in my baby steps in inflammasome biology; Louise Kerry, for always caring; Carrie Mullineaux-Sanders for making sure I don't get lost during lab outings; and Rachael Barry for always checking up on me; and all of you for answering my (many) silly questions.

I would like to thank all of my friends back home, for entertaining me and encouraging me to continue. Special thanks to my housemates Alexandra, Stef, and Zoe. I would not have returned to the UK if weren't for you and my labmates. Alexandra, you proved to be a closer friend than my closest friends and I hope to have been worthy of this.

I could not have done this PhD without my mom, Sophia, and my sister, Rallou. Mom, your unconditional love, support, and readiness for endless conversations about everything was what made me carry on. I am proud to have you as my mother and thank you for everything you have taught me. Ralloukaki, I may not even have a "pla", but I know I will always have you by my side no matter what. And for that, could I *be* any more thankful? Also, credits to my cats for absorbing my emotions and tolerating my hugs and squeezes.

I would like to take a moment and thank those I lost during this time. My grandmother for always believing in me and for filling my insatiable appetite for chocolate; my first cat Tigis for teaching me to love unconditionally and making me realise that cats are my alter ego; and my baby cat Piki for being an excellent writing buddy for as long as you made it – I will always miss having you on my desk.

And finally, my Dad. I would not have reached this stage if it wasn't for you. You were my best friend, always providing me with endless strength and advice on absolutely everything. Your encyclopaedic knowledge, elegance, thirst for life, open-mindedness, always being a loving figure have made you a role model to aspire to. Your loss has been unbearable, but I promise you to carry on. You have been the best father I could have ever asked for, and for that I am eternally thankful.

Table of Contents

Abstract 3

Declaration of originality 4

Copyright declaration 4

Acknowledgments 5

Table of Contents 7

List of Figures 11

List of Tables 14

Abbreviations 15

Publications 17

1 Introduction 19

1.1 *Salmonella enterica* species 19

1.1.1 Taxonomy and nomenclature 19

1.1.2 Pathogenesis in humans 20

1.1.3 Typhoidal *Salmonella* and their epidemiology 21

1.1.3.1 *Salmonella* Typhi 23

1.1.3.2 *Salmonella* Paratyphi A 23

1.1.3.3 *Salmonella* Paratyphi B, Paratyphi C and Sendai 26

1.2 Diagnosis, treatment, and vaccination for enteric fever 26

1.3 Models to study enteric fever 28

1.4 *Salmonella* evolution 29

1.5 *Salmonella* infection mechanism 30

1.6 *Salmonella* key virulence factors 32

1.6.1 *Salmonella* type III secretion systems 32

1.6.1.1 SPI-1 T3SS 33

1.6.1.2 SPI-2 T3SS 35

1.6.1.3 Role in virulence 36

1.6.2 Vi antigen in *S.* Typhi 38

1.6.3 O-antigen in *S.* Paratyphi A 39

1.6.4 Flagella 41

1.6.5 Adhesins 41

1.6.6 Toxins 42

1.7 The carrier state of enteric fever 44

1.8 Bile during *Salmonella* infection 46

1.8.1 Bile composition and functions 46

1.8.2 Antimicrobial properties of bile 47
1.8.3 *Salmonella* mechanisms of bile tolerance and resistance 47
1.8.4 *Salmonella* virulence gene regulation in response to bile 48
1.9 The inflammasome host immune response to *Salmonella* 50
1.9.1 Pattern recognition receptors and inflammatory signalling 50
1.9.2 Host innate immunity to *Salmonella* – an overview 51
1.9.3 Inflammasome activation during *Salmonella* infection 52
1.9.3.1 Inflammatory caspases 53
1.9.3.2 IL-1β and IL-18 pro-inflammatory cytokines 54
1.9.3.3 Pyroptosis and Gasdermin-D 54
1.9.3.4 Inflammasome signalling 55
1.9.3.5 The NLRP3 inflammasome 57
1.9.3.6 The NLRC4 inflammasome 59
1.9.3.7 Caspase-8 and inflammasomes 61
1.9.3.8 Non-canonical inflammasome activation 62
1.10 Project aims 63
2 Materials & Methods 65
2.1 Bacterial culture and strains 65
2.1.1 Bacterial culture 65
2.1.2 Bacterial strains and mutagenesis 67
2.1.3 Slide agglutination test 68
2.2 Cell lines and cell culture 71
2.2.1 Human cell lines used in this study 71
2.2.2 HeLa cell culture 71
2.2.3 THP-1 cell culture 72
2.2.4 Isolation of primary human monocyte-derived macrophages (MDMs) 72
2.3 THP-1 and MDM cell treatments 72
2.4 Cell infections 73
2.4.1 HeLa invasion and HeLa replication assays 74
2.4.2 THP-1 gentamicin protection and chloroquine resistance assays 74
2.4.3 PI uptake-based cell death assay 74
2.4.4 Immunofluorescence 74
2.4.5 Enzyme linked immunosorbent assay (ELISA) 75
2.4.6 Sample preparation for SDS-PAGE and immunoblotting 75
2.5 Bacterial protein expression analysis 76
2.6 Transcriptome analysis 76

2.6.1 RNA extraction 76
2.6.2 RNA sequencing (RNA-Seq) and data analysis 76
2.6.3 Real Time-quantitative PCR (RT-qPCR) 77
2.7 Crude LPS preparation and silver staining 78
2.8 SPI-1 secretion assay 78
2.9 β-lactamase Translocation assays 79
2.10 Bile tolerance assays 79
2.11 Motility assays 79
2.12 Bioinformatics analysis 80
2.13 Statistical analysis 80
3 The Salmonella Paratyphi A response to bile 81
3.1 *S.* Paratyphi A invades HeLa cells in a SPI-1-dependent manner 82
3.2 *S.* Paratyphi A becomes more invasive in epithelial cells following growth in bile 84
3.3 Overview of changes in *S.* Paratyphi A transcriptome in response to bile 88
3.4 Bile-mediated differential gene regulation in *S.* Typhi and *S.* Paratyphi A 91
3.5 Shared responses to bile between *S.* Typhi and *S.* Paratyphi A 93
3.6 Differential regulation of bile-tolerance and resistance genes 97
3.7 Effect of exposure to bile on SPI-1 and adhesin expression 100
3.8 Effect of bile on *S.* Paratyphi A motility 103
3.9 Effect of bile on *S.* Paratyphi A-specific genes 105
3.10 Effect of bile on *S.* Paratyphi A metabolism 107
3.11 Role of glyoxylate cycle genes in host cell infection 110
3.12 Discussion 113
4 Inflammasome activation during infection with typhoidal Salmonella 121
4.1 Typhoidal *Salmonella* induce cell death in THP-1 cells 122
4.2 Typhoidal *Salmonella* induces caspase-dependent pyroptosis 125
4.3 Caspase-4 and ASC contribute to cell death triggered by *S.* Paratyphi A 128
4.4 The role of the NLRP3 inflammasome during infection with typhoidal *Salmonella* 132
4.5 The role of NLRC4 during typhoidal *Salmonella*-induced pyroptosis 135
4.6 The role of caspase-8 during THP-1 cell infection with *S.* Paratyphi A 139
4.7 Caspase-4 is activated upstream of NLRP3 and caspase-8 during infection with *S.* Paratyphi A 140
4.8 Clinical *S.* Paratyphi A isolates induce efficient macrophage cell death and inflammasome activation 141
4.9 Clinical *S.* Paratyphi A isolates induce caspase-1/4-, caspase-8- and NLRP3-mediated pyroptosis 144

4.10 *S.* Typhi induces SPI-1-dependent, Vi-independent macrophage cell death 146
4.11 The role of *S.* Typhi-specific T3SS effector protein StoD in early host cell death 151
4.12 *S.* Typhi H58 triggers similar levels of pyroptosis compared to non-H58 strains 153
4.13 SPI-1 T3SS overexpression leads to increased cell death during *S.* Paratyphi A infection . 155
4.14 *S.* Paratyphi A induces SPI-1 T3SS-dependent cell death and inflammasome activation, which is restricted by very long LPS O-antigen chains 157
4.15 FepE-dependent reduction in *S.* Paratyphi A-induced cell death is not mediated by interference with immune signalling priming 161
4.16 Complementation of Δ*fepE* restores the WT phenotype 162
4.17 Very long O-antigen chains trigger ASC-dependent cell death during infection with *S.* Paratyphi A 165
4.18 The role of very long O-antigen chains in inflammasome activation by *S.* Typhimurium infection 169
4.19 *S.* Paratyphi A-induced inflammasome activation in human monocyte-derived macrophages (MDMs) 171
4.20 The role of very long O-antigen chains during infection of MDMs with *Salmonella* 179
4.21 *fepE* expression inversely correlates with pyroptosis during infection with *Salmonella* ... 183
4.22 Discussion 184
5 Final conclusions and future perspectives 193
References 198
Appendix 225

List of Figures

Figure 1.1 **Enteric fever global incidence in 2017.** 22
Figure 1.2 **Evolution of *Salmonella*.** 29
Figure 1.3 **Typhoidal Salmonella infection mechanism.** 31
Figure 1.4 **Type III secretion systems in Salmonella.** 34
Figure 1.5 **Salmonella gallbladder colonisation models.** 45
Figure 1.6 **Canonical inflammasome assembly.** 53
Figure 1.7 **Human inflammasome activation during macrophage infection with *S.* Typhimurium.** . 58
Figure 3.1 **The SPI-1 T3SS of S. Paratyphi A is active during growth in aerobic conditions to late exponential phase.** 83
Figure 3.2 **The presence of 3% bile in the growth media does not affect S. Paratyphi A growth.** 85
Figure 3.3 **Exposure to bile renders S. Paratyphi A 9150 more invasive to HeLa cells in a SPI-1-dependent manner.** 86
Figure 3.4 **Effect of bile on S. Paratyphi A SPI-1 expression and invasion in HeLa cells.** 88
Figure 3.5 **Overview of transcriptomic changes induced by bile.** 90
Figure 3.6 **Shared responses to bile between S. Typhi and S. Paratyphi A.** 92
Figure 3.7 **Bile tolerance of S. Typhi and S. Paratyphi A.** 99
Figure 3.8 **Effect of bile on S. Paratyphi SPI-1 expression.** 101
Figure 3.9 **Exposure to bile downregulates expression of SPI-4 in S. Paratyphi A.** 102
Figure 3.10 **Effect of bile on S. Paratyphi A motility.** 104
Figure 3.11 **Effect of bile on S. Paratyphi A clinical isolates motility.** 105
Figure 3.12 **Validation of bile effect on S. Paratyphi A metabolic genes.** 108
Figure 3.13 **Glyoxylate cycle in *Salmonella*.** 109
Figure 3.14 **Loss of glyoxylate cycle enzymes does not affect invasion or intracellular replication of S. Paratyphi A in epithelial cells** 111
Figure 3.15 **Effect of glyoxylate enzyme gene deletion on intracellular replication of S. Paratyphi A in human macrophages.** 112
Figure 4.1 **S. Typhi induces THP-1 cell death in a time-dependent manner.** 123
Figure 4.2 **S. Paratyphi A 9150 induces lower levels of THP-1 cell death than S. Typhi Ty2.** 124
Figure 4.3 **S. Paratyphi A infection rate of THP-1 cells is similar at MOI 50 and 15.** 125
Figure 4.4 **S. Paratyphi A and S. Typhi induce caspase-dependent cell death.** 126
Figure 4.5 **Validation of GSDMD^{miR} THP-1 cells.** 127
Figure 4.6 **Typhoidal *Salmonella* induce GSDMD-dependent pyroptotic cell death** 127
Figure 4.7 **Effect of irreversible inhibition of caspase-4 on typhoidal *Salmonella*-induced cell death.** 128
Figure 4.8 **CASP4^{miR} and ASC^{miR} THP-1 cell validation** 129
Figure 4.9 **S. Paratyphi A induces caspase-4-dependent pyroptosis.** 130
Figure 4.10 **S. Paratyphi A induces ASC-dependent cell death in THP-1 cells.** 130
Figure 4.11 **S. Paratyphi A induces ASC-dependent, caspase-4 independent caspase-1 activation.** 131
Figure 4.12 **MCC950 efficiently blocks NLRP3 activation in THP-1 cells.** 132

Figure 4.13 **Effect of MCC950-mediated NLRP3 inhibition on *Salmonella*-induced cell death.** 133
Figure 4.14 **IFNγ priming of THP-1 cells induces NLRP3-dependent increase in cell death by typhoidal *Salmonella*.** 134
Figure 4.15 **The role of NAIP silencing in typhoidal *Salmonella*-induced cell death.** 135
Figure 4.16 **The role of NAIP silencing in inflammasome activation during THP-1 infection with typhoidal *Salmonella*.** 136
Figure 4.17 **Sequence alignment of PrgJ, PrgI, and FliC of S. Paratyphi A, S. Typhi, and S. Typhimurium.** 138
Figure 4.18 **The role of caspase-8 during infection with typhoidal *Salmonella*.** 139
Figure 4.19 **Caspase-4 is activated upstream of NLRP3 and caspase-8 during S. Paratyphi A infection.** 140
Figure 4.20 **Clinical S. Paratyphi A isolates trigger more cell death than 9150.** 141
Figure 4.21 **Clinical S. Paratyphi A isolates induce higher levels of inflammasome activation.** 142
Figure 4.22 **Clinical S. Paratyphi A isolates induce higher production of IL-1β compared to 9150.** 143
Figure 4.23 **Clinical S. Paratyphi A isolates induce caspase-dependent pyroptosis.** 144
Figure 4.24 **Activation of caspase-4 and caspase-8 is shared among S. Paratyphi A strains.** 145
Figure 4.25 **S. Paratyphi A clinical isolates induce NLRP3-dependent cell death** 146
Figure 4.26 **The Vi capsule of S. Typhi limits epithelial cell invasion.** 146
Figure 4.27 **S. Typhi induces SPI-1-dependent, Vi capsule-independent macrophage cell death** ... 147
Figure 4.28 **The role of the Vi antigen during infection of THP-1 cells with S. Typhi.** 148
Figure 4.29 **S. Typhi escapes to the cytosol independently of SPI-1 T3SS and the Vi capsule.** 149
Figure 4.30 **Host cell priming does not affect S. Typhi-induced cell death.** 150
Figure 4.31 **S. Typhi induces SPI-1 T3SS-dependent ASC speck formation** 151
Figure 4.32 **StoD is a T3SS-dependent effector not involved in S. Typhi-induced early host cell death.** 152
Figure 4.33 **S. Typhi H58 clinical isolates cause similar cell death in comparison to S. Typhi Ty2, depending on the levels of SPI-1 expression.** 154
Figure 4.34 **S. Typhi H58 clinical isolates cause similar levels of cell death compared to S. Typhi genotype 3.3.** 155
Figure 4.35 **Overexpression of SPI-1 T3SS expression induces higher epithelial cell invasion by S. Paratyphi A 9150.** 156
Figure 4.36 **Overexpression of SPI-1 T3SS results in elevated THP-1 cell death and bacterial internalisation during infection with S. Paratyphi A 9150.** 157
Figure 4.37 **Deletion of fepE does not impact bacterial growth.** 158
Figure 4.39 **Very long LPS O-antigen chains suppress macrophage cell death independently of bacterial internalisation during infection with S. Paratyphi A.** 159
Figure 4.38 **Loss of very long O-antigen chains results in increased epithelial cell invasion during infection with S. Paratyphi A.** 159
Figure 4.40 **Loss of very long O-antigen chains in S. Paratyphi A triggers increased inflammasome activation in THP-1 cells.** 160

Figure 4.41 **S. Paratyphi A cytosolic escape relies on SPI-1 T3SS but is not affected by very long O-antigen chains.** 161
Figure 4.42 **Loss of very long LPS O-antigen chains in S. Paratyphi A does not interfere with THP-1 cell priming.** 162
Figure 4.43 **Complementation of ΔfepE in S. Paratyphi A recovers epithelial cell invasion.** 163
Figure 4.44 **Complementation of loss of very long O-antigen LPS chains in S. Paratyphi A recovers cell death level in THP-1 cells.** 164
Figure 4.45 **Loss of very long O-antigen chains mediates increased IL-1β secretion independently of host cell priming during infection with S. Paratyphi A.** 165
Figure 4.46 **S. Paratyphi A ΔfepE-induced cell death is mediated by ASC.** 166
Figure 4.47 **ASC speck formation occurs independently of SPI-1 T3SS or very long O-antigen chains during infection with S. Paratyphi A.** 167
Figure 4.48 **ASC speck formation is not NLRP3-dependent during infection with S. Paratyphi A** ... 168
Figure 4.49 **Caspase-4 mediates the increased cell death induced by S. Paratyphi A 9150 ΔfepE** .. 169
Figure 4.50 **FepE-mediated very long O-antigen chains limit S. Typhimurium invasion into HeLa cells.** 170
Figure 4.51 **Very long O-antigen chains limit S. Typhimurium-induced pyroptosis.** 171
Figure 4.52 **S. Paratyphi A induces SPI-1-dependent cell death in MDMs.** 172
Figure 4.53 **S. Paratyphi A ED199 triggers higher levels of cell death in MDMs compared to S. Paratyphi A 9150.** 172
Figure 4.54 **S. Paratyphi A ED199 triggers higher levels of IL-1β in MDMs compared to S. Paratyphi A 9150, independently of cell priming.** 173
Figure 4.55 **S. Paratyphi A triggers caspase-dependent cell death in MDMs** 174
Figure 4.56 **NAIP expression in MDMs is significantly higher than in THP-1 cells.** 175
Figure 4.57 **Effect of NAIP silencing on MDM infection with S. Paratyphi A.** 176
Figure 4.58 **Effect of NLRP3 and caspase-8 inhibition in MDM infection with S. Paratyphi A.** 177
Figure 4.59 **Effect of siRNA-mediated caspase-4 silencing on MDM infection with S. Paratyphi A.** 178
Figure 4.60 **The role of very long O-antigen chains during MDMs infection with S. Paratyphi A 9150.** 179
Figure 4.61 **The role of very long O-antigen chains in cytokine secretion by MDMs during infection with S. Paratyphi A 9150.** 180
Figure 4.63 **Effect of fepE overexpression on S. Paratyphi A ED199-induced cytokine production by MDMs.** 181
Figure 4.62 **The effect of fepE overexpression on S. Paratyphi A ED199-induced MDMs cell death.** 181
Figure 4.64 **The role of very long O-antigen chains during infection of MDMs with S. Typhimurium.** 182
Figure 4.65 **fepE expression inversely correlates with *Salmonella*-induced THP-1 pyrotposis.** 183
Figure 4.66 **Proposed model for S. Paratyphi A inflammasome activation in THP-1 cells.** 186
Figure Appendix.1 **Representative sample of quality checks for RNA-Seq reads.** 225
Figure Appendix.2 **S. Typhi H58-triggered pyroptosis in THP-1 cells.** 226

List of Tables

Table 1.1 **Typhoidal *Salmonella* O and H antigens.** 22
Table 1.2 **Comparison of *S.* Typhi and *S.* Paratyphi A – an overview of their main characteristics** .. 24
Table 2.1 **Strains and plasmids used in this study** 66
Table 2.2 ***S.* Typhi and *S.* Paratyphi A clinical isolate strains from Nepal.** 67
Table 2.3 **Primers used in this study** 69
Table 2.4 **Cell lines used in this study.** 71
Table 2.5 **SMART Pool siRNA sequences** 73
Table 2.6 **Fluorescence antibodies used in this study** 75
Table 2.7 **Western blot antibodies used in this study** 77
Table 3.1 **Read alignment and RNA types in RNA-Seq sample analysis.** 89
Table 3.2 **Number of genes differentially regulated in response to bile.** 91
Table 3.3 **GO enrichment analysis of biological processes differentially expressed in typhoidal *Salmonella* following exposure to bile.** 93
Table 3.4 **Shared upregulated genes in bile between Ty2, 9150, and ED199** 94
Table 3.5 **Shared downregulated genes in bile between Ty2, 9150, and ED199.** 96
Table 3.6 **Genes linked to bile tolerance and/or resistance in *Salmonella*.** 98
Table 3.7 **Expression change of *S.* Paratyphi A genes in bile found as pseudogenes in *S.* Typhi.** 106
Table Appendix.1 **Bile-mediated change in expression of genes in S. Typhi Ty2, S. Paratyphi A 9150 or ED199.** 227

Abbreviations

AIM2	Absent in Melanoma 2
ALR	AIM2-like receptor
AMP	Antimicrobial peptide
ASC	Apoptosis-associated speck-like protein
BIR	Baculoviral inhibitor-of-apoptosis protein repeat-containing
BSA	Bovine serum albumin
CARD	Caspase recruitment domain
CFU	Colony forming unit
CLR	C-type lectin receptor
DAMP	Danger-associated molecular pattern
dsDNA	Double stranded DNA
ECA	Enterobacterial common antigen
EHEC	Enterohaemorrhagic *E. coli*
ELISA	Enzyme-linked immunosorbent assay
EPEC	Enteropathogenic *E. coli*
EV	Empty vector
FBS	Foetal bovine serum
GBP	Guanylate binding protein
GO	Gene ontology
GSDMD	Gasdermin-D
H58	Haplotype 58
HSE	Health & safety executive
IEC	Intestinal epithelial cells
IFN	Interferon
IL	Interleukin
iNTS	Invasive non-typhoidal *Salmonella*
LB	Lysogeny broth
LPS	Lipopolysaccharide
LRR	Leucine rich repeat
M cells	Microfold cells
MAPK	Mitogen-activated protein kinase
MCSF	Macrophage colony stimulating factor
MDM	Monocyte-derived macrophage
MDR	Multi-drug resistance
MIC	Minimum inhibitory concentration
miR	miRNA30E-based stable silencing
MOI	Multiplicity of infection
MyD88	Myeloid differentiation protein 88

ns	Not significant
NAIP	NLR family apoptosis inhibitor protein
NBD	Nucleotide binding domain
Neu5Ac	N-acetylneuramic acid
Neu5Gc	N-glycolylneuramic acid
NF-κB	Nuclear factor kappa-light-chain enhancer of activated B cells
NLR	NOD-leucine-rich repeat
NLRC4	NLR family CARD-containing protein 4
NLRP3	NLR family pyrin domain containing protein 3
NOD	Nucleotide-binding and oligomerisation domain
NTS	Non-typhoidal *Salmonella*
OD	Optical density
ORF	Open reading frame
PAMP	Pathogen-associated molecular pattern
PBS	Phosphate buffered saline
PCA	Principal component analysis
PCR	Polymerase chain reaction
PFA	Paraformaldehyde
PI	Propidium iodide
PIT	Pore-induced intracellular trap
PMA	Phorbol 12-myristate 13-acetate
PRR	Pattern recognition receptor
PYD	Pyrin domain
RFP	Red fluorescence protein
ROS	Reactive oxygen species
RT	Room temperature
siRNA	Small interfering RNA
SCV	*Salmonella* containing vacuole
Sif	*Salmonella*-induced filaments
SNP	Single nucleotide polymorphism
SPI	*Salmonella* pathogenicity island
T3SS	Type III secretion system
TCA	Tricarboxylic acid cycle
TLR	Toll-like receptor
TNF	Tumour necrosis factor
WT	Wild type
XDR	Extensive drug resistance

Publications

Mylona, E., Sanchez-Garrido, J., Baker, S., Hoang Thu, T. H., Dongol, S., Karkey, A., Shenoy A.R., Frankel G. Working title: Very long O-antigen chains of *Salmonella* Paratyphi A inhibit invasion, pyroptosis, and inflammasome activation [Manuscript in preparation].

McDowell, M.A., Byrne, A.M.P., **Mylona, E.**, Johnson R., Sagfors, A., Crepin V.F., Lea, S., Frankel, G. (2019) The *S.* Typhi effector StoD is an E3/E4 ubiquitin ligase which binds K48- and K63-linked diubiquitin. *Life Science Alliance*. 2 (3).

Johnson, R., **Mylona, E.**, Frankel, G. (2018) Typhoidal *Salmonella*: distinctive virulence factors and pathogenesis. *Cellular Microbiology*. 20 (9), e. 12939.

1

Introduction

1.1 *Salmonella enterica* species

1.1.1 Taxonomy and nomenclature

Salmonella is a Gram-negative, rod-shaped, facultative anaerobic bacterium, named after Theobald Salmon, who first isolated and described it in 1884 (Su & Chiu, 2007). Based on the current Centre for Disease Control and Prevention nomenclature system, the *Salmonella* genus belongs to the *Enterobacteriaceae* family and comprises two species, *S. enterica* and *S. bongori* (Brenner *et al.*, 2000; Grimont & Weill, 2007). Based on biochemical and genomic homology, the use of six subspecies belonging to *S. enterica* has been approved: subspecies *enterica* (subsp. I), *salamae* (subsp. II), *arizonae* (subsp. IIIa), *diarizonae* (subsp. IIIb), *houtenae* (subsp. IV), and *indica* (subsp. VI) (Brenner *et al.*, 2000; Grimont & Weill, 2007). The Kauffmann-White scheme subdivides subspecies into serovars based on serologic identification of O (somatic) and H (flagellar) antigens; more than 2,500 *Salmonella* serovars have been recognised (Brenner *et al.*, 2000; Grimont & Weill, 2007).

S. enterica subsp. *enterica* is of particular importance, causing extensive morbidity and mortality in both humans and other vertebrates (Coburn, Grassl & Finlay, 2007). Based on the disease they cause in humans, serovars belonging to this subspecies are broadly divided into typhoidal, such as serovars Typhi and Paratyphi A, and non-typhoidal *Salmonella* (NTS) serovars, such as serovar Typhimurium. For simplicity, in this report the name will be shortened into the genus and serovar format, i.e. *Salmonella enterica* subsp. *enterica* serovar Paratyphi A will be *Salmonella* Paratyphi A or *S.* Paratyphi A (Brenner *et al.*, 2000).

1.1.2 Pathogenesis in humans

The majority of *S. enterica* subsp. *enterica* serovars are pathogenic for warm-blooded animals. Serovars may be either generalists (with a broad host range) such as *S.* Typhimurium and *S.* Enteritidis, infecting humans, poultry and cattle alike, or host-restricted, such as *S.* Paratyphi A and *S.* Typhi that only infect humans, and *S.* Dublin that only infects cattle (Gal-Mor, 2019).

Acute enteric (typhoid or paratyphoid) fever is endemic in areas with poor sanitation and is caused by typhoidal *Salmonella* ingested with contaminated water or food. There are 11–27 million cases annually, from which > 120,000 are fatal (Buckle, Walker & Black, 2012; Darton, Blohmke & Pollard, 2014; Stanaway *et al.*, 2019; Mogasale *et al.*, 2014; Antillón *et al.*, 2017; WHO, 2018; Baker *et al.*, 2011). There is a higher incidence among children and teenagers in endemic areas (WHO, 2003; Crump & Mintz, 2010; Stanaway *et al.*, 2019). Infection with typhoidal serovars is invasive, where bacteria enter the bloodstream and disseminate systemically (Dougan & Baker, 2014; Raffatellu *et al.*, 2008). Symptoms typically include prolonged fever, headache, muscle and stomach aches, malaise, and diarrhoea or constipation. In rare occasions, complications such as intestinal bleeding (10–20% of cases) and perforation (1–3%), encephalopathy (2–40%) or sepsis and septic shock are reported (Bhan, Bahl & Bhatnagar, 2005; Parry *et al.*, 2002; WHO, 2003; Crump *et al.*, 2015). Rose spots may also develop on the chest and abdomen of < 25% of patients (WHO, 2003; Crump *et al.*, 2015). Enteric fever has a long incubation period of 5–14 days, depending on the infectious dose, and usually lasts for 3 weeks (Raffatellu *et al.*, 2008; Levine, Tacket & Sztein, 2001; Raffatellu *et al.*, 2006; Crump *et al.*, 2015). Colonisation of systemic sites allows the establishment of chronic carriage in the gallbladder in 1–5% of patients (WHO, 2003; Dougan & Baker, 2014; Gunn *et al.*, 2014; Gonzalez-Escobedo & Gunn, 2013a).

Foodborne human infection with NTS results in > 80 million cases per year and > 150,000 deaths are attributed to *Salmonella*-associated gastroenteritis (Majowicz *et al.*, 2010). NTS serovars such as *S.* Typhimurium and *S.* Enteritidis are prevalent worldwide (Hohmann, 2001; Majowicz *et al.*, 2010). In healthy humans, NTS infection remains localised in the ileum and colon, typically resulting in gastroenteritis (Zhang *et al.*, 2003). Symptoms include watery diarrhoea, abdominal pain, nausea and

vomiting (Hohmann, 2001; Gal-Mor, Boyle & Grassl, 2014). Symptoms develop within an incubation period of 6–72 h, last < 10 days and do not commonly require antibiotic treatment to resolve (Hohmann, 2001; Raffatellu *et al.*, 2008, 2006). The risk increases in patients with a weak immune system, such as young children and the elderly, patients undergoing immunosuppression, following gastric surgery, as well as individuals with a disrupted intestinal microbiome (Feasey *et al.*, 2012; Gal-Mor, Boyle & Grassl, 2014; Hohmann, 2001; Crump *et al.*, 2015). A fraction of patients (~5%) with NTS-caused gastroenteritis, who are usually immunocompromised individuals, may develop bacteraemia (Hohmann, 2001; Crump *et al.*, 2015). Recently, the emergence of invasive NTS (iNTS) in sub-Saharan Africa, such as *S.* Typhimurium ST313, has led to invasive systemic infections with > 20% mortality rate among immunocompromised patients suffering from HIV, malaria, or malnutrition (Feasey *et al.*, 2012; Kingsley *et al.*, 2009). ST313 isolates exhibit commonalities with *S.* Typhi and *S.* Paratyphi A, such as increased genome degradation and systemic dissemination (Feasey *et al.*, 2012; Kingsley *et al.*, 2009).

1.1.3 Typhoidal *Salmonella* and their epidemiology

Enteric fever is caused by typhoidal *Salmonella* serovars Typhi, Paratyphi A, Paratyphi B, Paratyphi C and Sendai (Gal-Mor, Boyle & Grassl, 2014; Raffatellu *et al.*, 2008); their O and H antigens are listed in Table 1.1. Enteric fever is endemic in South and Southeast Asia and sub-Saharan Africa, with Asia having the highest incidence and mortality rates (Figure 1.1) (Crump *et al.*, 2015; Thanh *et al.*, 2016; Stanaway *et al.*, 2019; Baker *et al.*, 2011). However, sparse data and poor surveillance in several countries complicate estimations of actual numbers of enteric fever cases (Stanaway *et al.*, 2019). *S.* Typhi is the most common etiologic agent of enteric fever (Stanaway *et al.*, 2019). However, the rate of *S.* Paratyphi A isolation has been rising in the recent years, partly due to the use of the Vi vaccine against *S.* Typhi (Zellweger *et al.*, 2017; Sahastrabuddhe *et al.*, 2013) (Table 1.2). Currently, *S.* Paratyphi A may cause > 40% of enteric fever cases in India, Nepal, and Pakistan (Zhou *et al.*, 2014; Zellweger *et al.*, 2017; Sahastrabuddhe *et al.*, 2013) and about a third globally (Stanaway *et al.*, 2019). In addition, the incidence of *S.* Paratyphi A may be underestimated due to the unavailability of appropriate diagnostic tools (Sahastrabuddhe *et al.*, 2013). While the incidence and mortality rates of enteric fever have shown a decline over the last three decades, possibly owing to economic improvement of endemic countries and the associated development of sanitation and food handling (Stanaway *et al.*, 2019), enteric fever incidence remains high in many regions supporting development of vaccination policies (Marchello, Hong & Crump, 2019).

Table 1.1 **Typhoidal *Salmonella* O and H antigens.**

Table adapted from WHO, 2003; Grimont & Weill, 2007. Antigens used in agglutination assays for each serovar are shown in bold. *S.* Typhi Phase 2 H antigen z66 is rarely found. *S.* Paratyphi A does not typically express Phase 2 H antigens. *S.* Typhimurium is presented as an example NTS for comparison.

Serovar	O antigen	H antigen (Phase 1 : Phase 2)	Serogroup
S. Typhi	**9**, 12, Vi	**d**, j : z66	D1
S. Paratyphi A	1, **2**, 12	**a** : (1, 5)	A
S. Paratyphi B	1, **4**, (5), 12	**b** : 1, 2	B
S. Paratyphi C	**6**, **7**, (Vi)	**c** : 1, 5	C1
S. Sendai	1, 9, 12	a : 1, 5	D1
S. Typhimurium	1, 4, 5, 12	i : 1, 2	B

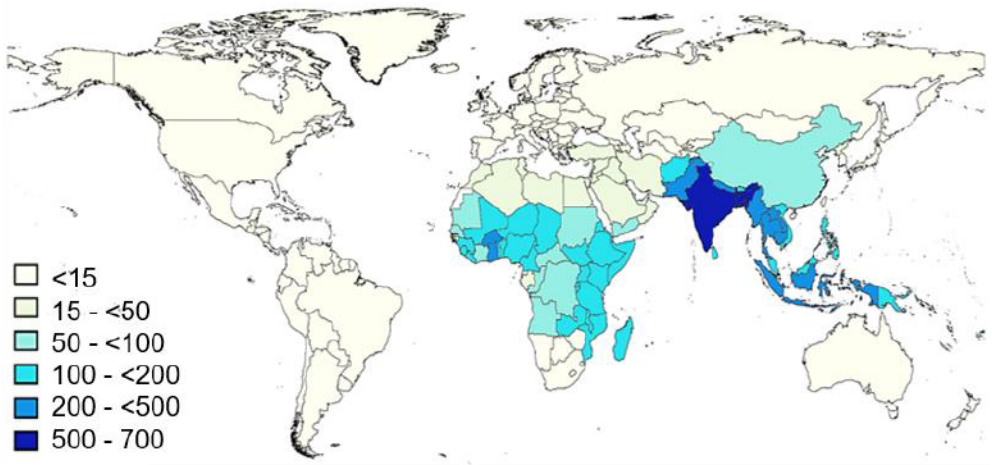


Figure 1.1 **Enteric fever global incidence in 2017.**

Key shows number of cases per 100,000. Adapted from Stanaway *et al.*, 2019.

1.1.3.1 *Salmonella* Typhi

S. Typhi is the main cause of enteric fever (Table 1.2). Of interest is Haplotype 58 (H58), which is a recently emerged subclade and is responsible for the ongoing typhoid epidemic in Asia and Africa (Feasey *et al.*, 2015; Wong *et al.*, 2015). Phylogeographical analysis suggests that H58 has clonally expanded and disseminated globally, unlike other subclades of *S.* Typhi that have remained geographically restricted (Feasey *et al.*, 2015; Wong *et al.*, 2015, 2016). *S.* Typhi multi-drug resistance (MDR) is associated with H58 in most countries, although this is likely not the only contributing factor to the success of this genotype and the underlying mechanisms remain largely unknown (Feasey *et al.*, 2015; Thanh *et al.*, 2016; Wong *et al.*, 2015; Johnson, Mylona & Frankel, 2018).

1.1.3.2 *Salmonella* Paratyphi A

S. Paratyphi A is an important though-neglected pathogen in Asia (Woods *et al.*, 2006). *S.* Paratyphi A infects young children less often than *S.* Typhi (Sahastrabuddhe *et al.*, 2013), which may partly explain the lower numbers of fatal cases attributed to *S.* Paratyphi A. Like *S.* Typhi, *S.* Paratyphi A strains with reduced susceptibility to currently used antimicrobials and MDR have emerged (Sahastrabuddhe *et al.*, 2013), further increasing the alarm for this pathogen. Extreme drug resistance (XDR) seen in *S.* Typhi (Klemm *et al.*, 2018) may soon be replicated in *S.* Paratyphi A while it spreads globally. Phylogenetic studies on *S.* Paratyphi A have discovered worldwide spread on multiple occasions and have classified isolated strains into seven lineages A–G (Zhou *et al.*, 2014). Lineages A and C are the progenitors of most extant isolates and currently the most common (Zhou *et al.*, 2014). A clinical isolate belonging to lineage C (ED199 or NVGH308) is currently used in human challenge studies providing the basis for assessing vaccine efficacy (Dobinson *et al.*, 2017; McCullagh *et al.*, 2015). The lack of a paratyphoid vaccine, the increasing global incidence of *S.* Paratyphi A, and the growing MDR (Table 1.2), allow the prediction of *S.* Paratyphi A becoming the major cause of enteric fever within the next few years (Baker, Karkey & Parry, 2014; Woods *et al.*, 2006; Zellweger *et al.*, 2017; Zhou *et al.*, 2014; Crump & Mintz, 2010; Sahastrabuddhe *et al.*, 2013).

Table 1.2 **Comparison of *S.* Typhi and *S.* Paratyphi A – an overview of their main characteristics**

Characteristic	*S.* Typhi	*S.* Paratyphi A	Notes
Host range	Human-restricted	Human-restricted	-
Clinical syndrome	Typhoid fever	Paratyphoid fever	Clinically indistinguishable, occasionally paratyphoid is milder (Maskey *et al.*, 2006; Dobinson *et al.*, 2017)
Cases in 2017	9,343-12,597 x10^3	2,666-4,184 x10^3	(Stanaway *et al.*, 2019)
Carrier state	Yes	Yes	(Dongol *et al.*, 2012)
Treatment	Fluoroquinolones (e.g. ciprofloxacin, gatifloxacin); Third-generation cephalosporins; Azithromycin; Chloramphenicol		(Crump et al., 2015) Reduced susceptibility/resistance against most of these reported
MDR	Yes XDR also reported (XDR=MDR + fluoroquinolones and third-generation cephalosporins)	Yes	MDR = ampicillin, chloramphenicol, trimethoprim-sulfamethoxazole resistance (Parry *et al.*, 2015; Klemm *et al.*, 2018; Sahastrabuddhe *et al.*, 2013)
Infectious dose	10^3 CFUs	0.7-5 × 10^3 CFUs	(Waddington *et al.*, 2014; Levine, Tacket & Sztein, 2001; Dobinson *et al.*, 2017)
Median age	16 years	20 years	Children < 5 y affected more often by typhoid than paratyphoid (Karkey *et al.*, 2010; Sahastrabuddhe *et al.*, 2013)
Vaccine(s)	Attenuated live Ty21a vaccine, Vi Polysaccharide Vaccine (ViPS), Tetanus toxoid conjugated Vi Vaccine (TCV)	Currently no licensed vaccine	(WHO, 2018; McCullagh *et al.*, 2015)
Genome degradation	> 4%	> 4%	< 1% in S. Typhimurium (Holt *et al.*, 2009; Sabbagh *et al.*, 2010; McClelland *et al.*, 2004)
Pseudogenes	> 150 pseudogenes in Ty2 only	> 135 pseudogenes in 9150 only	
	~65 pseudogenes shared		
Capsule	Vi antigen	No capsule	-
Serogroup / O-antigen	D1 / O9, O12	A / O2, O12	(Grimont & Weill, 2007)
***Salmonella* pathogenicity islands (SPIs)**	SPI-1 to SPI-12 and SPI-15 to SPI-18	SPI-1 to SPI-6, SPI-8 to SPI-12, SPI-16, 17, 18	(Desai *et al.*, 2013; Sabbagh *et al.*, 2010)
Typhoid toxin	Yes	Yes	(Haghjoo & Galán, 2004; den Bakker *et al.*, 2011)

HlyE/ClyA toxin		Yes	Yes	(Oscarsson *et al.*, 2002)
Motility (flagellar)		Monophasic (mutation in *fljB;* lack of *hin*) Less motile than *S.* Paratyphi A	Monophasic (mutation in *hin*)	(McClelland *et al.*, 2004; Elhadad *et al.*, 2015a)
In	**high body temp**	Impaired motility	Impaired motility	(Elhadad *et al.*, 2015b)
	bile	**Increased** expression of flagellar genes	Unknown	(Johnson *et al.*, 2018)
Immune evasion strategies	**Immune recognition evasion by modulation of SPI-1/flagellin expression**	TviA-mediated SPI-1 and flagellin expression reduction, reduction of invasion Response to environmental stimuli (see SPI-1 regulation)	Reduction of SPI-1 expression and invasion following response to environmental stimuli (see SPI-1 regulation) Reduction of flagellin expression – mechanism to be determined	(Hiyoshi *et al.*, 2018b; Raffatellu *et al.*, 2005a; Wilson *et al.*, 2008; Winter *et al.*, 2015; Wangdi *et al.*, 2014; Wilson *et al.*, 2011; Elhadad *et al.*, 2015a; Winter *et al.*, 2008, 2009a) Intestinal inflammation also blunted by typhoid toxin? (Del Bel Belluz *et al.*, 2016; Gibani *et al.*, 2019)
	Complement inhibition	Vi-mediated inhibition of complement deposition	Atypical O2 and very long O-antigen chains prevent antibody binding	
	Neutrophil respiratory burst inhibition	Vi antigen-mediated inhibition of antibody-mediated recognition	Very long O-antigen chains prevent antibody binding	
	Immune signalling	Vi and TviA-mediated inhibition of PRR signalling	?	
SPI-1 regulation	**Response to O_2**	SopE-mediated invasion decreases in low O_2 availability	High O_2 reduce SPI-1 expression and epithelial cell invasion	(Elhadad *et al.*, 2016; Johnson *et al.*, 2017)
	Response to high body temperatures	Decreased invasion	Decreased SPI-1 expression, decreased invasion	Fever suggests systemic dissemination, SPI-1 may no longer be required (Elhadad *et al.*, 2015b; Johnson, Mylona & Frankel, 2018)
	Response to the intestinal epithelium	Osmoregulation via TviA-mediated reduction of SPI-1 expression Butyrate-mediated SPI-1 repression	Intraepithelial increase in O_2 levels limit SPI-1 expression (unknown mechanism) Butyrate-mediated SPI-1 repression	Reduction of SPI-1 expression to limit intestinal inflammation (Bronner *et al.*, 2018; Haneda *et al.*, 2009; Winter *et al.*, 2014, 2009b, 2010)
	Response to bile	Increased expression and invasion	Unknown	Adaptation to/colonisation of the gallbladder? (Johnson *et al.*, 2018)
Requirement of SPI-2		None found during infection of cultured cells or of humanised mouse model	? / increased expression and required for intracellular replication in feverlike temperatures	(Forest *et al.*, 2010; Karlinsey *et al.*, 2019; Elhadad *et al.*, 2015b)

1.1.3.3 *Salmonella* Paratyphi B, Paratyphi C and Sendai

The remaining typhoidal *Salmonella* serovars are beyond the scope of this project and are only briefly discussed. *S.* Paratyphi B comprises clones of different phylogenetic origin, mainly of lineage Java and *sensu stricto*; the former is mostly associated with gastroenteritis, while the latter with enteric fever (Higginson *et al.*, 2018; Barker *et al.*, 1988). The incidence of *S.* Paratyphi B *sensu stricto* has declined over the last decades (Levine *et al.*, 2007), but its occurrence may increase following the use of vaccines against *S.* Typhi and those under development against *S.* Paratyphi A (Higginson *et al.*, 2018). *S.* Paratyphi C is often misidentified due to the high similarity to *S.* Cholerasuis, a swine-adapted serovar (Grimont & Weill, 2007; Liu *et al.*, 2009), so its incidence may be difficult to estimate. *S.* Paratyphi C is more similar to *S.* Cholerasuis than to *S.* Paratyphi A and *S.* Typhi (Liu *et al.*, 2009) . However, unlike *S.* Paratyphi A and B, *S.* Paratyphi C carries the Vi antigen similar to *S.* Typhi (Bäumler *et al.*, 1998; Bueno *et al.*, 2004) (Table 1.1; for Vi see Section 1.6.2). *S.* Sendai is rarely isolated from patients and it recently diverged from *S.* Paratyphi A (see also Figure 1.2B) (Feng *et al.*, 2019).

1.2 Diagnosis, treatment, and vaccination for enteric fever

The lack of effective diagnostics tools and treatment options represent major obstacles in controlling enteric fever. Cases are commonly confirmed following persisting fever and bacteria isolation and culture (Crump *et al.*, 2015; Parry *et al.*, 2011). Bone marrow culture is the gold standard owing to its increased sensitivity (> 80%), but due to practical reasons the less sensitive (40–60%) blood culture is the mainstay method, while polymerase chain reaction (PCR)-based diagnostics have the benefit of requiring few or even dead organisms (WHO, 2003; Crump & Mintz, 2010; Crump *et al.*, 2015; WHO, 2018; Parry *et al.*, 2011). However, detection of typhoidal organisms is hindered by the presence of antibiotics, a small specimen volume, inappropriate laboratory media, and/or the time of collection (WHO, 2003; Crump *et al.*, 2015; Parry *et al.*, 2011). Insufficient microbiology facilities often act as an added obstacle in endemic countries (Parry *et al.*, 2011). Serological tests (e.g. Widal test, Typhidot test, and variations of these) detect antibodies against O (lipopolysaccharide [LPS]) and H (flagella) antigens, against the Vi antigen or outer membrane protein antigens, but their sensitivity and reliability are reduced by background levels of the tested antibodies in endemic regions, due to Vi vaccine use and due to similarities of the antigens with other *Salmonella* serovars or enteric bacteria (WHO, 2003; Crump *et al.*, 2015; Parry *et al.*, 2011). Importantly, detection of chronic carriers is hindered by the fact that ~25% of carriers do not report any clinical symptoms prior to developing chronic carriage (WHO, 2003; Gunn *et al.*, 2014; Gal-Mor, 2019; Dongol *et al.*, 2012).

Timely treatment with antibiotics is essential for minimising the mortality rate and complications of enteric fever (Crump & Mintz, 2010; Gibani, Britto & Pollard, 2018; WHO, 2003;

Butler, 2011). However, available options of antimicrobials against enteric fever (Table 1.2) suffer from decreased antibiotic susceptibility that is increasingly being identified among typhoidal *Salmonella* (Crump & Mintz, 2010; Butler, 2011; Wong *et al.*, 2015; Thanh *et al.*, 2016). Other than MDR (Table 1.2), *S.* Typhi and *S.* Paratyphi A resistance to nalidixic acid and fluoroquinolones like ciprofloxacin and ofloxacin has frequently been reported (Parry *et al.*, 2015; Crump *et al.*, 2015; Sahastrabuddhe *et al.*, 2013; Dongol *et al.*, 2012; Zellweger *et al.*, 2017). Extended-spectrum cephalosporins are used to treat MDR *Salmonella*, which, however, require longer time for fever clearance (Parry *et al.*, 2015). Another alternative for uncomplicated enteric fever is the azalide antimicrobial azithromycin, with few resistance cases to this antimicrobial class having been reported to date (Crump *et al.*, 2015; Parry *et al.*, 2015). Alarmingly, plasmid-borne XDR (Table 1.2) in *S.* Typhi isolates from Pakistan leaves limited alternative treatment options (Klemm *et al.*, 2018). Antimicrobial treatment is also hindered by the limited ability of such substances to target intracellular sites in the reticuloendothelial system and the gallbladder (Crump *et al.*, 2015). Antibiotic treatment of chronic carriers is rarely successful (WHO, 2003; Gunn *et al.*, 2014); an extended course of antibiotic administration and/or cholecystectomy, i.e. surgical removal of the gallbladder, may increase the success rate (Crump *et al.*, 2015).

The most efficient prevention and control strategies are the improvement of sanitation, securing the safety of water and food supply, implementation of mass vaccination strategies and development of tools to identify and manage chronic carriers (Crump & Mintz, 2010; Crump *et al.*, 2015; Pitzer *et al.*, 2014; WHO, 2018). As there are no animal reservoirs for *S.* Typhi and Paratyphi A, their elimination may be feasible. Three licensed vaccines against *S.* Typhi are available (Table 1.2). However, Ty21a and ViPS vaccines are licensed for use in children aged ≥ 6 and ≥ 2 years respectively and immunity weakens after three years requiring re-vaccination (Crump & Mintz, 2010; WHO, 2003; Pitzer *et al.*, 2014; WHO, 2018). The recently licensed TCV is suggested to have longer-lasting protection and is safe for people aged ≥ 6 months and ≤ 45 years old (Baker, Karkey & Parry, 2014; Pitzer *et al.*, 2014; WHO, 2018). However, vaccination remains scarce in endemic countries (Stanaway *et al.*, 2019), although routine vaccination of infants would have the strongest long-term effect in reducing typhoid incidence (Pitzer *et al.*, 2014). Importantly, there are no licensed vaccines against *S.* Paratyphi A yet. Vaccine development against paratyphoid is essential, an ideal solution being a bivalent vaccine conferring protection against both *S.* Typhi and *S.* Paratyphi A (Crump *et al.*, 2015; Crump & Mintz, 2010; Sahastrabuddhe *et al.*, 2013). Live-attenuated *S.* Paratyphi A or conjugate O-antigen-based vaccines are in various stages of development (Sahastrabuddhe *et al.*, 2013; Xiong *et al.*, 2015; Martin *et al.*, 2016), but their protective effect remains undefined (Baker, Karkey & Parry, 2014). Understanding the immune response against *S.* Paratyphi A is thus vital for this purpose.

1.3 Models to study enteric fever

The molecular pathogenesis of *S.* Paratyphi A has been poorly investigated. Although *S.* Typhi has been investigated more, most of the current knowledge on typhoidal *Salmonella* infection is extrapolated from studies on *S.* Typhimurium. *S.* Typhi and *S.* Typhimurium share about 89% genomic homology (Sabbagh *et al.*, 2010) and infection of susceptible mouse strains with *S.* Typhimurium leads to a typhoid-like disease (Broz, Ohlson & Monack, 2012; Higginson, Simon & Tennant, 2016; Tsolis *et al.*, 2011). Also, in contrast to the hazard group 2 *S.* Typhimurium, *S.* Paratyphi A and *S.* Typhi are classified as hazard group 3 organisms by the Health & Safety Executive (HSE) and are listed under Schedule 5 of the Anti-terrorism, Crime and Security Act (2001), which complicates research with these pathogens, as a biosafety level 3 lab and proper training are required.

Due to the host restriction of typhoidal *Salmonella*, there are few appropriate *in vivo* models (Song *et al.*, 2010; Firoz Mian *et al.*, 2011) and thus most studies are performed *in vitro*. An approach has been to introduce *S.* Typhi-specific factors, such as the Vi, into *S.* Typhimurium, which have contributed to our understanding of such factors, but mechanistic differences between the two serovars remain unaddressed (Tsolis *et al.*, 2011). *S.* Typhimurium and typhoidal serovars differ on their host adaptation and the distinct clinical syndromes caused in humans, which are driven by differentially evolved effectors, the degree of genome degradation, differential regulation of virulence factors and typhoidal-specific virulence factors (Dougan & Baker, 2014; Johnson, Mylona & Frankel, 2018; Eswarappa *et al.*, 2008; Holt *et al.*, 2009; Raffatellu *et al.*, 2008; Hiyoshi *et al.*, 2018a; Gal-Mor, Boyle & Grassl, 2014; Jennings, Thurston & Holden, 2017; Sabbagh *et al.*, 2010), which cannot be replicated in a *S.* Typhimurium-infected mouse model of enteric fever (Song *et al.*, 2010). Given that *S.* Paratyphi A and *S.* Typhi are unable to infect common mouse strains (Carter & Collins, 1974), permissive humanised mice, which are engrafted with human hematopoietic stem cells, have been developed as experimental animal models (Libby *et al.*, 2010; Song *et al.*, 2010; Firoz Mian *et al.*, 2011). In these animals, *S.* Typhi is recovered from systemic sites like the liver and spleen, occasionally neurological symptoms may manifest, and an immune response highly similar to humans is elicited in some of the mice (Firoz Mian *et al.*, 2011; Song *et al.*, 2010; Libby *et al.*, 2010). Recently, using this model, Karlinsey *et al.* (2019) demonstrated key differences between *S.* Typhi and *S.* Typhimurium during infection, supporting these models as a useful tool for elucidating the pathogenic mechanisms of typhoidal *Salmonella*. However, limitations of the use of the humanised mouse model so far include the fact that only hematopoietic cells are human while other like epithelial cells are murine, the intraperitoneal delivery of the infecting organisms instead of the natural oral route, and the restriction of the study to the early bacteraemic phase only (Wang, Knodler & Strugnell, 2019).

Human challenge systems have been developed with the main aim being vaccine development (Levine, Tacket & Sztein, 2001; Dobinson *et al.*, 2017; McCullagh *et al.*, 2015; Waddington *et al.*, 2014). Recently, one such system was used to demonstrate that typhoid toxin is not involved in symptom development, in contrast to what was predicted by mouse studies (Gibani *et al.*, 2019; Song, Gao & Galán, 2013), demonstrating that mouse models may be misleading for studying enteric fever. Due to ethical restrictions, human challenge systems present limitations (Wang, Knodler & Strugnell, 2019). Treatment is required when symptoms manifest or at day 14 (Gibani *et al.*, 2019), much earlier than the onset of complications. Therefore, later stages of the disease, including chronic carriage, and serious enteric fever complications cannot be studied in humans (Wang, Knodler & Strugnell, 2019). The lack of an appropriate enteric fever model is thus clear.

1.4 *Salmonella* evolution

The acquisition of *Salmonella* pathogenicity islands (SPIs) have been central to *Salmonella* evolution. SPIs were acquired through horizontal gene transfer and modified via genome degradation (Bäumler, 1997; Bäumler *et al.*, 1998; Liu *et al.*, 2009; Didelot *et al.*, 2007; Fookes *et al.*, 2011; Holt *et al.*, 2009; Desai *et al.*, 2013). Following a single acquisition of SPI-1, the *Salmonella* genus diverged from *Escherichia coli* > 100 million years ago (Bäumler, 1997). Further divergence into the two *Salmonella* species, *S. bongori* and *S. enterica*, was mediated by the acquisition of SPI-2 by *S. enterica* about 25–40 million years ago (Shea *et al.*, 1996; Ochman & Groisman, 1996; Fookes *et al.*, 2011; Bäumler *et al.*, 1998) (Figure 1.2A). SPI-1 and SPI-2 encode for two Type III secretion systems further described in Section 1.5.1.

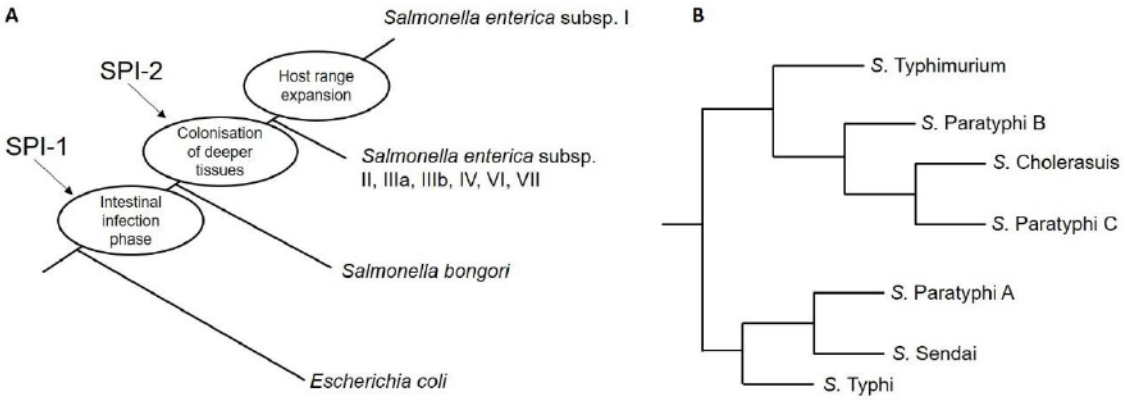


Figure 1.2 **Evolution of *Salmonella*.**

(**A**) Acquisition of genes leading to evolution of *S. enterica* subsp. *enterica* (subsp. I) capable of infecting warm-blooded vertebrates. (**B**) Evolutionary relationship between *S.* Paratyphi A and indicated serovars (not scaled). Panels adapted from Bäumler, 1997; Bäumler *et al.*, 1998; Holt *et al.*, 2009; Liu *et al.*, 2009; Feng *et al.*, 2019.

S. enterica serovars are classified based on their antigenic profile; however, other differences between serovars are found at the genomic level, which are responsible for serovar pathogenicity and host specificity, despite close similarity in nucleotide and amino acid sequences between serovars (Holt *et al.*, 2009; Brown *et al.*, 2003; Bäumler *et al.*, 1998; Liu *et al.*, 2009; Desai *et al.*, 2013; Zhou *et al.*, 2014; Coburn, Grassl & Finlay, 2007). The human-restricted typhoidal serovars *S.* Paratyphi A and *S.* Typhi, which are the focus of this project, have independently evolved within the *S. enterica* species (Didelot *et al.*, 2007), and may share recent common ancestry (den Bakker *et al.*, 2011). They are highly clonal and monomorphic, as well as being relatively distinct from other *Salmonella* serovars (Didelot *et al.*, 2007; Holt *et al.*, 2009; Deng *et al.*, 2003; Holt *et al.*, 2008; Kidgell *et al.*, 2002) (Figure 1.2B). The carrier state (discussed in detail in Section 1.7), which is defined by asymptomatic chronic carriage and shedding of bacteria, is suggested to have largely determined evolution of typhoidal *Salmonella* (Roumagnac *et al.*, 2006; Kidgell *et al.*, 2002; Hiyoshi *et al.*, 2018a). Convergence via homologous recombination and parallel, recent, and extensive genome degradation has occurred during the evolution of *S.* Paratyphi A and *S.* Typhi. Genome degradation (Table 1.2) has largely mediated host restriction and adaptation of typhoidal serovars (Holt *et al.*, 2009; Liu *et al.*, 2009; Holt *et al.*, 2008; Sabbagh *et al.*, 2010; Zhou *et al.*, 2014; Achtman, 2008; Didelot *et al.*, 2007). In fact, host-restriction mediated by genome degradation is common among human-restricted pathogens evolving from a generalist progenitor, such as *Yersinia pestis* and *Mycobacterium leprae* (Feasey *et al.*, 2012). A few pseudogenes shared between *S.* Typhi and *S.* Paratyphi A were acquired via recombination between the two serovars, while the majority were independently formed through adaptive mutation(s) (Holt *et al.*, 2009; Zhou *et al.*, 2014) (Table 1.2). These processes led to independent evolution of the extra-intestinal and systemic lifestyle of typhoidal *Salmonella* serovars (Holt *et al.*, 2009).

1.5 *Salmonella* infection mechanism

Human infection with *Salmonella* typically occurs following consumption of contaminated food or water and is transmitted faecal-orally (Coburn, Grassl & Finlay, 2007). Based on human challenge studies, the infectious dose of *S.* Paratyphi A is typically 1–5 × 10^3 colony forming units (CFU) causing disease in 60% of patients, but as few as 700 CFU may lead to acute enteric fever (Dobinson *et al.*, 2017). Similarly, enteric fever was caused in 55% of individuals infected with 10^3 *S.* Typhi bacteria, with the infectious dose correlating to infection rate and inversely correlating to incubation period (Waddington *et al.*, 2014; Levine, Tacket & Sztein, 2001). In *S.* Typhimurium outbreaks, 10^1–10^4 bacteria were calculated to have been ingested (Blaser & Newman, 1982).

Salmonella survives the stomach and reaches the small intestine, where it crosses the intestinal epithelium and enters the submucosa (Figure 1.3) (Fàbrega & Vila, 2013; Foster & Hall, 1991; Parry *et al.*, 2002). Crossing of the epithelial barrier occurs via different routes: *Salmonella* may invade epithelial cells, be translocated through microfold (M) cells, phagocytosed by macrophages or be taken up by dendritic cell extensions between epithelial cell tight junctions (Parry *et al.*, 2002; Jepson & Clark, 2001; Fàbrega & Vila, 2013; Rescigno *et al.*, 2001; Dougan & Baker, 2014). At the submucosa, NTS infection triggers an extensive exudative inflammatory response, characterised by recruitment of macrophages and dendritic cells and by neutrophil infiltration (Tükel *et al.*, 2006; Zhang *et al.*, 2003). High levels of cytokines like IFNγ, TNF, IL-18, and IL-12 are detected (Santos *et al.*, 2009). Inflammation typically remains localised in the intestine, and results in loss of intestinal barrier integrity and profuse watery diarrhoea (Zhang *et al.*, 2003). Additionally, NTS-induced intestinal inflammation is thought to disrupt the native microbiota to the benefit of *Salmonella* (Stecher *et al.*, 2007). On the other hand,

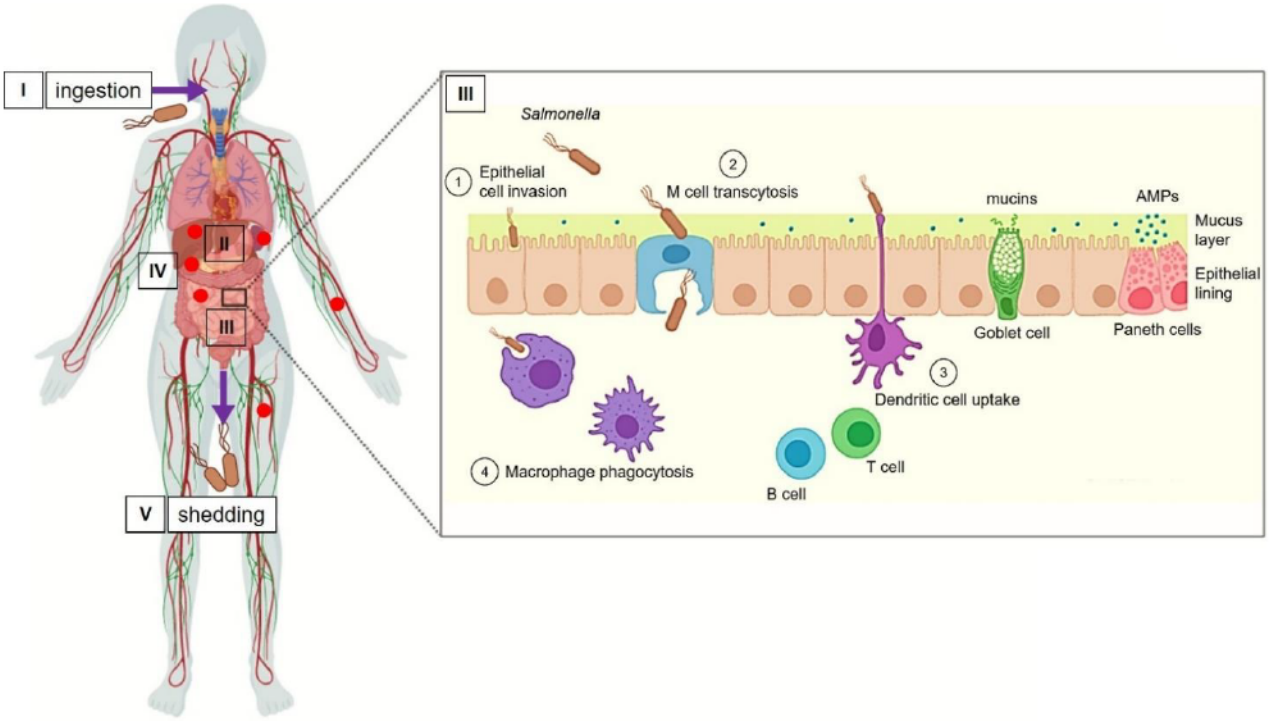


Figure 1.3 **Typhoidal *Salmonella* infection mechanism.**

Following ingestion (I), *Salmonella* passes through the stomach (II) and enters the small intestine (III). Crossing of the epithelial barrier to the submucosa occurs via epithelial cell invasion (1), M cell transcytosis (2), uptake by extending processes of dendritic cells (3), and/or via phagocytosis by macrophages (4). *Salmonella* undergoes intramacrophage replication and migrates to mesenteric lymph nodes, from where it disseminates (IV) via the reticuloendothelial system to systemic sites (red dots) such as the bloodstream, liver, spleen, gallbladder and bone marrow. Establishment of chronic carriage in these organs and reinfection of the gut from the gallbladder leads to shedding (V) and ultimately transmission of enteric fever. Image designed with Biorender.

typhoidal *Salmonella* undergo limited replication in the intestine before reaching the mesenteric lymph nodes, which, together with uptake by macrophages, allow systemic dissemination (Figure 1.3) (Parry *et al.*, 2002; Dougan & Baker, 2014; Raffatellu *et al.*, 2008). IFNγ elevation is observed during infection with *S.* Paratyphi A or *S.* Typhi, along with moderate production of TNF, IL-6 and IL-8 (Gal-Mor, Boyle & Grassl, 2014). However, typhoidal *Salmonella* succeed in systemic dissemination by evading host recognition and immune response activation (Table 1.2) by mechanisms such as the Vi antigen in *S.* Typhi (Winter *et al.*, 2014; Wangdi *et al.*, 2014; Winter *et al.*, 2009b; Raffatellu *et al.*, 2005a; Wilson *et al.*, 2011) and the very long LPS uncommon O-antigen chains in *S.* Paratyphi A (Hiyoshi *et al.*, 2018b). The limited intestinal inflammation during typhoidal *Salmonella* infection (Table 1.2), characterised by mononuclear cell infiltrates while neutrophils are scarce, also explains the long incubation period of enteric fever (Raffatellu *et al.*, 2008). Passage of a small number of typhoidal bacteria, surviving intracellularly, into the bloodstream leads to systemic dissemination via the reticuloendothelial system, reaching other organs such as the gallbladder, liver, spleen, and bone marrow (Figure 1.3) (Gal-Mor, 2019; Dougan & Baker, 2014; Hiyoshi *et al.*, 2018a). Colonisation of such organs facilitates development of the chronic carrier state (Section 1.7), during which reinfection of the gut and bacterial shedding promote transmission of enteric fever (Dougan & Baker, 2014; Gal-Mor, 2019; Gonzalez-Escobedo, Marshall & Gunn, 2011). Clearly, the different clinical presentation of gastroenteritis and enteric fever reflects differences in infection mechanisms and interactions of typhoidal and NTS serovars with the host immune system (Hiyoshi *et al.*, 2018a; Keestra-Gounder, Tsolis & Bäumler, 2015).

1.6 *Salmonella* key virulence factors

1.6.1 *Salmonella* type III secretion systems

Bacterial secretion systems allow bacteria to secrete proteins into the environment, host target cells or other bacteria during competition and are thus considered essential virulence factors for many pathogenic bacteria, as they manipulate host cell processes and promote bacterial survival (Green & Mecsas, 2016; Raymond *et al.*, 2013). Type III secretion systems (T3SS) are involved in pathogenicity of many Gram-negative bacteria such as pathogenic *E. coli*, *Shigella*, and *Yersinia*. T3SS are referred to as injectisomes or molecular syringes as they translocate effector proteins directly from within bacteria to target host cells (Figure 1.4) (Green & Mecsas, 2016; Ramos-Morales, 2012; Coburn, Sekirov & Finlay, 2007). T3SSs are multiprotein complexes, evolutionarily related to flagellar systems, formed by a basal body of two protein rings embedded in the inner and outer bacterial membranes, while a needle spans the space between the bacterium and the host cell (Diepold & Armitage, 2015).

A translocon pore at the tip of the needle creates a port of entry to the target eukaryotic host cell (Figure 1.4) (Deng *et al.*, 2017; Kubori *et al.*, 1998). Effectors generally have a secretion signal directing them to the T3SS and a chaperone may facilitate this transport process within the bacterial cell (Green & Mecsas, 2016; Ramos-Morales, 2012). Chaperones may have diverse roles, such as maintaining the protein in an unfolded state and promoting its stability (Ehrbar *et al.*, 2003; Stebbins & Galán, 2003; Ghosh, 2004).

S. enterica, including *S.* Typhimurium, *S.* Paratyphi A and *S.* Typhi, possess two T3SSs, encoded by SPI-1 and SPI-2. These T3SSs secrete effectors which are involved in host cell invasion, manipulate host cell processes, promote immune evasion and mediate the formation and maturation of a permissive replicative niche termed *Salmonella*-containing vacuole (SCV) inside host cells (McGhie *et al.*, 2009; Jennings, Thurston & Holden, 2017; Fàbrega & Vila, 2013; Ramos-Morales, 2012; Hume *et al.*, 2017). A list of effectors found in *S.* Typhimurium, *S.* Paratyphi A and *S.* Typhi, along with their known functions was recently published (Johnson, Mylona & Frankel, 2018; Jennings, Thurston & Holden, 2017). The repertoire of functional effectors may influence the characteristics of the serovars; for example, many *S.* Typhimurium effectors, such as SopD2 and SlrP, are found as pseudogenes or are differentially evolved in the human-adapted *S.* Typhi and *S.* Paratyphi A, possibly pointing to a reduced requirement for these effectors in these infections (Johnson, Mylona & Frankel, 2018; Sabbagh *et al.*, 2010; Eswarappa *et al.*, 2008). Pseudogenisation of many effector genes has been suggested as a mechanism of host restriction and adaptation of typhoidal *Salmonella* as opposed to NTS (Johnson, Mylona & Frankel, 2018). *S.* Typhimurium encodes for additional effectors not found in the other serovars, such as GtgE, AvrA, and SseJ (Johnson, Mylona & Frankel, 2018), whilst, interestingly, our lab recently identified a T3SS effector found in *S.* Typhi but absent from *S.* Typhimurium and *S.* Paratyphi A with a yet unidentified role (McDowell *et al.*, 2019; Johnson, Mylona & Frankel, 2018). Considering these in addition to the minor differences between *S.* Typhi and *S.* Paratyphi A effector pools (Johnson, Mylona & Frankel, 2018), the different virulence mechanisms employed by the three serovars are further supported.

1.6.1.1 SPI-1 T3SS

Most structural components of the SPI-1 T3SS (Figure 1.4), effectors, chaperones, and regulators are encoded with the SPI-1 pathogenicity island (Fàbrega & Vila, 2013; Lou *et al.*, 2019). The SPI-1 is activated by the conditions in the intestinal milieu, namely low oxygen and high osmolarity (Drecktrah *et al.*, 2006; Kröger *et al.*, 2013; Fàbrega & Vila, 2013). Based on studies with *S.* Typhimurium, SPI-1 T3SS-secreted effectors are typically exploited during the intestinal phase of infection; they mediate invasion into host cells by inducing cytoskeletal rearrangements and membrane ruffling. These actions allow bacterial internalisation by the host cell and formation of the SCV (Srikanth *et al.*, 2011; McGhie

et al., 2009). *S.* Paratyphi A, *S.* Typhi and *S.* Typhimurium all require the SPI-1 T3SS to invade host cells *in vitro* (Galan & Curtiss III, 1989; Bishop *et al.*, 2008; Elhadad *et al.*, 2016). *In vivo*, the SPI-1 may be dispensable following intraperitoneal inoculation, while it is suggested to be important after oral inoculation (Galan & Curtiss III, 1989). Although SPI-1-independent invasion mechanisms have been described in *S.* Typhimurium (Hume *et al.*, 2017), this T3SS is required for mucosal inflammation and development of diarrhoea (Zhang *et al.*, 2003; Fàbrega & Vila, 2013).

The regulation of SPI-1 is complex and occurs at many levels. It involves numerous genetic regulators and is directed by environmental stimuli (Lou *et al.*, 2019; Fàbrega & Vila, 2013). Briefly, the regulatory network for SPI-1 in *S.* Typhimurium is centred around three transcriptional regulators HilD, RtsA and HilC, with HilD being at the top of the hierarchy; their combined action and environmental

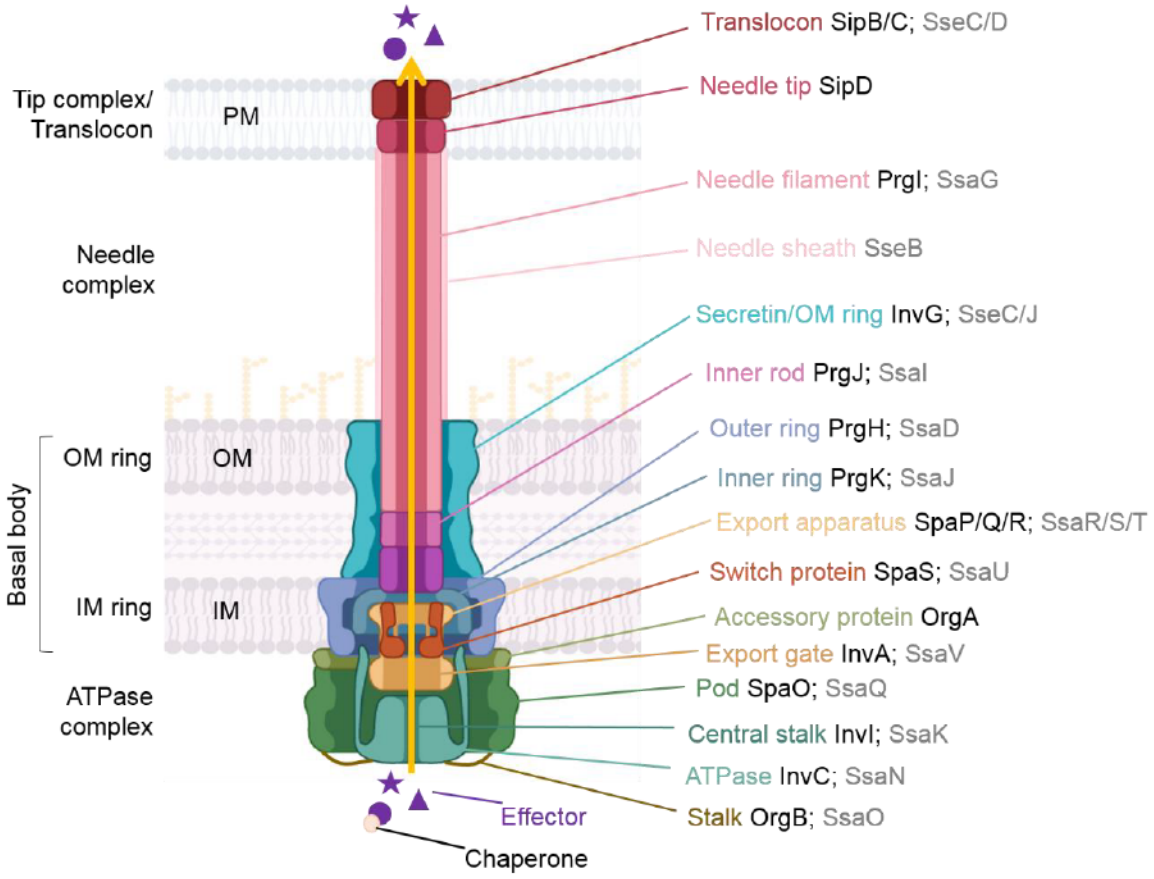


Figure 1.4 **Type III secretion systems in *Salmonella*.**

T3SS are composed of a basal body, a needle filament, and a transolocon that inserts itself in the target eukaryotic cell membrane. The basal body is embedded in the inner and outer membranes and consists of an inner and an outer ring. An ATPase at the base of the basal body energises the secretory process, while a sorting complex mediates the targeting of the effectors via the T3SS. The needle filament spans the space between the bacterium and the target cell. Effector delivery to the T3SS is often mediated by chaperones. Protein names in black represent SPI-1 T3SS proteins, while in grey SPI-2 T3SS proteins. PM, eukaryotic plasma membrane; IM, inner membrane; OM, Outer membrane. Image partially designed with Biorender.

signals result in activation of HilA which is the master positive SPI-1regulator, activating the expression of structural and effector genes (Fàbrega & Vila, 2013). HilD, RtsA and HilC receive positive or negative signals from other regulatory systems allowing communication with other virulence strategies. *hilD*, *hilC*, and *hilA* are encoded within the SPI-1, while *rtsA* and *hilE* (involved in *hilA* downregulation) are present at separate genomic loci (Fàbrega & Vila, 2013; Lou ***et al.***, 2019). Regulation of SPI-1 is important to minimise the energetic cost required for its synthesis and to limit recognition by the immune system (Table 1.2) (Johnson, Mylona & Frankel, 2018; Fàbrega & Vila, 2013).

SPI-1 regulation in response to stimuli such as bile, oxygen availability, and temperature, often differs between NTS and typhoidal *Salmonella*, as well as between *S.* Paratyphi A and *S.* Typhi (Table 1.2). For example, *S.* Typhimurium limits expression of SPI-1 genes following exposure to bile, while *S.* Typhi upregulates these genes (Johnson ***et al.***, 2018; Prouty & Gunn, 2000). Furthermore, SPI-1 in *S.* Typhimurium shows similar expression patterns in aerobic and microaerobic growth and it becomes more invasive following aerobic growth (Ibarra ***et al.***, 2010). In contrast, *S.* Paratyphi A invasiveness increases in microaerobic conditions (Elhadad ***et al.***, 2016). Invasion and motility of typhoidal serovars are downregulated in response to fever-like temperatures (39–42 °C) compared to 37 °C, while these virulence strategies do not show marked changes in *S.* Typhimurium, likely reflecting the ability to sense dissemination to systemic sites by typhoidal serovars (Elhadad ***et al.***, 2015b). Differences in SPI-1 regulation between typhoidal and NTS likely reflect different sites of infection and/or adaptation to systemic sites and immune evasion by typhoidal *Salmonella* (Johnson ***et al.***, 2018; Johnson, Mylona & Frankel, 2018; Elhadad ***et al.***, 2015b; Ibarra ***et al.***, 2010; Elhadad ***et al.***, 2016; Johnson ***et al.***, 2017).

1.6.1.2 SPI-2 T3SS

SPI-2 encodes structural genes (Figure 1.4), effectors and chaperones for a second T3SS which is important for intracellular survival. Expression of SPI-2 is induced by the intracellular environment, particularly that of macrophages, where the presence of nutrients is scarce (Fass & Groisman, 2009). The SPI-2 T3SS mediates the formation of *Salmonella*-induced filaments (Sifs) which position the SCV in a juxtanuclear position exploiting the host cell cytoskeleton. Maturation of SCV is mediated by SPI-2, promoting bacterial intracellular proliferation and survival (Steele-Mortimer, 2008; Jennings, Thurston & Holden, 2017). SPI-2 effectors mediate interactions of the SCV with the Golgi apparatus, ensure protection by stabilizing the SCV membrane, interact with the actin cytoskeleton, modulate lysosome function, and are involved in immune signalling (Jennings, Thurston & Holden, 2017).

Expression of the SPI-2 is regulated primarily by the SPI-2-encoded SsrAB two component system in *S.* Typhimurium. Upon activation by acidic pH or the macrophage intracellular milieu, SsrB promotes SPI-2 gene expression by binding to the promoters of SPI-2 genes and by counteracting the

silencing activity of H-NS, which generally represses horizontally acquired genes (Walthers *et al.*, 2007; Fass & Groisman, 2009). Cross-talk between the regulatory elements of SPI-1 and SPI-2 via HilD and SsrB allows the switch from the SPI-1 T3SS to the SPI-2 T3SS (Bustamante *et al.*, 2008).

The role of the SPI-2 T3SS during infection with typhoidal *Salmonella* serovars remains unclear. The highly host-adapted *S.* Typhi and *S.* Paratyphi A carry many SPI-2 effectors as pseudogenes that are present and intact in other gastrointestinal serovars, or lack them altogether (Jennings, Thurston & Holden, 2017; Johnson, Mylona & Frankel, 2018). *S.* Paratyphi A exhibited a significant increase in SPI-2 expression and intracellular replication in response to high temperatures (42 °C) possibly implying switching to intracellular survival following systemic dissemination (Elhadad *et al.*, 2015b). *S.* Typhi SPI-2 has been shown to be upregulated in macrophages (Faucher *et al.*, 2006). However, it has been suggested to be dispensable for *S.* Typhi survival within macrophages (Forest *et al.*, 2010); this was recently corroborated in a humanised mouse model of typhoid fever where SPI-2 mutants were recovered from systemic sites equally as well as wild-type (WT) bacteria (Karlinsey *et al.*, 2019). The role of SPI-2 during infection with typhoidal *Salmonella* requires further investigation.

1.6.1.3 Role in virulence

The SPI-1 and SPI-2 T3SSs have multiple roles in *Salmonella* virulence. They mediate host cell invasion, SCV formation and maturation, immune evasion and induction of host cell death.

During infection, *Salmonella* adheres to the host cell surface and translocates effectors in a SPI-1 T3SS-dependent manner. Briefly, effectors such as SipA, SipC, SopA, SopB, SopD and SopE/SopE2 induce host cytoskeletal rearrangements to mediate bacterial uptake by membrane ruffling. SipC and SipA manipulate actin polymerisation and bundling, while SopB promotes membrane ruffling and SopE/SopE2 activates Rho GTPases Cdc42 and Rac1 (Raffatellu *et al.*, 2005b; McGhie *et al.*, 2009; Hayward & Koronakis, 1999; McGhie, Hayward & Koronakis, 2001; Friebel *et al.*, 2001; Zhou, Mooseker & Galán, 1999; Finn *et al.*, 2017; Stender *et al.*, 2000). In this manner, *Salmonella* manipulates several cytoskeleton-associated pathways, myosin-mediated contraction pathways, and vesicle trafficking pathways (Hume *et al.*, 2017). Subsequently, the antagonistic actions of *S.* Typhimurium SptP with SopE promote the recovery of the cytoskeleton to a steady state (Kubori & Galán, 2003). However, despite the high similarity between *S.* Typhi and *S.* Typhimurium, SptP appears to be non-functional in *S.* Typhi (Johnson *et al.*, 2017). SPI-1 T3SS effectors also modulate tight junctions between epithelial cells, which leads to epithelial barrier disruption and diarrhoea (Ramos-Morales, 2012).

Following internalisation into the host cell, *Salmonella* resides within a vacuole or phagosome. The SPI-1 T3SS effectors mediate the early steps of phagosome conversion to SCV soon after infection, with SopB and SopE playing major roles, while SPI-2 T3SS effectors such as SseF, SseG, SseJ, PipB2, SifA

among others, mediate positioning the SCV close to the nucleus, intracellular replication and Sif formation (Bakowski, Braun & Brumell, 2008; McGhie *et al.*, 2009; Steele-Mortimer, 2008). The SCV offers a protective and permissive niche for *Salmonella* to replicate intracellularly. Altogether, the SCV and SPI-2 T3SS effectors protect intracellular *Salmonella* from reactive oxygen species (ROS) generated in response to infection, modulate host cell death and interfere with antigen presentation among other functions (Bakowski, Braun & Brumell, 2008; Ibarra *et al.*, 2010; Ramos-Morales, 2012; Knodler & Steele-Mortimer, 2003; Jennings, Thurston & Holden, 2017). Sifs carry late endocytic markers and have been suggested to support perinuclear positioning of the SCV in close proximity to the Golgi apparatus; the association with the Golgi apparatus may allow nutrient and/or membrane uptake (Srikanth *et al.*, 2011; McGhie *et al.*, 2009). Naturally, some intracellular *Salmonella* do not reside in the SCV and are either targeted by autophagy or escape the vacuole and either replicate in the cytosol or are degraded by host cell defence mechanisms (Bakowski, Braun & Brumell, 2008). SPI-2-independent *S.* Typhimurium intracellular growth has been observed to occur outside the SCV primarily in cultured epithelial cells (Brumell *et al.*, 2002; Malik-Kale, Winfree & Steele-Mortimer, 2012; Beuzón, Salcedo & Holden, 2002).

The *Salmonella* T3SS have important roles in modulating and evading host immune responses (McGhie *et al.*, 2009). The initial inflammatory response elicited by *S.* Typhimurium is induced by the activities of SPI-1 T3SS effectors. For example, manipulation of Rho GTPases like Cdc42 by SopE/E2 is sensed by the host cell, resulting in activation of NF-κB and AP-1 pathways leading to transcriptional upregulation of pro-inflammatory genes and stimulation of immune cell migration (Patel & Galán, 2006; Patel & McCormick, 2014). T3SS effectors also interact with cell death pathways (Ramos-Morales, 2012; Wemyss & Pearson, 2019). *Salmonella* secretes both pro-apoptotic (e.g. SpvB and SlrP) and anti-apoptotic (e.g. AvrA and SopB) effectors into epithelial cells, which collectively facilitate intramacrophage replication following establishment of its intracellular niche (Ramos-Morales, 2012; Finn *et al.*, 2017; Wemyss & Pearson, 2019). *S.* Typhimurium suppresses necroptosis, which is a lytic, caspase-independent form of cell death, via the secretion of T3SS effectors (SseK1-3), which also inhibit apoptosis and NF-κB-dependent signalling (Günster *et al.*, 2017; Wemyss & Pearson, 2019). Macrophages have evolved intracellular immune surveillance mechanisms such as the inflammasomes, which can detect effectors and T3SS structural components such as PrgJ and PrgI and promote pyroptotic cell death and inflammation (see also Section 1.9.3) (Wemyss & Pearson, 2019). *S.* Typhimurium thus expresses several T3SS effectors that dampen the immune response by inhibiting inflammatory signalling such as SptP, AvrA and SseL (McGhie *et al.*, 2009). Some effectors linked to modulation of inflammatory responses are interestingly absent (e.g. AvrA) or pseudogenes (e.g. SlrP) in *S.* Typhi and *S.* Paratyphi A (Sabbagh *et al.*, 2010; Johnson, Mylona & Frankel, 2018).

Although the SPI-1 T3SS is thought to be involved in invasion and SPI-2 T3SS in intracellular survival, there is a temporal and spatial overlap in their functions (Brawn, Hayward & Koronakis, 2007; Srikanth *et al.*, 2011; McGhie *et al.*, 2009; Finn *et al.*, 2017). The SPI-1 T3SS has also been involved in intracellular replication and SCV biogenesis (Steele-Mortimer *et al.*, 2002), while some effectors can be secreted by both T3SSs and SPI-1 T3SS-dependent effectors may persist within the host cells until late stage of infection, when SPI-2 is active. Finally, in some cases both systems may be required simultaneously (Srikanth *et al.*, 2011; McGhie *et al.*, 2009; Brawn, Hayward & Koronakis, 2007).

1.6.2 Vi antigen in *S.* Typhi

S. Typhi produces a virulence polysaccharidic capsule named Vi antigen; Vi-positive *S.* Typhi strains are more virulent than strains lacking the Vi (Parry *et al.*, 2002) and thus the majority of primary *S.* Typhi isolates from humans express the Vi (Raffatellu *et al.*, 2006). Vi is encoded by the *viaB* locus found within the SPI-7 (Pickard *et al.*, 2003). A highly similar *SPI-7* is present in *S.* Paratyphi C and *S.* Dublin, while is absent from *S.* Paratyphi A, as well as *S.* Typhimurium and other gastroenteritis-causing serovars (Raffatellu *et al.*, 2005a; Parkhill *et al.*, 2001; Pickard *et al.*, 2003; Bueno *et al.*, 2004).

The *viaB* locus encodes genes necessary for its transcriptional regulation (*tviA*), Vi biosynthesis (*tviBCDE*), and export and retention of the Vi on the bacterial cell surface (*vexABCDE*) (Virlogeux *et al.*, 1995). TviB and TviC catalyse the formation of the Vi building blocks, while TviD and TviE facilitate the polymer synthesis and assembly (Virlogeux *et al.*, 1995; Wetter *et al.*, 2012). VexBC form an ABC transporter, VexA is an outer membrane polysaccharide export protein, VexD is a polysaccharide co-polymerase protein, while VexE is a lipid anchor, important for deposition and retention of the Vi antigen on the bacterial surface (Wetter *et al.*, 2012; Liston, Ovchinnikova & Whitfield, 2016; Virlogeux *et al.*, 1995). The regulator TviA is a *viaB* locus activator (Virlogeux *et al.*, 1995), and a negative regulator for SPI-1 T3SS and flagellin expression through repression of the flagellar regulator *flhDC* (Winter *et al.*, 2009b). Therefore, absence of *tviA* results in increased invasion to host cells (Winter *et al.*, 2009b), while absence of Vi synthesis and export genes leads to variable invasion capacity based on the cultured cell type being tested (Bishop *et al.*, 2008; Winter *et al.*, 2009b). TviA availability increases in low osmolarity and is thought to physiologically translate as such: low TviA during intestinal epithelial invasion downregulates Vi expression and allows flagellar motility and SPI-1 T3SS activity, while Vi upregulation in tissues promotes immune evasion (Winter *et al.*, 2009b; Arricau *et al.*, 1998; Virlogeux *et al.*, 1994; Pickard *et al.*, 1994) as discussed next.

TviA dampens pro-inflammatory NF-κB-mediated responses by downregulating SPI-1 T3SS upon tissue entry and introduction of TviA in *S.* Typhimurium has the same effect (Winter *et al.*, 2014). Similarly, TviA-mediated repression of flagellin expression is responsible for preventing inflammasome

activation, as indicated by reduced levels of pyroptosis, an inflammatory form of cell death, and IL-1β (Winter *et al.*, 2015). *S.* Typhi is less cytotoxic for primary human macrophages compared to *S.* Typhimurium in a flagellin-dependent manner (Kortmann, Brubaker & Monack, 2015). Also, TviA-mediated reduction of flagellin production and secretion results in reduced levels of MAP kinase (MAPK) signalling and secretion of the chemoattractant IL-8 by human epithelial cells, while the presence of the capsule *per se* is not required for this immunomodulatory mechanism (Winter *et al.*, 2008; Raffatellu *et al.*, 2005a). Importantly, introduction of the *viaB* locus in *S.* Typhimurium leads to reduced inflammation in a murine mouse model (Haneda *et al.*, 2009).

The presence of Vi confers increased resistance to human serum and phagocytosis (Wilson *et al.*, 2011), likely by limiting antibody binding to O-antigens (Wangdi *et al.*, 2014; Hart *et al.*, 2016). The Vi may bind to prohibitin molecules on the host cell surface, thus dampening inflammation through MAPK signalling and IL-8 production (Sharma & Qadri, 2004). Also, Vi prevents recognition of LPS by toll-like receptor (TLR) 4 and flagellin by TLR5, thereby reducing secretion of TNF and IL-8 leading to low levels of neutrophil influx, a characteristic of *S.* Typhi infection (Raffatellu *et al.*, 2005a; Wilson *et al.*, 2008; Winter *et al.*, 2008). In contrast to *S.* Typhimurium, human neutrophils do not respond to the presence of *S.* Typhi by forming pseudopods *in vitro*, as the Vi interferes with complement activation and complement-dependent chemotactic neutrophils responses (Wangdi *et al.*, 2014).

In summary, the *viaB* locus mediates evasion of both intracellular immunity by TivA-dependent downregulation of the SPI-1 T3SS and flagellin expression, and of extracellular immune mechanisms by the Vi acting as a physical shield, interfering with immune recognition and complement deposition on the bacterial surface (Winter *et al.*, 2015; Wangdi *et al.*, 2014; Wilson *et al.*, 2008, 2011).

1.6.3 O-antigen in *S.* Paratyphi A

The highly variable O-antigen is an oligo- or polysaccharide composed of repeating heteropolymers of 2–8 monosaccharides, attached to the LPS core structure and extending towards the environment (Alexander & Rietschel, 2001; Lerouge & Vanderleyden, 2002). The O-antigen is involved in protection from recognition by immune receptors and antibodies, as well as from phagocytic cell uptake and complement activation (Lerouge & Vanderleyden, 2002; Alexander & Rietschel, 2001). Therefore, the O-antigen is under strong selection by the host immune system and, along with lipid A, serves as a virulence determinant (Alexander & Rietschel, 2001) and as an important immunogen resulting in an antibody-mediated response (Reyes *et al.*, 2012). Modifications are hence essential to be able to evade host immune responses (Reyes *et al.*, 2012); these may also affect bacterial adherence and host colonisation (Reyes *et al.*, 2012; Lerouge & Vanderleyden, 2002).

The LPS of *Salmonella* serogroups A and D to which *S.* Paratyphi A and *S.* Typhi belong to respectively (Table 1.1), together with the LPS of serogroup B, is composed of the same minor O-antigen (O12) which has a trisaccharide D-mannose–L-rhamnose–D-galactose backbone (Fierer & Guiney, 2001; Liu *et al.*, 2014). The serogroups diverge at the branching sugar attached on the mannose: group A has a paratose, group D a tyvelose, and group B an abequose, which is the main structural difference between these O antigens (Fierer & Guiney, 2001; Liu *et al.*, 2014). *S.* Typhi carries the O9 antigen (tyvelose), and the NTS *S.* Typhimurium the O4 antigen (abequose) (Table 1.1). However, *rfbE*, the gene encoding the enzyme responsible for converting CDP-Paratose to CDP-Tyvelose, is mutated and non-functional in *S.* Paratyphi A; therefore, a paratose residue, i.e. the O2 antigen, replaces tyvelose (Hiyoshi *et al.*, 2018b; McClelland *et al.*, 2004; Liu *et al.*, 2014). A few non-human NTS serovars carry the O2 antigen, suggesting that this is not an adaptation to humans (Grimont & Weill, 2007; Hiyoshi *et al.*, 2018b). Structural diversity of the O-antigen additionally increases by lateral modifications (e.g. glycosylation or acetylation) (Liu *et al.*, 2014; Reyes *et al.*, 2012).

S. Paratyphi A does not carry the Vi (Bueno *et al.*, 2004), but instead produces very long LPS O-antigen chains, mediated by the polysaccharide co-polymerase FepE, which is a pseudogene in *S.* Typhi (Hiyoshi *et al.*, 2018b). In fact, the loss of function in *fepE* is important for allowing Vi formation and Vi-mediated inflammation suppression by *S.* Typhi (Crawford *et al.*, 2013). The very long O-antigen chains are thought to mediate immune evasion strategies, for which the Vi antigen is responsible in *S.* Typhi (Hiyoshi *et al.*, 2018a) (Table 1.2). Regulation of O-antigen chain length is also important for *S.* Typhimurium virulence and very long O-antigen chains may interfere with bacterial uptake by mouse macrophages *in vitro* (Murray, Attridge & Morona, 2003, 2006). Very long O-antigen chains also contribute to complement resistance in *S.* Typhimurium (Murray, Attridge & Morona, 2005; Hölzer *et al.*, 2009; Murray, Attridge & Morona, 2003). Similar to O-chain length regulation by FepE in *S.* Typhimurium, the very long O-chains on the bacterial surface of *S.* Paratyphi A prevent antibody-mediated complement activation by masking surface structures. Additionally, the *S.* Paratyphi A O2-polysaccharide averts IgM antibody binding due to the inability of IgM to bind to the O2 antigen. In contrast, the O9 antigen of *S.* Typhi is bound by IgM but this is hindered by the presence of the Vi (Hiyoshi *et al.*, 2018b; Hart *et al.*, 2016). Therefore, the ability of both pathogens to prevent antibody binding, the complement bactericidal effects and the induced phagocyte respiratory burst, was acquired independently through convergent evolution (Hiyoshi *et al.*, 2018b). It thus appears that the production of a capsule, be it the Vi in *S.* Typhi or the very long O-polysaccharides of *S.* Paratyphi A, is important for manifestation of enteric fever (Johnson, Mylona & Frankel, 2018; Hiyoshi *et al.*, 2018a).

1.6.4 Flagella

The majority of *S. enterica* serovars are motile, having multiple peritrichous flagella, a structure essential for motility and chemotaxis. Compared to *S.* Typhimurium, typhoidal *Salmonella* serovars Paratyphi A, Typhi and Sendai are significantly less motile, expressing the motility-chemotaxis regulon at lower levels (Elhadad *et al.*, 2015a). The flagellar filament is composed of flagellin monomers; *S.* Typhimurium encodes for two alternating, antigenically distinct flagellins (FliC and FljB) regulated by a phase variation mechanism (Simon *et al.*, 1980). On the other hand, *S.* Paratyphi A and *S.* Typhi are generally considered monophasic (McClelland *et al.*, 2004; Sabbagh *et al.*, 2010). *S.* Typhi has only one gene encoding for flagellin FliC of antigen H:*d* and lacks the gene responsible for phase switching (*hin*). *S.* Paratyphi A has a frameshift mutation in *hin*, disabling phase switching (McClelland *et al.*, 2004). However, *S.* Typhi H:*j* antigenic variants have been isolated in Indonesia, a variation of H:*d* due to an in-frame deletion (Frankel *et al.*, 1989; Baker *et al.*, 2008). Indonesian *S.* Typhi isolates have also been observed to be biphasic, expressing a plasmid-encoded FljB analogue of the H:*z66* antigen (Baker *et al.*, 2007a), as well as a FliC repressor (Baker *et al.*, 2007a) repressing *fliC* expression making *z66* the dominant antigen (Baker *et al.*, 2007b). H:*j* and H:*z66* antigenic variants are thought to have recently emerged during *S.* Typhi evolution (Baker *et al.*, 2008), due to immune selection in the Indonesian region, where *S.* Typhi incidence is high (Baker *et al.*, 2007a). This additional variation is thought to be important for immune response evasion by *S.* Typhi (Schreiber *et al.*, 2015). A similar phenomenon has not been reported in *S.* Paratyphi A yet.

Flagellar-mediated motility facilitates host cell invasion by both typhoidal (Elhadad *et al.*, 2015a; Liu *et al.*, 1988) and NTS (Van Asten *et al.*, 2000; Elhadad *et al.*, 2015a). Flagellin is a potent activator of the immune system for most bacterial pathogens (Miao *et al.*, 2007), recognised by immune receptors, resulting in (pro)inflammatory cytokine secretion (Hayashi *et al.*, 2001; Miao *et al.*, 2007, 2006; Kortmann, Brubaker & Monack, 2015; Reyes Ruiz *et al.*, 2017). However, *S.* Typhi and *S.* Paratyphi A exploit high, fever-like temperatures as a cue to attenuate host cell invasion and bacterial motility, which is hypothesised to promote persistence within the host (Elhadad *et al.*, 2015b).

1.6.5 Adhesins

Interactions with and adhesion to host cells are often facilitated by fimbriae, pili and other adhesive proteins found on the bacterial surface, which are critical for intestinal colonisation. *Salmonella* expresses an array of fimbrial operons, which are dependent on the serovar (Townsend *et al.*, 2001; Sabbagh *et al.*, 2010; Azriel *et al.*, 2017). Differences in the adhesin repertoire in serovars contributes to differences in their infection mechanisms. For example, unlike *S.* Typhimurium that preferentially invades M cells, *stg*-depleted *S.* Typhi shows preferential entry in enterocytes over M cells *in vitro* in an *stg*-dependent manner (Gonzales, Wilde & Roland, 2017). This can in part be

explained by the absence of Lpf (long polar fimbriae) in *S.* Typhi, which mediates M cell recognition and attachment in *S.* Typhimurium (Gonzales, Wilde & Roland, 2017). Furthermore, the fimbrial repertoire and allelic variation observed in fimbrial operons have been suggested to play a role in defining serovar host specificity and tissue tropism (Townsend *et al.*, 2001; Bishop *et al.*, 2008; Yue *et al.*, 2012; Sabbagh *et al.*, 2010; Yue *et al.*, 2015), but the selective pressures driving this selection are not always clear. For example, allelic variation in the adhesin of the *fim* operon, as well as low binding point mutations, are suggested to be involved in host-specific interactions in *S.* Typhimurium, while absence of variation in *S.* Typhi, in addition to high binding, restricts it to binding to human cells (Yue *et al.*, 2015, 2012; Kisiela *et al.*, 2012). Also, pseudogenisation and degradation of fimbrial genes is thought to be implicated in host restriction and adaptation (Yue *et al.*, 2012). *S.* Typhi and Paratyphi A share pseudogenisation or loss of genes in fimbrial operons, which are found active in *S.* Typhimurium and other NTS and may be related to the inability of typhoidal serovars to infect other hosts (Liu *et al.*, 2009; McClelland *et al.*, 2001; Townsend *et al.*, 2001; Parkhill *et al.*, 2001; Yue *et al.*, 2012), while few operons remain fully functional in both serovars (McClelland *et al.*, 2004). Additionally, the presence of pseudogenes has been hypothesised to be a mechanism of energy preservation for *S.* Typhi, as fimbrial production is an energetically costly process (Dufresne, Saulnier-Bellemare & Daigle, 2018). However, our understanding of the role of most fimbrial operons during infection remains limited (Sabbagh *et al.*, 2010), particularly in the context of *S.* Paratyphi A infection. Their expression varies between laboratory growth conditions (Dufresne, Saulnier-Bellemare & Daigle, 2018; Azriel *et al.*, 2017), which further complicates functional investigation and characterisation.

1.6.6 Toxins

The typhoid toxin is a virulence factor expressed by both *S.* Typhi and *S.* Paratyphi A (Haghjoo & Galán, 2004; den Bakker *et al.*, 2011), however, it has been extensively studied only in *S.* Typhi. The typhoid toxin islet is absent from *S.* Typhimurium and *S.* Enteritidis, but is found in other NTS serovars like *S.* Javiana, *S.* Montevideo and *S.* Schwarzengrund (den Bakker *et al.*, 2011; Suez *et al.*, 2013; Rodriguez-Rivera *et al.*, 2015; Miller & Wiedmann, 2016). Mice systemically administered with purified active typhoid toxin developed typhoid symptoms, although not fever, suggesting that typhoid toxin may be responsible for symptom manifestation during human infection, while they also exhibited a drop in immune cell numbers and neutrophil circulation (Song, Gao & Galán, 2013), in line with the possible role of typhoid toxin in modulating the host immune response as assessed in humans (Gibani *et al.*, 2019). Before the typhoid toxin can exert its toxicity, *S.* Typhi must be intracellular and within the SCV (Haghjoo & Galán, 2004; Spanò, Ugalde & Galán, 2008; Fowler & Galán, 2018). Toxin sorting and packaging in vesicles from the SCV requires interaction with a N-acetylneuramic acid (Neu5Ac)-terminated receptor in the SCV lumen (Chang, Song & Galán, 2016). Typhoid toxin then enters target

cells through binding to Neu5Ac-terminated glycans, which is a human-specific moiety, on surface glycoproteins (Song, Gao & Galán, 2013; Deng *et al.*, 2014). Most non-human mammals, such as chimpanzees and mice, have mainly N-glycolylneuramic acid (Neu5Gc) moieties on their glycans, and are thus resistant to typhoid toxin activity. This specificity is underlined by the resistance shown by human cells induced to display Neu5Gc instead of Neu5Ac, as well as mice engineered to constitutively express Neu5Gc (Deng *et al.*, 2014). The specificity of typhoid toxin for human-specific sialic acid modifications may be accountable to a certain extent for the lack of typhoid fever symptom development in other species (Deng *et al.*, 2014). Furthermore, following binding to cell receptors, the toxin enters the cells and the active subunit targets the nucleus exerting its DNA-damaging effect, causing G_2/M cell cycle arrest (Spanò, Ugalde & Galán, 2008; Haghjoo & Galán, 2004; Ibler *et al.*, 2019; Miller & Wiedmann, 2016; Rodriguez-Rivera *et al.*, 2015). In an *in vitro* study, typhoid toxin caused extensive single-stranded DNA formation, triggering an atypical DNA damage response, which ultimately led to senescence of the intoxicated cell, which is thought to increase cell susceptibility to *S.* Typhi infection thus promoting chronic infection (Ibler *et al.*, 2019; Miller & Wiedmann, 2016). However, typhoid toxin was recently shown not to mediate infection and manifestation of the clinical presentation of typhoid fever in a human challenge model, while its role in systemic disease and chronic carriage in humans remains to be elucidated (Gibani *et al.*, 2019).

S. Paratyphi A and *S.* Typhi also express the less well-studied, transmembrane pore-forming hemolysin HlyE (or ClyA), whose role in pathogenicity remains elusive (Faucher *et al.*, 2009; Oscarsson *et al.*, 2002; Wallace *et al.*, 2000). This toxin is absent from *S.* Typhimurium, but present in some other NTS serovars (Faucher *et al.*, 2009; den Bakker *et al.*, 2011; Oscarsson *et al.*, 2002; Fuentes *et al.*, 2008), as well as *E. coli* and *Shigella* (Wallace *et al.*, 2000). HlyE and the typhoid toxin are often both present in *Salmonella* serovars (den Bakker *et al.*, 2011). The *hlyE* gene is within the SPI-18 alongside an invasin (Typhi-associated invasion A, *taiA*). TaiA promotes phagocytosis by macrophages, while HlyE limits bacterial growth within macrophages (Faucher *et al.*, 2009). If indeed macrophages offer a shielded environment for bacteria during systemic dissemination, this complementary action of the two proteins may promote chronic infection (Faucher *et al.*, 2009). HlyE has also been suggested to promote invasion in human epithelial cells *in vitro* via an unknown mechanism (Fuentes *et al.*, 2008; Faucher *et al.*, 2009). Ectopic expression of *hlyE* in *S.* Typhimurium facilitated colonisation of liver and spleen in mice, pointing towards a role in systemic stages of infection (Fuentes *et al.*, 2008). Typhoid toxin and HlyE may thus be contributing to some of the infection characteristics that distinguish *S.* Typhi and *S.* Paratyphi A from *S.* Typhimurium.

1.7 The carrier state of enteric fever

The carrier state describes typically asymptomatic patients who, after convalescence, are contagious by intermittently shedding high levels of bacteria in faeces and urine one year after infection (Crawford *et al.*, 2010; Gunn *et al.*, 2014; Khatri *et al.*, 2009; Gal-Mor, 2019; Dongol *et al.*, 2012). The carrier state has been explored mainly with *S.* Typhi, while it is less investigated in *S.* Paratyphi A infection (Khatri *et al.*, 2009; Gal-Mor, Boyle & Grassl, 2014; Dongol *et al.*, 2012). However, both pathogens can establish chronic carriage in secondary organs, resulting in approximately 2–5% of the infected population becoming carriers in endemic areas (Levine *et al.*, 1982; Khatri *et al.*, 2009). Considering the host restriction of typhoidal *Salmonella*, faecal shedding of bacteria is thought to promote enteric fever transmission and persistence in endemic areas with carriers acting as reservoirs (Gunn *et al.*, 2014; Khatri *et al.*, 2009; Pitzer *et al.*, 2014; Saul, Smith & Maire, 2013; Gal-Mor, 2019). Notorious examples of carriers come from workers in food services such as "Typhoid Mary the cook" and "Mr. N the milker" who, although healthy themselves, were responsible for more than 200 cases of typhoid fever (Ledingham, 1999; Brooks, 1996). More recently, a *S.* Paratyphi A outbreak among Israeli travellers was possibly traced back to food handlers at a site they visited in Nepal (Gal-Mor *et al.*, 2012; Meltzer *et al.*, 2014). It is worth noting that, although NTS shedding is evident for some weeks after infection, long-term carriage of NTS is rare and symptomatic (Gal-Mor, 2019; Marzel *et al.*, 2016).

Extraintestinal infection suggests crossing of the intestinal epithelial barrier, efficient immune evasion and invasion and/or colonisation of a permissive, immune-privileged niche (Gunn *et al.*, 2014; Gal-Mor, 2019; Raffatellu *et al.*, 2008). Although other systemic sites are also colonised during the carrier state (Figure 1.3), the biliary tract and gallbladder are thought to be the primary sites (Gonzalez-Escobedo, Marshall & Gunn, 2011; Gal-Mor, 2019; Gonzalez-Escobedo, La Perle & Gunn, 2013). Typhoidal *Salmonella* may exploit different mechanisms to persist in the gallbladder (Figure 1.5). Gallbladder colonisation may be promoted by formation of biofilms by *S.* Typhi on gallstones when cholesterol is present (Crawford *et al.*, 2010; Prouty, Schwesinger & Gunn, 2002; Crawford *et al.*, 2008). This is supported by the high correlation of gallstones and the carrier state (Gonzalez-Escobedo, Marshall & Gunn, 2011; SchiøLer *et al.*, 1983), and the difficulty in treating chronic carriage with antimicrobials (Gunn *et al.*, 2014; González *et al.*, 2018). In fact, human gallstones covered with *S.* Typhi biofilms have been observed microscopically (Gunn *et al.*, 2014; Marshall *et al.*, 2014). Almost 90% of *S.* Typhi carriers suffer from gallstones (SchiøLer *et al.*, 1983), while about 3.5% of patients undergoing cholecystectomy in endemic regions carried *S.* Paratyphi A or *S.* Typhi (Dongol *et al.*, 2012; Ristori *et al.*, 1982). *S.* Typhi may form biofilms also on the gallbladder epithelium (Gonzalez-Escobedo & Gunn, 2013a) and *S.* Typhi aggregates on this epithelium have been observed in patients from endemic countries (Basnyat & Baker, 2015). Alternatively, growth in the gallbladder lumen or invasion

and replication within epithelial cells are other mechanisms possibly exploited by *S.* Typhi to persist in the gallbladder (Gonzalez-Escobedo & Gunn, 2013a; Menendez ***et al.***, 2009). Bacterial detachment from biofilms formed in the gallbladder and shedding, as well as bacterial release following cell death of infected host cells, possibly mediate reinfection of the gut (Gunn ***et al.***, 2014; Gal-Mor, 2019; Knodler ***et al.***, 2010; Crawford ***et al.***, 2010; Gonzalez-Escobedo & Gunn, 2013a). Many of these mechanisms remain to be demonstrated with *S.* Paratyphi A. Nevertheless, the ability of *S.* Typhi and *S.* Paratyphi A to colonise the gallbladder indicates mechanisms to tolerate the antimicrobial properties of bile (Section 1.8.2) (van Velkinburgh & Gunn, 1999; Johnson ***et al.***, 2018), while interestingly, genomic organisation reflects the ability of *S.* Typhi and *S.* Paratyphi A to colonise the gallbladder. Chromosomal re-arrangements, which may slow down growth, are associated with gallbladder colonisation, where the need for a fast growth rate during competition with native microbiota is minimal (Hiyoshi ***et al.***, 2018a), further supporting the adaptation of typhoidal *Salmonella* to the gallbladder environment.

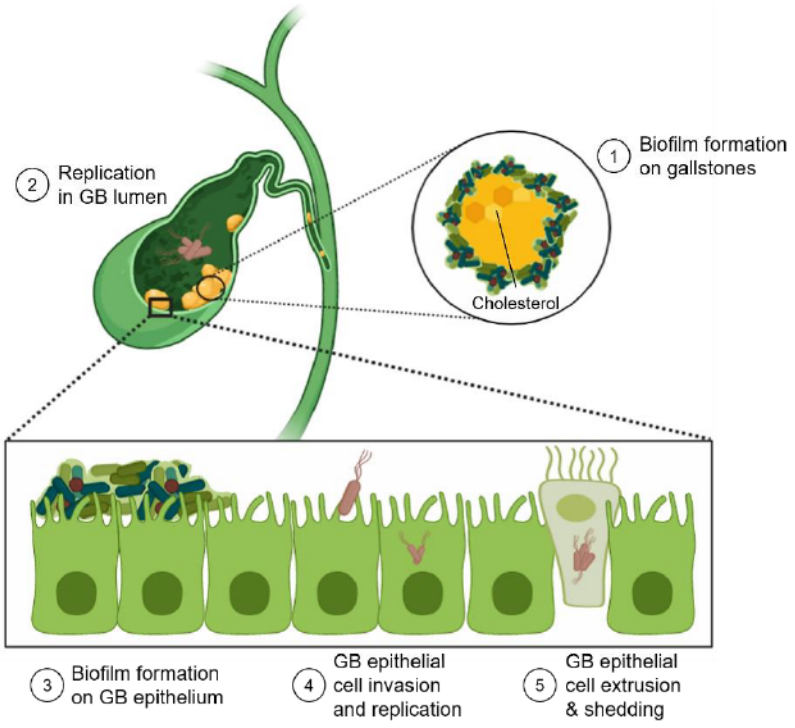


Figure 1.5 ***Salmonella*** **gallbladder colonisation models.**

There are different models proposed by which *Salmonella* may colonise the gallbladder during the carrier state. *Salmonella* may form biofilms on cholesterol-containing gallstone surfaces (1), replicate in the gallbladder lumen (2), or form biofilms on the gallbladder epithelium when gallstones are present (3). Alternatively, *Salmonella* may invade the gallbladder epithelium and replicate intracellularly (4) which may lead to host cell death, cell extrusion and bacterial shedding (5). GB, gallbladder. Image created using Biorender.

On the host side, risk factors promoting chronic carriage are gender, age, and the presence of gallstones. The carrier state is more common among women than men, while the risk seems to increase with age (Levine *et al.*, 1982; Gal-Mor, 2019; Gunn *et al.*, 2014; SchiøLer *et al.*, 1983; Crawford *et al.*, 2010). Gallstone-induced inflammation in the gut, possibly aids *Salmonella* in colonising an already compromised epithelium (Gonzalez-Escobedo & Gunn, 2013a). Chronic carriage has been correlated with malignancies associated with the gallbladder (Nath *et al.*, 2008; Caygill *et al.*, 1995; Ristori *et al.*, 1982; Nath, Singh & Shukla, 1997); chronic inflammation and damage in the gallbladder by bacteria and gallstones possibly increases the risk of cancer (Gunn *et al.*, 2014; Scanu *et al.*, 2015; Gonzalez-Escobedo, La Perle & Gunn, 2013). It is unclear whether the bacteria mediate the damage or whether the damaged tissue serves as a permissive niche for bacterial colonisation, but an acute inflammatory response is induced by the presence of *S.* Paratyphi A or *S.* Typhi (Dongol *et al.*, 2012).

1.8 Bile during *Salmonella* infection

1.8.1 Bile composition and functions

Bile is a prolonged stress factor for *Salmonella*, as the bacterium is exposed to bile in the small intestine during infection and at higher concentrations in the gallbladder during chronic infection (Gunn, 2000; van Velkinburgh & Gunn, 1999; Sistrunk *et al.*, 2016). Bile is an aqueous, sterile, slightly basic, dark yellow digestive secretion, produced and secreted in the intestinal tract by the liver and stored in the gallbladder in high concentrations following water removal by the gallbladder epithelium (Hofmann, 1999; Boyer, 2013). Bile is composed mainly of bile acids, cholesterol and phospholipids, while pigments such as bilirubin and biliverdin are responsible for its colour. The primary role of bile is to aid in emulsification and solubilisation of lipids during digestion and to promote excretion of cholesterol, as well as harmful substances, including insoluble or protein-bound and drug metabolites (Begley, Gahan & Hill, 2005; Hofmann, 1999; Boyer, 2013). Primary bile acids are synthesised in hepatocytes as the end products of cholesterol degradation and the main ones in humans are cholate and chenodeoxycholate (Hofmann, 1999; Urdaneta & Casadesús, 2017). To prevent damage to biliary epithelial cell membranes, bile acids form micelles with phospholipids (Hofmann, 1999). Furthermore, bile acids are conjugated with glycine or taurine that further hinders their ability to penetrate cell membranes. Bile acids may be modified by intestinal microbiota giving rise to secondary bile acids deoxycholate and litocholate, which facilitate reabsorption and bile acid cycling in the hepatic circulation (Hofmann, 1999; Urdaneta & Casadesús, 2017). Finally, as discussed in the following section, bile has antimicrobial properties, which along with the continuous flow of fresh bile going through, maintain the biliary tract relatively free from microorganisms (Gunn *et al.*, 2014).

1.8.2 Antimicrobial properties of bile

Due to its amphipathic nature, bile has antimicrobial properties as it can dissolve membrane lipids, thus disrupting membrane integrity and causing intracellular material leakage (Begley, Gahan & Hill, 2005; Urdaneta & Casadesús, 2017). Bile also affects the conformation and stability of molecules such as DNA and various proteins (Begley, Gahan & Hill, 2005; Urdaneta & Casadesús, 2017). Nucleotide mutations and chromosomal rearrangements may become more frequent in *Salmonella*, as well as oxidative DNA damage in the presence of bile (Prieto, Ramos-Morales & Casadesús, 2004, 2006). IgA and mucus are also present in bile, hindering bacterial growth and adhesion (Hofmann, 1999; Boyer, 2013; Begley, Gahan & Hill, 2005). In addition, bile acids promote intestinal homeostasis by inducing the production of protective host molecules that are not a component of bile, such as antimicrobial peptides from biliary epithelial cells (Urdaneta & Casadesús, 2017). Moreover, bile acids may chelate ions like iron and calcium that are important for bacterial survival (Urdaneta & Casadesús, 2017).

1.8.3 *Salmonella* mechanisms of bile tolerance and resistance

The range of bile concentration varies from 0.2–2% w/v in the small intestine to up to 8% w/v in the gallbladder (Gunn, 2000). However, to promote survival in these environments, enteric pathogens have evolved a multitude of mechanisms to sense, respond, and tolerate the antimicrobial effects of bile listed above (Sistrunk ***et al.***, 2016; Urdaneta & Casadesús, 2017; Gunn, 2000; Begley, Gahan & Hill, 2005). Gram-negative bacteria are more resistant to bile than Gram-positive bacteria, possibly due to their outer membrane structure (Begley, Gahan & Hill, 2005; Sengupta, Ray & Chowdhury, 2014). *Salmonella* is considered to be inherently resistant to bile and to individual bile salts (van Velkinburgh & Gunn, 1999). *S.* Paratyphi A can grow relatively well in bile concentrations of ≤ 5%, while it shows a significant growth defect when bile concentration reaches 15% (Zhou ***et al.***, 2016). The minimum inhibitory concentration (MIC) for *S.* Typhi and *S.* Typhimurium is 12% and 18%, respectively, while the minimum bacteriostatic concentration is 18% and 60% (van Velkinburgh & Gunn, 1999), exceeding the concentrations encountered in the human body (Gunn, 2000). Sublethal bile concentrations allow adaptation of *Salmonella* to bile, increasing its survival in high concentrations (van Velkinburgh & Gunn, 1999; Hernández ***et al.***, 2012). *S.* Paratyphi A and *S.* Typhi have been isolated from bile of cholecystectomy patients, with median loads of 9.3×10^4 CFU/mL and 5.2×10^4 CFU/mL, respectively (Dongol ***et al.***, 2012). Therefore, the ability of *Salmonella* to replicate within the gallbladder lumen and to form biofilms on gallstones (Figure 1.5), support that this pathogen is capable of survival in high bile concentrations, which is required for its lifestyle (Menendez ***et al.***, 2009; Gonzalez-Escobedo & Gunn, 2013a; Crawford ***et al.***, 2010; Prouty, Schwesinger & Gunn, 2002; Basnyat & Baker, 2015).

Gene products involved in bacterial resistance to bile include envelope structures, porins, efflux pumps, and proteins involved in stress responses and DNA repair mechanisms (Begley, Gahan &

Hill, 2005; Sistrunk *et al.*, 2016; Urdaneta & Casadesús, 2017; Gunn, 2000; Álvarez-Ordóñez *et al.*, 2011). To counteract the membrane damaging effects of bile, bacterial species may change their membrane composition and architecture (e.g. fatty acid composition and lipid fluidity) (Begley, Gahan & Hill, 2005). In particular, *Salmonella* withstands exposure to bile via several mechanisms (Sistrunk *et al.*, 2016): (i) multiple bile-sensitive bacterial mutants are linked to membrane integrity including Tol genes (Ramos-Morales *et al.*, 2003; Prouty *et al.*, 2002) and loss of the LPS O-antigen, as well as the enterobacterial common antigen (ECA), renders *Salmonella* bile-sensitive (Prouty *et al.*, 2002; Ramos-Morales *et al.*, 2003; Crawford *et al.*, 2012), (ii) the downregulation of porins in *S.* Typhimurium in combination with the upregulation of efflux pumps regulate bile salt entry and transport out of the bacterium, like the AcrAB pump and the TolC efflux pump (Prouty *et al.*, 2004a; Langridge *et al.*, 2009; Sengupta, Ray & Chowdhury, 2014), while (iii) *Salmonella* also induces DNA repair mechanisms including Dam and RecABCD in response to bile (Prieto, Ramos-Morales & Casadesús, 2004, 2006; Langridge *et al.*, 2009). Although their role in bile resistance is not well understood, the two-component PhoPQ system, which is important for virulence in both *S.* Typhi and *S.* Typhimurium, is essential for *Salmonella* survival in bile, as loss of PhoPQ increases susceptibility to bile killing, while overexpression of this system increases survival in high bile concentrations (van Velkinburgh & Gunn, 1999). Although most of these studies have been performed in *S.* Typhimurium, a study showed that survival of *S.* Typhi in 10% bile requires many of these genes, such as *acrAB*, *tolC*, *dam*, genes involved in O-antigen biosynthesis, and *phoPQ* (Langridge *et al.*, 2009). Additionally, *S.* Typhi immunogenic antigens in typhoid carriers were identified using an immunoscreening method and these included membrane proteins, lipoproteins and proteins assisting in ion efflux (Charles *et al.*, 2013).

1.8.4 *Salmonella* virulence gene regulation in response to bile

Enteric bacterial pathogens including *Shigella flexneri*, *Vibrio cholerae*, pathogenic *E. coli*, and *S.* Typhimurium exploit bile as an environmental cue to sense their location within the host and adjust the expression of virulence genes (Sengupta, Ray & Chowdhury, 2014; Sistrunk *et al.*, 2016; Álvarez-Ordóñez *et al.*, 2011). Examples of virulence-specific responses to bile include *Shigella* activating biofilm-formation, invasion and adherence genes in response to bile (Pope, Reed & Payne, 1995; Nickerson *et al.*, 2017; Faherty *et al.*, 2012). The T3SS tip protein (IpaD) undergoes conformational changes upon binding to deoxycholate, which leads to recruitment of the translocator protein (IpaB) promoting T3SS-dependent epithelial cell invasion (Olive *et al.*, 2007; Stensrud *et al.*, 2008; Dickenson *et al.*, 2011). On the other hand, *V. cholerae* represses transcription of virulence-associated genes including cholera toxin, while it activates motility for effective colonisation (Gupta & Chowdhury, 1997; Schuhmacher & Klose, 1999). Enterohemorrhagic *E. coli* (EHEC) O157:H7 may downregulate the LEE (locus of enterocyte effacement) pathogenicity island, which is important for virulence and adhesion,

in response to bile in order to prevent adhesion in the small intestine as opposed to the colon where there is no bile (Hamner *et al.*, 2013).

S. Typhimurium downregulates expression of SPI-1 proteins and effector secretion following exposure to bile, which lead to decreased epithelial cell invasion (Prouty *et al.*, 2004b; Prouty & Gunn, 2000; Johnson *et al.*, 2018; van Velkinburgh & Gunn, 1999). Motility is also decreased in response to bile, as flagellar and chemotaxis genes are downregulated (Prouty *et al.*, 2004b; Johnson *et al.*, 2018). Bile salts bind to the T3SS tip protein (SipD), like in *Shigella*, although the consequence of this remains unknown (Wang *et al.*, 2010b). Although the regulatory mechanisms of *S.* Typhimurium virulence in response to bile remain poorly understood; the stability of the SPI-1 regulator HilD is affected in the presence of bile which might partially explain the bile-mediated effect on SPI-1 expression (Eade *et al.*, 2016). The current model for *S.* Typhimurium suggests that bile is sensed in the intestinal lumen leading to repression of invasion-associated genes, where bile concentrations are high. When bile concentrations drop as *S.* Typhimurium traverses the intestinal mucus layer and approaches the intestinal epithelium, these genes are derepressed to facilitate invasion (Prouty & Gunn, 2000).

Salmonella forms biofilms on gallstones during establishment of the carrier state (Figure 1.5). Therefore, unsurprisingly, when grown *in vitro* in bile *S.* Typhimurium upregulates genes responsible for biofilm formation, flagella, outer membrane proteins, quorum sensing and ECA synthesis genes (Prouty, Schwesinger & Gunn, 2002; Marshall *et al.*, 2014; Crawford *et al.*, 2008; Crawford, Reeve & Gunn, 2010; Gonzalez-Escobedo & Gunn, 2013b). In fact, the presence of bile is essential for induction of biofilm formation in *S.* Typhi and *S.* Typhimurium, with the most important constituent being cholesterol (Prouty, Schwesinger & Gunn, 2002; Crawford *et al.*, 2008; Marshall *et al.*, 2014).

Although the importance of bile during systemic infection has long been recognised (Gunn, 2000; Gonzalez-Escobedo, Marshall & Gunn, 2011), the response of typhoidal serovars to bile remains poorly investigated. *S.* Typhi can survive in the gallbladder (Section 1.7), suggesting that it possesses mechanisms to withstand high bile concentrations and adjust its gene expression accordingly (Langridge *et al.*, 2009; Johnson *et al.*, 2018). Although there was early evidence that *S.* Typhimurium and *S.* Typhi respond differently to bile (van Velkinburgh & Gunn, 1999), it was only until recently that transcriptomic analysis revealed that *S.* Typhi behaves unlike *S.* Typhimurium in response to bile. More specifically, bile induces upregulation of SPI-1, motility and chemotaxis genes in *S.* Typhi, leading to higher levels of HeLa cell invasion (Johnson *et al.*, 2018). The mechanistic details have yet to be determined, but, in contrast to *S.* Typhimurium (Eade *et al.*, 2016), *S.* Typhi HilD stability increases during exposure to bile (Johnson *et al.*, 2018). Interestingly, the increased SPI-1 expression and invasion phenotype is amplified with a H58 clinical strain, which is more bile resistant than the

reference *S.* Typhi Ty2 strain (Johnson *et al.*, 2018). The *S.* Typhi behaviour in response to bile may reflect adaptation to the gallbladder environment during chronic infection and thus may have facilitated H58 dissemination (Johnson *et al.*, 2018; Johnson, Mylona & Frankel, 2018). This is also suggested by the unique genotype of carrier strains and the improved ability of a carrier compared to an outbreak strain to form biofilms (Kalai Chelvam, Chai & Thong, 2014; Charles *et al.*, 2013; Hatta *et al.*, 2011). Bile-induced DNA damage may be one of the driving forces of mutagenesis and adaptation within the gallbladder (Prieto, Ramos-Morales & Casadesús, 2006, 2004). Also, increase in the expression of metabolic genes exploiting bile components as substrates, such as glycerophospholipids, further demonstrate that typhoidal *Salmonella* are well adapted to the gallbladder milieu (Johnson *et al.*, 2018; Antunes *et al.*, 2011). Despite these insights in the behaviour of *S.* Typhimurium and *S.* Typhi upon exposure to bile, the effect of bile on *S.* Paratyphi A remains unknown.

1.9 The inflammasome host immune response to *Salmonella*

1.9.1 Pattern recognition receptors and inflammatory signalling

The host innate immunity is the first line of defence, as it can mount an immediate response against infection, within minutes to hours (Medzhitov, 2007). The first step in responding to an infection is being able to detect the pathogen, as well as the associated danger signals. This role is carried out by pattern recognition receptors (PRRs) recognising pathogen (PAMPs) or danger-associated molecular patterns (DAMPs), leading to downstream pro-inflammatory responses (Kumagai, Takeuchi & Akira, 2008; Medzhitov, 2007; Sellge & Kufer, 2015). PRRs include receptors belonging to the TLR or C-type lectin receptor (CLR) families, which can recognise specific conserved structures on pathogens. These are membrane-bound receptors present on the host cell plasma membrane and on intracellular compartments like endosomes, sensing PAMPs found in the extracellular environment or inside endosomes/lysosomes. Cytoplasmic receptors belonging to the nucleotide binding and oligomerisation domain (NOD)-leucine-rich repeat protein (NLR), retinoic acid-inducible gene-I (RIG-I)-like receptor/helicase (RLR/RLH), and AIM2 (absent in melanoma 2)-like receptor (ALR) families detect ligands in the host cell cytosol (Kumagai, Takeuchi & Akira, 2008; Sellge & Kufer, 2015; Takeuchi & Akira, 2010; Iwasaki & Medzhitov, 2015). PRRs are expressed primarily in immune cells such as macrophages and dendritic cells, but non-immune cells frequently exposed to the external environment like epithelial cells also express several of these PRRs (Kumagai, Takeuchi & Akira, 2008; Takeuchi & Akira, 2010). Aberrant activation of PRRs, for example when they fail to distinguish between self and non-self-molecules, can lead to autoimmune diseases, making the tight regulation of these pathways essential (Medzhitov, 2007; Takeuchi & Akira, 2010).

Upon recognition of the activating signal, PRRs induce intracellular signal transduction cascades, triggering the expression of pro-inflammatory, such as TNF and pro-IL-1β, and/or activation of programmed cell death pathways, such as apoptosis or pyroptosis. For example, once stimulated, membrane-bound TLRs recruit adaptor proteins like myeloid differentiation protein 88 (MyD88) or TIR-domain-containing adaptor protein inducing IFN-β (TRIF), triggering activation of NF-κB, mitogen-activated protein (MAP) kinase and IRF-dependent transcriptional upregulation of genes leading to production of proinflammatory cytokines and/or type I interferons (IFNs) (Kawai & Akira, 2010; Takeuchi & Akira, 2010; Haraga, Ohlson & Miller, 2008). The intracellular NLRs are composed of a NOD and a leucine-rich-repeat (LRR) domain at the C terminus. NLRs are distinguished based on their N-terminal domain which can be a caspase-recruitment domain (CARD; e.g. NLRC4), a pyrin domain (PYD; e.g. NLRP3), or a baculoviral inhibitor-of-apoptosis protein repeat-containing (BIR) domain (e.g. NAIP [NLR Family Apoptosis Inhibitory Protein]) (Medzhitov, 2007). ALRs such as AIM2 contains a PYD at the N-terminus and a HIN200 domain at the C terminus (Hornung ***et al.***, 2009) (Figure 1.6). NLRs and ALRs are not involved in transcriptional activation of genes involved in the inflammatory response (Medzhitov, 2007). Instead, NLRs and ALRs are examples of sensors that assemble into intracellular multiprotein complexes known as inflammasomes, which result in caspase-1 activation, pyroptosis and secretion of proinflammatory cytokines IL-18 and IL-1β as described in Section 1.9.3.

1.9.2 Host innate immunity to *Salmonella* – an overview

The host immune response to *Salmonella* has been mostly studied with *S.* Typhimurium as a model organism, both in cells and using the typhoid-like murine model of infection *in vivo*. Following ingestion, *Salmonella* first encounters opposition from physical barriers and immune responses in the small intestine. These include a thick mucus layer composed mucins, as well as antimicrobial peptides (AMPs) secreted by Paneth cells which target different bacterial cell components (Figure 1.3) (Broz, Ohlson & Monack, 2012). Infection with non-invasive NTS results in a stereotypical host response, characterised by neutrophil influx following recognition of *Salmonella* by PRRs (Raffatellu ***et al.***, 2008; Broz, Ohlson & Monack, 2012). Expression of PRRs on the basolateral side of epithelial cells and on macrophages and dendritic cells in the lamina propria allows the host to discriminate *Salmonella* from resident bacteria of the microbiota (Raffatellu ***et al.***, 2008; Franchi ***et al.***, 2012). Multiple TLRs are involved in recognition of Gram-negative bacteria including *Salmonella*. For example, TLR4 recognises LPS, TLR5 flagellin, and TLR9 binds to unmethylated CpG repeats on bacterial DNA (Kawasaki & Kawai, 2014). Breach of the epithelial barrier expose *Salmonella* to resident macrophages and dendritic cells in the submucosa (Broz, Ohlson & Monack, 2012). Phagocyte-mediated defences are important for limiting systemic dissemination of NTS (Hiyoshi ***et al.***, 2018a), through phagocytosis and signalling to other immune cells (Broz, Ohlson & Monack, 2012). During *S.* Typhimurium infection, an extensive

inflammatory response occurs in the intestinal mucosa, which includes the production of several interleukins, such as IL-22, IL-18, IL-1β, IFNγ, as well as chemokines like IL-8 that attract neutrophils (Broz, Ohlson & Monack, 2012). Bacterial clearance is mediated by cell death by pyroptosis, release of intracellular bacteria and neutrophil killing of extracellular *Salmonella* (Broz, Ohlson & Monack, 2012; Gal-Mor, Boyle & Grassl, 2014).

Typhoidal *Salmonella* are adept at evading host immune responses and moderating intestinal inflammation (Table 1.2). While cytokines such as IFNγ are detected during acute enteric fever, levels of IL-1β and TNF are considered low (Gal-Mor, Boyle & Grassl, 2014; Gal-Mor *et al.*, 2012) and, as mentioned earlier, infection with typhoidal *Salmonella* is not characterised by a neutrophil infiltration (Raffatellu *et al.*, 2008; Gal-Mor, Boyle & Grassl, 2014), which allows their systemic dissemination (Figure 1.3). The requirement of a strong immune response against NTS is highlighted by the increased susceptibility of immunocompromised patients and patients with immune deficiencies (e.g. IL-12/IL-23 axis), who, however, are not susceptible to typhoidal *Salmonella*, further supporting the existence of major differences in the immune response against the two types of serovars (Gal-Mor, Boyle & Grassl, 2014; Raffatellu *et al.*, 2008). Macrophages are important for both typhoidal and non-typhoidal *Salmonella* serovars, particularly for systemic dissemination. However, the interactions of macrophages with *S.* Paratyphi A have been investigated only recently and in a very limited manner.

1.9.3 Inflammasome activation during *Salmonella* infection

Inflammasomes are multimeric protein assemblies, acting as cytosolic platforms for proteolytic cleavage and activation of caspase-1, which in turn processes pro-inflammatory cytokines and cell death mediators (Eldridge & Shenoy, 2015; Broz & Dixit, 2016; Schroder & Tschopp, 2010). They play an essential role in antibacterial innate immunity, but inflammasome dysregulation can also lead to the development of multiple autoinflammatory syndromes (Fusco & Duncan, 2018; Medzhitov, 2007; He, Hara & Núñez, 2016). Inflammasomes have been mostly studied in macrophages, however they have been also shown to be active in neutrophils and dendritic cells, in addition to non-professional immune cells such as epithelial cells (Sellin, Müller & Hardt, 2018; Schroder & Tschopp, 2010), and may perform distinct functions in different cell types (Vance, 2015). Canonical activation of inflammasomes (Sections 1.9.3.5, 1.9.3.6) leads to caspase-1-mediated maturation and secretion of proinflammatory cytokines pro-IL-18 and pro-IL-1β, and cell death by Gasdermin-D (GSDMD)-mediated pyroptosis which are described in Sections 1.9.3.2 and 1.9.3.3, respectively. Non-canonical inflammasome activation may also occur and induce pyroptotic cell death via caspase-4/5 (Section 1.9.3.8).

1.9.3.1 Inflammatory caspases

Caspases are cysteine-dependent aspartate-specific proteases and are distinguished into apoptotic (initiator caspase-2, -8, -9, and -10 and executioner caspase-3, -6, and -7) and inflammatory (caspase-1, -4, -5, and -11) (Fernández & Lamkanfi, 2015). Inflammatory caspases are involved in maturation and secretion of pro-inflammatory cytokines IL-18, IL-1β, and IL-1α, cell death by pyroptosis and elimination of pathogens (Sanchez-Garrido *et al.*, 2020).

Caspase-1 is important for mediating clearance of intracellular pathogens including *S.* Typhimurium (Miao *et al.*, 2010a; Mariathasan *et al.*, 2004; Broz & Monack, 2011; Raupach *et al.*, 2006; Lara-Tejero *et al.*, 2006; Broz *et al.*, 2010b). Caspase-1 recruitment to the inflammasome complex at high concentrations allows the dimerization of caspase-1 monomers which leads to autoproteolysis and activation (Boucher *et al.*, 2018; Datta *et al.*, 2013; Srinivasula *et al.*, 2002). Caspase-1 is synthesised as a 45 kDa monomeric zymogen containing a CARD at the N-terminus and p20/p10 (20 kDa/10 kDa) subunits at the C-terminus (Figure 1.6) (Thornberry *et al.*, 1992; Wilson *et al.*, 1994). Although the active species of caspase-1 has long been thought to be a tetramer of two p20 and two p10 subunits (p20/p10), it was recently proposed that the full length p45 and a transient heterodimer p33/p10 enable caspase-1 activity (Boucher *et al.*, 2018; Wilson *et al.*, 1994). p33/p10 undergoes autoprocessing releasing p20/p10 disrupting the stability of the dimer, which results in

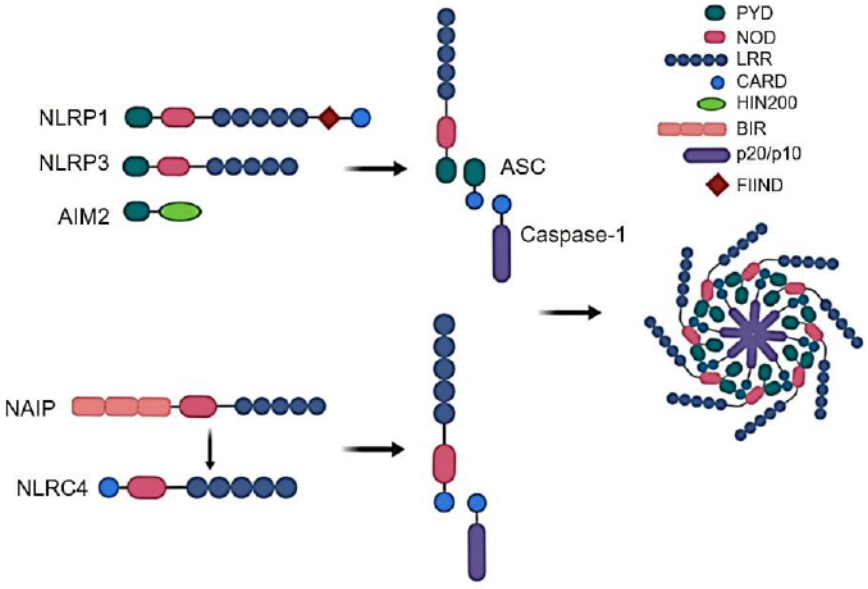


Figure 1.6 **Canonical inflammasome assembly.**

Schematic showing domain composition of selected human NLRs and AIM2. Homotypic interactions between domains lead to caspase-1 recruitment and activation. Molecules that do not contain a CARD bind to caspase-1 via ASC; CARD-containing NLRs can activate caspase-1 in the absence of ASC, but caspase-1-mediated processing of cytokines is compromised. Assembly of inflammasomes into multiprotein platform allows downstream events, such as cleavage of cytokines and GSDMD (not shown). Image created using Biorender.

termination of caspase-1 protease activity, serving as an intrinsic mechanism to regulate and deactivate inflammasomes (Boucher *et al.*, 2018).

The other inflammasome-associated inflammatory caspase is caspase-11 in mice, which corresponds to caspase-4 and caspase-5 in humans (Fernández & Lamkanfi, 2015). Caspase-4 and caspase-5 are possibly the result of gene duplication of the ancestral caspase-11-like gene (Martinon & Tschopp, 2004). These caspases are involved in cytosolic LPS recognition in the non-canonical inflammasome pathway (Kayagaki *et al.*, 2015; Shi *et al.*, 2015; Casson *et al.*, 2015; Hagar *et al.*, 2013; Aachoui *et al.*, 2013; Shi *et al.*, 2014), which is described in Section 1.9.3.8. Caspase-4 binds to LPS via its CARD domain, leading to its activation without complete autoprocessing and resulting in p32 fragments (Shi *et al.*, 2014; Casson *et al.*, 2015; Yang, Zhao & Shao, 2015).

1.9.3.2 IL-1β and IL-18 pro-inflammatory cytokines

The pro-inflammatory cytokines IL-18 and IL-1β are synthesised as the inert precursors pro-IL-18 and pro-IL-1β, respectively. Caspase-1-mediated maturation into their active forms (p18 and p17, respectively) is required for their unconventional secretion (Chan & Schroder, 2019). IL-1β belongs to the so-called leaderless proteins, as it does not have a signal sequence to direct its secretion via the endoplasmic reticulum and Golgi apparatus canonical secretory pathway (Eder, 2009). As both IL-18 and IL-1β are leaderless proteins with similar modes of regulation, the secretion of IL-18 is assumed to follow a similar route to IL-1β, although it has not been well studied. It is thought that their release occurs through GSDMD pores (see also 1.9.3.3) via their pore function or via passive secretion upon cell lysis (together with their pro-forms) (Evavold *et al.*, 2018; Chan & Schroder, 2019; Broz, Pelegrín & Shao, 2019). These cytokines may also be secreted independently of pyroptosis, such as by neutrophils during *S.* Typhimurium infection and by monocytes upon exposure to LPS or *S.* Typhimurium, or during hyperactivated macrophages (Diamond *et al.*, 2017; Gaidt *et al.*, 2016; Chen *et al.*, 2014; Evavold *et al.*, 2018). Following maturation, IL-1β and IL-18 bind to their receptor, triggering signalling that results in production of inflammatory mediators and recruitment of other immune cells, promoting local inflammation (Joosten, Netea & Dinarello, 2013; Dinarello *et al.*, 2013).

1.9.3.3 Pyroptosis and Gasdermin-D

Pyroptosis is a pro-inflammatory, lytic form of cell death, accompanied by cell swelling and release of cell contents (Bergsbaken, Fink & Cookson, 2009; Shi, Gao & Shao, 2017; Jorgensen & Miao, 2015). It is thought to disrupt the intracellular replication niche of pathogens, allowing killing by extracellular immune mechanisms, such as through pore-induced intracellular traps (PITs) (Jorgensen *et al.*, 2016). Pyroptosis hence allows secretion of pro-inflammatory cytokines, as well as DAMPs, and promotes cell

extrusion and release of intracellular pathogens (Sellin *et al.*, 2014; Knodler *et al.*, 2014; Miao *et al.*, 2010a; Man, Karki & Kanneganti, 2017; Hayward *et al.*, 2018).

GSDMD belongs to the human Gasdermin family, which consists of six proteins with different expression profiles (Broz, Pelegrín & Shao, 2019). GSDMD, expressed in most tissues, has been identified as the caspase substrate inducing membrane rupture and cell death by swelling and osmotic lysis (Liu *et al.*, 2016; Kayagaki *et al.*, 2015; Shi *et al.*, 2015; Ding *et al.*, 2016; Broz, Pelegrín & Shao, 2019; He *et al.*, 2015). GSDMD was first identified as the mediator of pyroptosis, during caspase-1 and caspase-11 cell death in murine macrophages (Kayagaki *et al.*, 2015; Shi *et al.*, 2015; He *et al.*, 2015). Since then, caspase-8 has also been shown to cleave GSDMD (Orning *et al.*, 2018). Therefore, pyroptosis has been redefined as Gasdermin-mediated programmed necrotic cell death (Broz, Pelegrín & Shao, 2019). GSDMD is cleaved by caspases into its N- (p30) and C-terminal domains (Shi *et al.*, 2015; Liu *et al.*, 2016; Aglietti *et al.*, 2016). Full-length GSDMD remains inactive by structural autoinhibition of the C-terminal domain that folds on the N-terminal domain; this activity inhibition mechanism is conserved among most Gasdermins (Ding *et al.*, 2016; Rathkey *et al.*, 2017; Shi *et al.*, 2015).

Caspase-mediated cleavage of GSDMD is required to trigger pyroptosis. Cleavage between the N and C-domains allows the release of the N from the C-domain, which can then translocate to the plasma membrane to form pores of 10-16 nm (Shi *et al.*, 2015; Liu *et al.*, 2016; Broz, Pelegrín & Shao, 2019; Ding *et al.*, 2016). In agreement with the inhibitory role of the C-terminus, ectopic expression of the GSDMD N-domain alone is sufficient to induce pyroptosis by selectively binding lipids found on the inner leaflet of the plasma membrane and oligomerising to form pores (Liu *et al.*, 2016; Ding *et al.*, 2016; Aglietti *et al.*, 2016; Shi *et al.*, 2015; Mulvihill *et al.*, 2018), while mutation of the interdomain cleavage site blocks GSDMD-mediated pyroptosis (Liu *et al.*, 2016; Rathkey *et al.*, 2017). The GSDMD N-domain can also bind to cardiolipin, which is found on bacterial membranes, and thus GSDMD may also have direct bactericidal properties (Liu *et al.*, 2016; Ding *et al.*, 2016). Supporting GSDMD pore-mediated cytokine secretion, the size of the pores suggests mature IL-1β and IL-18 passage through them, while their precursors are too large to pass (Liu *et al.*, 2016; Ding *et al.*, 2016; Aglietti *et al.*, 2016). Following GSDMD-mediated pore formation combined with overwhelming the ability of the cell to naturally repair the membrane (Rühl *et al.*, 2018), the cell swells and undergoes osmotic lysis and eventually pyroptosis (Ding *et al.*, 2016; Shi, Gao & Shao, 2017; Aglietti *et al.*, 2016; Sborgi *et al.*, 2016).

1.9.3.4 Inflammasome signalling

Inflammasome assembly relies on homotypic interactions between protein domains of the different components (Figure 1.6). For example, NLRC4 can directly interact with pro-caspase-1 through CARD-CARD interactions and lead to pyroptotic cell death (Duncan & Canna, 2018). For receptors that lack a

CARD domain, like NLRP3, an adaptor molecule named ASC (apoptosis-associated speck-like protein) is recruited. ASC is a bipartite molecule containing a PYD and CARD and serves as a bridge between the PYD of the NLR and the CARD of pro-caspase-1 (Hara *et al.*, 2013; Fernandes-Alnemri *et al.*, 2007). Recruitment of ASC leads to formation of a single ASC-speck in the host cell, which is visible by microscopy (Broz *et al.*, 2010b; Mariathasan *et al.*, 2004; Man *et al.*, 2014b; Bryan *et al.*, 2009).

Inflammasomes are often described as requiring two signals in order to be fully activated. Signal 1, the priming signal, involves activation of pro-inflammatory signalling pathways by microbial components, cytokines or interferons. Specific microbial ligands and/or homeostatic perturbations often caused by infection are examples of signal 2, the activating signal. Bacterial infection can thus provide both signal 1 and 2, and lead to robust inflammasome activation (Schroder & Tschopp, 2010; He, Hara & Núñez, 2016; Bauernfeind *et al.*, 2009). NLRs recognise a variety of signals related to infection, both directly (e.g. T3SS components) and indirectly (e.g. mitochondrial damage), while AIM-2 directly binds to intracellular dsDNA, and PYRIN responds to modifications of Rho GTPases induced by bacteria. Following recognition of signal 2, inflammasome-associated receptors oligomerise and form a single multimeric complex (Eldridge & Shenoy, 2015; Broz, 2019; Sharma & Kanneganti, 2016). The outcomes of inflammasome activation, namely maturation and secretion of pro-inflammatory cytokines and pyroptosis are essential for promoting inflammation and aiding in limiting the pathogen burden (Hayward *et al.*, 2018).

Inflammasome-associated proteins are also regulated at the post-translational level. Briefly, phosphorylation of inflammasome components, proteolysis or binding to an activating ligand are key for activation or contribute to optimal activity (Fusco & Duncan, 2018). Guanylate binding proteins (GBPs) are a family of GTPases that control bacterial replication and enhance inflammasome activation (Kim *et al.*, 2012; Shenoy *et al.*, 2012; Meunier *et al.*, 2015). These molecules are IFNγ-induced and their actions after macrophage IFNγ priming promote inflammasome activation during infection with *S.* Typhimurium (Shenoy *et al.*, 2012; Meunier *et al.*, 2014; Santos *et al.*, 2018; Santos & Broz, 2018; Fisch *et al.*, 2019a; Pilla *et al.*, 2014). GBPs may have different activities during inflammasome activation, such as mediating bacteria-containing vacuole disruption, or promoting LPS binding to caspase-11 to enable oligomerisation (Eldridge & Shenoy, 2015; Santos & Broz, 2018).

Inflammasomes have been extensively studied in infection with *S.* Typhimurium; however, most of our understanding comes from murine studies and inflammasome responses in human cells remain poorly investigated (Bierschenk, Boucher & Schroder, 2017). The main inflammasomes known to be activated by *S.* Typhimurium are NLRP3 (Section 1.9.3.5), NLRC4 (Section 1.9.3.6), and the non-canonical pathway (Section 1.9.3.8), while caspase-8 (Section 1.9.3.7) also contributes to these

pathways (Figure 1.7). Other known inflammasomes are NLRP1, AIM2, PYRIN, and NLRP6. N-terminal cleavage of Nlrp1b results in destabilisation and proteasomal degradation which leads to release of the C-terminal FIIND and CARD domain which interacts with and activates caspase-1. Although Nlrp1b can respond to bacterial proteins that cause its N-terminal cleavage, such as proteases (anthrax toxin) or ubiquitin ligases (*Shigella* IpaH7.8), (Sandstrom *et al.*, 2019; Hayward *et al.*, 2018; Mitchell, Sandstrom & Vance, 2019; Xu *et al.*, 2019), such *Salmonella*-associated factors have not been identified yet. The AIM2 inflammasome detects the presence of dsDNA in the cytosol following infection with a virus or an intracellular bacterium (Hornung *et al.*, 2009; Fernandes-Alnemri *et al.*, 2010; Rathinam *et al.*, 2010; Sagulenko *et al.*, 2013; Jones *et al.*, 2010; Warren *et al.*, 2010). The HIN200 domain of AIM2 directly binds to dsDNA independently of the DNA sequence (Roberts *et al.*, 2009). AIM2 is not involved in caspase-1 activation nor IL-1β secretion during infection with *S.* Typhimurium (Fernandes-Alnemri *et al.*, 2010; Rathinam *et al.*, 2010; Jones *et al.*, 2010), but it may have inflammasome-independent roles. Mice deficient in AIM2 succumb to infection with *S.* Typhimurium significantly faster than WT mice. This was shown to be due to the protective role of AIM2 against *Salmonella*-mediated disruption of the intestinal epithelium integrity by promoting the expression of tight junction proteins (Hu *et al.*, 2016). Activation of PYRIN during *S.* Typhimurium infection has not been reported so far (Wemyss & Pearson, 2019), while NLRP6 and NLRP12 appear to act in an inflammasome-independent manner and dampen innate immune signalling, and mice deficient in NLRP6 or NLRP12 are resistant to infection (Zaki *et al.*, 2014; Anand *et al.*, 2012). However, the mechanism and/or ligands underlying their activation by *S.* Typhimurium remain to be found.

The main inflammasome activation activated during *Salmonella* infection are next described with a focus on their role during *S.* Typhimurium infection. The role of inflammasomes during infection with *S.* Typhi has been investigated in a limited manner and will be outlined as well, while inflammasome activation induced by *S.* Paratyphi A had not been investigated until this study to the best of my knowledge.

1.9.3.5 The NLRP3 inflammasome

Despite extensive research on the NLRP3 inflammasome, the specific trigger is still to be defined. Due to the low amount of NLRP3 in resting conditions to prevent unnecessary excessive activation, NLRP3 usually requires signal 1 to be expressed and to undergo post-translational modification by de-ubiquitination to be ready for activation by signal 2 (Bauernfeind *et al.*, 2009; Juliana *et al.*, 2012; Py *et al.*, 2013). Other cellular processes also contribute to NLRP3 priming, such as caspase-8 (Gurung *et al.*, 2014), and thus signal 1 for NLRP3 activity may be more complicated than originally thought (He, Hara & Núñez, 2016). Multiple activating signals (signal 2) have been shown to induce NLRP3 activity, including extracellular ATP, bacterial pore-forming toxins, and dysfunctional mitochondria (He, Hara

& Núñez, 2016; Swanson, Deng & Ting, 2019). Additionally, NLRP3 can be activated by the non-canonical pathway (Section 1.9.3.8). Due to the plethora of NLRP3 activation signals, it is thought that NLRP3 does not interact directly with a specific ligand but rather these diverse signals act on a common cellular process which causes NLRP3 activation (He *et al.*, 2016; Swanson, Deng & Ting, 2019). There are several suggested such processes, such as K^+ efflux (Yang *et al.*, 2015; Muñoz-Planillo *et al.*, 2013; Pétrilli *et al.*, 2007), Ca^{2+} efflux (Lee *et al.*, 2012), release of oxidised mtDNA (Shimada *et al.*, 2012), production of ROS by mitochondria (Zhou *et al.*, 2011), and lysosomal rupture accompanied by

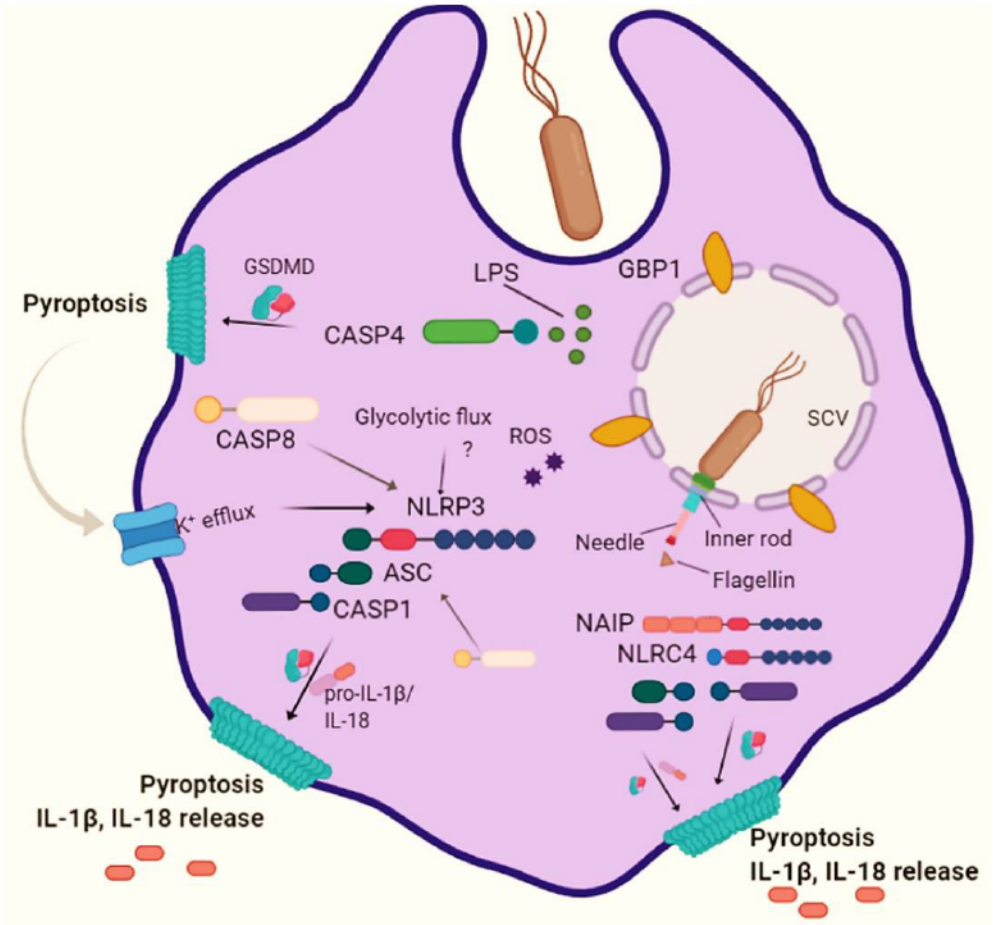


Figure 1.7 **Human inflammasome activation during macrophage infection with *S.* Typhimurium.**

Following infection, *Salmonella* mainly resides in the SCV. The needle and inner rod proteins of the SPI-1 T3SS, as well as inadvertent flagellin secretion into the host cell cytosol, are recognised by the single human NAIP, which in turn activates NLRC4. NLRC4 oligomerisation can occur independently of ASC resulting in caspase-1 activation and GSDMD cleavage and pyroptosis. However, ASC recruitment is required for optimal maturation and release of cytokines. GBP-mediated SCV disruption results in cytosolic LPS, which is recognised by caspase-4 leading to pyroptosis. Also, the resulting K^+ efflux is sensed by the NLRP3, along with other proposed signals, resulting in its activation and ASC recruitment, which in turn leads to caspase-1-mediate cytokine maturation and pyroptotic cell death. Finally, caspase-8 has been suggested to be involved in priming of NLRP3 and/or to be recruited to the inflammasome complex. A large complex consisting of NLRP3, NLRC4, ASC, and caspase-1/8 may form during infection with *S.* Typhimurium (not shown). Image created with Biorender.

cathepsin release (Hornung & Latz, 2010). K^+ efflux is the result of many NLRP3 activation pathways that involve pore formation, like treatment with the toxin nigericin and ATP stimulation, and thus is considered a universal trigger of NLRP3 (Muñoz-Planillo *et al.*, 2013). However, the mechanistic details of K^+ efflux and NLRP3 activation are not fully elucidated (He, Hara & Núñez, 2016) and some K^+ efflux-independent NLRP3 activation pathways have also been described. For example, NLRP3 activation via caspase-8 in human monocytes resulted in caspase-1 and IL-1β maturation without K^+ efflux and in the absence of signal 2 (Gaidt *et al.*, 2016).

During *S.* Typhimurium infection, NLRP3 contributes to IL-1β and IL-18 secretion, together with NLRC4 and caspase-8, and these molecules are recruited to the same complex in macrophages (Man *et al.*, 2014b, 2013; Broz *et al.*, 2010b; Qu *et al.*, 2016; Bierschenk *et al.*, 2019). Also, human monocytes respond to *S.* Typhimurium infection by activating the NLRP3 inflammasome and secreting IL-1β without undergoing pyroptosis possibly acting as a sustained signal for other immune cells (Diamond *et al.*, 2017). The NLRP3 inflammasome has been suggested to be important during the systemic stages of *S.* Typhimurium infection in mice, as low expression of SPI-1 T3SS induces NLRP3 inflammasome via an undetermined signal (Broz *et al.*, 2010b; Sellin *et al.*, 2014). Also, *S.* Typhimurium-mediated disruption of glycolytic flux by utilising host cell glucose leads to reduced NADH and increased mitochondrial ROS production, which has been suggested to activate NLRP3 (Sanman *et al.*, 2016). CARD9, a protein associated with immune signalling and cytokine synthesis, limits NLRP3 and IL-1β activation by interfering with ASC and caspase-8 recruitment to the inflammasome; however, upon exposure to *S.* Typhimurium CARD9 expression is downregulated in mouse macrophages promoting increased production of IL-1β (Pereira *et al.*, 2016). On the other hand, *S.* Typhimurium oxidative metabolism has been proposed as an evasion mechanism of NLRP3 activation to promote systemic virulence (Wynosky-Dolfi *et al.*, 2014). NLRP3 activation is complex and the activating signal is not always clear. It is therefore unsurprising that the trigger for NLRP3 activation upon *S.* Typhimurium exposure is not established (Sanchez-Garrido *et al.*, 2020) and warrants further investigation.

1.9.3.6 The NLRC4 inflammasome

The NLRC4 inflammasome has been extensively implicated in the immune response against *S.* Typhimurium, and is also involved in many other enteric bacterial infections such as *S. flexneri* (Bierschenk, Boucher & Schroder, 2017; Zhao & Shao, 2015; Sanchez-Garrido *et al.*, 2020). The NLRC4 inflammasome complex is formed following recognition of the cognate ligand of NAIP molecules leading to hetero-oligomerisation of NAIP and NLRC4 (Figure 1.6) (Yang *et al.*, 2013; Hu *et al.*, 2015; Zhang *et al.*, 2015; Kofoed & Vance, 2011). NAIP molecules undergo conformational changes recruiting and activating NLRC4, which in turns self-oligomerises with other NLRC4 molecules (Hu *et al.*, 2015; Zhang *et al.*, 2015; Diebolder *et al.*, 2015; Halff *et al.*, 2012). Humans have a single *NAIP* gene, while

mice encode seven (*Naip1–7*). The human NAIP has been shown to recognise cytosolic *Salmonella* flagellin (FliC), T3SS rod (PrgJ) and needle (PrgI) proteins (Figure 1.7) (Reyes Ruiz *et al.*, 2017; Kortmann, Brubaker & Monack, 2015; Yang *et al.*, 2013), while mouse Naip1 recognises the T3SS needle protein, Naip2 the T3SS rod, and Naip5/6 recognise flagellin monomers (Yang *et al.*, 2013; Zhao *et al.*, 2011; Broz *et al.*, 2010b; Man *et al.*, 2014b; Miao *et al.*, 2006; Franchi *et al.*, 2006; Kofoed & Vance, 2011; Lightfield *et al.*, 2008; Rayamajhi *et al.*, 2013; Miao *et al.*, 2010b). *S.* Typhi induces caspase-1 activation and pyroptosis in both human primary macrophages and the THP-1 cell line (Kortmann, Brubaker & Monack, 2015; Winter *et al.*, 2015). This response is thought to be flagellin-dependent in primary cells suggesting that NLRC4 is implicated (Kortmann, Brubaker & Monack, 2015), although further studies are required to confirm this. Similarly, during THP-1 cell infection, TviA-mediated reduction of flagellin has been suggested as a mechanism to limit pyroptosis (Winter *et al.*, 2015).

The ability of a single NAIP to recognise different ligands is probably explained by the structural similarity of the C-terminus of these proteins. More specifically, the C-terminal helical hairpin structure of the T3SS needle protein is highly similar to that of the rod protein and flagellin (Yang *et al.*, 2013; Zhao & Shao, 2015; Miao *et al.*, 2010b; Lightfield *et al.*, 2008; Reyes Ruiz *et al.*, 2017). Due to the evolutionary relatedness of T3SS and flagellar apparatus, it is suggested that flagellin is inadvertently secreted to the host cell cytosol via the SPI-1 T3SS (Zhao & Shao, 2015) and a functional SPI-1 T3SS is required for flagellin-induced caspase-1 activation (Sun, Rolán & Tsolis, 2007). The SPI-2 T3SS rod and needle proteins are not recognised by NAIP due to their distinct structures, which possibly serves as an immune evasion strategy at later stages of infection, together with downregulation of SPI-1 proteins and flagellin (Miao *et al.*, 2010b; Reyes Ruiz *et al.*, 2017; Miao *et al.*, 2006, 2010a). The SPI-2 T3SS has been also shown to counteract the SPI-1 T3SS-mediated inflammasome activation implying an immune evasion mechanism by *S.* Typhimurium at infection stages when SPI-2 is active (Bierschenk *et al.*, 2019). It is unclear whether typhoidal *Salmonella* exploit a similar evasion mechanism, as SPI-2 may not be required during infection with S. Typhi (Karlinsey *et al.*, 2019; Forest *et al.*, 2010).

During *S.* Typhimurium infection, NLRP3 and NLRC4 are recruited to a single macromolecular complex together with caspase-1 and may be functionally redundant in mouse cells, although their activating signals differ (Broz *et al.*, 2010b; Man *et al.*, 2014b; Qu *et al.*, 2016). In support of this, NLRC4-deficient mice can clear *S.* Typhimurium infection similarly to WT mice, while mice lacking both inflammasomes are more susceptible to *S.* Typhimurium infection (Broz *et al.*, 2010b). In human primary macrophages and a macrophage-like cell line, pharmacological inhibition of NLRP3 alone does not decrease caspase-1 activation and inflammasome-induced cell death, and both NLRC4 and NLRP3 are thought to contribute to pyroptosis and cytokine secretion (Bierschenk *et al.*, 2019; Yang *et al.*,

2013; Kortmann, Brubaker & Monack, 2015). NLRC4 contains a CARD and thus does not rely on ASC to form an inflammasome complex capable of recruiting caspase-1 and NLRC4 can cause caspase-1-dependent downstream signalling without caspase-1 undergoing autoproteolysis (Broz *et al.*, 2010a). However, ASC is required for optimal NLRC4 inflammasome activity ensuring cytokine maturation and secretion (Broz *et al.*, 2010a).

Studies in murine models have shown that NLRC4 activation leads to several downstream events during infection with *S.* Typhimurium. NAIP/NLRC4 activation in murine intestinal epithelial cells (IECs) is essential for limiting dissemination to systemic sites (Hausmann *et al.*, 2020), as it results in expulsion of such cells in the intestinal lumen promoting elimination of the pathogen (Sellin *et al.*, 2014; Rauch *et al.*, 2017). Also, NLRC4 inflammasome activation results in cytoskeletal rearrangements leading to cell stiffness and reduced bacterial uptake by host cells *in vitro*, limiting host cell infection and pathogen intracellular survival (Man *et al.*, 2014a). NLRC4-mediated cytokine secretion recruits immune cells to the intestinal lumen and neutrophil-mediated elimination of *S.* Typhimurium, while eicosanoid release as a result of cell expulsion promotes fluid accumulation to promote flushing of the pathogen (Miao *et al.*, 2010a; Franchi *et al.*, 2012; Rauch *et al.*, 2017). Activity of NLRC4 in intestinal macrophages and dendritic cells in response to *S.* Typhimurium allows discrimination between commensals and pathogens in the intestine, underlining the important role of this inflammasome in host intestinal defence (Franchi *et al.*, 2012).

1.9.3.7 Caspase-8 and inflammasomes

Caspase-8 is traditionally considered an apoptotic caspase (Fernández & Lamkanfi, 2015; Feltham, Vince & Lawlor, 2017). However, its role in inflammasome activation and modulation, as well as in tissue homeostasis, is becoming increasingly apparent. Its many roles in inflammation include promoting NLRP3 inflammasome priming and TLR-mediated cytokine production (Gurung *et al.*, 2014; Philip *et al.*, 2014, 2016), as well as being involved in NLRP3-induced IL-1β secretion (Antonopoulos *et al.*, 2015). Importantly, caspase-8 can directly cleave pro-IL-1β at the same site as caspase-1, albeit less efficiently (Maelfait *et al.*, 2008). Similarly, Fas-dependent signalling, a TNF family receptor, can induce caspase-8-dependent, inflammasome-independent IL-1β and IL-18 maturation (Bossaller *et al.*, 2012). In support of this, caspase-8 contains a death effector domain (DED) domain which can interact with the PYD domain of ASC, pointing towards caspase-8 recruitment to the inflammasome platform (Sagulenko *et al.*, 2013; Vajjhala *et al.*, 2015). Indeed, in the absence of caspase-1, NLRP3 activation can induce ASC-caspase-8 polymerisation and caspase-8-dependent apoptosis (Antonopoulos *et al.*, 2015; Vajjhala *et al.*, 2015; Sagulenko *et al.*, 2013). Caspase-8 is involved in inflammasome activation following infection with various pathogens. *Francisella tularensis* induces release of IL-18 in a caspase-1-independent, caspase-8-depedent manner via AIM2-ASC (Pierini *et al.*, 2013). Caspsase-8 is essential

for host defence against *Yersinia*, as inflammasome activation engages caspase-8, which mediates caspase-1 processing while it also directly cleaves GSDMD (Orning *et al.*, 2018; Philip *et al.*, 2014). As mentioned earlier, during *S.* Typhimurium infection caspase-8 is recruited to the NLRP3 and NLRC4-containing inflammasome complex, where caspase-8 is proteolytically activated and contributes to cytokine production and processing, while it does not seem to affect pyroptosis of mouse macrophages (Man *et al.*, 2014b, 2013). During *in vivo* infection, caspase-8 is also activated downstream of NLRC4 in an ASC-dependent manner in IECs promoting *S.* Typhimurium-infected cell expulsion independently of caspase-1 and GSDMD (Rauch *et al.*, 2017).

1.9.3.8 Non-canonical inflammasome activation

The NLRP3 inflammasome can be activated via a non-canonical pathway during *S.* Typhimurium infection upon recognition of cytosolic LPS (Figure 1.7). This recognition occurs by human caspase-4 and caspase-5 or by mouse caspase-11, independently of TLR4 (Yang, Zhao & Shao, 2015; Shi *et al.*, 2014; Casson *et al.*, 2015; Baker *et al.*, 2015; Kayagaki *et al.*, 2013, 2011; Hagar *et al.*, 2013; Schmid-Burgk *et al.*, 2015; Aachoui *et al.*, 2013). The CARD domains of caspase-4 and caspase-11 contain Lipid A-binding sites allowing for direct recognition of cytosolic LPS by these caspases (Shi *et al.*, 2014), leading to caspase oligomerisation and activation (Shi *et al.*, 2014; Yang, Zhao & Shao, 2015). Hexa- or penta-acylated lipid A is recognised by caspase-11, while tetra-acylated lipid A is only recognised by human caspase-4 (Hagar *et al.*, 2013; Lagrange *et al.*, 2018). Caspase-4/11 activation leads to GSDMD cleavage and pyroptotic cell death, while IL-18 and IL-1β maturation is driven mainly by NLRP3-mediated active caspase-1 (Kayagaki *et al.*, 2011, 2015; Schmid-Burgk *et al.*, 2015). K^+ efflux during non-canonical activation has been proposed as the mechanism underlying NLRP3 activation, directly caused by GSDMD pores or triggered by caspase-11-mediated pannexin-1 cleavage (Swanson, Deng & Ting, 2019; Yang, Zhao & Shao, 2015; Rühl & Broz, 2015). GBPs are involved in the exposure of LPS to the host cytosol during infection with Gram-negative bacteria (including *S.* Typhimurium) by mediating disruption of the bacteria-containing vacuoles (Yang, Zhao & Shao, 2015; Santos *et al.*, 2018; Fisch *et al.*, 2019a; Meunier *et al.*, 2014; Shenoy *et al.*, 2012). In support of this requirement of GBPs, IFNγ-treated human macrophages respond to *S.* Typhimurium by recruiting caspase-4 in a GBP-1-mediated manner promoting pyroptosis, while untreated macrophages do not respond to *S.* Typhimurium in a caspase-4-dependent manner (Fisch *et al.*, 2019a). In addition to caspase-4, caspase-5 has also been found to mediate cell death and IL-1β release during infection of human macrophages with *S.* Typhimurium, in contrast to what is seen with LPS transfection alone where caspase-5 does not have a role (Baker *et al.*, 2015).

1.10 Project aims

S. Paratyphi A is a neglected pathogen that may soon become the leading cause of enteric fever. Understanding its virulence mechanisms and the ensuing host immune response is critical for vaccine development. Important gaps in our knowledge include the interaction of *S.* Paratyphi A with the host at the anatomical and cellular levels. The main aim of this project was to study *S.* Paratyphi A-host interactions; in particular, I aimed to:

- Investigate *S.* Paratyphi A responses to bile
- Study the interaction of *S.* Paratyphi A with human epithelial cells and macrophages
- Elucidate the activation of cell death and inflammasome activation pathways in human macrophages during *S.* Paratyphi A infection
- Investigate infection with *S.* Paratyphi A clinical isolates

2

Materials & Methods

2.1 Bacterial culture and strains

2.1.1 Bacterial culture

Salmonella strains used in this study are listed in Table 2.1 and clinical isolates in Table 2.2. *Salmonella* strains were routinely cultured in Lennox Lysogeny Broth (LB) at 37 °C with agitation (200 rpm) and aeration, unless otherwise stated. Where necessary, growth media were supplemented with antibiotics (Sigma) at the required concentrations: 50 µg/mL kanamycin (kan), 100 µg/mL spectinomycin (Spec), or 100 µg/mL ampicillin (Amp). SPI-1 expression was induced either by sub-culturing saturated cultures 1:33 to late exponential phase (optical density at A_{600} (OD_{600}) ≈1.8), or by growth in microaerobic conditions, where bacteria were incubated as static cultures for 16–18 h in LB Miller (OD_{600} ≈1.0). Where applicable, Lennox LB was supplemented with 3% (w/v) filter-sterilised ox bile (Sigma B3883/Merck 1037560500). For growth curves, bacteria were grown for 16 h before being sub-cultured 1:50, and the OD_{600} was monitored every hour.

Table 2.1 **Strains and plasmids used in this study**

Strains			
Name		**Genotype**	**Source**
S. Typhi	Ty2	WT	G. Dougan (Wellcome Sanger Institute, UK)
		Δ*invA*::Kan^r	(Johnson *et al.*, 2017)
		Δ*tviB*::Kan^r	Frankel Group (R. Johnson)
		Δ*stoD*::Kan^r	(McDowell et al., 2019)
	H58	ERL12148	G. Dougan (Wellcome Sanger Institute, UK)
		129-0238	G. Dougan (Wellcome Sanger Institute, UK)
S. Paratyphi A	ATCC 9150	WT	Ohad Gal-Mor (Tel Aviv University, Israel)
		Δ*fepE*::Kan^r	This study
		Δ*invA*::Kan^r	Frankel Group (R. Johnson)
		Δ*aceA*::Kan^r	This study
		Δ*aceB*::Kan^r	This study
		Δ*aceBA*::Kan^r	This study
S. Typhimurium	ATCC 14028	WT	ATCC
		Δ*prgH*::Tn5	(Johnson *et al.*, 2017)
		Δ*prgH*Δ*ssaV*::Kan^r	Sophie Helaine, Imperial College
		Δ*fepE*::Kan^r	This study
Plasmids			
Name		**Comments/Selection**	**Source**
pWSK29-Spec	Empty vector (EV)	Spec^r	(Johnson *et al.*, 2017)
	pWSK29-*hilA*	9150 *hilA* gene, T3 promoter Spec^r	This study
	pWSK29-*fepE*	9150 *fepE* gene, T3 promoter Spec^r	This study
	pWSK29-*sopD*-TEM-1	Spec^r	This study
	pWSK29-*stoD*-TEM-1	Spec^r	This study
	pWSK29-TEM-1 EV	Spec^r	This study
pKD4		Kan^r cassette-expressing plasmid, used as template	(Datsenko & Wanner, 2000)
pKD46		Expressing λ-red recombinase under the arabinose-inducible *araBAD* promoter which is temperature-sensitive, Amp^r	(Datsenko & Wanner, 2000)

2.1.2 Bacterial strains and mutagenesis

Salmonella deletion mutants were generated using the λ-red recombinase system as previously described (Datsenko & Wanner, 2000). Briefly, the kanamycin resistance (Kanʳ)-encoding cassette was amplified from pKD4 plasmid using primers (Table 2.3) complementary to the Kanʳ cassette-region with approximately 50 base-pair overhang regions complementary to the upstream or downstream

Table 2.2 ***S.* Typhi and *S.* Paratyphi A clinical isolate strains from Nepal.**

Strains were kindly provided by Prof Stephen Baker during work in OUCRU, Vietnam. All strains were isolated from patients with acute typhoid in Nepal in the stated year (Dolecek *et al.*, 2008; Arjyal *et al.*, 2016). *S.* Typhi isolates were tested for Vi and O9, and *S.* Paratyphi A for O2 by slide agglutination (See Section 2.1.3).

Serovar	Genotype/Lineage	ID/Name	Isolation Date, Age, Sex	Agglutination test
S. Typhi	Genotype 4.3.1 (H58)	01TY052	2008, 4, M	Vi+, O9+
		01TY061	2008, 16, M	Vi+, O9+
		01TY065	2008, 23, F	Vi+, O9+
		01TY066	2008, 11, F	Vi+, O9+
		01TY069	2008, 24, M	Vi+, O9+
		01TY073	2008, 24, F	Vi+, O9+
		01TY077	2008, 6, F	Vi+, O9+
		01TY083	2009, 6, F	Vi+, O9+
		01TY088	2009, 19, M	Vi+, O9+
		01TY095	2009, 16, M	Vi+, O9+
		01TY096	2009, 15, M	Vi+, O9+
		01TY102	2009, 18, M	Vi+, O9+
		01TY301	2010, 16, M	Vi+, O9+
		01TY426	2010, 17, M	Vi+, O9+
		01TY433	2010, 19, M	Vi+, O9+
		01TY441	2010, 28, M	Vi+, O9+
		01TY481	2010, 17, M	Vi+, O9+
	Genotype 3.3	01TY086	2009, 13, M	Vi+, O9+
		01TY151	2009, 6, F	Vi+, O9+
		01TY154	2009, 17, F	Vi+, O9+
		01TY257	2009, 19, M	Vi+, O9+
S. Paratyphi A	Lineage A	02TY129	2013, 6, M	O2+
		02TY221	2014, 24, M	O2+
		02TY224	2014, 27, M	O2+
		ED293	2006, 24, M	O2+
	Lineage C	ED199	2006, 35, F	O2+

regions of the gene of interest. PCR products were DpnI-digested and purified. *Salmonella* carrying pKD46 was grown at 30 °C to saturation before sub-culturing to mid-log phase (OD_{600} ≈0.4-0.6) and λ-red recombinase was induced with the addition of 10 mM arabinose for 30 min prior to washing three times with ice-cold 15% v/v glycerol. *Salmonella* was transformed with 1 µg Kan^r-gene flanking products by electroporation (2.5 kV, 200Ω, 25 µF). Transformants were recovered in 1 mL SOC media and incubated at 30 °C for at least 1 h. Kan^r-only mutants were selected by growth on kanamycin-containing agar plates and screened by sequencing using Up/Down primers (Table 2.3). Positive clones were cured of pKD46 by 16 h growth at 42 °C and loss of the plasmid was confirmed by selection of Kan-resistant, Amp-sensitive clones. Gene deletions were confirmed by sequencing (GATC/Eurofins) using Up/Down primers (Table 2.3).

The *hilA* overexpression and *fepE* complementation plasmids were constructed by Gibson assembly (NEB) following the manufacturer's instructions. The TEM-1 plasmids were generated by first constructing a pWSK29-Spec plasmid containing the TEM-1 β-lactamase by Gibson assembly (NEB) according to the manufacturer's instructions and using primers listed in Table 2.3. The indicated *S.* Typhi Ty2 genes were cloned as a C-terminal fusion to TEM-1 (Table 2.3) into pWSK29-Spec-TEM-1. Plasmid inserts were amplified with Q5 polymerase (Table 2.3) and confirmed by sequencing using standard M13 primers. To transform plasmids into *Salmonella*, the indicated bacterial strains were grown overnight and sub-cultured to mid-log phase. Bacteria were washed two times with ice cold 15% glycerol and transformed with 100 ng of plasmid by electroporation. Bacteria were recovered for 1 h at 37 °C and transformants were selected by growth on antibiotic agar plates.

2.1.3 Slide agglutination test

Clinical isolate strains were tested for the presence of Vi and O9 antigen for S. Typhi, and O2 antigen for S. Paratyphi A by slide agglutination as follows. A drop of 0.9% NaCl solution on a glass slide was mixed with 3-4 colonies of bacteria. 2-3 drops of Vi, O9, or O2 rabbit antisera (Remel) was mixed with each bacteria-containing droplet. The droplets were visually inspected for clump formation and a positive/negative readout was recorded.

Table 2.3 **Primers used in this study**

Name	Sequence
Deletion mutants	
9150 Δ*fepE* For	TCATTGGATAAAGTTTTCAGGTCATACGGCATGCCATCTCTTAATGT AAAACGTGTAGGCTGGAGCTGCTTC
Tm Δ*fepE* For	TCATTGGATAAATTTTTCAGGTCATACGGCATGCCATCTCTTAATGT AAAACGTGTAGGCTGGAGCTGCTTC
9150/Tm Δ*fepE* Rev	GGATATCGCTATCCGGCTTTTCGGGTAAATCAGACTAACCGTTCATC TACATATGAATATCCTCCTTAG
Δ*invA* For	ACTTAACAGTGCTCGTTTACGACCTGAATTACTGATTCTGGTACTAA TGGGTGTAGGCTGGAGCTGCTTC (Johnson *et al.*, 2017)
Δ*invA* Rev	GCTATCTGCTATCTCACCGAAAGATAAAACCTCCAGATCCGGAAAAC GACCCATATGAATATCCTCCTTAG (Johnson *et al.*, 2017)
Δ*aceA* For	CACCACATAACAATATGGAGCATCTGCACATGAAAACCCGTACTCA ACTGTGTAGGCTGGAGCTGCTTCG
Δ*aceA* Rev	CGGTAAGCGCAGCGCCACCGGGCATCAATCAAAACTGCGATTCTTC GGCATATGAATATCCTCCTTAG
Δ*aceB* For	ATCTGGATCAACAACGAGGAGCTGCATGATGAATCCACAGGCAACC ACTGTGTAGGCTGGAGCTGCTTCG
Δ*aceB* Rev	GTGCAGATGCTCCATATTGTTATGTGGTGAATTAAGCCAGTAAGCG ATAGCCATATGAATATCCTCCTTAG
Sequencing primers (gene deletion confirmation)	
fepE Up	AGGCAAGTTTAATTCCGAATATTTAGC
fepE Down	TATGGGCTGCGCTGTATGATTATC
invA Up	GTTACGTAGTATGACCGATATTGC (Johnson *et al.*, 2017)
invA Down	CCTCCAATTAATGAAGGATCGC (Johnson *et al.*, 2017)
aceA Up	CGATGCCGCACGTCTGATG
aceA Down	GGTTTGAGCAATCAGTAATTCCAG
aceB Up	TGGAAATTGTTTTGATTTTG
aceB Down	ACGGGCGGGTGATGCCTTC
Gibson assembly primers	
hilA For	GCTCCACCGCGGTGGCGGCCATGCCACATTTTAATCCTG
hilA Rev	GGATCCACTAGTTCTAGAGCTTACCGTAATTTAATCAAGCG
pWSK29-Spec For (*hilA* vector)	GCTCTAGAACTAGTGGATC
pWSK29-Spec Rev (*hilA* vector)	GGCCGCCACCGCGGTGGA
fepE For	CTCCACCGCGATGCCATCTCTTAATGTAAAAC
fepE Rev	TACCGGGCCCTCAGACTAACCGTTCATC
pWSK29-Spec For (*fepE* vector)	GTTAGTCTGAGGGCCCGGTACCCAATTC
pWSK29-Spec Rev (*fepE* vector)	GAGATGGCATCGCGGTGGAGCTCCAGCT
pWSK29-Spec EV For (TEM1 fusion vector)	GATATCAAGCTTATCGATACCG
pWSK29-Spec EV Rev (TEM1 fusion vector)	AATTCCTGCAGCCCGGGGGA
TEM1 For	TCCCCCGGGCTGCAGGAATTCGCACCCAGAAACGCTGGTG
TEM1 Rev	GTATCGATAAGCTTGATATCTTACCAATGCTTAATCAGTGAGGCACC
Restriction digest primers	
Ty2 *sopD* For (NotI)	CATGGCGGCCGCATGCCAGTCACTTTAAGCTTCG
Ty2 *sopD* Rev (EcoRI)	CGGAATTCCGTGTCAGTAATATATTACGACTG

stoD For (BamHI)	CGCGGATCCAGAAGGAGATATACCTACGTAATGTTCTTAACATTTCC TAATGTAG
stoD Rev (EcoRI)	CGCGGATCCAGAAGGAGATATACCTACGTAATGTTCTTAACATTTCC TAATGTAG
qRT-PCR primers	
ftsZ For	GTATCACCGAGCTGTCCAAG (Johnson *et al.*, 2018)
ftsZ Rev	CTGCGATACCCTGAACCG (Johnson *et al.*, 2018)
hilA For	CATGGCTGGTCAGTTGGAG (Johnson *et al.*, 2018)
hilA REV	CGTAATTCATCGCCTAAACG (Johnson *et al.*, 2018)
sopB FOR	GCCTGGAATTGTAAAAGCGG (Johnson *et al.*, 2018)
sopB REV	TTTTCTGTCCACCGCTATCC (Johnson *et al.*, 2018)
hilD For	TGCACTTATCCCAAACGAGC (Johnson *et al.*, 2018)
hilD Rev	GGCAGGAAAGTCAGGTGTATAG (Johnson *et al.*, 2018)
fadE For	TCGTCACTTCCCGCTTAAC (Johnson *et al.*, 2018)
fadE Rev	TCCTACCGACAAACATTCCAC (Johnson *et al.*, 2018)
hilC For	GTGGGTTTGATTTCCTTGAGC (primer designed by R. Johnson)
hilC Rev	CCAGTTTTCGCTTCAGACTTG (primer designed by R. Johnson)
rtsA For	TGTTTAATCCCTCACCTGTCC (primer designed by R. Johnson)
rtsA Rev	GATTTCCTCTGCCAGTTTTGC (primer designed by R. Johnson)
fliZ For	GGGAATATGTCGTGCGTTTAC (primer designed by R. Johnson)
fliZ Rev	TCATCGAGAAAACCGTCCTG (primer designed by R. Johnson)
cysJ For	CTGTTGGTGATAGTGACGTCC (primer designed by R. Johnson)
cysJ Rev	ATTCATAAGAGGTGTCGCCG (primer designed by R. Johnson)
aceB For	TGAAGGCGAACGTACAGAAG
aceB Rev	CCTCCATCAGACCGTAAATCG
aceA For	AGAAAGAGTGGACACAACCG
aceA Rev	GTAATTTCACCACCTCCTCCG
iclR For	CGGGCAGGTTCAGTCTTTAA
iclR Rev	GGTGAGTCGTGGAATTAGGC
sodA For	GTGCTGAAAGGTGACAAACTG
sodA Rev	TTCAGATAGTAAGCGTGTTCCC
fliE For	GCTGCGCTGGATCGTATTAG
fliE Rev	TCGGCCATCACGTCATTAAG
sipA For	ACGTCAGAAAAGGGCACTAC
sipA Rev	TTCACAATCTCTGCCGTCTG
fepE For	GGGTTGCTTCTGTCCTTTCTG
fepE Rev	TTACCTCCATATCCAACACGC
16S For	TGTAGCGGTGAAATGCGTAG (primer designed by R. Johnson)
16S Rev	CAAGGGCACAACCTCCAAG (primer designed by R. Johnson)

2.2 Cell lines and cell culture

2.2.1 Human cell lines used in this study

Human cell lines used in this study are listed in Table 2.4. All cell lines were maintained at 37 °C in 5% (v/v) CO_2 and were confirmed to be mycoplasma-negative (MycoAlert mycoplasma detection kit, Lonza). The retroviral-transduced NAIP^{miR} cell line was generated as previously described (Eldridge ***et al.***, 2017) by P. Goddard, and the plasmid was designed by J. Sanchez-Garrido (Shenoy Group, Imperial College London).

2.2.2 HeLa cell culture

HeLa cells were maintained in **Dulbecco's modified Eagle medium** (DMEM) with 4500 mg/L glucose (Sigma), 10% (v/v) heat-inactivated foetal bovine serum (FBS; Gibco) and 1% (v/v) GlutaMAX (ThermoFisher Scientific). For harvesting, media were removed, cells were washed once with **Dulbecco's Phosphate Buffer Saline** (DPBS, Sigma) and treated with 0.2% EDTA (Sigma) supplemented with 2% Trypsin (Sigma) for 5 min at 37 °C/5% (v/v) CO_2. FBS-containing media was added to inactivate trypsin and cells were harvested by centrifugation at 1,200 rpm. Cells were seeded at 7×10^4 cells/well in 24-well plates for invasion assays or 3.5×10^4 cells/well in black wall/clear bottom 96-well plates for translocation assays 24 h prior to infection.

Table 2.4 **Cell lines used in this study**.

Cell line	Genotype	Selection	Source
HeLa ATCC	WT	N/A	ATCC
THP-1	WT	N/A	John MacMicking laboratory (Yale School of Medicine) (Shenoy ***et al.***, 2012)
THP-1 GSDMD^{miR}	pMX-CMV-YFP-GSDMD^{miR} 5'-TACACATTCATTGAGGTGCTGG-3'	Puromycin	(Eldridge et al., 2017)
THP-1 ASCmiR	pMX-CMV-YFP-ASC-miR30E 5'-CAGCTCTTCAGTTTCACACCAG-3'	Puromycin	(Goddard et al., 2019)
THP-1 CASP4^{miR}	pMX-CMV-YFP-CAS4-miR30E 5'-ATATCTTGTCATGGACAGTCGT-3'	Puromycin	(Pallett et al., 2016; Goddard et al., 2019)
THP-1 NAIP^{miR}	pMX-CMV-YFP-NAIP^{miR} 5'-ATTCACAAAGTTCACCACGGCT-3'	Puromycin	Oligomer design by P. Goddard, cell line construction by J. Sanchez-Garrido, A. Shenoy group
THP-1 CTRL^{miR}	pMX-CMV-YFP-LacZ^{miR} 5'-TCACGACGTTGTAATACGACGT-3'	Puromycin	(Eldridge et al., 2017)
THP-1 ASC^{mRFP}	pMX-ASC-mRFP	Puromycin	(Goddard et al., 2019)

2.2.3 THP-1 cell culture

THP-1 cells were routinely cultured in suspension in RPMI-1640 (Sigma) supplemented with 10% (v/v) heat-inactivated FBS, 1 mM Sodium Pyruvate (Sigma), 10 mM HEPES solution (Sigma) and 100 U/100 µg/mL penicillin/streptomycin (Sigma). Retroviral plasmid transduced cell lines (miR) were maintained with 2 µg/mL Puromycin (Sigma).

Cells were seeded at 1.5×10^5 cells/well in 96-well black-wall clear-bottom plates for cell death assays and CFU assays, at 4.5×10^5 cells/well in 48-well plates for western blotting, or at 5×10^5 cells/well on glass coverslips in 24-well plates for immunofluorescence. For all assays, THP-1 cells were seeded 3 days prior to infection and differentiated to macrophage-like cells with 100 ng/mL phorbol 12-myristate 13-acetate (PMA; Sigma) for 48 h. 24 h before infection PMA was withdrawn and antibiotic-containing media was replaced with antibiotic-free media. For cell death assays, cell treatments and infections were carried out specifically in complete RPMI media lacking phenol red (Gibco) to prevent interference of the dye with propidium iodide (PI).

2.2.4 Isolation of primary human monocyte-derived macrophages (MDMs)

Primary MDMs were prepared as previously described by CD14+ enrichment by MACS (Magnetic-activated cell sorting, Miltenyi Biotec) (Goddard et al., 2019). Briefly, leukocyte cones were obtained either from the NHS blood and transfusion service or from anonymous healthy donors. Buffy coats containing white blood cells were prepared by diluting blood from each donor in PBS and using 50 mL LeucoSep tubes (Greiner Bio-one) and centrifugation at 1000 × g for 20 min at RT (no breaks, to prevent disturbance of blood layers). Following three washes with 20 mL of pre-warmed RPMI and two washes with 20 mL of MACS buffer (50 mg/mL BSA, 2 mM EDTA in PBS), CD14+ cells were isolated using biotinylated anti-CD14+ antibody and anti-biotin microbeads following the manufacturer's guidelines (Miltenyi Biotec). CD14+ cells were confirmed by flow cytometry (85-95%; performed by J. Sanchez-Garrido) and were seeded and cultured for 7-8 days in RPMI supplemented with 20 ng/mL human macrophage colony-stimulating factor (MCSF) to promote differentiation to macrophages. Media was replenished every 3 days. MCSF and antibiotics were removed 24 h prior to infection.

2.3 THP-1 and MDM cell treatments

THP-1 or MDM cells were incubated with chemical inhibitors 1 h prior to infection or treatment at the following concentrations: Z-VAD-FMK (R&D Systems, FMK001) at 50 µM, Z-YVAD-FMK (R&D Systems, FMK005) at 50 µM, Z-IETD-FMK (R&D Systems, FMK007) at 50 µM, and MCC950 (Tocris Bioscience, 5479) at 2 µM for THP-1 cells or 5 µM for MDMs.

For LPS plus nigericin controls (LPS/Nig), THP-1 cells were primed with 250 ng/mL Ultra-pure *E. coli* O111:B4 LPS-EB (Invivogen, tlrl-3pelps) for 3 h prior to treatment with 25 µM nigericin (Sigma) for 1 h. When required, caspase-4 activation was induced in unprimed cells by transfecting LPS (5 µg/mL) with Lipofectamine 2000 transfection reagent [1% (v/v)] (Life Technologies). Caspase-8 activation was induced by treating unprimed cells with 2 µM staurosporine for 5 h (Sigma).

For small interfering RNA (siRNA)-mediated transient knockdown of CASP4, NAIP, and GSDMD in MDM cells, ON-target Plus SMARTpool (Dharmacon) was used with siRNAs listed in Table 2.5, 72 h post seeding. Transfection was performed with the Transit-X2 Transfection Reagent (Mirus) according to manufacturer's guidelines at a final siRNA concentration of 30 nM. Cells were incubated for 5-6 h post transfection and media was supplemented with MCSF as described above.

Table 2.5 **SMART Pool siRNA sequences**

siRNA sequence	Cat. No	Source
siRNA ON-TARGETplus non-targeting	Dharmacon, D-001810-10	(Goddard *et al.*, 2019)
- UGGUUUACAUGUCGACUAA -	D-001810-01	
- UGGUUUACAUGUUGUGUGA -	D-001810-02	
- UGGUUUACAUGUUUUCUGA -	D-001810-03	
- UGGUUUACAUGUUUUCCUA -	D-001810-04	
siRNA CASP4	Dharmacon, L-004404-00	(Goddard *et al.*, 2019)
- GGACUAUAGUGUAGAUGUA -	L-004404-05	
- CAACGUAUGGCAGGACAAA -	L-004404-06	
- GAACUGUGCAUGAUGAGAA -	L-004404-07	
- UAACAUAGACCAAAUAUCC -	L-004404-08	
siRNA NAIP	Dharmacon, L-004389-00	A. Shenoy
- GCAUCGAACUCCAUUUAAA -	J-004389-06	
- GAACAUUAUCCAGCAGUUA -	J-004389-07	
- GAGCGAAAUUUAGCUGAAA -	J-004389-08	
- GUACAAGAUUCCCUGUCUA -	J-004389-09	
siRNA GSDMD	Dharmacon, J-016207-00	Q. Zhong, Frankel Group
- CCACGUGCUUGCAGGGUGA -	J-016207-05	
- GUCCUUCUCUUCCCGGAUA -	J-016207-06	
- GCACCUCAAUGAAUGUGUA -	J-016207-07	
- GGAACUCGCUAUCCCUGUU -	J-016207-08	

2.4 Cell infections

For THP-1 infections and infections with bile-grown bacteria, bacterial cultures were washed twice in PBS and diluted to achieve the appropriate multiplicity of infection (MOI). CFUs were confirmed by retrospective plating. Following infection, cells were centrifuged at 600 × *g* for 10 min in order to synchronise the infection.

2.4.1 HeLa invasion and HeLa replication assays

All HeLa infections were performed at an MOI of 100 for all *Salmonella* serovars. Following infection, invasion was allowed for 30 min at 37 °C/5% (v/v) CO_2. Cells were washed twice with DPBS and media supplemented with 100 µg/mL gentamicin (Sigma) was added to the cells for 2 h post infection. For longer infection timepoints, gentamicin was reduced to 20 µg/mL. Cells were harvested following washing twice with DPBS and incubating in ice cold DPBS supplemented with 0.1% Triton X100 for 5 min at RT. Cell lysates were mixed and serially diluted before plating in triplicate on LB agar plates for CFU enumeration.

2.4.2 THP-1 gentamicin protection and chloroquine resistance assays

For gentamicin protection assays, THP-1 or MDM cells were treated with Z-VAD-FMK prior to infection in order to prevent loss of internalised bacteria due to cell death. Cells were infected and at 30 min of bacterial uptake by THP-1 cells, cells were washed once with DPBS and media supplemented with 100 µg/mL gentamicin was added. At 1.5 h post infection, cells were washed twice with PBS, lysed in 0.5% Triton X-100 for 5 min at room temperature and serially diluted in sterile PBS. Dilutions were plated in triplicate onto LB agar plates and CFUs were enumerated. To determine the percentage of cytosolic bacteria, $GSDMD^{miR}$ THP-1 cells were used in order to minimise cell death. At 30 min post infection gentamicin (100 µg/mL) was added. For the 1.5 h post infection time point, chloroquine (200 µg/mL; Sigma) was additionally added to the cells for 1 h (Goddard ***et al.***, 2019), before lysing and plating CFUs. For the 3 h post infection time point, gentamicin was reduced to 20 µg/mL and chloroquine (200 µg/mL) was added at 2 h post infection and left for 1 h to ensure killing of vacuolar bacteria. Cells were lysed and CFUs were determined as above.

2.4.3 PI uptake-based cell death assay

Prior to infection, cell media was replaced with full media supplemented with 5 µM PI (Sigma). Cells were infected as described and PI uptake was monitored one a FLUOstar Omega plate reader (BMG Labtech) with 530 nm emission/ 620 nm excitation filters. Gentamicin was added 30 min post infection to all wells at a final concentration of 200 µg/mL. For 100% cell death control cells, cells were treated with 0.05% Triton X100 (defined as maximal cell lysis). Unless otherwise stated, experimental values of PI uptake were blanked with uninfected cell values. Cell death was calculated as the percentage of the average value of maximal cell lysis.

2.4.4 Immunofluorescence

For minimising cell death, seeded cells were treated with Z-VAD-FMK prior to infection. Cells were infected and treated with gentamicin as above. At the desired time points, cells were washed three times with PBS. For inside/outside staining cells were transferred to ice and saturated with 2% Bovine

SerumAlbumin(BSA;Si gma)for5min,beforeaddinganti -CSAantibody(1:200;InsightBiotechnology) for35 -45min .Allproceedingstepswerecarriedout atroomtemperature (RT).Cellswerewashed with PBS and the secondary antibody (1:200 donkey anti -goat immunoglobulin -Cy2; Jackson ImmunoResearch) was added in 2% BSA for 30 min, before washing with PBS and fixing with 4% Paraformaldehyde(PFA,ThermoFisherScientific)inPBSfor20min .PFAwasremoved andcellsw ere washed three times with PBS before quenching amines with 50 mM NH_4Cl for 10 min. Cells were permeabilisedwith0.2%TritonX -100(Sigma)for4min.CoverslipswereblockedinBSA (Sigma)for5 min before staining bacteria with primary antibody in 2% BSA for 45 min. Cells were washed and blockedoncemore,beforea ddingsecondaryantibody,Hoechst(1:1,000),andphalloidin -tetramethyl rhodamineisocyanate(1:100;Invitrogen)for30min. Fortotalstaining,coverslipswerefixedinPFAat the desired time points and stained as above. All fluorescence antibodies are l isted in Table 2.6. CoverslipswerewashedinPBSbeforemountingwithProLongGoldantifadereagent(ThermoFisher Scientific)onmicroscopicslidesand visualizedusingaZeissAxioObserverZ1microscopeat40 x or63 x magnification atconsistentexposuretimes .Imageswereprocessedusingtheassociated CarlZeissZen Bluesoftware.

Table 2.6 **Fluorescenceantibodiesusedinthisstudy**

Antibody	Source	Identifier
Goatanti -CSA-1	InsightBiotechnology	01-91-99
PhalloidinAlexa647	Startech	23127-AAT
Hoechst33258	Sigma-Aldrich	94403
Donkeyanti -goat immunoglobulin-Cy2	JacksonImmunoResearch	705-225-147, RRID:AB_2307341

2.4.5 Enzyme linked immunosorbent assay (ELISA)

CellswereinfectedasforPIuptakeassaysandsupernatantswerecollectedat3hpostinfection. IL-1β or TNFwasmeasuredusingthehuma nTNF -α ELISA kit orthehumanIL -1betaELISAkit (ThermoFischer Scientific) following the manufacturer's guidelines. Absorbance was measured using a FLUOstar Omega plate reader (BMG Labtech) at 450 nm, and absorbance at 540 nm was subtracted for well correction.

2.4.6 Sample preparation for SDS-PAGE and immunoblotting

30 min prior to treatment/infection THP -1 cells were washed three times with non -supplemented RMPI,andmediawasreplacedwithserum -freeOptiMEMsupplementedwith1mMsodiumpyruvate, in which subsequent procedures were completed. For detection of secreted proteins, supernatants werecollectedandproteinswereprecipitate dinacetone [1:5 (v/v)] at -20°Covernight,followedby centrifugation at 15,000 × *g* for 15 min. Pellets were air -dried and re -suspended in 2X SDS loading

buffer (4% SDS, 20% Glycerol, 120 mM Tris pH 6.8, bromophenol blue). Cell lysates were prepared in ice-cold RIPA buffer (60 mM Tris pH 8.0, 150 mM NaCl, 1% NP-40, 0.5% sodium-deoxycholate, 1 mM EDTA, 5% β-mercaptoethanol; Sigma) supplemented with Protease inhibitor (Pierce protease inhibitor mini tablets, EDTA-free, ThermoScientific), and 1 mM phenylmethylsulfonyl fluoride (PMSF) and resuspended in 1X SDS loading buffer. Supernatant and lysate samples were vortexed and boiled for 10-15 min and centrifuged. Proteins were separated by SDS polyacrylamide gel electrophoresis (SDS-PAGE) and transferred onto 0.2 µm PVDF membranes (GE Healthcare) by semi-dry transfer (BioRad TransBlot) at 25 V for 30 min. Membranes were blocked in 10% milk in PBS-T before incubation with primary and secondary antibodies as listed in Table 2.7. Membranes were imaged using ECL Prime western blotting detection reagent (GE Healthcare) with a BioRad ChemiDoc XRS+.

2.5 Bacterial protein expression analysis

Bacteria were grown under desired conditions in liquid culture and the OD_{600} was recorded. 1 mL of culture was collected by centrifugation and re-suspended in appropriate amount of 2X SDS loading buffer (1M Tris pH 6.8, 2% SDS, 20% glycerol, 5% β-mercaptoethanol, bromophenol blue), i.e. 100 µL per 1 of OD_{600} unit. Samples were processed, separated by SDS-PAGE and transferred to PVDF membranes as above, before membranes were incubated in 5% milk followed by primary antibody (Table 2.7) in 5% milk at 4 °C overnight. Membranes were imaged as above.

2.6 Transcriptome analysis

2.6.1 RNA extraction

Bacteria were cultured overnight in LB or LB supplemented with 3% (w/v) ox bile, before being diluted 1:33 and grown to late exponential phase. Approximately 6 x 10^8 bacteria in duplicate for each strain for RNAseq were treated with RNAprotect reagent (Qiagen) and digested with 15 mg/mL lysozyme (Sigma) and 2 mg/mL proteinase K (Qiagen) for 20 min according to manufacturer's instructions. RNA extraction was performed using the RNeasy Mini Kit (Qiagen) following the manufacturer's guidelines.

2.6.2 RNA sequencing (RNA-Seq) and data analysis

At least 40 µg of RNA from each strain was treated with DNase (Promega) as per the manufacturer's instructions, excepting a longer sample incubation at 37 °C for 1 h, before adding an additional 1 µl of DNase and incubating for a further of 1 h. RNasIN (Promega) was added for the duration of incubation to maintain the integrity of RNA. Duplicates were pooled and RNA-Seq was performed over three biological replicates. Depletion of rRNA was performed using Ribo-zero (Illumina) and RNA-Seq was

performed in Wellcome Sanger Institute by D. Pickard. mRNA libraries were multiplexed and prepared following the Illumina TruSeq protocol before sequencing via paired-end methodology on the Illumina HiSeq platform. Each lane of Illumina sequence was assessed for quality on the basis of adapter contamination, average base read quality, and any unusual G-C bias using FastQC. Quality control was performed for each of the sequences (sense and antisense of each sample) using the interactive version of FastQC (Andrews, 2010), see Figure Appendix.*1*. Quality checks were conducted for adapter contamination, average base read quality, GC distribution, and sequence content. All sequences passed the quality control giving a median Phred score > 32. Investigation of differential expression was performed using the Rockhopper tool (McClure ***et al.***, 2013) with default settings and by aligning all sequences to the *S*. Paratyphi A ATCC 9150 (NC_006511) genome. When indicated, *S*. Typhi Ty2 samples were aligned to *S*. Typhi Ty2 (NC_004631). The expression value in Bile of each strain was divided by the expression value in LB of each strain and converted to $\log_2$ in order to give the $\log_2$ fold change ($\log_2$FC).

2.6.3 Real Time-quantitative PCR (RT-qPCR)

RNA was extracted from 6 x 10^8 bacteria for each strain as described above. 2 µg of RNA was treated with DNase (Promega) as per the manufacturer's instructions, with prolonged incubation time of 1 h.

Table 2.7 **Western blot antibodies used in this study**

Antibody		Source/Identifier
SipA	Rabbit anti-SipA (*Salmonella*)	V Koronakis Lab (Johnson ***et al.***, 2017)
SipC	Rabbit anti-SipC (*Salmonella*)	V Koronakis Lab (Johnson ***et al.***, 2017)
SipD	Rabbit anti-SipD (*Salmonella*)	V Koronakis Lab (Johnson ***et al.***, 2017)
DnaK	Mouse anti-DnaK (E.coli) mAb (8E2/2)	Enzo, ADI-SPA-880-D RRID:AB_10619012
Caspase-1	Mouse anti-Caspase-1 (p20) (human) mAb (Bally-1)	AdipoGen, AG-20B-0048 RRID:AB_2490257
Caspase-4	Mouse anti-human caspase-4 (4B9)	Santa Cruz Biotechnology, sc-56056, RRID:AB_781828
IL-18	Anti-IL-18 (Human) pAb	MBL International, PM014 RRID:AB_592017
NAIP	Mouse anti-human NAIP	R&D Systems, MAB829
GSDMD	Mouse Anti-Human GSDMDC1 Monoclonal Antibody, Unconjugated, Clone 64-Y	Santa Cruz Biotechnology, sc-81868, RRID:AB_2263768
GAPDH	Rabbit anti-GAPDH	Abcam, ab9485
ASC	anti-Asc pAb (AL177) antibody	Adipogen, AG-25B-0006, RRID:AB_2490440
Secondary anti-mouse	Peroxidase AffiniPure Goat Anti-Mouse IgG	Jackson Immunoresearch, 115-035-008 RRID: AB_2313585
Secondary anti-rabbit	Peroxidase AffiniPure Goat Anti-Rabbit IgG	Jackson Immunoresearch, 111-035-008 RRID: AB_2337937

17.125 µL of DNase-treated sample was incubated with 2 µL random primers (Promega) at 75 °C for 5 min to melt secondary RNA structures and immediately transferred to ice to prevent secondary structures from reforming. Reverse transcription was then performed with M-MLV reverse transcriptase (Promega) according to the manufacturer's instructions, followed by second strand synthesis with further incubation at 72 °C for 10 min. RT-qPCR was then performed using the PowerUp master mix (Applied Biosystems) on the Applied Biosystems StepOnePlus system using 20 ng of cDNA and forward and reverse primers (Table 2.3) at a final concentration of 0.2 µM. As negative controls, samples without reverse transcription were used. For bile studies, *ftsZ* was used as the reference gene as it has been shown not to be affected by bile (Johnson *et al.*, 2018). For *fepE* expression comparison across strains, the conserved *16S* rRNA gene was used as the housekeeping gene. qPCR was performed in duplicate for at least three biological repeats as indicated. Primers designed in this study were tested for their efficiency on a range of cDNA concentrations and determining their efficiency using the qPCR efficiency calculator of ThermoFisher.

2.7 Crude LPS preparation and silver staining

1.5 mL of overnight bacterial culture was centrifuged at 10,000 × g and resuspended in 100 µL 1X SDS loading buffer, before boiling at 100 °C for 5 min. Proteinase K (Qiagen) was added at 1 mg/mL and samples were incubated at 60 °C for 2 h, prior to the addition of 5% β-mercaptoethanol and further incubation for 5 min at 100 °C. Acrylamide gels loaded with crude LPS samples were fixed in 10% acetic acid/30% ethanol overnight. Gels were handled at room temperature and incubations were performed with slow agitation. Gels were oxidised in oxidative solution (10% acetic acid, 30% ethanol, 1% periodic acid) for 10 min and washed three times for 15 min in water. Gels were stained for 30 min in silver stain solution (0.2 mg/mL silver nitrate) and briefly rinsed in water. Developer solution (10% acetic acid, 30% ethanol, 0.02% formaldehyde) was applied before stopping the reaction with 1% acetic acid.

2.8 SPI-1 secretion assay

Bacteria were grown under SPI-1 inducing conditions in 50 mL growth media in the presence or absence of 3% bile. A SPI-1 secretion assay was performed as previously described (Kaniga *et al.*, 1995). Briefly, 1 mL of culture was pelleted by centrifugation for 1 min and resuspended in an appropriate amount of 2X SDS buffer as described above. The remaining culture was centrifuged at 4000 × *g* for 20 min at 4 °C and filtered through a 0.22 µm filter. Proteins in 5 mL of supernatant were then precipitated overnight in 10% trichloroacetic acid (TCA, Sigma) at 4 °C. Precipitated proteins were collected by centrifugation at 15,000 × *g* for 15 min and washed twice in 100% acetone at 4 °C, before air drying

and resuspension in the same volume of 2X SDS buffer as the respective pellet fractions. Both supernatant and pellet samples were boiled at 100 °C for at least 10 min, before western blotting as described above; Antibodies used are listed in Table 2.7.

2.9 β-lactamase Translocation assays

HeLa cells were infected as described above. A group of blank (medium-only) and a group of uninfected controls were included. The plate was centrifuged at 600 × *g* for 5 min and bacterial invasion was allowed for 1 h at 37 °C/5% (v/v) CO_2. The following steps were performed in the dark. Media were removed and 100 µL of 3 mM probenecid solution (Sigma)-20 mM HEPES (Sigma) in HBSS pH 7.3 (Gibco) (probenecid-HEPES-HBSS) was added. TEM-1 substrate (CCF2-AM-LiveBLAzer-FRET B/G loading kit, Invitrogen) was added and cells were incubated at RT for 3 h post infection. Cells were washed and left with 100 µL probenecid-HEPES-HBSS. Fluorescence was measured with a FLUOstar Optima plate reader (BMG Labtech), set at an excitation wavelength of 410 nm; emission was recorded at 450 nm (blue) and 520 nm (green). Blanked average green and blue backgrounds calculated were subtracted from respective emissions of all samples giving the net green or blue signal. Blue to green ratio was calculated for each sample and divided by the average of the same ratio for the uninfected controls to obtain the response ratio.

2.10 Bile tolerance assays

Bacteria were grown in LB overnight as previously described and their OD_{600} was measured. Cultures were normalised to the lowest value and 15 µL were added in 1.5 mL bile solution of varied concentration as stated. Bacterial growth was allowed for 16 h, before recording their growth by OD_{600} readings and CFU enumeration by serially diluting and plating the bile cultures.

2.11 Motility assays

Motility was assessed by inoculating a single colony of bacterial strains grown in standard LB agar plates onto 0.3% Bacto Difco Agar (Scientific Laboratory Supplies) with or without 1% (w/v) ox bile, and incubated at 37 °C for the indicated duration. A lower percentage of bile was used, as higher concentrations interfered with agar setting. Motility was assessed by measuring the diameter of swimming.

2.12 Bioinformatics analysis

Bioinformatics analysis tools were used for gene sequence acquisition, primer design and at various stages of the transcriptomic analysis. All gene sequences were obtained from KEGG genes. Gene alignment was performed using Clustal Omega multiple sequencing alignment tool (Madeira et al., 2019). Heat maps were performed with Morpheus heat map design tool (Wenger & Coon, 2013). GO analysis was carried out with Panther GO annotation tool (Mi *et al.*, 2017). PCA analysis was performed in Perseus (Tyanova *et al.*, 2016).

2.13 Statistical analysis

No statistical methods were used to determine sample size. All experiments were repeated independently as indicated in figure legends. Cell death assays, gentamicin protection and chloroquine resistance assays, and ELISAs were performed with at least two technical repeats for each biological repeat and means from independent experiments were analysed. For immunofluorescence analysis, > 100 cells were counted from randomly selected fields, % cells showing events were obtained for each biological repeat and means were compared statistically. When required, data were log-transformed (CFU experiments) or logit-transformed (PI death assays). Normal distribution was determined with the Shapiro-Wilk normality test. Paired two-tailed t-tests, repeated measures one-way or two-way ANOVA were applied to analyse data as indicated in the figure legends. Multiple comparisons were corrected by the Tukey test or the False Discovery Rate (FDR) approach of Benjamini, Krieger and Yekutieli. All statistical analyses were performed using GraphPad Prism 8 (Graphpad Software Inc.).

3

The *Salmonella* Paratyphi A response to bile

Enteric pathogens have evolved mechanisms to respond and tolerate bile in the small intestine (Section 1.8.3; Sistrunk ***et al.***, 2016). *Salmonella* encounters high concentrations of bile in the gallbladder upon systemic dissemination and establishment of chronic infection (Gonzalez-Escobedo & Gunn, 2013a; Gunn, 2000). Typhoidal *Salmonella* colonisation of the gallbladder and survival in bile require efficient tolerance and/or resistance mechanisms towards bile. Therefore, typhoidal *Salmonella* are expected to be able to sense bile to regulate gene expression. While it is well accepted that chronic carriage is important during the infection cycle of typhoidal *Salmonella* (Gal-Mor, 2019; Gonzalez-Escobedo & Gunn, 2013a; Dougan & Baker, 2014), the behaviour of typhoidal *Salmonella* in bile has not been extensively investigated. Our laboratory recently showed that, while *S.* Typhimurium downregulates genes associated with SPI-1 and motility in response to bile (Prouty & Gunn, 2000; Prouty ***et al.***, 2004b; Johnson ***et al.***, 2018; Hernández ***et al.***, 2012), *S.* Typhi upregulates these genes

becoming more virulent by increased host cell invasion (Johnson *et al.*, 2018). The response of *S.* Paratyphi A to bile remains unknown. While it is speculated that it may be highly similar to that of *S.* Typhi, differences between the two serovars (Table 1.2) may be responsible for distinct responses. Therefore, we aimed to investigate the transcriptomic profile of *S.* Paratyphi A in response to bile, while comparing it to *S.* Typhi as a control. The strains used for this purpose were the sequenced reference *S.* Paratyphi A ATCC 9150 (henceforth referred to as *S.* Paratyphi A 9150) and the clinical *S.* Paratyphi A isolate ED199 (Dolecek *et al.*, 2008). *S.* Typhi Ty2 was used as a control (Johnson *et al.*, 2018). The specific objectives thus were to:

- Establish a HeLa infection model for *S.* Paratyphi A which would allow to next
- Examine the effect of bile on SPI-1 activity in *S.* Paratyphi A;
- Identify bile-mediated changes in the *S.* Paratyphi A transcriptome;
- Determine regulation of genes involved in bile tolerance;
- Determine the effect of bile on virulence genes;
- Examine potentially *S.* Paratyphi A-specific responses.

3.1 *S.* Paratyphi A invades HeLa cells in a SPI-1-dependent manner

The first aim was to establish a HeLa infection model for *S.* Paratyphi A in our lab. *S.* Paratyphi A induces SPI-1 expression during both aerobic and microaerobic conditions (Elhadad *et al.*, 2016). Aerobic conditions are created by agitation, where bacteria are grown overnight and then sub-cultured to late exponential phase. Microaerobic conditions involve growth in static cultures for 16 h, after which bacteria reach stationary phase. *S.* Paratyphi A has been shown to be more invasive during microaerobic conditions (Elhadad *et al.*, 2016). However, bacterial growth is compromised in microaerobic conditions in the presence of bile (King, Ferenci & Szabo, 2003 and R. Johnson, unpublished data). Alternatively, bacterial aggregates may form in static conditions, as has been observed with *Shigella* (Nickerson *et al.*, 2017), either because of the longer incubation time or the lack of agitation allowing bacteria to aggregate more easily. Therefore, to exclude any growth defects and/or variation in downstream analyses, *S.* Paratyphi A 9150 or ED199 were grown in aerobic conditions overnight and sub-cultured. To test when SPI-1 was expressed during these conditions, bacterial pellets were collected at various readings of OD_{600} and bacterial pellets were probed for the SPI-1 T3SS protein SipD. SipD is detectable at an OD_{600} of 1.4, and no further increase in SipD

abundance is observed after OD_{600} of 2.0 (Figure 3.1A). Therefore, both *S.* Paratyphi A strains express SPI-1 at detectable levels at late exponential phase (OD_{600} of 1.7-2.0, Figure 3.1A), similarly to *S.* Typhi (Johnson ***et al.***, 2017, 2018) and *S.* Typhimurium (Kröger ***et al.***, 2013).

To further test SPI-1 activity during anaerobic growth, the ability of *S.* Paratyphi A to invade epithelial cells was next determined. HeLa cells were infected with *S.* Paratyphi A 9150 grown to late exponential phase in aerobic conditions, while *S.* Typhi Ty2 was used as a control. Bacterial invasion was assessed following a gentamicin protection assays by CFU enumeration at 2 h post infection. Similar to *S.* Typhi Ty2, *S.* Paratyphi A 9150 invade HeLa cells in a SPI-1-dependent manner, as a Δ*invA* mutant strain lacking a functional SPI-1 T3SS, failed to invade HeLa cells in these settings (Figure 3.1B), in line with a previous report (Elhadad ***et al.***, 2016). Interestingly, *S.* Paratyphi A 9150 WT invades HeLa cells at significantly lower levels than *S.* Typhi Ty2 WT (Figure 3.1B), suggesting that *S.* Paratyphi A shows lower SPI-1 activity than *S.* Typhi when grown under these conditions.

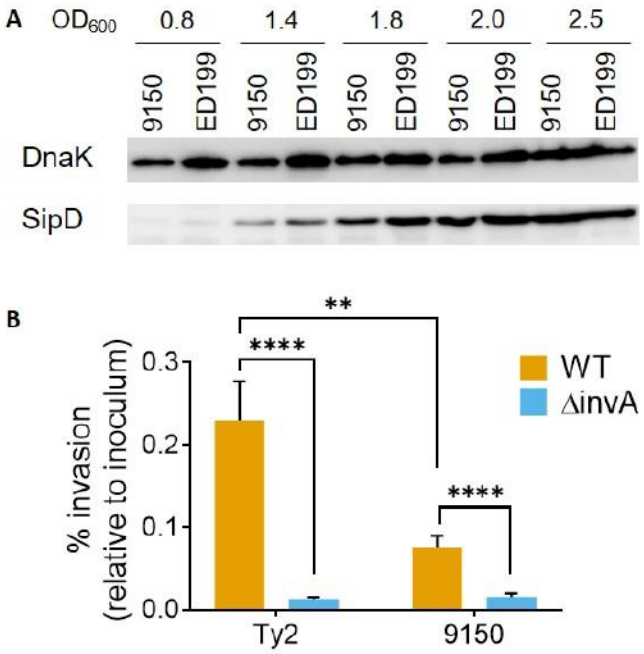


Figure 3.1 **The SPI-1 T3SS of *S.* Paratyphi A is active during growth in aerobic conditions to late exponential phase.**

(A) *S.* Paratyphi A 9150 or ED199 were sub-cultured and bacterial pellet samples were collected at various growth stages from mid to late exponential phase. SPI-1 expression was assessed by immunoblotting for the SPI-1 T3SS protein SipD. DnaK was used as a loading control. Image representative of two independent repeats. **(B)** HeLa cells were infected with *S.* Typhi Ty2 and *S.* Paratyphi A 9150 WT and Δ*invA* mutants (MOI 80-100) and invasion efficiency was assessed at 2 h post infection by gentamicin protection assays. Bars show means ± SEM from five independent repeats and were analysed by two-way ANOVA. **, $p < 0.01$; ****, $p < 0.0001$

3.2 *S.* Paratyphi A becomes more invasive in epithelial cells following growth in bile

S. Typhimurium becomes less invasive into host epithelial cells following exposure to bile, while *S.* Typhi becomes more invasive (Johnson *et al.*, 2018; Prouty & Gunn, 2000). In order to investigate whether the latter is shared between typhoidal *Salmonella*, the invasiveness of *S.* Paratyphi A following exposure to bile was tested. First, the effect of bile on *S.* Paratyphi A growth was assessed to eliminate any variation due to a possible growth defect. *S.* Paratyphi A 9150 or ED199 were grown in standard LB media with or without the addition of 3% ox bile and their growth was assessed by monitoring OD_{600} over time. This concentration more closely reflects bile concentrations encountered in the small intestine than in the gallbladder, but it was chosen for this analysis to aid comparisons with the published bile-induced transcriptome of *S.* Typhi and because it has been previously shown not to affect growth of *S.* Typhi and *S.* Typhimurium (Johnson *et al.*, 2018). Importantly, 3% bile has been shown to influence both the *S.* Typhi and *S.* Typhimurium transcriptome (Johnson *et al.*, 2018; Prouty & Gunn, 2000; Prouty *et al.*, 2004a).

The presence of 3% bile in growth media does not affect growth of *S.* Paratyphi A 9150 (Figure 3.2A) or ED199 (Figure 3.2B), as determined by OD_{600}. To independently verify that bile does not hinder *S.* Paratyphi A growth in the conditions that were used in further experiments (i.e. growth to late exponential phase), *S.* Paratyphi A was grown in the presence or absence of 3% bile and CFUs were enumerated. To determine whether this phenomenon is consistent across *S.* Paratyphi A strains, five more clinical isolates were included in the analysis. The clinical isolates tested were *S.* Paratyphi A ED199, 02TY129, 02TY221, 02TY224, or ED293, all tested for the O2 antigen by slide agglutination and were isolated from adult patients with acute typhoid between 2006 and 2014 in Nepal (Arjyal *et al.*, 2016; Dolecek *et al.*, 2008) (Table 2.2). *S.* Typhi Ty2 and *S.* Typhimurium were used as controls (Johnson *et al.*, 2018). Consistent with the *S.* Paratyphi A 9150 and ED199 growth curves (Figure 3.2A-B), bile did not influence the growth of any *Salmonella* strain tested, with all strains reaching similar CFU/mL in the presence or absence of bile (Figure 3.2C) when grown to late exponential phase in aerobic conditions. These results suggest that *S.* Paratyphi A can grow equally well in media with or without bile.

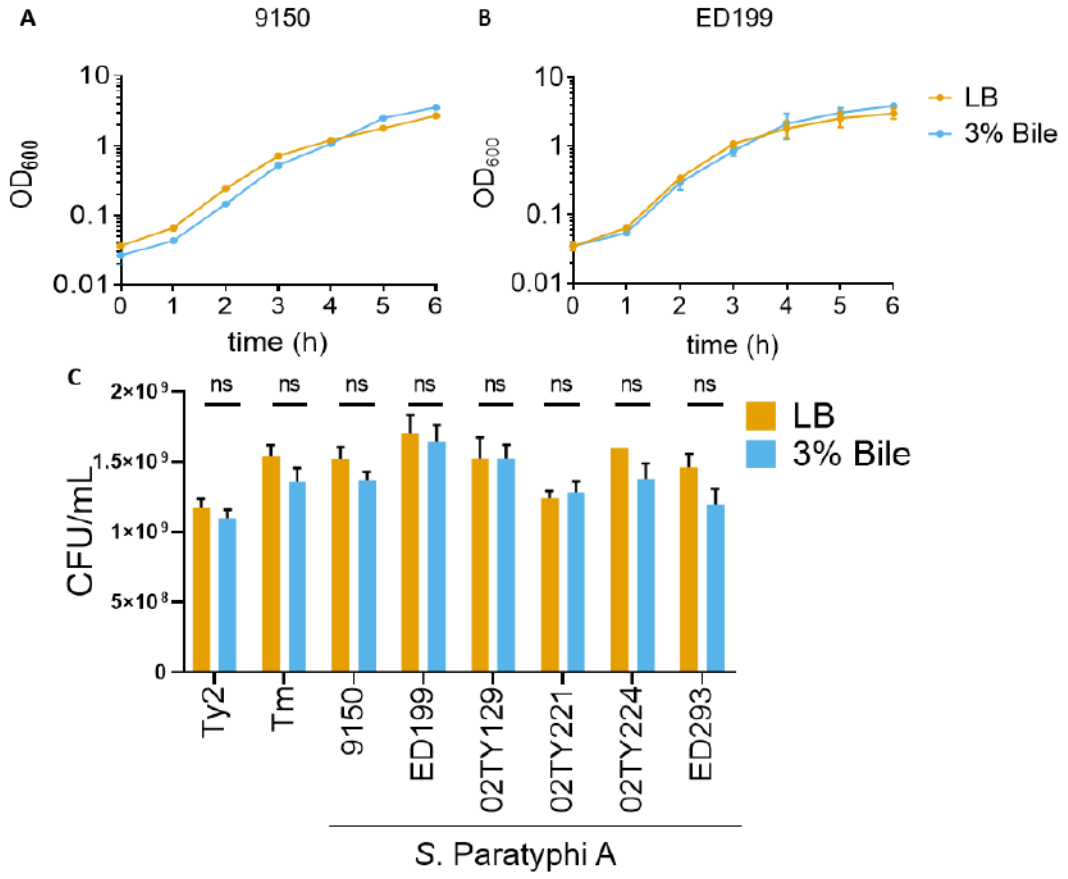


Figure 3.2 **The presence of 3% bile in the growth media does not affect *S.* Paratyphi A growth.**

(A) *S.* Paratyphi A 9150 (9150) or **(B)** ED199 (ED199) were grown in the absence (LB) or presence (3% Bile) of 3% ox bile and their growth was assessed by measuring the OD_{600} over time. **(C)** CFUs were enumerated in cultured bacteria grown aerobically to late exponential phase in the presence or absence of bile. Bars show means ± SEM from (A) three, (B) two, or (C) five independent repeats. Statistical analysis by two-way ANOVA followed by correction for multiple comparisons. ns, not significant.

Next, the effect of bile on *S.* Paratyphi A SPI-1 activity was determined. Because the impact of bile on *S.* Typhimurium invasiveness has long been known (Johnson *et al.*, 2018; Prouty & Gunn, 2000), WT *S.* Typhimurium was used as a control in addition to *S.* Typhi Ty2. In line with previous reports (Prouty & Gunn, 2000; Prouty *et al.*, 2004b; Johnson *et al.*, 2018), *S.* Typhimurium invasiveness was found to be over 60% lower following exposure to bile (Figure 3.3A). Conversely, but as expected (Johnson *et al.*, 2018), invasion of *S.* Typhi Ty2 was higher following growth in bile compared to LB (Figure 3.3A). Similar to *S.* Typhi Ty2, *S.* Paratyphi A 9150 was significantly more invasive in HeLa cells after exposure to bile (Figure 3.3A). Bile resulted in a > 1.6-fold increase in *S.* Paratyphi A 9150 invasion as compared to the > 3.3-fold increase in *S.* Typhi Ty2 invasion (Figure 3.3A). Both *S.* Typhi and *S.* Paratyphi A 9150 Δ*invA* deletion mutants invaded HeLa cells equally in the presence and absence of bile, suggesting that the increase in invasiveness was SPI-1-dependent (Figure 3.3A). The increased

invasiveness in response to bile points to a typhoidal serovar-specific response to bile, as opposed to NTS.

The SPI-1-dependent increase in invasiveness in bile suggested that SPI-1 is upregulated after exposure to bile. Also, previous research has confirmed that expression of SPI-1 T3SS proteins is upregulated in *S.* Typhi in response to bile (Johnson ***et al.***, 2018). Therefore, induction of SPI-1 expression was verified by blotting for SPI-1 proteins in bacterial whole lysates. Indeed, *S.* Paratyphi A 9150 expressed both the SPI-1 T3SS structural (SipD, SipC) and effector (SipA) proteins at higher levels in the presence to 3% bile as opposed to LB alone, like *S.* Typhi Ty2 (Figure 3.3B). The difference in SPI-

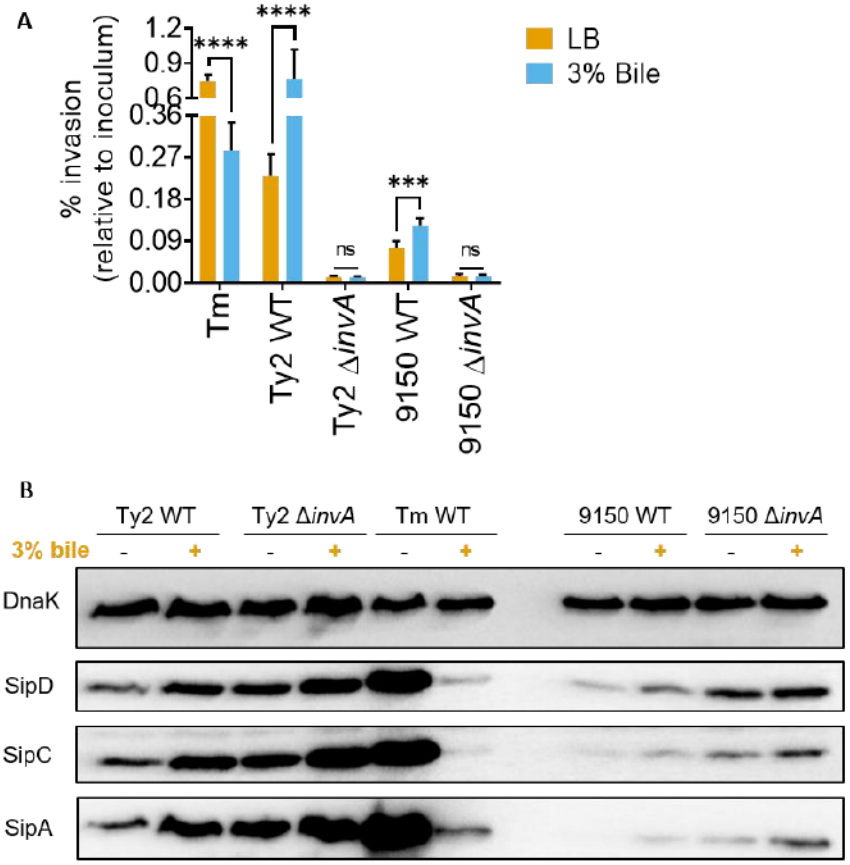


Figure 3.3 **Exposure to bile renders *S.* Paratyphi A 9150 more invasive to HeLa cells in a SPI-1-dependent manner.**

(A) S. Typhimurium (Tm), S. Typhi Ty2 (Ty2) or S. Paratyphi A 9150 (9150) were grown to late exponential phase in the presence or absence of 3% bile and HeLa cells were infected (MOI 100). Intracellular bacteria were quantified by CFU enumeration at 2 h post infection by gentamicin protection assays. **(B)** SPI-1 T3SS protein expression was tested by Western Blotting in bacterial pellets form bacteria grown to late exponential phase in the presence or absence of bile. Immunoblot representative of three independent repeats. Bars show means ± SEM from five independent repeats. Statistical analysis by two-way ANOVA followed by correction for multiple comparisons. ***, $p < 0.001$; ****, $p < 0.0001$; ns, not significant

1 protein expression between LB and bile conditions was greater in the Δ*invA* mutants, as SPI-1 proteins are expected to be retained within bacteria and not secreted. *S.* Typhimurium WT was used as a control to confirm the action of bile, which, as expected, repressed the expression of the SPI-1 proteins tested (Figure 3.3B). *S.* Paratyphi A appears to express SPI-1 T3SS proteins at low levels compared to *S.* Typhi Ty2 and *S.* Typhimurium (Figure 3.3). This may suggest low overall SPI-1 expression, which would be consistent with the low invasiveness of *S.* Paratyphi A WT into HeLa cells (Figure 3.1A and Figure 3.3A). The low abundance of SPI-1 proteins in bacterial lysates may also indicate efficient secretion of SPI-1 proteins from *S.* Paratyphi A, which would then not be detected in whole cell lysates; this is supported by the higher levels of SPI-1 proteins detected in the *S.* Paratyphi A 9150 SPI-1 mutant Δ*invA* in comparison to WT, although SPI-1 protein levels are still less than in *S.* Typhi Ty2 Δ*invA* (Figure 3.3B).

To examine whether the bile-mediated increase in invasion into HeLa cells, as well as the higher SPI-1 protein expression observed in *S.* Paratyphi A 9150, is shared between *S.* Paratyphi A clinical isolates, the invasiveness and SPI-1 expression of multiple strains were tested following exposure to bile. Like *S.* Paratyphi A 9150, all clinical isolates tested herein became significantly more invasive, by > 1.4-fold on average, following growth in LB media supplemented with 3% bile compared to growth in unsupplemented LB media (Figure 3.4A). However, in contrast to observations with *S.* Paratyphi A 9150 and *S.* Typhi Ty2 (Figure 3.3), where increased invasion correlated with increase in SPI-1 expression, all clinical strains showed a decrease in SPI-1 protein expression following growth in bile (Figure 3.4B).

Notably all *S.* Paratyphi A clinical isolates were significantly more invasive than 9150 following growth in standard LB media (Figure 3.4A), which correlated with higher expression of SPI-1 proteins in clinical isolates compared to *S.* Paratyphi A 9150 (Figure 3.4B). These results suggest that clinical strains are more virulent than the reference *S.* Paratyphi A strain in terms of SPI-1 T3SS activity.

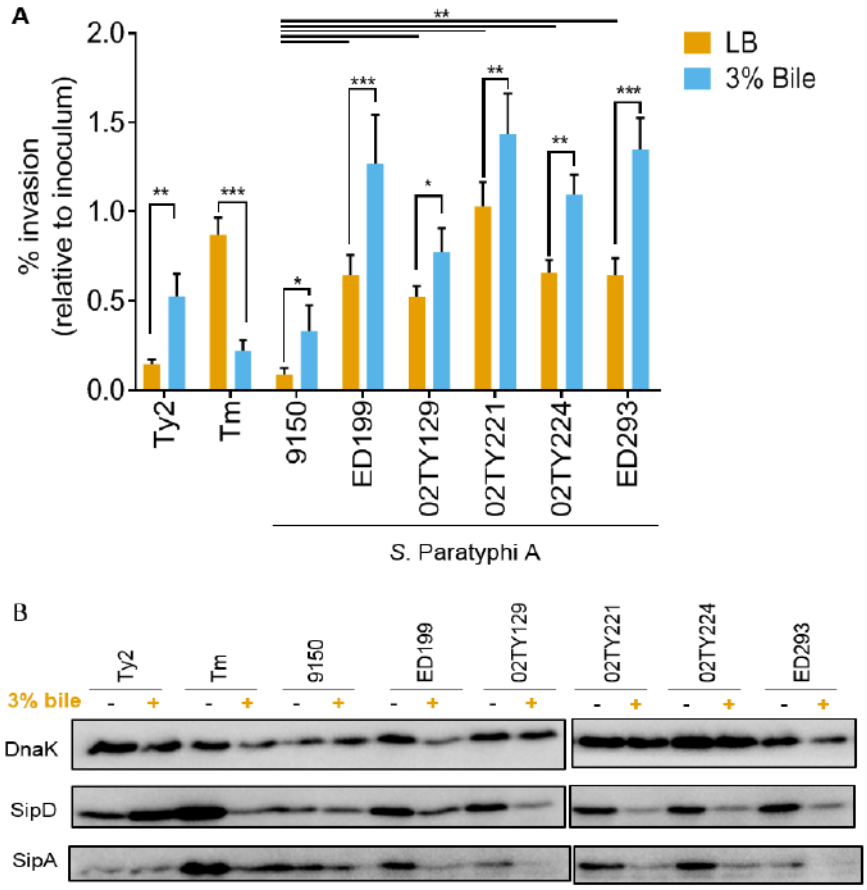


Figure 3.4 **Effect of bile on *S.* Paratyphi A SPI-1 expression and invasion in HeLa cells.**

(A) HeLa cells were infected (MOI 100) with *S.* Paratyphi A strains grown in LB or LB supplemented with 3% bile and internalised CFU were enumerated at 2 hpi by gentamicin protection assays. **(B)** Expression of SPI-1 proteins SipD and SipA was determined in bacterial pellets grown to late exponential phase. Representative image of four independent repeats. Statistical analysis by two-way ANOVA followed by correction for multiple comparisons or repeated-measures one-way ANOVA for LB comparisons. Bars show means ± SEM from seven (Ty2, Tm, 9150) or five (clinical isolates) independent experiments. *, $p < 0.05$; **, $p < 0.01$; ***, $p < 0.001$.

3.3 Overview of changes in *S.* Paratyphi A transcriptome in response to bile

The above results suggested that the behaviour of *S.* Paratyphi A changes in bile and therefore we next aimed to understand the underlying mechanisms. Global changes in gene expression in response to bile in *S.* Paratyphi A were examined by performing RNA-Seq analysis on RNA isolated from the reference *S.* Paratyphi A strain 9150 and the clinical isolate ED199, along with *S.* Typhi Ty2 acting as a control (Johnson ***et al.***, 2018). As previously, strains were grown in the absence (LB) or presence of 3% ox bile (Bile) to late exponential phase. Following sequencing of RNA reads, ribosomal RNA was depleted from all samples, as it is the most abundant RNA species in the total content of RNA and may skew downstream analyses if retained in the sample (both steps conducted by D. Pickard, Sanger

Institute; see also Section 2.6.2), while by removing rRNA a greater proportion of the sequencing library will be mRNA.

RNA-Seq analysis was performed using the sequenced and annotated genome of *S.* Paratyphi A 9150 (McClelland ***et al.***, 2004). Reads from all samples were aligned to this genome to facilitate comparisons using the Rockhopper analysis tool, which is specifically designed for bacterial genomes (McClure ***et al.***, 2013). More than 87% of reads were successfully aligned in all strains, while very low levels of ribosomal (and other species of) RNA (< 2%) were detected, suggesting a good representation of mRNA in all samples (Table 3.1). In agreement with this, > 84% of reads were aligned to protein-coding genes in all samples. On average, 7% of reads were aligned to unannotated regions in all strains (Table 3.1), possibly due to poor annotation of this genome. Unannotated regions represent reads aligning to intergenic regions, sRNAs or, alternatively, may align to open reading frames (ORFs) that have not been identified or characterised yet. These sequences may warrant further investigation and may reveal unknown regulatory regions and/or genomic regions with other unknown functions.

Table 3.1 **Read alignment and RNA types in RNA-Seq sample analysis.**

RNA reads were aligned to the *S.* Paratyphi A 9150 genome using the Rockhopper analysis tool and the output of the fractions of different RNA types are presented here. Three values per strain/condition represent three independent repeats.

Reads	*S.* Typhi Ty2						*S.* Paratyphi A 9150						*S.* Paratyphi A ED199					
	LB			Bile			LB			Bile			LB			Bile		
Total (10^7)	2.2	1.9	1.8	2.2	2.0	1.8	2.3	2.3	2.3	2.1	1.8	2.1	1.8	2.4	1.6	2.0	2.4	1.8
% Success-fully aligned	89	89	88	87	89	87	94	94	94	94	94	95	93	95	94	94	94	95
% Protein-coding genes	87	86	85	85	86	86	87	87	86	87	85	84	86	85	84	86	86	87
% Ribosomal RNA	1	0	1	1	1	1	0	1	1	1	2	1	1	1	2	1	1	1
% Transfer RNA	0	0	0	0	0	0	0	0	0	0	0	0	0	0	0	0	0	0
% Misc. RNA	5	7	8	6	6	6	6	5	6	5	6	10	6	6	6	6	5	6
% Unannotated regions	7	7	7	7	7	7	7	7	7	7	7	7	7	8	7	7	7	7

A heat map of normalised read abundance in individual samples is shown in Figure 3.5A. *S.* Typhi Ty2 LB and Bile samples clustered together, separately from *S.* Paratyphi A samples. *S.* Paratyphi A ED199 samples were also clustered separately, although one bile sample is more closely positioned to LB samples than to other bile samples (Figure 3.5A). *S.* Paratyphi A 9150 samples exhibited a mixed relatedness with other samples, which may indicate variation between repeats. However, analysis of the normalised abundance of all reads in all samples by Principal Component Analysis (PCA) showed clustering of *S.* Typhi and of *S.* Paratyphi A separately, when the first two components explaining 67.1% of the variation were plotted (Figure 3.5B). The LB and Bile samples of each strain broadly clustered separately as well, indicating that there is a clear variation between gene expression in the two conditions. *S.* Paratyphi A samples grouped separately, suggesting a serovar-specific response as well (Figure 3.5A). Combining the results from the heat map and the PCA in Figure 3.5, which cluster data by slightly different methods, it was decided not to exclude any sample from the downstream analysis as this may have led to bias towards identifying 'outliers'. Preparation of all samples was performed in a similar manner and there were no obvious variations or deviations in order to further support exclusion of one or more samples.

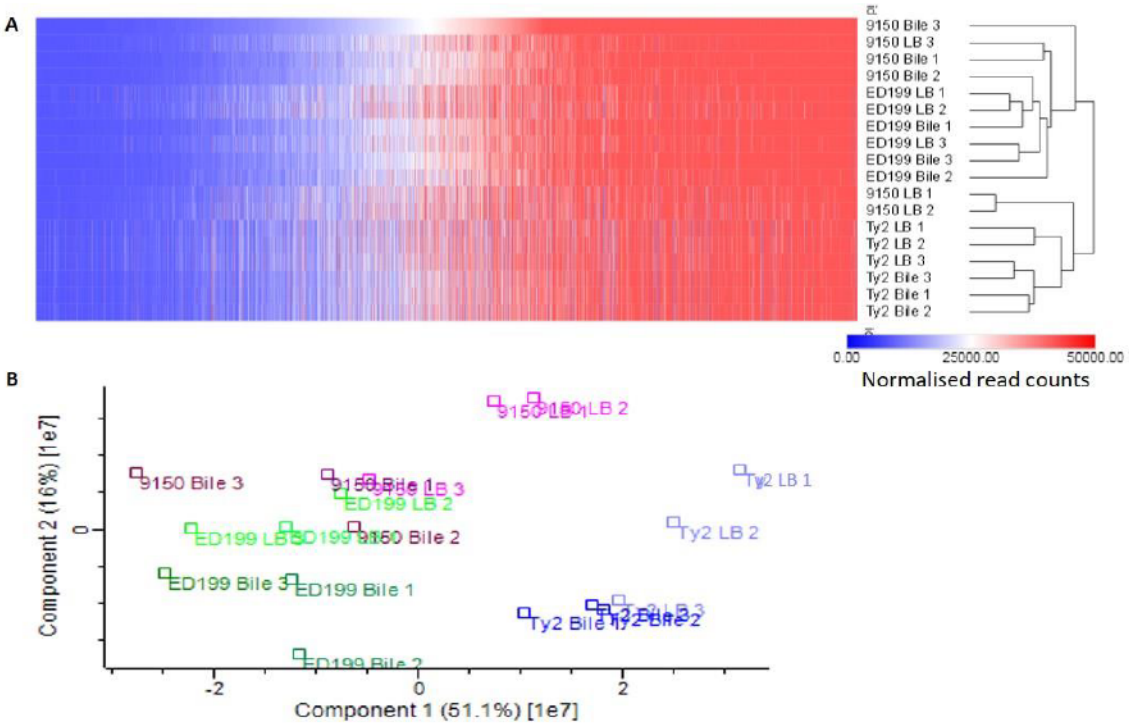


Figure 3.5 **Overview of transcriptomic changes induced by bile.**

(A) Heat map showing normalised read counts in all individual samples and hierarchical clustering of these. **(B)** PCA scatterplot of Ty2, 9150, and ED199 transcriptomes in LB and Bile. Each repeat is shown as a square, and numbers match the repeats across strains. These graphs were produced with the help of C. Mullineaux-Sanders (Frankel group).

Bile-mediated differential gene expression was considered in genes that showed a ≥ 2-fold change and were statistically significant (adjusted *p* value or $q \leq 0.05$). These genes were selected for downstream analysis, unless otherwise stated. The total number of genes shown to be differentially regulated at the transcription level in bile compared to standard growth media were 164 in *S.* Typhi Ty2, 293 in *S.* Paratyphi A 9150 and 243 in ED199 (Table 3.2). These numbers corresponded to approximately 6% of the total number of coding sequences in *S.* Paratyphi A (Table 3.2). This value was lower in *S.* Typhi Ty2 (3.7%), but this was possibly the result of aligning the transcriptome reads to *S.* Paratyphi A 9150 genome. When the *S.* Typhi Ty2 RNA-Seq data were aligned to the sequenced *S.* Typhi Ty2 genome, the total number of differentially regulated genes was 157, which corresponded to 3.4% of total coding sequences of the Ty2 genome. Therefore, aligning the *S.* Typhi Ty2 samples to the *S.* Paratyphi A 9150 genome should not affect downstream analyses.

Table 3.2 **Number of genes differentially regulated in response to bile.**

Percentages of coding sequences correspond to the *S.* Paratyphi A 9150 genome, and in parentheses to S. Typhi Ty2 genome.

Serovar	Strain	Number of genes differentially regulated			Approx. % of coding sequences
		Total	Up	Down	
S. Typhi	**Ty2**	164	103	61	3.7 (3.4)
S. Paratyphi A	**9150**	293	127	166	6.6
	ED199	243	129	114	5.5

3.4 Bile-mediated differential gene regulation in *S.* Typhi and *S.* Paratyphi A

To identify common and discrete responses to bile between *S.* Typhi and *S.* Paratyphi A, the pools of upregulated or downregulated genes from the three strains tested were compared. The two *S.* Paratyphi A strains (9150 and ED199) shared more upregulated or downregulated genes than either did with *S.* Typhi Ty2 (Figure 3.6). The majority of differentially expressed genes in bile in *S.* Typhi were not commonly regulated in either of the two *S.* Paratyphi A strains. Also, *S.* Typhi Ty2 shared a fraction of differentially expressed genes (either upregulated or downregulated) with only one of the two *S.* Paratyphi A strains. Most genes (≈60%) activated by bile were shared by both *S.* Paratyphi A strains, while fewer (33% and 48% for ED199 and 9150, respectively) were commonly downregulated in both strains. These comparisons suggest that bile may exert strain-specific effects on gene regulation, while similarities between typhoidal serovars point towards shared responses.

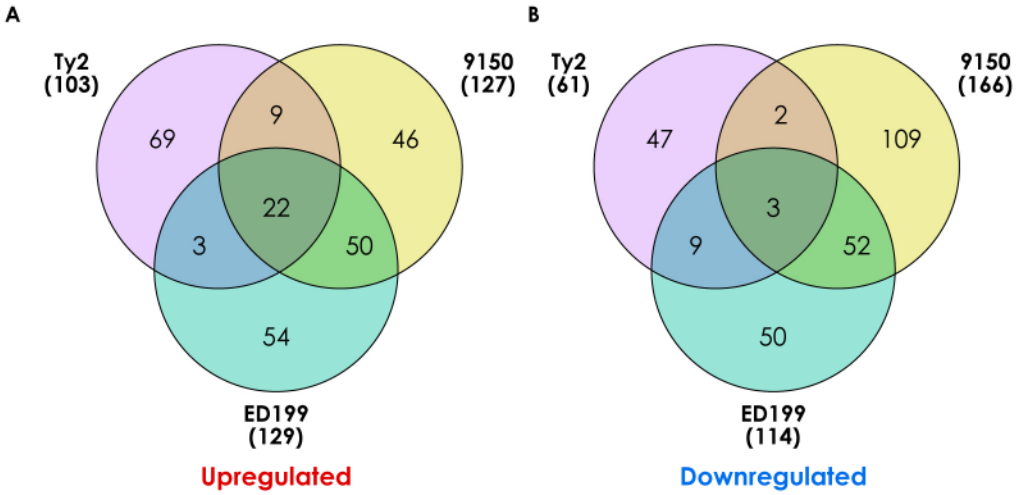


Figure 3.6 **Shared responses to bile between *S.* Typhi and *S.* Paratyphi A.**

Venn diagrams comparing significantly differentially **(A)** upregulated or **(B)** downregulated genes in response to bile across the three strains tested.

Of all significantly upregulated genes by > 2-fold, 22 were shared between all three strains tested, accounting for about 7.5–13.4% of all differentially regulated genes per strain (Figure 3.6A). The overlap in downregulated genes in all three strains was small; only 3 downregulated genes were shared between *S.* Typhi Ty2, *S.* Paratyphi A 9150 and ED199, accounting for less than 2% of the total differentially regulated genes in each strain in response to bile (Figure 3.6B). These shared changes in gene expression are further discussed in the next sections.

Gene Ontology (GO) enrichment analysis was performed on the pools of differentially regulated genes, in order to gain insights into what biological pathways and functions are affected by exposure to bile in *S.* Paratyphi A. A summary of significantly enriched GO terms are listed in Table 3.3. As expected (Johnson *et al.*, 2018), *S.* Typhi upregulated flagellar-mediated motility and chemotaxis (Table 3.3). Along with flagellar motility-associated genes, Johnson *et al.* (2017) previously showed that SPI-1 T3SS-associated genes were also upregulated, which are important for virulence. Genes associated with SPI-1 did not come up in the analysis herein; however, as it is discussed later, all SPI-1-related genes were upregulated, but possibly due to variation in individual samples (see also Figure 3.5), this effect was shown not to be statistically significant. When grown in bile, *S.* Paratyphi A significantly downregulated various metabolic processes (Table 3.3). Among the pathways downregulated in *S.* Paratyphi A 9150 were genes linked to sulphate metabolism, glyoxylate cycle, and removal of superoxide radicals, and the majority of these pathways were shared with *S.* Paratyphi A ED199 (Table 3.3). Interestingly, genes associated with hydrogen sulphide biosynthetic process, sulphate transport and assimilation, and the tricarboxylic acid cycle (TCA) were found to be activated

by bile in *S.* Typhimurium and *S.* Typhi in the Johnson ***et al.***, (2017) study. Collectively these results suggested that S. Paratyphi A and S. Typhi may be exploiting different metabolic pathways in bile.

3.5 Shared responses to bile between *S.* Typhi and *S.* Paratyphi A

22 genes were significantly upregulated in all three strains by more than 2-fold (Figure 3.6; Table 3.4), which represents a small proportion of the total number of differentially expressed genes in all strains (< 20% of upregulated genes). It is worth noting, however, that the genes shown in Figure 3.6 to be upregulated in *S.* Typhi and only one of the two *S.* Paratyphi A strain, are also upregulated in the other one albeit not significantly.

Table 3.3 **GO enrichment analysis of biological processes differentially expressed in typhoidal *Salmonella* following exposure to bile.**

GO terms significantly enriched in the three strains tested within gene pools upregulated or downregulated are shown. Pathways in colour are to indicate shared responses between indicated strains.

	***S.* Typhi**	***S.* Paratyphi A 9150**	***S.* Paratyphi A ED199**
Upregulated	• Bacterial-type flagellum assembly • Chemotaxis • Bacterial-type flagellum-dependent cell motility		• Haem transport • Cytochrome complex assembly • Anaerobic respiration
Downregulated	• Proton transmembrane transport	• Hydrogen sulphide biosynthetic process • 'de novo' IMP biosynthetic process • Sulphate assimilation • Sulphate reduction • Sulphate transmembrane transport • ATP hydrolysis coupled anion transmembrane transport • Glyoxylate cycle • Arginine catabolic process to succinate • Removal of superoxide radicals • Mo-molybdopterin cofactor biosynthetic process	• Hydrogen sulphide biosynthetic process • 'de novo' IMP biosynthetic process • Sulphate assimilation • Sulphate reduction • Sulphate transmembrane transport • ATP hydrolysis coupled anion transmembrane transport • Glyoxylate cycle • Cysteine biosynthetic process • GMP biosynthetic process

Table 3.4 **Shared upregulated genes in bile between Ty2, 9150, and ED199.**

q < 0.05; FC, fold change; OM, outer membrane; IM, inner membrane

Gene name	Product	ID		Log_2FC			Known function(s)/Notes
		9150	Ty2	Ty2	9150	ED199	
yhcN	hypothetical protein	SPA3228	t3276	4.0211	2.4232	2.7994	Putative OM protein; peroxide/acid stress response protein; DUF1471 domain-containing protein (unknown function) – representatives of this family play roles in cellular processes including stress response, and biofilm formation (Eletsky *et al.*, 2014; Lee *et al.*, 2010)
ynfM	membrane transport protein	SPA1368	t1407	3.0753	2.3496	2.4854	IM transport protein, putative major facilitator transport (MFS) protein, facilitates movement of small solutes across membranes
-	hypothetical protein	SPA3229	t3277	3.0959	2.0809	2.4500	Putative periplasmic protein
glpD	aerobic glycerol-3-phosphate dehydrogenase	SPA3384	t3987	2.6724	3.8718	3.3088	*glp* genes (*glpF*, *glpK*, *glpD*) involved in glycerol utilisation, required for bile tolerance in *Salmonella* (Langridge *et al.*, 2009); involved in persister cell formation and multidrug tolerance of biofilms in *E. coli* (Spoering, Vulić & Lewis, 2006)
-	hypothetical protein	SPA1308	t1475	2.3648	3.1043	1.2912	Acid stress chaperone HdeB; role as acid protective chaperone (Dahl *et al.*, 2015)
ybiJ	hypothetical protein	SPA1930	t2065	2.2352	1.1615	1.5166	Putative periplasmic protein; DUF1471 domain-containing protein (see also entry for yhcN); role in biofilm formation/motility in UPEC (Hancock, Vejborg & Klemm, 2010)
yeiA	dihydropyrimidine dehydrogenase	SPA0664	t0668	1.9069	1.2772	1.6549	Role in swarming motility in *E. coli* (involved in energy production and conversion) (Inoue *et al.*, 2007), pseudogene in Ty2
-	putative transcriptional regulator	SPA2654	t2692	1.7630	4.6049	4.8675	ArsR family transcriptional regulator
glpF	glycerol uptake facilitator protein	SPA3930	t3531	2.1998	3.3142	1.4438	Diffusion of glycerol, see also entry for glpD
-	hypothetical protein	SPA1831	t1967	1.4656	1.6674	1.9038	Small peptide of 35 amino acid long, present in very few *Salmonella* serovars
-	oxidoreductase	SPA0665	t0669	1.8616	2.3116	2.0704	Dihydropyrimidine dehydrogenase (NAD+) subunit PreT; differentially regulated in response to stress (Shah *et al.*, 2013)

marA	multiple antibiotic resistanceprotein/ DNA-binding transcriptional activator	SPA1336	t1440	1.5969	1.8320	1.8689	*marRAB* operonactivatedinresponsetobile; confersantibiotictolerancebyactivatingmultidrug effluxpumps;importantforsurvival inbile (Gunn, 2000;Begley ,Gahan&Hill,2005;Prouty *etal.* , 2004a)
glgS	glycogensynthesis proteinGlgS	SPA3065	t3117	1.6197	1.9696	1.3310	Surfacecompositionregulator;upregulatedin responsetostarvationstressinE.coli ; overexpression resultsin glycogensynthesis (Hengge - Aronis&Fischer,1992)
tdcC	HAAAP family,L -threonine/L -serine permease, anaerobically inducible	SPA3112	t3163	1.5392	3.0063	2.4412	Threoninetransporter, roleinnutrientuptake ; pseudogeneinTy2
marR	multipleantibiotic resistanceprotein/ DNA-binding transcriptional repressor	SPA1335	t1441	1.3479	2.2072	2.0453	(seealsomarAentry) marRencodesarepressorof *marRAB* transcriptionandcontrolstheproduction ofMarAinresponsetoenvironmentalsignals ; directlyinteractswithdeoxycholate (Prouty *etal.* , 2004a)
ygaP	hypotheticalprotein	SPA2655	t2693	1.3702	4.3148	4.5152	Membrane transportprotein ;thiosul phatesul phur transferase
dmsC	anaerobicdimethyl sulphoxidereductase subunitC	SPA1832	t4214	1.2500	1.6046	1.6439	Roleinbacterialsurvivalinanaerobicconditions; detectedasdifferentiallyexpressedin *S.* Paratyphi A *invivo* vs *exvivo* possiblyduetoadaptationofthe macrophageenvironment (Sheikh *etal.* ,2010)
dmsB	anaerobic dimethyl sulphoxidereductase subunitB	SPA1357	t1418	1.2928	1.4099	1.6599	Roleinbacterialsurvivalinanaerobicconditions
tdcB	catabolic threonine dehydratase	SPA3113	t3164	1.6755	3.6990	2.5319	Involvedin L-threonine catabolism
slsA	hypotheticalprotein	SPA3611	t3757	1.0753	2.1594	3.8629	Predicted IM protein; encoded withinSPI -3
apbA	2-dehydropantoate 2-reductase	SPA2289	t2430	1.0199	1.3123	1.2689	Potentialvirulence -associatedgeneinTy;involved inthiaminebiosynthesis
hypC	Putative hydrogenase expression/ formationprotein	SPA2714	t2758	1.0027	1.8776	1.8701	UpregulatedinTminresponsetophysiologicalbile (Antunes *etal.* ,2012)

The shared upregulated genes among *S.* Typhi Ty2, *S.* Paratyphi A 9150 and ED199 include genes involved in transport across the inner or outer membrane, metabolic processes, biofilm formation and stress responses. Genes such as *glp* genes (Langridge *et al.*, 2009) those in the *marRAB* operon (Prouty *et al.*, 2004a) were expected to be upregulated in response to bile (see also Table 3.6). Genes linked to stress responses (e.g. *yhcN*, *glpS*, *SPA1308*) were upregulated in all three strains, in keeping with bile acting as a stress factor enabling the induction of a stress response (Begley, Gahan & Hill, 2005; Hernández *et al.*, 2012; Urdaneta & Casadesús, 2017; Walawalkar, Vaidya & Nayak, 2016). A few genes (*yeiA*, *glpD*, *ybiJ*) with putative roles in biofilm formation and/or motility, which is associated with biofilms, were also included in this list, consistent with the biofilm-inducing capacity of bile in *Salmonella* (Gonzalez-Escobedo & Gunn, 2013a).

Three genes are significantly downregulated in all *S.* Paratyphi A 9150, *S.* Paratyphi A ED199, and *S.* Typhi Ty2 (Table 3.5). All three encode confirmed or putative membrane proteins. Expression of the porin-encoding gene *ompF* showed the greatest reduction in response to bile in all three strains tested (Table 3.5). As listed in Table 3.6 as well, mutation in *ompF* in *E. coli* leads to increased resistance towards bile (Thanassi, Cheng & Nikaido, 1997). The decrease in *ompF* expression in bile in all three strains tested here is consistent with upregulation of *marR* and *marA* in all strains (Table 3.4), which are involved in *ompF* downregulation (Hernández *et al.*, 2012; Villarreal *et al.*, 2014; Prouty *et al.*, 2004a). *marB* of the *marRAB* operon was significantly upregulated in both *S.* Paratyphi A strains; expression in *S.* Typhi was also increased in bile, although not significantly. Less is known about the other two shared downregulated genes in bile (*yajG* and *ygjU*) as shown in Table 3.5.

Table 3.5 **Shared downregulated genes in bile between Ty2, 9150, and ED199**.

$q < 0.05$; FC, fold change; OM, outer membrane

Gene name	Product	ID		Log_2FC			Known function/Notes
		9150	Ty2	Ty2	9150	ED199	
ompF	outer membrane protein F	SPA1799	t1935	-4.640	-6.331	-5.534	Downregulation induced by marRAB; linked to survival in and resistance towards bile; downregulated in response to deoxycholate (Hernández *et al.*, 2012; Villarreal *et al.*, 2014; Prouty *et al.*, 2004a)
yajG	lipoprotein	SPA2277	t2415	-1.083	-1.199	-1.012	Putative OM lipoprotein; associated with oxidative stress response in *S.* Kentucky during chicken infection (Cheng *et al.*, 2015); downregulated in *S.* Typhimurium in bile (Johnson *et al.*, 2018)
ygjU	membrane transport protein	SPA3094	t3145	-1	-1.409	-1.159	Putative dicarboxylate permease; serine/threonine transporter SstT (import of ser/thr, import of Na; symporter); upregulated in *S.* Typhimurium and in *S.* Typhi in bile previously (Johnson *et al.*, 2018)

To identify serovar-specific responses to bile, genes upregulated in *S.* Typhi and downregulated in *S.* Paratyphi A strains and *vice versa* were next compared. No genes were significantly repressed in bile in *S.* Typhi and upregulated in both *S.* Paratyphi A strains, while one gene was significantly upregulated in response to bile in *S.* Typhi and was downregulated in *S.* Paratyphi A. This gene was *aceB*, which encodes a malate synthase A and is one of the enzymes of the glyoxylate bypass of the Krebs cycle. Expression of *aceB* in *S.* Typhi in bile is consistent with the report by Johnson *et al.* (2017), which also showed an upregulation of *aceB* in response to bile in *S.* Typhimurium. This points towards a possible *S.* Paratyphi A-specific response.

Other than *aceB*, *S.* Typhi upregulated *SPA0307* (*t0297*; $\log_2$FC=2.56) and *SPA1728* (*t1798*; $\log_2$FC=2.53), which were significantly downregulated in *S.* Paratyphi A ED199 (*SPA307* $\log_2$FC= -4.17; *SPA1728* $\log_2$FC=-1.15). Both genes showed a slight decrease in expression in *S.* Paratyphi A 9150, although this was not statistically significant. *SPA0307* encodes for *cadA*, a lysine decarboxylase involved in lysine metabolism, while SPA1728 is a hypothetical protein. Similarly, *S.* Paratyphi A 9150 downregulated *SPA1372* ($\log_2$FC=-1.31), also known as *ydgF*, which was upregulated in *S.* Typhi (*t1402*; $\log_2$FC=1.10) and encodes for a hypothetical protein. This gene was also downregulated in *S.* Paratyphi A ED199, although not significantly. There were no genes differentially expressed between the two *S.* Paratyphi A strains (9150 and ED199) significantly by ≥ 2-fold in response to bile.

In the following sections, genes not evidently exhibiting a similar response among all three strains but that are of interest are discussed, such as with regards to virulence or bile tolerance, and whose changes are not necessarily statistically significant or ≥ 2-fold, in order to ensure complete coverage of the transcriptomic changes in these strains and to gain insights into these processes.

3.6 Differential regulation of bile-tolerance and resistance genes

As described in Sections 1.8.2 and 1.8.3, bile has antimicrobial properties to which many bacterial pathogens have developed resistance (Gunn, 2000; Sistrunk *et al.*, 2016; Urdaneta & Casadesús, 2017). Genes known to be involved in bile resistance and tolerance include the *Tol* genes, efflux pumps, porins, and several regulatory genes (Table 3.6). The predicted or known regulation of these genes in response to bile, along with changes observed in their expression in response to bile in *S.* Paratyphi A are shown in Table 3.6 and Figure 3.7A. *S.* Typhi and *S.* Paratyphi A show a highly similar regulation of these genes when grown in bile, in line with their generally conserved role. Based on hierarchical clustering, *S.* Paratyphi A 9150 and ED199 are more similar, possibly due to the similar magnitude in changes of expression. Both typhoidal *Salmonella* serovars regulated all tolerance and resistance-associated genes as expected/predicted (Table 3.6 and Figure 3.7A). Significant increase in the

expression of *acrR*, *marR*, and *marA* in response to bile was observed in all three strains tested (Figure 3.7A). Conversely, as discussed earlier, *ompF* was downregulated in all strains. Also, *tolQ* and *tolR* were significantly downregulated in the two *S.* Paratyphi A strains; the decrease in expression of these genes

Table 3.6 **Genes linked to bile tolerance and/or resistance in *Salmonella*.**

ECA; enterobacterial common antigen; Tm, Typhimurium; Pt, Paratyphi A; Ty, Typhi.

	Gene name	Function/mechanism of resistance/tolerance	Known/predicted regulation in bile	Reference
Tol	*tolQRA tolC*	Efflux pump function Cell envelope Mutants sensitive to bile	No marked change in expression	(Prouty *et al.*, 2002; Langridge *et al.*, 2009)
Efflux pumps	*acrAB*	Efflux pump Mutants sensitive to bile	Upregulation	(Prouty *et al.*, 2004a; Langridge *et al.*, 2009)
	acrR			
	emrA	Efflux pump (present in Tm and Pt, partial presence in Ty) *E. coli acrAemrB* mutant highly sensitive to bile	Upregulation	(Thanassi, Cheng & Nikaido, 1997)
	emrB			
	ermR			
Regulatory genes	*phoPQ*	Two component system Mutants sensitive to bile	No induction/ upregulation, some phoPQ-regulated genes important for virulence	(van Velkinburgh & Gunn, 1999; Langridge *et al.*, 2009)
	marR	Regulatory genes Upregulation in bile particularly by deoxycholate (interacts with marR); Mutants sensitive to bile	Upregulation	(Prouty *et al.*, 2004a)
	marA			
	marB			
	rpoS	General stress response Mutant sensitive to bile	Upregulation	(Begley, Gahan & Hill, 2005)
Porins	*ompF*	*E. coli* mutant more resistant to bile	Downregulation	(Thanassi, Cheng & Nikaido, 1997; Hernández *et al.*, 2012; Villarreal *et al.*, 2014)
	ompC	*E. coli* mutant sensitive to bile	Downregulation	
DNA repair	*dam*	DNA adenine methylase Mutant sensitive to bile	Upregulation?	(Prieto, Ramos-Morales & Casadesús, 2004)
	recA, B, C, D	DNA repair Mutants sensitive to bile	Upregulation?	(Prieto, Ramos-Morales & Casadesús, 2006)
ECA	*wecD*	Biosynthesis and assembly of ECA; Putative protective role against bile salts Mutants sensitive to bile	Upregulation?	(Prouty *et al.*, 2002; Ramos-Morales *et al.*, 2003)
	wecA			

in *S.* Typhi Ty2 was not statistically significant. Remaining genes largely showed insignificant changes in response to bile.

S. Typhi and *S.* Typhimurium have been shown to be inherently resistant to high bile concentrations with a MIC of 12% and 18%, respectively (van Velkinburgh & Gunn, 1999). As shown in Figure 3.2A-B, the growth rate of *S.* Paratyphi A 9150 and ED199 was not affected by the presence of 3% bile in the growth media, like *S.* Typhi and *S.* Typhimurium (Johnson *et al.*, 2018). To further investigate bile tolerance of *S.* Paratyphi A in high concentrations, bacteria were grown for 16 h in a gradient of bile concentrations (5–30%) and growth was assessed relative to LB-grown bacteria by CFU enumeration. *S.* Typhi Ty2 growth was affected at high bile concentrations (15–30%), consistent with

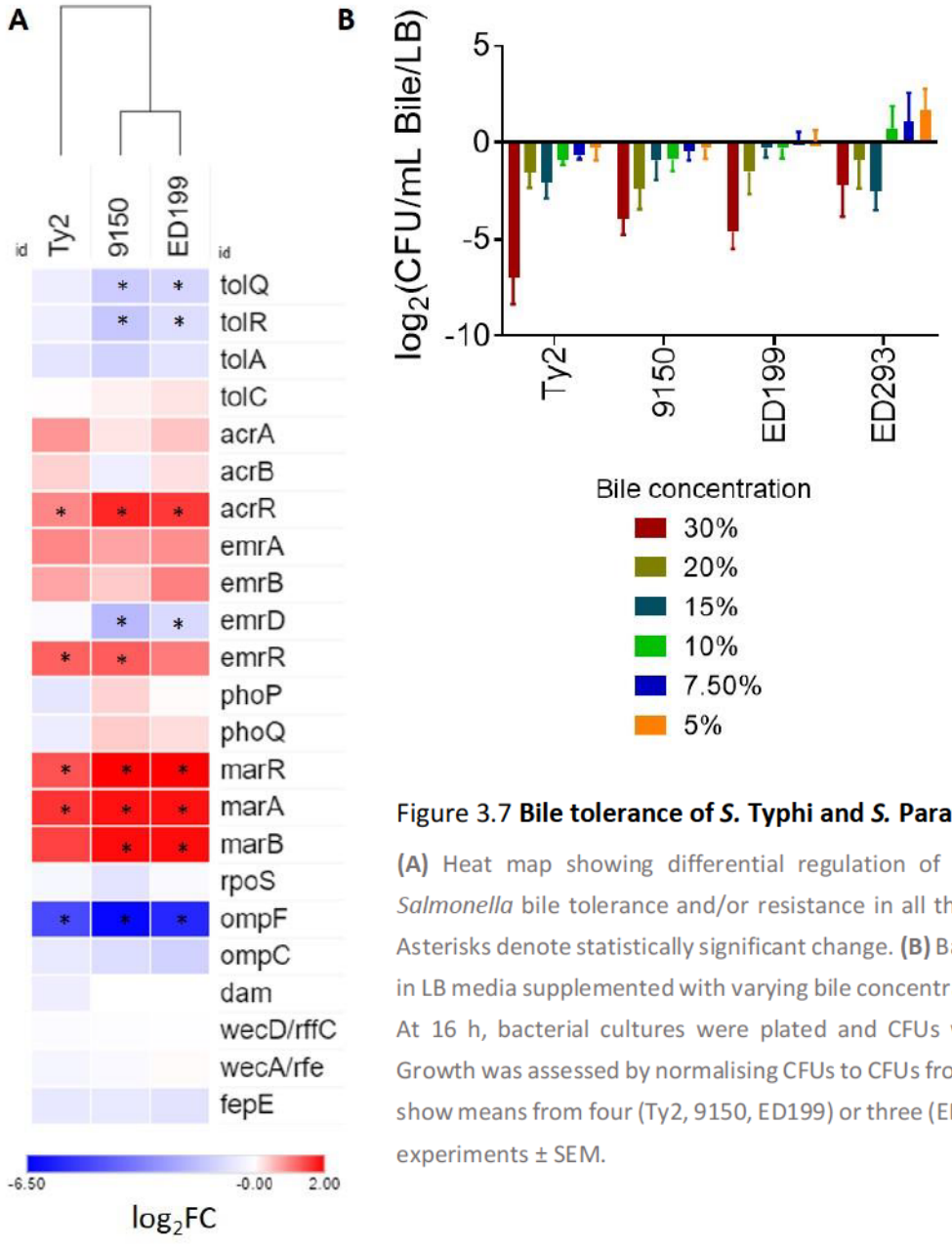


Figure 3.7 **Bile tolerance of *S.* Typhi and *S.* Paratyphi A.**

(A) Heat map showing differential regulation of genes involved in *Salmonella* bile tolerance and/or resistance in all three strains tested. Asterisks denote statistically significant change. **(B)** Bacteria were grown in LB media supplemented with varying bile concentrations as indicated. At 16 h, bacterial cultures were plated and CFUs were enumerated. Growth was assessed by normalising CFUs to CFUs from LB cultures. Bars show means from four (Ty2, 9150, ED199) or three (ED293) independent experiments ± SEM.

its published MIC, and its growth in bile relative to standard LB remains unaffected in 5–7.5% bile (Figure 3.7B). *S.* Paratyphi A 9150 tolerated similar bile concentrations to *S.* Typhi Ty2, although its growth was less limited at high concentrations (Figure 3.7). *S.* Paratyphi ED199 is able to withstand concentrations reaching 15% more readily than *S.* Paratyphi A and *S.* Typhi Ty2 (Figure 3.7B). To test whether the ability of *S.* Paratyphi A to tolerate high bile concentrations is shared with other clinical isolates, *S.* Paratyphi A ED293 was also included in this analysis. This strain tolerated high bile concentrations better than all other strains tested. Its growth was enhanced in bile concentrations ranging 5–10%, while 15–30% bile only mildly affected its growth compared to *S.* Typhi Ty2 and other strains of *S.* Paratyphi A (Figure 3.7B). These results suggested that *S.* Paratyphi A may be more tolerant than *S.* Typhi in high bile concentrations, while clinical isolates exhibit an amplified phenotype of bile tolerance, which has also been observed with an *S.* Typhi clinical isolate compared to Ty2 (Johnson ***et al.***, 2018)

3.7 Effect of exposure to bile on SPI-1 and adhesin expression

It was shown above that exposure to bile results in increased invasiveness by *S.* Paratyphi A. Also, a key difference between *S.* Typhimurium and *S.* Typhi in their response to bile is disparate SPI-1 regulation (Johnson ***et al.***, 2018). Bile-mediated changes in expression of SPI-1-encoded genes and other SPI-1 T3SS-dependent effectors encoded outside the SPI-1 in *S.* Typhi Ty2 and *S.* Paratyphi A 9150 and ED199 are shown in Figure 3.8A. As expected (Johnson ***et al.***, 2018), all SPI-1-associated genes were upregulated in bile in *S.* Typhi Ty2; this change in expression was statistical significant for some of these genes. Similarly, *S.* Paratyphi A 9150 upregulated all SPI-1 associated genes, with a few showing a statistically significant increase (Figure 3.8A). Strikingly, *S.* Paratyphi A ED199 showed an overall decrease in expression of SPI-1-associated genes, with a few exceptions, such as *hilD* and *hilC* which were mildly, although not significantly, upregulated (Figure 3.8A). Hierarchical clustering suggested a closer similarity between *S.* Typhi Ty2 and *S.* Paratyphi A 9150 than between the two *S.* Paratyphi A strains (9150 and ED199).

To validate these findings, the transcription of the SPI-1 regulators *hilA*, *hilC* and *hilD* (Fàbrega & Vila, 2013), as well as *rtsA* which is encoded outside the genomic island (Ellermeier & Slauch, 2003), along with the effectors *sopB* and *sipA* was tested via RT-qPCR. For better comparison, the individual values of $\log_2$ fold change obtained from each repeat in RNA-Seq analysis were plotted separately for these genes (Figure 3.8B). RT-qPCR corroborated results obtained from RNA-Seq analysis regarding all four regulators tested (*hilA*, *hilC*, *hilD*, and *rtsA*). While the genes encoding these proteins were upregulated in both *S.* Typhi Ty2 and *S.* Paratyphi A 9150, RT-qPCR analysis showed a minimal change in expression in *S.* Paratyphi A ED199, but the trend was in line with the RNA-Seq data (Figure 3.8C).

sopB and *sipA* were upregulated in *S.* Typhi Ty2 and *S.* Paratyphi A 9150 as shown by both RNA-Seq and RT-qPCR analysis (Figure 3.8A-B). However, differential expression of *sopB* and *sipA* in *S.* Paratyphi A ED199 in response to bile as shown by RNA-Seq was not corroborated with RT-qPCR (Figure 3.8B). The overall lack of differential expression of SPI-1 regulators between LB and bile growth conditions of *S.* Paratyphi A ED199 may explain the variation seen in expression of SPI-1 T3SS-dependent

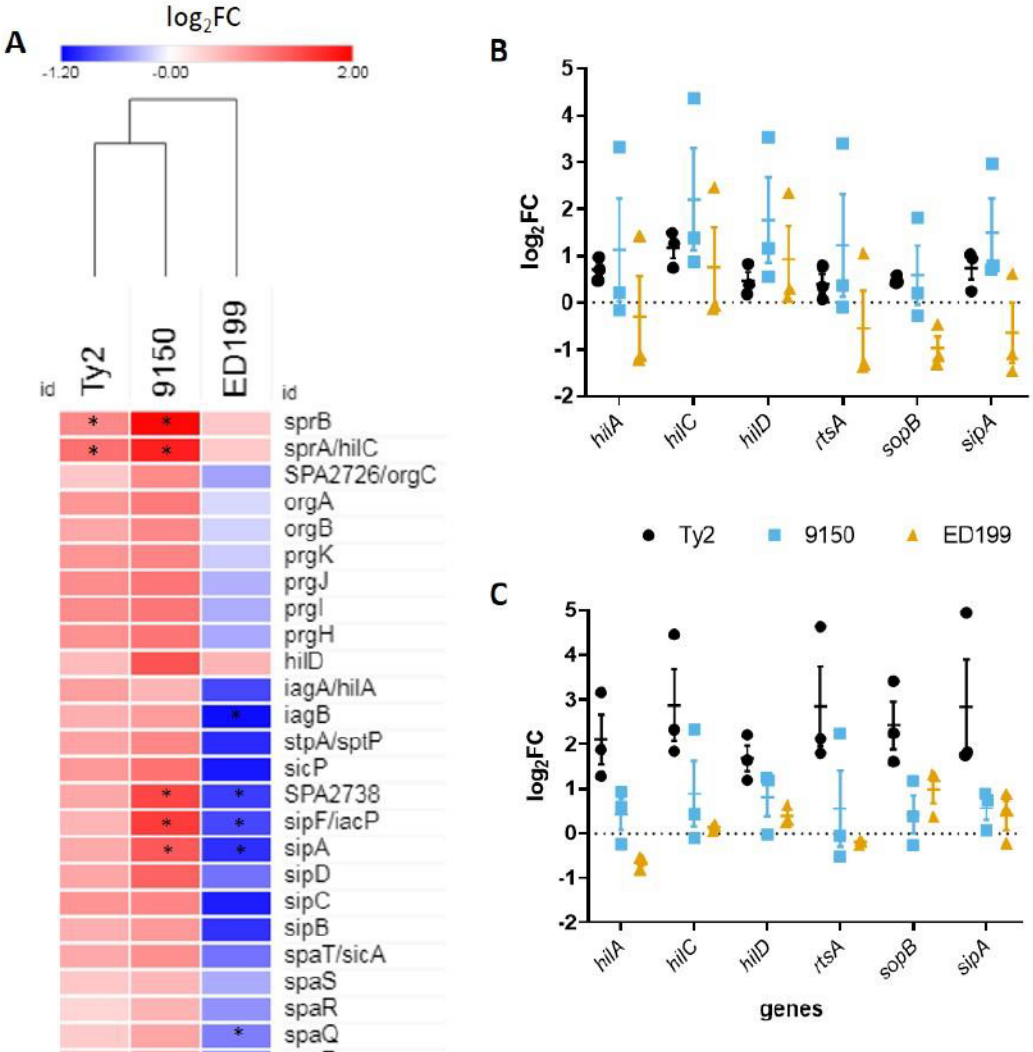


Figure 3.8 **Effect of bile on *S.* Paratyphi SPI-1 expression.**

(A) Heat map showing changes in SPI-1 gene expression in response to bile in Ty2, 9150 and ED199. Asterisks indicate statistically significant changes in gene expression in each strain. **(B)** Individual RNA-Seq-derived $\log_2$ fold change values and **(C)** validation of changes in SPI-1 gene expression following exposure to 3% bile by RT-qPCR. (B) and (C) were performed with different sets of samples.

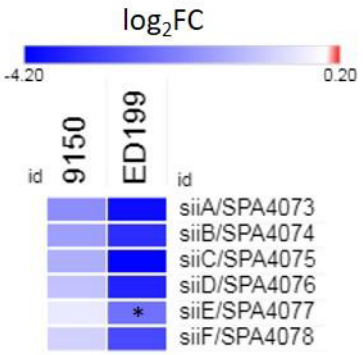


Figure 3.9 **Exposure to bile downregulates expression of SPI-4 in *S.* Paratyphi A.**

Heat map showing log_2 fold change in expression levels of SPI-4 genes in *S.* Paratyphi A 9150 and ED199. Asterisk indicates statistical significance.

effectors. Additionally, *S.* Paratyphi A ED199 is more variable than the reference strains across biological replicates, which may be a result of adaptation of the latter to laboratory conditions and may indicate an overall absence of an effect of bile on SPI-1 regulation in ED199.

Downregulation or small change in expression of SPI-1-associated genes in *S.* Paratyphi A ED199 comes in sharp contrast to the HeLa cell invasion data, but is in line with the SPI-1 protein expression levels (Figure 3.4). It is possible that clinical *S.* Paratyphi A isolates exploit other molecules to promote invasion into host cell upon exposure to bile. An obvious candidate would be adhesins, which facilitate bacterial proximity and adhesion to the host cell, as well as biofilm formation which is important for survival in the gallbladder (Fàbrega & Vila, 2013; Kline *et al.*, 2009; Gonzalez-Escobedo & Gunn, 2013a). A large non-fimbrial T1SS-secreted adhesin, SiiE, which is encoded within SPI-4 is suggested to be important in *in vitro* invasion of *S.* Typhimurium by promoting a close interaction of epithelial cells and thus efficient translocation of SPI-1 proteins (Gerlach *et al.*, 2007; Sabbagh *et al.*, 2010; Gerlach *et al.*, 2008). Also, in *S.* Typhimurium, SprB activates the SPI-4 (Saini & Rao, 2010; Main-Hester *et al.*, 2008); *sprB* was significantly upregulated in *S.* Paratyphi A 9150 (log_2FC=1.94), as well as in *S.* Paratyphi A ED199 although not significantly. However, all SPI-4 genes (*siiA-F/SPA4073-78*) were downregulated in *S.* Paratyphi A 9150 and ED199, where this reduction in expression was statistically significant and more than 5-fold (log_2FC=-2.34) in *SPA4077/siiE* in *S.* Paratyphi A ED199. The SiiE adhesin-associated genes are found as pseudogenes in *S.* Typhi Ty2 (Parkhill *et al.*, 2001; Sabbagh *et al.*, 2010). Furthermore, most fimbrial operon genes did not exhibit differential regulation in response to bile, such as *sef*, *ste*, *stb*, *tcf*, and *sth* and the curli *csg*. *fimA* of the *fim* operon and *stdC* of the *std* operon were significantly downregulated in *S.* Paratyphi A ED199 (Table Appendix.1). All these genes showed no difference in expression following exposure to bile in *S.* Paratyphi A 9150 (Table Appendix.1). Taken together, bile-mediated changes in expression of genes that promote host cell attachment and invasion did not fit a model whereby they would assist in increased invasion compensating for downregulation of SPI-1; however, as the role of adhesins is unknown in most cases, it is impossible to conclude how *S.* Paratyphi A ED199 exploits these changes to modulate host cell

invasion. Another possibility is that regulation of motility-associated gene expression in *S.* Paratyphi A clinical strains allows for increased invasion.

3.8 Effect of bile on *S.* Paratyphi A motility

Following exposure to bile, *S.* Typhimurium downregulates genes associated with flagellar motility, while *S.* Typhi upregulates these genes (Johnson ***et al.***, 2018). The increase in expression of motility-associated genes in *S.* Typhi was observed here as well, where the majority of genes showed a statistically significant increase of more than 2-fold in expression following exposure to bile (Figure 3.10A). Interestingly, genes linked to flagellar motility and chemotaxis were among the genes shown to be significantly upregulated in *S.* Typhi Ty2, but not in *S.* Paratyphi A strains (Figure 3.6). *S.* Paratyphi A 9150 showed a modest upregulation in the majority of genes associated with motility and chemotaxis, although this change in expression was not statistically significant (Figure 3.10A). Surprisingly, *S.* Paratyphi A ED199 showed a small change in expression of most genes, while the majority of genes showed a decrease in expression, with downregulation of ***fliE*** (log_2FC=-1.04) and ***flhE*** (log_2FC=-0.68) being statistically significant. In order to confirm this disparate modulation of gene expression between the three strains tested here, the expression of ***fliE***, which was significantly downregulated in *S.* Paratyphi A ED199, and of ***fliZ***, which was upregulated in all strains, was confirmed by RT-qPCR. Indeed, the trend of the expression of these genes seen with RNA-Seq (Figure 3.10A-B) was corroborated with RT-qPCR (Figure 3.10C). *S.* Paratyphi A 9150 showed more variation in expression of these two genes when investigated both with RNA-Seq and with RT-qPCR, suggesting that bile probably has an insignificant effect on the motility of this strain.

To verify these results, motility was tested in standard motility agar supplemented with 1% bile. A slightly lower concentration was used, as 3% bile concentration interfered with agar setting. Measuring the swimming diameter of *S.* Typhi Ty2, *S.* Paratyphi A 9150 and ED199 in motility agar in the presence or absence of 1% bile confirmed that the impact of bile on motility is in line with the gene expression results. In particular, *S.* Typhi Ty2 became significantly more motile in the presence of bile (Figure 3.10D), while the motility of *S.* Paratyphi A 9150 did not change in the presence of bile (Figure 3.10E), as suggested by the expression data (Figure 3.10B-C). *S.* Paratyphi A ED199 was significantly less motile in bile (Figure 3.10F), in line with the overall downregulation of flagellar genes (Figure 3.10A). Direct comparisons between the motility profiles of these strains cannot be made, due to the different incubation times used for *S.* Typhi (16h), *S.* Paratyphi A 9150 (24 h) and ED199 (8 h), owing to marked strain-to-strain variation in motility in swimming agar. However, *S.* Paratyphi A ED199 is markedly more motile with a swimming diameter of 4.6 cm on average, i.e. greater than double that

of 2 cm of *S.* Paratyphi A 9150 in a third of the time. *S.* Paratyphi A has been previously shown to be more motile than *S.* Typhi, although the strains tested were different that those tested in this project (Elhadad ***et al.***, 2015a). Also, *S.* Paratyphi A clinical isolates may exploit increased motility for survival within the host, which is consistent with data with an outbreak strain from an independent study (Gal-Mor ***et al.***, 2012). However, upon encounter of bile, which may act as an environmental cue, motility

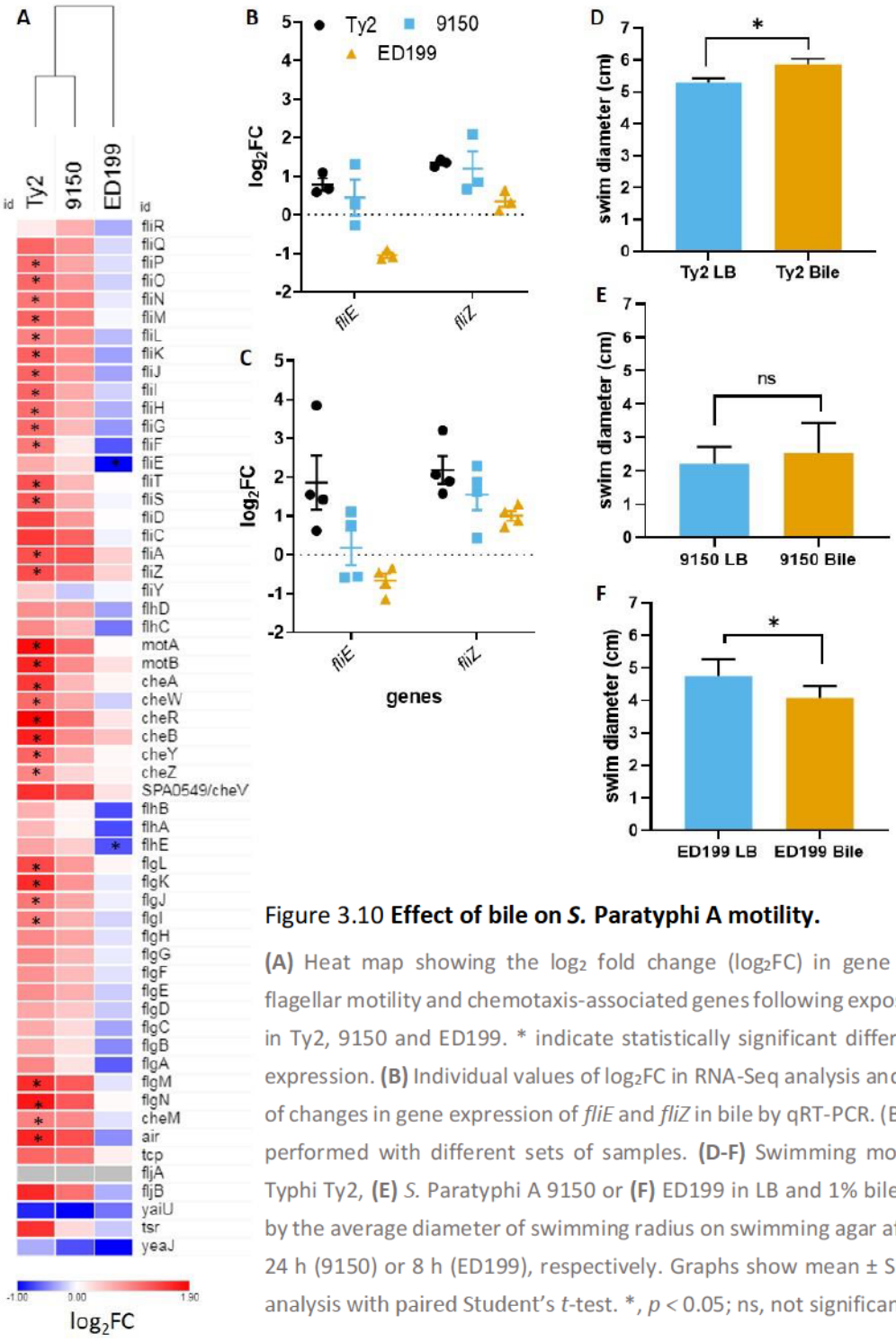


Figure 3.10 **Effect of bile on *S.* Paratyphi A motility.**

(A) Heat map showing the log_2 fold change (log_2FC) in gene expression of flagellar motility and chemotaxis-associated genes following exposure to 3% bile in Ty2, 9150 and ED199. * indicate statistically significant differences in gene expression. **(B)** Individual values of log_2FC in RNA-Seq analysis and **(C)** validation of changes in gene expression of *fliE* and *fliZ* in bile by qRT-PCR. (B) and (C) were performed with different sets of samples. **(D-F)** Swimming motility of **(D)** *S.* Typhi Ty2, **(E)** *S.* Paratyphi A 9150 or **(F)** ED199 in LB and 1% bile was assessed by the average diameter of swimming radius on swimming agar after 16 h (Ty2), 24 h (9150) or 8 h (ED199), respectively. Graphs show mean ± SEM. Statistical analysis with paired Student's *t*-test. *, $p < 0.05$; ns, not significant.

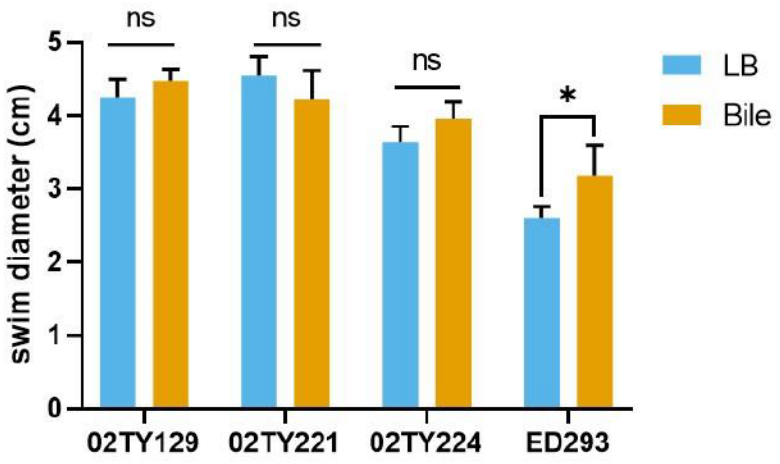


Figure 3.11 **Effect of bile on *S.* Paratyphi A clinical isolates motility.**

Swimming motility of *S.* Paratyphi A clinical strains in LB and 1% bile assessed by the average swimming diameter on swimming agar after 8 h. Graphs show mean ± SEM from five independent repeats. Statistical analysis by two-way ANOVA followed by correction for multiple comparisons. *, $p < 0.05$; ns, not significant.

may be limited to evade recognition by the immune system. To examine whether this increased motility was shared with other clinical *S.* Paratyphi A isolates, swimming motility was tested in the other clinical strains as well. Interestingly, bile did not affect the motility of *S.* Paratyphi A 02TY129, 02TY221 and 02TY224, while it promoted motility for *S.* Paratyphi A ED293 (Figure 3.11). It is currently unclear why the *S.* Paratyphi A clinical isolates may regulate their motility differently in response to bile, but indicates within-serovar variation in flagellar motility and/or flagellin proteins.

3.9 Effect of bile on *S.* Paratyphi A-specific genes

Genes only found in *S.* Paratyphi A and not in *S.* Typhi were next investigated, as these may be implicated in different strategies to establish chronic carriage between the two serovars. A list of these genes (*SPA2394-2431, SPA2469, SPA2472-3, SPA2601-13, SPA2623-25, SPA4289-91*) was found in Holt (2009). Although the comparison was made between other reference strains than those used herein, namely *S.* Typhi CT18 and *S.* Paratyphi A AKU_12601, most of these genes were found in other *S.* Paratyphi A strains tested in that study including 9150. None of these genes were differentially regulated in response to bile in any of the two *S.* Paratyphi A strains tested.

The genomes of both *S.* Paratyphi A and *S.* Typhi are characterised by extensive genome degradation (McClelland et al., 2004; Holt et al., 2009). Although *S.* Typhi and *S.* Paratyphi A share some of their pseudogenes (Table 1.2), there are also pseudogenes that are not shared between the two serovars. Pseudogenes in *S.* Typhi Ty2 that are intact in *S.* Paratyphi A 9150 were examined for differential regulation to bile, which may drive disparate responses between the two serovars. From

Table 3.7 **Expression change of *S.* Paratyphi A genes in bile found as pseudogenes in *S.* Typhi.**

Genes that are intact in *S.* Paratyphi A and pseudogenes in S. Typhi Ty2 were examined for differential regulation in response to bile. Those that exhibited a statistically significant change in expression in one of the two or both *S.* Paratyphi A strains are presented here. log_2FC values are shown only when $q < 0.05$.

Gene ID	Gene name	Function	*S.* Paratyphi A log_2FC, q < 0.05	
			9150	ED199
SPA0186	*panD*	aspartate 1-decarboxylase	-1.25873	
SPA0375	-	-	1.189825	
SPA0664	*yeiA*	putative dihydropyrimidine dehydrogenase	1.277228	1.654865
SPA0712	*yegS*	putative diacylglycerol kinase catalytic domain	-0.83289	
SPA1133	*oppC*	ABC superfamily (membrane), oligopeptide transport protein	-0.87932	
SPA1326	-	putative outer membrane protein	4.095924	
SPA1340	*ydeI*	putative periplasmic protein	-1.09516	
SPA1356	*dmsA*	putative dimethyl sulphoxide reductase subunit	1.553598	
SPA1479	*ynhG*	putative LysM domain	-0.92093	
SPA1540	*astA*	arginine succinyltransferase	-3.41504	
SPA1555	*yeaD*	putative enzymes related to aldose 1-epimerase		1.352672
SPA1723	-	putative sodium/glucose cotransporter	-0.78727	
SPA1923	*glnH*	glutamine-binding periplasmic protein precursor	1.6458	1.544171
SPA2040	*speF*	ornithine decarboxylase isozyme, inducible		2.918162
SPA2080	-	putative cytoplasmic protein		1.329705
SPA2333	*aroM*	protein of aro operon, regulated by aroR		-1
SPA2357	*yahO*	probable secreted protein	-2.83094	-1.8679
SPA2650	*gabP*	GabA permease (4-amino butyrate transport carrier)	-2.63559	
SPA2652	*ygaU*	putative LysM domain	-1.10745	
SPA3112	*tdcC*	HAAAP family, L-threonine/ L-serine permease, anaerobically inducible	3.006277	2.441227
SPA3369	*yhgF*	putative transcription accessory protein	-1.23195	
SPA3456	-	-	-0.9094	
SPA3612	*cigR*	putative inner membrane protein	-0.68589	-0.97763
SPA4286	*yjgB*	putative alcohol dehydrogenase	-1.97797	

the ~200 genes (McClelland *et al.*, 2004), 24 showed statistically significant upregulation or downregulation in response to bile in any of the two *S.* Paratyphi A strains (Table 3.7). The response to bile of some of these genes was shared between the two *S.* Paratyphi A strains. Most genes with a known function have catalytic activity in metabolic pathways, although these showed a varying response to bile between the two *S.* Paratyphi A strains. Based on the current annotation (GO analysis) of this pool of genes, it was suggested that they are not involved in a specific arm of metabolism that is targeted by bile. Bile also triggered changes in expression of genes encoding membrane proteins that may be involved in bile components uptake or efflux or have other regulatory purposes. Genes belonging to this pool with unknown or not well investigated functions may prove to be unique *S.* Paratyphi A strategies for survival and/or virulence following exposure to bile.

3.10 Effect of bile on *S.* Paratyphi A metabolism

Most of the biological processes repressed in response to bile in *S.* Paratyphi A 9150 and ED199 included pathways involved in metabolic processes (Table 3.3). Although not statistically enriched, these pathways showed the opposite response in *S.* Typhi (not shown). Many of these pathways are biosynthetic processes; downregulation of such pathways in response to bile may indicate an arrest in certain metabolic processes in the harsh environment created by bile.

GO analysis (Table 3.3) indicated that sulphate assimilation and reduction involved genes encoded by the *cys* operon. Genes belonging to the *cys* operon are implicated in *Salmonella* oxidative stress (Wang *et al.*, 2010a) and in *S.* Typhi tolerance to bile (Langridge *et al.*, 2009). *cys* genes are also involved in hydrogen sulphide biosynthetic process, which has been implicated in defences against oxidative stress in bacteria (Shatalin *et al.*, 2011). As previously mentioned, bile results in oxidative stress in bacteria (Walawalkar, Vaidya & Nayak, 2016); therefore, it is intriguing that *S.* Paratyphi A would reduce these genes in response to bile. A similar response was observed with a *S.* Typhi H58 strain (Johnson *et al.*, 2018). Bile-triggered downregulation of a *cys* gene (*cysJ*) was corroborated in *S.* Paratyphi A strains, although the magnitude was smaller than that observed with RNA-Seq (Figure 3.12A-B). However, *cysJ* expression in *S.* Typhi could not be validated. Another gene involved in protection from oxidative stress in *Salmonella* is *sodA* (Langridge *et al.*, 2009), and a similar trend in its expression in response to bile was observed in the Johnson *et al* (2017) study, namely it was upregulated in *S.* Typhi Ty2, but downregulated in a clinical strain. While its expression levels remained unchanged in *S.* Typhi Ty2 in the present study, it showed a tendency to be downregulated in *S.* Paratyphi A (Figure 3.12A-B). As decreases in expression observed by RNA-Seq were not always corroborated with RT-qPCR, a gene that was observed to be upregulated by RNA-Seq in all three strains

tested was examined. The upregulation of *fadE*, which is involved in fatty acid metabolism (Wolfe, 2005), was examined by qPCR and validated in all three strains. It remains unknown why the RNA-Seq data were not always corroborated with RT-qPCR in this case. Nevertheless, this discrepancy may suggest overall non-significant changes in expression in response to bile of the genes tested.

The glyoxylate bypass (also known as glyoxylate shunt or cycle) of the TCA cycle (Figure 3.13A) mediates the utilisation of acetate and fatty acids as carbon sources when glucose is scarce. The CO_2-producing reactions are bypassed during activation of the glyoxylate cycle and maintains the number of carbon atoms (Figure 3.13A). The enzymes involved in the glyoxylate shunt are AceA, which is an isocitrate lyase catalysing the conversion of isocitrate to glyoxylate and succinate, and AceB, a malate synthase A, which catalyses the formation of malate from glyoxylate. To determine cycle flow through the glyoxylate cycle instead of the TCA cycle, AceA competes for the same substrate with IcdA, the

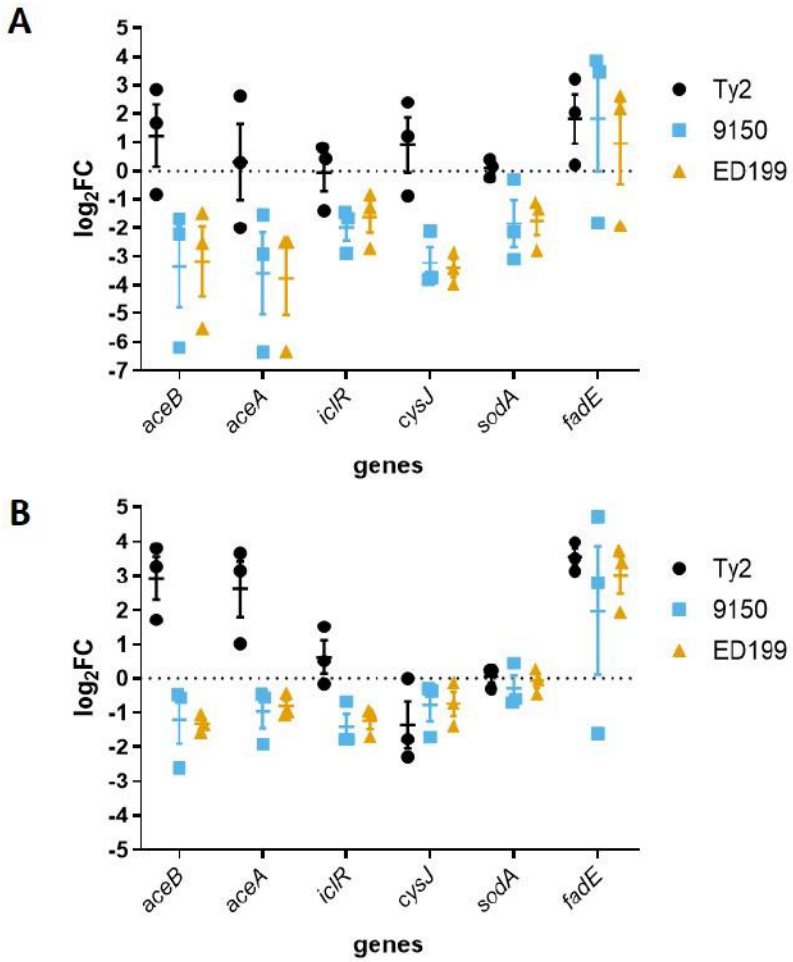


Figure 3.12 **Validation of bile effect on *S.* Paratyphi A metabolic genes**.

(A) Individual log_2FC values from RNA-Seq analysis of indicated genes showing expression change in bile over LB. **(B)** Validation of expression of indicated genes in bile with RT-qPCR. (A) and (B) were performed with different sets of samples.

isocitrate dehydrogenase converting isocitrate to α-Ketoglutarate, as AceA has a lower affinity for isocitrate than IcdA. Their activity is controlled by AceK, the isocitrate dehydrogenase kinase/phosphatase that phosphorylates and inactivates IcdA, allowing AceA to direct flux through the glyoxylate cycle (Cozzone, 1998; Wolfe, 2005).

The genes involved in this pathway are encoded by the *aceBAK* operon (Figure 3.13B) in *Salmonella* and *E. coli*. In *S.* Paratyphi A, *aceK* is a pseudogene due to a mutation resulting in a stop codon at base 96 (McClelland *et al.*, 2004; Wilson & Maloy, 1987). Expression of *aceB* and *aceA* were significantly downregulated in response to bile in both *S.* Paratyphi A 9150 and ED199 by more than 4-fold ($log_2FC > 2.3$) (Figure 3.12A). In contrast, *S.* Typhi Ty2 significantly repressed expression of *aceB*; expression of *aceA* was unchanged. To validate these results, transcription of these genes was

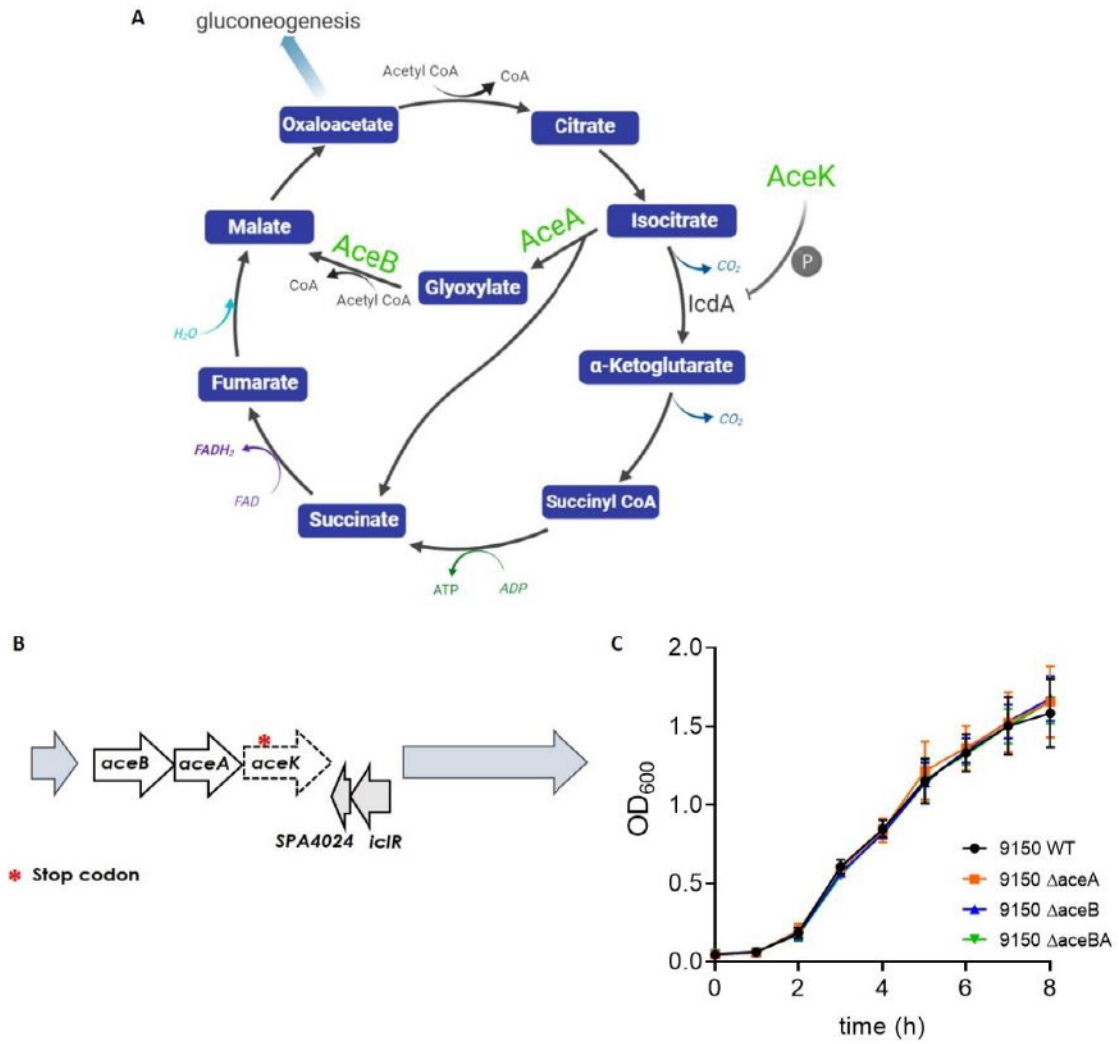


Figure 3.13 **Glyoxylate cycle in *Salmonella*.**

(A) The glyoxylate bypass of the Krebs cycle. Glyoxylate cycle enzymes are shown in green. Graphic produced with Biorender. **(B)** the *aceBAK* operon in *S.* Paratyphi A. **(C)** *S.* Paratyphi A was grown in standard LB media and growth was assessed by monitoring OD_{600} over time. Results show means from three independent repeats.

assessed by RT-qPCR. As shown in Figure 3.12B, both *aceB* and *aceA* were downregulated in the *S.* Paratyphi A strains, while they were induced by bile in *S.* Typhi Ty2. It is worth noting that none of the TCA cycle enzymes were significantly differentially expressed in bile in any of the three strains (Table Appendix.1), suggesting that regulation of the glyoxylate cycle by bile is not because of changes in the TCA cycle activity. As *aceB* was the only gene to be significantly differentially regulated by bile between *S.* Typhi and *S.* Paratyphi A (see Section 3.5), it was further investigated as shown in the following sections. Deletion of *aceA*, *aceB*, or *aceBA* did not affect *S.* Paratyphi A 9150 growth in standard LB media (Figure 3.13C). It is worth noting that another pathway downregulated in the two *S.* Paratyphi A strains was a catabolic process resulting in succinate (Table 3.1), which is in line with downregulation of the glyoxylate pathway and production of the intermediate molecules. Collectively, these results suggest that *S.* Paratyphi A may have a distinct metabolic profile in bile compared to *S.* Typhi.

3.11 Role of glyoxylate cycle genes in host cell infection

The enzymes involved in the glyoxylate cycle have been shown to influence interactions of bacteria with host cells. AceA is involved in persistence during chronic infection, but not in acute infection of mice with *S.* Typhimurium, suggesting *S.* Typhimurium dependence on fatty acids at the persistent phase of infection (Fang *et al.*, 2005). A transcriptomic analysis found induction of *aceA* during *S.* Typhi infection of human macrophages after 12 h of infection (Faucher *et al.*, 2006). These suggest that AceA may be important for long-term survival in macrophages. Additionally, AceA is involved in modulation of NLRP3 inflammasome during infection with *S.* Typhimurium (Wynosky-Dolfi *et al.*, 2014). *S.* Paratyphi A interactions with macrophages are examined in Chapter 4 and the glyoxylate cycle appears to be relevant for the systemic phase of infection. Therefore, the next aim was to explore whether this pathway has a role during *S.* Paratyphi A infection of human cells. To test whether deletion of *aceA* or *aceB* affect interactions of *S.* Paratyphi A 9150 with host cells, HeLa and differentiated macrophage-like THP-1 cells were infected with *S.* Paratyphi A 9150, Δ*aceA*, Δ*aceB*, and Δ*aceBA*.

HeLa cells were infected and internalised bacteria were determined at 2 h post infection to assess invasion levels. Deletion of either *aceA*, *aceB*, or both *aceBA* did not affect invasion of *S.* Paratyphi A, as these invaded HeLa cells at comparable levels to WT (Figure 3.14A). The ability of these mutants to replicate within HeLa cells was determined by infecting HeLa cells and assessing bacterial numbers at 20 h post infection. The deletion of either or both genes had no significant effect on intracellular replication compared to WT bacteria (Figure 3.14B). These results suggest that the glyoxylate bypass is not required for interactions of *S.* Paratyphi A 9150 with HeLa cells. This is in line

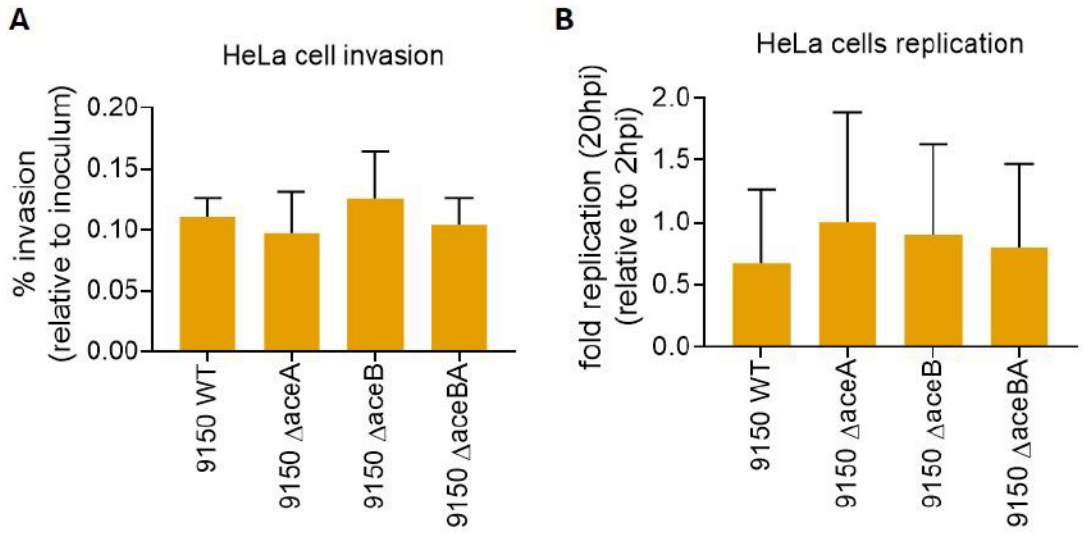


Figure 3.14 **Loss of glyoxylate cycle enzymes does not affect invasion or intracellular replication of *S.* Paratyphi A in epithelial cells.**

HeLa cells were infected (MOI 100) with *S.* Paratyphi A 9150 and **(A)** invasion was determined at 2 h post infection, and **(B)** replication at 20 h post infection by enumeration of intracellular CFUs by gentamicin protection assays. Bars represent means ± SEM from two independent repeats.

with a study investigating the metabolic requirements of *S.* Typhimurium during infection of HeLa cells (Bowden *et al.*, 2014).

AceA is important for long-term survival of *S.* Typhimurium in macrophages. Therefore, THP-1 cells were infected with *S.* Paratyphi A 9150 WT, Δ*aceA*, Δ*aceB*, and Δ*aceBA* in macrophages in which cell death was blocked to more accurately assess bacterial loads at several timepoints. The establishment of the infection conditions for THP-1 cell line are presented in Chapter 4. Bacterial loads were determined at 1.5 h, 3 h, and 20 h post infection. Due to CL3 biosafety regulations, an intermediate time point could not be included in the analysis. Disruption of the glyoxylate cycle did not affect survival and replication within macrophages compared to bacteria with an intact glyoxylate pathway at 3 or 20 h post infection (Figure 3.15A). Bacterial loads at 3 and 20 h post infection were also analysed as fold change in bacterial numbers compared to those at 1.5 h post infection. Fold change of glyoxylate cycle enzyme mutants was similar to that of WT bacteria at both time points tested at 3 h (Figure 3.15B) and 20 h post infection (Figure 3.15C). Interestingly, *S.* Paratyphi A intracellular replication begins later than 3 h post infection, while it reaches > 5-fold higher numbers at 20 h post infection. Collectively, these results suggest that the inability to utilise the glyoxylate shunt does not impact on interactions of *S.* Paratyphi A with host cells.

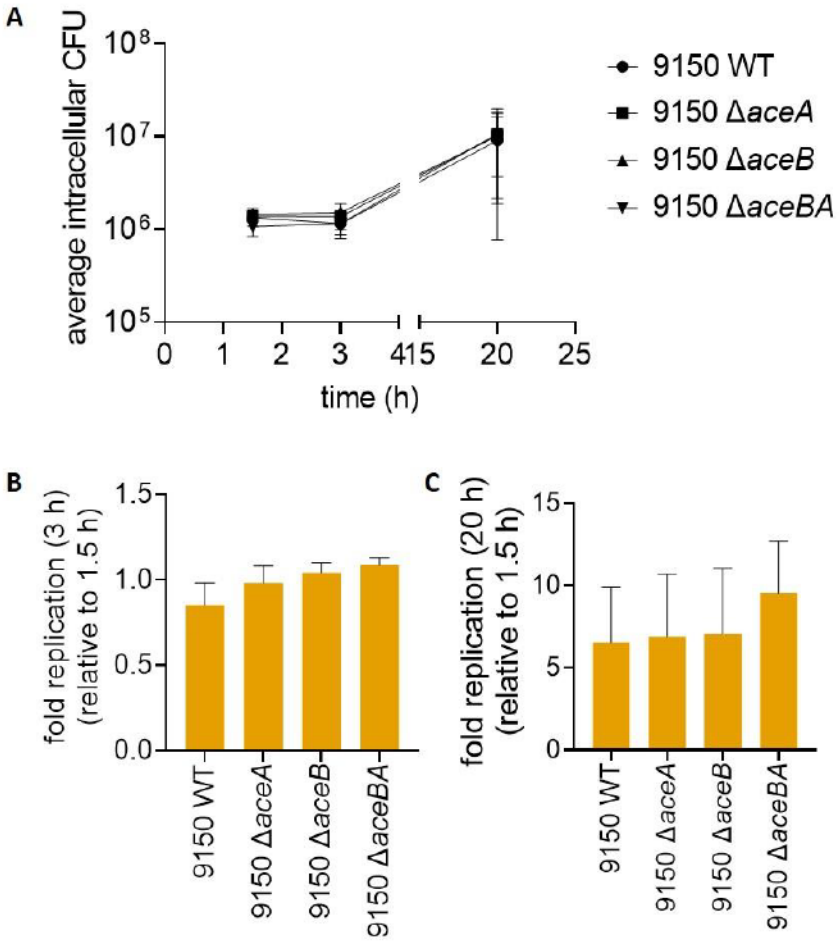


Figure 3.15 **Effect of glyoxylate enzyme gene deletion on intracellular replication of *S.* Paratyphi A in human macrophages.**

(A) GSDMD^{miR} THP-1 cells were infected with *S.* Paratyphi A 9150 (MOI 50) as indicated and numbers of intracellular bacteria were determined at 1.5, 3 and 20 h post infection. Based on these numbers, fold replication of bacteria at **(B)** 3 h and **(C)** 20 h relative to 1.5 h post infection were calculated. Bars show means ± SEM from two independent repeats. Statistical analysis by one-way ANOVA showed statistically not significant differences between strains.

3.12 Discussion

Infection with typhoidal *Salmonella* often results in asymptomatic chronic carriage in the gallbladder (Gal-Mor, 2019). *Salmonella* encounters bile both within the small intestine and in the gallbladder in high concentrations. Despite the importance of the chronic carrier state, the response of typhoidal *Salmonella* to bile, a major environmental cue for enteric pathogens, has been poorly studied. *S.* Typhimurium responds to bile by downregulating many virulence-associated genes (Prouty *et al.*, 2004b; Prouty & Gunn, 2000; Johnson *et al.*, 2018). In contrast, Johnson *et al.* (2017) recently showed that *S.* Typhi upregulates these genes, becoming more invasive into epithelial cells, a response that is amplified with a clinical *S.* Typhi strain (H58). However, the molecular mechanisms of *S.* Paratyphi A, the other major causative agent of typhoid fever in humans (Stanaway *et al.*, 2019), for survival and behaviour in bile remain unknown. In the present study, the sequenced *S.* Paratyphi A 9150 strain was used to investigate the response of *S.* Paratyphi A to bile, alongside a clinical isolate *S.* Paratyphi A ED199 (Dolecek *et al.*, 2008). In an attempt to elucidate the underlying mechanisms of *S.* Paratyphi A behaviour to bile, a transcriptomic analysis was performed comparing changes in expression of *S.* Typhi and *S.* Paratyphi A in response to bile. The transcriptome of *S.* Typhi Ty2 in bile was used as a control (Johnson *et al.*, 2018), as well as a way to investigate common and disparate responses within typhoidal *Salmonella* serovars.

Overall, all three strains tested herein regulated many genes linked to bile tolerance and resistance (e.g. *ompF, marA, glpD*), as well as several stress responses, in a similar manner, further supporting the conserved role of most of these genes between bacterial species (Sistrunk *et al.*, 2016; Begley, Gahan & Hill, 2005; Gunn, 2000). For example, the *marRAB* operon has previously been shown to be activated by bile, and more specifically by the bile salt deoxycholate, and encodes proteins important for survival as it mediates antibiotic tolerance by activating the transcription of efflux pumps facilitating efflux of harmful bile substances (Prouty *et al.*, 2004a). Furthermore, OmpF is a major porin downregulated in response to treatment with antibiotics (Choi *et al.*, 2018). Activation of *marRAB* leads to downregulation of *ompF*, both responses observed herein, and decreased production of OmpF results in reduced influx, in line with a role in limiting influx of harmful substances (Villarreal *et al.*, 2014; Prouty *et al.*, 2004a; Hernández *et al.*, 2012). Like in *S.* Paratyphi A, expression of *ompF* is also significantly downregulated in *S.* Typhimurium in bile (Johnson *et al.*, 2018), suggesting that this unified change in *ompF* expression is a shared robust mechanism of bile resistance, common among *Salmonella* serovars. Similarly, *S.* Typhi and *S.* Typhimurium have previously been shown to be inherently resistant to bile, tolerating concentrations that exceed those encountered *in vivo* (van Velkinburgh & Gunn, 1999). This was also shown for *S.* Paratyphi A, with clinical isolates exhibiting an enhanced ability to survive in high bile concentrations. This increased bile tolerance may be beneficial

for *S.* Paratyphi A circulating within the human population for establishment of chronic carriage in the gallbladder, a phenotype frequently seen with this pathogen in endemic areas (Dongol *et al.*, 2012).

Other genes that were commonly upregulated in all three strains tested herein and have unknown functions (e.g. *SPA3229*, *SPA2654*, *SPA1831*, and *slsA*) warrant further investigation in this context. For example, *slsA* is encoded within the SPI-3 pathogenicity island. SPI-3 contains proteins seemingly unrelated functionally, as its genes are involved in processes from initial attachment to survival upon systemic dissemination (Fàbrega & Vila, 2013). Such investigations may reveal novel typhoidal *Salmonella* factors involved in chronic carriage establishment and/or bile tolerance.

S. Typhi Ty2 and *S.* Paratyphi A 9150 showed similarities in the regulation of gene classes such as SPI-1-associated genes and motility and chemotaxis genes. Similar to *S.* Typhi (Johnson *et al.*, 2018) and in contrast to *S.* Typhimurium (Prouty & Gunn, 2000; Prouty *et al.*, 2004b; Eade *et al.*, 2016), the ability of *S.* Paratyphi A 9150 to invade HeLa cells increased following exposure to bile, which correlated with an increase in SPI-1 expression both at the transcriptional and at the translational level. Increase in virulence following exposure to bile is observed with other pathogenic bacteria to enhance infection, such as *S. flexneri* (Pope, Reed & Payne, 1995; Stensrud *et al.*, 2008; Olive *et al.*, 2007; Faherty *et al.*, 2012) and *V. cholerae* (Gupta & Chowdhury, 1997; Schuhmacher & Klose, 1999).

Although bile induced higher invasiveness of clinical *S.* Paratyphi A isolates into HeLa cells, SPI-1 protein expression was seemingly reduced when grown in bile. The apparent decrease in SPI-1 protein levels was in line with lower transcription of the respective genes in *S.* Paratyphi A ED199. The underlying mechanism for the increase in invasiveness is unknown but may be via increased motility, although infection was synchronised via centrifugation under the conditions tested, or via increased expression of other molecules mediating invasiveness such as adhesins and fimbriae. However, most adhesin proteins as well as flagellar-associated genes, which promote approach, adherence and invasion into host cells (Humphries *et al.*, 2001; Fàbrega & Vila, 2013; Townsend *et al.*, 2001) were downregulated in response to bile. It is possible that other uncharacterised molecules involved in adhesion and attachment may be involved. The role of several adhesin proteins is not fully characterised and their downregulation may in fact allow bacterial proximity to the host cell (Forest *et al.*, 2007; Dufresne, Saulnier-Bellemare & Daigle, 2018; Townsend *et al.*, 2001). However, it should be considered that the plethora of pseudogenised fimbrial operons in typhoidal *Salmonella* (McClelland *et al.*, 2004; Holt *et al.*, 2009; Parkhill *et al.*, 2001; Townsend *et al.*, 2001) indicate that these may be dispensable for interaction with host tissue (Nuccio & Bäumler, 2014). In the experiments performed here, the protein and RNA samples were taken at the point prior to cell infection, under SPI-1 inducing conditions. These *in vitro* conditions may not be ideal to measure

adhesin expression, as an *in vivo* model is often required to enable their transcription (Humphries *et al.*, 2003), which is in keeping with their often undetectable expression levels in our datasets. Furthermore, bile may serve as a cue to downregulate SPI-1 and flagellar genes in clinical *S.* Paratyphi A to escape immune recognition by the host cells, while the protein levels of these genes in *S.* Paratyphi A 9150 are already low.

Importantly, given the already higher invasiveness of clinical isolates compared to *S.* Paratyphi A 9150 even following growth in LB only, suggest underlying differences in SPI-1 expression and/or activity in the clinical isolates compared to the lab strain. Clinical and lab strains may differ at their sequence level via accumulation of mutations under growth in lab conditions. An alternative scenario is that SNPs within regulatory or other genes acquired during circulation within the human population may be driving such differences, as is the case with, for example, *S.* Typhi H58 and non-H58 strains (Wong *et al.*, 2015). Also, translation and/or protein modifications, as well as differences in stability or regulatory mechanisms may be influencing the final protein levels and/or the strain-specific behaviour during interactions with host cells and under stress conditions. For example, the stability of HilD, which only differs at two amino acids between *S.* Typhimurium and *S.* Typhi, greatly increases in *S.* Typhi following exposure to bile, unlike *S.* Typhimurium, which may provide an explanation for the differences observed in SPI-1 expression (Johnson *et al.*, 2018; Eade *et al.*, 2016). Additionally, SPI-1 structural and effector proteins may have longer half-lives or assemble more efficiently within bile in *S.* Paratyphi A ED199 compared to 9150 and thus slower transcription would be required to maintain SPI-1 expression and protein levels. An analogous example is seen with *Shigella*, where bile salts trigger conformational changes in the translocon protein facilitating assembly and an activation-ready state of the T3SS (Stensrud *et al.*, 2008). SPI-1 dependent secretion/translocation may be optimised during exposure to bile by *S.* Paratyphi A clinical isolates, in order to minimise energy spent on producing proteins and allow this saved energy to be exploited in other processes (e.g. bile tolerance strategies). To address these points in the future, a translocation assay, assessing the levels of SPI-1 effectors translocated in the host cells, and determining the stability and/or conformational changes of SPI-1 proteins could provide further elucidation into this matter. Finally, while HeLa cells serve as a tool to study SPI-1 T3SS activity, interactions with epithelial cells need to be confirmed in an intestinal epithelial cell model. Additionally, in order to truly understand the interactions of *S.* Paratyphi A and bile, especially to confirm whether clinical strains behave differently to reference strains, more clinical isolates from diverse geographical regions should be included in any future analyses.

The main difference between *S.* Typhi Ty2 and both *S.* Paratyphi A strains were the bile-mediated downregulation of several metabolic pathways. Surprisingly, many of the genes involved in

these pathways have been linked to bile tolerance by *S.* Typhi (Langridge ***et al.***, 2009) or aid in nutrient utilisation within bile (such as phospholipids by ***fad*** genes) by *S.* Typhimurium (Antunes ***et al.***, 2011). Downregulation of many of these genes was also observed in a clinical *S.* Typhi strain in response to bile (Johnson ***et al.***, 2018). It is currently unclear why these strains limit responses that may be protective towards bile, while maintaining their ability to survive in high bile concentrations. Although *Salmonella* serovars share the majority of their metabolic traits, gastrointestinal and extraintestinal serovars can be distinguished by their content or degradation of genes linked to aerobic metabolism (Nuccio & Bäumler, 2014) and serovars generally may be differentiated in their cell wall and membrane-associated metabolism, as well as their transport and catabolism of specific nutrients (Seif ***et al.***, 2018). Indeed, many of the genes that showed differential regulation in bile between the two serovars are involved in these pathways and, thus, considering that modifications after the transcription step may occur, metabolomics studies on these strains following exposure to bile are required to elucidate the metabolic requirements and response of typhoidal *Salmonella* in bile.

Furthermore, several *S.* Paratyphi A genes found as pseudogenes in *S.* Typhi showed differential regulation in response to bile, suggesting that these genes may be partly responsible for distinct responses between the two serovars. Indeed, the majority of these genes are associated with the membrane leaflet and/or are involved in metabolic pathways, whose bile-induced regulation overall differs between *S.* Paratyphi A and *S.* Typhi. For example, ***SPA2357*** was downregulated in both *S.* Paratyphi A strains and encodes for the periplasmic protein YahO, whose function is unknown. It is a DUF1471 domain-containing protein and, although the function of this domain is unexplored, members of this family are involved in stress responses (Eletsky ***et al.***, 2014). Indeed in *S.* Typhimurium, ***yahO*** is regulated by RpoS, a known regulator involved in stress responses (Ibanez-Ruiz ***et al.***, 2000), while it is repressed by the same porin regulator as ***ompF*** (Corcoran ***et al.***, 2012), making this protein a possible candidate for the stress response to bile. Alternatively, its repression may be a result of ***ompF*** downregulation observed here. Furthermore, ***SPA1326***, which was greatly upregulated in response to bile in *S.* Paratyphi A 9150, encodes for a putative outer membrane protein. The ortholog of this gene in *S.* Typhimurium encodes for phosphoporin PhoE. PhoE is part of a complex in the bacterial membrane leaflet induced upon phosphate limitation and allowing phosphate transport into the cell promoting intra-macrophage non-replicating *S.* Typhimurium (Choi ***et al.***, 2019). Another gene of this group, ***glnH***, was greatly upregulated in both *S.* Paratyphi A strains. In *S.* Typhimurium, GlnH has been shown to be involved in survival within macrophages (Bai ***et al.***, 2014). Induction of these genes may be essential during dissemination and/or chronic carriage, during which *Salmonella* must be able to survive within macrophages. Finally, ***tdcC***, which showed a great increase in expression in both strains, is involved in nutrient uptake (Sumantran, Schweizer & Datta, 1990), which may be important

in the nutrient limiting environment of bile. The activator of the *tdc* operon, *tdcA*, was also significantly and greatly upregulated in both *S.* Paratyphi A strains. This operon, through the activity of *tdcA*, has been shown to be important for intracellular replication and *in vivo* virulence of *S.* Typhimurium (Lim *et al.*, 2010), which may be important upon sensing bile during systemic dissemination. Given that these are pseudogenes in *S.* Typhi, their role in *S.* Paratyphi A tolerance to bile and induced virulence warrant further investigation. Also, gene products of unknown functions may prove to be unique *S.* Paratyphi A virulence factors, at least during exposure to bile, and may therefore offer productive research avenues in the future.

The only gene that was significantly upregulated in *S.* Typhi Ty2 and significantly downregulated in both *S.* Paratyphi A strains was *aceB*, a malate synthase involved in the glyoxylate bypass of the TCA cycle. Interestingly, bile has been shown to influence genes involved in central metabolism in *S.* Typhimurium, such as repressing the TCA cycle and switching to alternative respiratory systems (Antunes *et al.*, 2012). Given that the glyoxylate cycle has been linked to persistence and survival during chronic infection (Fang *et al.*, 2005; Mckinney *et al.*, 2000), it may be surprising that *S.* Paratyphi A would downregulate the associated genes upon exposure to bile. In an attempt to see whether this gene and/or pathway may be important for bile growth, a reporter strain under the control of the promoter of the *aceBA(K)* operon was constructed and *S.* Paratyphi A 9150 growth was determined in different conditions (LB, bile, acetate); however, differential activity of the reporter strain between different growth conditions could not be determined (not shown). Similarly, *S.* Paratyphi A growth in acetate as the sole carbon source is already very low, possibly due to the lack of AceK (Cozzone, 1998), and thus differences between the WT strain and the *aceBA* mutants were not detectable within 8 h of growth (not shown). It is possible that *S.* Paratyphi A exploits redundant pathways; acetate assimilation may be slow under aerobic growth, as has been observed for *S.* Typhimurium compared to *E. coli* (Sargo *et al.*, 2015), and longer times would be required to observe differences in growth. Also, low expression of the *ace* genes in *S.* Typhimurium compared to *E. coli* (Wilson & Maloy, 1987) and the pseudogenisation of *aceK* in *S.* Paratyphi A (McClelland *et al.*, 2004) suggests that regulation of the Krebs cycle may be different in this pathogen.

During persistence, *Mycobacterium tuberculosis* is suggested to exploit the glyoxylate shunt to metabolise lipids in the lung environment, where carbohydrates may not be available (Mckinney *et al.*, 2000). Deletion of isocitrate lyase disrupts *M. tuberculosis* persistence, while it does not affect bacterial growth during acute infection (Mckinney *et al.*, 2000). As interactions of *S.* Paratyphi A with host cells is a topic that concerns the next chapter as well, it was also investigated whether the genes involved in the glyoxylate pathway in *S.* Paratyphi A 9150 were involved in these processes. However, *aceB* and *aceA* deletion mutants behaved in a similar manner as the WT counterpart during infection

of host cells with *S.* Paratyphi A. The role of the glyoxylate cycle in persistent infection and as a virulence factor remains controversial. While it has been shown to promote persistence in *S.* Typhimurium infections (Fang *et al.*, 2005), an *aceA* deletion mutant maintained its virulence in mice (Yimga *et al.*, 2006) and no role for *aceA* was found in HeLa cell invasion and replication (Bowden *et al.*, 2014), which is in keeping with the results presented here. Similarly, *aceA* was not identified as a gene linked to persistence in a microarray screen (Lawley *et al.*, 2006). These findings suggest that there are complex interactions between metabolic pathways and virulence strategies, and often redundant pathways are in place, which may explain the lack of an essential role of glyoxylate cycle enzymes during *in vitro S.* Paratyphi A infection of host cells. Also, *in vitro* infection does not always require the same cellular processes that are important for *in vivo* virulence (Lorenz & Fink, 2002). The glyoxylate cycle may be important for virulence but not act as a virulence factor itself (Lorenz & Fink, 2002). Future studies may exploit *in vivo* enteric fever models to further investigate the role of this pathway during infection with *S.* Paratyphi A (with regards to systemic infection, cell interactions and in response to bile). However, as the focus of this project shifted towards the interactions of *S.* Paratyphi A and inflammasomes (Chapter 4), the role of the glyoxylate cycle became deprioritised and further attempts to understand it in *S.* Paratyphi A were not performed.

This study provided insights into pathways that may be differentially expressed between *S.* Typhi and S. Paratyphi A in response to bile. A limitation of the GO analysis is that only ORFs with known gene names were analysed, and the *S.* Typhimurium gene naming was used for this purpose as it is the only one currently available for this type of analysis, which may occasionally differ between serovars. While the expression of various genes known to be differentially expressed by bile (either involved in bile tolerance or in virulence) were independently investigated, other unidentified pathways may also be regulated differently in bile. Also, despite the fact that the bile concentration used in this study more closely reflects the concentrations encountered in the small intestine (Gunn, 2000), 3% bile was chosen for this study as it does not affect bacterial growth *in vitro* making results reproducible, and this concentration was used in the recent study by our lab (Johnson *et al.*, 2018) so comparisons could be made more easily. Increasing bile concentrations is challenging for *in vitro* studies; to circumvent this and to truly understand the behaviour of typhoidal *Salmonella* in the environment of the gallbladder, including high bile concentrations, limiting nutrient milieu, and different type of epithelial cells, future research should focus on investigating the response of clinical strains isolated from chronic carriers. Previous findings suggest that isolates from chronic carriers may have increased ability to form biofilms, while they may be genetically distinct with many genotypes circulating among carriers in a given location (Kalai Chelvam, Chai & Thong, 2014; Charles *et al.*, 2013; Hatta *et al.*, 2011). In line with this, this study used ox bile, which is commonly selected for the study

of the response of bacterial pathogens to bile (Begley, Gahan & Hill, 2005). Ox bile was chosen for this study as it was used in the Johnson ***et al.*** (2017) study, so comparisons could be facilitated. It is worth noting that discrepancies in the magnitudes of induced changes in expression observed with that study may be the result of ox bile originating from different manufacturers. Furthermore, differences between commercial and physiological bile preparations are generally expected to be seen (Antunes ***et al.***, 2012). Nevertheless, as typhoidal *Salmonella* serovars are human-restricted, human bile would be required to better elucidate their behaviour, as they may respond differently to bile originating from animals. In fact, it was recently shown that genes encoding curli fimbriae, involved in biofilm formation on gallstones, were induced when *S.* Typhi was exposed to human bile, while these genes were repressed when grown in animal bile (ox or mouse) (González ***et al.***, 2019). Finally, *in vitro* studies should be combined with *in vivo*/*ex vivo* analyses as much as it is feasible, given the lack of appropriate enteric fever models, to corroborate these findings.

In summary, it is evident that bile affects gene expression in *S.* Paratyphi A, inducing changes in > 5% of the genome, which in turn leads to changes in interactions with host cells and may reflect adaptation to the gallbladder. Differences observed between *S.* Typhi and *S.* Paratyphi A require further elucidation; understanding these responses may facilitate understanding of chronic carriage and the molecular mechanisms underlying its establishment during enteric fever.

4

Inflammasome activation during macrophage infection with typhoidal *Salmonella*

Macrophages are professional phagocytes required for mounting a host immune response by sensing and responding to infection. They achieve this by engulfing invading pathogens and activating inflammatory pathways, such as inflammasomes, upon recognition of intracellular bacteria and cytosolic PAMPs (Eldridge & Shenoy, 2015; Broz & Dixit, 2016). Moreover, macrophages play an important role during infection with typhoidal *Salmonella*, as *Salmonella* can survive intracellularly and disseminate to systemic sites (Dougan & Baker, 2014). Most inflammasome studies in the context of *Salmonella* infection and pathogenesis have utilised *S.* Typhimurium and mouse macrophages as model systems. Thus, very little is known about the role of inflammasomes in typhoidal *Salmonella* infection. *S.* Typhi leads to caspase-1 activation and pyroptosis in human macrophages (Winter ***et al.***,

2015; Kortmann, Brubaker & Monack, 2015), but the underlying mechanisms remain largely unexplored. The function of inflammasomes during *S.* Paratyphi A infection remains unknown. The aim of this chapter was to explore interactions of *S.* Paratyphi A with macrophages and to determine if and how this pathogen leads to inflammasome activation. *S.* Typhi was included to provide a comparison between the two most prevalent causes of enteric fever. *S.* Typhimurium was used as a control, as it is a well-studied pathogen in terms of inflammasome activation. However, as inflammasome signalling remains poorly studied in the context of *S.* Typhimurium infection of human macrophages, this study also offers novel insights in this aspect. The specific objectives of this chapter thus were to:

- Establish an infection model in human macrophages with typhoidal *Salmonella;*
- Investigate what host-driven inflammasome signalling pathways are activated in response to infection with typhoidal *Salmonella;*
- Examine the role of SPI-1 T3SS in inflammasome activation by S. Typhi and whether Vi antigen contributes to modulation of inflammasome activation;
- Examine the role of SPI-1 T3SS in inflammasome activation by *S.* Paratyphi A and whether the FepE-mediated very long O-antigen chains contribute to modulation of inflammasome activation;
- Validate our findings in human MDMs.

4.1 Typhoidal *Salmonella* induce cell death in THP-1 cells

Interactions of typhoidal *Salmonella* with macrophages were studied in differentiated macrophage-like THP-1 cells infected with *S.* Paratyphi A or *S.* Typhi. As *S.* Typhi Ty2 was an established model in our lab, I first aimed to establish the infection conditions in THP-1 cells using this pathogen. *S.* Typhimurium was used as a control, as well as to provide a comparison of NTS infection and ensuing macrophage responses to those caused by typhoidal serovars. A hallmark of macrophage infection with bacterial pathogens is lytic cell death. This was measured by uptake of propidium iodide (PI): a sequence-independent intercalating fluorescent agent that can only access nucleic acids upon membrane disruption, such as during cell death by pyroptosis. PI is therefore used to identify the percentage of dead cells (Crowley *et al.*, 2016) through a simple *in vitro* assay.

THP-1 cells were infected at increasing MOIs with *S.* Typhi Ty2 or *S.* Typhimurium and cell death was determined at 5 h post infection. Both strains induced MOI-dependent cell death. However,

the differences between MOIs were smaller with *S.* Typhi Ty2 compared to *S.* Typhimurium which induced significantly higher cell death with higher MOIs (Figure 4.1A). Also at all MOIs tested, *S.* Typhimurium induced significantly more THP-1 cell death in comparison to *S.* Typhi Ty2 (Figure 4.1A). MOI 15 was therefore chosen for further analysis. THP-1 cells were infected with *S.* Typhi Ty2 or *S.* Typhimurium and cell death was monitored over time for 5 h. Both *S.* Typhi and *S.* Typhimurium-induced cell death increased during the first 120–150 min, with *S.* Typhimurium causing higher cell death levels at a faster rate, while cell death reached a plateau at later time points (Figure 4.1B). For this reason, downstream analyses were performed at 3 h post infection unless otherwise stated, serving as an indication of cell death early during infection.

THP-1 cells were next infected with *S.* Paratyphi A at a range of MOIs alongside *S.* Typhi Ty2. The range of MOIs tested was larger than those tested with *S.* Typhi Ty2 above, as initial experiments showed that *S.* Paratyphi A 9150-induced cytotoxicity was undetectable at MOI 15. Preliminary experiments showed that *S.* Typhi and *S.* Paratyphi A induced SPI-1-dependent cell death (see also Sections 4.10 and 4.15), similarly to *S.* Typhimurium (Mariathasan ***et al.***, 2004; Miao ***et al.***, 2006; Bierschenk ***et al.***, 2019; Casson ***et al.***, 2015). Therefore, SPI-1 mutants (Δ*invA*) of both *S.* Paratyphi A 9150 and *S.* Typhi Ty2 were used in parallel. This served as a way to determine the upper and lower limits of SPI-1-induced experimental cell death levels; when WT and Δ*invA*-induced cell death becomes similar, this may be due to overwhelming the cells with a high bacterial load.

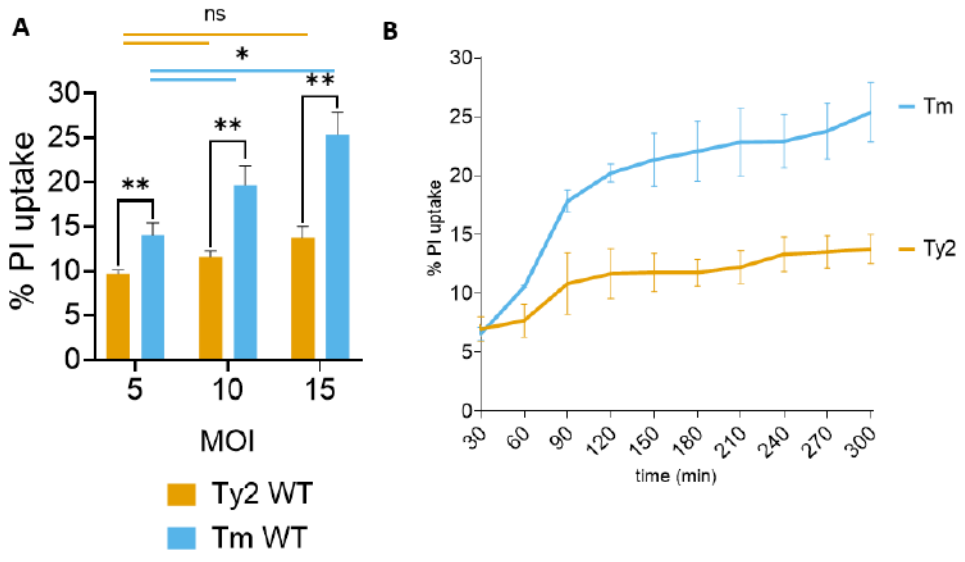


Figure 4.1 ***S.* Typhi induces THP-1 cell death in a time-dependent manner.**

(A) THP-1 cells were infected at increasing MOIs with *S.* Typhi Ty2 (Ty2) or *S.* Typhimurium (Tm) and cell death was determined at 5 h post infection. **(B)** THP-1 cells were infected as indicated at MOI 15 and cell death was determined by PI uptake over time. Bars show means ± SEM from three independent repeats. Statistical analysis by matched two-way ANOVA. *, $p < 0.05$; **, $p < 0.01$. ns, not significant.

S. Paratyphi A 9150 induced low levels of cell death even at high MOIs (Figure *4.2*A). However, high MOIs (e.g. MOI 100) induced SPI-1-independent cell death by both typhoidal *Salmonella* serovars, indicating that the infected cells became overwhelmed and died independently of a *Salmonella*-specific pathogenicity mechanism. *S.* Paratyphi A 9150 MOI of 50 induced similar levels of cell death as that induced by *S.* Typhi Ty2 at MOI of 15, while cell death remained SPI-1-dependent (Figure 4.2A). Thus, MOI of 50 was selected for further experiments with *S.* Paratyphi A. This experiment also indicated that both *S.* Paratyphi A and *S.* Typhi-induced cell death in THP-1 cells was SPI-1 T3SS-dependent, as the Δ*invA* mutants induced significantly less cell death than WT at MOI 50 or MOI 15, respectively ($p < 0.05$, compared by two-tailed Student's *t*-test; see also Section 4.15) (Figure 4.2A). THP-1 cells were also infected with WT *S.* Paratyphi A 9150 at MOI 50 and cell death was monitored over time. Similar to *S.* Typhi Ty2 and *S.* Typhimurium (Figure 4.1), *S.* Paratyphi-A-induced cell death increased with time and reached a plateau after 180 min post infection, showing only a mild increase after this timepoint (Figure 4.2B).

The above results show that *S.* Paratyphi A 9150 required > 3-fold higher MOI to cause similar levels of macrophage cell death compared to *S.* Typhi Ty2. To test whether this difference between cell death induced by *S.* Paratyphi A 9150 at MOI 50 and MOI 15 is due to higher bacterial

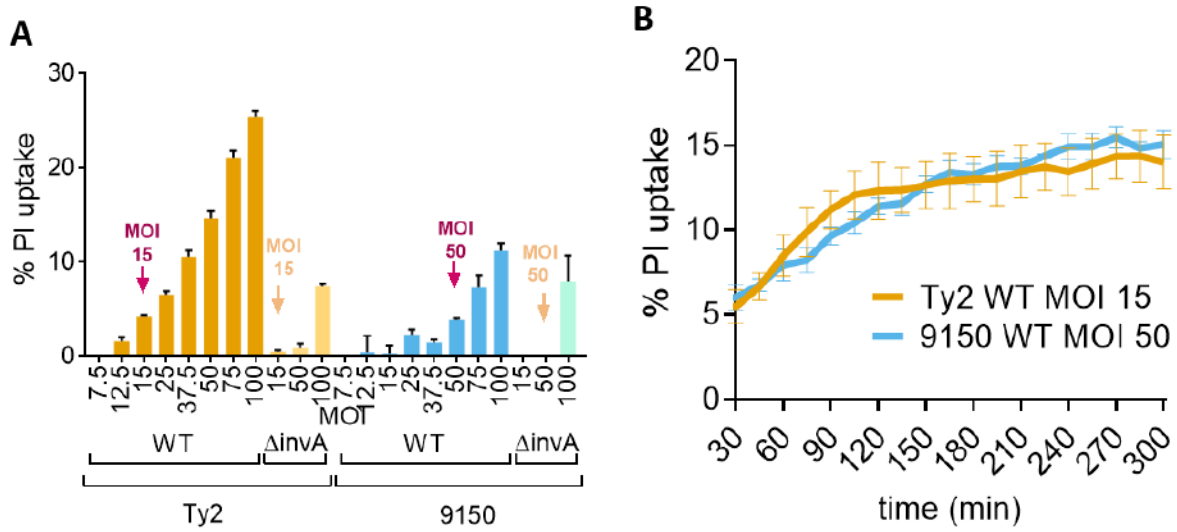


Figure 4.2 ***S.* Paratyphi A 9150 induces lower levels of THP-1 cell death than S. Typhi Ty2.**

(A) THP-1 cells were infected with WT or Δ*invA S.* Typhi Ty2 (Ty2) or *S.* Paratyphi A 9150 (9150) at increasing MOIs as indicated and cell death was measured by PI uptake. **(B)** THP-1 cells were infected with WT *S.* Typhi Ty2 (MOI 15) and *S.* Paratyphi A (MOI 50) and cell death was monitored over time by PI uptake. Bars show means ± SEM from (A) two or (B) three independent repeats.

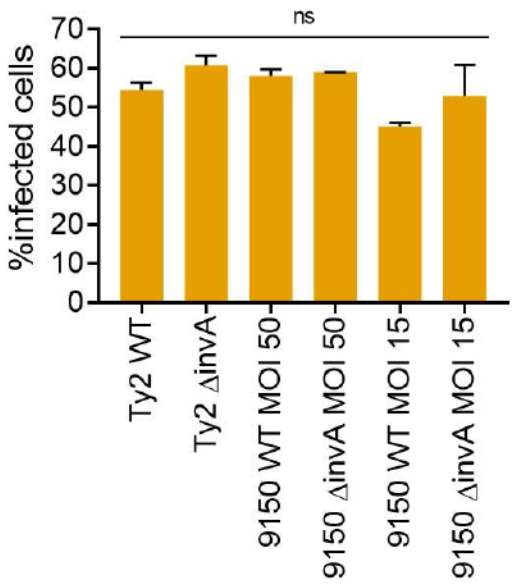


Figure 4.3 ***S.* Paratyphi A infection rate of THP-1 cells is similar at MOI 50 and 15.**

THP-1 cells were treated with Z-VAD-FMK prior to infection with WT or Δ*invA S.* Typhi Ty2 (Ty2; MOI 15) or *S.* Paratyphi A 9150 (9150) at the indicated MOIs. At 30 min post infection, extracellular and total bacteria were stained; infected cells were quantified by fluorescent microscopy. Error bars show means ± SEM from two independent repeats. Means represent average percentages following quantification of > 100 cells from randomly selected slide fields per repeat. Statistical analysis by repeated measures one-way ANOVA following correction for multiple comparisons. ns, not significant

internalisation, Z-VAD-FMK-treated THP-1 cells were infected at the two different MOIs and stained for external and internal bacteria. Z-VAD-FMK is a pan-caspase inhibitor that efficiently blocks cell death induced by *Salmonella* (see also Section 4.2) and was thus exploited in these settings to minimise differences in cell death affecting quantification of intracellular bacteria. The higher cell death levels induced by *S.* Paratyphi A 9150 at MOI 50 did not correlate with significantly higher percentage of internalised bacteria (Figure 4.3). Also, WT and Δ*invA S.* Paratyphi A or *S.* Typhi were internalised similarly at these MOIs, further supporting that differences in cell death induction was not mediated by different levels of intracellular bacteria.

4.2 Typhoidal *Salmonella* induces caspase-dependent pyroptosis

S. Typhimurium-induced cell death is largely mediated by caspases (Wemyss & Pearson, 2019). To assess whether typhoidal *Salmonella* similarly induced caspase-dependent cell death in human macrophages, THP-1 cells were treated with the pan-caspase inhibitor Z-VAD-FMK prior to infection. The efficacy of Z-VAD-FMK activity was confirmed in cells primed with *E. coli* O111:B4 LPS and treated with nigericin, which activates the canonical NLRP3 inflammasome pathway leading to caspase-1-dependent pyroptotic cell death (Muñoz-Planillo *et al.*, 2013). As expected, Z-VAD-FMK completely inhibited the ability of nigericin to induce cell death in LPS-primed THP-1 cells (Figure 4.4A).

Z-VAD-FMK-treated THP-1 cells were then infected with *S.* Paratyphi A 9150 or *S.* Typhi Ty2 and cell death was determined at 3 h post infection. *S.* Typhimurium was used as a control. The pan-caspase Z-VAD-FMK inhibitor was able to entirely inhibit *Salmonella*-induced cell death at 3 h post

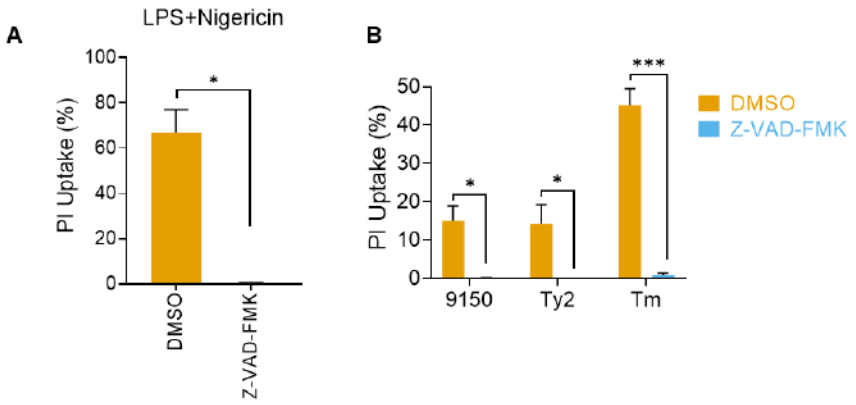


Figure 4.4 ***S.* Paratyphi A and *S.* Typhi induce caspase-dependent cell death.**

(A) THP-1 cells were primed with *E. coli* O111:B4 LPS for 3 h prior to treatment with DMSO (vehicle) or Z-VAD-FMK for 1 h. Nigericin was added for 1 h and cell death was assessed by PI uptake. **(B)** THP-1 cells treated with DMSO or Z-VAD-FMK were infected with *S.* Paratyphi A 9150 (9150; MOI 50), *S.* Typhi Ty2 (Ty2; MOI 15) or *S.* Typhimurium (Tm; MOI 15) and cell death was measured at 3 h post infection via PI uptake. Bars show means ± SEM from three independent repeats. Statistical analysis by (A) paired Student's *t*-test or (B) matched two-way ANOVA. *, $p < 0.05$; ***, $p < 0.001$.

infection (Figure 4.4B). These results suggest that both typhoidal *Salmonella* and NTS serovars induce caspase-dependent cell death in macrophages and thus this is a serovar-independent host response.

Macrophage infection with *S.* Typhimurium leads to pyroptotic cell death (Wemyss & Pearson, 2019). It is now well understood that the major mediator of pyroptosis is GSDMD (Broz, Pelegrín & Shao, 2019). Therefore, to ascertain whether cell death induced by typhoidal *Salmonella* was mediated by GSDMD-mediated pore formation and was thus pyroptotic, *GSDMD* was silenced in THP-1 cells using a miRNA30E-based plasmid (GSDMD^{miR}) (Goddard ***et al.***, 2019). As a control, CTRL^{miR} THP-1 cells expressing a non-targeting miRNA (*lacZ*) were used in parallel. *GSDMD* silencing was confirmed by Western blotting in lysates of uninfected cells (Figure 4.5A). To phenotypically validate these cell lines, CTRL^{miR} and GSDMD^{miR} cells were primed with *E. coli* O111:B4 LPS for 3 h, before treating with nigericin for 1 h and measuring cell death by PI uptake. As expected, *GSDMD* silencing prevented LPS+nigericin-induced cell death in THP-1 cells (Figure 4.5B).

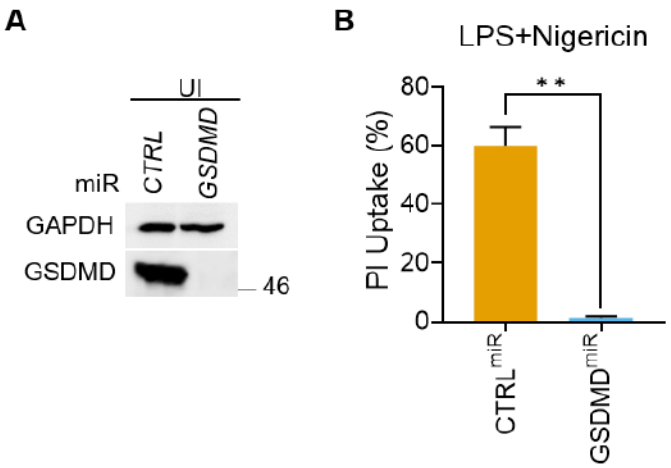


Figure 4.5 **Validation of GSDMD^{miR} THP-1 cells.**

(A) GSDMD was detected in uninfected (UI) THP-1 cells stably transduced with miRNA30E (miR) targeting GSDMD or a non-targeting control (CTRL). Blot produced by J. Sanchez-Garrido. **(B)** CTRL^{miR} and GSDMD^{miR} THP-1 cells were primed with *E. coli* O111:B4 LPS for 3 h before treating with nigericin for 1 h and measuring cell death by PI uptake. Error bars show means ± SEM from four independent repeats. Statistical analysis by paired Student's *t*-test. **, $p < 0.01$.

Next, CTRL^{miR} and GSDMD^{miR} THP-1 cells were infected with *S.* Paratyphi A 9150, *S.* Typhi Ty2, or *S.* Typhimurium and cell death was measured at 3 h post infection. GSDMD silencing entirely prevented *Salmonella*-induced cell death by all three serovars tested (Figure 4.6). This suggested that, similarly to *S.* Typhimurium, typhoidal *Salmonella* induces GSDMD-mediated pyroptosis at 3 h post infection. Additionally, pyroptosis is a hallmark of inflammasome activation during infection and it was thus implied that inflammasome pathways were indeed activated during infection with *S.* Paratyphi A or *S.* Typhi.

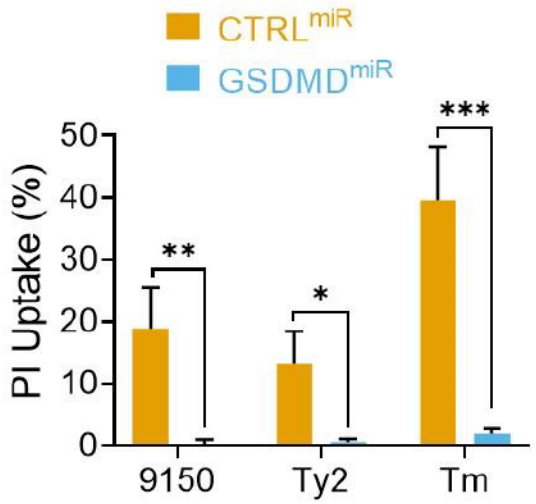


Figure 4.6 **Typhoidal *Salmonella* induce GSDMD-dependent pyroptotic cell death.**

CTRL^{miR} and GSDMD^{miR} THP-1 cells were infected with *S.* Paratyphi A 9150 (9150; MOI 50), *S.* Typhi Ty2 (Ty2; MOI 15), or *S.* Typhimurium (Tm; MOI 15) as a control. Cell death was determined at 3 h post infection by PI uptake. Bars show means ± SEM from four independent repeats. Statistical analysis by matched two-way ANOVA (C). *, $p < 0.05$; **, $p < 0.01$; ***, $p < 0.001$.

4.3 Caspase-4 and ASC contribute to cell death triggered by *S.* Paratyphi A

Activation of the canonical and/or non-canonical inflammasome pathways trigger pyroptosis through caspase-1 or caspase-4, respectively. As *S.* Paratyphi A and *S.* Typhi induce caspase- (Figure 4.4) and GSDMD-dependent pyroptosis (Figure 4.6), the contribution of caspase-1 and caspase-4 to cell death during infection with typhoidal *Salmonella* serovars was next investigated. For this purpose, THP-1 cells were treated with Z-YVAD-FMK prior to infection. Z-YVAD-FMK selectively inhibits mainly caspase-4, as well as caspase-1. To test the efficiency of Z-YVAD-FMK activity, THP-1 cells were treated with DMSO or Z-YVAD-FMK before transfecting with *E. coli* O111:B4 LPS and measuring cell death at 3 h post transfection. LPS transfection delivers LPS in the cytoplasm allowing for recognition of cytosolic LPS by caspase-4. Z-YVAD-FMK significantly reduced cell death induced by LPS transfection (Figure 4.7A), suggesting that this inhibitor prevented activation of caspase-4.

Z-YVAD-FMK-treated THP-1 cells were then infected with *S.* Paratyphi A 9150 or *S.* Typhi Ty2, as well as *S.* Typhimurium. Z-YVAD-FMK-mediated inhibition of caspase-1/4 significantly reduced *S.* Typhimurium-induced cell death (Figure 4.7B), although it did not completely inhibit it suggesting the involvement of additional cell death mediators (Wemyss & Pearson, 2019). Inhibition of caspase-1/4 by Z-YVAD-FMK resulted in a small but significant decrease in *S.* Paratyphi A 9150-induced cell death (Figure 4.7B). In contrast, *S.* Typhi Ty2-triggered macrophage cell death was not affected by Z-

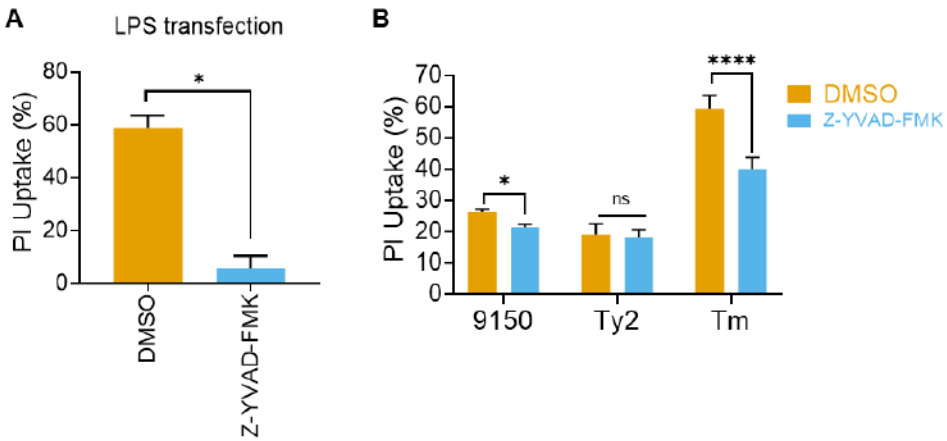


Figure 4.7 **Effect of irreversible inhibition of caspase-4 on typhoidal *Salmonella*-induced cell death.**

(A) THP-1 cells were treated with DMSO or Z-YVAD-FMK for 1 h prior to transfecting with *E. coli* O111:B4 LPS for 3 h and measuring cell death by PI uptake. **(B)** DMSO or Z-YVAD-FMK-treated THP-1 cells were infected with WT *S.* Paratyphi A 9150 (9150; MOI 50), *S.* Typhi Ty2 (Ty2; MOI 15) or *S.* Typhimurium (Tm; MOI 15) and cell death was measured by PI uptake at 3 h post infection. Bars show means ± SEM from (A) three or (B) four independent experiments. Statistical analysis by (A) paired Student's *t*-test or (B) matched two-way ANOVA. *, $p < 0.05$; ****, $p < 0.0001$.

YVAD-FMK treatment (Figure 4.7B), suggesting that *S.* Paratyphi A and *S.* Typhi may induce different pathways of inflammasome signalling in human macrophages.

To further examine the role of caspase-4, a THP-1 cell line with stable silencing of caspase-4 was employed (Goddard *et al.*, 2019). In addition, as ASC is readily recruited to inflammasome complexes formed during infection with *S.* Typhimurium (Man *et al.*, 2014b, 2013; Qu *et al.*, 2016; Broz *et al.*, 2010b), we aimed to determine the contribution of ASC in cell death induction by typhoidal *Salmonella*, which would indicate caspase-1 activation. Caspase-4 silencing was confirmed by immunoblotting for caspase-4 in CASP4^{miR} cell lysates (Figure 4.8A). Also, CASP4^{miR} THP-1 cells were unable to undergo pyroptosis when transfected with *E. coli* O111:B4 LPS for 3 h compared to CTRL^{miR} (Figure 4.8B). Furthermore, ASC^{miR} THP-1 cells (Goddard *et al.*, 2019) were confirmed to have ablated ASC expression by immunoblotting for ASC in cell lysates (Figure 4.8A) and ASC^{miR} THP-1 cells were shown to undergo significantly less cell death in response to LPS priming and nigericin treatment (Figure 4.8B).

CTRL^{miR} or CASP4^{miR} THP-1 cells were infected with *S.* Paratyphi A 9150, *S.* Typhi Ty2 or *S.* Typhimurium and cell death was determined at 3 h post infection. Silencing of caspase-4 markedly reduced *S.* Paratyphi A-induced pyroptosis by approximately 2-fold, while it did not affect THP-1 cell death triggered by *S.* Typhi Ty2 or *S.* Typhimurium (Figure 4.9A). Indeed, *S.* Typhimurium has been recently shown to induce caspase-4-dependent inflammasome activation only following treatment of THP-1 cells with IFNγ to induce GBP expression (Fisch *et al.*, 2019a, 2019b). These results suggest that

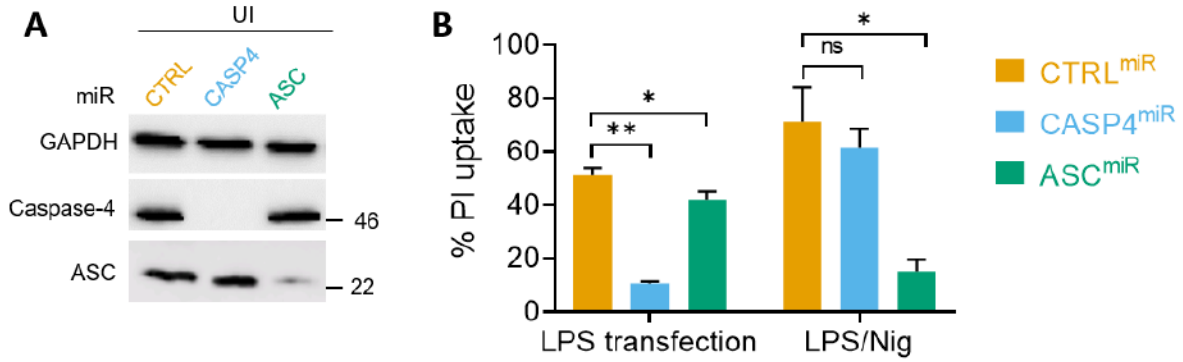


Figure 4.8 **CASP4^{miR} and ASC^{miR} THP-1 cell validation**.

(A) Stable silencing of caspase-4 and ASC in CASP4^{miR} and ASC^{miR} THP-1 cells, respectively, was confirmed by immunoblotting for the respective proteins in lysates of uninfected (UI) cells. Blot representative of three independent repeats. **(B)** CASP4^{miR} and ASC^{miR} THP-1 cells were either transfected with *E. coli* O111:B4 LPS for 3 h (LPS transfection) or primed with LPS for 3 h before treating with nigericin for 1 h (LPS/Nig) and cell death was measured. Graph shows means ± SEM from three independent repeats. Statistical analysis by two-way ANOVA followed by correction for multiple comparisons. *, $p < 0.05$; **, $p < 0.01$; ns, not significant.

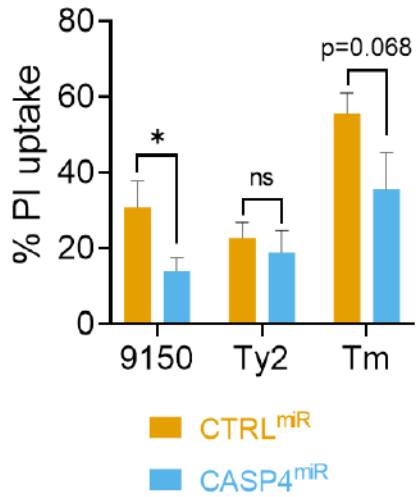


Figure 4.9 ***S.* Paratyphi A induces caspase-4-dependent pyroptosis.**

CTRL^{miR} or CASP4^{miR} THP-1 cells were infected with *S.* Paratyphi A 9150 (9150; MOI 50), *S.* Typhi Ty2 (Ty2; MOI 15) or *S.* Typhimurium (Tm; MOI 15) and cell death was determined at 3 h post infection. Graph shows means ± SEM from four independent repeats. Statistical comparison by matched two-way ANOVA. *, $p < 0.05$; ns, not significant.

caspase-4 plays an important role in pyroptosis during *S.* Paratyphi A infection and further support the data obtained with Z-YVAD-FMK-mediated inhibition of caspase-4, showing that *S.* Paratyphi A and *S.* Typhi possibly activate distinct pathways in inflammasome signalling.

ASC^{miR} THP-1 cells infected with *S.* Paratyphi A 9150 underwent pyroptosis at significantly lower levels compared to CTRL^{miR} (Figure 4.10). In contrast, although pyroptosis was lower in ASC^{miR} cells infected with *S.* Typhi Ty2 or *S.* Typhimurium compared to CTRL^{miR}, this was not statistically significant (Figure 4.10). ASC appeared to be dispensable for *S.* Typhimurium-induced cell death in these settings, which is in line with previous reports in human macrophages (Bierschenk ***et al.***, 2019), and previous work in mouse macrophages points towards a role for NLRC4 inflammasome in pyroptotic cell death in the absence of ASC (Broz ***et al.***, 2010a).

Given that *S.* Paratyphi A 9150-induced cell death was dependent on caspase-4 and ASC, we next investigated the effect of silencing either of these proteins on inflammasome activation during infection with *S.* Paratyphi A by immunoblotting. Caspase-4 silencing did not influence caspase-1

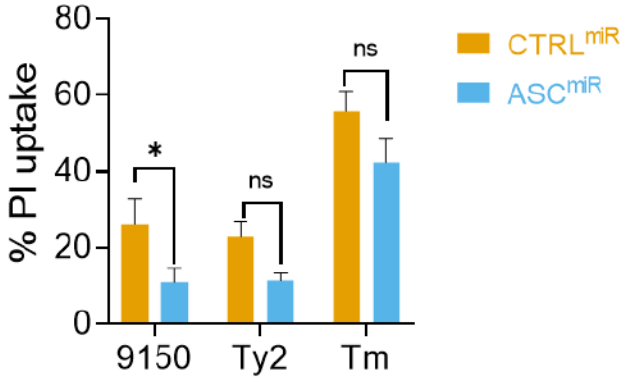


Figure 4.10 ***S.* Paratyphi A induces ASC-dependent cell death in THP-1 cells.**

CTRL^{miR} or ASC^{miR} THP-1 cells were infected with *S.* Paratyphi A 9150 (9150; MO I 50), *S.* Typhi Ty2 (Ty2; MOI 15) or *S.* Typhimurium (Tm; MOI 15) and cell death was determined at 3 h post infection. Bars show means ± SEM from four independent repeats. Statistical analysis by two-way ANOVA. *, $p < 0.05$; ns, not significant.

activation nor IL-18 cleavage, as the levels of their cleaved products in supernatants of infected cells were comparable between CTRL^{miR} and CASP4^{miR} THP-1 cells (Figure *4.11*). These results suggested that caspase-1 activation may occur in the absence of caspase-4, and that caspase-4 did not directly cleave IL-18, in keeping with previous publications (Kayagaki *et al.*, 2011, 2015; Schmid-Burgk *et al.*, 2015). Also, although activation of GSDMD was not determined here, it was suggested that caspase-4 directly induced pyroptosis independently of caspase-1 upon infection with *S.* Paratyphi A 9150. Furthermore, caspase-1 was cleaved at markedly lower levels in ASC^{miR} THP-1 cells compared to CTRL^{miR} during infection with *S.* Paratyphi A 9150. This also resulted in significantly lower IL-18 cleavage (Figure 4.11). A small reduction in caspase-4 activation was also observed, which may have been due to lower levels of cell death in ASC^{miR} THP-1 cells compared to CTRL^{miR}, leading to a lower level of caspase-4 release into the supernatant. Nevertheless, ASC was required for caspase-1 activation during THP-1 cell infection with *S.* Paratyphi A 9150, as well as for induction of cell death.

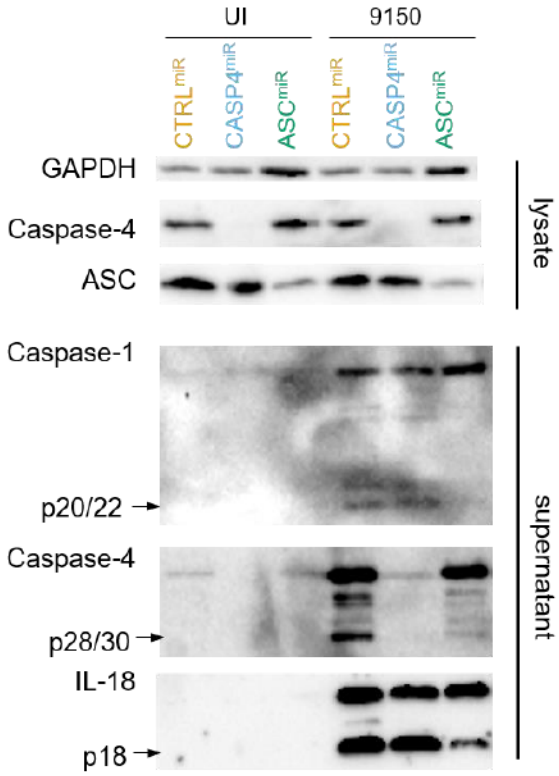


Figure 4.11 ***S.* Paratyphi A induces ASC-dependent, caspase-4 independent caspase-1 activation.**

THP-1 cells were infected with *S.* Paratyphi A 9150 (9150; MOI 50) inflammasome activation was assessed by immunoblotting for cleaved products of caspase-1, caspase-4 and IL-18 (indicated with arrows) in supernatants of infected cells. Uninfected (UI) cells were used as control. Blot representative of two independent repeats.

4.4 The role of the NLRP3 inflammasome during infection with typhoidal *Salmonella*

To test whether NLRP3 is involved during infection with typhoidal *Salmonella*, as is the case with *S.* Typhimurium (Man *et al.*, 2013, 2014b; Broz *et al.*, 2010b; Bierschenk *et al.*, 2019), THP-1 cells were treated with MCC950 prior to infection, which is a small NLRP3-specific inhibitor (Coll et al., 2015, 2019; Tapia-Abellán et al., 2019). The efficacy of the inhibitor was tested by the addition of nigericin to *E. coli* O111:B4 LPS-primed THP-1 cells pre-treated with MCC950. MCC950-mediated inhibition of NLRP3 completely abolished pyroptosis in THP-1 cells treated with nigericin (Figure 4.12A). Also, MCC950 pre-treatment of THP-1 cells entirely blocked caspase-1 cleavage induced by LPS priming and nigericin treatment (Figure 4.12B). These results suggested that MCC950 effectively blocks NLRP3 in THP-1 cells in conditions used here.

THP-1 cells were then treated with DMSO or MCC950 prior to infection with *S.* Paratyphi A 9150, *S.* Typhi Ty2, or *S.* Typhimurium and cell death was determined at 3 h post infection. In keeping with the importance of ASC in *S.* Paratyphi A 9150-induced THP-1 pyroptosis (Figure 4.10), inhibition of NLRP3 significantly reduced cell death triggered by *S.* Paratyphi A 9150 (Figure 4.13A). However, similarly to data shown in Figure 4.10, MCC950-mediated inhibition of NLRP3 did not prevent cell death triggered during infection with *S.* Typhi (Figure 4.13B) or *S.* Typhimurium (Figure 4.13C). Additionally, caspase-1 activation was reduced upon MCC950 treatment of THP-1 cells infected with *S.* Paratyphi A 9150, while caspase-4 activation remained unchanged (Figure 4.13D), suggesting that, as expected, caspase-4 is not activated downstream of NLRP3. To ascertain whether caspase-1 is

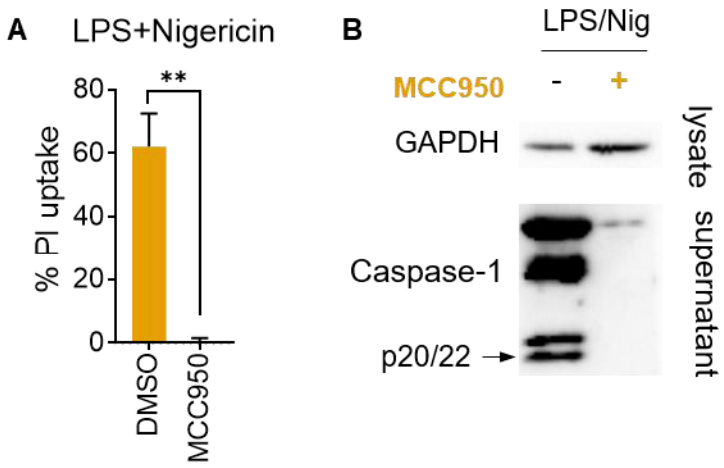


Figure 4.12 **MCC950 efficiently blocks NLRP3 activation in THP-1 cells.**

DMSO or MCC950-treated THP-1 cells were primed with *E. coli* O111:B4 LPS and treated with nigericin for 1 h prior to **(A)** measuring cell death by PI uptake and **(B)** determining caspase-1 activation by immunoblotting. Graph shows means ± SEM from four independent repeats, which were compared by paired Student's *t*-test. Blot is representative from three independent repeats. **, $p < 0.01$.

activated independently of NLRP3 during infection with *S.* Typhi Ty2 or *S.* Typhimurium, caspase-1 activation was also examined during infection with these pathogens. However, caspase-1 and caspase-4 activation did not change in response to NLRP3 inhibition during infection with *S.* Typhi (Figure 4.13D), further supporting the distinct inflammasome pathways activated during infection with *S.* Typhi and *S.* Paratyphi A. During *S.* Typhimurium infection, caspase-1 cleavage was decreased upon MCC950 treatment of THP-1 cells (Figure 4.13D). It is thus possible that other caspases activated during *S.* Typhimurium infection may have compensated for the inhibition of NLRP3 (such as caspase-8, see Section 4.6) and thus the similar levels of cell death between DMSO and MCC950-treated THP-

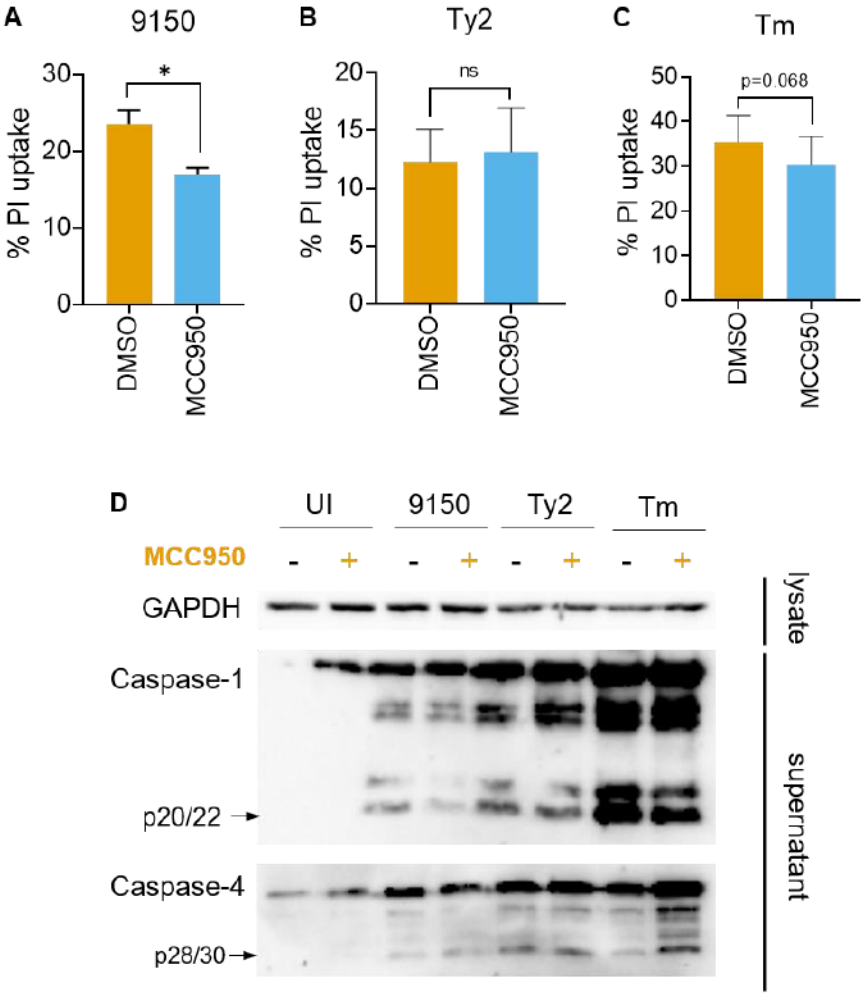


Figure 4.13 **Effect of MCC950-mediated NLRP3 inhibition on *Salmonella*-induced cell death.**

THP-1 cells were treated with DMSO or MCC950 prior to infection with **(A)** *S.* Paratyphi A 9150 (9150; MOI 50), **(B)** *S.* Typhi Ty2 (Ty2; MOI 15), or **(C)** *S.* Typhimurium (Tm; MOI 15) and cell death was determined at 3 h post infection. **(D)** DMSO or MCC950-treated THP-1 cells were infected as indicated and inflammasome activation was assessed by immunoblots of cleaved caspase-1 and caspase-4 products (indicated with arrows) in supernatants of infected cells. Blots representative from three independent repeats. Bars show means ± SEM from (A-B) six or (C) four independent repeats. Statistical analysis by paired Student's *t*-test. *, $p < 0.05$; ns, not significant

1 cells (Figure 4.13C). It should be noted that the higher caspase-4 cleavage in MCC950-treated THP-1 cells infected with S. Typhimurium is possibly a result of higher pro-caspase-4 present in the cells.

Furthermore, it has recently been reported that THP-1 cells primed with IFNγ prior to *S.* Typhimurium infection undergo increased cell death, as IFNγ activates GBP expression. GBPs enable disruption of the SCV and thus cytosolic bacteria are more readily recognised by inflammasomes in a caspase-4-dependent manner (Fisch ***et al.***, 2019a, 2019b). To test whether this was the case with typhoidal *Salmonella*, THP-1 cells were treated with IFNγ for 16 h prior to infection with WT *S.* Paratyphi A 9150, *S.* Typhi Ty2 or *S.* Typhimurium. IFNγ pre-treatment promoted increased cell death triggered by both typhoidal *Salmonella* serovars (Figure 4.14). Interestingly, this increase in cell death was mediated by NLRP3, as MCC950 treatment restored the levels of cell death to those observed with cells not receiving any treatment (Figure 4.14).

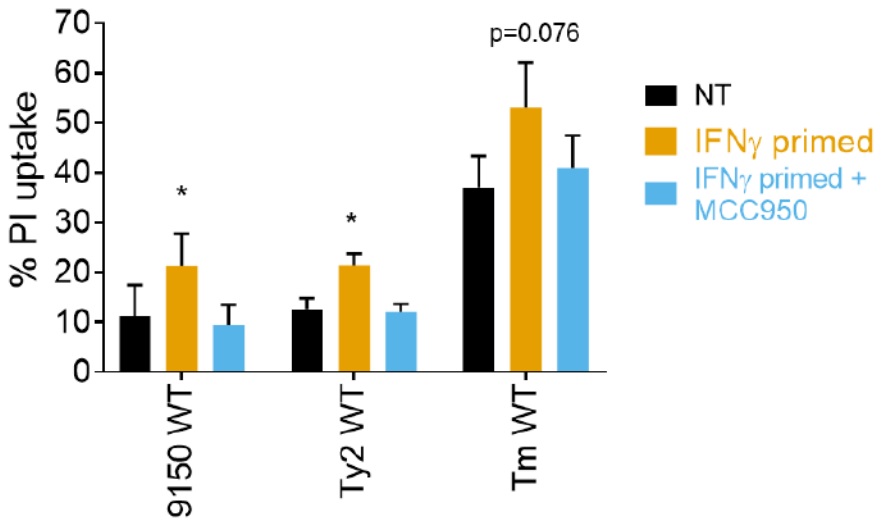


Figure 4.14 **IFNγ priming of THP-1 cells induces NLRP3-dependent increase in cell death by typhoidal *Salmonella*.**

THP-1 cells were primed with IFNγ for 16 h with or without MCC950 for 1 h prior to infection with *S.* Paratyphi A 9150 (9150; MOI50), *S.* Typhi Ty2 (Ty2; MOI 15) or *S.* Typhimurium (Tm; MOI 15). Cell death was determined at 3 h post infection. Bars show means ± SEM from three independent repeats. Statistical analysis by two-way ANOVA followed by correction for multiple comparisons. *, $p < 0.05$. NT, no treatment

4.5 The role of NLRC4 during typhoidal *Salmonella*-induced pyroptosis

It has been reported that *S.* Typhimurium leads to activation of NLRC4 through NAIP-dependent recognition of PAMPs in murine macrophages. NLRC4-dependent sensing of *S.* Typhimurium during murine macrophage infection, as well as transfection of the SPI-1 T3SS needle and rod proteins and flagellin monomers in human macrophages, triggers pyroptosis and cytokine processing (Yang *et al.*, 2013; Reyes Ruiz *et al.*, 2017; Kortmann, Brubaker & Monack, 2015; Miao *et al.*, 2010b; Zhao *et al.*, 2011; Franchi *et al.*, 2006; Rayamajhi *et al.*, 2013). Also, NLRP3 is recruited to the same macromolecular complex with NLRC4 during *S.* Typhimurium infection (Broz *et al.*, 2010b; Man *et al.*, 2013, 2014b). Pharmacological inhibition of NLRP3 did not completely inhibit cell death and caspase-1 activation (Figure 4.13). To ascertain whether NLRC4 activation contributes to pyroptosis and caspase-1 activation during infection with typhoidal *Salmonella*, *NAIP* was stably silenced in THP-1 cells (NAIP^{miR}). THP-1 cells expressing a non-targeting miRNA was used as a control (CTRL^{miR}). NAIP silencing was confirmed in NAIP^{miR} THP-1 cell lysates, which expressed NAIP at markedly lower abundance than CTRL^{miR} cells (Figure 4.16).

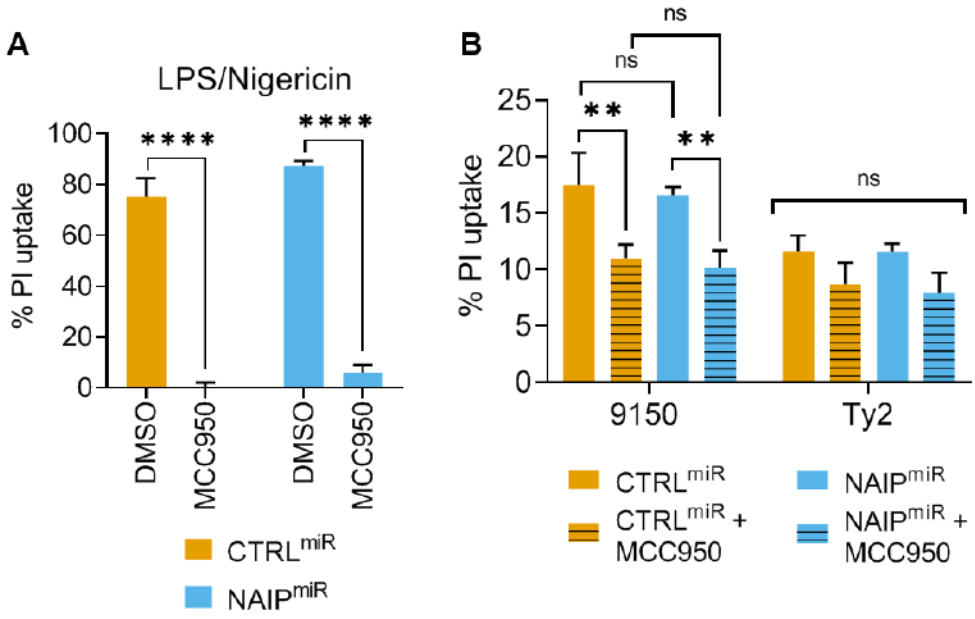


Figure 4.15 **The role of NAIP silencing in typhoidal *Salmonella*-induced cell death.**

(A) CTRL^{miR} and NAIP^{miR} THP-1 cells were primed with *E. coli* O111:B4 LPS before adding nigericin in cells pretreated with DMSO or MCC950. Cell death was determined at 1 h post nigericin addition by PI uptake. **(B)** CTRL^{miR} or NAIP^{miR} THP-1 cells with or without MCC950 pre-treatment, were infected with WT *S.* Paratyphi A 9150 (9150; MOI 50) or *S.* Typhi Ty2 (Ty2; MOI 15) and cell death was determined at 3 h post infection. Graphs show means ± SEM from three independent repeats. Statistical analysis by two-way ANOVA after correction for multiple comparisons (for B). **, $p < 0.01$; ****, $p < 0.0001$; ns, not significant

The effect of NAIP silencing on *S.* Paratyphi A or *S.* Typhi-induced pyroptosis and caspase-1 processing was tested in conjunction with MCC950-mediated NLRP3 inhibition to concomitantly test the role of both NLRP3 and NLRC4 sensors in typhoidal *Salmonella* macrophage infection. As cells were treated with DMSO or MCC950, the efficacy of NLRP3 inhibition by MCC950 was tested in cells primed with *E. coli* O111:B4 LPS and treated with nigericin. Nigericin-induced pyroptosis (Figure 4.15A) as well as caspase-1 cleavage was completely abolished following MCC950 treatment, independently of NAIP silencing (Figure 4.16).

CTRL^{miR} and NAIP^{miR} THP-1 cells were then infected with *S.* Paratyphi A 9150 or *S.* Typhi Ty2 and typhoidal *Salmonella*-induced pyroptosis was determined in CTRL^{miR} and NAIP^{miR} THP-1 cells with or without MCC950-mediated NLRP3 inhibition. NAIP silencing did not affect pyroptosis induction by *S.* Paratyphi A 9150 or *S.* Typhi Ty2, while NLRP3 inhibition significantly reduced pyroptosis levels only in *S.* Paratyphi A 9150-infected THP-1 cells (Figure 4.15B), in line with the observations presented in the previous section. As previously, *S.* Typhi Ty2 triggered similar levels of pyroptosis in both DMSO and MCC950-treated THP-1 cells (Figure 4.15B). To determine whether despite the lack of a contribution of NLRC4 during infection with typhoidal *Salmonella*, NAIP-NLRC4 mediated caspase-1 activation, caspase-1 and IL-18 cleavage were assessed in supernatants of infected CTRL^{miR} and NAIP^{miR}

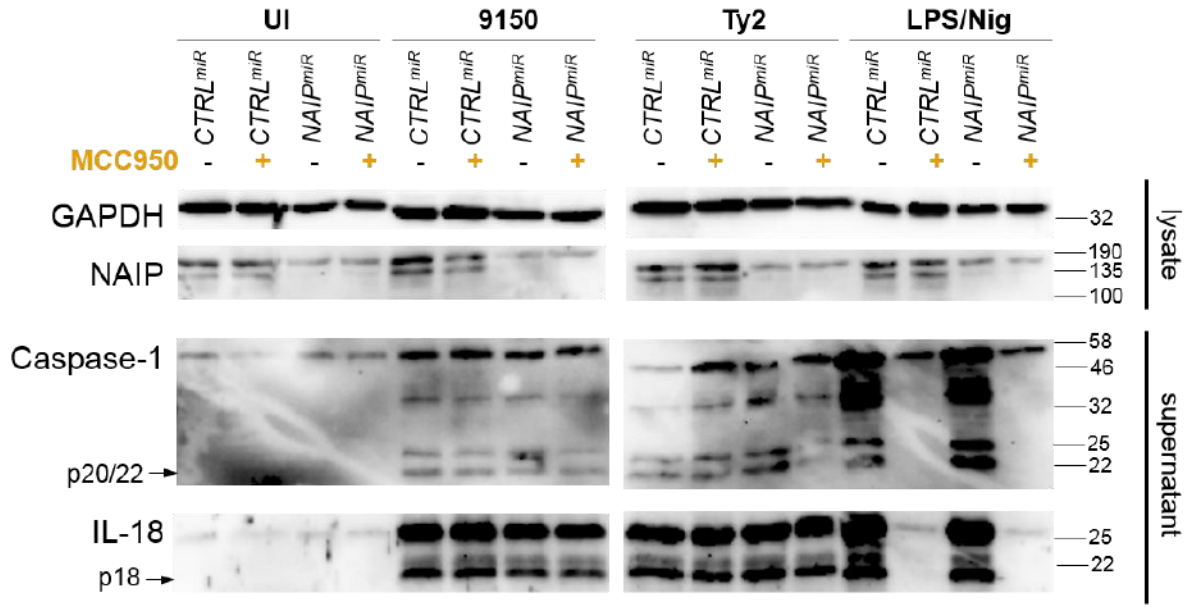


Figure 4.16 **The role of NAIP silencing in inflammasome activation during THP-1 infection with typhoidal *Salmonella*.**

NAIP expression was assessed in CTRL^{miR} and NAIP^{miR} cell lysates, while caspase-1 and IL-18 processing in supernatants from cells infected with S. Paratyphi A 9150 (9150; MOI 50) or S. Typhi Ty2 (Ty2; MOI 15). As a control form MCC950 inhibition, THP-1 cells were primed with *E. coli* O111:B4 LPS for 3 h and treated with nigericin for 1 h. Arrows indicate cleaved products. Blot representative from three independent repeats.

THP-1 cells. Activation of caspase-1 was similar in $CTRL^{miR}$ and $NAIP^{miR}$ THP-1 cells infected with *S.* Paratyphi A 9150 or *S.* Typhi Ty2, which also led to equivalent IL-18 processing as indicated by the levels of their cleaved products (Figure 4.16). Collectively, these results suggested that NLRC4 inflammasome did not play a major role in inflammasome activation and pyroptosis triggered by infection with *S.* Paratyphi A 9150 or *S.* Typhi Ty2.

As discussed earlier, the SPI-1 T3SS rod PrgJ and needle PrgI, as well as the flagellin monomer FliC have been demonstrated to activate inflammasomes during infection of human macrophages with *S.* Typhimurium (Reyes Ruiz *et al.*, 2017; Yang *et al.*, 2013; Kortmann, Brubaker & Monack, 2015). In order to test whether differences at the sequence level of these proteins in *S.* Paratyphi A 9150 and *S.* Typhi Ty2 were responsible for the apparent lack of NCLR4 involvement during macrophage infection, the amino acid sequence of these proteins were compared to those of *S.* Typhimurium. As *S.* Typhimurium SL1344 has been frequently used in published studies, its sequences were also included. C-terminus domains known to activate inflammasomes in *S.* Typhimurium do not differ at the sequence level in *S.* Typhi Ty2 or *S.* Paratyphi A 9150 (Figure 4.17). More specifically, V95, L98, L99 in PrgJ, I71, A74, I75 in PrgI and L502, L504, L505 in FliC (Zhao & Shao, 2015), suggested to be involved in recognition by Naip molecules, are conserved in all three serovars, indicating that any differences in the levels of inflammasome activation during *Salmonella* infection is not mediated by lack of receptor recognition.

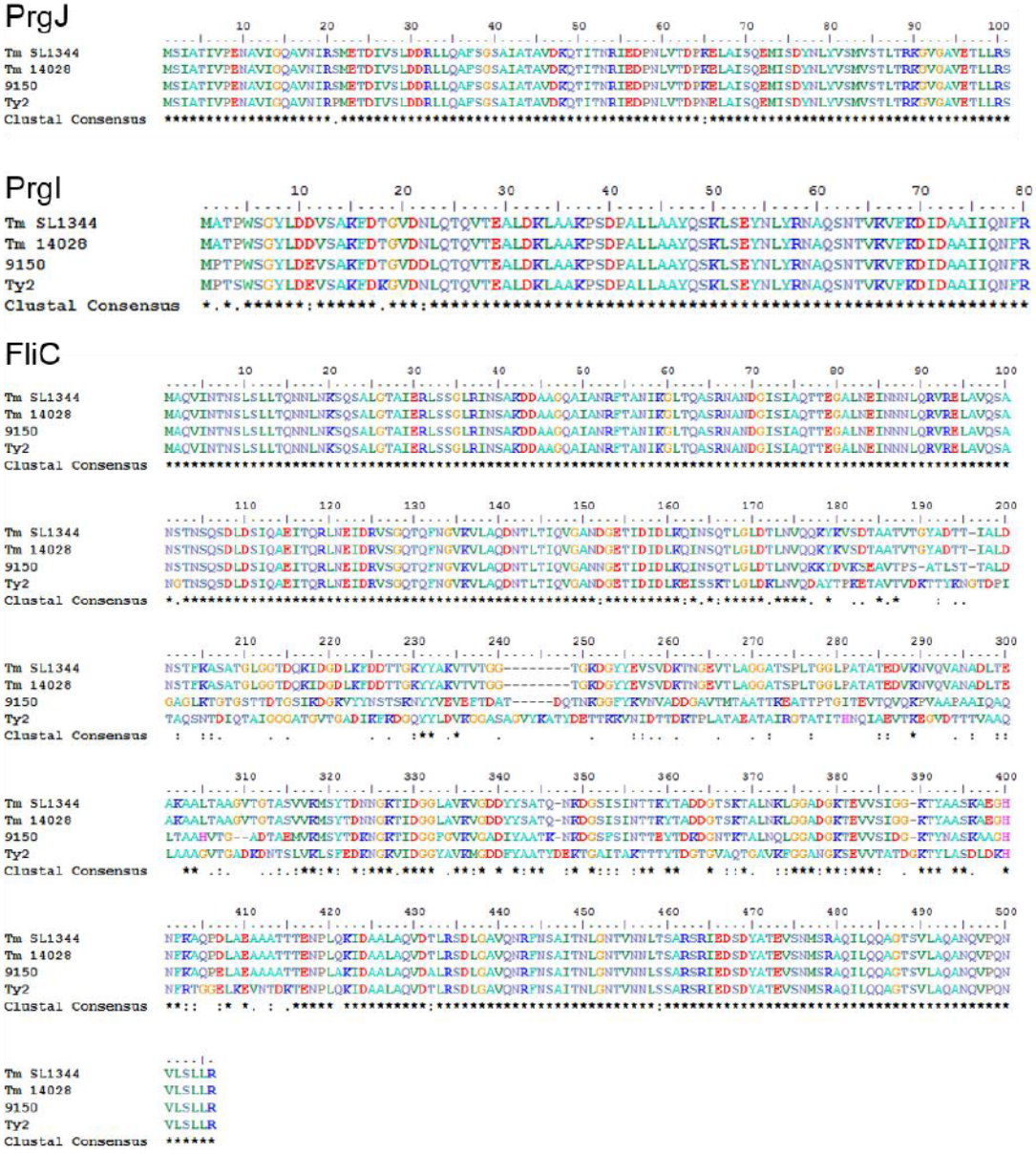


Figure 4.17 **Sequence alignment of PrgJ, PrgI, and FliC of *S.* Paratyphi A, *S.* Typhi, and *S.* Typhimurium.**

The amino acid sequences of SPI-1 T3SS rod PrgJ, needle PrgI, and flaggelin FliC proteins of *S.* Typhimurium (Tm) SL1233 and 14028 were aligned to the respective sequences of *S.* Paratyphi A 9150 (9150) and *S.* Typhi Ty2 (Ty2) reference strains using the CLUSTALW tool.

4.6 The role of caspase-8 during THP-1 cell infection with *S.* Paratyphi A

Given that caspase-4 stable silencing (Figure 4.9) or NLRP3 inhibition (Figure 4.13) did not completely inhibit cell death by *S.* Paratyphi A 9150, and neither failed to reduce *S.* Typhi Ty2-induced cell death, it was hypothesised that additional pathways are involved in pyroptosis during infection with typhoidal *Salmonella*. The role of caspase-8 in regulating and promoting inflammasome activation has become increasingly apparent; moreover, caspase-8 has also been shown to be able to cleave GSDMD (Man *et al.*, 2014b, 2013; Gurung *et al.*, 2014; Gurung & Kanneganti, 2015; Orning *et al.*, 2018; Van Opdenbosch *et al.*, 2017; Sarhan *et al.*, 2018). Therefore, the role of caspase-8 during infection with typhoidal *Salmonella* was investigated in THP-1 cells by pre-treating them with Z-IETD-FMK. Z-IETD-FMK is a narrow-spectrum caspase inhibitor specifically blocking caspase-8 activity. The efficiency of Z-IETD-FMK in inhibiting caspase-8 was tested by treating THP-1 cells with DMSO or Z-IETD-FMK before adding staurosporine for 5 h. Z-IETD-FMK-treated cells showed a significant reduction in cell death in response to staurosporine in comparison to DMSO-treated cells (Figure 4.18A).

Next, THP-1 cells were treated with Z-IETD-FMK, or DMSO as a control, and infected with *S.* Paratyphi A 9150, *S.* Typhi Ty2, or *S.* Typhimurium. Consistent with the known role of caspase-8 in S. Typhimurium-induced pyroptosis (Man *et al.*, 2013), inhibition of caspase-8 with Z-IETD-FMK significantly limited cell death induced by *S.* Typhimurium (Figure 4.18B). Interestingly, while Z-IETD-FMK-mediated inhibition of caspase-8 did not affect *S.* Typhi Ty2-induced pyroptosis, *S.* Paratyphi A 9150 triggered ~25% less pyroptosis in THP-1 cells pre-treated with Z-IETD-FMK compared to DMSO-treated cells (Figure 4.18B), indicating the contribution of caspase-8 to *S.* Paratyphi A-induced

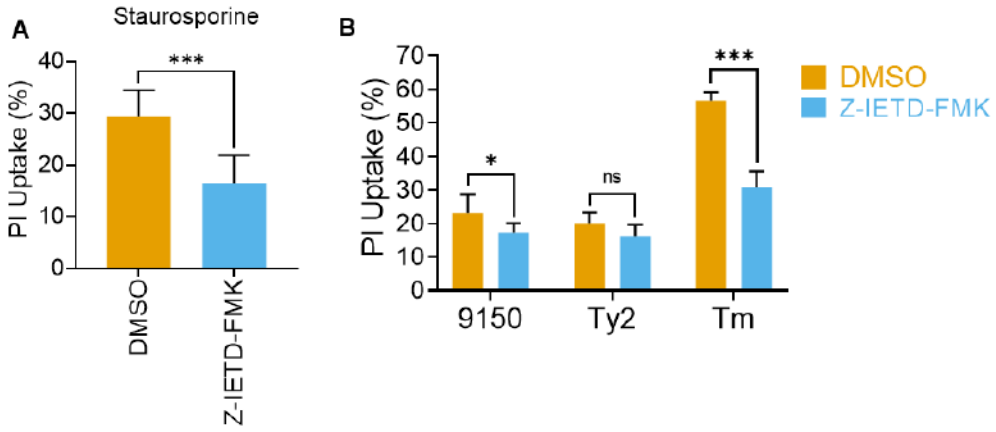


Figure 4.18 **The role of caspase-8 during infection with typhoidal *Salmonella*.**

(A) Staurosporine was added to DMSO (vehicle) or Z-IETD-FMK-treated THP-1 cells for 5 h and cell death was measured by PI uptake. **(B)** DMSO or Z-IETD-FMK-treated THP-1 cells were infected with WT S. Paratyphi A (9150; MOI 50), S. Typh Ty2 (Ty2; MOI 15) or S. Typhimurium (Tm; MOI 15) and cell death was determined at 3 h post infection. Bars show means ± SEM from three independent repeats. Statistical analysis by (A) paired Student's *t*-test or (B) matched two-way ANOVA. *, $p < 0.05$; ***, $p < 0.001$.

macrophage cell death. Also, similar to observations with caspase-4, the effect of caspase-8 blocking is different between infection with *S.* Paratyphi A and *S.* Typhi, further suggesting that the two pathogens activate different immune pathways in THP-1 cells.

4.7 Caspase-4 is activated upstream of NLRP3 and caspase-8 during infection with *S.* Paratyphi A

So far, caspase-4, caspase-8 and NLRP3 have been shown to be involved in pyroptotic cell death triggered during infection with *S.* Paratyphi A 9150, while NAIP-NLRC4 appeared to be dispensable in this process. To delineate whether only and in what order caspase-4, caspase-8 and NLRP3 were required for pyroptosis in *S.* Paratyphi A 9150 infection, these pathways were blocked in various combinations. To this end, CTRL^{miR} or CASP4^{miR} THP-1 cells were treated with Z-IETD-FMK and/or MCC950 prior to infection with *S.* Paratyphi A 9150 and cell death was measured at 3 h post infection. In line with previous observations (Figure 4.13 and Figure 4.18), pharmacological inhibition of caspase-8 or NLRP3 significantly limited *S.* Paratyphi A 9150-induced cell death in CTRL^{miR} THP-1 cells. Furthermore, inhibition of caspase-8 together with NLRP3 reduced pyroptosis by ~35% (Figure 4.19). Z-IETD-FMK and MCC950 treatment combined with the silencing of caspase-4 reduced cell death by ~75% (Figure 4.19). However, inhibition of caspase-8 or NLRP3 in CASP4^{miR} cells did not further reduce cell death than stable silencing of caspase-4 did (Figure 4.19). These results suggest that caspase-4 is activated upstream of caspase-8 and NLRP3. Therefore, together with the importance of ASC in *S.* Paratyphi A 9150-triggered pyroptosis (Figure 4.10), it is concluded that caspase-4 contributed to

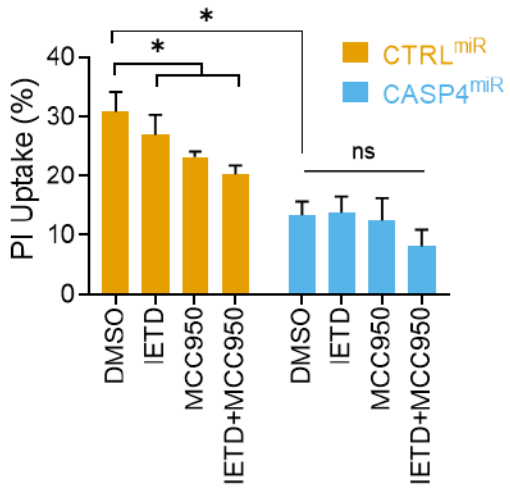


Figure 4.19 **Caspase-4 is activated upstream of NLRP3 and caspase-8 during *S.* Paratyphi A infection.**

CTRL^{miR} or CASP4miR THP-1 cells were infected with S. Paratyphi A 9150 (MOI 50) following treatment with Z-IETD-FMK and/or MCC950. Cell death was determined at 3 h post infection by PI uptake. Graph shows means ± SEM from four independent repeats. Statistical analysis was performed by two-way ANOVA following correction for multiple comparisons. *, $p < 0.05$; ns, not significant.

pyroptosis directly, as well as through non-canonical activation of NLRP3-ASC-caspase-1/caspase-8, while additional pathways are possible also involved.

4.8 Clinical *S.* Paratyphi A isolates induce efficient macrophage cell death and inflammasome activation

It is evident that *S.* Paratyphi A may be activating inflammasomes differently than *S.* Typhi (Figure 4.9, Figure 4.10, Figure 4.13). To ascertain whether the macrophage responses shown above are shared with other *S.* Paratyphi A strains, clinical *S.* Paratyphi A isolates were next tested for their ability to induce macrophage cell death. Five clinical bacterial strains isolated in Nepal (Dolecek ***et al.***, 2008; Arjyal ***et al.***, 2016) were used as a comparison to the prototype *S.* Paratyphi A 9150 strain. As mentioned earlier, one of these strains, ED199, is currently used in human challenge studies with the aim of vaccine development (McCullagh ***et al.***, 2015; Dobinson ***et al.***, 2017).

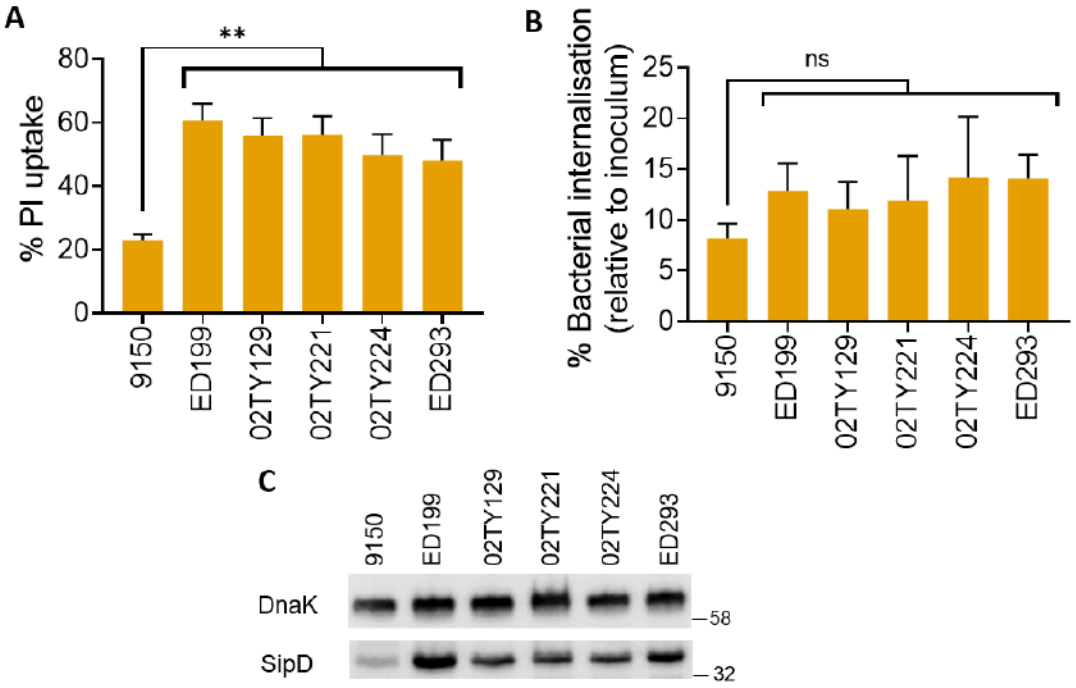


Figure 4.20 **Clinical *S.* Paratyphi A isolates trigger more cell death than 9150.**

(A) THP-1 cells were infected with *S.* Paratyphi A strains as indicated (MOI 50) and cell death was determined at 3 h post infection by PI uptake. **(B)** Z-VAD-FMK-treated THP-1 cells were infected with *S.* Paratyphi A and bacterial internalisation was assessed by gentamicin protection assays at 1.5 h post infection. **(C)** *S.* Paratyphi A strains were grown to late exponential phase and SPI-1 expression was determined by Western blotting for SipD and DnaK as a loading control in bacterial lysates. Blot representative of three independent repeats (samples used are the same as those used in Figure 3.4). Bars show means ± SEM from (A) five or (B) two independent repeats. Statistical analysis compared to *S.* Paratyphi A 9150 by repeated measures one-way ANOVA followed by correction for multiple comparisons. **, $p < 0.01$; ns, not significant.

THP-1 cells were infected with *S.* Paratyphi A and cell death was determined at 3 h post infection. Surprisingly, all five clinical isolates induced significantly higher cell death than 9150 by approximately 3-fold (Figure 4.20A), which is in line with higher invasiveness exhibited by these strains in HeLa cells (see Figure 3.4). Differences in bacterial internalisation by THP-1 cells were not significant between *S.* Paratyphi A clinical isolate strains and the reference strain (Figure 4.20B), indicating that induction of higher cell death was not mediated by higher bacterial uptake of clinical isolates by THP-1 cells. As discussed in Chapter 3, the abundance of SPI-1 proteins in these *S.* Paratyphi A clinical isolates was higher than in *S.* Paratyphi A 9150 (Figure 4.20C), suggesting that SPI-1 activity may be important for inflammasome activation during infection with *S.* Paratyphi A.

To investigate whether increased host cell death caused by *S.* Paratyphi A clinical isolates was associated with increased activation of inflammasome-associated proteins, THP-1 cells were infected with *S.* Paratyphi A and activation of caspase-1, caspase-4 and IL-18 was determined in supernatants of infected cells. Consistent with elevated host cell death, clinical *S.* Paratyphi A isolates induced increased activation of caspase-1, caspase-4 and IL-18 compared to the reference *S.* Paratyphi A 9150

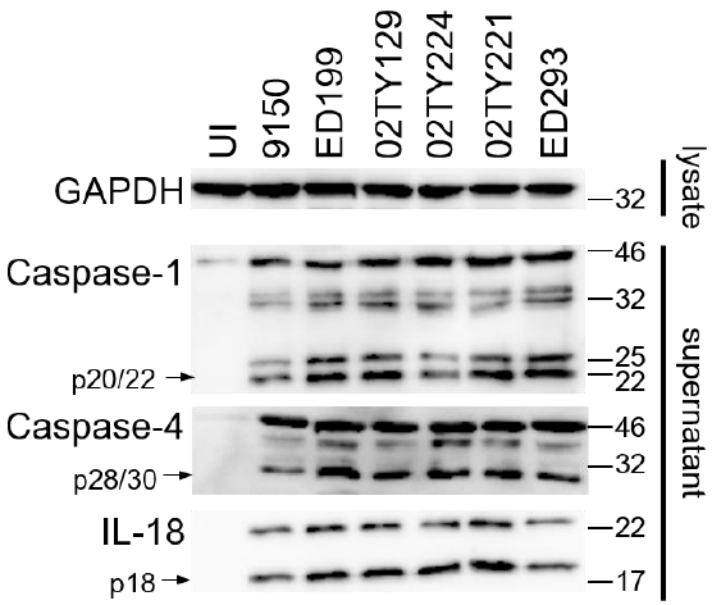


Figure 4.21 **Clinical S. Paratyphi A isolates induce higher levels of inflammasome activation.**

THP-1 cells were infected with S. Paratyphi A as indicated and inflammasome protein cleavage was determined by immunoblotting for the cleaved products in cell supernatants at 3 h post infection. Blot representative of two independent repeats.

strain (Figure 4.21), further supporting the increased immunogenicity of these strains in comparison to *S.* Paratyphi A 9150.

As an additional assessment of inflammasome activation during infection with *S.* Paratyphi A, production of the inflammasome-activated cytokine IL-1β during macrophage infection with clinical *S.* Paratyphi A isolates was assessed over time. All *S.* Paratyphi A strains induced markedly higher levels of IL-1β compared to UI cells, which increased with time (Figure 4.22A). Importantly, clinical *S.* Paratyphi A isolates induced evidently more IL-1β production compared to *S.* Paratyphi A 9150, which reached statistical significance at 3 h post infection (Figure 4.22A).

To determine whether the higher induction of macrophage cell death and inflammasome activation triggered by clinical isolates of *S.* Paratyphi A compared to *S.* Paratyphi A 9150 was due to increased host cell priming, secretion of the inflammasome-independent cytokine TNF was determined over time. As TNF is produced during infection following recognition of PAMPs, TNF was undetectable or detectable at very low levels at 1 h post infection. However, its production increased as infection progressed, and *S.* Paratyphi A 9150 induced the higher production of TNF compared to clinical isolates (Figure 4.22B). This was probably due to the higher cell death triggered by these strains earlier during infection compared to *S.* Paratyphi A 9150, which did not allow sufficient time for host cell priming and production of TNF. *S.* Typhimurium was included as a control given that this serovar induces rapid cell death early during infection. Indeed, infection with *S.* Typhimurium resulted in seemingly lower levels of TNF than *S.* Paratyphi A despite showing higher pyroptotic cell death (Figure 4.22B), supporting the hypothesis that the cells need to be alive to produce TNF. Therefore, it was

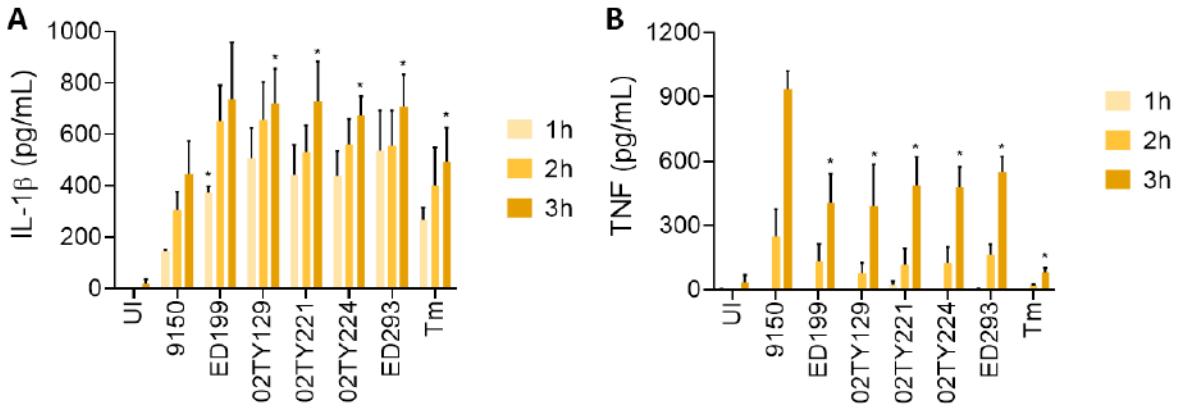


Figure 4.22 **Clinical *S.* Paratyphi A isolates induce higher production of IL-1β compared to 9150.**

THP-1 cells were infected with *S.* Paratyphi A as indicated, as well as *S.* Typhimurium (Tm) as a control and **(A)** IL-1β and **(B)** TNF secretion were monitored over time. Bars show means ± SEM from three independent repeats. Statistical analysis by repeated measures one-way ANOVA at each time point followed by corrections for multiple comparisons; comparisons made to 9150.

concluded that increased host cell priming by clinical *S.* Paratyphi A isolates was not driving increased cell death and inflammasome activation triggered by these compared to *S.* Paratyphi A 9150.

4.9 Clinical *S.* Paratyphi A isolates induce caspase-1/4-, caspase-8- and NLRP3-mediated pyroptosis

Given that clinical *S.* Paratyphi A isolates induced increased pyroptosis in THP-1 cells, it was next investigated whether the underlying mechanism is shared with that of *S.* Paratyphi A 9150. Indeed, Z-VAD-FMK pre-treatment of THP-1 cells prior to infection entirely abolished THP-1 cell death induced by all clinical *S.* Paratyphi A isolates tested (Figure 4.23A). Furthermore, stable silencing of GSDMD blocked cell death in THP-1 cells infected with clinical *S.* Paratyphi A isolates (Figure 4.23B). These results suggested that infection with *S.* Paratyphi A clinical isolates resulted in the same type of cell death induced by *S.* Paratyphi A 9150. As the clinical variants triggered elevated pyroptosis, the effect of caspase blocking (Z-VAD-FMK) or GSDMD silencing on inhibiting cell death in macrophages was more marked compared to *S.* Paratyphi A.

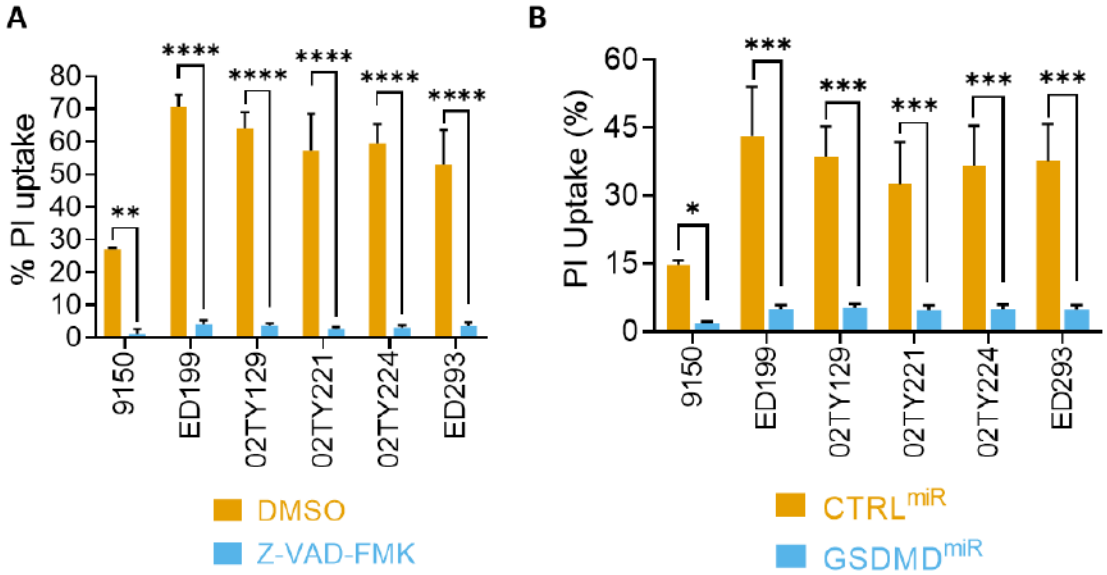


Figure 4.23 **Clinical *S.* Paratyphi A isolates induce caspase-dependent pyroptosis.**

(A) DMSO or Z-VAD-FMK-treated THP-1 cells were infected with *S.* Paratyphi A (MOI 50) as indicated and cell death was determined at 3 h post infection by PI uptake. **(B)** CTRL^{miR} or GSDMD^{miR} THP-1 cells were infected with *S.* Paratyphi A strains and cell death was determined at 3 h post infection. Graph shows means ± SEM from three independent repeats. Statistical analysis was performed by matched two-way ANOVA followed by correction for multiple comparisons. *, $p < 0.05$; **, $p < 0.01$; ***, $p < 0.001$; ****, $p < 0.0001$.

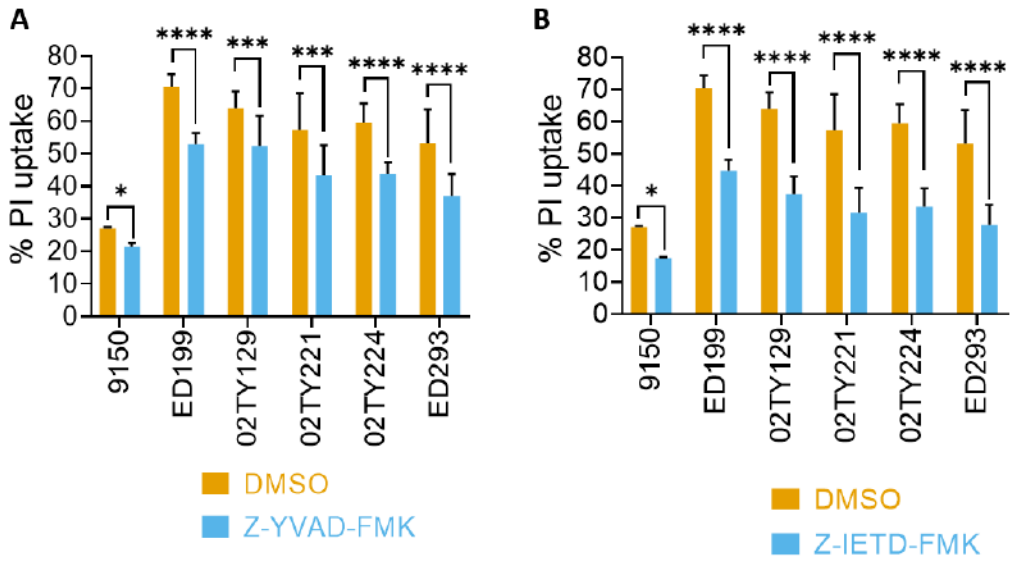


Figure 4.24 **Activation of caspase-4 and caspase-8 is shared among *S*. Paratyphi A strains.**

THP-1 cells pre-treated with DMSO or **(A)** Z-YVAD-FMK or **(B)** Z-IETD-FMK were infected with *S*. Paratyphi A as indicated and cell death was determined at 3 h post infection by PI uptake. Bars show means ± SEM from three independent repeats. Statistical analysis by matched two-way ANOVA followed by correction for multiple comparisons. *, $p < 0.05$; ***, $p < 0.001$; ****, $p < 0.0001$.

Pharmacological inhibition of caspase-4 or caspase-8, by Z-YVAD-FMK and Z-IETD-FMK respectively was next exploited to determine the contribution of these two caspases in pyroptosis during THP-1 infection with clinical *S*. Paratyphi A isolates. Similar to the ~21% reduction in *S*. Paratyphi A 9150-induced pyroptosis upon Z-YVAD-FMK treatment, Z-YVAD-FMK-mediated inhibition of caspase-1/4 significantly reduced pyroptosis induced by all *S*. Paratyphi A strains tested by 18-30% (Figure 4.24A). Caspase-8 inhibition via Z-IETD-FMK treatment of THP-1 cells significantly reduced induction of pyroptosis during infection with all clinical *S*. Paratyphi A strains by 34-47%, similarly to ~35.3% reduction in *S*. Paratyphi A-triggered pyroptosis (Figure 4.24B). These results further suggested that, similarly to inflammasome activation during infection with *S*. Paratyphi A 9150, caspase-4 and caspase-8 are both involved in pyroptosis during infection with other *S*. Paratyphi A strains.

Finally, to investigate whether activation of NLRP3 during macrophage infection with *S*. Paratyphi A was shared within this serovar, MCC950-treated THP-1 cells were infected with *S*. Paratyphi A clinical isolates. Indeed, NLRP3 inhibition significantly reduced pyroptosis induced by all *S*. Paratyphi A clinical variants tested by 23-28% compared to ~34.5% reduction in *S*. Paratyphi A 9150-induced pyrotptosis (Figure 4.25). These results collectively suggested that the mechanisms triggering pyroptosis in THP-1 cells are shared between *S*. Paratyphi A strains, where caspase-4, caspase-8 and NLRP3 contributed to *S*. Paratyphi A-induced pyroptosis.

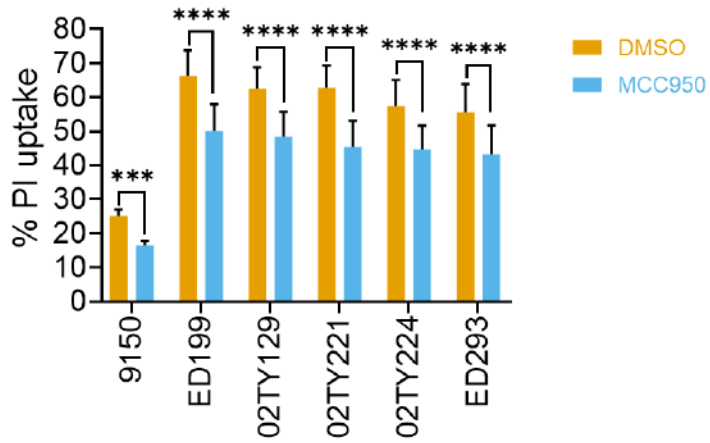


Figure 4.25 ***S.* Paratyphi A clinical isolates induce NLRP3-dependent cell death.**

DMSO or MCC950-treated THP-1 cells were infected with S. Paratyphi A as indicated and cell death was measured at 3 h post infection. Graph shows means ± SEM from three independent repeats and were statistically analysed by two-way ANOVA followed by correction for multiple comparison. ***, $p < 0.001$; ****, $p < 0.0001$.

4.10 *S.* Typhi induces SPI-1-dependent, Vi-independent macrophage cell death

So far, host-driven mechanisms underlying inflammasome activation were determined; therefore, investigation into how *S.* Typhi and *S.* Paratyphi A modulate cell death in human macrophages was next explored.

As previously mentioned, *S.* Typhi Ty2-induced pyroptosis required an active SPI-1 T3SS. On the other hand, the *S.* Typhi Vi capsule has been suggested to be involved in immune evasion mechanisms in different ways. One of them is via the regulatory protein TviA, which has been implicated in limiting inflammasome-mediated pyroptosis during *S.* Typhi infection (Winter et al., 2015). The mechanism underlying this reduction in pyroptosis has been suggested to be TviA-mediated flagellin downregulation; the actual capsule appears to have limited role in interfering with inflammasome activation in human macrophages (Winter et al., 2015). The necessity of SPI-1 in inducing pyroptosis and the requirement of the presence of the capsule in limiting induction of cell

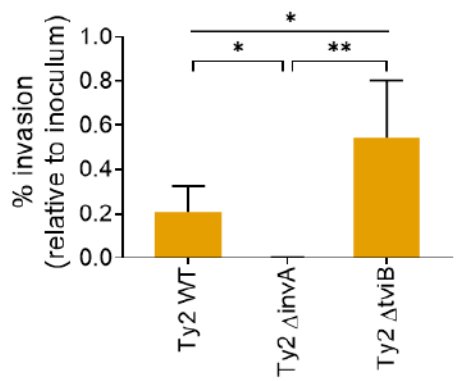


Figure 4.26 **The Vi capsule of *S.* Typhi limits epithelial cell invasion.**

HeLa cells were infected at MOI 100 with S. Typhi WT, Δ*invA* or Δ*tviB* and invasion was assessed at 2 h post infection via gentamicin protection assay and CFU enumeration. Bars show means ± SEM from three independent repeats. Statistical analysis by repeated measures one-way ANOVA. *, $p < 0.05$; **, $p < 0.01$.

death during macrophage infection with *S.* Typhi were next investigated. To this end, cells were infected with *S.* Typhi Δ*invA*, which is unable to secrete in a T3SS-dependent manner, or a Vi mutant *S.* Typhi Δ*tviB* which lacks the Vi capsule structural *tviB* gene and is thus unable to assemble the capsule on the bacterial surface (Virlogeux et al., 1995; Zhang et al., 2006). The role of the Vi was also tested, as the report by Winter *et al.* (2015) used conditions that were not SPI-1-inducing and examined inflammasome activation at later time points than those tested here.

Initially, to model whether the Vi capsule interferes with interactions with host cells, as has been previously reported (Raffatellu *et al.*, 2005a), the invasiveness of Δ*tviB* was assessed in HeLa cells by gentamicin protection assays. Consistent with previous findings (Johnson *et al.*, 2017), *S.* Typhi Ty2 invaded HeLa cells in a SPI-1 T3SS-dependent manner, as *S.* Typhi Ty2 Δ*invA* was unable to invade host epithelial cells (Figure 4.26). In contrast, *S.* Typhi Ty2 Δ*tviB* invaded HeLa cells significantly more than its WT counterpart (Figure 4.26), suggesting that the capsule had an impact on the interactions between *S.* Typhi and host cells, in keeping with previous reports (Bishop *et al.*, 2008). The absence of the capsule possibly allows the SPI-1 T3SS to more efficiently reach the host cells and mediate invasion.

THP-1 cells were then infected with *S.* Typhi WT, Δ*invA* or Δ*tviB*. Deletion of *invA* in *S.* Typhi Ty2 prevented induction of cell death in THP-1 cells (Figure 4.27A). Bacterial internalisation into THP-1 cells was not statistically different between WT *S.* Typhi Ty2 and Δ*invA* (Figure 4.27B). These results

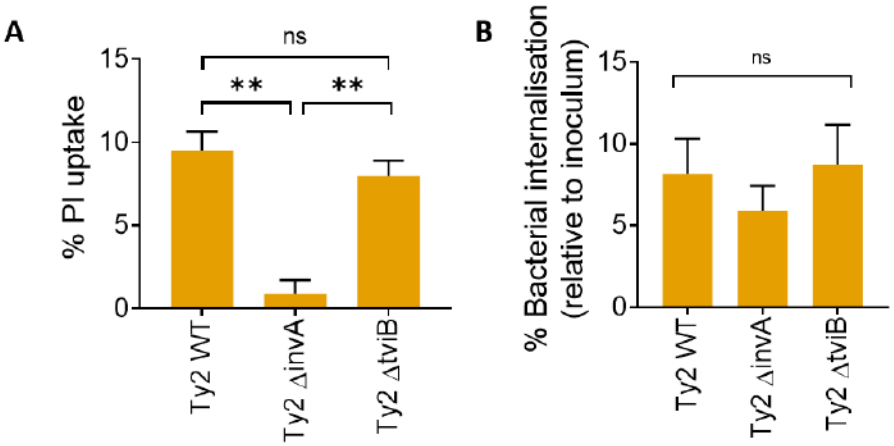


Figure 4.27 ***S.* Typhi induces SPI-1-dependent, Vi capsule-independent macrophage cell death.**

(A) THP-1 cells were infected with *S.* Typhi Ty2 (Ty2; MOI 15) as indicated. Cell death was measured at 3 h post infection via PI uptake. **(B)** Bacterial internalisation in THP-1 cells was determined via gentamicin protection assays at 1.5 h post infection in Z-VAD-FMK-treated cells. Bars show means ± SEM from (A) four or (B) five independent repeats. Statistical analysis by repeated measures one-way ANOVA for the indicated comparisons, after correction for multiple comparisons. **, $p < 0.01$; ns, not significant.

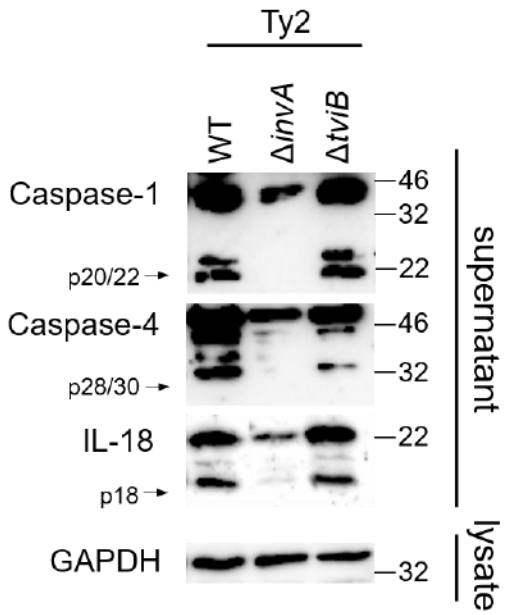


Figure 4.28 **The role of the Vi antigen during infection of THP-1 cells with *S*. Typhi.**

THP-1 cells were infected with S. Typhi Ty2 (Ty2; MOI 15) as indicated and activation of caspase-1, caspase-4 and IL-18 was determined via immunoblotting. Uninfected cells control is the same as in Figure 4.40. Arrows show cleaved products of caspase-1, caspase-4 and IL-18. Immunoblot representative of three independent repeats.

suggested SPI-1 was required for pyroptosis induction during THP-1 infection with *S.* Typhi Ty2, but *S.* Typhi Ty2 did not actively invade macrophages. Furthermore, lack of a functional SPI-1 T3SS rendered *S.* Typhi Ty2 unable to induce inflammasome activation in THP-1 cells (Figure 4.28). On the other hand, infection with *S.* Typhi Ty2 Δ*tviB* resulted in cell death (Figure 4.27A) and internalisation levels (Figure 4.27B) similar to those induced by its WT counterpart, suggesting that the Vi capsule did not play a role in modulating cell death in these settings. In support of this, *S.* Typhi Ty2 Δ*tviB* triggered similar levels of inflammasome activation in comparison to WT (Figure 4.28). Although caspase-4 cleavage was moderately lower during infection with *S.* Typhi Ty2 Δ*tviB*, pyroptosis was not influenced in CASP4^{miR} compared to CTRL^{miR} THP-1 cells (not shown).

Many immune mediators and immune sensors are present in the cytosol, including those involved in inflammasome activation. Therefore, bacterial escape from the vacuole to the cytosol was also determined. This was tested by a gentamicin and chloroquine-based assay; gentamicin targets bacteria that are not enclosed within a membrane (i.e. extracellular bacteria), while chloroquine kills vacuolar bacteria. In this way the assay allows quantification of cytosolic bacteria which, in combination with gentamicin-resistant bacteria, allows the fractions of intracellular bacterial populations can to calculated (Knodler, Nair & Steele-Mortimer, 2014; Goddard ***et al.***, 2019). This assay was performed in GSDMD^{miR} THP-1 cells to eliminate variation in recovered CFUs due to differences in cell death induction by different strains. The numbers of cytosolic *S.* Typhi Δ*invA* did not differ from those of WT at either 1.5 h or 3 h post infection (Figure 4.29A-B). Furthermore, in line with the lack of a role in interfering with pyroptosis, *S.* Typhi Ty2 Δ*tviB* escaped to the cytosol at similar rates to that of WT *S.* Typhi Ty2 (Figure 4.29A-B).

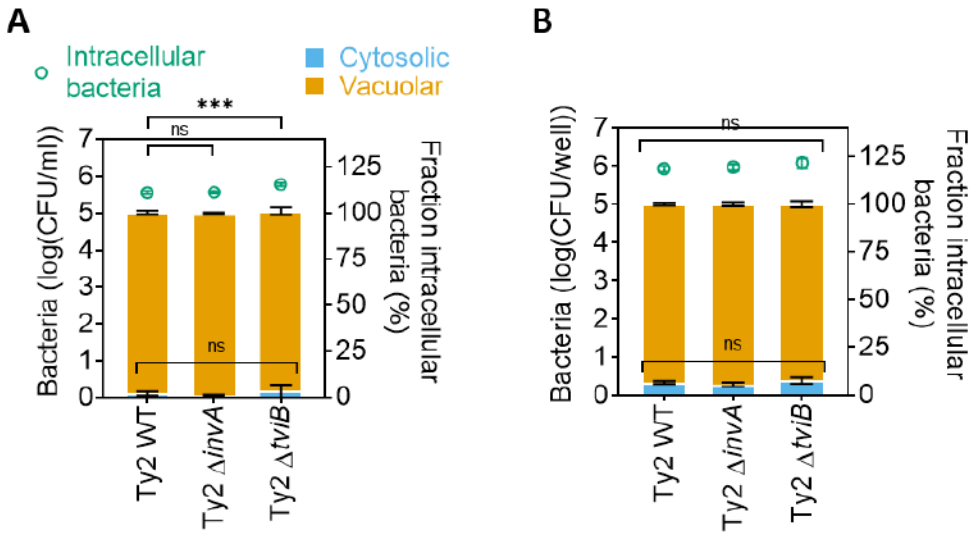


Figure 4.29 *S.* Typhi escapes to the cytosol independently of SPI-1 T3SS and the Vi capsule.

GSDMD^{miR} THP-1 cells were infected with S. Typhi Ty2 (Ty2; MOI 15) as indicated. Bacterial internalisation (left-axis) and the fraction of cytosolic escape as measured by chloroquine-resistance assay (right-axis) at **(A)** 1.5 h and **(B)** 3 h post infection. Graphs show means ± SEM from (A) six or (B) three independent repeats. Statistical analysis by repeated measures one-way ANOVA on the different data subsets. *, $p < 0.05$; **, $p < 0.01$; ***, $p < 0.001$; *ns*, not significant.

The low induction of cell death by *S.* Typhi Ty2 raised the possibility that macrophages are not primed at sufficient levels by these bacteria to induce expression of inflammasome components responsible for triggering pyroptosis. Low host cell priming may be exploited by *S.* Typhi as an immune evasion strategy. To test this hypothesis, THP-1 cells were primed with *E. coli* O111:B4 LPS prior to infection with WT *S.* Typhi Ty2 or *S.* Typhi Ty2 Δ*tviB*. Δ*tviB* was used to examine whether bacterial components become more readily available for recognition once the protective capsule is removed and host cells express immune sensors at high levels following LPS-mediated priming. However, LPS priming of THP-1 cells prior to infection with *S.* Typhi Ty2 did not result in increased host cell death during infection with neither WT nor Δ*tviB* (Figure 4.30A), indicating that inhibition of pro-inflammatory pathways may not be the mechanism followed by *S.* Typhi Ty2.

To independently investigate whether *S.* Typhi-mediated host cell priming differs between the strains tested, THP-1 cells were infected with *S.* Typhi Ty2 and secretion of the inflammasome-independent cytokine TNF was determined at 3 h post infection. TNF secretion was similar between *S.* Typhi Ty2 WT, Δ*invA* and Δ*tviB* (Figure 4.30B), further supporting that SPI-1-depedent cell death was mediated by the activity of SPI-1 T3SS and not by differences in host cell priming.

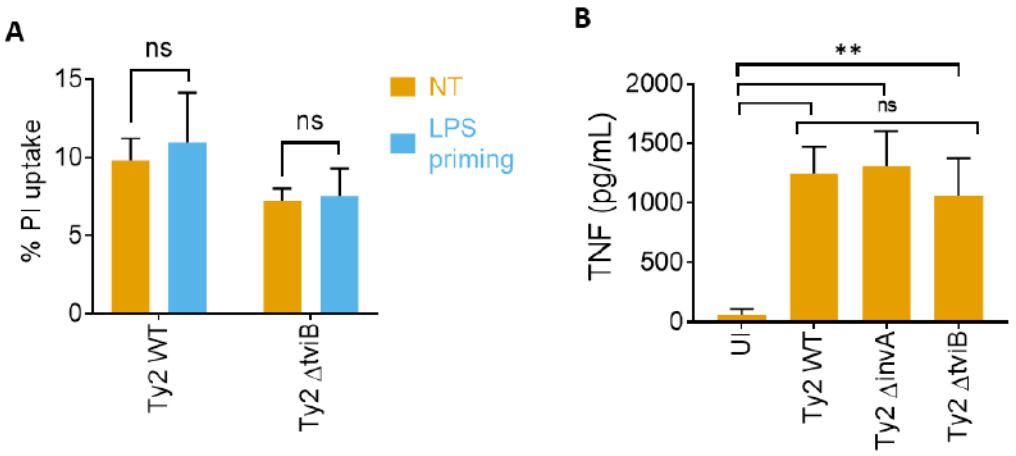


Figure 4.30 **Host cell priming does not affect *S.* Typhi-induced cell death.**

(A) THP-1 cells either received no treatment (NT) or primed with *E. coli* O111:B4 LPS before infection with S. Typhi Ty2 (Ty2; MOI 15) WT or Δ*tviB*. Cell death was determined at 3 h post infection by PI uptake. **(B)** THP-1 cells were infected with as indicated and TNF production was quantified by ELISA at 3 h post infection. Uninfected (UI) cells were used as a control. Bars show means ± SEM from (A) four or (B) three independent repeats. Statistical analysis by (A) matched two-way ANOVA or (B) repeated measures one-way ANOVA following correction for multiple comparisons. *, $p < 0.05$; **, $p < 0.01$; ns, not significant.

Given the SPI-1 T3SS-dependent induction of cell death by *S.* Typhi Ty2, it was next assessed whether inflammasome assembly is also induced in this manner. ASC-dependent inflammasome assembly can be visualised as ASC-specks by microscopy of fluorescently tagged ASC (ASC^{mRFP} THP-1 cells). ASC specks were observed in significantly higher numbers in cells infected with *S.* Typhi compared to uninfected cells (Figure 4.31A-B), confirming that *S.* Typhi was able to induce formation of ASC specks in infected cells. Importantly, infection with *S.* Typhi Ty2 triggered SPI-1 T3SS-dependent formation of ASC specks in THP-1 cells (Figure 4.31B). Although the percentage of infected cells was not quantified, ASC specks were not formed in all infected cells (see also Figure 4.3), but the percentage of cells with ASC specks correlated with the percentage of cell death determined by PI uptake. To investigate whether the ASC specks formed here were mediated by the NLRP3, ASC^{mRFP} cells were treated with MCC950 prior to infection with *S.* Typhi. However, MCC950-mediated inhibition of NLRP3 did not result in lower numbers of ASC specks being formed (Figure 4.31C), in line with the lack of a major role of NLRP3 during *S.* Typhi infection (Figure 4.13), and indicating at another activated inflammasome pathway.

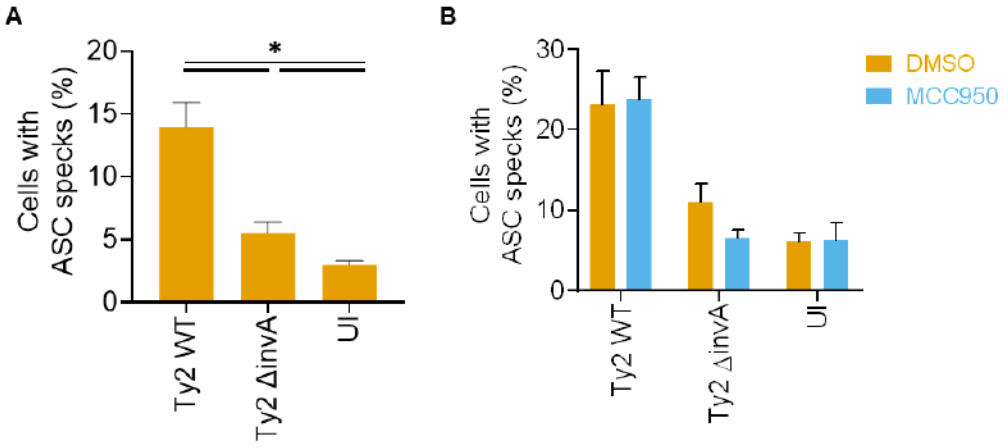


Figure 4.31 ***S.* Typhi induces SPI-1 T3SS-dependent ASC speck formation.**

(A) ASC^{mRFP} THP-1 cells were infected with *S.* Typhi Ty2 (Ty2; MOI 15) as indicated. **(B)** DMSO or MCC950-treated ASC^{mRFP} THP-1 cells were infected with *S.* Typhi Ty2. Cells with ASC specks were enumerated by fluorescent microscopy by counting > 120 cells from randomly selected slide fields per repeat. Graphs show means ± SEM from (A) four or (C) three independent repeats. Statistical analysis by (A) repeated measures one-way ANOVA or (B) matched two-way ANOVA. (A) was conducted together with Figure 4.47 and (B) was performed in conjunction with Figure 4.48; UI controls are shared between panels and statistical analysis was performed on all experimental conditions in each case. *, $p < 0.05$; ns, not significant.

Collectively, these results suggest that *S.* Typhi Ty2 is internalised by host cells and then escapes to the cytosol in a SPI-1-independent manner. However, cell death and ASC speck formation require a functional SPI-1 T3SS.

4.11 The role of *S.* Typhi-specific T3SS effector protein StoD in early host cell death

As the Vi antigen was not responsible for the moderate cell death levels induced by *S.* Typhi Ty2 in these settings, the role of another *S.* Typhi-specific virulence factor in host cell death was next tested. Recently identified by our laboratory, StoD is present in *S.* Typhi and absent from *S.* Typhimurium and *S.* Paratyphi A (Johnson, Mylona & Frankel, 2018). StoD is a homologue of the T3SS-dependent NleG proteins in EPEC and EHEC, which harbour a C-terminal region resembling the C-terminal U-box of eukaryotic E3 ubiquitin ligase and a N-terminal domain hypothesised to mediate substrate recognition and interaction (McDowell *et al.*, 2019; Wu *et al.*, 2010; Valleau *et al.*, 2018). However, the function of these proteins remains largely unknown.

It was confirmed that this effector is T3SS-dependent by performing a translocation and a secretion assay in *S.* Typhimurium. *S.* Typhimurium is a good model for this purpose compared to *S.* Typhi due to the higher efficiency in secretion and translocation; the latter could not be performed

successfully with *S.* Typhi using the same conditions possibly due to the already low levels of SPI-1 expression in *S.* Typhi. Using a WT and a Δ*prgH S.* Typhimurium strain expressing C-terminally tagged *S.* Typhi Ty2 StoD, it was shown that StoD was secreted in a SPI-1 T3SS-dependent manner, as it was secreted by the WT while it was absent from the supernatant of *S.* Typhimurium Δ*prgH* (Figure 4.32A). The non-secreted DnaK chaperone was used as a loading control, while the SPI-1 T3SS protein SipD was used as a positive control.

To corroborate whether StoD is efficiently translocated to host cells, a C-terminal fusion of StoD to TEM-1 expressed from a pWSK29 derivative plasmid was introduced into *S.* Typhimurium WT and Δ*prgH*Δ*ssaV*, a double SPI-1/SPI-2 T3SS mutant. As TEM-1 is an enzyme catabolising β-lactam-like

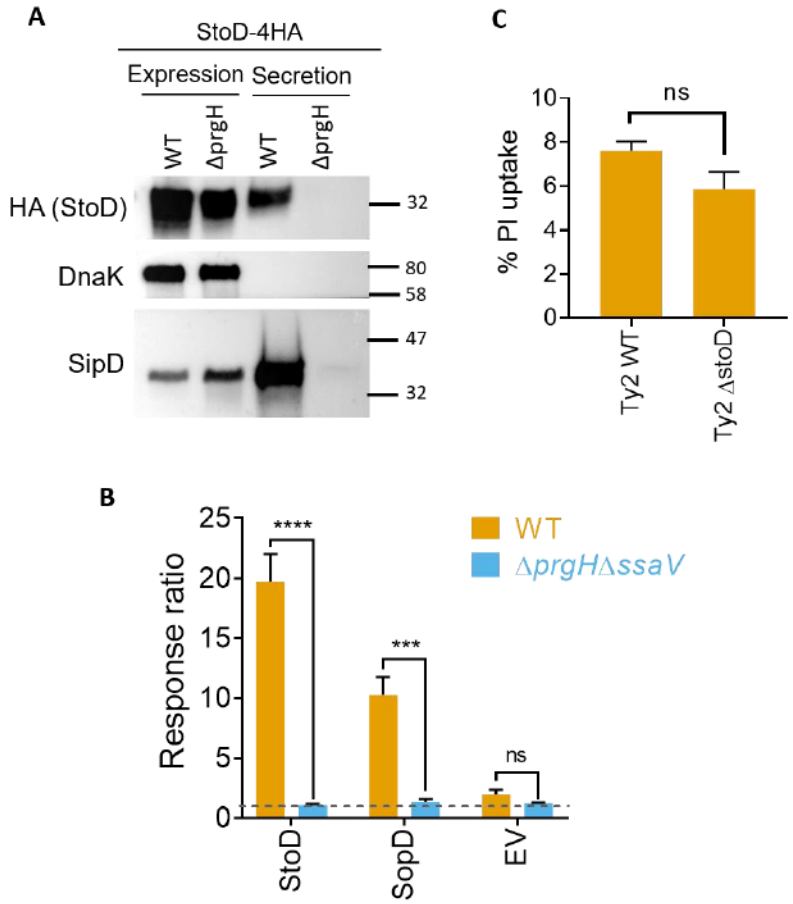


Figure 4.32 **StoD is a T3SS-dependent effector not involved in *S.* Typhi-induced early host cell death.**

(A) HeLa cells were infected at MOI 100 with *S.* Typhimurium WT or Δ*prgH*Δ*ssaV* expressing Ty2 StoD or, SopD as a control, fused to TEM1 and protein translocation was measured at 3 h post infection. **(B)** *S.* Typhimurium WT or Δ*prgH* expressing StoD-4HA was grown to SPI-1-inducing conditions and protein secretion via the SPI-1 T3SS was assessed by Western blotting. Image representative of two independent repeats. **(C)** THP-1 cells were infected with *S.* Typhi Ty2 WT or Δ*stoD* (MOI 15) and cell death was measured via PI uptake at 3 h post infection. Bars show means ±SEM from three independent repeats. Statistical analysis by (A) matched two-way ANOVA or (C) paired Student's *t*-test. ***, $p < 0.001$; ****, $p < 0.0001$; ns, not significant.

ampicillin, the derivative plasmid carried a spectinomycin resistance gene (Johnson *et al.*, 2017) instead of an ampicillin resistance gene which was previously used to test translocation of this effector (Byrne, 2017). The reason for this was to eliminate any β-lactamase, the product of the ampicillin-resistance gene on the plasmid, cleaving the substrate administered to cells during the assay. Empty vector (EV) carrying only the TEM-1 enzyme was used as a negative control, while *S.* Typhimurium expressing the SopD-TEM-1 fusion was used as a positive control, as SopD is expected to be translocated in a T3SS-dependent manner. Translocation of StoD into HeLa cells was completely abrogated by the Δ*prgH*Δ*ssaV* mutant compared to its WT counterpart, confirming StoD was translocated to HeLa cells during infection with *S.* Typhimurium in a T3SS-dependent manner (Figure 4.32B).

The role of StoD during infection remains unknown (McDowell *et al.*, 2019). It was tested herein whether it was involved in moderating *S.* Typhi-induced host cell death. However, loss of StoD did not lead to any significant difference in THP-1 cell death triggered by *S.* Typhi Ty2 compared to its WT counterpart, at least within this infection time frame (Figure 4.32C). Nevertheless, the small, although not significant, reduction in cell death may indicate a role in limiting cell death at later time points that were not within the scope of this project and may warrant further investigation in the future.

4.12 *S.* Typhi H58 triggers similar levels of pyroptosis compared to non-H58 strains

S. Typhi H58 clinical isolates have been shown to exhibit amplified virulence compared to *S.* Typhi Ty2 (Johnson *et al.*, 2018). Two clinical isolate strains belonging to genotype H58 (ERL12148 and 129-0238) available in our laboratory were used to test for differences in induction of macrophage cell death between *S.* Typhi Ty2 and clinical isolates. Interestingly, while bacterial internalisation by THP1 cells was similar between *S.* Typhi strains (Figure 4.33A), *S.* Typhi ERL12148 caused similar levels of cell death compared to Ty2, while 129-0238 was unable to cause pyroptosis to similar levels to those induced by *S.* Typhi Ty2 and was more similar to *S.* Typhi Δ*invA* (Figure 4.33B). However, assessment of the levels of SipD in bacterial lysates grown to late exponential phase revealed that the inability of *S.* Typhi 129-0238 was possibly mediated by very low levels of SPI-1 protein expression (Figure 4.33C). These results further support the serovar-wide importance of SPI-1 in *Salmonella*-induced cell death in host macrophages.

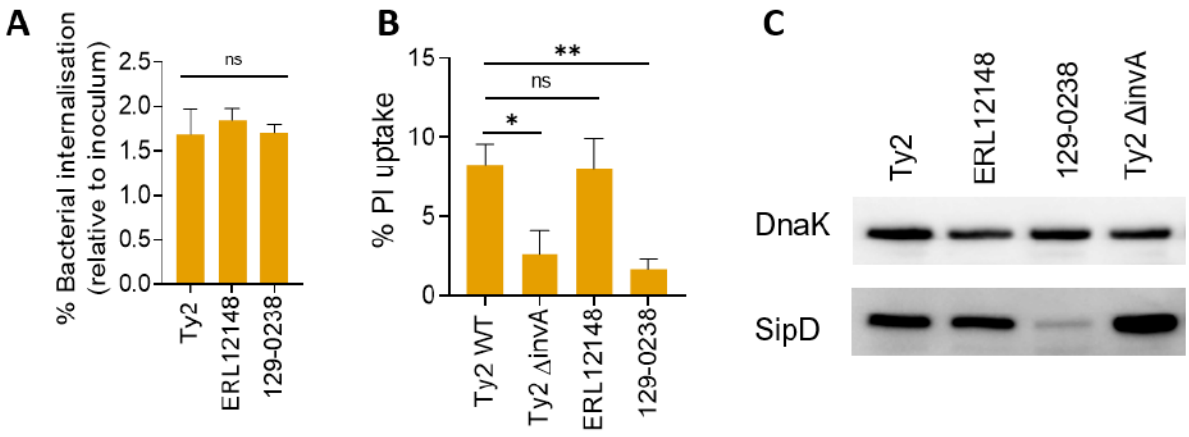


Figure 4.33 ***S.* Typhi H58 clinical isolates cause similar cell death in comparison to *S.* Typhi Ty2, depending on the levels of SPI-1 expression.**

(A) Z-VAD-FMK-treated THP-1 cells were infected with *S.* Typhi strains as indicated and bacterial internalisation was determined at 1.5 h post infection. **(B)** THP-1 cells were infected with *S.* Typhi and cell death was determined at 3 h post infection by PI uptake. **(C)** *S.* Typhi was grown to late exponential phase and SPI-1 expression was assessed by western blotting against SipD. Blot representative of three independent repeats. Bars indicate means ± SEM from (A) three or (B) six independent repeats. Statistical analysis by repeated measures one-way ANOVA. *, $p < 0.05$; **, $p < 0.01$; ns, not significant.

The *S.* Typhi strains belonging to H58 tested so far did not indicate an enhanced virulence in terms of inflammasome activation compared to *S.* Typhi Ty2. To test whether *S.* Typhi H58 (genotype 4.3.1) was more virulent than another circulating *S.* Typhi genotype (genotype 3.3) that circulates in endemic regions, several clinical isolates were obtained from our collaborator Stephen Baker. During a visit in the Oxford University Clinical Research Unit (OUCRU) in Vietnam, seventeen *S.* Typhi clinical isolates belonging to H58 and four clinical isolates belonging to genotype 3.3 (Pham, 2018) were used to infect THP-1 cells (Table 2.2). The median percentage value of cell death triggered by strains belonging to genotype 3.3 was lower than that of H58 clinical isolates; however this difference was not statistically significant (Figure 4.34A). Similarly, the median value of bacterial internalisation by THP-1 cells was statistically indistinguishable between *S.* Typhi H58 and genotype 3.3 strains (Figure 4.34B). A higher bacterial internalisation did not necessarily correlate with a higher cell death (compare symbol colours in Figure 4.34A and B). Also, SPI-1 expression was comparable between all strains (Figure Appendix.2). The individual values of PI uptake and bacterial internalisation by each strain are shown in Figure Appendix.2. Direct comparisons of these strains to *S.* Typhi Ty2 could not be made, as this strain was not available in OUCRU. Nevertheless, although more strains are required to draw conclusions (particularly more of genotype 3.3 or other non-H58) the comparable virulence of H58 strains to that of those belonging to other genotypes may further exemplify the requirement for

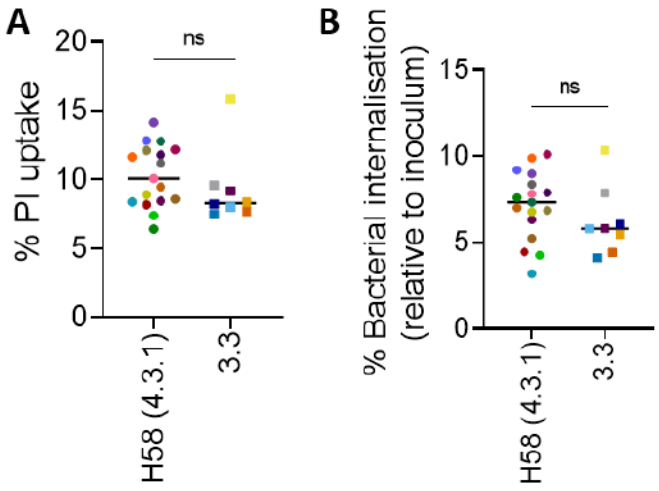


Figure 4.34 ***S.* Typhi H58 clinical isolates cause similar levels of cell death compared to *S.* Typhi genotype 3.3.**

THP-1 cells were infected with *S.* Typhi strains belonging to H58 or genotype 3.3 grown under microaerobic conditions to stationary phase, **(A)** cell death was determined at 3 h post infection by PI uptake and **(B)** bacterial internalisation at 1.5 h post infection. Each symbol represents the average mean from three biological repeats of cell death caused by each strain. Experiments were performed in two batches, where the same four genotype 3.3 strains were tested as a comparison and therefore each strain is represented by two squares. Lines show the median value of each genotype and symbol colour match the strains between the two panels. Statistical analysis by unpaired Student's *t*-test. These experiments were performed in OUCRU, Vietnam. ns, not significant.

immune evasion by *S.* Typhi, which also show that the success of *S.* Typhi H58 does not rely on more efficient immune evasion strategies compared to non-H58 *S.* Typhi.

4.13 SPI-1 T3SS overexpression leads to increased cell death during *S.* Paratyphi A infection

The next aim was to investigate how *S.* Paratyphi A modulates pyroptosis during infection of human macrophages. Comparison of SPI-1 T3SS protein expression between *Salmonella* serovars Typhi, Paratyphi A and Typhimurium shown in Figure 3.3, indicates that *S.* Paratyphi A 9150 expresses SPI-1 T3SS markedly lower than the other two serovars. Also, *S.* Paratyphi A 9150 WT invaded HeLa cells at very low levels (Figure 3.3). Therefore, it was hypothesised that reduced expression of SPI-1 proteins in *S.* Paratyphi A 9150 may be responsible for the lower cytotoxicity and ability to induce inflammasome activation, which is also supported by the data obtained with clinical isolates of *S.* Paratyphi A (Figure 4.20). To test this, the *hilA* gene, encoding for the positive regulator of SPI-1 T3SS HilA, was introduced on a plasmid under the control of a constitutive promoter into *S.* Paratyphi A WT and Δ*invA* as a control. HilA-mediated upregulation of SPI-1 T3SS-dependent proteins was confirmed

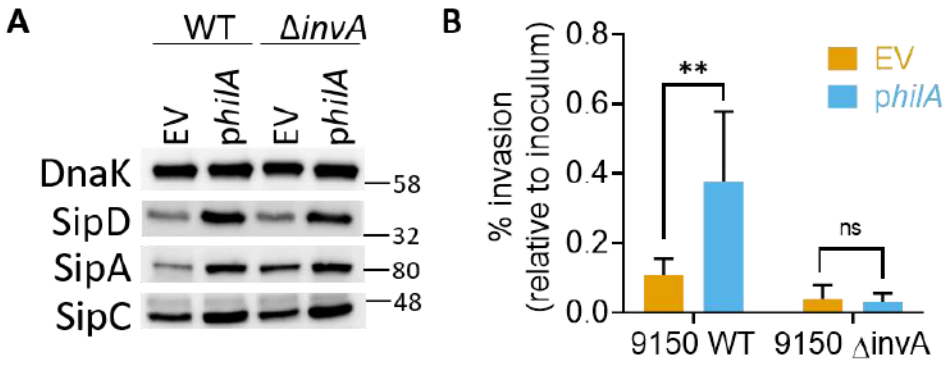


Figure 4.35 **Overexpression of SPI-1 T3SS expression induces higher epithelial cell invasion by *S.* Paratyphi A 9150.**

(A) *S.* Paratyphi A 9150 WT or Δ*invA* carrying an empty vector (EV) or a plasmid expressing *hilA* were grown to late exponential phase and abundance of SPI-1 proteins was determined via Western blotting in bacterial pellets. DnaK was used as a loading control. Immunoblot representative of two independent experiments. **(B)** HeLa cells were infected at MOI 100 with *S.* Paratyphi A 9150 WT or Δ*invA* as indicated and CFUs were enumerated at 2 h post infection via gentamicin protection assays. Bars show mean ± SEM from four independent repeats. Statistical analysis by matched two-way ANOVA. **, $p < 0.01$; ns, not significant.

by blotting against SPI-1 proteins in pellets of bacteria grown under SPI-1-inducing conditions. The abundance of SipD, SipA and SipC was markedly increased when HilA was introduced in WT and Δ*invA* *S.* Paratyphi A 9150 strains (Figure 4.35A). As a proof of concept, the invasiveness of these strains into HeLa cells was tested. As expected, and in correlation with the SPI-1 protein expression, when HilA was introduced into *S.* Paratyphi A 9150 WT, this became significantly more invasive compared to the counterpart strain carrying a pWSK29 empty vector (EV) (Figure 4.35B). This increase in invasiveness was not observed in the Δ*invA* mutant, confirming that this increase is mediated by HilA in a SPI-1 T3SS-dependent manner (Figure 4.35B). These observations also confirm that HilA has similar regulatory roles in *S.* Paratyphi A to these reported for *S.* Typhimurium, namely that HilA acts as a positive SPI-1 regulator, in line with previous reports (Elhadad ***et al.***, 2016).

Next, the effect of SPI-1 overexpression in *S.* Paratyphi A 9150 on THP-1 macrophage cell death was determined. Consistent with the hypothesis and the HeLa cell invasion results (Figure 4.35B), *S.* Paratyphi A 9150 WT expressing HilA on a plasmid induced significantly higher cell death levels in THP-1 compared to WT carrying the EV (Figure 4.36A). As a control, THP-1 cells were also infected with *S.* Paratyphi A 9150 Δ*invA* carrying EV or the HilA-expressing plasmid. HilA overexpression did not increase cell death levels induced by Δ*invA*, further corroborating that this phenotype is mediated by HilA-mediated SPI-1 overexpression. This increase in cell death induction by *S.* Paratyphi A 9150 when HilA was overexpressed was largely mediated by higher levels of bacterial internalisation by THP-1 cells (Figure 4.36B). This indicates that higher cell death is the result of increased bacterial numbers

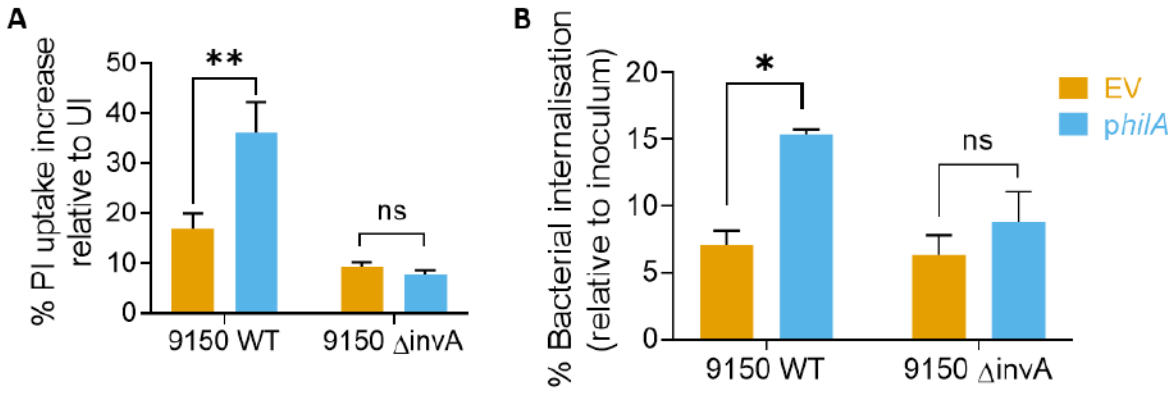


Figure 4.36 **Overexpression of SPI-1 T3SS results in elevated THP-1 cell death and bacterial internalisation during infection with *S.* Paratyphi A 9150.**

(A) THP1 cells were infected with *S.* Paratyphi A (MOI 50) with WT or Δ*invA* carrying an empty vector (EV) or expressing *hilA* on a plasmid. Cell death was measured by PI uptake at 3 h post infection. **(B)** Bacterial internalisation was determined in Z-VAD-FMK-treated THP-1 cells at 1.5 h post infection via a gentamicin protection assay. Bars show means ± SEM from three independent repeats. Statistical analysis by matched two-way ANOVA. *, $p < 0.05$; **, $p < 0.01$; ns, not significant

that are internalised, as *S.* Paratyphi A 9150 expressing SPI-1 T3SS proteins at higher levels is arguably better equipped to actively invade macrophages rather than being phagocytosed by host-mediated and/or SPI-1-independent mechanisms. This was also suggested by the results obtained with *S.* Typhimurium which both expresses higher SPI-1 and induced cell death at increased levels (Sections 3.3 and 4.1). These results indicate that, while *S.* Paratyphi A 9150 is able to potentially express SPI-1 proteins at high levels and SPI-1 T3SS is implicated in triggering pyroptosis, *S.* Paratyphi A 9150 limits expression of SPI-1 possibly as an immune evasion mechanism.

4.14 *S.* Paratyphi A induces SPI-1 T3SS-dependent cell death and inflammasome activation, which is restricted by very long LPS O-antigen chains

SPI-1 T3SS is necessary for inflammasome activation during *S.* Paratyphi A 9150 infection and the low levels of macrophage cell death induced by *S.* Paratyphi A 9150 were nevertheless SPI-1 dependent (Figure 4.2A). The next aim was thus to understand how *S.* Paratyphi A 9150 limits the induction of host cell death. *S.* Paratyphi A does not carry SPI-7 which encodes for the Vi antigen like *S.* Typhi (Bueno *et al.*, 2004). Instead, it produces very long O-antigen chains, which have been suggested to be involved in evading the respiratory burst triggered by neutrophils during infection with *S.* Paratyphi A (Hiyoshi *et al.*, 2018b). The underlying mechanism has been suggested to be interference with antibody-mediated recognition of the O-antigen and surface molecules (Hiyoshi *et al.*, 2018b). It was

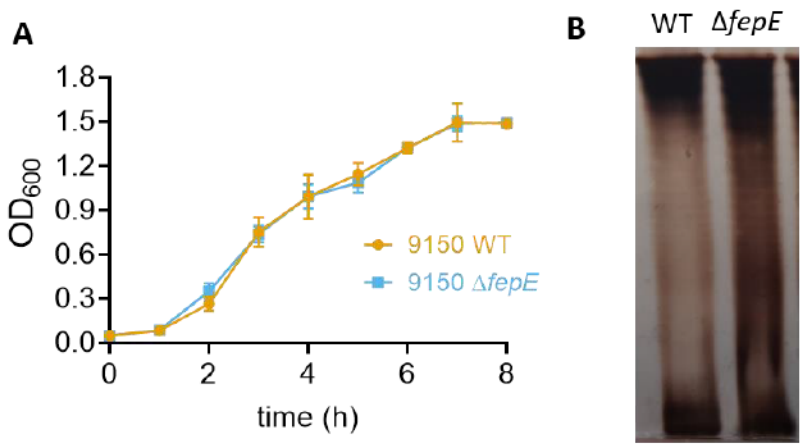


Figure 4.37 **Deletion of *fepE* does not impact bacterial growth.**

(A) *S.* Paratyphi A 9150 WT and Δ*fepE* were grown in standard LB media and optical density at 600 nm (OD_{600}) was monitored over time. Bars show means ± SEM from two independent repeats. **(B)** LPS was extracted from *S.* Paratyphi A WT and Δ*fepE*, separated by SDS-PAGE and silver stained. Stained acrylamide gel showing electrophoretic LPS mobility representative of three independent repeats.

thus hypothesised that very long O-antigen chains may impact on interactions of *S.* Paratyphi A with host cells and induction of macrophage cell death. To this end, an O-antigen chain length regulator, the polysaccharide co-polymerase FepE, was deleted in *S.* Paratyphi A 9150. Deletion of ***fepE*** did not affect growth of bacteria in standard LB media (Figure 4.37A). Reduced production of very long O-antigen polysaccharide polymers and altered LPS profile in *S.* Paratyphi A 9150 Δ***fepE*** compared to WT was confirmed by silver staining of total LPS (Figure 4.37B).

The effect of ***fepE*** deletion on interactions of *S.* Paratyphi A 9150 with epithelial cells was tested by assessing HeLa cell invasion. As shown earlier in Chapter 3, and as has been reported by Elhadad ***et al.*** (2016) following microaerobic growth, *S.* Paratyphi A 9150 invaded HeLa cells in a SPI-1 T3SS-dependent manner as indicated by the fact that Δ*invA* was unable to invade HeLa cells to the same levels as its WT counterpart (Figure 4.39). *S.* Paratyphi A Δ***fepE*** invasion into HeLa cells was ~6-fold higher than the parental WT (Figure 4.39). This suggests that, similar to loss of the Vi antigen, when very long O-antigen chains cannot be formed, *S.* Paratyphi A can invade host cells more efficiently. This may be due to better proximity of the SPI-1 T3SS to the host cell surface, as has been suggested for the *Shigella sonnei* T3SS when its capsule is absent (Watson ***et al.***, 2019).

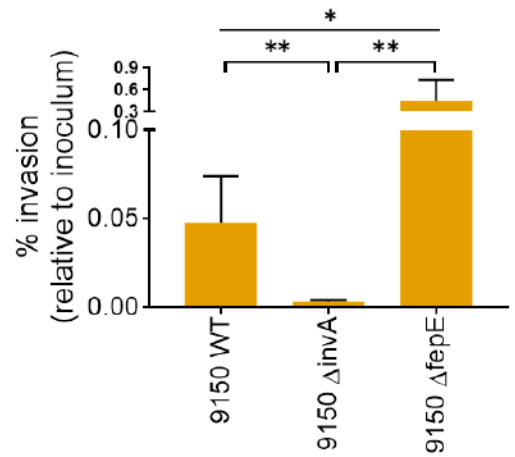


Figure 4.39 **Loss of very long O-antigen chains results in increased epithelial cell invasion during infection with *S.* Paratyphi A.**

HeLa cells were infected at MOI 100 with *S.* Paratyphi A 9150 as indicated and invasion was assessed at 2 h post infection via enumeration of gentamicin-resistant CFUs. Bars show means ± SEM from four independent repeats. Comparison by repeated measures one-way ANOVA. *, $p < 0.05$; **, $p < 0.01$.

The role of very long O-antigen chains on *S.* Paratyphi-A-induced macrophage cell death was investigated by infecting THP-1 cells and measuring cell death at 3 h post infection. As a control, *S.* Paratyphi A 9150 Δ*invA* triggered significantly lower amounts of cell death compared to WT, suggesting that cell death was SPI-1 T3SS-dependent during this infection time (Figure 4.38A). Infection with *S.* Paratyphi A Δ*fepE* resulted in significantly higher cell death in comparison to WT (Figure 4.38A), consistent with higher invasiveness of this mutant into HeLa cells (Figure 4.39). However, THP-1-mediated phagocytosis suggested that differences in host cell death between *S.* Paratyphi A 9150 WT and Δ*fepE* were not mediated by differential bacterial uptake of these strains (Figure 4.38B).

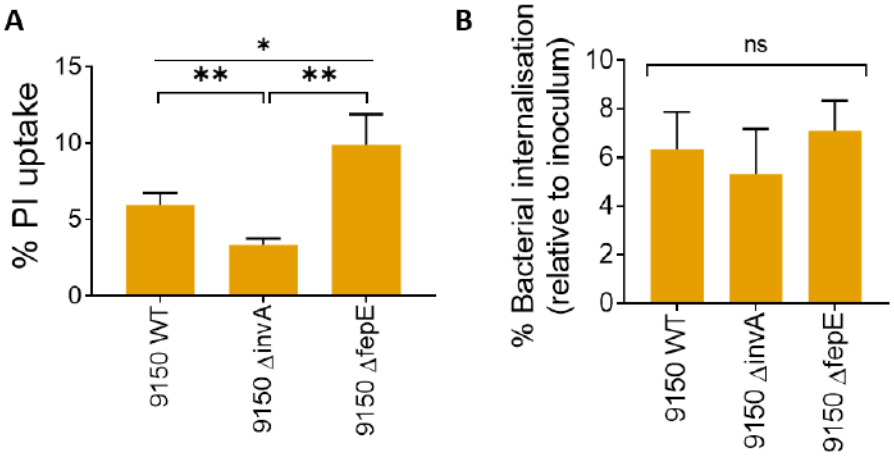


Figure 4.38 **Very long LPS O-antigen chains suppress macrophage cell death independently of bacterial internalisation during infection with *S.* Paratyphi A.**

(A) THP-1 cells were infected with *S.* Paratyphi A 9150 (9150; MOI 50) as indicated and cell death was measured at 3 h post infection via PI uptake. **(B)** Bacterial internalisation was determined via gentamicin protection assays at 1.5 h post infection in Z-VAD-FMK-treated cells. Bars show means ± SEM from five independent repeats. Statistical analysis by repeated measures one-way ANOVA. *, $p < 0.05$; **, $p < 0.01$; ns, not significant.

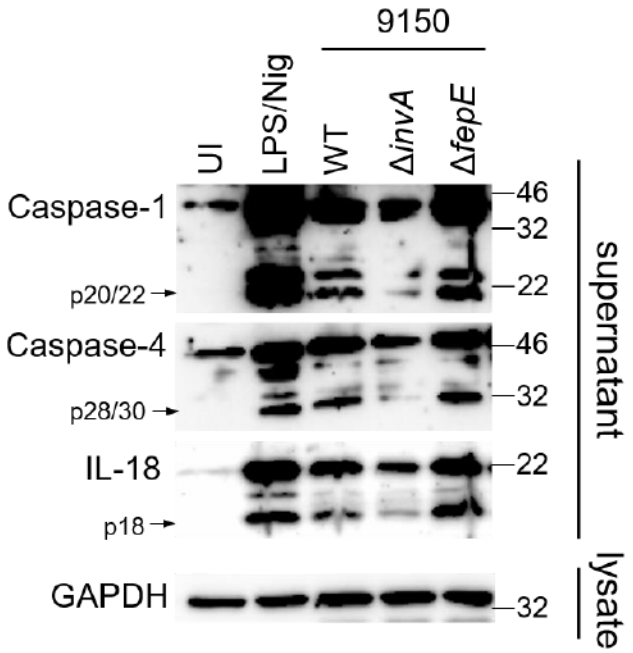


Figure 4.40 **Loss of very long O-antigen chains in *S.* Paratyphi A triggers increased inflammasome activation in THP-1 cells.**

THP-1 cells were infected with *S.* Paratyphi A 9150 (9150; MOI 50) as indicated and activation of caspase-1, caspase-4 and IL-18 was determined via immunoblotting. Uninfected (UI) cells were used as negative control, while cells treated with LPS+nigericin were used as positive control. Arrows show cleaved products of caspase-1, caspase-4 and IL-18. Immunoblot representative of three independent repeats.

Given that very long O-antigen chains in *S.* Paratyphi A 9150 limited pyroptosis, its role in inflammasome activation was next determined. THP-1 cells were infected with *S.* Paratyphi A 9150 WT, Δ*invA* and Δ*fepE* and activation of caspase-1 and caspase-4 and ensuing IL-18 cleavage, was determined by immunoblotting. *S.* Paratyphi A 9150 induced SPI-1 T3SS-dependent activation of caspase-1 and caspase-4 (Figure 4.40), consistent with the requirement of SPI-1 T3SS to induce cell death (Figure 4.38). Treatment with LPS followed by nigericin was used as a positive control for inflammasome activation. Loss of very long LPS O-antigen chains in *S.* Paratyphi A resulted in a moderate increase in caspase-1 and caspase-4 activation, which also resulted in increased pro-IL-18 cleavage (Figure 4.40). The enhanced inflammasome activation during infection with *S.* Paratyphi A 9150 Δ*fepE* in comparison to its WT counterpart correlated with increased THP-1 pyroptotic cell death (Figure 4.38).

As pyroptotic cell death requires cytosolic bacterial recognition by immune sensors, it was also tested whether *S.* Paratyphi A 9150 lacking very long O-antigen chains was able to escape the vacuole and enter the host cell cytosol at higher rates compared to WT. This would suggest a similar mechanism to that underlying higher HeLa cell invasion by *S.* Paratyphi A 9150 Δ*fepE* (Figure 4.39). Escape to the cytosol was assessed as previously by a chloroquine-based assay. After phagocytosis, the majority of *S.* Paratyphi A remained localised in vacuoles (Figure 4.41A). At 3 h post infection, *S.* Paratyphi A 9150 escaped to the cytosol in a SPI-1 T3SS-dependent manner (Figure 4.41B), suggesting that higher numbers of cytosolic WT *S.* Paratyphi A were responsible for higher pyroptosis and inflammasome activation compared to Δ*invA*. In contrast, the numbers of bacteria entering the

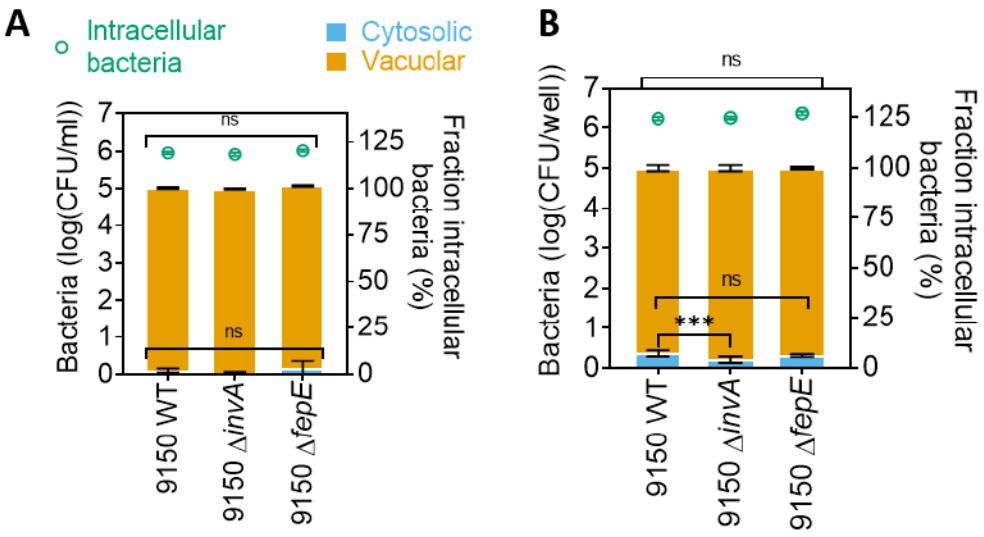


Figure 4.41 ***S.* Paratyphi A cytosolic escape relies on SPI-1 T3SS but is not affected by very long O-antigen chains.**

GSDMD^{miR} THP-1 cells were infected with *S.* Paratyphi A 9150 as indicated (MOI 50). Bacterial internalisation (left-axis) and fraction of cytosolic and vacuolar bacteria (right-axis) are shown at 1.5 h **(A)** and 3 h **(B)** post infection. Bars show means ± SEM from (A) five or (B) three independent repeats. Statistical analysis by repeated measures one-way ANOVA. ***, $p < 0.001$; ns, not significant

cytosol were not affected by loss of very long O-antigen chains (Figure 4.41B), despite the increase in cell death and inflammasome signalling.

These results collectively suggest that the reduced cell death induced by *S.* Paratyphi A 9150 Δ*invA* was partly mediated by slower escape to the cytosol, although it did not affect the initial bacterial uptake by THP-1 cells. Importantly, *S.* Paratyphi A 9150 limits cell death via production of very long O-antigen chains by a mechanism that does not affect phagocytosis or escape into the cytosol.

4.15 FepE-dependent reduction in *S.* Paratyphi A-induced cell death is not mediated by interference with immune signalling priming

Very long O-antigen chains may mask surface molecules (Hiyoshi *et al.*, 2018b). Also, LPS serves as a signal 1 during inflammasome activation, inducing NF-κB signalling and priming of inflammasome components (such as NLRP3). To test whether *S.* Paratyphi A 9150 WT induced less cell death than Δ*fepE* due to interference of very long O-antigen chains with host cell priming or due to an altered LPS profile of this mutant, THP-1 cells were primed with LPS prior to infection with *S.* Paratyphi A 9150 WT and Δ*fepE*. Pre-treatment of THP-1 with *E. coli* O111:B4 LPS ensures similar levels of signal-1-induced

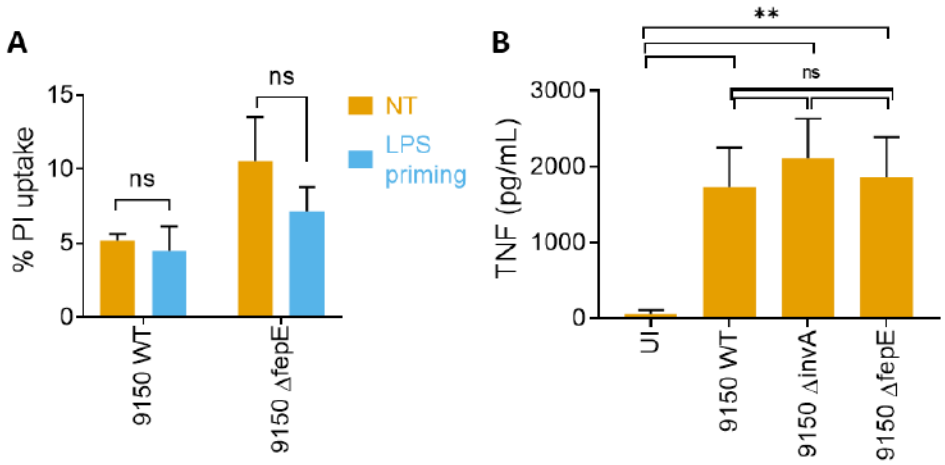


Figure 4.42 **Loss of very long LPS O-antigen chains in *S.* Paratyphi A does not interfere with THP-1 cell priming.**

(A) THP-1 cells were infected with *S.* Paratyphi A 9150 (9150; MOI 50) WT and Δ*fepE* following no-treatment (NT) or *E. coli* O111:B4 LPS priming for 3 h. Cell death was measured at 3 h post infection by PI uptake. **(B)** TNF quantification by ELISA in culture supernatants of unprimed THP-1 cells infected with *S.* Paratyphi A as indicated for 3 h. Bars show means ± SEM from (A) four or (B) three independent repeats. Statistical analysis by (A) matched Two-way ANOVA or (B) repeated measures one-way ANOVA following correction for multiple

signalling. Macrophage cell death triggered by *S.* Paratyphi A 9150 WT or Δ*fepE* was not affected by LPS priming prior to infection (Figure 4.42A).

To further validate that loss of very long O-antigen chains did not interfere with host cell priming, the levels of the inflammasome-independent TNF cytokine were quantified. Secretion of TNF following infection with *S.* Paratyphi A 9150 WT and Δ*fepE* was similar, like Δ*invA* which was used as a control (Figure 4.42B). All strains induced significantly higher TNF secretion compared to uninfected cells (Figure 4.42B). These findings show that very long O-antigen chains of LPS in *S.* Paratyphi A modulate cell death independently of interference with host cell priming and induction of pro-inflammatory signalling.

4.16 Complementation of Δ*fepE* restores the WT phenotype

To verify that very long O-antigen chains were responsible for the observed increase in epithelial cell invasion, macrophage cell death and inflammasome activation, the *fepE* deletion mutant was complemented in *S.* Paratyphi A 9150 with plasmid-encoded *fepE,* where *fepE* expression was under the control of a constitutive promoter. *S.* Paratyphi A 9150 Δ*fepE* carrying an empty vector (EV) vector was used as a control. Indeed, complementation of *fepE* restored the LPS electrophoretic mobility to a similar to the WT counterpart (Figure 4.43A). The banding was more extreme to the upper and lower

range in the complemented strain compared to WT, possibly due to higher levels of *fepE* expression under the control of the constitutive promoter (Murray, Attridge & Morona, 2005). Invasion in HeLa cells revealed that, while Δ*fepE* and Δ*fepE* carrying the EV invaded HeLa cells significantly more than WT, complementation of *fepE* restored invasion into HeLa cells to WT levels (Figure 4.43B). These results suggest that indeed loss of very long LPS O-antigen chains was responsible for limiting *S.* Paratyphi A 9150 invasion into host cells.

The effect of *fepE* complementation on macrophage pyroptosis and inflammasome activation was next tested. Upon *fepE* complementation, cell death levels were restored to those induced by WT (Figure 4.44A). Specifically, while *S.* Paratyphi A 9150 Δ*fepE* with or without EV induced significantly higher cell death in THP-1 cells compared to WT, complemented Δ*fepE* triggered comparable cell death to that of WT (Figure 4.44A). The exaggerated phenotype observed with the complemented strain was possibly due to excessive FepE production. This phenotype was not mediated by differences in bacterial uptake by THP-1 cells, as differences in phagocytosis between the strains were not significant compared to WT (Figure 4.44B). These results suggest that FepE-mediated formation of very long O-antigen chains and/or additional unidentified roles that this gene may have were responsible for

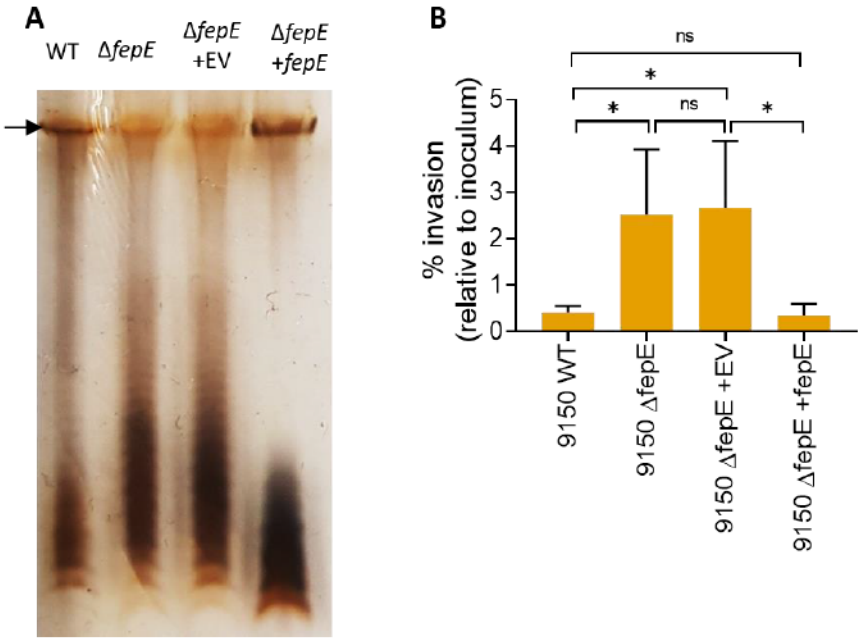


Figure 4.43 **Complementation of Δ*fepE* in *S.* Paratyphi A recovers epithelial cell invasion.**

(A) Silver stained acrylamide gel showing electrophoretic LPS mobility of the indicated strains. Very long O-chains indicated by arrow. Image representative of two independent repeats. **(B)** HeLa cells were infected with *S.* Paratyphi A 9150 (9150; MOI 100) as indicated and invasion was determined at 2 h post infection by gentamicin protection assays. Bars show means ± SEM from three independent repeats. Statistical analysis by repeated measures one-way ANOVA corrected for multiple comparisons. *, $p < 0.05$; ns, not significant

limiting *S.* Paratyphi A 9150-induced cell death in host cells. THP-1 cells were infected with *S.* Paratyphi A WT, Δ*fepE*, and the complemented strain and inflammasome activation was determined in the supernatant of infected cells. As observed above, loss of very long LPS O-antigen chains led to higher levels of caspase-1 and caspase-4 activation in comparison to WT (Figure 4.44C), and IL-18 cleavage reflected the levels of caspase-1 activation (Figure 4.44C). However, activation of these inflammasome-associated proteins was markedly reduced upon complementation of Δ*fepE* (Figure 4.44C). The complemented strain induced slightly lower cleavage of caspase-4 than that induced by WT, possibly due to overexpression of *fepE*. These results implicate an inflammasome activation interfering mechanism by the presence of very long O-antigen chains.

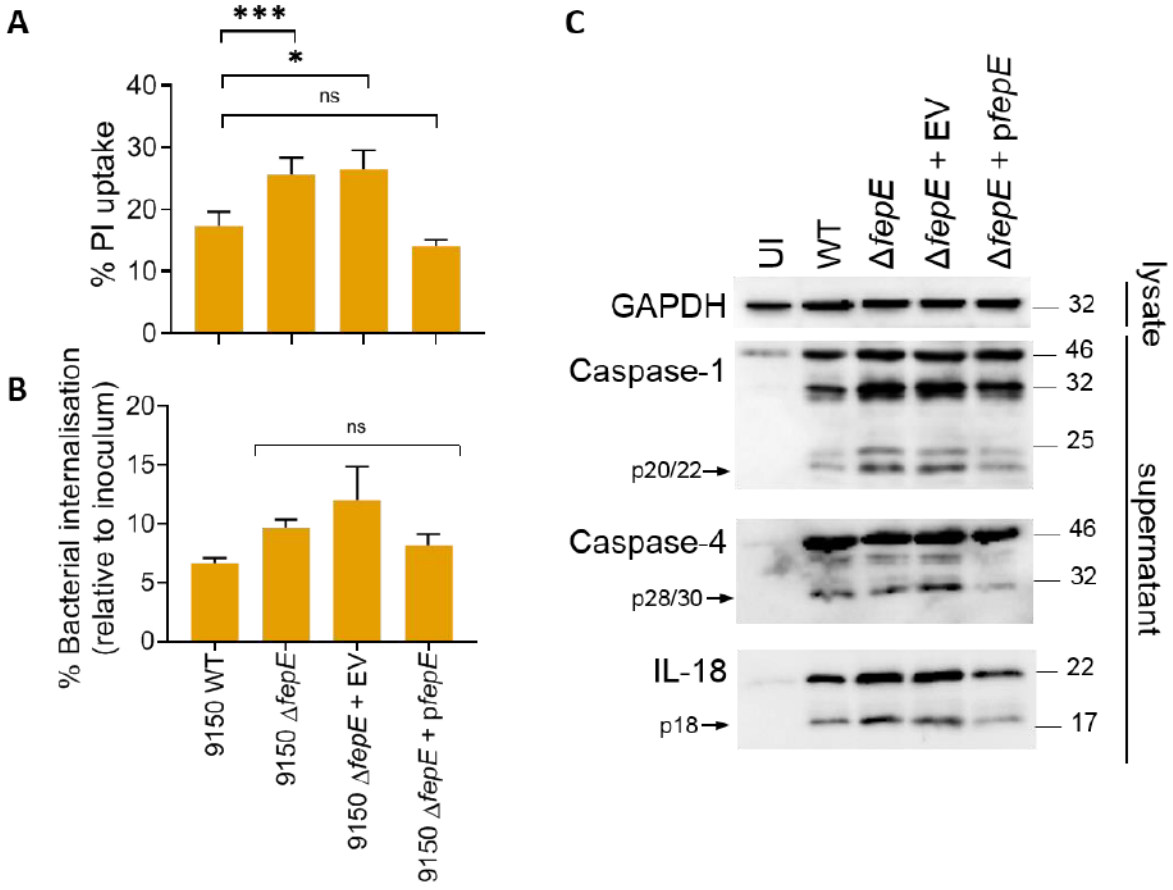


Figure 4.44 **Complementation of loss of very long O-antigen LPS chains in *S.* Paratyphi A recovers cell death level in THP-1 cells.**

(A) THP-1 cells were infected at MOI 50 with *S.* Paratyphi A 9150 as indicated and cell death was assessed by PI uptake at 3 h post infection. **(B)** Bacterial internalisation was determined at 1.5 h post infection in Z-VAD-FMK treated THP-1 cells. **(C)** THP-1 cells were infected at MOI 50 and inflammasome activation was determined by immunoblotting of indicated proteins at 3 h post infection. Arrows indicate cleaved products. Image representative of two independent repeats. Bars show means ± SEM from three independent repeats. Statistical analysis by repeated measures one-way ANOVA. *, $p < 0.05$; ***, $p < 0.001$; ns, not significant

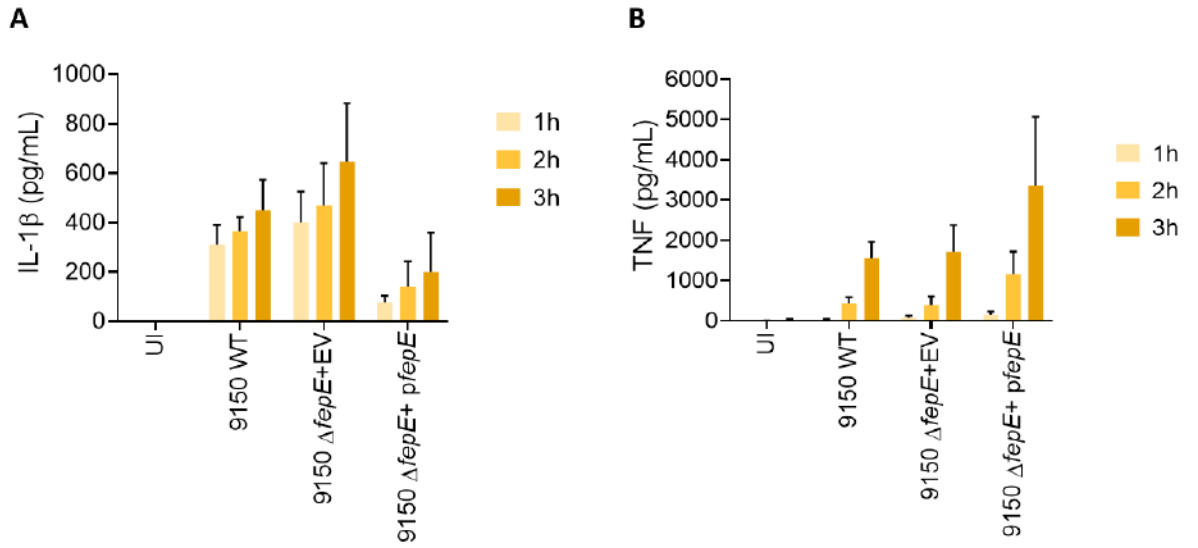


Figure 4.45 **Loss of very long O-antigen chains mediates increased IL-1β secretion independently of host cell priming during infection with *S.* Paratyphi A.**

THP-1 cells were infected with *S.* Paratyphi A 9150 (9150; MOI 50) as indicated and **(A)** IL-1β and **(B)** TNF secretion were determined in supernatants of infected cells. Graphs show ± SEM from three independent repeats.

Furthermore, *S.* Paratyphi A 9150 Δ*fepE* induced mildly higher IL-1β secretion than WT throughout the infection. In contrast, the complemented strain triggered markedly lower levels of IL-1β than WT and Δ*fepE* (Figure 4.45A). The differences in inflammasome activation between *S.* Paratyphi A 9150 WT and Δ*fepE* were not mediated by differences in immune cell priming at any point during infection, as assessed by TNF secretion from infected cells (Figure 4.45B). In fact, the complemented strain, which overexpressed *fepE*, triggered higher production of TNF at 2 and 3 h post infection (Figure 4.45B) possibly due to lower rate of cell death induced by this strain. These results support that FepE-mediated very long LPS O-antigen chains were responsible for limiting cell death and inflammasome activation induced by *S.* Paratyphi A 9150 in macrophages.

4.17 Very long O-antigen chains trigger ASC-dependent cell death during infection with *S.* Paratyphi A

Loss of very long O-antigen chains resulted in higher inflammasome activation and pyroptosis. It has already been shown in this report that NLRP3, ASC, caspase-4 and caspase-8 significantly contributed to inflammasome activation and pyroptosis by *S.* Paratyphi A. Results shown in sections 4.3, 4.4, 4.6, and 4.7, suggest that *S.* Paratyphi A induces inflammasome activation directly via caspase-4 or through NLRP3-ASC and caspase-8 via NLRP3-ASC or directly. In order to examine how *S.* Paratyphi A 9150

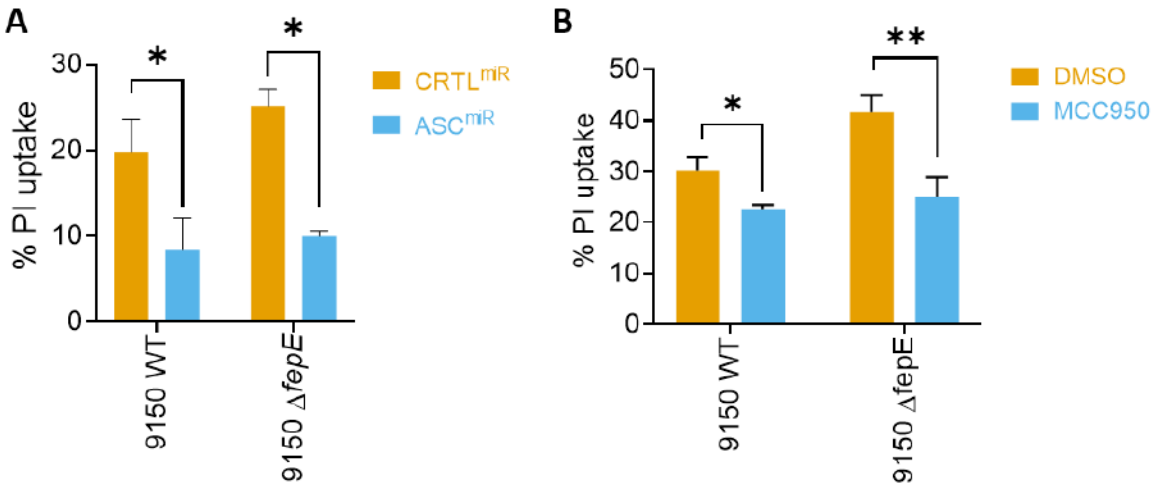


Figure 4.46 ***S.* Paratyphi A Δ*fepE*-induced cell death is mediated by ASC.**

(A) CTRL^{miR} or ASC^{miR} THP-1 cells were infected with *S.* Paratyphi A 9150 (9150; MOI 50) WT or Δ*fepE* and cell death was determined at 3 h post infection. **(B)** DMSO or MCC950-treated THP-1 cells were infected as indicated and cell death was determined at 3 h post infection. Bars show means ± SEM from three independent repeats. Statistical analysis was performed by two-way ANOVA. *, $p < 0.05$; **, $p < 0.01$.

Δ*fepE* triggers the enhanced inflammasome response, the contribution of these pathways was next tested. Silencing of ASC revealed that pyroptosis during infection with *S.* Paratyphi A 9150 Δ*fepE* was driven by ASC by ~60%, similarly to *S.* Paratyphi A 9150 WT, where ASC contributed by ~58% (Figure *4.46*A). Additionally, pharmacological inhibition of NLRP3 via MCC950 resulted in significant reduction of pyroptosis during infection with *S.* Paratyphi A Δ*fepE* by ~40%, comparable to the reduction seen during infection with WT (Figure *4.46*B).

In order to investigate whether the enhanced inflammasome response to *S.* Paratyphi A 9150 Δ*fepE* was also reflected in ASC speck formation, ASC^{mRFP} THP-1 cells were infected with *S.* Paratyphi A 9150 WT, Δ*invA* and Δ*fepE*. Infection with all three strains induced significantly higher numbers of cells with ASC specks than basal levels (UI cells) (Figure 4.47A-B). Representative images of infected cells and ASC specks are shown in Figure 4.47A. Infection with *S.* Paratyphi A 9150 WT resulted in elevated numbers of ASC specks compared to Δ*invA*, although this was not significantly different (Figure 4.47B). Nevertheless, it was evident that SPI-1 T3SS was required for assembly of ASC specks in the majority of cells. While *S.* Paratyphi A 9150 Δ*fepE* induced higher levels of pyroptosis (Figure 4.42) and inflammasome activation (Figure 4.43) compared to the parental WT, the number of ASC specks formed within macrophages was only slightly higher that that formed during infection with WT *S.* Paratyphi A 9150 (Figure 4.47B). These results suggest that the increased inflammasome activation

triggered by loss of very long O-antigen chains was not mainly mediated by an ASC-dependent mechanism.

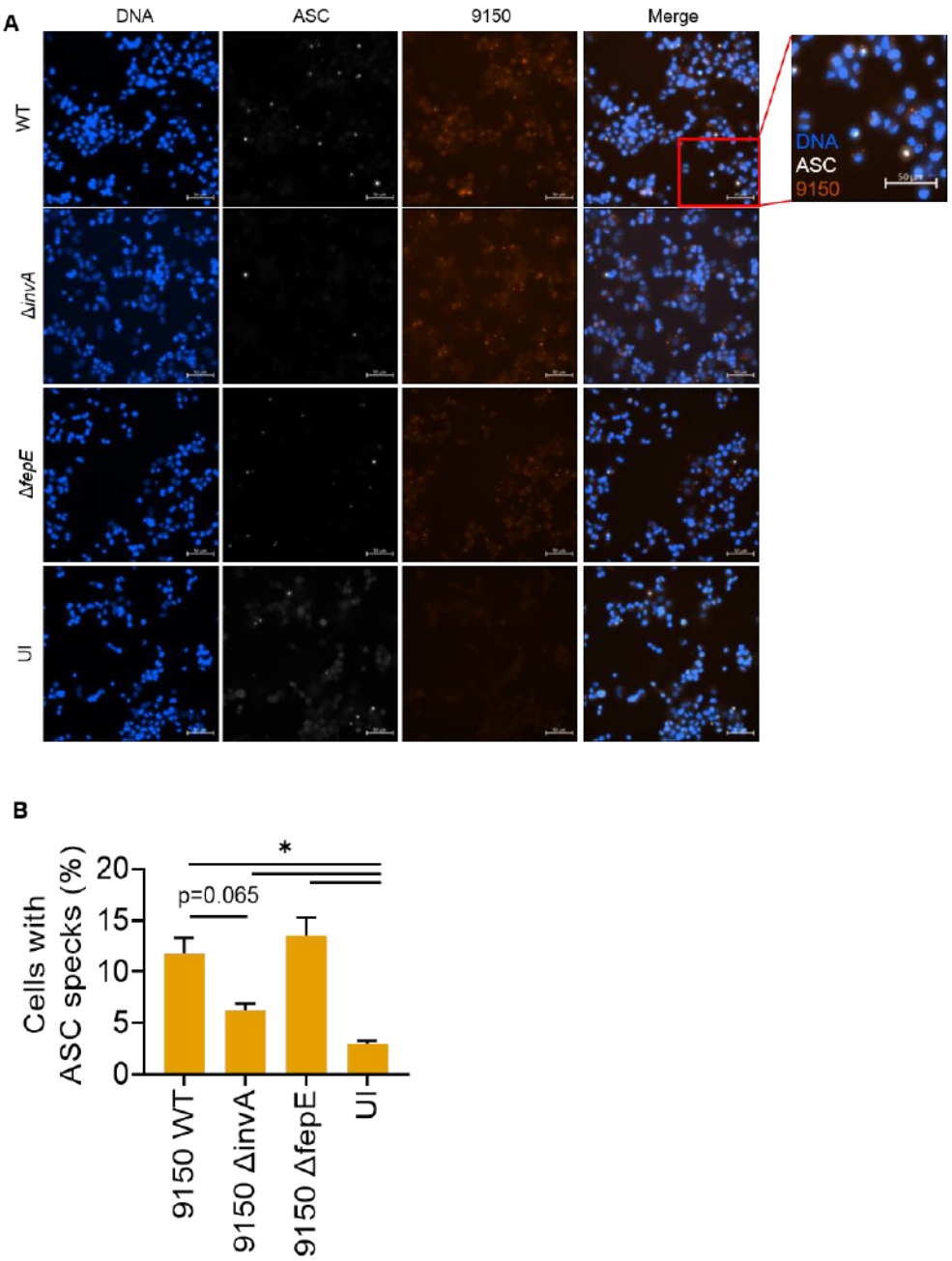


Figure 4.47 **ASC speck formation occurs independently of SPI-1 T3SS or very long O-antigen chains during infection with *S.* Paratyphi A.**

Z-VAD-FMK-treated ASC^{mRFP} THP-1 cells were infected with *S.* Paratyphi A 9150 (9150; MOI 50) as indicated. **(A)** Representative images and **(B)** quantification of cells with ASC-specks from four independent repeats. These were conducted along Figure 4.32 and UI controls are shared between panels, while statistical analysis was performed on all experimental conditions. Scale bar 50 µm. Bars show means ± SEM from four independent repeats. Statistical analysis by repeated measures one-way ANOVA. *, $p < 0.05$.

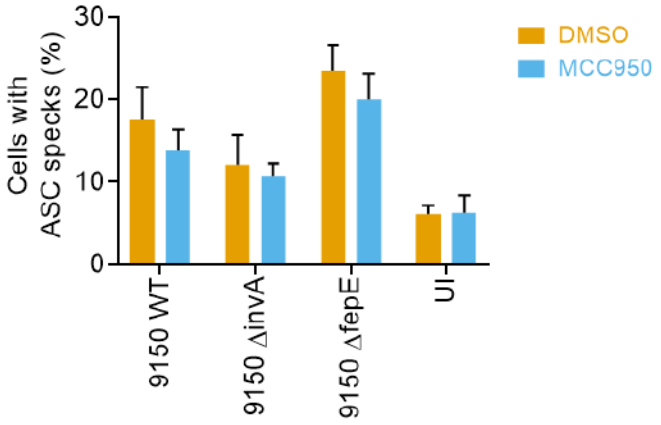


Figure 4.48 **ASC speck formation is not NLRP3-dependent during infection with *S*. Paratyphi A.**

Z-VAD-FMK-treated ASC^{mRFP} THP-1 cells were treated with DMSO or MCC950 prior to infection with *S.* Paratyphi A 9150 (9150; MOI 50) as indicated. Cells with ASC specks were enumerated by fluorescent microscopy by counting >120 cells from randomly selected slide fields per repeat. Graph shows means ± SEM from three independent repeats. Statistical analysis by two-way ANOVA followed by correction for multiple comparisons. These were conducted along Figure 4.32 and UI controls are shared between panels, while statistical analysis was performed on all experimental conditions.

Given the contribution of NLRP3 to pyroptosis (Figure 4.13A) and inflammasome activation (Figure 4.13D) during infection with *S.* Paratyphi A 9150, ASC^{mRFP} THP-1 cells were then treated with MCC950 prior to infection, in order to ascertain whether ASC speck formation was mediated by NLRP3 activation. Inhibition of NLRP3 via MCC950 resulted in a very moderate, albeit not statistically significant, decrease in the number of cells with ASC specks during infection with *S.* Paratyphi A 9150 WT, Δ*invA* or Δ*fepE* (Figure *4.48*). These results suggested that other inflammasome pathways induce the formation of ASC specks within THP-1 cells, independently of NLRP3, during infection with *S.* Paratyphi A 9150.

To verify whether caspase-4 has a dominant role in detecting cytosolic Δ*fepE* bacteria, CTRL^{miR} and CASP4^{miR} THP-1 cells were infected with *S.* Paratyphi A 9150 WT and Δ*fepE*. Cell death was significantly reduced during infection with both WT and Δ*fepE*, while the levels pyroptosis that CASP4^{miR} cells underwent was similar during infection with WT or Δ*fepE* (Figure *4.49*A). Additionally, pharmacological inhibition of NLRP3 and caspase-8 in CASP4^{miR} cells did not further reduce cell death induced by *S.* Paratyphi A 9150 Δ*fepE* (Figure *4.49*B). Moreover, while *S.* Paratyphi A 9150 Δ*fepE* induced ASC-dependent cell death (Figure 4.46), this reduction was comparable to the reduction observed with WT *S.* Paratyphi A 9150 (Figure 4.10). These results, in combination with the similar

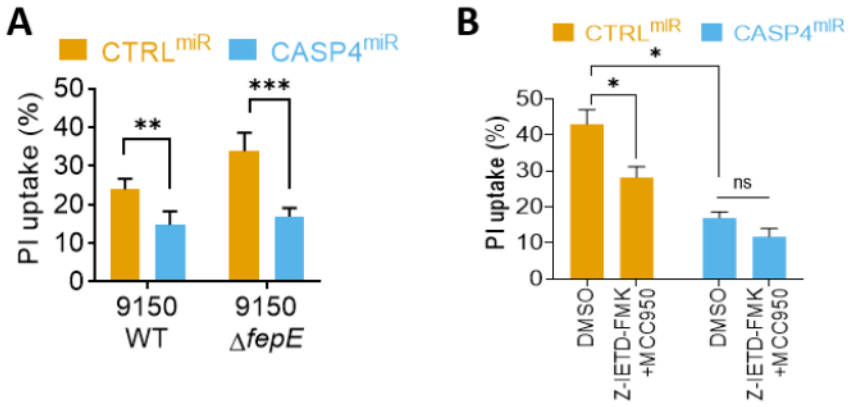


Figure 4.49 **Caspase-4 mediates the increased cell death induced by *S.* Paratyphi A 9150 Δ*fepE*.**

(A) CTRL^{miR} or CASP4^{miR} THP-1 cells were infected with *S.* Paratyphi A 9150 WT or Δ*fepE* and cell death was determined at 3 h post infection. **(B)** DMSO or Z-IETD-FMK and MCC950-treated CTRL^{miR} or CASP4^{miR} THP-1 cells were infected with *S.* Paratyphi A 9150 Δ*fepE* and cell death was determined at 3 h post infection. Graphs show means ± SEM from (A) six or (B) four independent repeats. Statistical analysis was performed by two-way ANOVA. *, $p < 0.05$; **, $p < 0.01$; ***, $p < 0.001$; ns, not significant.

numbers of cells with ASC specks during infection with *S.* Paratyphi A WT and Δ*fepE* (Figure 4.49), suggest that the higher pyroptotic cell death induced by S. Paratyphi A Δ*fepE* is a result of increased caspase-4 activation, as opposed to requiring downstream activation of the NLRP3-ASC-caspase-1 inflammasome.

4.18 The role of very long O-antigen chains in inflammasome activation by *S.* Typhimurium infection

FepE is also present in *S.* Typhimurium and is highly similar between *S.* Paratyphi A and *S.* Typhimurium, differing in only one amino acid at the protein sequence level, while *S.* Typhi carries a pseudogenised *fepE* allele. The role of very long O-antigen chains during infection of *S.* Typhimurium has previously been studied in the context of complement resistance (Murray, Attridge & Morona, 2005; Hölzer *et al.*, 2009) and virulence in mouse models (Murray, Attridge & Morona, 2003, 2006). Therefore, it was next investigated whether very long O-antigen chains in *S.* Typhimurium have the same role in dampening inflammasome activation and cell death in macrophages as they do during infection with *S.* Paratyphi A 9150. It was hypothesised that introduction of plasmid-borne *fepE* into *S.* Typhimurium WT would interfere with invasion of HeLa cells by *S.* Typhimurium. Indeed, overexpression of *fepE* markedly reduced the ability of *S.* Typhimurium WT to invade HeLa cells (Figure 4.50A). In contrast, and in keeping with data obtained with *S.* Paratyphi A 9150, deletion of *fepE* in *S.* Typhimurium significantly promoted invasion into HeLa cells by > 2-fold (Figure 4.50B). Complementation of

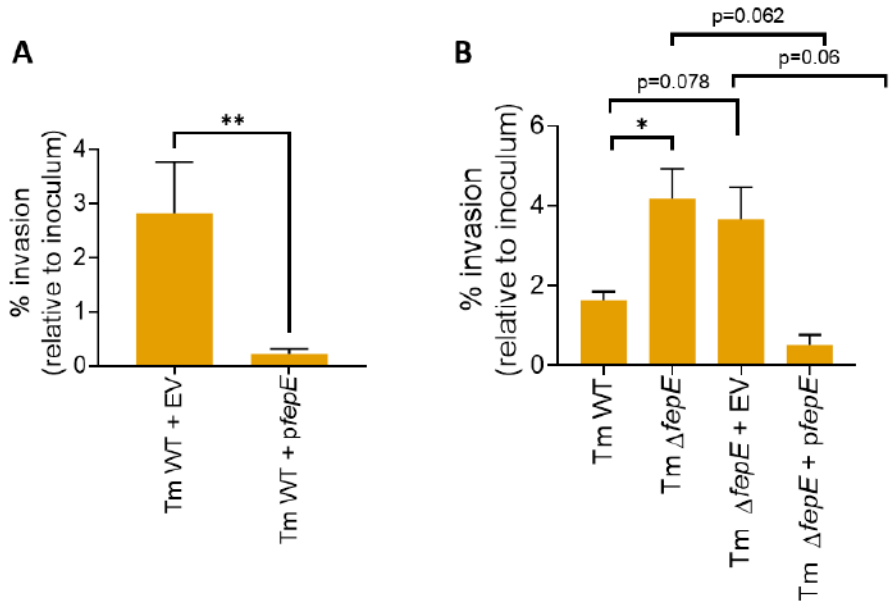


Figure 4.50 **FepE-mediated very long O-antigen chains limit *S.* Typhimurium invasion into HeLa cells.**

(A) HeLa cells were infected with *S.* Typhimurium WT carrying an empty vector (EV) or overexpressing *fepE* (p*fepE*) and invasion was assessed at 2 h post infection by gentamicin protection assays. **(B)** HeLa cells were infected with *S.* Typhimurium WT and Δ*fepE*, as well as the complemented strain and invasion was determined at 2 h post infection. Bars shown means ± SEM from (A) four or (B) three independent repeats. Statistical analysis by (A) paired student's *t*-test or (B) repeated measures one-way ANOVA followed by correction for multiple comparisons. *, $p < 0.05$; **, $p < 0.01$.

S. Typhimurium Δ*fepE* resulted in invasion levels comparable to those demonstrated by its WT counterpart (Figure 4.50B), further supporting the role of FepE in interfering with invasion.

The effect of *fepE*-mediated very long O-antigen chains on pyroptosis and inflammasome activation during *S.* Typhimurium infection of THP-1 cells was next investigated. Preliminary experiments suggested that overexpression of *fepE* in WT *S.* Typhimurium indeed prevented induction of pyroptosis in THP-1 cells, as well as activation of caspase-1 and IL-18, as well as caspase-4 (not shown), further supporting the hypothesis that very long O-antigen chains interfere with inflammasome activation in macrophages. To further validate the findings with *S.* Paratyphi A, the effect of the loss of very long O-antigen chains on inflammasome activation was next investigated. Similarly to the role of very long O-antigen chains during infection with *S.* Paratyphi A, deletion of *fepE* resulted in a small, but statistically significant, increase in cell death triggered by *S.* Typhimurium, which was restored to WT levels upon complementation with plasmid-borne *fepE* (Figure 4.51A).

Bacterial internalisation of *S.* Typhimurium WT and Δ*fepE* by THP-1 cells was indistinguishable, suggesting that loss of very long O-antigen chains did not promote phagocytosis (Figure 4.51B). Phagocytosis by THP-1 cells revealed that the complemented strain was internalised at lower rates

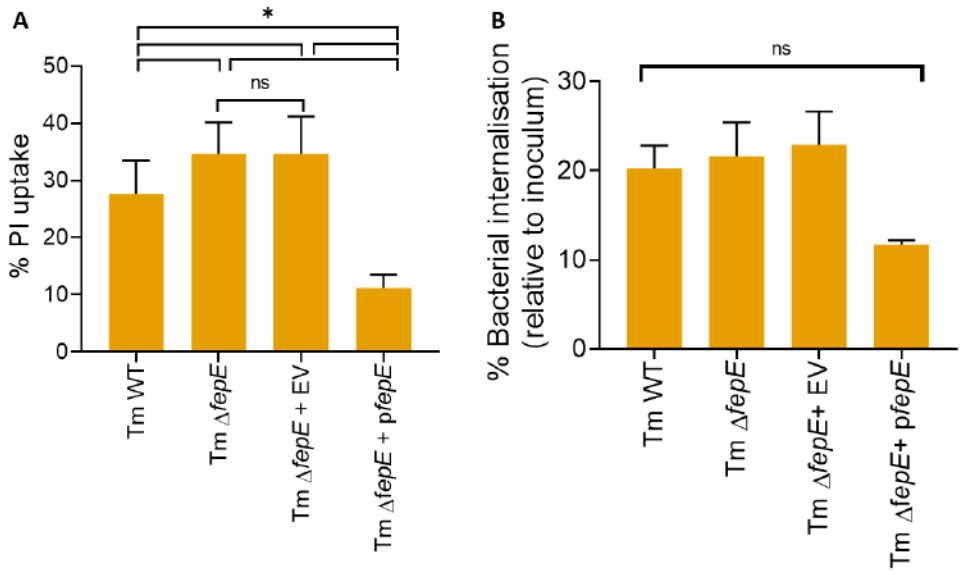


Figure 4.51 **Very long O-antigen chains limit *S.* Typhimurium-induced pyroptosis.**

(A) THP-1 cells were infected with *S.* Typhimuirum (Tm; MOI 15) as indicated and pyroptosis was determined at 3 h post infection by PI uptake. **(B)** Z-VAD-FMK-treated THP-1 cells were infected with as indicated and bacterial internalisation was assessed by gentamicin protection assays at 1.5h post infection. Graphs show means ± SEM from three independent repeats. Statistical analysis by repeated measures one-way ANOVA followed by correction for multiple comparisons. *, $p < 0.05$; ns, not significant. These experiments were conducted by J. Sanchez-Garrido.

compared to WT *S.* Typhimurium, although this difference was not found to be statistically significant (Figure 4.51B). This response was probably due to excessive production of FepE. These results suggest that interfering with inflammasome activation and pyroptosis in a manner dependent on FepE-mediated production of very long O-antigen LPS chains is shared by typhoidal and NTS serovars.

4.19 *S.* Paratyphi A-induced inflammasome activation in human monocyte-derived macrophages (MDMs)

The interactions of *S.* Paratyphi A with MDMs remain poorly investigated. Therefore, it was next aimed to examine whether observations in THP-1 cells are replicated in primary MDMs. Preliminary data with *S.* Typhi showed that MDMs are not responsive to infection with typhoidal *Salmonella* to the same levels as THP-1 cells; MOI of 15 triggered undetectable levels of cell death compared to uninfected cells, in contrast to infection with *S.* Typhimurium which leads to > 30% cell death in MDMs at MOI 15 (not shown). MOI of 30 triggered ~21% cell death in MDM infected with *S.* Typhi Ty2 (one repeat, not shown). Therefore, to ascertain what MOI would be optimal for investigation of pyroptotic cell death during *S.* Paratyphi A 9150 infection in these cells, MDMs were infected with *S.* Paratyphi A 9150 WT and Δ*invA* at various MOIs. These experiments revealed that *S.* Paratyphi A 9150 triggered low cell

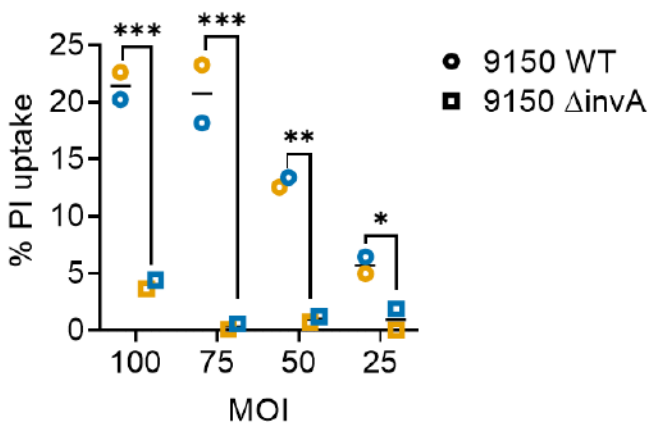


Figure 4.52 ***S.* Paratyphi A induces SPI-1-dependent cell death in MDMs.**

MDMs were infected with *S.* Paratyphi A WT or Δ*invA* at serial MOIs and cell death was determined by PI uptake at 3 h post infection. Symbol colours match donors. Lines show means from two repeats. Statistical analysis by matched two-way ANOVA followed by correction for multiple comparisons. *, $p < 0.05$; **, $p < 0.01$; ***, $p < 0.001$.

death even at high MOIs (MOI 100); however, the effect of MOI increase on cell death reached a plateau as MOIs increased, and infections at MOI 100 and MOI 75 induced similar levels of cell death (Figure 4.52). Further, *S.* Paratyphi A 9150 induced SPI-1 T3SS-dependent cell death even at low MOIs (Figure 4.52). Therefore, MOI 75 was selected for further experiments in MDMs, which is higher than MOI 50 which was previously used in THP-1 cells.

MDMs were next infected with *S.* Paratyphi A 9150 or *S.* Paratyphi A ED199 to compare the ability of the two strains to induce cell death in MDMs. *S.* Paratyphi A ED199 induced significantly more

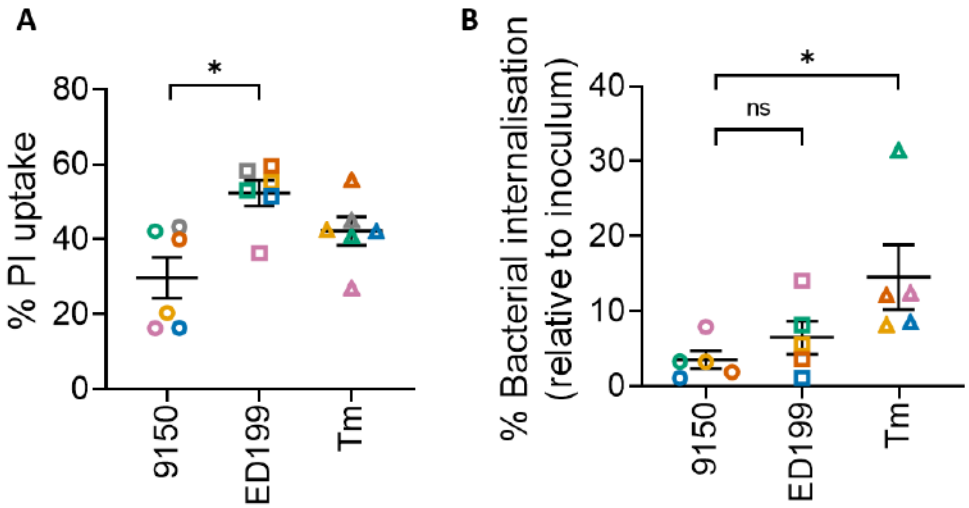


Figure 4.53 ***S.* Paratyphi A ED199 triggers higher levels of cell death in MDMs compared to *S.* Paratyphi A 9150.**

(A) MDMs were infected with *S.* Paratyphi A 9150 (9150; MOI 75) or ED199 (ED199; MOI 75) or *S.* Typhimurium (Tm; MOI 15) and cell death was determined at 3 h post infection. **(B)** Z-VAD-FMK-treated MDMs were infected as indicated and bacterial internalisation was assessed by gentamicin protection assays at 1.5 h post infection. Symbol colours match donors across both panels. Bars show means ± SEM. Statistical analysis by repeated measures one-way ANOVA. *, $p < 0.05$; ns, not significant.

cell death in MDMs compared to *S.* Paratyphi A (Figure 4.53A), which was not mediated by increased bacterial internalisation by MDMs (Figure 4.53B). As a comparison, MDMs were infected with *S.* Typhimurium at a lower MOI (MOI 15) and, although it was phagocytosed more than *S.* Paratyphi A ED199 (Figure 4.53B), it caused slightly lower cell death (Figure 4.53A).

Similarly, *S.* Paratyphi A ED199 led to higher secretion of IL-1β in comparison to *S.* Paratyphi A 9150 (Figure 4.54A), although *S.* Paratyphi A 9150 and ED199 induced similar levels of TNF secretion (Figure 4.54B). Infection of MDMs with *S.* Typhimurium led to robust IL-1β secretion (Figure 4.54A), while TNF secretion was more varied between donors (Figure 4.54B) and was similar to the low TNF secretion seen with THP-1 cells during *S.* Typhimurium infection. These results suggested that *S.* Paratyphi A ED199 (as well as *S.* Typhimurium) triggered higher inflammasome activation in comparison to *S.* Paratyphi A 9150, in keeping with the results obtained with THP-1 cells and further supporting that clinical *S.* Paratyphi A isolates are more immunogenic in human macrophages than *S.* Paratyphi A 9150, which is a highly attenuated strain.

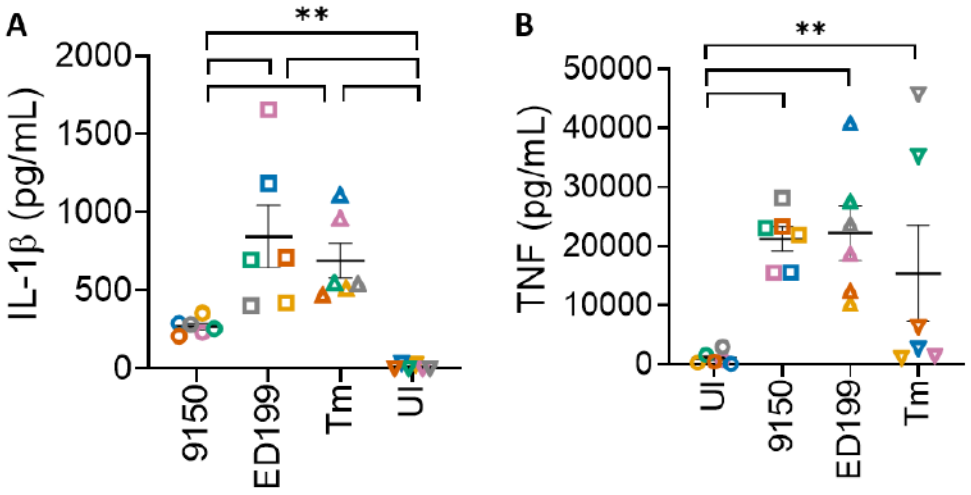


Figure 4.54 ***S.* Paratyphi A ED199 triggers higher levels of IL-1β in MDMs compared to *S.* Paratyphi A 9150, independently of cell priming.**

MDMs were infected with *S.* Paratyphi A 9150 or ED199 (MOI 75) or *S.* Typhimurium (Tm; MOI 15) and **(A)** IL-1β and **(B)** TNF production was determined at 3 h post infection. Symbol colours match donors across both panels. Bars show means ± SEM from six donors. Statistical analysis by repeated measures one-way ANOVA, followed by correction for multiple comparisons. **, $p < 0.01$.

It was next investigated whether MDMs respond to infection with *S.* Paratyphi A through a similar mechanism as THP-1 cells. To confirm that MDMs undergo caspase-dependent pyroptosis, MDMs were treated with Z-VAD-FMK. Initial experiments indicated that cell death at 3 h post infection did not result in a significant difference in cell death between DMSO and Z-VAD-FMK-treated MDMs, and therefore cell death was monitored over time. As Z-VAD-FMK is an irreversible caspase inhibitor, high expression of caspases in MDMs may have resulted in Z-VAD-FMK not being able to efficiently inhibit caspases at later timepoints at the administered concentration. Indeed, blocking of cell death was detectable at earlier time points during infection with *S.* Paratyphi A (Figure 4.55A). An earlier timepoint was thus chosen for comparison; Z-VAD-FMK-treatment of MDMs significantly reduced cell death induced by *S.* Paratyphi A 9150 or *S.* Paratyphi A ED199 at 90 min post infection (Figure 4.55B), suggesting that cell death was caspase-dependent similarly to THP-1 cell death triggered by *S.* Paratyphi A.

Additionally, silencing of *GSDMD* by small interfering RNA (siRNA) in MDMs was also attempted in order to verify its contribution to pyroptosis during infection with *S.* Paratyphi A. However, efficient silencing could not be attained, as assessed by immunoblotting against GSDMD in MDM lysates, and thus conclusions could not be drawn (not shown). Partial silencing in MDMs obtained from one donor suggested a reduction in cell death, indicating that *S.* Paratyphi A-triggered cell death in MDMs is pyroptotic. To validate these findings, testing in cells from multiple donors and following optimization of GSDMD-targeting siRNA concentration should be carried out in the future.

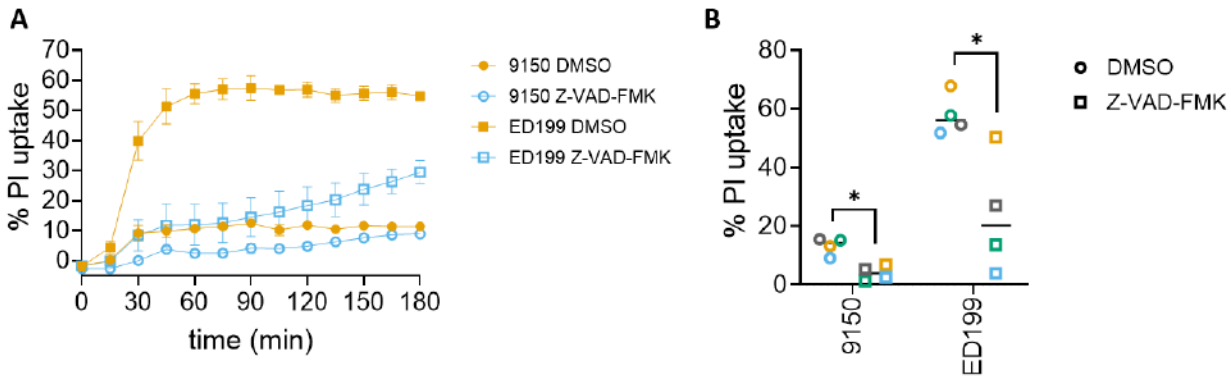


Figure 4.55 ***S.* Paratyphi A triggers caspase-dependent cell death in MDMs.**

(A) DMSO or Z-VAD-FMK-treated MDMs were infected with *S.* Paratyphi A 9150 or ED199 (MOI 75) and cell death was monitored over time. **(B)** Cell death at 90 min post infection is shown. Symbol colours match donors. Statistical comparison by two-way ANOVA. Bars show means ± SEM from four independent repeats. *, $p < 0.05$.

Despite the known robust activation of Naip-NLRC4 in murine macrophages during infection with *S.* Typhimurium (Yang *et al.*, 2013; Man *et al.*, 2013, 2014b; Broz *et al.*, 2010b; Reyes Ruiz *et al.*, 2017), a similar role for the human NAIP-NLRC4 inflammasome could not be observed with THP-1 cells during infection with *S.* Paratyphi A or *S.* Typhi. It was hypothesized that the lower expression of NAIP in THP-1 cells compared to primary MDMs (Kortmann, Brubaker & Monack, 2015), was responsible for the lack of a role of NAIP-NLRC4 during infection of THP-1 cells with typhoidal *Salmonella*. Indeed, MDMs exhibited a markedly higher expression of NAIP compared to THP-1 cells (Figure 4.56).

Therefore, to next ascertain whether NAIP-NLRC4 was activated during infection of MDMs with *S.* Paratyphi A, NAIP was silenced in MDMs by siRNA prior to infection. MDMs were also treated with DMSO or MCC950, in order to investigate the effect of silencing both NLRP3 and NLRC4. The efficiency of NAIP silencing was variable between donors (Figure 4.57A), which may have been a result of differential NAIP expression in different donors. Infection of MDMs with *S.* Paratyphi A 9150 resulted in very low levels of cell death, which was either dependent on the donors or the level of SPI-1 induction in this experiment (as well as that presented in Figure 4.59 in which MDMs originated from the same three donors). Nevertheless, MDM infection with *S.* Paratyphi A ED199 or *S.* Typhimurium resulted in robust cell death permitting comparisons between treatments. Silencing of NAIP and/or pharmacological inhibition of NLRP3 did not affect pyroptosis triggered by either *S.* Paratyphi A ED199 or *S.* Typhimurium (Figure 4.57B). Furthermore, IL-1β secretion was similar between MDMs treated with NAIP-targeting siRNA or non-targeting CTRL siRNA (Figure 4.57C), suggesting that NAIP-NLRC4 did not contribute to cell death of MDMs upon infection with *S.* Paratyphi A ED199 or *S.* Typhimurium, in line with observations with THP-1 cells presented here.

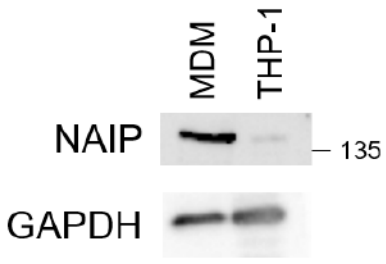


Figure 4.56 **NAIP expression in MDMs is significantly higher than in THP-1 cells.**

Expression of NAIP in MDM and THP-1 cells was determined by immunoblotting of NAIP in cell lysates of uninfected cells. This blot was produced by J. Sanchez-Garrido.

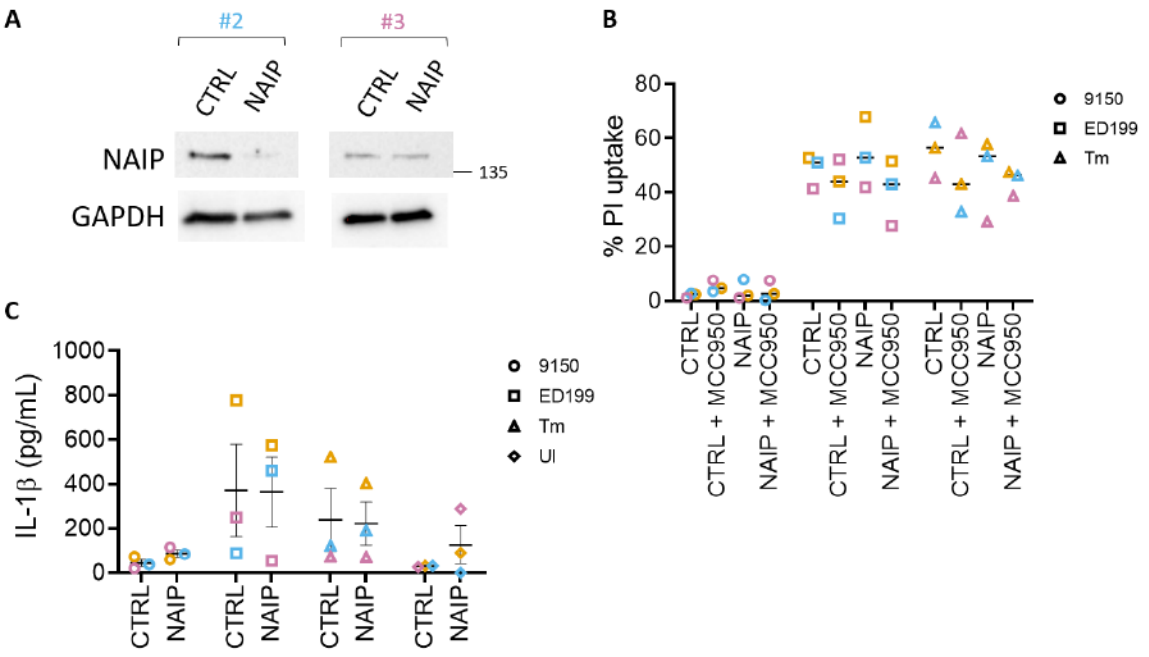


Figure 4.57 **Effect of NAIP silencing on MDM infection with *S.* Paratyphi A.**

(A) siRNA-mediated silencing of NAIP in MDMs was assessed by immunoblotting of NAIP in cell lysates. Sample preparation and blot by J. Sanchez-Garrido. **(B)** MDMs pre-treated with CTRL or NAIP-targeting siRNA were treated with DMSO or MCC950 prior to infection with *S.* Paratyphi A 9150 (9150; MOI 75), *S.* Paratyphi A ED199 (ED199; MOI 75) or *S.* Typhimurium (Tm; MOI 15) and cell death was determined at 3 h post infection. **(C)** MDMs treated with CTRL or NAIP-targeting siRNA were infected as in B and IL-1β secretion was determined at 3 h post infection. Graphs show means ± SEM from three independent repeats. Statistical analysis by two-way ANOVA. Symbol colours indicate donors and are matched across all panels.

To further investigate the role of NLRP3, as well as caspase-8, in cell death induction in MDMs by *S.* Paratyphi A, MDMs were treated with MCC950 and/or Z-IETD-FMK prior to infection. MCC950-mediated inhibition resulted in a significant reduction in pyroptosis triggered by *S.* Paratyphi A 9150 in MDMs, while it did not have a similar effect on *S.* Paratyphi A ED199-induced cell death (Figure 4.58A). Caspase-8 inhibition resulted only in a moderate reduction of cell death during MDM infection with *S.* Paratyphi A 9150 (Figure 4.58A). IL-1β secretion during MDM infection with *S.* Paratyphi A 9150 or *S.* Paratyphi A ED199 was appeared to be unaffected by treatment with MCC950 or Z-IETD-FMK, likely due to the high variation between donors (Figure 4.58B). Although it did not reach statistical significance, Z-IETD-FMK treatment led to a moderate reduction of IL-1β secretion by MDMs during infection, suggesting that caspase-8 may not directly affect pyroptosis but it may influence cytokine maturation and secretion during MDM infection with *S.* Paratyphi A.

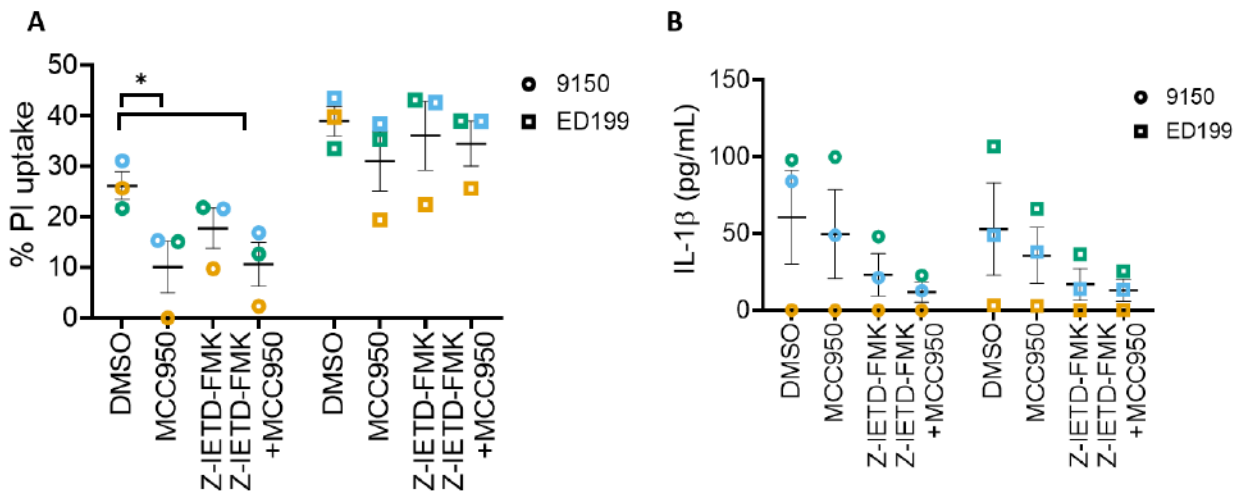


Figure 4.58 **Effect of NLRP3 and caspase-8 inhibition in MDM infection with *S.* Paratyphi A.**

MCC950 and/or Z-IETD-FMK-treated MDMs were infected with *S.* Paratyphi A 9150 or ED199 (MOI 75). **(A)** Cell death and **(B)** IL-1β secretion were determined at 3 h post infection. Bars show means ± SEM. Symbol colours indicate donors (matching across panels). Statistical analysis by matched two-way ANOVA followed by correction for multiple comparisons. *, $p < 0.05$.

Data obtained with THP-1 cells suggested that caspase-4 played an important role during infection with *S.* Paratyphi A. Therefore, the role of caspase-4 in MDM infection was next tested. Caspase-4 was silenced via siRNA in MDMs; efficient silencing was shown by immunoblotting against caspase-4 in MDM cell lysate (Figure 4.59A). Additionally, MDM cells transfected with *E. coli* O111:B4 LPS for 3 h showed a marked reduction of > 2-fold in cells with siRNA-mediated caspase-4 silencing (Figure 4.59B), indicating functional silencing of caspase-4. MDM cells pre-treated with non-targeting siRNA or siRNA against caspase-4 with or without the addition of MCC950 were infected with *S.* Paratyphi A 9150, *S.* Paratyphi A ED199 or *S.* Typhimurium. However, silencing of caspase-4 and/or pharmacological inhibition of NLRP3 did not affect cell death induced by any of the bacterial strains tested (Figure 4.59C). Similarly, siRNA-mediated caspase-4 silencing did not impact on IL-1β secretion triggered by *S.* Paratyphi A strains or *S.* Typhimurium (Figure 4.59D). *S.* Typhimurium has previously been shown to rely on IFNγ treatment of MDMs in order to induce caspase-4-dependent pyroptosis (Fisch ***et al.***, 2019a, 2019b), which is in line with findings presented here. Therefore, it is possible that a similar priming would have been required prior to *S.* Paratyphi A infection of MDMs in order to trigger caspase-4-dependent pyroptosis. It is worth noting that, despite increasing the administered MCC950 concentration to 5 µM compared to 2 µM given to THP-1 cells, MCC950 had a variable effect on MDMs from different donors (compare Figure 4.57, Figure 4.58, and Figure 4.59). The reason for this might have been differences in NLRP3 expression between donors.

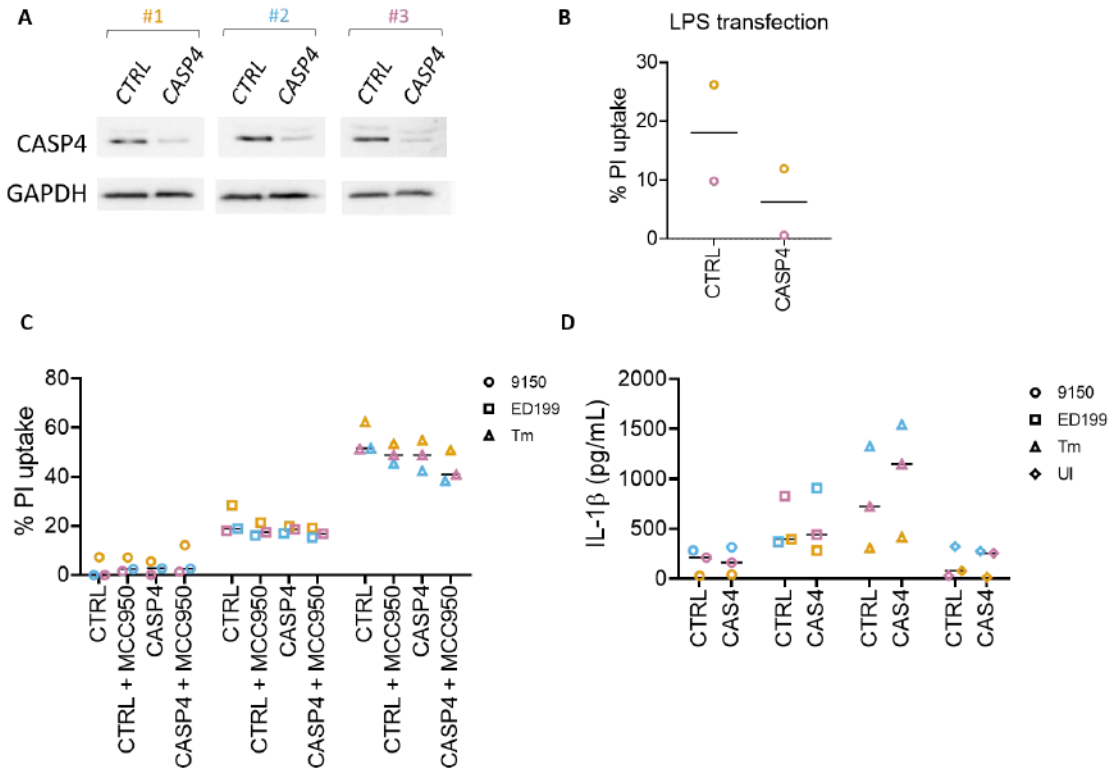


Figure 4.59 **Effect of siRNA-mediated caspase-4 silencing on MDM infection with *S.* Paratyphi A.**

(A) siRNA-mediated silencing of NAIP in MDMs was assessed by immunoblotting of caspase-4 in cell lysates from all donors. Blot was produced by J. Sanchez-Garrido. **(B)** MDMs pre-treated with CTRL or CASP4-targeting siRNA were transfected with *E. coli* O111:B4 LPS for 3 h and cell death was determined. **(C)** MDMs pre-treated with CTRL or CASP4-targeting siRNA were treated with DMSO or MDD950 prior to infection with *S.* Paratyphi A 9150 (9150; MOI 75), *S.* Paratyphi A ED199 (ED199; MOI 75) or *S.* Typhimurium (Tm; MOI 15) and cell death was determined at 3 h post infection. **(D)** MDMs treated with CTRL or CASP4-targeting siRNA were infected as in (C) and IL-1β secretion was determined at 3 h post infection. Error bars show means ± SEM from three independent repeats. Statistical analysis by two-way ANOVA. Symbol colours indicate donors and are matched across all panels.

4.20 The role of very long O-antigen chains during infection of MDMs with *Salmonella*

The role of very long O-antigen chains during infection of MDMs with *S.* Paratyphi A 9150 was next sought. Loss of very long O-antigen chains resulted in only a moderate increase in *S.* Paratyphi A 9150-induced cell death in MDM cells (Figure 4.60A). However, complementation of the mutant strain triggered significantly lower cell death in MDMs compared to the WT counterpart (Figure 4.60A), which was probably a result of excessive production of FepE in this strain mediating interference with induction of host cell death. All *S.* Paratyphi A 9150 *fepE* strains were similarly phagocytosed by MDMs (Figure 4.60B); thus very long O-antigen chains play no role in interfering with bacterial uptake by host MDMs. Similarly, infection of MDMs with *S.* Paratyphi A 9150 Δ*fepE* and the complemented strain resulted in similar levels of IL-1β production (Figure 4.61A), as well as TNF production (Figure 4.61B), suggesting that increases in LPS O-antigen chain length did not affect host cell priming. All strains induced significantly higher production of IL-1β and TNF compared to UI cells (Figure 4.61A-B), showing that cells are sufficiently recognised by MDMs.

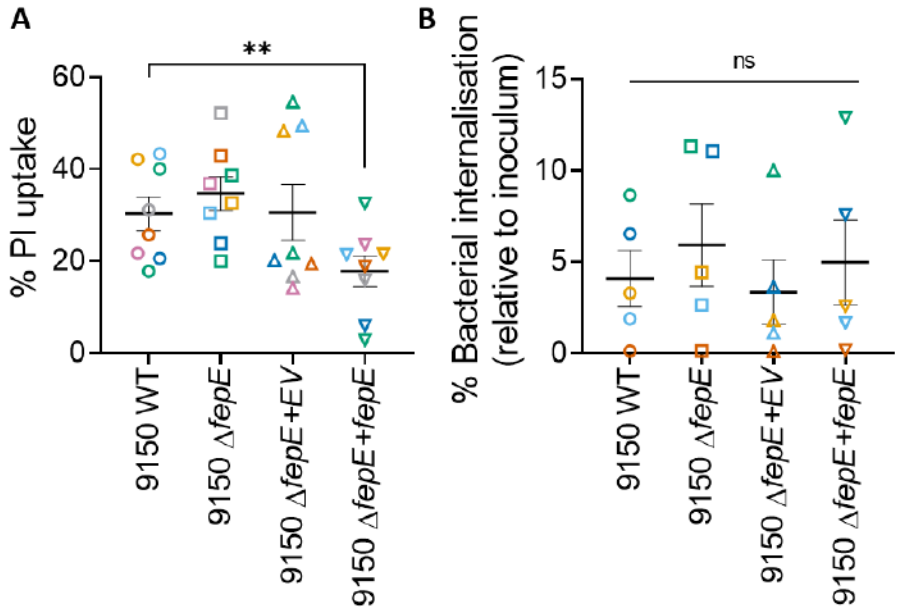


Figure 4.60 **The role of very long O-antigen chains during MDMs infection with *S.* Paratyphi A 9150.**

(A) MDMs were infected with *S.* Paratyphi A 9150 (9150; MOI 75) as indicated and cell death was determined by PI uptake at 3 h post infection. **(B)** Z-VAD-FMK-treated MDMs were infected as indicated and phagocytosis was determined at 1.5 h post infection. Symbol colours represent donors matched across both panels. Graphs show means ± SEM and statistical analysis was performed by repeated measures one-way ANOVA. **, $p < 0.01$; ns, not significant.

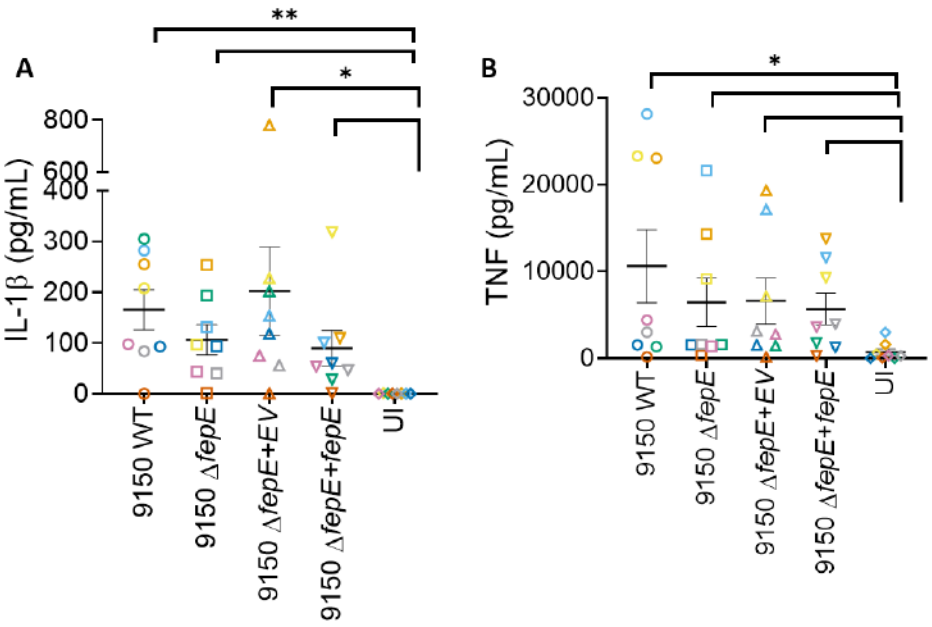


Figure 4.61 **The role of very long O-antigen chains in cytokine secretion by MDMs during infection with *S.* Paratyphi A 9150.**

MDMs were infected with *S.* Paratyphi A 9150 (9150; MOI 75) as indicated and **(A)** IL-1β secretion and **(B)** TNF secretion were determined at 3 h post infection. Symbol colours represent donors matched across both panels. Error bars show means ± SEM and statistical analysis was performed by repeated measures one-way ANOVA followed by correction for multiple comparisons. *, $p < 0.05$; **, $p < 0.01$.

Given that overexpression of *fepE* appeared to be interfering with triggering of pyroptosis in MDMs during infection with *S.* Paratyphi A 9150, it was next hypothesised that overexpression of *fepE* in *S.* Paratyphi A ED199 may limit enhanced pyroptosis in MDMs. To this end, plasmid-encoded *fepE* was introduced into *S.* Paratyphi A ED199 and MDMs were infected. However, MDMs infected with *S.* Paratyphi A ED199 overexpressing *fepE* underwent similar levels of pyroptosis as MDMs infected with *S.* Paratyphi A expressing only endogenous *fepE* (Figure 4.63A). MDMs phagocytosed *S.* Paratyphi A ED199 overexpressing *fepE* at lower, but not significant, levels (Figure 4.63B).

Additionally, the levels of IL-1β produced by MDMs during infection with *S.* Paratyphi A ED199 with or without overexpressing *fepE* were similar (Figure 4.62A), as were the levels of TNF production (Figure 4.62B), suggesting that overexpression of FepE did not lead to different host cell priming. Indeed, overexpression of *fepE* in *S.* Paratyphi A ED199 only slightly affected the electrophoretic mobility of LPS in this strain (Figure 4.62C), suggesting that either this strain has additional regulatory mechanisms for LPS O-antigen length or exogenous *fepE* could not be assimilated in the endogenous regulatory network.

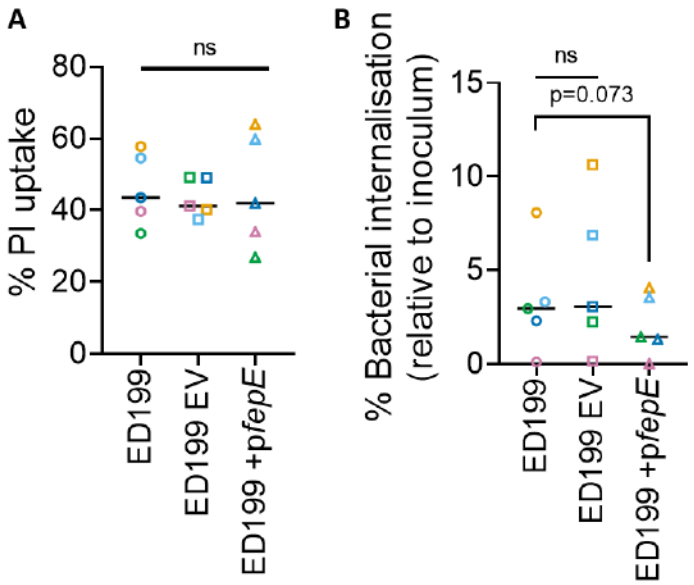


Figure 4.63 **The effect of *fepE* overexpression on *S.* Paratyphi A ED199-induced MDMs cell death.**

(A) MDMs were infected with *S.* Paratyphi A ED199 (ED199; MOI75) as indicated and cell death was determined at 3 h post infection. **(B)** Z-VAD-FMK-treated MDMs were infected with *S.* Paratyphi A ED199 and bacterial internalisation was assessed by gentamicin-resistant assays at 1.5 h post infection. Error bars show means ± SEM. Symbol colours indicate donors, which match across both panels. Statistical analysis by repeated measures one-way ANOVA. ns, not significant.

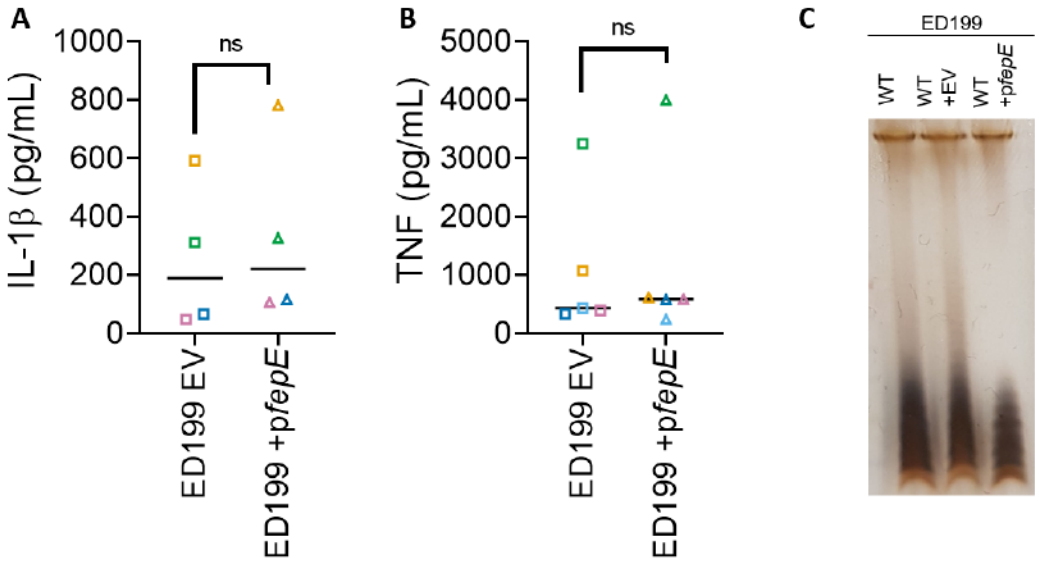


Figure 4.62 **Effect of *fepE* overexpression on *S.* Paratyphi A ED199-induced cytokine production by MDMs.**

MDMs were infected with *S.* Paratyphi A ED199 (ED199; MOI75) as indicated and **(A)** IL-1β and (B) TNF secretion were determined at 3 h post infection. (C) Electrophoretic mobility of total LPS of indicated *S.* Paratyphi A ED199 strains assessed by SDS-PAGE and silver staining. Error bars show means ± SEM. Symbol colours indicate donors, which match across both panels. Statistical analysis by paired Student's *t*-test. ns, not significant.

Finally, the role of very long O-antigen in pyroptosis induction was investigated during MDM infection with *S.* Typhimurium. Similar to observations with THP-1 cells, loss of very long O-antigen chains allowed induction of moderately higher pyroptosis in MDMs, while infection with the complemented strain resulted in significantly lower cell death compared to WT (Figure 4.64A). The differences observed in cell death levels between *S.* Typhimurium WT, Δ*fepE* and the complemented strain were not mediated by differences in phagocytosis by MDMs (Figure 4.64B). It is worth noting that the complemented strain was internalised moderately less than WT *S.* Typhimurium and Δ*fepE*, although this reduction did not reach statistical significance. These results suggest that very long O-antigen chains are capable of limiting pyroptosis during infection with *S.* Typhimurium in a similar manner to *S.* Paratyphi A.

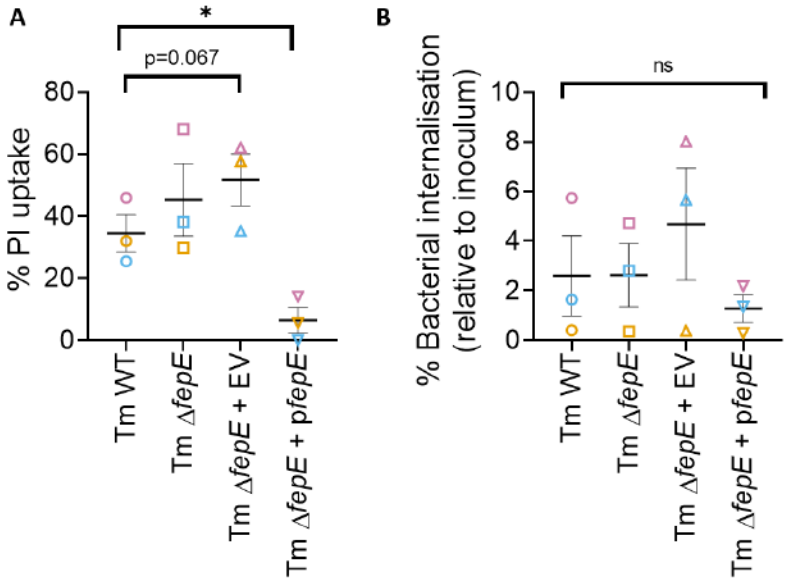


Figure 4.64 **The role of very long O-antigen chains during infection of MDMs with *S.* Typhimurium.**

(A) MDMs were infected with *S.* Typhimurium (Tm; MOI 15) as indicated and cell death was determined by PI uptake at 3 h post infection. **(B)** Z-VAD-FMK-treated MDMs were infected as indicated and phagocytosis was determined at 1.5 h post infection. Symbol colours represent donors matched across both panels. Error bars show means ± SEM and statistical analysis was performed by repeated measures one-way ANOVA. *, $p < 0.05$; ns, not significant.

4.21 *fepE* expression inversely correlates with pyroptosis during infection with *Salmonella*

Experiments presented above suggested that both *S.* Paratyphi A ED199 and *S.* Typhimurium induced higher inflammasome activation and cell death compared to *S.* Paratyphi A 9150, while overexpression of *fepE* in the complemented ΔfepE strains resulted in exaggerated phenotypes, particularly in *S.* Typhimurium. To see whether the difference in cell death induced by *S.* Paratyphi A 9150, ED199 and *S.* Typhimurium was true at the different MOIs used in previous experiments, THP-1 cells were infected at MOI 50, which has been used for *S.* Paratyphi A, MOI 15, which has been used for *S.* Typhimurium, and MOI 25 as an intermediate infection condition, and cell death and IL-1β production was determined at 3 h post infection. *S.* Paratyphi A 9150 triggered lower cell death (Figure 4.65A) and IL-1β (Figure 4.65B) secretion at all MOIs tested compared to *S.* Paratyphi A ED199 and *S.* Typhimurium. Therefore, given that *fepE*-mediated production of very long O-antigen chains prevented pyroptosis, it was hypothesised that *S.* Paratyphi A 9150 may be eliciting a low inflammasome signalling response due to high expression of *fepE*. To test this, *fepE* expression was

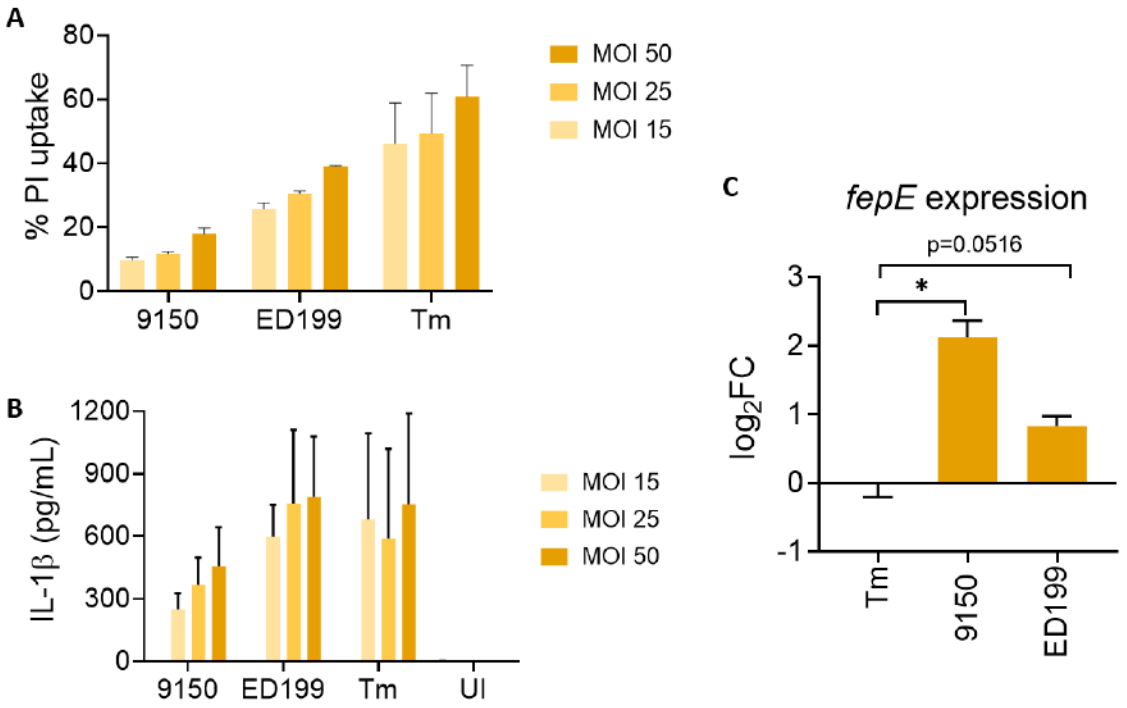


Figure 4.65 ***fepE* expression inversely correlates with *Salmonella*-induced THP-1 pyrotposis.**

THP-1 cells were infected with *S.* Paratyphi A 9150 (9105), *S.* Paratyphi A ED199 (ED199) and *S.* Typhimurium (Tm) at increasing MOIs. **(A)** Cell death and **(B)** IL-1β secretion were determined at 3 h post infection. **(C)** *fepE* expression was determined by RT-qPCR on bacteria grown to late exponential phase. The log value of the fold change is expressed as change of S. Paratyphi A 9150 or ED199 compared to *S.* Typhimurium *fepE* expression. Bars show means ± SEM from (A-B) two or (C) four independent repeats. Statistical analysis by (A-B) two-way ANOVA or (C) repeated measures one-way ANOVA. *, $p < 0.05$.

determined in *S.* Paratyphi A 9150 and *S.* Paratyphi A ED199 compared to *S.* Typhimurium. Indeed, *S.* Paratyphi A 9150 expressed ***fepE*** at significantly higher levels than *S.* Typhimurium (Figure 4.65C). *S.* Paratyphi ED199, which triggered higher cell death than *S.* Paratyphi A 9150 but lower than *S.* Typhimurium, expressed ***fepE*** at intermediate levels between the two strains (Figure 4.65C). These results thus suggest that ***fepE*** expression inversely correlates with inflammasome activation and pyroptosis induced by *Salmonella* (independently of the serovar); higher expression of ***fepE*** results in lower levels of pyroptotic cell death.

4.22 Discussion

The mechanisms of typhoidal *Salmonella*, and particularly *S.* Paratyphi A, pathogenesis are poorly understood. The results in this chapter demonstrate that both *S.* Paratyphi A and *S.* Typhi trigger pyroptotic cell death in human macrophages. However, cell death is considerably lower than that induced by the NTS *S.* Typhimurium, in line with previous reports for *S.* Typhi (Kortmann, Brubaker & Monack, 2015; Winter ***et al.***, 2015) and in keeping with the ability of typhoidal *Salmonella* to evade innate immunity (Hiyoshi ***et al.***, 2018a; Johnson, Mylona & Frankel, 2018). Limiting of pyroptosis by *S.* Paratyphi A and *S.* Typhi is speculated to be beneficial for the pathogen to either escape killing by extracellular mechanisms following cell death and release of the bacteria [such as pore-induced intracellular traps, PITs (Jorgensen ***et al.***, 2016)] and/or, more likely, to promote survival of the host cell and thus increase dissemination of the pathogen within macrophages to systemic sites. Interestingly, it was found that macrophage pyroptosis is modulated in a disparate manner both by the host and by either *S.* Paratyphi A or *S.* Typhi. Furthermore, this study, as well as other reports (Bierschenk ***et al.***, 2019; Kortmann, Brubaker & Monack, 2015; Yang ***et al.***, 2013), suggest that murine and human macrophages may exploit inflammasome signalling in different ways in response to bacterial pathogen.

S. Typhi induced caspase-dependent pyroptosis; however, a dominant role for a specific inflammasome pathway could not be identified, suggesting that redundant pathways are at play. Simultaneous inhibition of both NLRP3 and NAIP-NLRC4 activation seem to result in slightly lower activation of caspase-1, which however does reflect on cell death or IL-18 maturation. Upon IFNγ priming, which results in GBP-mediated vacuole disruption (Shenoy ***et al.***, 2012; Fisch ***et al.***, 2019a; Santos ***et al.***, 2018), *S.* Typhi Ty2 was recognized by NLRP3. This may have been the result of caspase-4-mediated recognition of the pathogen upstream of NLRP3, similar to observations previously made

with *S.* Typhimurium (Fisch et al., 2019a). Testing the effect of IFNγ priming on CASP4^{miR} cells will aid in determining whether this is the case.

The virulence of *S.* Typhi clinical isolates could not be directly compared to the reference strain (Ty2). However, it was observed that, although *S.* Typhi H58 clinical isolate have been suggested to be more virulent than non-H58 strains (Johnson *et al.*, 2018), this was not the case here in terms of induction of pyroptosis in comparison with another circulating *S.* Typhi genotype, suggesting that the success of this clade may lie on other strategies such as antibiotic resistance (Holt *et al.*, 2011, 2007), and/or enhanced survival and virulence in bile and thus upon the development of the carrier state (Johnson *et al.*, 2018).

S. Paratyphi A induced caspase-dependent pyroptosis in human macrophages. More specifically, the activities of caspase-1, caspase-4 and caspase-8, mainly via NLRP3, resulted in activation of inflammasomes and GSDMD-mediated cell death during infection with *S.* Paratyphi A 9150 (Figure 4.66). These proteins have also been implicated in pyroptosis by *S.* Typhimurium (Broz *et al.*, 2010b; Man *et al.*, 2014b; Reyes Ruiz *et al.*, 2017; Man *et al.*, 2013; Kayagaki *et al.*, 2015; Shi *et al.*, 2015; Fisch *et al.*, 2019a; Casson *et al.*, 2015; Fisch *et al.*, 2019b; Broz *et al.*, 2010a, 2012; Gurung *et al.*, 2012). Pharmacological and genetic silencing support the roles of caspase-4 in detecting bacteria and activating the NLRP3-ASC-caspase-1/8 inflammasome. In this study, ASC was shown to have an important role during inflammasome activation by *S.* Paratyphi A; while ASC may be dispensable for pyroptosis triggered by *S.* Typhimurium in human macrophages, as it was found here and reported by Bierschenk *et al.* (2019), it is required for pyroptosis induced by *S.* Paratyphi A. Caspase-4 was shown to be upstream of caspase-8 and/or NLRP3, but it was not investigated at what level ASC is specifically involved. It is expected to be recruited by NLRP3, but it may also be recruited by an unidentified sensor or at different levels of the signalling pathway. ASC has been shown to be recruited in a large inflammasome complex during infection with *S.* Typhimurium, together with NLRP3, NLRC4, caspase-1 and caspase-8 (Man *et al.*, 2014b, 2013). However, a dominant role of the NAIP-NLRC4 inflammasome could not be identified during infection with *S.* Paratyphi A, despite its involvement in *S.* Typhimurium infection (Yang *et al.*, 2013; Broz *et al.*, 2010b; Man *et al.*, 2014b; Kortmann, Brubaker & Monack, 2015; Reyes Ruiz *et al.*, 2017; Zhao *et al.*, 2011). Inhibition of both NLRP3 and NLRC4 did not completely abolish caspase-1 activation or pyroptosis during infection with *S.* Paratyphi A, suggesting the activation of an alternative pyroptotic cell death pathway. Experiments with a caspase-8 inhibitor revealed that caspase-8 also contributed to cell death by *S.* Paratyphi A. This may be explained by the known ability of caspase-8 to induce GSDMD cleavage (Orning et al., 2018; Sarhan et al., 2018); alternatively, caspase-8 may contribute to priming and/or posttranslational modification of

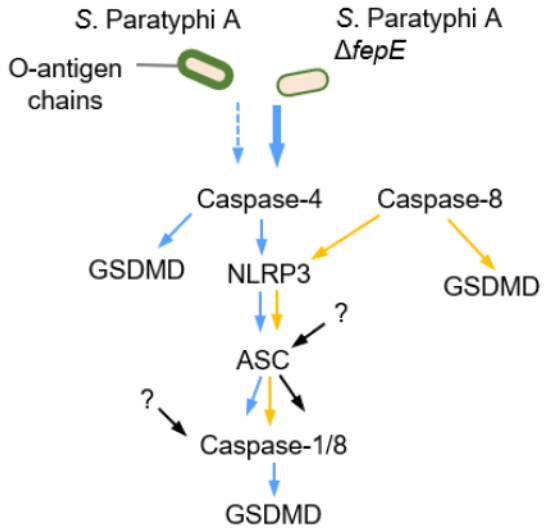


Figure 4.66 **Proposed model for *S*. Paratyphi A inflammasome activation in THP-1 cells.**

S. Paratyphi A triggers caspase-4 dependent inflammasome activation which results in pyroptotic cell death, as well as activation of NLRP3 and/or caspase-8. ASC is required for pyroptosis by *S.* Paratyphi A via NLRP3 and possibly via another as of yet unidentified mechanism. Caspase-8 may contribute to inflammasome activation via NLRP3 priming and/or direct GSDMD cleavage. A caspase-4-independent, ASC and/or caspase1/8-dependent pathway is also suggested to be activated. Loss of very long O-antigen chains regulated via FepE results in enhanced inflammasome activation during infection of human macrophages with *S.* Paratyphi A 9150.

NLRP3 (Gurung et al., 2014; Van Opdenbosch et al., 2017). As simultaneous inhibition of caspase-4, caspase-8, and NLRP3 did not completely prevent pyroptosis during *S.* Paratyphi A infection, other pathways, possibly through ASC, may be involved in detecting *S.* Paratyphi A infection (Figure 4.69), which warrant further investigation.

On the pathogen side, the SPI-1 T3SS in both *S.* Paratyphi A and *S.* Typhi is required for inflammasome activation and induction of pyroptosis, similar to what has been reported for *S.* Typhimurium (Mariathasan ***et al.***, 2004; Miao ***et al.***, 2006; Bierschenk ***et al.***, 2019; Casson ***et al.***, 2015). The importance of SPI-1 T3SS in immune recognition is shared with clinical isolates belonging to either typhoidal *Salmonella* serovar, and thus clinical variants with higher expression of SPI-1 result in higher levels of cell death during infection of human macrophages. Although SPI-1 T3SS did not mediate initial bacterial uptake of *S.* Paratyphi A or *S.* Typhi by macrophages, it facilitated *S.* Paratyphi A escape to the cytosol, while *S.* Typhi escaped to the cytosol independently of SPI-1, possibly suggesting a pathogen-independent mechanism for phagosome disruption. Nevertheless, the low typhoidal *Salmonella* escape to the cytosol correlates with lower activation of inflammasomes, which may indicate a mechanism of evading pathogen recognition by intracellular host cell sensors. Although inherent differences between serovars in the SPI-1 structural proteins may partly mediate this, as is the case of the highly similar SipC of *S.* Typihmurium and the homolog IpaC in *Shigella* (Du ***et al.***, 2016), it is more likely that higher SPI-1 expression and/or T3SS activity are responsible. In keeping with this, the higher level of SPI-1 expression in *S.* Paratyphi A clinical isolates was consistent with their ability to cause more pyroptosis. Furthermore, although escape to the cytosol by clinical variants or by overexpressing the SPI-1 in *S.* Paratyphi A 9150 remains to be determined, *S.* Paratyphi A 9150

internalization by macrophages was enhanced once SPI-1 was overexpressed by HilA, which in turn resulted in more cell death. These results collectively suggest that *S.* Paratyphi A 9150 may limit SPI-1 expression as an immune evasion mechanism, which may also explain the lack of a significant role for NAIP-NLRC4 in inflammasome activation and cell death.

A major difference between *S.* Paratyphi A and *S.* Typhi is the presence of the Vi antigen in the latter, while *S.* Paratyphi A produces very long O-antigen chains regulated by FepE. Although the Vi antigen of *S.* Typhi interfered with invasion in HeLa cells (Bishop ***et al.***, 2008), a role in limiting inflammasome activation was not identified in the settings tested herein. This suggests that the presence of the Vi antigen does not prevent intracellular recognition of *S.* Typhi by inflammasomes, in line with a previous report (Winter ***et al.***, 2015), even upon inducing efficient SPI-1 expression. Thus, while the TviA regulator may have an important role in limiting induction of pyroptosis by *S.* Typhi indirectly (Winter et al., 2015), the physical presence of the Vi and/or intracellular expression and production of the capsule is not directly involved in intracellular shielding of the pathogen. *S.* Typhi may therefore have additional immune evasion strategies against inflammasome activation. To this end, the role of the *S.* Typhi-specific T3SS effector StoD was investigated; however, a role of this effector in pyroptosis induction or prevention was not identified. The role of other virulence factors, and possibly putative T3SS effectors (Frankel and Pupko groups, unpublished data), in modulating inflammasome activation warrant further investigation.

On the other hand, very long O-antigen chains produced by *S.* Paratyphi A were shown to interfere with host cell-pathogen interactions. Very long LPS O-antigen chains are produced by the polysaccharide copolymerase FepE. It was shown here that *S.* Paratyphi A very long O-antigen chains interfered with host epithelial cell invasion. Overexpression of ***fepE*** interferes with host cell invasion in a similar manner to *S. sonnei* overexpressing its O antigen capsule (Caboni ***et al.***, 2015). Importantly, the very long LPS O-antigen chains suppressed *S.* Paratyphi A-induced inflammasome activation and pyroptosis without promoting escape from the vacuole to the cytosol. The O-antigen chains have been shown to limit the accessibility of the *S.* Typhimurium (Hölzer et al., 2009), *S. flexneri* (West et al., 2005) and *S. sonnei* (Caboni ***et al.***, 2015) T3SS to the host lipid bilayer and is thus speculated that very long O-antigen chains in *S.* Paratyphi A may have a similar role. It should, however, be noted that it is unclear why this would impact only non-phagocytic cell invasion and not uptake by macrophages or intracellular escape from the vacuole, suggesting distinct mechanisms of internalisation into macrophages and triggering epithelial cell invasion. Expression of ***fepE*** when *S.* Paratyphi A is intracellular is unknown. Very long O-antigen chains may be required for survival of *S.* Typhimurium in SCVs as modelled by growth in minimal media *in vitro* (Silva ***et al.***, 2018). Therefore, given its role in

immune evasion, it would be expected that *S.* Paratyphi A expresses ***fepE*** intracellularly. In fact, it is possible that the differences in caspase-4 contribution during infection with *S.* Paratyphi A and *S.* Typhi may have to do with intracellular expression of ***fepE*** and Vi genes. To determine the effect of very long O-antigen chains on the assembly and activity of SPI-1 T3SS, translocation of T3SS effector proteins into host cells upon deletion of ***fepE*** should be tested in the future, as well as the intracellular ***fepE*** expression. Alternatively, during epithelial cell infection, very long O-antigen chains may impact on the proximity of other attachment and invasion virulence factors to the host cell membrane.

Consistent with a role in evading inflammasome activation, very long O-antigen chains in *S.* Paratyphi A have been shown to reduce antibody-mediated recognition by the host and respiratory burst in neutrophils (Hiyoshi ***et al.***, 2018b). Additionally, synthesis of very long O-antigen chains has been shown to be important for *S.* Typhimurium virulence, as they contribute to complement resistance, bile acid tolerance and interactions with host cells during *S.* Typhimurium infection (Hölzer ***et al.***, 2009; Murray, Attridge & Morona, 2003, 2006, 2005; Crawford ***et al.***, 2012). Importantly, it was found that ***fepE*** expression is inversely correlated with pyroptosis induced by ***Salmonella*** strains. The exaggerated phenotype seen during infection with S. Typhimurium ***fepE***-complemented strain, compared to that seen in S. Paratyphi A 9150, where pyroptosis levels were much lower than the WT levels, is possibly a result of the lower basal levels of ***fepE*** expression in *S.* Typhimurium in comparison to *S.* Paratyphi A 9150. Therefore, overexpression of ***fepE*** in this strain exceeded the endogenous levels of ***fepE*** in *S.* Typhimurium and hence the enhanced immune evasion ability of the complemented strain.

Altogether, loss of very long O-antigen chains resulted in enhanced inflammasome activation, which was independent of macrophage priming, bacterial uptake or vacuolar escape. Although the activating signals of NLRP3 and caspase-8 remain to be elucidated, these signalling pathways were amplified in the absence of very long O-antigen chains in *S.* Paratyphi A. As caspase-4 was shown to be active upstream of these molecules, it is likely that ***fepE***-mediated evasion of inflammasome activation is achieved at the caspase-4 level. Human macrophages have previously been shown to detect LPS through caspase-4 during infection with *S.* Typhimurium (Fisch ***et al.***, 2019b, 2019a; Baker ***et al.***, 2015; Casson ***et al.***, 2015), EPEC (Goddard ***et al.***, 2019), ***Yersinia*** (Casson ***et al.***, 2015), and ***Francisella*** (Lagrange ***et al.***, 2018). During *S.* Paratyphi A infection, the length of LPS sugar chains might sterically hinder caspase-4-mediated recognition of lipid-A in the cytosol (Shi et al., 2014). Thus the modification of LPS O-antigen polysaccharide length, which is dispensable for caspase-4 binding (Kayagaki et al., 2013; Hagar et al., 2013), can indirectly reduce caspase-4 LPS recognition and activation and help bacteria evade detection in human cells. Bacterial modifications of LPS acylation,

for example by *Helicobacter*, *Francisella* and *Yersinia*, has previously been reported to suppress caspase-4/11 activation in human and mouse macrophages (Hagar et al., 2013; Lagrange et al., 2018; Shi et al., 2014; Kayagaki et al., 2013). However, unlike mouse caspase-11, human caspase-4 can detect hypo-acylated LPS from *Francisella*, which indicate species-specific differences that need to be taken into account (Lagrange et al., 2018). Other mechanisms of subverting caspase-4 in epithelial cells include T3SS effectors that inhibit it, such as OspC3 from *Shigella* and NleF from EPEC and EHEC (Kobayashi et al., 2013; Pallett et al., 2016), but no such effectors have been described in *Salmonella* to date (Sanchez-Garrido *et al.*, 2020). O-antigen-mediated inhibition of caspase-4 activation may also be used by *S. sonnei* (Watson *et al.*, 2019); whether other bacteria that regulate very long O antigen chains, such as *S.* Dublin and *S.* Enteritidis (Murray, Attridge & Morona, 2003), *Pseudomonas aeruginosa* (Kintz et al., 2008) and *S. flexneri* (Morona, Daniels & Van Den Bosch, 2003; Hong & Payne, 1997), may also evade caspase-4 detection should be investigated in the future. A key experiment would be to determine caspase-4 recruitment (Thurston *et al.*, 2016; Fisch *et al.*, 2019a) to intracellular WT *S.* Paratyphi A and compare it to that of *S.* Paratyphi A Δ*fepE*. Furthermore, a partially reduced LPS O-antigen chain length (e.g. via deletion of the regulator *wzzB*) (Hölzer *et al.*, 2009) should also be studied for its effect on inflammasome activation, which would further enhance the findings presented here. Additionally, although caspase-5 is suggested to play a minimal role in *S.* Typhimurium-induced inflammasome activation in human macrophages (Fisch *et al.*, 2019b; Baker *et al.*, 2015), given the disparate host cell responses to these pathogens its role should be determined in the context of *S.* Paratyphi A infection in the future.

The role of very long O-antigen chains in interfering with pyroptosis was also demonstrated during MDM infection with either *S.* Paratyphi A or *S.* Typhimurium, further supporting their contribution in immune evasion irrespective of other virulence factors promoting or preventing inflammation which are not shared between the two serovars. Importantly, MDMs require a larger bacterial inoculum to respond to infection with *S.* Paratyphi A (and *S.* Typhi) via pyroptotic cell death, which may reflect the ability of typhoidal *Salmonella* to escape inflammatory signalling. It would be interesting to test survival of these serovars within MDMs in the future. However, experiments in MDMs suggested that inflammasome signalling may differ between THP-1 cells and MDMs in response to *S.* Paratyphi A infection. We were unable to verify the contribution of caspase-4 in inflammasome activation and pyroptosis by *S.* Paratyphi A, and the caspase-4-independent pathway already suggested in THP-1 cells may have a more prominent role in MDMs. Given the higher expression of all inflammasome proteins (e.g. caspases, NAIP) in MDMs compared to THP-1 cells, it is possible that other pathways compensate for the lack of one arm of the signalling pathway. Therefore, critical

experiments to be performed in the future would be silencing and/or pharmacologically inhibiting more than one sensor at a time in MDMs and testing their role in *S.* Paratyphi A infection.

Similar to observations in Chapter 3, it is also reported in this Chapter that clinical *S.* Paratyphi A isolates are more virulent than the prototype *S.* Paratyphi A 9150 strain in terms of macrophage cytotoxicity, likely driven by enhanced SPI-1 activity, prompting the re-evaluation of the suitability of the reference strain. Possible SNPs in *S.* Paratyphi A clinical isolates may be within genes responsible for immune activation. Unfortunately, clinical isolates are often unsuitable for genetic manipulation, due to the high rate of secondary mutations. Nevertheless, the data presented herein showed that *S.* Paratyphi A ED199, which has been used in clinical human challenge studies (McCullagh et al., 2015; Dobinson et al., 2017), largely corresponds with the pathogenicity of other clinical variants in terms of macrophage invasion and inflammasome activation. Studies presented here should be thus corroborated with this clinical isolate, as well as clinical variants isolated in different geographical regions to reflect possible adaptation.

Despite the importance of the results presented here, this study had limitations that should be addressed in future studies. Although implications about the interactions of *S.* Paratyphi A with epithelial cells are made with the use of HeLa cells, it is understood that this is not the optimal model for such investigations. HeLa cells are not a good representation of intestinal epithelial cells, as they do not originate from this tissue and they are not polarised; however, they serve as a good model to investigate the activity of SPI-1. To further understand interactions of *S.* Paratyphi A with epithelial cells, other cell lines should be used and test whether the phenotypes observed here are physiologically relevant. Furthermore, while *S.* Paratyphi A 9150 has more frequently been used in published studies and hence it was chosen for experiments presented herein, given its highly attenuated profile, a low-passage clinical isolate or another more virulent reference strain should be used, such as *S.* Paratyphi A AKU12601. As the genomes of more isolates become available these can also be exploited. Mutants made with clinical isolates should be sequenced to verify the lack of secondary mutations prior to experiments.

In summary, this chapter has shown that *S.* Paratyphi A induces inflammasome-dependent cell death during infection of human macrophages and serves as a novel characterisation of pyroptosis induction during infection with *S.* Paratyphi A. This process is dependent on the SPI-1 T3SS and is limited by production of very long O-antigen chains in both THP-1 cells and MDMs. Very long O-antigen chains can also modulate pyroptosis during infection of THP-1 cells and MDMs by *S.* Typhimurium and, critically, a higher expression of ***fepE*** is correlated with a lower induction of pyroptosis. The model proposed by the data obtained here involves *S.* Paratyphi A leading to caspase-4-dependent pyroptosis

and NLRP3-ASC-capsase-1 activation during which caspase-8 also contributes, likely via NLRP3 priming, GSDMD cleavage and/or in an unidentified inflammasome pathway. Additional caspase-independent and/or ASC-dependent pathways may also be involved. Thus, *S.* Paratyphi A interacts with human immune cells through mechanisms distinct to other *Salmonella* serovars. In the future, each pathway shown in Figure 4.69 should be targeted in a more systematic way by effective genetic manipulation (e.g. siRNA) in MDMs to verify its contribution to inflammasome activation by S. Paratyphi A. Nevertheless, observations such as those outlined here are critical for understanding how *S.* Paratyphi A (and other invasive *Salmonella*) stimulate infection and evade immune recognition and thus provide important insights as to how we can circumvent these pathways. The increasing prevalence of *S.* Paratyphi A and the efforts for a universal vaccine development against enteric fever, support the need for future studies to focus on better understanding of the virulence mechanisms of *S.* Paratyphi A and its interactions with host immune cells.

5

Final conclusions and future perspectives

Enteric fever remains a major public health problem in middle and low-income countries (Woods *et al.*, 2006; Stanaway *et al.*, 2019; Sahastrabuddhe *et al.*, 2013; Zellweger *et al.*, 2017). Although improvements in sanitation are of particular importance and often the most effective route to limit transmission of enteric fever (Baker *et al.*, 2011; Stanaway *et al.*, 2019; Marchello, Hong & Crump, 2019), this often entails large scale reorganisation. Therefore, it is crucial to develop strategies to target the causing agents. Comprehending the mechanisms by which *S.* Paratyphi A and *S.* Typhi interact with the host, lead to disease, and evade host immunity are essential for facilitating the undertaking of such strategies. However, much of the understanding of typhoidal *Salmonella* pathogenesis and virulence comes from studies in murine models infected with NTS serovars such as

S. Typhimurium, despite the multitude of differences between the two classes of serovars (Sabbagh *et al.*, 2010; Johnson, Mylona & Frankel, 2018; Gal-Mor, 2019; Gal-Mor, Boyle & Grassl, 2014). Furthermore, as *S.* Typhi is the main cause of enteric fever in endemic countries, the molecular pathogenesis of *S.* Paratyphi A has attracted little interest. Many epidemiological studies now indicate the surge in the incidence of *S.* Paratyphi A (Zellweger *et al.*, 2017; Zhou *et al.*, 2014; Sahastrabuddhe *et al.*, 2013; Karkey *et al.*, 2013), as well as in MDR frequency (Sahastrabuddhe *et al.*, 2013; Dongol *et al.*, 2012; Zellweger *et al.*, 2017), thus raising the possibility of it becoming the next main cause of enteric fever within the next few years (Baker, Karkey & Parry, 2014).

Most studies so far have focused on the epidemiology of *S.* Paratyphi A (Karkey *et al.*, 2013; Zellweger *et al.*, 2017; Zhou *et al.*, 2014); hence, systematic characterisation of *S.* Paratyphi A in terms of its molecular virulence and pathogenesis is lacking (Hiyoshi *et al.*, 2018b; Elhadad *et al.*, 2016, 2015b, 2015a; Gal-Mor *et al.*, 2012). The main aims of this study were thus to investigate the pathogenic mechanisms used by *S.* Paratyphi A during exposure to bile and during interactions with host cells, focussing on macrophages, two aspects that may prove to be useful for understanding the systemic phase of enteric fever. Throughout this project, *S.* Paratyphi A was compared to *S.* Typhi. This is due to the fact that, while *S.* Typhi and *S.* Paratyphi A have undergone extensive convergent evolution to independently acquire characteristics leading to the same clinical syndrome and to their common extraintestinal lifestyle, the two serovars are phenotypically and genetically distinct (Didelot *et al.*, 2007; Holt *et al.*, 2009; McClelland *et al.*, 2004). Therefore, identifying differences and commonalities between the two will deepen our understanding of enteric fever in order to develop appropriate strategies to target these pathogens.

Chronic carriage during enteric fever is more frequently associated with colonisation of the gallbladder rather than other systemic sites by *S.* Typhi and *S.* Paratyphi A (Dongol *et al.*, 2012; Gal-Mor, 2019), although this may partially be caused by the increased frequency of detection due to medical procedures such as cholecystectomy. Nonetheless, molecular mechanisms that promote survival and virulence in this environment are required to be elucidated to begin to understand how typhoidal *Salmonella* establish carriage. Recently our lab showed that, in the presence of bile, *S.* Typhi behaves very differently to *S.* Typhimurium, the long-standing model of *Salmonella* behaviour in response to bile, exemplifying that the typhoidal and NTS exploit bile in a disparate manner to adjust their virulence and evidently exploit different infection strategies (Johnson *et al.*, 2018). The present study sought to investigate whether *S.* Paratyphi A and *S.* Typhi behave in a similar manner in the presence of bile, as it may represent common strategies upon systemic infection. It was demonstrated that bile affects gene expression in *S.* Paratyphi A, resulting in > 5% of the genome to be differentially

expressed in the presence of bile. While *S.* Typhi and *S.* Paratyphi A regulated many genes in a shared manner, it was interesting to observe differences in regulation of metabolic genes and genes that are thought to be useful for bile tolerance, suggesting that the two pathogens adapt to bile by different mechanisms. Indeed, many genes that differ between the two serovars (e.g. pseudogenes, unique genes, etc.) are involved in metabolism, in line with the idea that the main differences between serovars may lie in their metabolic traits (Seif ***et al.***, 2018). In keeping with this idea, several S. Typhi pseudogenes that are intact in S. Paratyphi A may be involved in metabolic processes and the expression of many of them was regulated by bile. Future studies investigating regulation of metabolism in response to bile may elucidate useful infection strategies exploited by typhoidal *Salmonella* serovars.

The innate immune pathway has numerous PRRs to sense bacteria, in order to elicit a protective immune response (Medzhitov, 2007). While both typhoidal serovars examined in this project are skilled at evading immunity (Raffatellu ***et al.***, 2008; Hiyoshi ***et al.***, 2018a), they do so using different strategies. For example, while it was recently proposed that the Vi antigen in *S.* Typhi and the very long O-antigen chains in *S.* Paratyphi A may fulfil analogous roles during evading the phagocytic respiratory burst (Hiyoshi ***et al.***, 2018b), such an analogy could not be determined in terms of dampening inflammasome activation by the two pathogens. The fact that the majority of pseudogenes and virulence strategies were acquired by convergent evolution between *S.* Typhi and *S.* Paratyphi A implies that the underlying mechanisms may differ (Hiyoshi ***et al.***, 2018a). These need to be understood and delineated by direct comparisons between the two pathogens in order to understand enteric fever and develop strategies to target it. It was further shown here that, while *S.* Typhi may be inducing less pyroptosis than *S.* Typhimurium by limiting flagellin and/or SPI-1 expression in a TviA-dependent manner (Winter ***et al.***, 2015; Kortmann, Brubaker & Monack, 2015), the main strategies to limit inflammasome activation in human macrophages by *S.* Paratyphi A are probably mediated by synthesising very long O-antigen chains intracellularly and by tightly regulating its SPI-1 expression via an unknown mechanism.

The O-antigen is recognised by the immune system and results in antibody production (Martin ***et al.***, 2016). Thus it would not be surprising (Seif ***et al.***, 2019) if, despite the defining feature of carrying the uncommon O2 antigen in *S.* Paratyphi A (Kothari ***et al.***, 2014; Hiyoshi ***et al.***, 2018b), the O-antigen is under selection, and variations in the gene clusters responsible for its synthesis may be observed between clinical isolates. FepE expression in *S.* Paratyphi A ED199 was lower than that in 9150 which led to the hypothesis that overexpressing ***fepE*** into ED199 would result in excessive production of very long O chains and reduce pyroptosis. As this was not seen, it is speculated that differences in O-antigen

biosynthesis and regulation pathways are at play. Future analyses on understanding O-antigen variation in *S.* Paratyphi A would be pivotal for determining its effect(s) on virulence and immunity, and ultimately help in an informed vaccine design (Sahastrabuddhe ***et al.***, 2013; Martin ***et al.***, 2016).

S. Paratyphi A 9150 currently remains the most frequently used strain in *in vitro* studies of interactions between host cells and *S.* Paratyphi A and this, combined with the possibility of genetically manipulating it, is why it was chosen for this study. Strikingly, transcriptomic analysis of *S.* Paratyphi A 9150 and the recently isolated *S.* Paratyphi A ED199, as well as investigations on host cell invasion and inflammasome signalling, revealed that clinical variants may be behaving differently to the reference strain. The clinical isolates used in this study exhibit enhanced virulence in terms of invasiveness, motility and inflammasome activation compared to *S.* Paratyphi A 9150. *S.* Paratyphi A 9150 appears to be highly attenuated, as suggested by the low epithelial cell invasion, motility and induction of cell death; its low *in vitro* virulence will make clinical isolates seem more virulent compared to the reference strain. These results are consistent with data generated with an outbreak *S.* Paratyphi A isolate in Israel, which was more invasive and motile than *S.* Paratyphi A 9150 (Gal-Mor et al., 2012). It is likely that *in vitro* adaptation over time has attenuated *S.* Paratyphi A 9150, in a manner comparable to *S.* Typhi (Johnson ***et al.***, 2018). Alternatively, the phenotypes displayed by the clinical isolates may be a result of adaptation by SNP acquisition within the geographical region they were isolated, similarly to observations with differing *S.* Typhi genotypes (Wong ***et al.***, 2015; Frankel ***et al.***, 1989). Comparative studies between *S.* Paratyphi A 9150 and AKU 12601, another available sequenced reference strain, may facilitate selection of the more appropriate strain to use in *in vitro* assays. Alternatively, as more genomes become available, a more relevant clinical isolate may replace the currently available reference strains, such as *S.* Paratyphi A ED199. However, it should be taken into account that *in vitro* studies do not necessarily imply an increased virulence *in vivo*. Where possible, additional studies with primary human cells and/or *in vivo* models will be required to confirm the phenotypes observed in this project. Furthermore, the clinical variants used in this study are all from one geographical region and they may not be truly representative of the circulating *S.* Paratyphi A; increasing the number of isolates coming from different endemic regions is pivotal for determining how representative the responses observed here are of *S.* Paratyphi A infection.

This study also provided insights into the differences in host cell invasion and evasion of the immune system between typhoidal and NTS. *S.* Paratyphi A may have unique virulence mechanisms compared to *S.* Typhi, as well as to *S.* Typhimurium, and therefore their infection strategies should not be assumed to be identical. This was exemplified in terms of SPI-1 regulation, inflammasome activation and FepE-mediated immune evasion. This further supports that *S.* Typhimurium infection of human

cells/tissues is evidently not the suitable model for typhoidal *Salmonella* (both *S.* Paratyphi A and *S.* Typhi) (Johnson, Mylona & Frankel, 2018), and, while it is of immediate interest due to the importance of NTS-induced gastroenteritis in public health, enteric fever is a much more dangerous disease that actually requires treatment to resolve. It was surprising that, while *S.* Paratyphi A and *S.* Typhimurium may potentially share an immune evasion strategy, the very long O-antigen chains (Murray, Attridge & Morona, 2003, 2006, 2005; Hölzer *et al.*, 2009), *S.* Paratyphi A exploits this in a distinct manner to *S.* Typhimurium by expressing the gene at higher levels so by having more very long O-antigen chains (than long chains) allow to moderate intracellular inflammasome activation, as well as the respiratory burst (Hiyoshi *et al.*, 2018b). This, combined with the uncommon O2 antigen, demonstrates that *S.* Paratyphi A evades immune mechanisms by exploiting unique strategies compared to other human-infecting *Salmonella* serovars. For example, the increased *fepE* expression in *S.* Paratyphi A may be a result of the different infection strategy compared to *S.* Typhimurium, promoting immune evasion and migration from the intestinal tissue by *S.* Paratyphi A. Open questions to be addressed in the future include the expression profile of *fepE* as well as other O-chain length regulators, their regulation in *S.* Paratyphi A, and whether these differ from *S.* Typhimurium, which may shed light on the infection stages that this immune evasion method is used.

While the two typhoidal serovars share several genes, unlike other *Salmonella* genomes, there are generally no obvious candidates that can be linked to their common lifestyle (McClelland *et al.*, 2004; Holt *et al.*, 2009). Both *S.* Paratyphi A and *S.* Typhi have loss-of-function mutations in genes linked to survival in the intestine, such as the operon responsible for butyrate metabolism (Bronner *et al.*, 2018), or genes potentially associated with their human restriction (Spanò & Galán, 2012; Solano-Collado, Rofe & Spanò, 2018). However, sharing many of the strategies shown to facilitate, for instance, the suppression of intestinal inflammation, such as downregulation of SPI-1 and flagellin expression (Table 1.2), or aversion of complement activation and the respiratory burst (Hart *et al.*, 2016; Hiyoshi *et al.*, 2018b; Wangdi *et al.*, 2014; Wilson *et al.*, 2011), does not necessarily mean sharing the underlying mechanisms, as is becoming clear in many instances (Vi versus FepE; TviA versus unknown mechanism to downregulate SPI-1 and flagellar expression, etc.). Therefore, as we move into an era of mass *S.* Typhi vaccination, and given the increasing rates of *S.* Paratyphi A infections, we need to quickly identify and comprehend the common and distinct mechanisms of virulence exhibited by these two serovars, which will offer avenues for future research and will contribute to developing novel vaccination strategies targeting both pathogens.

References

Aachoui, Y., Leaf, I.A., Hagar, J.A., Fontana, M.F., et al. (2013) Caspase-11 Protects Against Bacteria That Escape the Vacuole. *Science*. 339 (6122), 975–978.

Achtman, M. (2008) Evolution, Population Structure, and Phylogeography of Genetically Monomorphic Bacterial Pathogens. *Annual Review of Microbiology*. 62 (1), 53–70.

Aglietti, R.A., Estevez, A., Gupta, A., Ramirez, M.G., et al. (2016) GsdmD p30 elicited by caspase-11 during pyroptosis forms pores in membranes. *Proceedings of the National Academy of Sciences of the United States of America*. 113 (28), 7858–7863.

Alexander, C. & Rietschel, E.T. (2001) Bacterial lipopolysaccharides and innate immunity. *Journal of Endotoxin Research*. 7 (3), 167–202.

Álvarez-Ordóñez, A., Begley, M., Prieto, M., Messens, W., et al. (2011) *Salmonella* spp. survival strategies within the host gastrointestinal tract. *Microbiology*.157 (12) pp.3268–3281.

Anand, P.K., Subbarao Malireddi, R.K., Lukens, J.R., Vogel, P., et al. (2012) NLRP6 negatively regulates innate immunity and host defence against bacterial pathogens. *Nature*.488 (7411) pp.389–393.

Andrews, S. (2010) *No Title*. 2010. FastQC: a quality control tool for high throughput sequence data. Available from: https://www.bioinformatics.babraham.ac.uk/projects/fastqc/.

Antillón, M., Warren, J.L., Crawford, F.W., Weinberger, D.M., et al. (2017) The burden of typhoid fever in low- and middle-income countries: A meta-regression approach Marilia Sá Carvalho (ed.). *PLoS Neglected Tropical Diseases*. 11 (2), e0005376.

Antonopoulos, C., Russo, H.M., El Sanadi, C., Martin, B.N., et al. (2015) Caspase-8 as an effector and regulator of NLRP3 inflammasome signaling. *Journal of Biological Chemistry*. 290 (33), 20167–20184.

Antunes, L.C.M., Andersen, S.K., Menendez, A., Arena, E.T., et al. (2011) Metabolomics reveals phospholipids as important nutrient sources during *Salmonella* growth in bile in vitro and in vivo. *Journal of Bacteriology*. 193 (18), 4719–4725.

Antunes, L.C.M., Wang, M., Andersen, S.K., Ferreira, R.B.R., et al. (2012) Repression of *Salmonella* enterica phop expression by small molecules from physiological bile. *Journal of Bacteriology*. 194 (9), 2286–2296.

Arjyal, A., Basnyat, B., Nhan, H.T., Koirala, S., et al. (2016) Gatifloxacin versus ceftriaxone for uncomplicated enteric fever in Nepal: An open-label, two-centre, randomised controlled trial. *The Lancet Infectious Diseases*. 16 (5), 535–545.

Arricau, N., Hermant, D., Waxin, H., Ecobichon, C., et al. (1998) The RcsB-RcsC regulatory system of *Salmonella* typhi differentially modulates the expression of invasion proteins, flagellin and Vi antigen in response to osmolarity. *Molecular Microbiology*. 29 (3), 835–850.

Van Asten, F.J.A.M., Hendriks, H.G.C.J.M., Koninkx, J.F.J.G., Van Der Zeijst, B.A.M., et al. (2000) Inactivation of the flagellin gene of *Salmonella* enterica serotype Enteritidis strongly reduces invasion into differentiated Caco-2 cells. *FEMS Microbiology Letters*. 185 (2), 175–179.

Azriel, S., Goren, A., Shomer, I., Aviv, G., et al. (2017) The Typhi colonization factor (Tcf) is encoded by multiple non-typhoidal *Salmonella* serovars but exhibits a varying expression profile and interchanging contribution to intestinal colonization. *Virulence*. 1–17.

Bai, J., Kim, S.I., Ryu, S. & Yoon, H. (2014) Identification and characterization of outer membrane vesicle-associated proteins in *Salmonella* enterica serovar Typhimurium. *Infection and Immunity*. 82 (10), 4001–4010.

Baker, P.J., Boucher, D., Bierschenk, D., Tebartz, C., et al. (2015) NLRP3 inflammasome activation downstream of cytoplasmic LPS recognition by both caspase-4 and caspase-5. *European Journal of Immunology*. 45 (10), 2918–2926.

Baker, S., Hardy, J., Sanderson, K.E., Quail, M., et al. (2007a) A novel linear plasmid mediates flagellar variation in *Salmonella* Typhi. *PLoS Pathogens*. 3 (5), 0605–0610.

Baker, S., Holt, K., Van De Vosse, E., Roumagnac, P., et al. (2008) High-throughput genotyping of

Salmonella enterica serovar Typhi allowing geographical assignment of haplotypes and pathotypes within an urban district of Jakarta, Indonesia. *Journal of Clinical Microbiology*. 46 (5), 1741–1746.

Baker, S., Holt, K., Whitehead, S., Goodhead, I., et al. (2007b) A linear plasmid truncation induces unidirectional flagellar phase change in H:z66 positive *Salmonella* Typhi. *Molecular Microbiology*. 66 (5), 1207–1218.

Baker, S., Holt, K.E., Clements, A.C.A., Karkey, A., et al. (2011) Combined high-resolution genotyping and geospatial analysis reveals modes of endemic urban typhoid fever transmission. *Open Biology*. 1 (OCTOBER).

Baker, S., Karkey, A. & Parry, C. (2014) Are we adequately prepared for the emergence of *Salmonella* enterica serovar Paratyphi A? *The Lancet Global Health*.2 (4) pp.e195–e196.

den Bakker, H.C., Moreno Switt, A.I., Govoni, G., Cummings, C.A., et al. (2011) Genome sequencing reveals diversification of virulence factor content and possible host adaptation in distinct subpopulations of *Salmonella* enterica. *BMC Genomics*. 12 (1), 425.

Bakowski, M.A., Braun, V. & Brumell, J.H. (2008) *Salmonella*-containing vacuoles: Directing traffic and nesting to grow. *Traffic*. 9 (12), 2022–2031.

Barker, R.M., Kearney, G.M., Nicholson, P., Blair, A.L., et al. (1988) Types of *Salmonella* paratyphi B and their phylogenetic significance. *J. Med. Microbiol*.26.

Basnyat, B. & Baker, S. (2015) Typhoid carriage in the gallbladder. *The Lancet*. 386 (9998), 1074.

Bauernfeind, F.G., Horvath, G., Stutz, A., Alnemri, E.S., et al. (2009) Cutting Edge: NF-κB Activating Pattern Recognition and Cytokine Receptors License NLRP3 Inflammasome Activation by Regulating NLRP3 Expression. *The Journal of Immunology*. 183 (2), 787–791.

Bäumler, A.J. (1997) The record of horizontal gene transfer. *Trends Microbiol.* 5 (8), 318–322.

Bäumler, A.J., Tsolis, E.M., Ficht, T.A. & Adams, L.G. (1998) Evolution of Host Adaptation in *Salmonella* enterica. *Infection and immunity*. 66 (10), 4579–4587.

Begley, M., Gahan, C.G.M. & Hill, C. (2005) The interaction between bacteria and bile. *FEMS Microbiology Reviews*. 29 (4), 625–651.

Del Bel Belluz, L., Guidi, R., Pateras, I.S., Levi, L., et al. (2016) The Typhoid Toxin Promotes Host Survival and the Establishment of a Persistent Asymptomatic Infection. *PLoS Pathogens*. 12 (4).

Bergsbaken, T., Fink, S.L. & Cookson, B.T. (2009) Pyroptosis: host cell death and inflammation. *Nature Reviews Microbiology*. 7 (2), 99–109.

Beuzón, C.R., Salcedo, S.P. & Holden, D.W. (2002) Growth and killing of a *Salmonella* enterica serovar Typhimurium sifA mutant strain in the cytosol of different host cell lines. *Microbiology*. 148 (9), 2705–2715.

Bhan, M., Bahl, R. & Bhatnagar, S. (2005) Typhoid and paratyphoid fever. *The Lancet*. 36, 749–762.

Bierschenk, D., Boucher, D. & Schroder, K. (2017) *Salmonella*-induced inflammasome activation in humans. *Molecular Immunology*. 86, 38–43.

Bierschenk, D., Monteleone, M., Moghaddas, F., Baker, P.J., et al. (2019) The *Salmonella* pathogenicity island-2 subverts human NLRP3 and NLRC4 inflammasome responses. *Journal of Leukocyte Biology*. 105 (2), 401–410.

Bishop, A., House, D., Perkins, T., Baker, S., et al. (2008) Interaction of *Salmonella* enterica serovar Typhi with cultured epithelial cells: Roles of surface structures in adhesion and invasion. *Microbiology*. 154 (7), 1914–1926.

Blaser, M.J. & Newman, L.S. (1982) A Review of Human Salmonellosis I Infective Dose. *Reviews of Infectious Diseases*. 4 (6), 1096–1106.

Bossaller, L., Chiang, P.-I., Schmidt-Lauber, C., Ganesan, S., et al. (2012) Cutting Edge: FAS (CD95) Mediates Noncanonical IL-1β and IL-18 Maturation via Caspase-8 in an RIP3-Independent Manner. *The Journal of Immunology*. 189 (12), 5508–5512.

Boucher, D., Monteleone, M., Coll, R.C., Chen, K.W., et al. (2018) Caspase-1 self-cleavage is an intrinsic mechanism to terminate inflammasome activity. *Journal of Experimental Medicine*. 215 (3), 827–840.

Bowden, S.D., Hopper-Chidlaw, A.C., Rice, C.J., Ramachandran, V.K., et al. (2014) Nutritional and Metabolic Requirements for the Infection of HeLa Cells by *Salmonella* enterica Serovar Typhimurium. *PLoS ONE*. 9 (5), 96266.

Boyer, J.L. (2013) Bile formation and secretion. *Comprehensive Physiology*. 3 (3), 1035–1078.

Brawn, L.C., Hayward, R.D. & Koronakis, V. (2007) *Salmonella* SPI1 Effector SipA Persists after Entry and Cooperates with a SPI2 Effector to Regulate Phagosome Maturation and Intracellular Replication. *Cell Host and Microbe*. 1 (1), 63–75.

Brenner, F.W., Villar, R.G., Angulo, F.J., Tauxe, R., et al. (2000) *Salmonella* Nomenclature. *Journal of Clinical Microbiology*. 38 (7), 2465–2467.

Bronner, D.N., Faber, F., Olsan, E.E., Byndloss, M.X., et al. (2018) Genetic Ablation of Butyrate Utilization Attenuates Gastrointestinal *Salmonella* Disease. *Cell Host & Microbe*. 23 (2), 266-273.e4.

Brooks, J. (1996) The sad and tragic life of Typhoid Mary. *CMAJ*.154 (6) pp.915–916.

Brown, E.W., Mammel, M.K., LeClerc, J.E. & Cebula, T.A. (2003) Limited boundaries for extensive horizontal gene transfer among *Salmonella* pathogens. *Proceedings of the National Academy of Sciences of the United States of America*. 100 (26), 15676–15681.

Broz, P. (2019) Recognition of Intracellular Bacteria by Inflammasomes. *Microbiology Spectrum*. 7 (2).

Broz, P. & Dixit, V.M. (2016) Inflammasomes: mechanism of assembly, regulation and signalling. *Nature Reviews Immunology*. 16 (7), 407–420.

Broz, P., Von Moltke, J., Jones, J.W., Vance, R.E., et al. (2010a) Differential requirement for caspase-1 autoproteolysis in pathogen-induced cell death and cytokine processing. *Cell Host and Microbe*. 8 (6), 471–483.

Broz, P. & Monack, D. (2011) Molecular Mechanisms of Inflammasome Activation during Microbial Infections. *Immunol Rev*. 243 (1), 174–190.

Broz, P., Newton, K., Lamkanfi, M., Mariathasan, S., et al. (2010b) Redundant roles for inflammasome receptors NLRP3 and NLRC4 in host defense against *Salmonella*. *The Journal of Experimental Medicine*. 207 (8), 1745–1755.

Broz, P., Ohlson, M.B. & Monack, D.M. (2012) Innate immune response to *Salmonella* typhimurium, a model enteric pathogen. *Gut Microbes*. 3 (2), 62–70.

Broz, P., Pelegrín, P. & Shao, F. (2019) The gasdermins, a protein family executing cell death and inflammation. *Nature Reviews Immunology*.pp.1–15.

Broz, P., Ruby, T., Belhocine, K., Bouley, D.M., et al. (2012) Caspase-11 increases susceptibility to *Salmonella* infection in the absence of caspase-1. *Nature*. 490 (7419), 288–291.

Brumell, J.H., Tang, P., Zaharik, M.L. & Finlay, B.B. (2002) Disruption of the *Salmonella*-containing vacuole leads to increased replication of *Salmonella* enterica serovar typhimurium in the cytosol of epithelial cells. *Infection and immunity*. 70 (6), 3264–3270.

Bryan, N.B., Dorfleutner, A., Rojanasakul, Y. & Stehlik, C. (2009) Activation of Inflammasomes Requires Intracellular Redistribution of the Apoptotic Speck-Like Protein Containing a Caspase Recruitment Domain. *The Journal of Immunology*. 182 (5), 3173–3182.

Buckle, G.C., Walker, C.L.F. & Black, R.E. (2012) Typhoid fever and paratyphoid fever: Systematic review to estimate global morbidity and mortality for 2010. *Journal of Global Health*. 2 (1), 1.

Bueno, S.M., Santiviago, C.A., Murillo, A.A., Fuentes, J.A., et al. (2004) Precise Excision of the Large Pathogenicity Island, SPI7, in *Salmonella* enterica Serovar Typhi. *Journal of Bacteriology*. 186 (10), 3202–3213.

Bustamante, V.H., Martínez, L.C., Santana, F.J., Knodler, L.A., et al. (2008) HilD-mediated transcriptional cross-talk between SPI-1 and SPI-2. *Proceedings of the National Academy of Sciences of the United States of America*. 105 (38), 14591–14596.

Butler, T. (2011) *Treatment of typhoid fever in the 21st century: promises and shortcomings*.

Byrne, A.M.P. (2017) *Identification and Characterisation of Novel T3SS Effector Proteins of Salmonella enterica serovar Typhi*. Imperial College London.

Caboni, M., Pédron, T., Rossi, O., Goulding, D., et al. (2015) An O Antigen Capsule Modulates Bacterial

Pathogenesis in Shigella sonnei. *PLoS Pathogens*. 11 (3), 1–26.
Carter, P.B. & Collins, F.M. (1974) Growth of typhoid and paratyphoid bacilli in intravenously infected mice. *Infection and immunity*. 10 (4), 816–822.
Casson, C.N., Yu, J., Reyes, V.M., Taschuk, F.O., et al. (2015) Human caspase-4 mediates noncanonical inflammasome activation against gram-negative bacterial pathogens. *Proceedings of the National Academy of Sciences*. 112 (21), 6688–6693.
Caygill, C., Braddick, M., Hill, M., Knowles, R., et al. (1995) The association between typhoid carriage, typhoid infection and subsequent cancer at a number of sites . 1995.pdf. *Eur J Cancer Prev*. 4, 187–193.
Chan, A.H. & Schroder, K. (2019) Inflammasome signaling and regulation of interleukin-1 family cytokines. *The Journal of experimental medicine*. 217 (1).
Chang, S.J., Song, J. & Galán, J.E. (2016) Receptor-Mediated Sorting of Typhoid Toxin during Its Export from *Salmonella* Typhi-Infected Cells. *Cell Host and Microbe*. 20 (5), 682–689.
Charles, R.C., Sultana, T., Alam, M.M., Yu, Y., et al. (2013) Identification of Immunogenic *Salmonella* enterica Serotype Typhi Antigens Expressed in Chronic Biliary Carriers of S. Typhi in Kathmandu, Nepal. *PLoS Neglected Tropical Diseases*. 7 (8).
Chen, K.W., Groß, C.J., Sotomayor, F., Stacey, K.J., et al. (2014) The Neutrophil NLRC4 Inflammasome Selectively Promotes IL-1β Maturation without Pyroptosis during Acute *Salmonella* Challenge. *Cell Reports*. 8 (2), 570–582.
Cheng, Y., Pedroso, A.A., Porwollik, S., McClelland, M., et al. (2015) rpoS-regulated core genes involved in the competitive fitness of *Salmonella* enterica serovar kentucky in the intestines of chickens. *Applied and Environmental Microbiology*. 81 (2), 502–514.
Choi, K.M., Kim, M.H., Cai, H., Lee, Y.J., et al. (2018) Salicylic Acid Reduces OmpF Expression, Rendering *Salmonella* enterica Serovar Typhimurium More Resistant to Cephalosporin Antibiotics . *Chonnam Medical Journal*. 54 (1), 17.
Choi, S., Choi, E., Cho, Y.J., Nam, D., et al. (2019) The *Salmonella* virulence protein MgtC promotes phosphate uptake inside macrophages. *Nature Communications*. 10 (1).
Coburn, B., Grassl, G.A. & Finlay, B. (2007) *Salmonella*, the host and disease: a brief review. *Immunology and Cell Biology*. 85, 112–118.
Coburn, B., Sekirov, I. & Finlay, B.B. (2007) Type III secretion systems and disease. *Clinical Microbiology Reviews*. 20 (4), 535–549.
Coll, R.C., Hill, J.R., Day, C.J., Zamoshnikova, A., et al. (2019) MCC950 directly targets the NLRP3 ATP-hydrolysis motif for inflammasome inhibition. *Nature Chemical Biology*. 15 (6), 556–559.
Coll, R.C., Robertson, A.A.B., Chae, J.J., Higgins, S.C., et al. (2015) A small-molecule inhibitor of the NLRP3 inflammasome for the treatment of inflammatory diseases. *Nature Medicine*. 21 (3), 248–255.
Corcoran, C.P., Podkaminski, D., Papenfort, K., Urban, J.H., et al. (2012) Superfolder GFP reporters validate diverse new mRNA targets of the classic porin regulator, MicF RNA. *Molecular Microbiology*. 84 (3), 428–445.
Cozzone, A.J. (1998) Regulation of acetate metabolism by protein phosphorylation in enteric bacteria. *Annual Review of Microbiology*. 52 (1), 127–164.
Crawford, R.W., Gibson, D.L., Kay, W.W. & Gunn, J.S. (2008) Identification of a bile-induced exopolysaccharide required for *Salmonella* biofilm formation on gallstone surfaces. *Infection and Immunity*. 76 (11), 5341–5349.
Crawford, R.W., Keestra, A.M., Winter, S.E., Xavier, M.N., et al. (2012) Very Long O-antigen Chains Enhance Fitness during *Salmonella*-induced Colitis by Increasing Bile Resistance. *PLoS Pathogens*. 8 (9).
Crawford, R.W., Reeve, K.E. & Gunn, J.S. (2010) Flagellated but Not Hyperfimbriated *Salmonella* enterica Serovar Typhimurium Attaches to and Forms Biofilms on Cholesterol-Coated Surfaces. *JOURNAL OF BACTERIOLOGY*. 192 (12), 2981–2990.
Crawford, R.W., Rosales-Reyes, R., Ramírez-Aguilar, M. de la L., Chapa-Azuela, O., et al. (2010)

Gallstones play a significant role in *Salmonella* spp. gallbladder colonization and carriage. *Proceedings of the National Academy of Sciences of the United States of America*. 107 (9), 4353–4358.

Crawford, R.W., Wangdi, T., Spees, A.M., Xavier, M.N., et al. (2013) Loss of very-long O-antigen chains optimizes capsule-mediated immune evasion by *Salmonella* enterica serovar Typhi. *mBio*. 4 (4).

Crowley, L.C., Scott, A.P., Marfell, B.J., Boughaba, J.A., et al. (2016) Measuring cell death by propidium iodide uptake and flow cytometry. *Cold Spring Harbor Protocols*. 2016 (7), 647–651.

Crump, J.A. & Mintz, E.D. (2010) Global trends in typhoid and paratyphoid Fever. *Clinical infectious diseases*. 50 (2), 241–246.

Crump, J.A., Sjölund-Karlsson, M., Gordon, M.A. & Parry, C.M. (2015) Epidemiology, clinical presentation, laboratory diagnosis, antimicrobial resistance, and antimicrobial management of invasive *Salmonella* infections. *Clinical Microbiology Reviews*.28 (4) pp.901–937.

Dahl, J.U., Koldewey, P., Salmon, L., Horowitz, S., et al. (2015) HdeB functions as an acid-protective chaperone in bacteria. *Journal of Biological Chemistry*. 290 (1), 65–75.

Darton, T.C., Blohmke, C.J. & Pollard, A.J. (2014) Typhoid epidemiology, diagnostics and the human challenge model. *Current opinion in gastroenterology*. 30 (1), 7–17.

Datsenko, K.A. & Wanner, B.L. (2000) One-step inactivation of chromosomal genes in Escherichia coli K-12 using PCR products. *Proceedings of the National Academy of Sciences*. 97 (12), 6640–6645.

Datta, D., McClendon, C.L., Jacobson, M.P. & Wells, J.A. (2013) Substrate and inhibitor-induced dimerization and cooperativity in caspase-1 but not caspase-3. *Journal of Biological Chemistry*. 288 (14), 9971–9981.

Deng, L., Song, J., Gao, X., Wang, J., et al. (2014) Host adaptation of a bacterial toxin from the human pathogen *Salmonella* typhi. *Cell*. 159 (6), 1290–1299.

Deng, W., Liou, S.-R., Plunkett Iii, G., Mayhew, G.F., et al. (2003) Comparative Genomics of *Salmonella* enterica Serovar Typhi Strains Ty2 and CT18. *JOURNAL OF BACTERIOLOGY*. 185 (7), 2330–2337.

Deng, W., Marshall, N.C., Rowland, J.L., McCoy, J.M., et al. (2017) Assembly, structure, function and regulation of type III secretion systems. *Nature Reviews Microbiology*. 15 (6), 323–337.

Desai, P.T., Porwollik, S., Long, F., Cheng, P., et al. (2013) Evolutionary genomics of *Salmonella* enterica subspecies. *mBio*. 4 (2).

Diamond, C.E., Leong, K.W.K., Vacca, M., Rivers-Auty, J., et al. (2017) *Salmonella* typhimurium-induced IL-1 release from primary human monocytes requires NLRP3 and can occur in the absence of pyroptosis. *Scientific Reports*. 7 (1), 6861.

Dickenson, N.E., Zhang, L., Epler, C.R., Adam, P.R., et al. (2011) Conformational Changes in IpaD from Shigella flexneri upon Binding Bile Salts Provide Insight into the Second Step of Type III Secretion. *Biochemistry*. 50 (2), 172–180.

Didelot, X., Achtman, M., Parkhill, J., Thomson, N.R., et al. (2007) A bimodal pattern of relatedness between the *Salmonella* Paratyphi A and Typhi genomes: Convergence or divergence by homologous recombination? *Genome Research*. 17 (1), 61–68.

Diebolder, C.A., Halff, E.F., Koster, A.J., Huizinga, E.G., et al. (2015) Cryoelectron Tomography of the NAIP5/NLRC4 Inflammasome: Implications for NLR Activation. *Structure*. 23 (12), 2349–2357.

Diepold, A. & Armitage, J.P. (2015) Type III secretion systems: the bacterial flagellum and the injectisome. *Philosophical Transactions of the Royal Society B*. 370 (1679), 20150020.

Dinarello, C.A., Novick, D., Kim, S. & Kaplanski, G. (2013) Interleukin-18 and IL-18 binding protein. *Frontiers in Immunology*. 4 (OCT), 1–10.

Ding, J., Wang, K., Liu, W., She, Y., et al. (2016) Pore-forming activity and structural autoinhibition of the gasdermin family. *Nature*. 535 (7610), 111–116.

Dobinson, H.C., Gibani, M.M., Jones, C., Thomaides-Brears, H.B., et al. (2017) Evaluation of the Clinical and Microbiological Response to *Salmonella* Paratyphi A Infection in the First Paratyphoid Human Challenge Model. *Clinical Infectious Diseases*. 64 (8), 1066–1073.

Dolecek, C., La, T.T.P., Rang, N.N., Phuong, L.T., et al. (2008) A multi-center randomised controlled trial of gatifloxacin versus azithromycin for the treatment of uncomplicated typhoid fever in children

and adults in Vietnam. *PLoS ONE*. 3 (5).

Dongol, S., Thompson, C.N., Clare, S., Nga, T.V.T., et al. (2012) The Microbiological and Clinical Characteristics of Invasive *Salmonella* in Gallbladders from Cholecystectomy Patients in Kathmandu, Nepal. *PLoS ONE*. 7 (10).

Dougan, G. & Baker, S. (2014) *Salmonella* enterica serovar typhi and the pathogenesis of typhoid fever. *Annual Review of Microbiology*. 68, 317–336.

Drecktrah, D., Knodler, L.A., Ireland, R. & Steele-Mortimer, O. (2006) The mechanism of *Salmonella* entry determines the vacuolar environment and intracellular gene expression. *Traffic*. 7 (1), 39–51.

Du, J., Reeves, A.Z., Klein, J.A., Twedt, D.J., et al. (2016) The type III secretion system apparatus determines the intracellular niche of bacterial pathogens. *Proceedings of the National Academy of Sciences*. 113 (17), 4794–4799.

Dufresne, K., Saulnier-Bellemare, J. & Daigle, F. (2018) Functional Analysis of the Chaperone-Usher Fimbrial Gene Clusters of *Salmonella* enterica serovar Typhi. *Frontiers in Cellular and Infection Microbiology*. 8 (8).

Duncan, J.A. & Canna, S.W. (2018) The NLRC4 Inflammasome. *Immunological reviews*.281 (1) pp.115–123.

Eade, C.R., Hung, C.-C., Bullard, B., Gonzalez-Escobedo, G., et al. (2016) Bile Acids Function Synergistically To Repress Invasion Gene Expression in *Salmonella* by Destabilizing the Invasion Regulator HilD. *Infection and Immunity*. 84 (8), 2198–2208.

Eder, C. (2009) Mechanisms of interleukin-1beta release. *Immunobiology*. 214 (7), 543–553.

Ehrbar, K., Friebel, A., Miller, S.I. & Hardt, W.-D. (2003) Role of the *Salmonella* Pathogenicity Island 1 (SPI-1) Protein InvB in Type III Secretion of SopE and SopE2, Two *Salmonella* Effector Proteins Encoded Outside of SPI-1. *JOURNAL OF BACTERIOLOGY*. 185 (23), 6950–6967.

Eldridge, M.J.G., Sanchez-Garrido, J., Hoben, G.F., Goddard, P.J., et al. (2017) The Atypical Ubiquitin E2 Conjugase UBE2L3 Is an Indirect Caspase-1 Target and Controls IL-1β Secretion by Inflammasomes. *Cell Reports*. 18 (5), 1285–1297.

Eldridge, M.J.G. & Shenoy, A.R. (2015) Antimicrobial inflammasomes: Unified signalling against diverse bacterial pathogens. *Current Opinion in Microbiology*.23 pp.32?41-41.

Eletsky, A., Michalska, K., Houliston, S., Zhang, Q., et al. (2014) Structural and Functional Characterization of DUF1471 Domains of *Salmonella* Proteins SrfN, YdgH/SssB, and YahO Paul C. Driscoll (ed.). *PLoS ONE*. 9 (7), e101787.

Elhadad, D., Desai, P., Grassl, G.A., McClelland, M., et al. (2016) Differences in host cell invasion and *Salmonella* pathogenicity island 1 expression between *Salmonella* enterica serovar Paratyphi A and nontyphoidal S. Typhimurium. *Infection and Immunity*. 84 (4), 1150–1165.

Elhadad, D., Desai, P., Rahav, G., McClelland, M., et al. (2015a) Flagellin is required for host cell invasion and normal *Salmonella* pathogenicity island 1 expression by *Salmonella* enterica serovar Paratyphi A. *Infection and Immunity*. 83 (9), 3355–3368.

Elhadad, D., McClelland, M., Rahav, G. & Gal-Mor, O. (2015b) Feverlike temperature is a virulence regulatory cue controlling the motility and host cell entry of typhoidal *Salmonella*. *Journal of Infectious Diseases*. 212 (1), 147–156.

Ellermeier, C.D. & Slauch, J.M. (2003) RtsA and RtsB coordinately regulate expression of the invasion and flagellar genes in *Salmonella* enterica serovar typhimurium. *Journal of Bacteriology*. 185 (17), 5096–5108.

Eswarappa, S.M., Janice, J., Nagarajan, A.G., Balasundaram, S. V, et al. (2008) Differentially Evolved Genes of *Salmonella* Pathogenicity Islands: Insights into the Mechanism of Host Specificity in *Salmonella*. *PLoS ONE*. 3 (12).

Evavold, C.L., Ruan, J., Tan, Y., Xia, S., et al. (2018) The Pore-Forming Protein Gasdermin D Regulates Interleukin-1 Secretion from Living Macrophages. *Immunity*. 48 (1), 35-44.e6.

Fàbrega, A. & Vila, J. (2013) *Salmonella* enterica serovar Typhimurium skills to succeed in the host: Virulence and regulation. *Clinical Microbiology Reviews*. 26 (2), 308–341.

Faherty, C.S., Redman, J.C., Rasko, D.A., Barry, E.M., et al. (2012) Shigella flexneri effectors OspE1 and OspE2 mediate induced adherence to the colonic epithelium following bile salts exposure. *Molecular Microbiology*. 85 (1), 107–121.

Fang, F.C., Libby, S.J., Castor, M.E. & Fung, A.M. (2005) Isocitrate lyase (AceA) is required for *Salmonella* persistence but not for acute lethal infection in mice. *Infection and immunity*. 73 (4), 2547–2549.

Fass, E. & Groisman, E.A. (2009) Control of *Salmonella* pathogenicity island-2 gene expression. *Current Opinion in Microbiology*.12 (2) pp.199–204.

Faucher, S.P., Forest, C., Béland, M. & Daigle, F. (2009) A novel PhoP-regulated locus encoding the cytolysin ClyA and the secreted invasin TaiA of *Salmonella* enterica serovar Typhi is involved in virulence. *Microbiology*. 155 (2), 477–488.

Faucher, S.P., Porwollik, S., Dozois, C.M., McClelland, M., et al. (2006) Transcriptome of *Salmonella* enterica serovar Typhi within macrophages revealed through the selective capture of transcribed sequences. *Proceedings of the National Academy of Sciences*. 103 (6), 1906–1911.

Feasey, N.A., Dougan, G., Kingsley, R.A., Heyderman, R.S., et al. (2012) Invasive non-typhoidal *Salmonella* disease: an emerging and neglected tropical disease in Africa. *Lancet*. 379 (9835), 2489–2499.

Feasey, N.A., Gaskell, K., Wong, V., Msefula, C., et al. (2015) Rapid Emergence of Multidrug Resistant, H58-Lineage *Salmonella* Typhi in Blantyre, Malawi. *PLoS Neglected Tropical Diseases*. 9 (4).

Feltham, R., Vince, J.E. & Lawlor, K.E. (2017) Caspase-8: Not so silently deadly. *Clinical and Translational Immunology*.6 (1).

Feng, Y., Lin, E., Zou, S., Chen, C.L., et al. (2019) Complete genome sequence of *Salmonella* enterica serovar Sendai shows H antigen convergence with S. Miami and recent divergence from S. Paratyphi A. *BMC Genomics*. 20 (1).

Fernandes-Alnemri, T., Wu, J., Yu, J.W., Datta, P., et al. (2007) The pyroptosome: A supramolecular assembly of ASC dimers mediating inflammatory cell death via caspase-1 activation. *Cell Death and Differentiation*. 14 (9), 1590–1604.

Fernandes-Alnemri, T., Yu, J.-W., Juliana, C., Solorzano, L., et al. (2010) The AIM2 inflammasome is critical for innate immunity to Francisella tularensis. *Nature Publishing Group*. 11 (5). Available from: doi:10.1038/ni.1859 [Accessed: 23 June 2019].

Fernández, D.J. & Lamkanfi, M. (2015) Inflammatory caspases: Key regulators of inflammation and cell death. *Biological Chemistry*. 396 (3), 193–203.

Fierer, J. & Guiney, D.G. (2001) Diverse virulence traits underlying different clinical outcomes of *Salmonella* infection. *Journal of Clinical Investigation*.107 (7) pp.775–780. Available from: doi:10.1172/JCI12561 [Accessed: 14 March 2018].

Finn, C.E., Chong, A., Cooper, K.G., Starr, T., et al. (2017) A second wave of *Salmonella* T3SS1 activity prolongs the lifespan of infected epithelial cells. *PLOS Pathogens*. 13 (4), e1006354.

Firoz Mian, M., Pek, E.A., Chenoweth, M.J. & Ashkar, A.A. (2011) Humanized mice are susceptible to *Salmonella* typhi infection. *Cellular & Molecular Immunology*. 852 (10), 83–87.

Fisch, D., Bando, H., Clough, B., Hornung, V., et al. (2019a) Human GBP1 is a microbe-specific gatekeeper of macrophage apoptosis and pyroptosis. *The EMBO Journal*. 38 (13), e100926. Available from: doi:10.15252/embj.2018100926 [Accessed: 16 July 2019].

Fisch, D., Clough, B., Domart, M.-C., Bando, H., et al. (2019b) Differential spatiotemporal targeting of Toxoplasma and *Salmonella* by GBP1 assembles caspase signalling platforms. *bioRxiv*. 792804.

Fookes, M., Schroeder, G.N., Langridge, G.C., Blondel, C.J., et al. (2011) *Salmonella* bongori provides insights into the evolution of the *Salmonella*e. *PLoS Pathogens*. 7 (8).

Forest, C., Faucher, S.P., Poirier, K., Houle, S., et al. (2007) Contribution of the stg Fimbrial Operon of *Salmonella* enterica Serovar Typhi during Interaction with Human Cells. *INFECTION AND IMMUNITY*. 75 (11), 5264–5271. Available from: doi:10.1128/IAI.00674-07 [Accessed: 14 March 2018].

Forest, C.G., Ferraro, E., Sabbagh, S.C. & Daigle, F. (2010) Intracellular survival of *Salmonella* enterica serovar Typhi in human macrophages is independent of *Salmonella* pathogenicity island (SPI)-2.

Microbiology. 156 (12), 3689–3698.

Foster, J.W. & Hall, H.K. (1991) Inducible pH homeostasis and the acid tolerance response of *Salmonella* typhimurium. *Journal of Bacteriology*. 173 (16), 5129–5135.

Fowler, C.C. & Galán, J.E. (2018) Decoding a *Salmonella* Typhi Regulatory Network that Controls Typhoid Toxin Expression within Human Cells. *Cell host & microbe*. 23 (1), 65-76.e6.

Franchi, L., Amer, A., Body-Malapel, M., Kanneganti, T.-D., et al. (2006) Cytosolic flagellin requires Ipaf for activation of caspase-1 and interleukin 1β in *Salmonella*-infected macrophages. *Nature Immunology*. 7 (6), 576–582.

Franchi, L., Kamada, N., Nakamura, Y., Burberry, A., et al. (2012) NLRC4-driven production of IL-1β discriminates between pathogenic and commensal bacteria and promotes host intestinal defense. *Nature Immunology*. 13 (5), 449–456. Available from: doi:10.1038/ni.2263 [Accessed: 24 September 2017].

Frankel, G., Newton, S.M., Schoolnik, G.K. & Stocker, B.A. (1989) Intragenic recombination in a flagellin gene: characterization of the H1-j gene of *Salmonella* typhi. *The EMBO journal*. 8 (10), 3149–3152.

Friebel, A., Ilchmann, H., Aepfelbacher, M., Ehrbar, K., et al. (2001) SopE and SopE2 from *Salmonella* typhimurium Activate Different Sets of RhoGTPases of the Host Cell. *Journal of Biological Chemistry*. 276 (36), 34035–34040.

Fuentes, J.A., Villagra, N., Castillo-Ruiz, M. & Mora, G.C. (2008) The *Salmonella* Typhi hlyE gene plays a role in invasion of cultured epithelial cells and its functional transfer to S. Typhimurium promotes deep organ infection in mice. *Research in Microbiology*. 159 (4), 279–287.

Fusco, W.G. & Duncan, J.A. (2018) Novel aspects of the assembly and activation of inflammasomes with focus on the NLRC4 inflammasome. *International Immunology*.30 (5) pp.183–193. Available from: doi:10.1093/intimm/dxy009 [Accessed: 10 July 2018].

Gaidt, M.M., Ebert, T.S., Chauhan, D., Schmidt, T., et al. (2016) Human Monocytes Engage an Alternative Inflammasome Pathway. *Immunity*. 44 (4), 833–846. Available from: doi:10.1016/j.immuni.2016.01.012 [Accessed: 24 November 2017].

Gal-Mor, O. (2019) Persistent Infection and Long-Term Carriage of Typhoidal and Nontyphoidal *Salmonella*e. *Clinical Microbiology Reviews*. 32 (1).

Gal-Mor, O., Boyle, E.C. & Grassl, G.A. (2014) Same species, different diseases: How and why typhoidal and non-typhoidal *Salmonella* enterica serovars differ. *Frontiers in Microbiology*.5 (AUG).

Gal-Mor, O., Suez, J., Elhadad, D., Porwollik, S., et al. (2012) Molecular and Cellular Characterization of a *Salmonella* enterica Serovar Paratyphi A Outbreak Strain and the Human Immune Response to Infection. *Clinical and Vaccine Immunology*. 19 (2), 146–156. Available from: doi:10.1128/cvi.05468-11 [Accessed: 6 January 2018].

Galan, J.E. & Curtiss III, R. (1989) Cloning and molecular characterization of genes whose products allow *Salmonella* typhimurium to penetrate tissue culture cells. *Proceedings of the National Academy of Sciences of the United States of America*. 86 (16), 6383–6387. Available from: doi:10.1073/pnas.86.16.6383 [Accessed: 15 April 2017].

Gerlach, R.G., Cláudio, N., Rohde, M., Jäckel, D., et al. (2008) Cooperation of *Salmonella* pathogenicity islands 1 and 4 is required to breach epithelial barriers. *Cellular Microbiology*. 10 (11), 2364–2376. Available from: doi:10.1111/j.1462-5822.2008.01218.x [Accessed: 31 January 2020].

Gerlach, R.G., Jäckel, D., Geymeier, N. & Hensel, M. (2007) *Salmonella* Pathogenicity Island 4-Mediated Adhesion Is Coregulated with Invasion Genes in *Salmonella* enterica. *INFECTION AND IMMUNITY*. 75 (10), 4697–4709. Available from: doi:10.1128/IAI.00228-07 [Accessed: 24 May 2019].

Ghosh, P. (2004) Process of Protein Transport by the Type III Secretion System. *Microbiology and Molecular Biology Reviews*. 68 (4), 771–795.

Gibani, M.M., Britto, C. & Pollard, A.J. (2018) Typhoid and paratyphoid fever: a call to action. *Current Opinion in Infectious Diseases*. 31 (5), 1. Available from: doi:10.1097/QCO.0000000000000479.

Gibani, M.M., Jones, E., Barton, A., Jin, C., et al. (2019) Investigation of the role of typhoid toxin in acute typhoid fever in a human challenge model. *Nature Medicine*.25 (7) pp.1082–1088.

Goddard, P.J., Sanchez-Garrido, J., Slater, S.L., Kalyan, M., et al. (2019) Enteropathogenic Escherichia coli Stimulates Effector-Driven Rapid Caspase-4 Activation in Human Macrophages. *Cell Reports*. 27 (4), 1008-1017.e6. Available from: doi:10.1016/j.celrep.2019.03.100.

Gonzales, A.M., Wilde, S. & Roland, K.L. (2017) New insights into the roles of long polar fimbriae and Stg fimbriae in *Salmonella* interactions with enterocytes and M cells. *Infection and Immunity*. 85 (9).

Gonzalez-Escobedo, G. & Gunn, J.S. (2013a) Gallbladder epithelium as a niche for chronic *Salmonella* carriage. *Infection and Immunity*. 81 (8), 2920–2930.

Gonzalez-Escobedo, G. & Gunn, J.S. (2013b) Identification of *Salmonella* enterica serovar typhimurium genes regulated during biofilm formation on cholesterol gallstone surfaces. *Infection and Immunity*. 81 (10), 3770–3780.

Gonzalez-Escobedo, G., Marshall, J.M. & Gunn, J.S. (2011) Chronic and acute infection of the gall bladder by *Salmonella* Typhi: understanding the carrier state. *Nat Rev Microbiol*. 9 (1), 9–14.

Gonzalez-Escobedo, G., La Perle, K.M.D. & Gunn, J.S. (2013) Histopathological Analysis of *Salmonella* Chronic Carriage in the Mouse Hepatopancreatobiliary System Herbert B. Tanowitz (ed.). *PLoS ONE*. 8 (12), e84058. Available from: doi:10.1371/journal.pone.0084058 [Accessed: 17 November 2019].

González, J.F., Alberts, H., Lee, J., Doolittle, L., et al. (2018) Biofilm Formation Protects *Salmonella* from the Antibiotic Ciprofloxacin in Vitro and in Vivo in the Mouse Model of chronic Carriage. *Scientific Reports*. 8 (1).

González, J.F., Tucker, L., Fitch, J., Wetzel, A., et al. (2019) Human Bile-Mediated Regulation of *Salmonella* Curli Fimbriae. *Journal of Bacteriology*. 201 (18). Available from: doi:10.1128/jb.00055-19 [Accessed: 25 April 2019].

Green, E.R. & Mecsas, J. (2016) Bacterial Secretion Systems: An Overview. *Microbiology Spectrum*. 4 (1), 1–32.

Grimont, P.A.D. & Weill, F.-X. (2007) Antigenic formulae of the *Salmonella* serovars, 9th edition. *WHO Collaborating Centre for Reference and Research on Salmonella, Geneva, Switzerland.*

Gunn, J.S. (2000) Mechanisms of bacterial resistance and response to bile. *Microbes and Infection*.2 (8) pp.907–913.

Gunn, J.S., Marshall, J.M., Baker, S., Dongol, S., et al. (2014) *Salmonella* chronic carriage: Epidemiology, diagnosis, and gallbladder persistence. *Trends in Microbiology*.22 (11) pp.648–655.

Günster, R.A., Matthews, S.A., Holden, D.W. & Thurston, T.L.M. (2017) SseK1 and SseK3 type III secretion system effectors inhibit NF-κB signaling and necroptotic cell death in *Salmonella*-infected macrophages. *Infection and Immunity*. 85 (3).

Gupta, S. & Chowdhury, R. (1997) Bile Affects Production of Virulence Factors and Motility of Vibrio cholerae. *INFECTION AND IMMUNITY*.65 (3). Available from: http://iai.asm.org/ [Accessed: 19 November 2019].

Gurung, P., Anand, P.K., Malireddi, R.K.S., Vande Walle, L., et al. (2014) FADD and caspase-8 mediate priming and activation of the canonical and noncanonical Nlrp3 inflammasomes. *Journal of immunology (Baltimore, Md. : 1950)*. 192 (4), 1835–1846. Available from: doi:10.4049/jimmunol.1302839 [Accessed: 16 July 2019].

Gurung, P. & Kanneganti, T.D. (2015) Novel Roles for Caspase-8 in IL-1β and Inflammasome Regulation. *American Journal of Pathology*. 185 (1), 17–25.

Gurung, P., Subbarao Malireddi, R.K., Anand, P.K., Demon, D., et al. (2012) Toll or interleukin-1 receptor (TIR) domain-containing adaptor inducing interferon-β (TRIF)-mediated caspase-11 protease production integrates toll-like receptor 4 (TLR4) protein- and Nlrp3 inflammasome-mediated host defense against enteropathogens. *Journal of Biological Chemistry*. 287 (41), 34474–34483.

Hagar, J.A., Powell, D.A., Aachoui, Y., Ernst, R.K., et al. (2013) Cytoplasmic LPS Activates Caspase-11: Implications in TLR4-Independent Endotoxic Shock. *Science*. 341 (6151), 1250–1253.

Haghjoo, E. & Galán, J.E. (2004) *Salmonella* typhi encodes a functional cytolethal distending toxin that

is delivered into host cells by a bacterial-internalization pathway. *Proceedings of the National Academy of Sciences of the United States of America*. 101 (13), 4614–4619.

Halff, E.F., Diebolder, C.A., Versteeg, M., Schouten, A., et al. (2012) Formation and structure of a NAIP5-NLRC4 inflammasome induced by direct interactions with conserved N- and C-terminal regions of flagellin. *Journal of Biological Chemistry*. 287 (46), 38460–38472.

Hamner, S., McInnerney, K., Williamson, K., Franklin, M.J., et al. (2013) Bile Salts Affect Expression of Escherichia coli O157:H7 Genes for Virulence and Iron Acquisition, and Promote Growth under Iron Limiting Conditions. *PLoS ONE*. 8 (9), 1–14.

Hancock, V., Vejborg, R.M. & Klemm, P. (2010) Functional genomics of probiotic Escherichia coli Nissle 1917 and 83972, and UPEC strain CFT073: Comparison of transcriptomes, growth and biofilm formation. *Molecular Genetics and Genomics*. 284 (6), 437–454.

Haneda, T., Winter, S.E., Butler, B.P., Wilson, R.P., et al. (2009) The Capsule-Encoding viaB Locus Reduces Intestinal Inflammation by a *Salmonella* Pathogenicity Island 1-Independent Mechanism. *INFECTION AND IMMUNITY*. 77 (7), 2932–2942.

Hara, H., Tsuchiya, K., Kawamura, I., Fang, R., et al. (2013) Phosphorylation of the adaptor ASC acts as a molecular switch that controls the formation of speck-like aggregates and inflammasome activity. *Nature Immunology*. 14 (12), 1247–1255.

Haraga, A., Ohlson, M.B. & Miller, S.I. (2008) *Salmonella*e interplay with host cells. *Nature Reviews Microbiology*.6 (1) pp.53–66. Available from: doi:10.1038/nrmicro1788.

Hart, P.J., O'Shaughnessy, C.M., Siggins, M.K., Bobat, S., et al. (2016) Differential killing of *Salmonella* enterica serovar Typhi by antibodies targeting VI and lipopolysaccharide O:9 antigen. *PLoS ONE*. 11 (1).

Hatta, M., Pastoor, R., Scheelbeek, P.F.D., Sultan, A.R., et al. (2011) Multi-locus variable-number tandem repeat profiling of *Salmonella* enterica serovar Typhi isolates from blood cultures and gallbladder specimens from Makassar, South-Sulawesi, Indonesia. *PLoS ONE*. 6 (9).

Hausmann, A., Böck, D., Geiser, P., Berthold, D.L., et al. (2020) Intestinal epithelial NAIP/NLRC4 restricts systemic dissemination of the adapted pathogen *Salmonella* Typhimurium due to site-specific bacterial PAMP expression. *Mucosal Immunology*. 1–15.

Hayashi, F., Smith, K.D., Ozinsky, A., Hawn, T.R., et al. (2001) The innate immune response to bacterial flagellin is mediated by Toll- like receptor 5. *Nature*. 410 (6832), 1099-103.

Hayward, J.A., Mathur, A., Ngo, C. & Man, S.M. (2018) Cytosolic Recognition of Microbes and Pathogens: Inflammasomes in Action. *Microbiology and Molecular Biology Reviews*. 82 (4), 1–40. Available from: doi:10.1128/mmbr.00015-18 [Accessed: 14 September 2018].

Hayward, R.D. & Koronakis, V. (1999) Direct nucleation and bundling of actin by the SipC protein of invasive *Salmonella*. *The EMBO Journal*.18 (18).

He, yuan, Zeng, M.Y., Yang, D., Motro, B., et al. (2016) NEK7 is an essential mediator of NLRP3 activation downstream of potassium efflux. *Nature*. 530 (7590), 354–357. Available from: doi:10.1038/nature16959 [Accessed: 28 October 2018].

He, W.T., Wan, H., Hu, L., Chen, P., et al. (2015) Gasdermin D is an executor of pyroptosis and required for interleukin-1β secretion. *Cell Research*. 25 (12), 1285–1298. Available from: doi:10.1038/cr.2015.139 [Accessed: 25 August 2017].

He, Y., Hara, H. & Núñez, G. (2016) Mechanism and Regulation of NLRP3 Inflammasome Activation. *Trends in Biochemical Sciences*. 41 (12), 1012–1021.

Hengge-Aronis, R. & Fischer, D. (1992) Identification and molecular analysis of glgS, a novel growth-phase-regulated and rpoS-dependent gene involved in glycogen synthesis in Escherichia coli. *Molecular Microbiology*. 6 (14), 1877–1886.

Hernández, S.B., Cota, I., Ducret, A., Aussel, L., et al. (2012) Adaptation and preadaptation of *Salmonella* enterica to bile. *PLoS Genetics*. 8 (1).

Higginson, E.E., Ramachandran, G., Hazen, T.H., Kania, D.A., et al. (2018) *Improving Our Understanding of Salmonella enterica Serovar Paratyphi B through the Engineering and Testing of a Live Attenuated Vaccine Strain*. Available from: doi:10.1128/mSphere.00474-18 [Accessed: 24 May

2019].

Higginson, E.E., Simon, R. & Tennant, S.M. (2016) *Animal Models for Salmonellosis: Applications in Vaccine Research*. Available from: doi:10.1128/CVI.00258-16 [Accessed: 15 November 2019].

Hiyoshi, H., Tiffany, C.R., Bronner, D.N. & Baumler, A.J. (2018a) Typhoidal *Salmonella* serovars: ecological opportunity and the evolution of a new pathovar. *FEMS Microbiology Reviews*. 024, 527–541.

Hiyoshi, H., Wangdi, T., Lock, G., Saechao, C., et al. (2018b) Mechanisms to Evade the Phagocyte Respiratory Burst Arose by Convergent Evolution in Typhoidal *Salmonella* Serovars. *Cell Reports*. 22 (7), 1787–1797.

Hofmann, A.F. (1999) Bile Acids: The Good, the Bad, and the Ugly. *News Physiol. Sci.* •.14. Available from: www.physiology.org/journal/physiologyonline [Accessed: 24 May 2019].

Hohmann, E.L. (2001) *Nontyphoidal Salmonellosis*. Available from: www.cdc.gov/ncidod/dbmd/foodnet/ [Accessed: 4 November 2019].

Holt, K.E. (2009) *Genomic variation and evolution of Salmonella enterica serovars Typhi and Paratyphi A*.

Holt, K.E., Dolecek, C., Chau, T.T., Duy, P.T., et al. (2011) Temporal fluctuation of multidrug resistant *Salmonella* typhi haplotypes in the mekong river delta region of Vietnam. *PLoS Neglected Tropical Diseases*. 5 (1). Available from: doi:10.1371/journal.pntd.0000929 [Accessed: 13 April 2018].

Holt, K.E., Parkhill, J., Mazzoni, C.J., Roumagnac, P., et al. (2008) High-throughput sequencing provides insights into genome variation and evolution in *Salmonella* Typhi. *Nature genetics*. 40 (8), 987–993.

Holt, K.E., Thomson, N.R., Wain, J., Langridge, G.C., et al. (2009) Pseudogene accumulation in the evolutionary histories of *Salmonella* enterica serovars Paratyphi A and Typhi. *BMC Genomics*. 10, 36.

Holt, K.E., Thomson, N.R., Wain, J., Phan, M.D., et al. (2007) Multidrug-Resistant Salmonella enterica Serovar Paratyphi A Harbors IncHI1 Plasmids Similar to Those Found in Serovar Typhi. *JOURNAL OF BACTERIOLOGY*. 189 (11), 4257–4264.

Hölzer, S.U., Schlumberger, M.C., Jäckel, D. & Hensel, M. (2009) Effect of the O-Antigen Length of Lipopolysaccharide on the Functions of Type III Secretion Systems in *Salmonella* enterica. *INFECTION AND IMMUNITY*. 77 (12), 5458–5470. Available from: doi:10.1128/IAI.00871-09 [Accessed: 14 March 2019].

Hong, M. & Payne, S.M. (1997) Effect of mutations in Shigella flexneri chromosomal and plasmid-encoded lipopolysaccharide genes on invasion and serum resistance. *Molecular Microbiology*. 24 (4), 779–791.

Hornung, V., Ablasser, A., Charrel-Dennis, M., Bauernfeind, F., et al. (2009) AIM2 recognizes cytosolic dsDNA and forms a caspase-1-activating inflammasome with ASC. *Nature*. 458 (7237), 514–518. Available from: doi:10.1038/nature07725 [Accessed: 30 May 2019].

Hornung, V. & Latz, E. (2010) Critical functions of priming and lysosomal damage for NLRP3 activation. *European Journal of Immunology*. 40 (3), 620–623.

Hu, G.-Q., Song, P.-X., Li, N., Chen, W., et al. (2016) AIM2 contributes to the maintenance of intestinal integrity via Akt and protects against *Salmonella* mucosal infection. *Mucosal Immunology*. 9 (5), 1330–1339. Available from: doi:10.1038/mi.2015.142 [Accessed: 25 August 2017].

Hu, Z., Zhou, Q., Zhang, C., Fan, S., et al. (2015) Structural and biochemical basis for induced self-propagation of NLRC4. *Science*. 350 (6259), 399–404. Available from: doi:10.1126/science.aac5489 [Accessed: 30 May 2019].

Hume, P.J., Singh, V., Davidson, A.C. & Koronakis, V. (2017) Swiss army pathogen: The *Salmonella* entry toolkit. *Frontiers in Cellular and Infection Microbiology*.7 (AUG) p.348. Available from: doi:10.3389/fcimb.2017.00348 [Accessed: 23 December 2019].

Humphries, A.D., Raffatellu, M., Winter, S., Weening, E.H., et al. (2003) The use of flow cytometry to detect expression of subunits encoded by 11 *Salmonella* enterica serotype Typhimurium fimbrial operons. *Molecular Microbiology*. 48 (5), 1357–1376. Available from: doi:10.1046/j.1365-

2958.2003.03507.x [Accessed: 28 March 2020].

Humphries, A.D., Townsend, S.M., Kingsley, R. a, Nicholson, T.L., et al. (2001) *Role of fimbriae as antigens and intestinal colonization factors of Salmonella serovars*. 201, 121–125.

Ibanez-Ruiz, M., Robbe-Saule, V., Hermant, D., Labrude, S., et al. (2000) Identification of RpoS (σ(S))-regulated genes in *Salmonella* enterica serovar typhimurium. *Journal of Bacteriology*. 182 (20), 5749–5756.

Ibarra, J.A., Knodler, L.A., Sturdevant, D.E., Virtaneva, K., et al. (2010) Induction of *Salmonella* pathogenicity island 1 under different growth conditions can affect *Salmonella*-host cell interactions in vitro. *Microbiology (Reading, England)*. 156 (Pt 4), 1120–1133.

Ibler, A.E.M., ElGhazaly, M., Naylor, K.L., Bulgakova, N.A., et al. (2019) Typhoid toxin exhausts the RPA response to DNA replication stress driving senescence and *Salmonella* infection. *Nature Communications*. 10 (1).

Inoue, T., Shingaki, R., Hirose, S., Waki, K., et al. (2007) Genome-wide screening of genes required for swarming motility in Escherichia coli K-12. *Journal of Bacteriology*. 189 (3), 950–957. Available from: doi:10.1128/JB.01294-06 [Accessed: 5 January 2020].

Iwasaki, A. & Medzhitov, R. (2015) Control of adaptive immunity by the innate immune system. *Nature Immunology*.16 (4) pp.343–353.

Jennings, E., Thurston, T.L.M. & Holden, D.W. (2017) *Salmonella* SPI-2 Type III Secretion System Effectors: Molecular Mechanisms And Physiological Consequences. *Cell Host and Microbe*. 22 (2), 217–231. Available from: doi:10.1016/j.chom.2017.07.009.

Jepson, M.A. & Clark, M.A. (2001) The role of M cells in *Salmonella* infection. *Microbes and Infection*. 3.

Johnson, R., Byrne, A., Berger, C.N., Klemm, E., et al. (2017) The type III secretion system effector SptP of *Salmonella* enterica serovar Typhi. *Journal of Bacteriology*. 199 (4), JB.00647-16.

Johnson, R., Mylona, E. & Frankel, G. (2018) Typhoidal *Salmonella*: distinctive virulence factors and pathogenesis. *Cellular Microbiology*. 20 (9), e12939. Available from: doi:10.1111/cmi.12939.

Johnson, R., Ravenhall, M., Pickard, D., Dougan, G., et al. (2018) Comparison of *Salmonella* enterica serovars Typhi and Typhimurium reveals typhoidal serovar-specific responses to bile. *Infection and Immunity*. 86 (3), IAI.00490-17.

Jones, J.W., Kayagaki, N., Broz, P., Henry, T., et al. (2010) Absent in melanoma 2 is required for innate immune recognition of Francisella tularensis. *Proceedings of the National Academy of Sciences*. 107 (21), 9771–9776. Available from: doi:10.1073/pnas.1003738107 [Accessed: 2 January 2019].

Joosten, L.A.B., Netea, M.G. & Dinarello, C.A. (2013) Interleukin-1β in innate inflammation, autophagy and immunity. *Seminars in Immunology*. 25 (6), 416–424. Available from: doi:10.1016/j.smim.2013.10.018.

Jorgensen, I. & Miao, E.A. (2015) Pyroptotic cell death defends against intracellular pathogens. *Immunological Reviews*.265 (1) pp.130–142. Available from: doi:10.1111/imr.12287 [Accessed: 23 September 2017].

Jorgensen, I., Zhang, Y., Krantz, B.A. & Miao, E.A. (2016) Pyroptosis triggers pore-induced intracellular traps (PITs) that capture bacteria and lead to their clearance by efferocytosis. *Journal of Experimental Medicine*. 213 (10), 2113–2128.

Juliana, C., Fernandes-Alnemri, T., Kang, S., Farias, A., et al. (2012) Non-transcriptional priming and deubiquitination regulate NLRP3 inflammasome activation. *Journal of Biological Chemistry*. 287 (43), 36617–36622.

Kalai Chelvam, K., Chai, L.C. & Thong, K.L. (2014) Variations in motility and biofilm formation of *Salmonella* enterica serovar Typhi. *Gut Pathogens*. 6 (1).

Kaniga, K., Tucker, S., Trollinger, D. & Galan, J.E. (1995) Homologs of the Shigella IpaB and IpaC invasins are required for *Salmonella* typhimurium entry into cultured epithelial cells. *Journal of Bacteriology*. 177 (14), 3965–3971.

Karkey, A., Arjyal, A., Anders, K.L., Boni, M.F., et al. (2010) The Burden and Characteristics of Enteric Fever at a Healthcare Facility in a Densely Populated Area of Kathmandu Lorenz von Seidlein

(ed.). *PLoS ONE*. 5 (11), e13988. Available from: doi:10.1371/journal.pone.0013988 [Accessed: 10 November 2019].

Karkey, A., Thompson, C.N., Tran Vu Thieu, N., Dongol, S., et al. (2013) Differential Epidemiology of *Salmonella* Typhi and Paratyphi A in Kathmandu, Nepal: A Matched Case Control Investigation in a Highly Endemic Enteric Fever Setting John Andrew Crump (ed.). *PLoS Neglected Tropical Diseases*. 7 (8), e2391.

Karlinsey, J.E., Stepien, T.A., Mayho, M., Kingsley, R.A., et al. (2019) Genome-wide Analysis of *Salmonella* enterica serovar Typhi in Humanized Mice Reveals Key Virulence Features. *Cell Host and Microbe*. Available from: doi:10.1016/j.chom.2019.08.001.

Kawai, T. & Akira, S. (2010) The role of pattern-recognition receptors in innate immunity: update on Toll-like receptors. *Nature Publishing Group*. 11. Available from: doi:10.1038/ni.1863 [Accessed: 3 June 2017].

Kawasaki, T. & Kawai, T. (2014) Toll-like receptor signaling pathways. *Frontiers in Immunology*.5 (SEP).

Kayagaki, N., Stowe, I.B., Lee, B.L., O'Rourke, K., et al. (2015) Caspase-11 cleaves gasdermin D for non-canonical inflammasome signalling. *Nature*. 526 (7575), 666–671.

Kayagaki, N., Warming, S., Lamkanfi, M., Walle, L. Vande, et al. (2011) Non-canonical inflammasome activation targets caspase-11. *Nature*. 479 (7371), 117–121.

Kayagaki, N., Wong, M.T., Stowe, I.B., Ramani, S.R., et al. (2013) Noncanonical Inflammasome Activation by Intracellular LPS Independent of TLR4. *Science*. 341 (6151), 1246–1249.

Keestra-Gounder, A.M., Tsolis, R.M. & Bäumler, A.J. (2015) Now you see me, now you don't: the interaction of *Salmonella* with innate immune receptors. *Nature reviews. Microbiology*. 13 (4), 206–216. Available from: doi:10.1038/nrmicro3428.

Khatri, N.S., Maskey, P., Poudel, S., Jaiswal, V.K., et al. (2009) Gallbladder Carriage of *Salmonella* Paratyphi A May Be an Important Factor in the Increasing Incidence of This Infection in South Asia. *Annals of Internal Medicine*. 150 (8), 567. Available from: doi:10.7326/0003-4819-150-8-200904210-00017 [Accessed: 28 December 2018].

Kidgell, C., Reichard, U., Wain, J., Linz, B., et al. (2002) *Salmonella* typhi, the causative agent of typhoid fever, is approximately 50,000 years old. *Infection, Genetics and Evolution*. 2 (1), 39–45.

Kim, B.H., Shenoy, A.R., Kumar, P., Bradfield, C.J., et al. (2012) IFN-inducible GTPases in host cell defense. *Cell Host and Microbe*.12 (4) pp.432–444. Available from: doi:10.1016/j.chom.2012.09.007 [Accessed: 14 September 2018].

King, T., Ferenci, T. & Szabo, E.A. (2003) The effect of growth atmosphere on the ability of Listeria monocytogenes to survive exposure to acid, proteolytic enzymes and bile salts. *International journal of food microbiology*. 84 (2), 133–143. Available from: doi:10.1016/s0168-1605(02)00404-x [Accessed: 3 February 2020].

Kingsley, R.A., Msefula, C.L., Thomson, N.R., Kariuki, S., et al. (2009) Epidemic multiple drug resistant *Salmonella* Typhimurium causing invasive disease in sub-Saharan Africa have a distinct genotype. *Genome Research*. 19 (12), 2279–2287. Available from: doi:10.1101/gr.091017.109 [Accessed: 14 January 2019].

Kintz, E., Scarff, J.M., DiGiandomenico, A. & Goldberg, J.B. (2008) Lipopolysaccharide O-antigen chain length regulation in Pseudomonas aeruginosa serogroup O11 strain PA103. *Journal of Bacteriology*. 190 (8), 2709–2716.

Kisiela, D.I., Chattopadhyay, S., Libby, S.J., Karlinsey, J.E., et al. (2012) Evolution of *Salmonella* enterica Virulence via point mutations in the fimbrial adhesin. *PLoS Pathogens*. 8 (6).

Klemm, E.J., Shakoor, S., Page, A.J., Qamar, F.N., et al. (2018) Emergence of an Extensively Drug-Resistant *Salmonella* enterica Serovar Typhi Clone Harboring a Promiscuous Plasmid Encoding Resistance to Fluoroquinolones and Third- Generation Cephalosporins. *mBio*. 9 (1).

Kline, K.A., Fälker, S., Dahlberg, S., Normark, S., et al. (2009) Bacterial Adhesins in Host-Microbe Interactions. *Cell Host and Microbe*.5 (6) pp.580–592.

Knodler, L.A., Crowley, S.M., Sham, H.P., Yang, H., et al. (2014) Noncanonical inflammasome activation of caspase-4/caspase-11 mediates epithelial defenses against enteric bacterial pathogens. *Cell*

Host and Microbe. 16 (2), 249–256.

Knodler, L.A., Nair, V. & Steele-Mortimer, O. (2014) Quantitative assessment of cytosolic *Salmonella* in epithelial cells. *PLoS ONE*. 9 (1).

Knodler, L.A. & Steele-Mortimer, O. (2003) Taking possession: biogenesis of the *Salmonella*-containing vacuole. *Traffic*. 4 (9), 587–599.

Knodler, L.A., Vallance, B.A., Celli, J., Winfree, S., et al. (2010) Dissemination of invasive *Salmonella* via bacterial-induced extrusion of mucosal epithelia. *Proceedings of the National Academy of Sciences of the United States of America*. 107 (41), 17733–17738.

Kobayashi, T., Ogawa, M., Sanada, T., Mimuro, H., et al. (2013) The Shigella OspC3 effector inhibits caspase-4, antagonizes inflammatory cell death, and promotes epithelial infection. *Cell Host and Microbe*. 13 (5), 570–583.

Kofoed, E.M. & Vance, R.E. (2011) Innate immune recognition of bacterial ligands by NAIPs determines inflammasome specificity. *Nature*. 477 (7366), 592–595.

Kortmann, J., Brubaker, S.W. & Monack, D.M. (2015) Cutting Edge: Inflammasome Activation in Primary Human Macrophages Is Dependent on Flagellin. *The Journal of Immunology*. 195 (3), 815–819.

Kothari, S., Kim, J.A., Kothari, N., Jones, C., et al. (2014) Purification of O-specific polysaccharide from lipopolysaccharide produced by *Salmonella* enterica serovar Paratyphi A. *Vaccine*. 32 (21), 2457–2462.

Kröger, C., Colgan, A., Srikumar, S., Händler, K., et al. (2013) An infection-relevant transcriptomic compendium for *Salmonella* enterica serovar typhimurium. *Cell Host and Microbe*. 14 (6), 683–695.

Kubori, T. & Galán, J.E. (2003) Temporal regulation of *Salmonella* virulence effector function by proteasome-dependent protein degradation. *Cell*. 115 (3), 333–342.

Kubori, T., Matsushima, Y., Nakamura, D., Uralil, J., et al. (1998) Supramolecular structure of the *Salmonella* typhimurium type III protein secretion system. *Science*. 280 (5363), 602–605. Available from: doi:10.1126/science.280.5363.602 [Accessed: 26 June 2016].

Kumagai, Y., Takeuchi, O. & Akira, S. (2008) Pathogen recognition by innate receptors. *Journal of Infection and Chemotherapy*.14 (2) pp.86–92.

Lagrange, B., Benaoudia, S., Wallet, P., Magnotti, F., et al. (2018) Human caspase-4 detects tetra-acylated LPS and cytosolic Francisella and functions differently from murine caspase-11. *Nature Communications*. 9 (1), 242. Available from: doi:10.1038/s41467-017-02682-y [Accessed: 22 January 2018].

Langridge, G.C., Phan, M.D., Turner, D.J., Perkins, T.T., et al. (2009) Simultaneous assay of every *Salmonella* Typhi gene using one million transposon mutants. *Genome Research*. 19 (12), 2308–2316.

Lara-Tejero, M., Sutterwala, F.S., Ogura, Y., Grant, E.P., et al. (2006) Role of the caspase-1 inflammasome in *Salmonella* typhimurium pathogenesis. *The Journal of Experimental Medicine*. 203 (6), 1407–1412.

Lawley, T.D., Chan, K., Thompson, L.J., Kim, C.C., et al. (2006) Genome-wide screen for *Salmonella* genes required for long-term systemic infection of the mouse. *PLoS Pathogens*. 2 (2), 0087–0100. Available from: doi:10.1371/journal.ppat.0020011.

Ledingham, J.C.G. (1999) Mr N the milker, and Dr Koch's concept of the healthy carrier. *Lancet*. 353, 1354–1356. Available from: https://ac.els-cdn.com/S0140673698113156/1-s2.0-S0140673698113156-main.pdf?_tid=92209a03-53e2-41b5-b627-afb45981878d&acdnat=1545930767_478861e1a92c55fd0ad5f2fcf8b52629 [Accessed: 27 December 2018].

Lee, G.S., Subramanian, N., Kim, A.I., Aksentijevich, I., et al. (2012) The calcium-sensing receptor regulates the NLRP3 inflammasome through Ca2+ and cAMP. *Nature*. 492 (7427), 123–127. Available from: doi:10.1038/nature11588.

Lee, J., Hiibel, S.R., Reardon, K.F. & Wood, T.K. (2010) Identification of stress-related proteins in

Escherichia coli using the pollutant cis-dichloroethylene. *Journal of Applied Microbiology*. 108 (6), 2088–2102. Available from: doi:10.1111/j.1365-2672.2009.04611.x [Accessed: 5 January 2020].

Lerouge, I. & Vanderleyden, J. (2002) O-antigen structural variation: Mechanisms and possible roles in animal/plant-microbe interactions. *FEMS Microbiology Reviews*.26 (1) pp.17–47. Available from: doi:10.1016/S0168-6445(01)00070-5 [Accessed: 13 November 2019].

Levine, M.M., Black, R.E., Lanata, C. & Committee, C.T. (1982) Precise Estimation of the Numbers of Chronic Carriers of *Salmonella* typhi in Santiago, Chile, an Endemic Area. *THE JOURNAL OF INFECTIOUS DISEASES*.146 (6).

Levine, M.M., Ferreccio, C., Black, R.E., Lagos, R., et al. (2007) Ty21a Live Oral Typhoid Vaccine and Prevention of Paratyphoid Fever Caused by *Salmonella* enterica Serovar Paratyphi B. *Clinical Infectious Diseases*. 45, 24–32. Available from: doi:10.1086/518141 [Accessed: 24 May 2019].

Levine, M.M., Tacket, C.O. & Sztein, M.B. (2001) Host-*Salmonella* interaction: Human trials. *Microbes and Infection*.3 (14–15) pp.1271–1279.

Libby, S.J., Brehm, M.A., Greiner, D.L., Shultz, L.D., et al. (2010) Humanized nonobese diabetic-scid IL2rγnull mice are susceptible to lethal *Salmonella* Typhi infection. *Proceedings of the National Academy of Sciences of the United States of America*. 107 (35), 15589–15594.

Lightfield, K.L., Persson, J., Brubaker, S.W., Witte, C.E., et al. (2008) Critical function for Naip5 in inflammasome activation by a conserved carboxy-terminal domain of flagellin. *Nature Immunology*. 9 (10), 1171–1178. Available from: doi:10.1038/ni.1646 [Accessed: 26 September 2017].

Lim, S., Kim, M., Choi, J. & Ryu, S. (2010) A Mutation in tdcA Attenuates the Virulence of *Salmonella* enterica Serovar Typhimurium. *Mol. Cells*. 29, 509–517. Available from: doi:10.1007/s10059-010-0063-6 [Accessed: 2 February 2020].

Liston, S.D., Ovchinnikova, O.G. & Whitfield, C. (2016) Unique lipid anchor attaches Vi antigen capsule to the surface of *Salmonella* enterica serovar Typh. *Proc Natl Acad Sci USA*. 113 (24), 6719–6724. Available from: doi:10.1371/journal.pone.0145945 [Accessed: 15 February 2018].

Liu, B., Knirel, Y.A., Feng, L., Perepelov, A. V., et al. (2014) Structural diversity in *Salmonella* O antigens and its genetic basis. *FEMS Microbiology Reviews*. 38 (1), 56–89.

Liu, S.-L., Ezaki, T., Miura, H., Matsui, K., et al. (1988) Intact Motility as a *Salmonella* typhi Invasion-Related Factor. *INFECTION AND IMMUNITY*. 1967–1973. Available from: http://iai.asm.org/content/56/8/1967.full.pdf [Accessed: 31 March 2018].

Liu, W.Q., Feng, Y., Wang, Y., Zou, Q.H., et al. (2009) *Salmonella* paratyphi C: Genetic divergence from *Salmonella* choleraesuis and pathogenic convergence with *Salmonella* typhi. *PLoS ONE*. 4 (2). Available from: doi:10.1371/journal.pone.0004510 [Accessed: 24 May 2019].

Liu, X., Zhang, Z., Ruan, J., Pan, Y., et al. (2016) Inflammasome-activated gasdermin D causes pyroptosis by forming membrane pores. *Nature*. 535 (7610), 153–158.

Lorenz, M.C. & Fink, G.R. (2002) Life and death in a macrophage: role of the glyoxylate cycle in virulence. *Eukaryotic cell*. 1 (5), 657–662. Available from: doi:10.1128/EC.1.5.657-662.2002 [Accessed: 16 February 2019].

Lou, L., Zhang, P., Piao, R. & Wang, Y. (2019) *Salmonella* Pathogenicity Island 1 (SPI-1) and Its Complex Regulatory Network. *Frontiers in Cellular and Infection Microbiology*. 9 (July), 1–12.

Madeira, F., Park, Y.M., Lee, J., Buso, N., et al. (2019) The EMBL-EBI search and sequence analysis tools APIs in 2019. *Nucleic acids research*. 47 (W1), W636–W641.

Maelfait, J., Vercammen, E., Janssens, S., Schotte, P., et al. (2008) Stimulation of Toll-like receptor 3 and 4 induces interleukin-1β maturation by caspase-8. *Journal of Experimental Medicine*. 205 (9), 1967–1973.

Main-Hester, K.L., Colpitts, K.M., Thomas, G.A., Ferric, †, et al. (2008) Coordinate Regulation of *Salmonella* Pathogenicity Island 1 (SPI1) and SPI4 in *Salmonella* enterica Serovar Typhimurium. *INFECTION AND IMMUNITY*. 76 (3), 1024–1035. Available from: doi:10.1128/IAI.01224-07 [Accessed: 24 May 2019].

Majowicz, S.E., Musto, J., Scallan, E., Angulo, F.J., et al. (2010) The Global Burden of Nontyphoidal

Salmonella Gastroenteritis. *Clinical Infectious Diseases*. 50 (6), 882–889.

Malik-Kale, P., Winfree, S. & Steele-Mortimer, O. (2012) The bimodal lifestyle of intracellular *Salmonella* in epithelial cells: Replication in the cytosol obscures defects in vacuolar replication. *PLoS ONE*. 7 (6).

Man, S.M., Ekpenyong, A., Tourlomousis, P., Achouri, S., et al. (2014a) Actin polymerization as a key innate immune effector mechanism to control *Salmonella* infection. *Proceedings of the National Academy of Sciences*. 111 (49), 17588–17593. Available from: doi:10.1073/pnas.1419925111 [Accessed: 11 July 2017].

Man, S.M., Hopkins, L.J., Nugent, E., Cox, S., et al. (2014b) Inflammasome activation causes dual recruitment of NLRC4 and NLRP3 to the same macromolecular complex. *Proceedings of the National Academy of Sciences*. 111 (20), 7403–7408.

Man, S.M., Karki, R. & Kanneganti, T.D. (2017) Molecular mechanisms and functions of pyroptosis, inflammatory caspases and inflammasomes in infectious diseases. *Immunological Reviews*.277 (1) pp.61–75.

Man, S.M., Tourlomousis, P., Hopkins, L., Monie, T.P., et al. (2013) *Salmonella* Infection Induces Recruitment of Caspase-8 to the Inflammasome To Modulate IL-1β Production. *The Journal of Immunology*. 191 (10), 5239–5246.

Marchello, C.S., Hong, C.Y. & Crump, J.A. (2019) Global typhoid fever incidence: A systematic review and meta-analysis. *Clinical Infectious Diseases*. 68, S105–S116.

Mariathasan, S., Newton, K., Monack, D.M., Vucic, D., et al. (2004) Differential activation of the inflammasome by caspase-1 adaptors ASC and Ipaf. *Nature*. 430 (6996), 213–218.

Marshall, J.M., Flechtner, A.D., Perle, L. & Gunn, K.M. (2014) Visualization of Extracellular Matrix Components within Sectioned *Salmonella* Biofilms on the Surface of Human Gallstones. *PLoS ONE*. 9 (2), 89243. Available from: doi:10.1371/journal.pone.0089243 [Accessed: 24 May 2019].

Martin, L.B., Simon, R., MacLennan, C.A., Tennant, S.M., et al. (2016) Status of paratyphoid fever vaccine research and development. *Vaccine*. 34 (26), 2900–2902. Available from: doi:10.1016/j.vaccine.2016.03.106.

Martinon, F. & Tschopp, J. (2004) Inflammatory caspases: Linking an intracellular innate immune system to autoinflammatory diseases. *Cell*. 117 (5), 561–574.

Marzel, A., Desai, P.T., Goren, A., Schorr, Y.I., et al. (2016) Persistent infections by nontyphoidal *Salmonella* in humans: Epidemiology and genetics. *Clinical Infectious Diseases*. 62 (7), 879–886.

Maskey, A.P., Day, J.N., Tuan, P.Q., Thwaites, G.E., et al. (2006) *Salmonella* enterica Serovar Paratyphi A and S. enterica Serovar Typhi Cause Indistinguishable Clinical Syndromes in Kathmandu, Nepal. *Clinical Infectious Diseases*. 42 (9), 1247–1253. Available from: doi:10.1086/503033 [Accessed: 20 August 2018].

McClelland, M., Sanderson, K.E., Clifton, S.W., Latreille, P., et al. (2004) Comparison of genome degradation in Paratyphi A and Typhi, human-restricted serovars of *Salmonella* enterica that cause typhoid. *Nature Genetics*. 36 (12), 1268–1274.

McClelland, M., Sanderson, K.E., Spieth, J., Clifton, S.W., et al. (2001) Complete genome sequence of *Salmonella* enterica serovar Typhimurium LT2. *Nature*. 413 (6858), 852–856. Available from: doi:10.1038/35101614 [Accessed: 16 March 2018].

McClure, R., Balasubramanian, D., Sun, Y., Bobrovskyy, M., et al. (2013) Computational analysis of bacterial RNA-Seq data. *Nucleic Acids Research*. 41 (14), e140–e140. Available from: doi:10.1093/nar/gkt444 [Accessed: 8 February 2020].

McCullagh, D., Dobinson, H.C., Darton, T., Campbell, D., et al. (2015) Understanding paratyphoid infection: Study protocol for the development of a human model of *Salmonella* enterica serovar Paratyphi A challenge in healthy adult volunteers. *BMJ Open*. 5 (6).

McDowell, M.A., Byrne, A.M.P., Mylona, E., Johnson, R., et al. (2019) The S. Typhi effector StoD is an E3/E4 ubiquitin ligase which binds K48- And K63-linked diubiquitin. *Life Science Alliance*. 2 (3).

McGhie, E.J., Brawn, L.C., Hume, P.J., Humphreys, D., et al. (2009) *Salmonella* takes control: effector-driven manipulation of the host. *Current Opinion in Microbiology*.12 (1) pp.117–124.

McGhie, E.J., Hayward, R.D. & Koronakis, V. (2001) Cooperation between actin-binding proteins of invasive *Salmonella*: SipA potentiates SipC nucleation and bundling of actin. *EMBO Journal*. 20 (9), 2131–2139.

Mckinney, J.D., Ho, K., Ner Zu Bentrup, È., Mun Ä Oz-Elõ Âas, E.J., et al. (2000) Persistence of Mycobacterium tuberculosis in macrophages and mice requires the glyoxylate shunt enzyme isocitrate lyase. *Nature*. 406, 735–738.

Medzhitov, R. (2007) Recognition of microorganisms and activation of the immune response. *Nature*.449 (7164) pp.819–826.

Meltzer, E., Stienlauf, S., Leshem, E., Sidi, Y., et al. (2014) A large outbreak of *Salmonella* paratyphi a infection among israeli travelers to Nepal. *Clinical Infectious Diseases*. 58 (3), 359–364.

Menendez, A., Arena, E.T., Guttman, J.A., Thorson, L., et al. (2009) *Salmonella* infection of gallbladder epithelial cells drives local inflammation and injury in a model of acute typhoid fever. *The Journal of infectious diseases*. 200 (11), 1703–1713.

Meunier, E., Dick, M.S., Dreier, R.F., Schürmann, N., et al. (2014) Caspase-11 activation requires lysis of pathogen-containing vacuoles by IFN-induced GTPases. *Nature*. 509 (7500), 366–370.

Meunier, E., Wallet, P., Dreier, R.F., Costanzo, S., et al. (2015) Guanylate-binding proteins promote activation of the AIM2 inflammasome during infection with Francisella novicida. *Nature Immunology*. 16 (5), 476–484.

Mi, H., Huang, X., Muruganujan, A., Tang, H., et al. (2017) PANTHER version 11: expanded annotation data from Gene Ontology and Reactome pathways, and data analysis tool enhancements. *Nucleic acids research*. 45.

Miao, E.A., Alpuche-Aranda, C.M., Dors, M., Clark, A.E., et al. (2006) Cytoplasmic flagellin activates caspase-1 and secretion of interleukin 1β via Ipaf. *Nature Immunology*. 7 (6), 569–575.

Miao, E.A., Andersen-Nissen, E., Warren, S.E. & Aderem, A. (2007) TLR5 and Ipaf: Dual sensors of bacterial flagellin in the innate immune system. *Seminars in Immunopathology*.29 (3) pp.275–288.

Miao, E.A., Leaf, I.A., Treuting, P.M., Mao, D.P., et al. (2010a) Caspase-1-induced pyroptosis is an innate immune effector mechanism against intracellular bacteria. *Nature Immunology*. 11 (12), 1136–1142.

Miao, E.A., Mao, D.P., Yudkovsky, N., Bonneau, R., et al. (2010b) Innate immune detection of the type III secretion apparatus through the NLRC4 inflammasome. *Proceedings of the National Academy of Sciences*. 107 (7), 3076–3080.

Miller, R.A. & Wiedmann, M. (2016) The cytolethal distending toxin produced by nontyphoidal *Salmonella* serotypes javiana, montevideo, oranienburg, and mississippi induces DNA damage in a manner similar to that of serotype Typhi. *mBio*. 7 (6).

Mitchell, P.S., Sandstrom, A. & Vance, R.E. (2019) The NLRP1 inflammasome: new mechanistic insights and unresolved mysteries. *Current Opinion in Immunology*. 60, 37–45. Available from: doi:10.1016/j.coi.2019.04.015.

Mogasale, V., Maskery, B., Ochiai, R.L., Lee, J.S., et al. (2014) Burden of typhoid fever in low-income and middle-income countries: A systematic, literature-based update with risk-factor adjustment. *The Lancet Global Health*. 2 (10), e570–e580.

Morona, R., Daniels, C. & Van Den Bosch, L. (2003) Genetic modulation of Shigella flexneri 2a lipopolysaccharide O antigen modal chain length reveals that it has been optimized for virulence. *Microbiology*.149 (4) pp.925–939.

Mulvihill, E., Sborgi, L., Mari, S.A., Pfreundschuh, M., et al. (2018) Mechanism of membrane pore formation by human gasdermin-D. *The EMBO Journal*. 37 (14), e98321. Available from: doi:10.15252/embj.201798321 [Accessed: 28 August 2018].

Muñoz-Planillo, R., Kuffa, P., Martínez-Colón, G., Smith, B., et al. (2013) K+ Efflux Is the Common Trigger of NLRP3 Inflammasome Activation by Bacterial Toxins and Particulate Matter. *Immunity*. 38 (6), 1142–1153.

Murray, G.L., Attridge, S.R. & Morona, R. (2006) Altering the length of the lipopolysaccharide O antigen

has an impact on the interaction of *Salmonella* enterica serovar typhimurium with macrophages and complement. *Journal of Bacteriology*. 188 (7), 2735–2739.

Murray, G.L., Attridge, S.R. & Morona, R. (2005) Inducible serum resistance in *Salmonella* typhimurium is dependent on wzzfepE-regulated very long O antigen chains. *Microbes and Infection*. 7 (13), 1296–1304.

Murray, G.L., Attridge, S.R. & Morona, R. (2003) Regulation of *Salmonella* typhimurium lipopolysaccharide O antigen chain length is required for virulence; identification of FepE as a second Wzz. *Molecular Microbiology*. 47 (5), 1395–1406.

Nath, G., Singh, H. & Shukla, V.K. (1997) Chronic typhoid carriage and carcinoma of the gallbladder. *European Journal of Cancer Prevention*.6 (6) pp.557–559.

Nath, G., Singh, Y.K., Kumar, K., Gulati, A.K., et al. (2008) Association of carcinoma of the gallbladder with typhoid carriage in a typhoid endemic area using nested PCR. *Journal of infection in developing countries*. 2 (4), 302–307.

Nickerson, K.P., Chanin, R.B., Sistrunk, J.R., Rasko, D.A., et al. (2017) Analysis of Shigella flexneri resistance, biofilm formation, and transcriptional profile in response to bile salts. *Infection and Immunity*. 85 (6).

Nuccio, S.P. & Bäumler, A.J. (2014) Comparative analysis of *Salmonella* genomes identifies a metabolic network for escalating growth in the inflamed gut. *mBio*. 5 (2).

Ochman, H. & Groisman, E.A. (1996) Distribution of Pathogenicity Islands in. *Microbiology*. 64 (12), 5410–5412.

Olive, A.J., Kenjale, R., Espina, M., Moore, D.S., et al. (2007) Bile salts stimulate recruitment of IpaB to the Shigella flexneri surface, where it colocalizes with IpaD at the tip of the type III secretion needle. *Infection and Immunity*. 75 (5), 2626–2629.

Van Opdenbosch, N., Van Gorp, H., Verdonckt, M., Saavedra, P.H.V., et al. (2017) Caspase-1 Engagement and TLR-Induced c-FLIP Expression Suppress ASC/Caspase-8-Dependent Apoptosis by Inflammasome Sensors NLRP1b and NLRC4. *Cell Reports*. 21 (12), 3427–3444.

Orning, P., Weng, D., Starheim, K., Ratner, D., et al. (2018) Pathogen blockade of TAK1 triggers caspase-8–dependent cleavage of gasdermin D and cell death. *Science*. 362 (6418), 1064–1069.

Oscarsson, J., Westermark, M., Löfdahl, S., Olsen, B., et al. (2002) Characterization of a pore-forming cytotoxin expressed by *Salmonella* enterica serovars Typhi and Paratyphi A. *Infection and Immunity*. 70 (10), 5759–5769. Available from: doi:10.1128/IAI.70.10.5759-5769.2002 [Accessed: 28 March 2018].

Pallett, M., Crepin, V., Serafini, N., Habibzay, M., et al. (2016) Bacterial virulence factor inhibits caspase-4/11 activation in intestinal epithelial cells. *Nature Publishing Group*. 10.

Parkhill, J., Dougan, G., James, K.D., Thomson, N.R., et al. (2001) Complete genome sequence of a multiple drug resistant *Salmonella* enterica serovar Typhi CT18. *Nature*. 413 (6858), 848–852.

Parry, C.M., Thieu, N.T.V., Dolecek, C., Karkey, A., et al. (2015) Clinically and microbiologically derived azithromycin susceptibility breakpoints for *Salmonella* enterica serovars Typhi and Paratyphi A. *Antimicrobial Agents and Chemotherapy*. 59 (5), 2756–2764.

Parry, C.M., Wijedoru, L., Arjyal, A. & Baker, S. (2011) The utility of diagnostic tests for enteric fever in endemic locations. *Expert Review of Anti-Infective Therapy*. 9 (6), 711–725.

Parry, M.C., Hien, T.T., Dougan, G., White, N.J., et al. (2002) Typhoid fever. *Medical Progress N Engl J Med*. 347 (22), 1770–1782.

Patel, J.C. & Galán, J.E. (2006) Differential activation and function of Rho GTPases during *Salmonella*-host cell interactions. *Journal of Cell Biology*. 175 (3), 453–463.

Patel, S. & McCormick, B.A. (2014) Mucosal inflammatory response to *Salmonella* typhimurium infection. *Frontiers in Immunology*. 5 (JUL), 1–10.

Pereira, M., Tourlomousis, P., Wright, J., P. Monie, T., et al. (2016) CARD9 negatively regulates NLRP3-induced IL-1β production on Salmonella infection of macrophages. *Nature Communications*. 7 (1), 12874. Available from: doi:10.1038/ncomms12874 [Accessed: 16 July 2019].

Pétrilli, V., Papin, S., Dostert, C., Mayor, A., et al. (2007) Activation of the NALP3 inflammasome is

triggered by low intracellular potassium concentration. *Cell Death and Differentiation*. 14 (9), 1583–1589.

Pham, T.D. (2018) *The Molecular Epidemiology of Enteric Fever in South and Southeast Asia*. The Open University.

Philip, N.H., DeLaney, A., Peterson, L.W., Santos-Marrero, M., et al. (2016) Activity of Uncleaved Caspase-8 Controls Anti-bacterial Immune Defense and TLR-Induced Cytokine Production Independent of Cell Death David Weiss (ed.). *PLOS Pathogens*. 12 (10), e1005910.

Philip, N.H., Dillon, C.P., Snyder, A.G., Fitzgerald, P., et al. (2014) Caspase-8 mediates caspase-1 processing and innate immune defense in response to bacterial blockade of NF-κB and MAPK signaling. *Proceedings of the National Academy of Sciences of the United States of America*. 111 (20), 7385–7390.

Pickard, D., Li, J., Roberts, M., Maskell, D., et al. (1994) Characterization of Defined ompR Mutants of *Salmonella* typhi: ompR Is Involved in the Regulation of Vi Polysaccharide Expression. *Infection and Immunity*. 62 (9), 3984–3993.

Pickard, D., Wain, J., Baker, S., Line, A., et al. (2003) Composition, acquisition, and distribution of the Vi exopolysaccharide-encoding *Salmonella* enterica pathogenicity island SPI-7. *Journal of Bacteriology*. 185 (17), 5055–5065.

Pierini, R., Perret, M., Djebali, S., Juruj, C., et al. (2013) ASC Controls IFN-γ Levels in an IL-18–Dependent Manner in Caspase-1–Deficient Mice Infected with Francisella novicida . *The Journal of Immunology*. 191 (7), 3847–3857.

Pilla, D.M., Hagar, J.A., Haldar, A.K., Mason, A.K., et al. (2014) Guanylate binding proteins promote caspase-11-dependent pyroptosis in response to cytoplasmic LPS. *Proceedings of the National Academy of Sciences*. 111 (16), 6046–6051.

Pitzer, V.E., Bowles, C.C., Baker, S., Kang, G., et al. (2014) Predicting the Impact of Vaccination on the Transmission Dynamics of Typhoid in South Asia: A Mathematical Modeling Study. *PLoS Neglected Tropical Diseases*. 8 (1), 40.

Pope, L.M., Reed, K.E. & Payne, S.M. (1995) Increased protein secretion and adherence to HeLa cells by Shigella spp. following growth in the presence of bile salts. *Infection and Immunity*. 63 (9), 3642–3648.

Prieto, A.I., Ramos-Morales, F. & Casadesús, J. (2004) Bile-induced DNA damage in *Salmonella* enterica. *Genetics*. 168 (4), 1787–1794.

Prieto, A.I., Ramos-Morales, F. & Casadesús, J. (2006) Repair of DNA damage induced by bile salts in *Salmonella* enterica. *Genetics*. 174 (2), 575–584.

Prouty, A.M., Brodsky, I.E., Falkow, S. & Gunn, J.S. (2004a) Bile-salt-mediated induction of antimicrobial and bile resistance in *Salmonella* typhimurium. *Microbiology*. 150 (4), 775–783.

Prouty, A.M., Brodsky, I.E., Manos, J., Belas, R., et al. (2004b) Transcriptional regulation of *Salmonella* enterica serovar Typhimurium genes by bile. *FEMS Immunology and Medical Microbiology*. 41 (2), 177–185.

Prouty, A.M. & Gunn, J.S. (2000) *Salmonella* enterica Serovar Typhimurium Invasion Is Repressed in the Presence of Bile. *Infection and Immunity*. 68 (12), 6763–6769.

Prouty, A.M., Schwesinger, W.H. & Gunn, J.S. (2002) Biofilm formation and interaction with the surfaces of gallstones by *Salmonella* spp. *Infection and Immunity*. 70 (5), 2640–2649.

Prouty, A.M., van Velkinburgh, J.C., John, S. & Gunn, J.S. (2002) *Salmonella* enterica Serovar Typhimurium Resistance to Bile : Identification and Characterization of the tolQRA Cluster. *JOURNAL OF BACTERIOLOGY*. 184 (5), 1270–1276.

Py, B.F., Kim, M.S., Vakifahmetoglu-Norberg, H. & Yuan, J. (2013) Deubiquitination of NLRP3 by BRCC3 Critically Regulates Inflammasome Activity. *Molecular Cell*. 49 (2), 331–338.

Qu, Y., Misaghi, S., Newton, K., Maltzman, A., et al. (2016) NLRP3 recruitment by NLRC4 during *Salmonella* infection. *The Journal of Experimental Medicine*. 213 (6), 877–885.

Raffatellu, M., Chessa, D., Wilson, R.P., Akçelik, M., et al. (2006) Capsule-Mediated Immune Evasion : a New Hypothesis Explaining Aspects of Typhoid Fever Pathogenesis. *INFECTION AND IMMUNITY*.

74 (1), 19–27.
Raffatellu, M., Chessa, D., Wilson, R.P., Dusold, R., et al. (2005a) The Vi Capsular Antigen of *Salmonella* enterica Serotype Typhi Reduces Toll-Like Receptor-Dependent Interleukin-8 Expression in the Intestinal Mucosa. *INFECTION AND IMMUNITY*. 73 (6), 3367–3374.
Raffatellu, M., Wilson, R.P., Chessa, D., Andrews-Polymenis, H., et al. (2005b) SipA, SopA, SopB, SopD, and SopE2 Contribute to *Salmonella* enterica Serotype Typhimurium Invasion of Epithelial Cells. *INFECTION AND IMMUNITY*. 73 (1), 146–154.
Raffatellu, M., Wilson, R.P., Winter, S.E. & Bäumler, A.J. (2008) Clinical pathogenesis of typhoid fever. *Journal of infection in developing countries*. 2 (4), 260–266.
Ramos-Morales, F. (2012) Impact of *Salmonella* enterica Type III Secretion System Effectors on the Eukaryotic Host Cell. *ISRN Cell Biology*. 2012, 1–36.
Ramos-Morales, F., Prieto, A.I., Beuzón, C.R., Holden, D.W., et al. (2003) Role for *Salmonella* enterica enterobacterial common antigen in bile resistance and virulence. *Journal of bacteriology*. 185 (17), 5328–5332. Available from: doi:10.1128/JB.185.17.5328 [Accessed: 21 November 2016].
Rathinam, V.A.K., Jiang, Z., Waggoner, S.N., Sharma, S., et al. (2010) The AIM2 inflammasome is essential for host defense against cytosolic bacteria and DNA viruses. *Nature Immunology*. 11 (5), 395–402.
Rathkey, J.K., Benson, B.L., Chirieleison, S.M., Yang, J., et al. (2017) Live-cell visualization of gasdermin D-driven pyroptotic cell death. *Journal of Biological Chemistry*. 292 (35), 14649–14658. Available from: doi:10.1074/jbc.M117.797217 [Accessed: 7 December 2018].
Rauch, I., Deets, K.A., Ji, D.X., von Moltke, J., et al. (2017) NAIP-NLRC4 Inflammasomes Coordinate Intestinal Epithelial Cell Expulsion with Eicosanoid and IL-18 Release via Activation of Caspase-1 and -8. *Immunity*. 46 (4), 649–659.
Raupach, B., Peuschel, S.K., Monack, D.M. & Zychlinsky, A. (2006) Caspase-1-mediated activation of interleukin-1β (IL-1β) and IL-18 contributes to innate immune defenses against *Salmonella* enterica serovar typhimurium infection. *Infection and Immunity*. 74 (8), 4922–4926. Available from: doi:10.1128/IAI.00417-06 [Accessed: 1 June 2017].
Rayamajhi, M., Zak, D.E., Chavarria-Smith, J., Vance, R.E., et al. (2013) Cutting edge: Mouse NAIP1 detects the type III secretion system needle protein. *Journal of immunology (Baltimore, Md. : 1950)*. 191 (8), 3986–3989.
Raymond, B., Young, J.C., Pallett, M., Endres, R.G., et al. (2013) Subversion of trafficking, apoptosis, and innate immunity by type III secretion system effectors. *Trends in Microbiology*.21 (8) pp.430–441. Available from: doi:10.1016/j.tim.2013.06.008.
Rescigno, M., Urbano, M., Valzasina, B., Francolini, M., et al. (2001) Dendritic cells express tight junction proteins and penetrate gut epithelial monolayers to sample bacteria. *Nature Immunology*. 2 (4), 361–367.
Reyes, R.E., Romo Gonzalez, C., Coria Jimenez, R., Ortiz Herrera, M., et al. (2012) Mechanisms of O-Antigen Structural Variation of Bacterial Lipopolysaccharide (LPS). *Intech*.
Reyes Ruiz, V.M., Ramirez, J., Naseer, N., Palacio, N.M., et al. (2017) Broad detection of bacterial type III secretion system and flagellin proteins by the human NAIP/NLRC4 inflammasome. *Proceedings of the National Academy of Sciences of the United States of America*. 114 (50), 13242–13247. Available from: doi:10.1073/pnas.1710433114 [Accessed: 5 January 2018].
Ristori, C., Rodriguez, H., Vicent, P., Lobos, H., et al. (1982) Investigation of the *Salmonella* typhi-paratyphi carrier state in cases of surgical intervention for gallbladder disease. *Bulletin of the Pan American Health Organization*. 16 (2), 161–171.
Roberts, T.L., Idris, A., Dunn, J.A., Kelly, G.M., et al. (2009) HIN-200 proteins regulate caspase activation in response to foreign cytoplasmic DNA. *Science*. 323 (5917), 1057–1060.
Rodriguez-Rivera, L.D., Bowen, B.M., Den Bakker, H.C., Duhamel, G.E., et al. (2015) Characterization of the cytolethal distending toxin (typhoid toxin) in non-typhoidal *Salmonella* serovars. *Gut Pathogens*. 7 (1).
Roumagnac, P., Weill, F.-X., Dolecek, C., Baker, S., et al. (2006) Evolutionary history of *Salmonella*

Typhi. *Science*. 314 (5803), 1301–1304.
Rühl, S. & Broz, P. (2015) Caspase-11 activates a canonical NLRP3 inflammasome by promoting K+ efflux. *European Journal of Immunology*. 45 (10), 2927–2936.
Rühl, S., Shkarina, K., Demarco, B., Heilig, R., et al. (2018) ESCRT-dependent membrane repair negatively regulates pyroptosis downstream of GSDMD activation. *Science*. 362 (6417), 956–960. Available from: doi:10.1126/science.aar7607 [Accessed: 25 January 2019].
Sabbagh, S.C., Forest, C.G., Lepage, C., Leclerc, J.M., et al. (2010) So similar, yet so different: Uncovering distinctive features in the genomes of *Salmonella* enterica serovars Typhimurium and Typhi. *FEMS Microbiology Letters*.305 (1) pp.1–13.
Sagulenko, V., Thygesen, S.J., Sester, D.P., Idris, A., et al. (2013) AIM2 and NLRP3 inflammasomes activate both apoptotic and pyroptotic death pathways via ASC. *Cell Death and Differentiation*. 20 (9), 1149–1160.
Sahastrabuddhe, S., Carbis, R., Wierzba, T.F. & Ochiai, R.L. (2013) Increasing rates of *Salmonella* Paratyphi A and the current status of its vaccine development. *Expert review of vaccines*. 12 (9), 1021–1031.
Saini, S. & Rao, C. V. (2010) SprB Is the molecular link between *Salmonella* pathogenicity island 1 (SPI1) and SPI4. *Journal of Bacteriology*. 192 (9), 2459–2462.
Sanchez-Garrido, J., Slater, S.L., Clements, A., Shenoy, A.R., et al. (2020) Vying for the control of inflammasomes: The cytosolic frontier of enteric bacterial pathogen-host interactions. *Cellular microbiology*. 22 (4), e13184. Available from: doi:10.1111/cmi.13184.
Sandstrom, A., Mitchell, P.S., Goers, L., Mu, E.W., et al. (2019) Functional degradation: A mechanism of NLRP1 inflammasome activation by diverse pathogen enzymes. *Science*. 364 (6435), eaau1330. Available from: doi:10.1126/science.aau1330 [Accessed: 13 March 2019].
Sanman, L.E., Qian, Y., Eisele, N.A., Ng, T.M., et al. (2016) Disruption of glycolytic flux is a signal for inflammasome signaling and pyroptotic cell death. *eLife*. 5 (MARCH2016).
Santos, J.C. & Broz, P. (2018) Sensing of invading pathogens by GBPs: At the crossroads between cell-autonomous and innate immunity. *Journal of Leukocyte Biology*. 8–10.
Santos, J.C., Dick, M.S., Lagrange, B., Degrandi, D., et al. (2018) LPS targets host guanylate-binding proteins to the bacterial outer membrane for non-canonical inflammasome activation. *The EMBO journal*. 37 (6).
Santos, R.L., Raffatellu, M., Bevins, C.L., Adams, L.G., et al. (2009) Life in the inflamed intestine, *Salmonella* style. *Trends in Microbiology*. 17 (11), 498–506.
Sargo, C.R., Campani, G., Silva, G.G., Giordano, R.C., et al. (2015) *Salmonella* typhimurium and Escherichia coli dissimilarity: Closely related bacteria with distinct metabolic profiles. *Biotechnology Progress*. 31 (5), 1217–1225.
Sarhan, J., Liu, B.C., Muendlein, H.I., Li, P., et al. (2018) Caspase-8 induces cleavage of gasdermin D to elicit pyroptosis during Yersinia infection. *Proceedings of the National Academy of Sciences of the United States of America*. 115 (46), E10888–E10897.
Saul, A., Smith, T. & Maire, N. (2013) Stochastic Simulation of Endemic *Salmonella* enterica Serovar Typhi: The Importance of Long Lasting Immunity and the Carrier State. *PLoS ONE*. 8 (9). Available from: doi:10.1371/journal.pone.0074097 [Accessed: 27 December 2018].
Sborgi, L., Rühl, S., Mulvihill, E., Pipercevic, J., et al. (2016) GSDMD membrane pore formation constitutes the mechanism of pyroptotic cell death. *The EMBO Journal*. 35 (16), 1766–1778. Available from: doi:10.15252/embj.201694696 [Accessed: 5 January 2019].
Scanu, T., Spaapen, R.M., Bakker, J.M., Pratap, C.B., et al. (2015) *Salmonella* Manipulation of Host Signaling Pathways Provokes Cellular Transformation Associated with Gallbladder Carcinoma. *Cell Host and Microbe*. 17 (6), 763–774.
SchiøLer, H., Christiansen, E.D., Høybye, G., Rasmussen, S.N., et al. (1983) Biliary Calculi in Chronic *Salmonella* Carriers and Healthy Controls: A Controlled Study. *Scandinavian Journal of Infectious Diseases*. 15 (1), 17–19.
Schmid-Burgk, J.L., Gaidt, M.M., Schmidt, T., Ebert, T.S., et al. (2015) Caspase-4 mediates non-

canonical activation of the NLRP3 inflammasome in human myeloid cells. *European Journal of Immunology*. 45 (10), 2911–2917.

Schreiber, F., Kay, S., Frankel, G., Clare, S., et al. (2015) The Hd, Hj, and Hz66 flagella variants of *Salmonella* enterica serovar Typhi modify host responses and cellular interactions. *Scientific Reports*. 5, 7947.

Schroder, K. & Tschopp, J. (2010) The Inflammasomes. *Cell*.140 (6) pp.821–832.

Schuhmacher, D.A. & Klose, K.E. (1999) Environmental signals modulate ToxT-dependent virulence factor expression in Vibrio cholerae. *Journal of bacteriology*. 181 (5), 1508–1514.

Seif, Y., Kavvas, E., Lachance, J.C., Yurkovich, J.T., et al. (2018) Genome-scale metabolic reconstructions of multiple *Salmonella* strains reveal serovar-specific metabolic traits. *Nature Communications*. 9 (1).

Seif, Y., Monk, J.M., Machado, H., Kavvas, E., et al. (2019) Systems Biology and Pangenome of *Salmonella* O-Antigens . *mBio*. 10 (4).

Sellge, G. & Kufer, T.A. (2015) PRR-signaling pathways: Learning from microbial tactics. *Seminars in Immunology*. 27 (2), 75–84. Available from: doi:10.1016/j.smim.2015.03.009.

Sellin, M.E., Müller, A.A., Felmy, B., Dolowschiak, T., et al. (2014) Epithelium-intrinsic NAIP/NLRC4 inflammasome drives infected enterocyte expulsion to restrict *Salmonella* replication in the intestinal mucosa. *Cell Host and Microbe*. 16 (2), 237–248. Available from: doi:10.1016/j.chom.2014.07.001 [Accessed: 25 August 2017].

Sellin, M.E., Müller, A.A. & Hardt, W.D. (2018) Consequences of Epithelial Inflammasome Activation by Bacterial Pathogens. *Journal of Molecular Biology*. 430 (2), 193–206. Available from: doi:10.1016/j.jmb.2017.03.031.

Sengupta, C., Ray, S. & Chowdhury, R. (2014) Fine tuning of virulence regulatory pathways in enteric bacteria in response to varying bile and oxygen concentrations in the gastrointestinal tract. *Gut pathogens*. 6 (1), 38. Available from: doi:10.1186/s13099-014-0038-9 [Accessed: 17 October 2016].

Shah, J., Desai, P.T., Chen, D., Stevens, J.R., et al. (2013) Preadaptation to cold stress in *Salmonella* enterica serovar typhimurium increases survival during subsequent acid stress exposure. *Applied and Environmental Microbiology*. 79 (23), 7281–7289.

Sharma, A. & Qadri, A. (2004) Vi polysaccharide of *Salmonella* typhi targets the prohibitin family of molecules in intestinal epithelial cells and suppresses early inflammatory responses. *Proceedings of the National Academy of Sciences of the United States of America*. 101 (50), 17492–17497.

Sharma, D. & Kanneganti, T.-D. (2016) The cell biology of inflammasomes: Mechanisms of inflammasome activation and regulation. *The Journal of cell biology*. 213 (6), 617–629. Available from: doi:10.1083/jcb.201602089 [Accessed: 16 July 2019].

Shatalin, K., Shatalina, E., Mironov, A. & Nudler, E. (2011) H2S: A universal defense against antibiotics in bacteria. *Science*. 334 (6058), 986–990.

Shea, J.E., Hensel, M., Gleeson, C. & Holden, D.W. (1996) Identification of a virulence locus encoding a second type III secretion system in *Salmonella* typhimurium. *Proceedings of the National Academy of Sciences of the United States of America*. 93 (6), 2593–2597.

Sheikh, A., Charles, R.C., Rollins, S.M., Harris, J.B., et al. (2010) Analysis of *Salmonella* enterica serotype paratyphi a gene expression in the blood of bacteremic patients in Bangladesh. *PLoS Neglected Tropical Diseases*. 4 (12), 1–10.

Shenoy, A.R., Wellington, D.A., Kumar, P., Kassa, H., et al. (2012) GBP5 Promotes NLRP3 Inflammasome Assembly and Immunity in Mammals. *Science*. 336 (6080), 481–485. Available from: doi:10.1126/science.1217032 [Accessed: 14 September 2018].

Shi, J., Gao, W. & Shao, F. (2017) Pyroptosis: Gasdermin-Mediated Programmed Necrotic Cell Death. *Trends in Biochemical Sciences*.42 (4) pp.245–254. Available from: doi:10.1016/j.tibs.2016.10.004 [Accessed: 5 January 2019].

Shi, J., Zhao, Y., Wang, K., Shi, X., et al. (2015) Cleavage of GSDMD by inflammatory caspases determines pyroptotic cell death. *Nature*. 526 (7575), 660–665.

Shi, J., Zhao, Y., Wang, Y., Gao, W., et al. (2014) Inflammatory caspases are innate immune receptors for intracellular LPS. *Nature*. 514 (7521), 187–192.

Shimada, K., Crother, T.R., Karlin, J., Dagvadorj, J., et al. (2012) Oxidized Mitochondrial DNA Activates the NLRP3 Inflammasome during Apoptosis. *Immunity*. 36 (3), 401–414. Available from: doi:10.1016/j.immuni.2012.01.009.

Silva, P. da, Manieri, F.Z., Herrera, C.M., Trent, M.S., et al. (2018) Novel Role of VisP and the Wzz System during O-Antigen Assembly in *Salmonella* enterica Serovar Typhimurium Pathogenesis. *Infection and Immunity*. 86 (8), e00319-18. Available from: doi:10.1128/IAI.00319-18 [Accessed: 16 February 2019].

Simon, M., Zieg, J., Silverman, M., Mandel, G., et al. (1980) Phase variation: evolution of a controlling element. *Science*. 209 (4463), 1370–1374.

Sistrunk, J.R., Nickerson, K.P., Chanin, R.B., Rasko, D.A., et al. (2016) Survival of the fittest: How bacterial pathogens utilize bile to enhance infection. *Clinical Microbiology Reviews*. 29 (4), 819–836.

Solano-Collado, V., Rofe, A. & Spanò, S. (2018) Rab32 restriction of intracellular bacterial pathogens. *Small GTPases*.9 (3) pp.216–223.

Song, J., Gao, X. & Galán, J.E. (2013) Structure and function of the *Salmonella* Typhi chimaeric A2B5 typhoid toxin. *Nature*. 499 (7458), 350–354.

Song, J., Willinger, T., Rongvaux, A., Eynon, E.E., et al. (2010) A mouse model for the human pathogen *Salmonella* typhi. *Cell host & microbe*. 8 (4), 369–376.

Spanò, S. & Galán, J.E. (2012) A Rab32-dependent pathway contributes to *Salmonella* typhi host restriction. *Science*. 338, 960–963.

Spanò, S., Ugalde, J.E. & Galán, J.E. (2008) Delivery of a *Salmonella* Typhi Exotoxin from a Host Intracellular Compartment. *Cell Host and Microbe*. 3 (1), 30–38.

Spoering, A.L., Vulić, M. & Lewis, K. (2006) GlpD and PlsB participate in persister cell formation in Escherichia coli. *Journal of Bacteriology*. 188 (14), 5136–5144.

Srikanth, C. V., Mercado-Lubo, R., Hallstrom, K. & McCormick, B.A. (2011) *Salmonella* effector proteins and host-cell responses. *Cellular and Molecular Life Sciences*.68 (22) pp.3687–3697.

Srinivasula, S.M., Poyet, J.L., Razmara, M., Datta, P., et al. (2002) The PYRIN-CARD protein ASC is an activating adaptor for caspase-1. *Journal of Biological Chemistry*. 277 (24), 21119–21122.

Stanaway, J.D., Reiner, R.C., Blacker, B.F., Goldberg, E.M., et al. (2019) The global burden of typhoid and paratyphoid fevers: a systematic analysis for the Global Burden of Disease Study 2017. *The Lancet Infectious Diseases*. 19 (4), 369–381.

Stebbins, C.E. & Galán, J.E. (2003) Priming virulence factors for delivery into the host. *Nature reviews. Molecular cell biology*. 4 (9), 738–743.

Stecher, B., Robbiani, R., Walker, A.W., Westendorf, A.M., et al. (2007) *Salmonella* enterica serovar typhimurium exploits inflammation to compete with the intestinal microbiota. *PLoS Biology*. 5 (10), 2177–2189.

Steele-Mortimer, O. (2008) The *Salmonella*-containing vacuole-Moving with the times. *Current Opinion in Microbiology*. 11 (1), 38–45.

Steele-Mortimer, O., Brumell, J.H., Knodler, L.A., Méresse, S., et al. (2002) The invasion-associated type III secretion system of *Salmonella* enterica serovar Typhimurium is necessary for intracellular proliferation and vacuole biogenesis in epithelial cells. *Cellular Microbiology*. 4 (1), 43–54.

Stender, S., Friebel, A., Linder, S., Rohde, M., et al. (2000) Identification of SopE2 from *Salmonella* typhimurium, a conserved guanine nucleotide exchange factor for Cdc42 of the host cell. *Molecular microbiology*. 36 (6), 1206–1221.

Stensrud, K.F., Adam, P.R., La Mar, C.D., Olive, A.J., et al. (2008) Deoxycholate interacts with IpaD of Shigella flexneri in inducing the recruitment of IpaB to the type III secretion apparatus needle tip. *Journal of Biological Chemistry*. 283 (27), 18646–18654.

Su, L.H. & Chiu, C.H. (2007) *Salmonella*: Clinical importance and evolution of nomenclature. *Chang Gung Medical Journal*.30 (3) pp.210–219.

Suez, J., Porwollik, S., Dagan, A., Marzel, A., et al. (2013) Virulence Gene Profiling and Pathogenicity Characterization of Non-Typhoidal *Salmonella* Accounted for Invasive Disease in Humans. *PLoS ONE*. 8 (3).

Sumantran, V.N., Schweizer, H.P. & Datta, P. (1990) A Novel Membrane-Associated Threonine Permease Encoded by the tdcC Gene of Escherichia coli. *JOURNAL OF BACTERIOLOGY*.

Sun, Y.H., Rolán, H.G. & Tsolis, R.M. (2007) Injection of flagellin into the host cell cytosol by *Salmonella* enterica serotype typhimurium. *Journal of Biological Chemistry*. 282 (47), 33897–33901.

Swanson, K. V., Deng, M. & Ting, J.P.Y. (2019) The NLRP3 inflammasome: molecular activation and regulation to therapeutics. *Nature Reviews Immunology*.19 (8) pp.477–489.

Takeuchi, O. & Akira, S. (2010) Pattern Recognition Receptors and Inflammation. *Cell*.140 (6) pp.805–820.

Tapia-Abellán, A., Angosto-Bazarra, D., Martínez-Banaclocha, H., de Torre-Minguela, C., et al. (2019) MCC950 closes the active conformation of NLRP3 to an inactive state. *Nature Chemical Biology*. 15 (6), 560–564. Available from: doi:10.1038/s41589-019-0278-6 [Accessed: 24 May 2019].

Thanassi, D.G., Cheng, L.W. & Nikaido, H. (1997) Active efflux of bile salts by Escherichia coli. *Journal of Bacteriology*. 179 (8), 2512–2518.

Thanh, D.P., Karkey, A., Dongol, S., Thi, N.H., et al. (2016) A novel ciprofloxacin-resistant subclade of h58. *Salmonella* typhi is associated with fluoroquinolone treatment failure. *eLife*. 5 (MARCH2016), 1–13.

Thornberry, N.A., Bull, H.G., Calaycay, J.R., Chapman, K.T., et al. (1992) A novel heterodimeric cysteine protease is required for interleukin-1βprocessing in monocytes. *Nature*. 356 (6372), 768–774.

Thurston, T.L.M., Matthews, S.A., Jennings, E., Alix, E., et al. (2016) Growth inhibition of cytosolic *Salmonella* by caspase-1 and caspase-11 precedes host cell death. *Nature Communications*. 7, 13292.

Townsend, S.M., Kramer, N.E., Edwards, R., Baker, S., et al. (2001) *Salmonella* enterica Serovar Typhi Possesses a Unique Repertoire of Fimbrial Gene Sequences. *INFECTION AND IMMUNITY*. 69 (5), 2894–2901.

Tsolis, R.M., Xavier, M.N., Santos, R.L. & Bäumler, A.J. (2011) How to become a top model: Impact of animal experimentation on human *Salmonella* disease research. *Infection and Immunity*.79 (5) pp.1806–1814.

Tükel, Ç., Raffatellu, M., Chessa, D., Wilson, R.P., et al. (2006) Neutrophil influx during non-typhoidal salmonellosis: Who is in the driver's seat? *FEMS Immunology and Medical Microbiology*. 46 (3), 320–329.

Tyanova, S., Temu, T., Sinitcyn, P., Carlson, A., et al. (2016) The Perseus computational platform for comprehensive analysis of (prote)omics data. *Nature Methods*.13 (9) pp.731–740.

Urdaneta, V. & Casadesús, J. (2017) Interactions between bacteria and bile salts in the gastrointestinal and hepatobiliary tracts. *Frontiers in Medicine*.4 (OCT) p.163.

Vajjhala, P.R., Lu, A., Brown, D.L., Pang, S.W., et al. (2015) The inflammasome adaptor ASC induces procaspase-8 death effector domain filaments. *Journal of Biological Chemistry*. 290 (49), 29217–29230.

Valleau, D., Little, D.J., Borek, D., Skarina, T., et al. (2018) Functional diversification of the NleG effector family in enterohemorrhagic Escherichia coli. *Proceedings of the National Academy of Sciences of the United States of America*. 115 (40), 10004–10009.

Vance, R.E. (2015) The NAIP/NLRC4 inflammasomes. *Current Opinion in Immunology*. 32, 84–89.

van Velkinburgh, J.C. & Gunn, J.S. (1999) PhoP-PhoQ-Regulated Loci Are Required for Enhanced Bile Resistance in *Salmonella* spp . *INFECTION AND IMMUNITY*. 67 (4), 1614–1622.

Villarreal, J.M., Becerra-Lobato, N., Rebollar-Flores, J.E., Medina-Aparicio, L., et al. (2014) The *Salmonella* enterica serovar Typhi ltrR-ompR-ompC-ompF genes are involved in resistance to the bile salt sodium deoxycholate and in bacterial transformation. *Molecular Microbiology*. 92 (5), 1005–1024.

Virlogeux, I., Waxin, H., Ecobichon, C., Lee, jade o, et al. (1994) Characterization of the rcsA and rcsB

Genes from *Salmonella* typhi: rcsB through tviA Is Involved in Regulation of Vi Antigen Synthesis. *Infection and Immunity*. 62 (9), 3984–3993.

Virlogeux, I., Waxin, H., Ecobichon, C. & Popoff, M.Y. (1995) Role of the viaB locus in synthesis, transport and expression of *Salmonella* typhi Vi antigen. *Microbiology*. 141 (12), 3039–3047.

Waddington, C.S., Darton, T.C., Jones, C., Haworth, K., et al. (2014) An outpatient, ambulant-design, controlled human infection model using escalating doses of *Salmonella* typhi challenge delivered in sodium bicarbonate solution. *Clinical Infectious Diseases*. 58 (9), 1230–1240.

Walawalkar, Y.D., Vaidya, Y. & Nayak, V. (2016) Response of *Salmonella* Typhi to bile-generated oxidative stress: implication of quorum sensing and persister cell populations. *Pathogens and disease*. 74 (8).

Wallace, A.J., Stillman, T.J., Atkins, A., Jamieson, S.J., et al. (2000) E. coli hemolysin E (Hlye, ClyA, SheA): X-ray crystal structure of the toxin and observation of membrane pores by electron microscopy. *Cell*. 100 (2), 265–276.

Walthers, D., Carroll, R.K., Navarre, W.W., Libby, S.J., et al. (2007) The response regulator SsrB activates expression of diverse *Salmonella* pathogenicity island 2 promoters and counters silencing by the nucleoid-associated protein H-NS. *Molecular Microbiology*. 65 (2), 477–493.

Wang, N., Knodler, L.A. & Strugnell, R.A. (2019) Typhoid Fever: The More We Learn, the Less We Know (Apologies, Albert Einstein). *Cell Host & Microbe*. 26 (3), 303–306.

Wang, S., Phillippy, A.M., Deng, K., Rui, X., et al. (2010a) Transcriptomic responses of *Salmonella* enterica serovars Enteritidis and Typhimurium to Chlorine-Based Oxidative Stress. *Applied and Environmental Microbiology*. 76 (15), 5013–5024.

Wang, Y., Nordhues, B., Zhong, D. & De Guzman, R. (2010b) NMR characterization of the interaction of the *Salmonella* type III secretion system protein SipD and bile salts. *Biochemistry*. 49 (19), 4220–4226.

Wangdi, T., Lee, C.-Y., Spees, A.M., Yu, C., et al. (2014) The Vi Capsular Polysaccharide Enables *Salmonella* enterica Serovar Typhi to Evade Microbe-Guided Neutrophil Chemotaxis. *PLoS Pathog*. 10 (8).

Warren, S.E., Armstrong, A., Hamilton, M.K., Mao, D.P., et al. (2010) Cutting Edge: Cytosolic Bacterial DNA Activates the Inflammasome via Aim2. *The Journal of Immunology*. 185 (2), 818–821.

Watson, J.L., Sanchez-Garrido, J., Goddard, P.J., Torraca, V., et al. (2019) Shigella sonnei O-Antigen Inhibits Internalization, Vacuole Escape, and Inflammasome Activation. *mBio*. 10 (6).

Wemyss, M.A. & Pearson, J.S. (2019) Host Cell Death Responses to Non-typhoidal *Salmonella* Infection. *Frontiers in immunology*.10 p.1758.

Wenger, C.D. & Coon, J.J. (2013) A proteomics search algorithm specifically designed for high-resolution tandem mass spectra. *Journal of Proteome Research*. 12 (3), 1377–1386.

West, N.P., Sansonetti, P., Mounier, J., Exley, R.M., et al. (2005) Optimization of virulence functions through glucosylation of Shigella LPS. *Science*. 307 (5713), 1313–1317.

Wetter, M., Goulding, D., Pickard, D., Kowarik, M., et al. (2012) Molecular Characterization of the viaB Locus Encoding the Biosynthetic Machinery for Vi Capsule Formation in *Salmonella* Typhi. *PLoS ONE*. 7 (9).

WHO (2003) Background document : The diagnosis, treatment and prevention of typhoid fever. *Communicable Disease Surveillance and Response Vaccines and Biologicals*. 2–48.

WHO (2018) Typhoid vaccines: WHO position paper, March 2018 – Recommendations. *WEEKLY EPIDEMIOLOGICAL RECORD*. 13 (93), 153–172.

Wilson, K.P., Black, J.A.F., Thomson, J.A., Kim, E.E., et al. (1994) Structure and mechanism of interleukin-lβ converting enzyme. *Nature*. 370 (6487), 270–275.

Wilson, R.B. & Maloy, S.R. (1987) Isolation and characterization of *Salmonella* typhimurium glyoxylate shunt mutants. *Journal of Bacteriology*. 169 (7), 3029–3034.

Wilson, R.P., Raffatellu, M., Chessa, D., Winter, S.E., et al. (2008) The Vi-capsule prevents Toll-like receptor 4 recognition of *Salmonella*. *Cellular Microbiology*. 10 (4), 876–890.

Wilson, R.P., Winter, S.E., Spees, A.M., Winter, M.G., et al. (2011) The Vi capsular polysaccharide

prevents complement receptor 3-mediated clearance of *Salmonella* enterica serotype Typhi. *Infection and Immunity*. 79 (2), 830–837.

Winter, S.E., Raffatellu, M., Wilson, P.R., Rüssmann, H., et al. (2008) The *Salmonella* enterica serotype Typhi regulator TviA reduces interleukin-8 production in intestinal epithelial cells by repressing flagellin secretion. *Cellular Microbiology*. 10 (1), 247–261.

Winter, S.E., Thiennimitr, P., Nuccio, S.P., Haneda, T., et al. (2009a) Contribution of flagellin pattern recognition to intestinal inflammation during *Salmonella* enterica serotype Typhimurium infection. *Infection and Immunity*. 77 (5), 1904–1916.

Winter, S.E., Winter, M.G., Atluri, V., Poon, V., et al. (2015) The flagellar regulator TviA reduces pyroptosis by *Salmonella* enterica serovar Typhi. *Infection and Immunity*. 83 (4), 1546–1555.

Winter, S.E., Winter, M.G., Godinez, I., Yang, H.J., et al. (2010) A rapid change in virulence gene expression during the transition from the intestinal lumen into tissue promotes systemic dissemination of *Salmonella*. *PLoS Pathogens*. 6 (8), 63–64.

Winter, S.E., Winter, M.G., Poon, V., Keestra, A.M., et al. (2014) *Salmonella* enterica Serovar Typhi Conceals the Invasion-Associated Type Three Secretion System from the Innate Immune System by Gene Regulation. *PLoS Pathogens*. 10 (7).

Winter, S.E., Winter, M.G., Thiennimitr, P., Gerriets, V.A., et al. (2009b) The TviA auxiliary protein renders the *Salmonella* enterica serotype Typhi RcsB regulon responsive to changes in osmolarity. *Molecular Microbiology*. 74 (1), 175–193.

Wolfe, A.J. (2005) The Acetate Switch. *Microbiology and Molecular Biology Reviews*. 69 (1), 12–50.

Wong, V.K., Baker, S., Connor, T.R., Pickard, D., et al. (2016) An extended genotyping framework for *Salmonella* enterica serovar Typhi, the cause of human typhoid. *Nature Communications*. 7, 12827.

Wong, V.K., Baker, S., Pickard, D.J., Parkhill, J., et al. (2015) Phylogeographical analysis of the dominant multidrug-resistant H58 clade of *Salmonella* Typhi identifies inter- and intracontinental transmission events. *Nature Genetics*. 47 (6), 632–639.

Woods, C.W., Murdoch, D.R., Zimmerman, M.D., Glover, W.A., et al. (2006) Emergence of *Salmonella* enterica serotype Paratyphi A as a major cause of enteric fever in Kathmandu, Nepal. *Transactions of the Royal Society of Tropical Medicine and Hygiene*. 100 (11), 1063–1067.

Wu, B., Skarina, T., Yee, A., Jobin, M.C., et al. (2010) NleG type 3 effectors from enterohaemorrhagic Escherichia coli are U-Box E3 ubiquitin ligases C. Erec Stebbins (ed.). *PLoS Pathogens*. 6 (6), e1000960.

Wynosky-Dolfi, M.A., Snyder, A.G., Philip, N.H., Doonan, P.J., et al. (2014) Oxidative metabolism enables *Salmonella* evasion of the NLRP3 inflammasome. *The Journal of Experimental Medicine*. 211 (4), 653–668.

Xiong, K., Chen, Z., Zhu, C., Li, J., et al. (2015) Safety and immunogenicity of an attenuated *Salmonella* enterica serovar Paratyphi A vaccine candidate. *International Journal of Medical Microbiology*. 305 (6), 563–571.

Xu, H., Shi, J., Gao, H., Liu, Y., et al. (2019) The N-end rule ubiquitin ligase UBR2 mediates NLRP1B inflammasome activation by anthrax lethal toxin. *The EMBO Journal*. 38 (13), 1–11.

Yang, D., He, Y., Muñoz-Planillo, R., Liu, Q., et al. (2015) Caspase-11 Requires the Pannexin-1 Channel and the Purinergic P2X7 Pore to Mediate Pyroptosis and Endotoxic Shock. *Immunity*. 43 (5), 923–932.

Yang, J., Zhao, Y. & Shao, F. (2015) Non-canonical activation of inflammatory caspases by cytosolic LPS in innate immunity. *Current Opinion in Immunology*. 32, 78–83.

Yang, J., Zhao, Y., Shi, J. & Shao, F. (2013) Human NAIP and mouse NAIP1 recognize bacterial type III secretion needle protein for inflammasome activation. *Proc Natl Acad Sci USA*. 110 (35), 14408–14413.

Yimga, M.T., Leatham, M.P., Allen, J.H., Laux, D.C., et al. (2006) Role of gluconeogenesis and the tricarboxylic acid cycle in the virulence of *Salmonella* enterica serovar typhimurium in BALB/c mice. *Infection and Immunity*. 74 (2), 1130–1140.

Yue, M., Han, X., Masi, L. De, Zhu, C., et al. (2015) Allelic variation contributes to bacterial host specificity. *Nature Communications*. 6.

Yue, M., Rankin, S.C., Blanchet, R.T., Nulton, J.D., et al. (2012) Diversification of the *Salmonella* Fimbriae: A model of macro- and microevolution. *PLoS ONE*. 7 (6).

Zaki, M.H., Man, S.M., Vogel, P., Lamkanfi, M., et al. (2014) *Salmonella* exploits NLRP12-dependent innate immune signaling to suppress host defenses during infection. *Proceedings of the National Academy of Sciences*. 111 (1), 385–390.

Zellweger, R.M., Basnyat, B., Shrestha, P., Prajapati, K.G., et al. (2017) A 23-year retrospective investigation of *Salmonella* Typhi and *Salmonella* Paratyphi isolated in a tertiary Kathmandu hospital. *PLOS Neglected Tropical Diseases*. 11 (11), e0006051.

Zhang, H., Zhou, Y., Bao, H. & Liu, H.W. (2006) Vi antigen biosynthesis in *Salmonella* typhi: Characterization of UDP-N-acetylglucosamine C-6 dehydrogenase (TviB) and UDP-N-acetylglucosaminuronic acid C-4 epimerase (TviC). *Biochemistry*. 45 (26), 8163–8173.

Zhang, L., Chen, S., Ruan, J., Wu, J., et al. (2015) Cryo-EM structure of the activated NAIP2-NLRC4 inflammasome reveals nucleated polymerization. *Science*. 350 (6259), 404–409.

Zhang, S., Kingsley, R.A., Santos, R.L., Andrews-Polymenis, H., et al. (2003) Molecular pathogenesis of *Salmonella* enterica serotype typhimurium-induced diarrhea. *Infection and Immunity*.71 (1) pp.1–12.

Zhao, Y. & Shao, F. (2015) The NAIP-NLRC4 inflammasome in innate immune detection of bacterial flagellin and type III secretion apparatus. *Immunological Reviews*. 265 (1), 85–102.

Zhao, Y., Yang, J., Shi, J., Gong, Y.-N., et al. (2011) The NLRC4 inflammasome receptors for bacterial flagellin and type III secretion apparatus. *Nature*. 477 (7366), 596–600.

Zhou, D., Mooseker, M.S. & Galán, J.E. (1999) Role of the S. typhimurium Actin-binding protein SipA in bacterial internalization. *Science*. 283 (5410), 2092–2095.

Zhou, L., Jones, C., Gibani, M.M., Dobinson, H., et al. (2016) Development and evaluation of a blood culture PCR assay for rapid detection of *Salmonella* paratyphi A in clinical samples Daniela Flavia Hozbor (ed.). *PLoS ONE*. 11 (3), e0150576.

Zhou, R., Yazdi, A.S., Menu, P. & Tschopp, J. (2011) A role for mitochondria in NLRP3 inflammasome activation. *Nature*. 469 (7329), 221–226.

Zhou, Z., McCann, A., Weill, F.-X., Blin, C., et al. (2014) Transient Darwinian selection in *Salmonella* enterica serovar Paratyphi A during 450 years of global spread of enteric fever. *Proceedings of the National Academy of Sciences*. 111 (33), 12199–12204.

Appendix

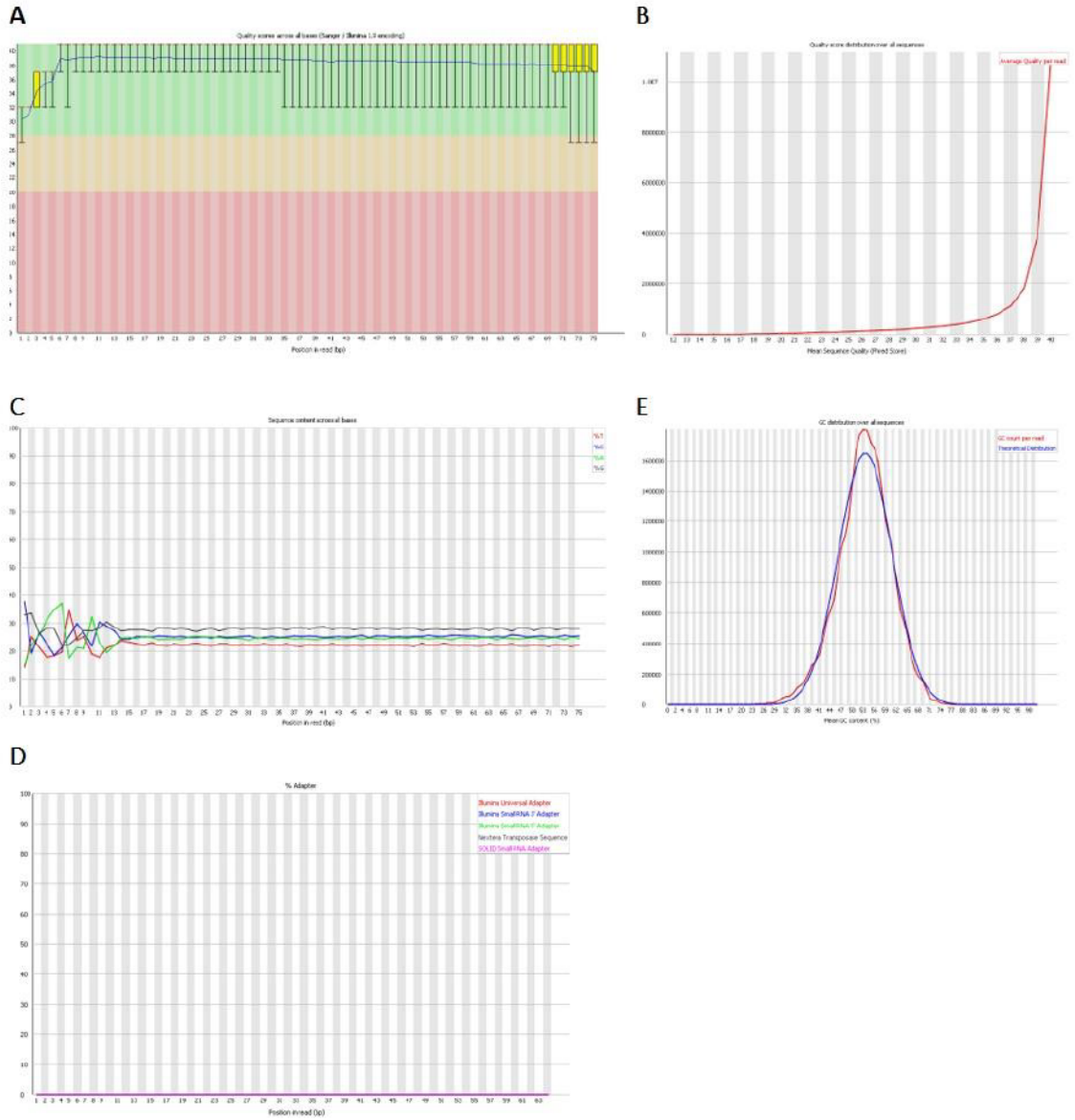


Figure Appendix.1 **Representative sample of quality checks for RNA-Seq reads.**

(A) Quality scores across all bases (Phred score in all read positions). (B) Quality score (Phred score) distribution over all sequences. (C) Sequence content across all bases in each read. (D) Adapter content in reads. (E) GC distribution over all sequences in the sample.

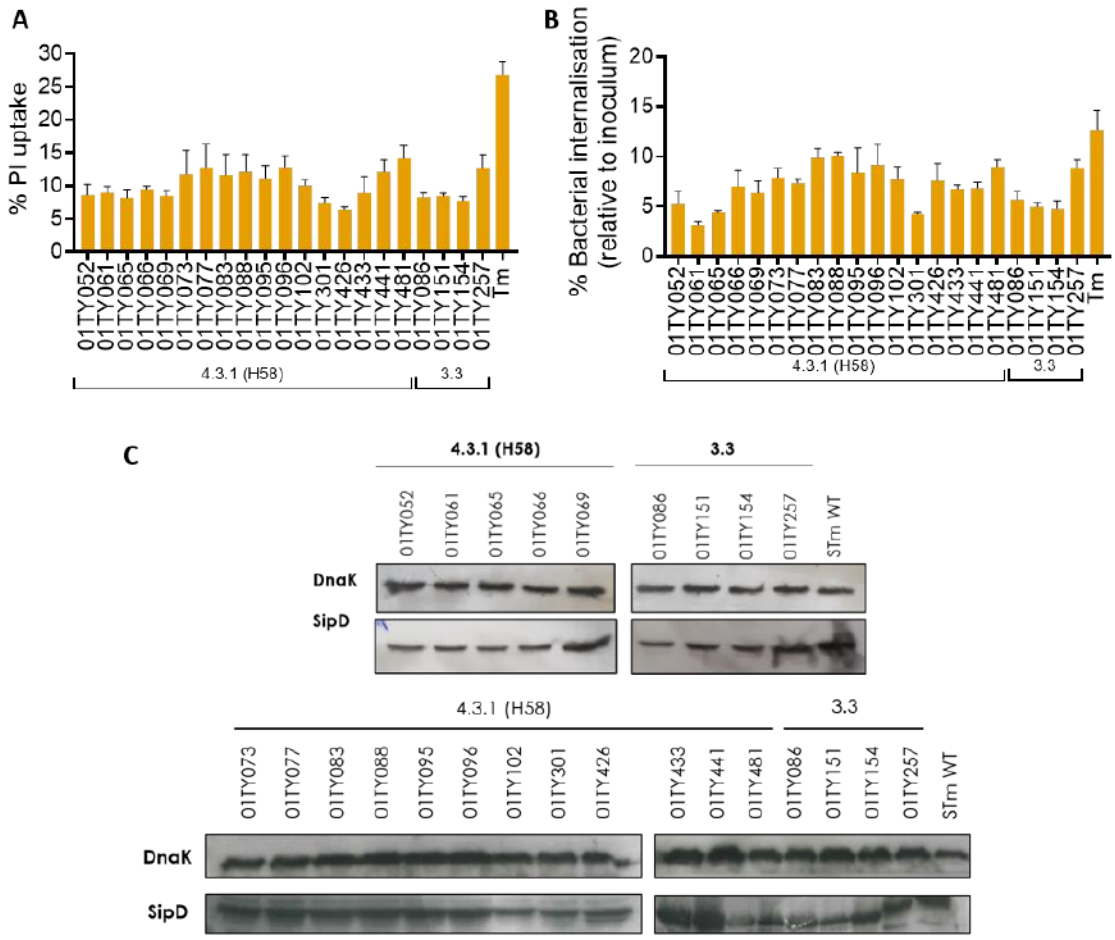


Figure Appendix.2 ***S.* Typhi H58-triggered pyroptosis in THP-1 cells.**

THP-1 cells were infected (MOI 15) with *S.* Typhi clinical isolates as indicated, while *S.* Typhimurium (Tm) was used as a control. **(A)** Cell death was determined at 3 h post infection by PI uptake and **(B)** bacterial internalisation at 1.5 h post infection by gentamicin protection assays. **(C)** *S.* Typhi was grown to late exponential phase and SPI-1 expression was determined by western blotting towards SipD. The samples and blots were produced by Trang Hguyen Hoang Thu (S. Baker group, OUCRU, Vietnam).

Table Appendix.1 **Bile-mediated change in expression of genes in *S.* Typhi Ty2, *S.* Paratyphi A 9150 or ED199.**

Name	Synonym	Product	Ty2		9150		ED199	
			qValue	log_2FC	qValue	log_2FC	qValue	log_2FC
thrL	SPA0001	thr operon leader peptide	0.2649	-0.4887	1	-0.0577	1	-0.2134
thrA	SPA0002	aspartokinase I/homoserine dehydrogenase I	1	-0.0566	1	-0.1444	1	0.5639
thrB	SPA0003	homoserine kinase	1	-0.0255	0.9063	-0.0833	1	0.47249
thrC	SPA0004	threonine synthase	1	0.06609	0.7381	-0.1436	1	0.20163
yaaA	SPA0005	hypothetical protein	1	-0.1831	1	0.34192	1	0.4021
talB	SPA0007	transaldolase B	1	-0.1116	1	-0.054	1	0.4085
mog	SPA0008	molybdopterin biosynthesis Mog protein	0.3674	-0.361	1	0.35509	1	0.01197
yaaH	SPA0009	hypothetical protein	1	-3	1	-2.3219	1	-2.3219
htgA	SPA0010	hypothetical protein	1	0	1	#DIV/0!	1	0
yaaI	SPA0011	hypothetical protein	1	-0.415	1	1	1	0
dnaK	SPA0012	DnaK protein (heat shock protein 70)	0.3449	-1.0307	1	0.07573	1	-0.0356
dnaJ	SPA0013	DnaJ protein	4E-05	-1.0238	1	-0.0931	1	0.18442
-	SPA0014	regulatory protein	1	-0.415	1	-1	1	-1
-	SPA0015	hypothetical protein	1	#DIV/0!	1	#DIV/0!	1	#DIV/0!
-	SPA0016	hypothetical protein	1	0	1	#DIV/0!	1	#DIV/0!
-	SPA0017	hypothetical protein	1	#NUM!	1	#DIV/0!	1	#DIV/0!
-	SPA0019	hydroxymethyltransferase	1	0	1	0	1	0
-	SPA0020	hypothetical protein	1	0	1	0	1	-1
bcfA	SPA0021	fimbrial subunit	1	-1.2224	1	-2.585	1	-1.3219
bcfB	SPA0022	fimbrial chaperone	1	#NUM!	1	#DIV/0!	1	#NUM!
bcfC	SPA0023	fimbrial usher	1	0	1	-1	1	-1
bcfD	SPA0024	fimbrial subunit	1	0	1	0	1	-0.585
bcfE	SPA0025	fimbrial subunit	1	1	1	0	1	0
bcfG	SPA0027	fimbrial chaperone	1	0	1	0	1	0
bcfH	SPA0028	hypothetical protein	1	-0.2224	1	-0.737	1	-0.3219
-	SPA0029	hypothetical protein	1	-0.3219	1	-1.585	1	-0.585
-	SPA0030	hypothetical protein	1	#DIV/0!	1	#DIV/0!	1	#DIV/0!
-	SPA0031	LysR family transcriptional regulator	1	#DIV/0!	1	#DIV/0!	1	#DIV/0!
-	SPA0032	transcriptional regulator	1	-1	1	-0.415	1	-0.415
-	SPA0033	sulfatase	1	#DIV/0!	1	#DIV/0!	1	#NUM!
-	SPA0034	5'-nucleotidase	1	-0.737	1	-0.737	1	-0.737
-	SPA0035	hypothetical protein	1	#DIV/0!	1	#DIV/0!	1	#DIV/0!
-	SPA0037	sulfatase regulatory protein	1	-1	1	0.41504	1	-0.737
-	SPA0038	hypothetical protein	1	0	1	0	1	0
-	SPA0039	sulfatase	1	-0.1926	1	-1.3219	1	-0.585
nhaA	SPA0040	Na(+)/H(+) antiporter 1	2E-05	-1.0506	1	-0.9359	1	-0.9143
nhaR	SPA0041	transcriptional activator protein NhaR	2E-05	-1	1	-0.6919	1	-0.387
-	SPA0042	glycosyl hydrolase	1	-0.3626	1	-0.6781	1	-0.6781
-	SPA0043	transporter	1	-1	1	#NUM!	1	#NUM!
rpsT	SPA0044	30S ribosomal protein S20	0.0018	-0.8002	0.5943	-0.284	0.334	-0.5579
yaaY	SPA0045	hypothetical protein	1	-0.3479	1	0	1	0.1375
ribF	SPA0046	riboflavin biosynthesis protein RibF	1	-0.1255	1	0.03747	1	0.22239
ileS	SPA0047	isoleucyl-tRNA synthetase	1	-0.1968	0.7836	-0.6219	1	0.02934
lspA	SPA0048	lipoprotein signal peptidase	0.4056	-0.3879	0.6808	-0.1965	1	-0.0429

fkpB	SPA0049	FkbB-type16 kDpeptidyl -prolyl cis-transi somerase	0.6124	-0.292	1	0.10599	0.8972	-0.3455
lytB	SPA0050	LytBpro tein	0.7453	-0.2201	1	0	1	-0.2944
-	SPA0051	hypotheticalprotein	1	-0.0802	1	-0.0589	1	0.22239
yaaF	SPA0052	nucleosidehydrolase	1	-0.1486	0.843	-0.1355	1	-0.1236
citB	SPA0053	transcriptionalregulatoryproteincitb	1	-0.1699	1	0.19265	1	-0.5475
-	SPA0054	transcriptionalregulator	1	0	1	0	1	-0.737
oadB	SPA0055	oxaloacetatedecarboxylasesubunitbeta	1	#NUM!	1	-1.585	1	0
oadA	SPA0056	oxaloacetatedecarboxylasesubunitalpha	1	0	1	-1	1	-1
oadG	SPA0057	oxaloacetatedecarboxylasesubunitgamma	1	#NUM!	1	0	1	#DIV/0!
-	SPA0058	citrate-sodium symporter	1	#NUM!	1	-1	1	#DIV/0!
citC	SPA0059	[citrate(pro -3S)-lyase]ligase	1	-1	1	0	1	#DIV/0!
citD	SPA0060	citrate lyaseacylcarrierprotein	1	-0.415	1	-0.415	1	#DIV/0!
citE	SPA0061	citrate lyasesubunitbeta	1	-0.3219	1	0	1	0
citF	SPA0062	citrate lyasesubunitalpha	1	-0.3219	1	0	1	0
-	SPA0063	hypotheticalprotein	1	0	1	-0.585	1	0
citG	SPA0064	CitGprotei n	1	0	1	0	1	0
dapB	SPA0065	dihydrodipicolinatereductase	1	-0.0911	1	-0.7244	1	-0.4005
carA	SPA0067	carbamoyl-phosphatesynthasesmallsubunit	0.9761	-0.1325	1	-1.8365	1	-1.5236
carB	SPA0068	carbamoyl-phosphatesynthase largesu bunit	0.0144	-0.8548	3E-10	-1.9359	1	-0.9125
caiF	SPA0069	transcriptionalactivatorCaiF	1	0.06105	0.0265	1.3151	0.2196	0.97566
caiE	SPA0070	carnitineoperonproteinCaiE	1	-0.8074	1	0	1	-0.263
caiD	SPA0071	carnitineracemase	1	-0.3626	1	0.078	1	-0.5525
caiC	SPA0072	crotonobetaine/carnitine-CoAl igase	1	0.26303	1	0.67807	1	0.48543
caiB	SPA0073	L-carnitinedehydratase	1	0.12553	1	0.73697	1	0.73697
caiA	SPA0074	carnitineoperonoxidoreductaseCaiA	1	0.12553	1	1	1	0.89308
caiT	SPA0075	carnitinetransporter	1	0	1	0	1	0
fixA	SPA0076	FixApro tein	1	-1.585	1	#DIV/0!	1	0
fixB	SPA0077	FixBpro tein	1	-0.585	1	0	1	1
fixC	SPA0078	FixCpro tein	1	-0.585	1	0	1	0
fixX	SPA0079	ferredoxinlikeproteinFixX	1	-0.585	1	-1	1	1
yaaU	SPA0080	metabolitetransportprotein	1	-0.415	1	0.58496	1	-0.585
-	SPA0081	lipoprotein	1	-0.737	1	-1	1	0.05063
-	SPA0082	secretedprotein	1	-0.415	1	-0.3219	1	-0.2224
-	SPA0083	secretedprotein	0.0005	1.08092	0.178	-0.5338	1	0.20401
-	SPA0084	hypotheticalprotein	1	#DIV/0!	1	#DIV/0!	1	#DIV/0!
-	SPA0085	sulfatase	1	-1	1	-0.585	1	-1
kefC	SPA0087	glutathione-regulatedpotassium -effluxsystemproteinKefC	1	-0.585	1	-1	1	0
folA	SPA0088	dihydrofolatereductasetypeI	1	-0.5525	1	-1.2224	1	-1.4854
apaH	SPA0089	bis(5'-nucleosyl)-tetraphosphatase	1	-0.1255	1	0.13993	1	-0.0573
apaG	SPA0090	CorDp rotein	0.9253	-0.1375	1	0.12338	1	0.16724
ksgA	SPA0091	dimethyladenosinetransferase	1	0.0199	1	0.06012	1	0.16724
pdxA	SPA0092	pyridoxal phosphate biosyntheticproteinPdxA	0.974	-0.2274	1	0.01759	1	0.13358
surA	SPA0093	survivalproteinSurA	1	-0.2091	0.9672	-0.3943	1	-0.1969
imp	SPA0094	organicsolventtoleranceprotein	1	-0.0995	0.9265	-0.3653	1	-0.054
djlA	SPA0095	DnaJ-like protein	0.7049	-0.1699	1	-0.0687	1	0
rluA	SPA0096	ribosomallargesubunitpseudouridinesynthaseA	1	-0.585	0.0011	-1.0506	1	-0.737
hepA	SPA0097	ATP-dependent helicaseHepA	1	-0.1155	0.0005	-1.3093	1	-0.7045
polB	SPA0098	DNApo lymeraseII	1	0.34792	1	0.41504	1	0.40054

-	SPA0099	ISele menttransposase	1	0	1	#DIV/0!	1	0
-	SPA0100	ISele menttransposase	1	-0.0791	1	-0.2224	1	-0.1635
-	SPA0101	hypotheticalprotein	1	-1	1	0	1	-0.585
-	SPA0102	hypotheticalprotein	1	#DIV/0!	1	#DIV/0!	1	#DIV/0!
araD	SPA0103	L-ribulose-5-phosphate 4-epimerase	1	1	1	0.58496	1	0
araA	SPA0104	L-arabinoseisomerase	1	0	1	0.48543	1	0
araB	SPA0105	L-ribulokinase	1	0	1	0.41504	1	-0.415
araC	SPA0106	arabinoseoperonregulatoryprotein	0.3683	-0.2895	1	0.29373	1	-0.3219
yabI	SPA0107	DedAf amilyintegralmembraneprotein	1	-0.2756	1	0.32193	1	-0.6167
yabJ	SPA0108	ABCtra nsporter	1	-0.5406	1	-0.3626	1	0
yabK	SPA0109	ABCtra nsporterintegralmembraneprotein	1	-0.2224	1	-0.585	1	0
tbpA	SPA0110	thiamine-bindingpe riplasmicprotein	1	0	1	-0.4475	1	-0.5146
yabN	SPA0111	ABCtra nsportersubstrate -bindingpro tein	1	0	1	-0.263	1	0.1375
leuD	SPA0112	3-isopropylmalatedehydratase	1	0.19931	1	-0.0444	1	0.19265
leuC	SPA0113	3-isopropylmalatedehydratase	1	0.39855	1	0.04064	1	0.32193
leuB	SPA0114	3-isopropylmalatedehydrogenase	1	0.33121	1	0.05247	1	0.71621
leuA	SPA0115	2-isopropylmalatesynthase	1	0.35364	1	0.11548	1	0.58496
leuL	SPA0116	leuope ronleaderpeptide	1	0	1	1	1	#DIV/0!
leuO	SPA0117	activator proteininleuABCDoperon	1	0	1	-1	1	0
ilvI	SPA0118	acetolactatesynthaseisozymeIIIlargesubunit	1	0.36257	1	-0.759	1	-0.152
ilvH	SPA0119	acetolactatesynthaseisozymeIIIsmallsubunit	1	0.22239	1	-0.9511	1	-0.3626
fruR	SPA0120	fructoserepressor	0.5431	-0.3504	1	0.56089	0.7698	0.67626
yabB	SPA0121	hypotheticalprotein	0.982	-0.1993	1	0.38918	1	0.33015
yabC	SPA0122	hypotheticalprotein	1	-0.0159	1	-0.1159	1	0.09516
ftsL	SPA0123	cell division proteinFts L	0.9856	-0.0868	0.5001	-0.3429	1	-0.0765
ftsI	SPA0124	penicillin-bindingpro tein3	0.293	-0.415	0.472	-0.3219	0.8249	-0.2701
murE	SPA0125	UDP-N-acetylmuramoylalanyl-D-glutamate--2,6-diamino pimligase	1	-0.0181	1	0.00734	0.9337	-0.3799
murF	SPA0126	UDP-N-acetylmuramoylalanyl-D-glutamyl-2,6-diamino pimelate--D-alanalan ylligase	1	-0.1319	1	-0.0605	1	-0.2665
mraY	SPA0127	phospho-N-acetylmuramoyl-pentapeptide- transferase	1	-0.1178	1	0.00692	1	-0.0736
murD	SPA0128	UDP-N-acetylmuramoyl-L-alanine:D-glutamateligase	1	-0.0339	1	-0.0654	1	-0.2288
ftsW	SPA0129	cell divisionproteinFtsW	1	-0.0199	0.7056	-0.1982	1	-0.1973
murG	SPA0130	UDP-N-acetylglucosamine:N-acetylmuramyl- (pentapeptide) pyrophosphoryl-undecaprenolN -acetylglucosamine transferase	1	0.02857	1	0.01815	1	-0.0765
murC	SPA0131	UDP-N-acetylmuramate:alanineligase	1	0.06711	1	0.20992	1	0.03602
ddlB	SPA0132	D-alanine--D-alanine ligase	1	-0.0172	1	0.08453	1	-0.096
ftsQ	SPA0133	cell divisionproteinFtsQ	1	-0.0931	1	0.05772	1	0
ftsA	SPA0134	cell divisionproteinFtsA	1	-0.0071	1	0.04422	1	-0.0787
ftsZ	SPA0135	cell divisionproteinFtsZ	1	-0.0147	1	0.01718	1	-0.2929
lpxC	SPA0136	UDP-3-O-[3-hydroxymyristoyl]N -acetylglucosaminedeacetylase	1	0.24734	1	0.25699	1	-0.0375
yacA	SPA0137	hypotheticalprotein	1	0.19855	1	-0.0671	1	0.07358
secA	SPA0138	preprotein translocaseSecAsubunit	1	0.02452	1	-0.231	1	-0.1612
mutT	SPA0139	7,8-dihydro-8-oxoguanine-triphosphatase	1	-0.3219	1	0.32193	1	0
-	SPA0140	aldo/ketoreductase	1	-0.5146	1	0.37851	1	0.37851
-	SPA0141	LysR-familytranscriptionalregulator	1	0.1375	1	0.17333	1	0.21022
yacG	SPA0142	hypotheticalprotein	1	-0.2572	0.8645	-0.1681	0.2885	-0.3607
yacF	SPA0143	hypotheticalprotein	1	-0.0291	0.8559	-0.2099	1	-0.1459
yacE	SPA0144	hypotheticalprotein	1	-0.5361	1	-0.0566	0.9351	-0.237
guaC	SPA0145	GMPre ductase	0.0544	-0.7388	0.2351	-0.7586	1	0.11382

hofC	SPA0146	proteintra nsportproteinHofC	1	#DIV/0!	1	#DIV/0!	1	#DIV/0!
hofB	SPA0147	proteintra nsportproteinHofB	1	#NUM!	1	0	1	0
ppdD	SPA0148	prepilin peptidasedependentproteinDprecursor	1	#DIV/0!	1	#DIV/0!	1	#DIV/0!
nadC	SPA0149	nicotinate-nucleotidepyrophosphorylase	0.3378	-0.3149	1	-0.1806	1	-0.0577
ampD	SPA0150	AmpDprotei n(anhydro -N-acetylmuramyl-tripeptide amidase)	1	0.20923	1	0.56884	1	0.4341
ampE	SPA0151	AmpEprotei n	1	-0.0597	1	0.47644	1	0.4039
-	SPA0152	glycosylhydrolase	1	0	1	-0.1155	1	-0.0995
-	SPA0153	symporter	1	0	1	0.26303	1	0.19265
aroP	SPA0154	aromaticaminoacidtransportproteinAroP	1	-0.387	1	-0.3219	1	-0.2016
pdhR	SPA0155	pyruvate dehydrogenasecomplexrepressor	0.0012	1.16146	0.2178	0.97085	0.1359	0.81714
aceE	SPA0156	pyruvate dehydrogenaseE1component	1	0.85664	1	1.12907	0.6121	1.09707
aceF	SPA0157	dihydrolipoamideacetyltransferasecomponent(E2)ofpyruvatedehydrogenase	0.994	0.77244	0.7381	1.12793	0.3685	1.26206
lpdA	SPA0158	dihydrolipoamidedehydrogenase	1	-0.0234	1	-0.292	0.9598	0.82204
-	SPA0159	secretedprotein	1	0.41504	1	1.58496	1	3
-	SPA0160	secretedprotein	1	1	1	-0.2996	1	0.58496
yacH	SPA0161	hypotheticalprotein	1	1.36257	1	0.05658	1	0.54057
acnB	SPA0162	aconitatehy dratase2	1	-0.0865	1	-0.5604	1	0.27627
yacL	SPA0163	hypotheticalprotein	1	0.09818	0.7381	0.73994	1	0.12168
kdgT	SPA0164	2-keto-3-deoxygluconatepermease	1	0	1	0.73697	1	0.32193
ygbK	SPA0165	hypotheticalprotein	1	0	1	0.36257	1	0.32193
-	SPA0166	PdxA-like protein	1	0	1	0.45251	1	0.37851
-	SPA0167	transcriptionalregulator	1	0	1	0.58496	1	0.39366
speD	SPA0168	S-adenosylmethioninedecarboxylase	1	0.18442	1	-0.0297	1	0.2115
speE	SPA0169	spermidinesynthase	1	-0.1856	1	-0.111	1	-0.0238
yacC	SPA0170	hypotheticalprotein	0.0008	-0.763	1	0.35755	1	0.26919
yacK	SPA0171	multicopperoxidase	6E-05	1.63543	0.1634	1.45868	0.0006	1.93794
gcd	SPA0172	glucosedehydrogenase	1	0	1	-0.922	1	0.41504
hpt	SPA0173	hypoxanthinephosphoribosyltransferase	0.3958	-0.3591	1	-0.5185	1	-0.3219
yadF	SPA0174	carbonicanhydrase	1	0.01168	0.0144	-1.1212	0.7963	-0.3198
yadG	SPA0175	ABCtra nsporterATP -bindingp rotein	1	0.09311	1	0.45943	1	0.54749
yadH	SPA0176	ABC transporter	1	-0.1203	1	0	1	0.44057
yadI	SPA0177	PTSsys temtransportersubunitIIA	0.4636	-0.278	0.0165	1.31487	0.6447	0.64981
yadE	SPA0178	hypotheticalprotein	1	0.02346	1	0.38529	1	0.18521
stkG	SPA0179	fimbrialprotein	1	#DIV/0!	1	0.16993	1	0.1375
stkF	SPA0180	fimbrialprotein	1	#DIV/0!	1	0.45943	1	-0.1699
stkE	SPA0181	fimbrialprotein	1	#DIV/0!	1	-0.152	1	-0.1926
stkD	SPA0182	fimbrialprotein	1	#DIV/0!	1	0	1	-0.585
stkC	SPA0183	outerme mbraneusherprotein	1	#DIV/0!	1	#DIV/0!	1	#DIV/0!
stkB	SPA0184	fimbriae;chaparone	1	#DIV/0!	1	#DIV/0!	1	#DIV/0!
stkA	SPA0185	majorf imbrialsubunit	1	#DIV/0!	1	#DIV/0!	1	#DIV/0!
panD	SPA0186	aspartate 1-decarboxylase	0.2807	-0.3883	4E-06	-1.2587	0.2112	-0.538
panC	SPA0187	pantoate:beta-alanine ligase	1	0.23947	0.0467	-0.6699	1	-0.0286
panB	SPA0188	3-methyl-2-oxobutanoatehydroxymethyltransferase	1	0.37084	0.3111	-0.3886	0.4207	-0.4709
folK	SPA0189	2-amino-4-hydroxy-6-hydroxymethyldihydropteridinepyrophosphokinase	1	-0.4557	0.0134	-0.8194	1	-0.6724
pcnB	SPA0190	poly(A) polymerase	1	-0.1013	0.0397	-0.8301	0.3022	-0.5198
yadB	SPA0191	glutamyl-tRNAs ynthetase	1	0	1	-0.4406	1	-0.5377
dksA	SPA0192	dosage-dependent dnaKsuppressorprotein	0.3265	-0.4946	1	-0.0859	1	-0.1044
sfsA	SPA0193	sugarf ermentationstimulationprotein	1	-0.0875	1	-0.1402	1	0.02203

ligT	SPA0194	2'-5'RNAl igase	1	-0.2937	1	0.06711	1	0.09954
hrpB	SPA0195	ATP-dependent helicaseHrpB	1	-0.2955	1	-0.6845	1	-0.415
mrcB	SPA0196	penicillin-bindingpro tein1b;peptidoglycansynthetase	1	-0.5052	0.094	-0.6951	1	-0.4854
fhuC	SPA0198	ferrichrometransportATP -binding proteinFhuC	1	0.58496	1	-0.6521	1	-0.3219
fhuD	SPA0199	ferrichrome-bindingpe riplasmicproteinprecursor	1	0	1	-0.737	1	-0.3626
fhuB	SPA0200	ferrichrometransportproteinFhuBprecursor	1	0	1	-1.585	1	-0.415
stfA	SPA0201	fimbrialsubunit	1	#DIV/0!	1	-1.585	1	0
stfD	SPA0203	periplasmicfimbrialchaperone	1	#DIV/0!	1	0	1	0
stfE	SPA0204	minorf imbrialsubunit	1	#DIV/0!	1	#DIV/0!	1	#DIV/0!
stfG	SPA0206	minorf imbrialsubunit	1	#DIV/0!	1	0	1	0.41504
-	SPA0207	hypotheticalprotein	1	#DIV/0!	1	0	1	-0.1926
hemL	SPA0208	glutamate-1-semialdehyde2,1 -aminomutase	1	-0.1825	0.6758	-0.1967	1	0.06634
yadQ	SPA0209	hypotheticalprotein	1	0	1	0.26303	1	0.1375
yadR	SPA0210	hypotheticalprotein	1	-0.152	1	-0.0941	1	-0.2654
yadS	SPA0211	hypotheticalprotein	1	-0.7162	1	-0.9511	1	-1
btuF	SPA0212	cobalaminperiplasmicbindingprotein	0.1872	-0.4525	1	-0.3344	1	-0.1203
mtn	SPA0213	MTA/SAHnucleosidase	0.4314	-0.4025	1	0	1	-0.1322
dgt	SPA0214	deoxyguanosinetriphosphatetriphosphohydrolase	1	0.17688	1	0.06413	1	0.55639
htrA	SPA0215	protease DOprecursor;heatshockproteinHtrA	1	-0.0079	1	-0.4322	1	-0.1091
yaeG	SPA0216	hypotheticalprotein	3E-09	1.65951	0.215	1.12618	1	0.39593
yaeH	SPA0217	hypotheticalprotein	0.0574	-0.8023	1	-0.0052	0.8469	-0.3948
-	SPA0218	innerme mbraneprotein	1	-0.4854	1	-0.3626	1	0
dapD	SPA0219	2,3,4,5-tetrahydropyridine-2-carboxylateN -succinyltransferase	0.6784	-0.277	1	-0.1453	1	0.19704
glnD	SPA0220	[protein-PII]uri dylyltransferase	1	0.18057	1	0.07306	1	0.35267
map	SPA0221	methionineaminopeptidase	1	0.11806	1	0.21632	1	0.18057
-	SPA0222	-	0.2817	-0.5552	0.2431	-0.5758	1	0.00165
rpsB	SPA0223	30Sribos omalproteinS2	1	-0.5713	1	-0.5603	1	-0.0156
tsf	SPA0224	elongationfactorTs	0.9659	-0.5204	1	-0.4499	1	0.20005
pyrH	SPA0225	uridine5' -monophosphatekinase	1	-0.1866	0.0847	-0.8036	0.5124	-0.4075
frr	SPA0226	ribosomerecyclingfactor	0.4284	-0.3976	0.7239	-0.3821	1	-0.1486
dxr	SPA0227	1-deoxy-D-xylulose5 -phosphate reductoisomerase	0.9721	-0.1699	0.2952	-0.4454	1	-0.111
uppS	SPA0228	undecaprenylpyrophosphatesynthetase	0.5332	-0.2701	0.0508	-0.6347	1	-0.2801
cdsA	SPA0229	phosphatidatecytidylyltransferase	0.2447	-0.341	0.0139	-0.737	1	-0.3668
yaeL	SPA0230	hypotheticalprotein	0.5856	-0.3551	0.5301	-0.3091	1	-0.0931
yaeT	SPA0231	outerme mbraneprotein	0.916	-0.3187	1	-0.343	1	-0.1639
ompH	SPA0232	outerme mbraneproteinOmpH	1	-0.2602	1	0.15654	1	0.06456
lpxD	SPA0233	UDP-3-O-[3-hydroxymyristoyl]glucosamine N-acyltransferase	1	-0.0992	1	0.24251	1	-0.0164
fabZ	SPA0234	(3R)-hydroxymyristoyl-ACPde hydratase	0.5865	-0.3639	0.635	-0.241	0.8387	-0.2832
lpxA	SPA0235	acyl-[acyl-carrier-protein]:UDP-N- acetylglucosamineO -acyltransferase	0.8659	-0.2751	0.724	-0.3088	0.8249	-0.3688
lpxB	SPA0236	lipid-A-disaccharidesynthase	0.3698	-0.4335	1	-0.1699	1	-0.2433
rnhB	SPA0237	ribonucleaseHII	0.3854	-0.3254	0.3293	-0.3312	1	-0.0813
dnaE	SPA0238	DNApo lymeraseIII,subunitalpha	0.4344	-0.4493	0.4731	-0.5059	1	-0.1255
accA	SPA0239	acetyl-coenzymeAcarboxylasecarboxyltransferasesubunitalpha	0.1488	-0.5783	0.7297	-0.3878	1	-0.1354
-	SPA0240	chitinase	1	-0.2224	1	-0.759	1	-0.241
ldcC	SPA0241	lysinedecarboxylase	1	0.02915	1	-0.1043	1	0.07595
yaeR	SPA0242	hypotheticalprotein	1	-0.117	1	-0.0451	1	0.09622
mesJ	SPA0243	cell cycleproteinMesJ	1	0.22239	1	-0.0431	1	0.1375
rof	SPA0244	ROFprote in	0.0595	-0.5684	0.6616	-0.262	1	-0.2925

yaeP	SPA0245	hypotheticalprotein	0.0786	-0.5461	0.7877	-0.2383	1	-0.2716
yaeQ	SPA0246	hypotheticalprotein	1	-0.3219	1	0.11103	1	-0.1926
yaeJ	SPA0247	releasefactor	1	0.026	1	0.19704	1	0.52083
cutF	SPA0248	copperho meostasisproteinCutFprecursor	1	0.36257	1	0.152	0.6456	0.69357
proS	SPA0249	prolyl-tRNAs ynthetase	0.8212	-0.2288	0.3106	-0.8978	0.3023	-0.5893
yaeB	SPA0250	hypotheticalprotein	1	-0.1605	1	-0.6015	1	-0.3049
rcsF	SPA0251	RcsFprot ein	0.0597	-0.5305	0.0246	-0.7141	0.0653	-0.6563
yaeC	SPA0252	lipoprotein	0.7744	-0.2426	1	-0.1142	0.6028	0.69491
yaeE	SPA0253	ABCtra nsporterpermease	1	0	1	0.81943	1	2.05889
abc	SPA0254	ABCtra nsporterATP -bindingp rotein	1	-0.0693	1	1.51937	8E-35	2.48938
yaeD	SPA0255	hypotheticalprotein	1	0.074	1	0.848	1	0.8625
rrsH	SPA0256	16Sribos omalRNA	1	0.00877	0.9033	0.59976	0.2027	-0.792
ileV	SPA0257	IletRN A	5E-06	-0.8962	1	0.07039	0.1162	-0.4745
alaV	SPA0258	AlatRN A	5E-07	-1.0228	1	-0.0377	0.3022	-0.463
rrlH	SPA0259	23Sribos omalRNA	1	0.03971	1	0.6059	0.9993	-0.5664
rrfH	SPA0261	5Sribosom alRNA	1	#DIV/0!	1	#DIV/0!	1	-1.585
-	SPA0262	hypotheticalprotein	1	#DIV/0!	1	-1.585	1	-1
kgtP	SPA0263	alpha-ketoglutaratepermease	1	0.41504	1	-0.0458	1	0.07039
yfiM	SPA0264	hypotheticalprotein	1	-0.0348	1	0.04731	1	-0.2824
pssA	SPA0265	CDP-diacylglycerol--serine O-phosphatidyltransferase	1	0.03562	1	-0.009	1	0.06751
yfiQ	SPA0266	acyl-CoAs ynthetase	1	-0.1315	1	0.2786	1	0.12374
yfiP	SPA0267	hypotheticalprotein	0.1466	-0.415	0.2351	-0.4594	0.0992	-0.585
yfiG	SPA0268	thioredoxin2	1	0.22827	0.2481	-0.3861	0.4209	-0.3883
yfiF	SPA0270	RNAm ethyltransferase	0.709	-0.2479	0.6712	-0.2439	1	-0.263
ung	SPA0271	uracil-DNAg lycosylase	1	0.18997	1	0.2115	1	0.33092
yfiD	SPA0272	hypotheticalprotein	1	0.63942	0.2829	1.52017	0.6545	0.9681
yfiK	SPA0273	hypotheticalprotein	1	-1	0.0026	-0.9773	1	-1.433
yfiE	SPA0274	LysR familytranscriptionalregulator	1	-0.0973	1	0.54543	0.0762	0.89308
srmB	SPA0275	ATP-dependent RNAhelicaseSrmB	1	0.03899	1	0.32931	0.5251	-0.4263
yfiC	SPA0276	hypotheticalprotein	1	-0.1019	1	-0.5639	1	-0.1468
nadB	SPA0277	L-aspartate oxidase(quinolinatesynthetaseB)	1	-0.415	1	0	1	0
rpoE	SPA0278	RNApo lymerasesigma -Efactor (sigma-24)	1	0.23329	0.322	1.12843	1	0.48153
rseA	SPA0279	sigma-Efac tornegativeregulatoryprotein	1	0.25092	0.4494	1.10897	1	0.30812
rseB	SPA0280	sigma-Efac torregulatoryproteinRseBprecursor	1	0.21324	1	0.42084	1	0.02647
rseC	SPA0281	sigma-Efac torregulatoryproteinRseC	1	0.20811	1	0.42663	1	-0.0336
lepA	SPA0282	GTP-bindingpro teinLepA	1	-0.1806	0.1266	-0.6666	0.5911	-0.4245
lepB	SPA0283	signalpeptidaseI	0.0038	-0.7678	0.0011	-1.0916	0.5477	-0.4796
rnc	SPA0284	ribonucleaseIII	1	0.11433	0.0914	-0.6271	0.9792	-0.3561
era	SPA0285	GTP-bindingpro tein	1	0.02076	0.0977	-0.8307	0.6284	-0.3515
recO	SPA0286	DNAre pairproteinRecO	0.6503	-0.2268	0.0256	-0.767	1	-0.1926
pdxJ	SPA0287	pyridoxalphosphatebiosyntheticprotein	1	0	1	0.32833	0.8236	0.59282
acpS	SPA0288	holo-(acyl-carrier-protein)s ynthase	1	-0.1293	1	0.40336	1	0.53605
yfhL	SPA0289	ferredoxin	1	-0.4854	1	-0.848	1	-2
-	SPA0290	transcriptionalregulator	1	-1	1	-0.585	1	-2.3219
-	SPA0291	transmembranetransportprotein	1	#DIV/0!	1	#DIV/0!	1	#DIV/0!
-	SPA0292	oxidoreductase	1	-0.6781	1	-1.2801	1	-0.737
yfhH	SPA0293	transcriptionalregulator	1	0.24101	1	0.80735	1	0.65711
-	SPA0294	phophosugarbindingprotein	1	-0.1444	1	-0.1844	1	0.34792

-	SPA0295	PTSsys temtransportersubunitIIBC	1	-0.2345	1	0	1	0.32193
yfhC	SPA0297	hypotheticalprotein	1	0	0.724	-0.2065	1	-0.1089
yfhD	SPA0298	hypotheticalprotein	1	0	1	-0.4854	1	-0.5146
-	SPA0299	hypotheticalprotein	1	0	1	#DIV/0!	1	0
purL	SPA0300	phosphoribosylformylglycineamidesynthetase	1	-0.3626	5E-23	-2.6107	3E-08	-1.6781
-	SPA0301	-	0.0544	-0.4713	1	-0.0759	0.0001	-1.166
yfhK	SPA0302	sensor kinaseprotein	1	-0.3103	1	0.50901	1	0.2115
yfhG	SPA0303	hypotheticalprotein	1	0	1	0.05344	1	0.29373
yfhA	SPA0304	transcriptionalregulator	1	0.03317	0.8559	-0.0982	1	0.30895
glnB	SPA0305	nitrogen regulatoryproteinp -II	0.1248	-0.5015	1	0.19137	1	-0.0937
yjdL	SPA0306	transmembranetransportprotein	1	2.58496	1	0	1	-2
cadA	SPA0307	lysine decarboxylase	4E-49	2.55722	1	-0.415	0	-4.1699
cadB	SPA0308	cadaverine/lysineantiporter	0.0319	1.30946	1	#DIV/0!	0	#NUM!
hmpA	SPA0310	flavohemoprotein	1	0.25678	1	-0.2801	1	0.27563
glyA	SPA0311	serine hydroxymethyltransferase	0.829	-0.4797	1	0.07196	1	-0.4063
hcaT	SPA0312	3-phenylpropionatepermease	1	-0.387	1	-0.926	1	-0.585
csiE	SPA0313	stationaryphaseinducibleproteinCsiE	1	0	1	0.36257	1	-0.1831
-	SPA0314	hypotheticalprotein	1	-0.3219	1	0	1	-0.0995
-	SPA0315	innerme mbrane protein	1	-0.2224	1	-0.1926	1	-0.2224
asrC	SPA0316	anaerobicsulfitereductasesubunitC	1	0.73697	1	1.80735	1	1.45066
asrB	SPA0317	anaerobicsulfitereductasesubunitB	1	0.70044	1	1.70044	1	1.39232
asrA	SPA0318	anaerobicsulfitereductase subunitA	1	1.05445	1	2	1	1.51937
-	SPA0319	hypotheticalprotein	1	-0.3219	1	0.32193	1	0
suhB	SPA0320	extragenicsuppressorproteinSuhB	1	0.17177	0.008	-0.8301	0.0093	-0.8797
-	SPA0321	RNAm ethyltransferase	1	0.19457	1	0.57455	1	-0.1926
yfhP	SPA0322	hypotheticalprotein	1	0.14861	0.0028	-1.5118	1	-0.1724
nifS	SPA0323	L-cysteinedesulfurase	1	-0.0155	0.0993	-1.5766	1	-0.3306
nifU	SPA0324	nifU-like protein	1	-0.1696	0.0038	-1.7288	0.1851	-0.7186
yfhF	SPA0325	hypotheticalprotein	0.7319	-0.2684	0.0002	-1.6084	0.0517	-0.7643
yfhE	SPA0326	chaperoneproteinHscB	1	-0.1262	0.0034	-1.1498	0.1843	-0.6435
hscA	SPA0327	chaperoneproteinHscA	1	-0.1303	0.0749	-1.4692	0.1718	-0.8468
fdx	SPA0328	ferredoxin	0.5276	-0.3606	5E-05	-1.5572	0.003	-1.0214
yfhJ	SPA0329	hypotheticalprotein	0.5339	-0.2976	0.0005	-1.2065	0.0556	-0.8666
yfhI	SPA0330	peptidaseB	1	0.08168	1	-0.2153	1	-0.3646
sseB	SPA0331	SseBpro tein	1	-0.086	0.5108	-0.2778	0.4378	-0.4425
-	SPA0332	-	1	-0.5594	1	-0.1255	1	-0.0825
-	SPA0333	hypotheticalprotein	1	0	1	0.22239	1	-0.0931
sseA	SPA0334	thiosulfatesulfurtransferase	0.8613	-0.2876	0.7442	0.69302	1	-0.0585
-	SPA0335	lipoprotein	0.4076	-0.5078	1	-0.0512	1	-0.0214
pbpC	SPA0336	penicillin-bindingpro tein1C	1	-0.2996	1	0.05658	1	-0.273
-	SPA0338	anaerobicreductasesubunit	1	0.16046	1	0.41504	1	0.22239
-	SPA0339	anaerobicreductasesubunit	1	0.41504	1	0	1	-0.415
-	SPA0340	polyferredoxin	1	0	1	0	1	0.58496
ndk	SPA0341	nucleosidediphosphatekinase	0.0007	-1.2441	1	-0.2443	1	-0.2361
yfgB	SPA0342	hypotheticalprotein	0.7284	-0.2801	0.0181	-0.949	0.0002	-1.2736
yfgA	SPA0343	DNA-bindingp rotein	1	0.06319	1	0.19907	1	0.16574
gcpE	SPA0344	GcpE protein(proteinE)	1	0.0902	1	-0.0139	1	0.29231
hisS	SPA0345	histidyl-tRNAs ynthetase	1	-0.0973	0.5819	-0.3889	1	-0.1539

yfgM	SPA0346	hypotheticalprotein	0.7613	-0.2609	0.4055	-0.4044	1	-0.1069
yfgL	SPA0347	lipoprotein	0.2685	-0.4955	0.2361	-0.5132	0.8236	-0.2553
engA	SPA0348	GTP-bindingpro tein	0.8581	-0.2065	0.0012	-1.1502	1	-0.585
yfgJ	SPA0349	hypotheticalprotein	1	-0.9434	1	-1.1806	1	-1.0473
sinI	SPA0351	hypotheticalprotein	1	0	1	0	1	-0.3923
ratA	SPA0352	hypotheticalprotein	1	0	1	-0.3626	1	-0.2224
xseA	SPA0355	exodeoxyribonucleaselargesubunit	1	0.36257	1	-0.1301	0.1663	-0.6641
guaB	SPA0356	inosine-5'-monophosphatedehydrogenase	1	0.22948	0.0007	-1.1538	4E-14	-2.0135
guaA	SPA0357	GMPs ynthase	0.1724	-0.5629	0.0038	-1.2252	0.0042	-1.0845
-	SPA0358	hypotheticalprotein	1	-1.585	1	-1	1	-1
-	SPA0359	hypotheticalprotein	2E-06	1.61374	0.0039	1.70645	0.7049	0.71422
-	SPA0360	hypotheticalprotein	1	-0.4854	1	-0.1926	1	0.28951
-	SPA0361	outerme mbranelipoprotein	1	-0.737	1	0.22239	1	0.152
-	SPA0362	hypotheticalprotein	1	-2	1	-1	1	-1
-	SPA0363	hypotheticalprotein	1	#NUM!	1	#DIV/0!	1	0
-	SPA0364	hypotheticalprotein	1	-0.8074	1	-1	1	-1
ppx	SPA0365	exopolyphosphatase	1	0.14684	0.3745	-0.3755	1	-0.0431
ppk	SPA0366	polyphosphatekinase	1	0.10825	1	-0.1839	1	0.24793
purN	SPA0367	phosphoribosylglycinamidinemyltransferase	0.3284	-0.3923	7E-13	-1.8007	5E-05	-1.0704
purM	SPA0368	phosphoribosylformylglycinamidinecyclo -ligase	0.9813	-0.152	3E-46	-2.4721	1E-13	-1.6897
upp	SPA0369	uracil phosphoribosyltransferase	0.0171	-0.6714	0.3443	-0.3902	0.0075	-0.9249
uraA	SPA0370	uracil permease(uraciltransporter)	1	-0.737	1	-1.5406	1	-1.2801
yfgE	SPA0371	hypotheticalprotein	1	0	0.4486	-0.3536	0.1151	-0.75
yfgD	SPA0372	arsenate reductase	1	-0.041	1	0.07782	1	-0.1694
-	SPA0373	hypotheticalprotein	1	0.16046	1	0.06711	1	0.24844
-	SPA0375	hypotheticalprotein	1	-0.585	0.0467	1.18982	1	1.12029
-	SPA0376	permease	1	#NUM!	1	1.28011	1	0.67807
-	SPA0377	hypotheticalprotein	1	0	1	-0.0255	0.4815	-0.4525
bcp	SPA0378	bacterioferritincomigratoryprotein	0.9437	-0.2547	1	-0.0937	1	0.0795
gcvR	SPA0379	glycinecleavagesystemtranscriptionalrepressor	1	-0.0176	1	0.35168	0.4695	0.79862
dapA	SPA0380	dihydrodipicolinatesynthase	1	-0.1147	1	-0.0419	1	0.31425
nlpB	SPA0381	lipoprotein	1	-0.1699	0.9979	-0.3698	1	0.21749
purC	SPA0382	phosphoribosylaminoimidazolesuccinocarboxamidesynthase	1	0.1481	2E-09	-1.655	1	-1
-	SPA0383	hypotheticalprotein	1	0.02425	0.4609	-0.3626	1	-0.2981
ypfI	SPA0384	hypotheticalprotein	1	-0.0242	0.4763	-0.2996	1	0.18556
-	SPA0385	hypotheticalprotein	1	-0.0283	0.8771	-0.1612	1	-0.2007
dapE	SPA0386	succinyl-diaminopimelatedesuccinylase	1	0.01963	0.6712	-0.2538	1	0.1822
yffB	SPA0387	hypotheticalprotein	0.9047	-0.1325	1	0.02346	1	0.25873
acrD	SPA0388	effluxpump	1	-0.3219	1	-1.5146	1	0.19265
aegA	SPA0390	oxidoreductase	1	0.24101	1	1.42884	1	1.55459
-	SPA0391	hypotheticalprotein	1	-0.1375	1	-0.7004	1	-0.2895
yffH	SPA0392	hypotheticalprotein	1	-0.1186	1	-0.1769	1	-0.6027
ypfG	SPA0393	hypotheticalprotein	1	0	1	-0.585	1	0
-	SPA0394	hypotheticalprotein	1	-0.5594	1	0.52083	1	-0.3561
tktB	SPA0395	transketolase	1	0.34792	0.0038	-1.2224	1	-0.1959
talA	SPA0396	transaldolaseA	1	0.41504	0.003	-1.1806	0.5275	-0.4448
maeB	SPA0397	NADP-dependentm alatedehydrogenase	1	-0.2146	1	0.33949	1	0.21068
eutS	SPA0398	ethanolamineutilizationproteinEutS	1	2	1	#DIV/0!	1	3

eutP	SPA0399	ethanolamine utilizationprotein	1	2.32193	1	2.32193	1	2.32193
eutQ	SPA0400	ethanolamineutilizationprotein	1	1.90689	1	1.87447	1	2.45943
eutT	SPA0401	cobalaminadenosyltransferase	1	2	1	1.80735	1	2.41504
eutD	SPA0402	phosphate acyltransferase	1	1.41504	1	1	1	2.22239
eutN	SPA0403	ethanolamineutilizationproteinEutN	1	0.5025	1	0.55254	1	0.5025
eutM	SPA0404	ethanolamineutilizationproteinEutN	1	0.65896	1	0.89308	1	1.32193
eutE	SPA0405	aldehyde dehydrogenase	1	0.64386	1	0.77761	1	1.19265
eutJ	SPA0406	ethanolamineutilizationproteinEutJ	1	0.73697	1	0.73697	1	1.22239
eutG	SPA0407	alchoholdehydrogenase	1	0.73697	1	1	1	0.41504
eutH	SPA0408	hypotheticalprotein	1	0	1	0	1	-0.415
eutA	SPA0409	ethanolamineutilizationproteinEutA	1	1	1	-0.4854	1	0
eutB	SPA0410	ethanolamineammonia -lyase heavychain	1	0.44746	1	-0.1699	1	0.12553
eutC	SPA0411	ethanolamineammonia -lyase lightchain	1	0.36257	1	-0.3219	1	-0.241
eutL	SPA0412	ethanolamineutilizationproteinEutL	1	0.21412	1	0.3744	1	0.25526
eutK	SPA0413	ethanolamineutilizationproteinEutK	1	0.32193	1	0.11548	1	0.10692
yfeG	SPA0414	ethanolamineoperontranscriptionalregulator	1	0	1	0.34792	1	0
hemF	SPA0415	coproporphyrinogenIIIoxidase	1	0.2115	1	0	1	0.10692
amiA	SPA0416	N-acetylmuramoyl-L-alanine amidase	1	0.27563	1	0.34395	1	0.22239
-	SPA0417	acetyltransferase	0.0016	-0.8099	0.4074	-0.3833	0.0028	-0.834
yfeZ	SPA0418	hypotheticalprotein	0.0013	-0.7182	1	-0.507	1	-0.5639
-	SPA0419	lipoprotein	0.2813	-0.4072	1	0.33949	1	-0.3219
-	SPA0420	hypotheticalprotein	0.8048	-0.229	1	0.66903	1	-0.2403
yfeF	SPA0421	oxidoreductase	1	0.38261	0.6023	1.25274	0.4378	0.95556
cysP	SPA0422	thiosulfate-bindingpro tein	1	0.14439	9E-208	-3.5064	0	-3.4811
cysU	SPA0423	sulfatetransportsystempermeaseCysT	1	0.36257	1E-181	-3.3775	0	-3.9449
cysW	SPA0424	sulfatetransportsystempermeaseCysW	1	1	8E-119	-3.1524	0	-3.8524
cysA	SPA0425	sulfatetransportATP -bindingpro teinCysA	1	1.5502	4E-55	-2.9023	0	-4.0377
cysM	SPA0426	cysteinesynthaseB	1	0.65208	3E-29	-2.2811	2E-50	-2.4475
yfeK	SPA0427	hypotheticalprotein	1	-0.1155	1	1.11548	1	0.55254
yfeJ	SPA0428	GMPs ynthase	1	-0.5025	1	-0.1444	1	-0.1699
ptsJ	SPA0429	transcriptionalregulator	1	-0.1926	1	-0.415	1	-0.2224
pdxK	SPA0430	pyridoxinekinase	1	-0.4594	1	-0.1926	1	-0.415
-	SPA0431	hypotheticalprotein	1	-0.4854	1	-0.3219	1	0
crr	SPA0432	ptssystem ,glucose -specificIIAcomponent	0.7029	-0.3211	1	-0.2915	1	0.08662
ptsI	SPA0433	hypothetical protein	1	-0.1507	1	-0.2755	1	-0.1284
ptsH	SPA0434	phosphocarrierproteinHPr	1	-0.1894	0.9732	-0.366	0.775	-0.4651
cysK	SPA0435	cysteinesynthaseA	0.3147	0.86195	1	-0.4021	1	-0.7558
cysZ	SPA0436	sulfatetransportproteinCysZ	1	-0.2955	1	-0.2801	1	0.04064
zipA	SPA0437	cell divisionprotein	0.4941	-0.3641	1	-0.1884	1	0.11126
ligA	SPA0438	DNAl igase	1	0.13006	0.4763	-0.3175	1	0.11784
ypeB	SPA0439	hypotheticalprotein	1	-0.0931	0.178	-0.372	1	-0.1605
yfeH	SPA0440	hypothetical protein	1	-1	1	-1.344	1	-1.1069
yfeR	SPA0441	transcriptionalregulator	1	-0.415	0.0006	-1.0458	2E-05	-1.1497
lysV	SPA0442	LystR NA	0.0163	-0.7294	0.4246	-0.3999	7E-11	-1.7266
valY	SPA0443	ValtRN A	0.0069	-0.7146	0.1396	-0.3638	2E-12	-1.7186
valX	SPA0444	ValtRN A	3E-05	-0.9087	0.4793	-0.3339	9E-15	-1.6142
valU	SPA0445	ValtRN A	0.0005	-0.887	0.3814	-0.2756	9E-10	-1.6122
gltX	SPA0446	glutamyl-tRNAs ynthetase	0.6595	-0.2796	0.8064	-0.5826	0.775	-0.4096

yfeD	SPA0447	hypotheticalprotein	1	-0.0057	6E-11	2.22729	3E-05	1.55753
yfeC	SPA0448	hypotheticalprotein	1	-0.1336	3E-11	2.23633	0.0001	1.54859
alaX	SPA0449	AlatRN A	1	-1.1375	1	0	1	0
yfeA	SPA0450	hypotheticalprotein	1	-0.1926	1	-0.372	1	-0.152
mntH	SPA0452	manganesetransport proteinMn tH	1	0.89308	1	-1.078	1	-0.1375
ypeC	SPA0453	hypotheticalprotein	0.9555	0.39993	1	0.0458	1	0.26793
-	SPA0454	ion-channel protein	1	0.13245	1	-0.0634	1	0.14439
-	SPA0455	decarboxylase	1	-0.152	5E-11	-1.9183	0.0274	-0.8365
-	SPA0456	hypotheticalprotein	0.0001	1.1964	1	0.21022	0.6225	0.65535
glk	SPA0457	glucokinase	0.9562	-0.2092	1	0.20353	1	0.34395
yfdZ	SPA0458	aminotransferase	1	-0.0843	0.0584	-1	1	-0.1598
ddg	SPA0459	acyltransferase	1	0.152	0.7163	0.74543	1	0.61005
-	SPA0460	hypotheticalprotein	1	0.05445	0.0158	1.01838	1	0.59946
pgtP	SPA0461	phosphoglyceratetransporterprotein	1	0	1	-1	1	-1
pgtC	SPA0462	phosphoglyceratetransportregulatoryproteinPgtCprecursor	1	0.32193	1	0.33342	0.0355	-0.8957
pgtA	SPA0464	phosphoglyceratetransportsystemtranscriptionalregulatoryproteinPgtA	1	0.35364	1	0	1	-0.3626
pgtE	SPA0465	outerme mbraneproteaseE	1	-0.3219	1	-0.8074	1	-0.2224
-	SPA0467	lipopolysaccharidemodificationacyltransferase	1	-0.263	1	-1.3219	1	-0.926
gtrB2	SPA0468	bactoprenolglucosyltransferase	1	0	1	-0.8231	1	-0.7004
gtrA	SPA0469	bactoprenol-linked glucosetransferase	1	-0.4854	1	-0.6374	1	-0.7965
-	SPA0470	ArgtRN A	1	-1	1	0	1	-1.585
yfdC	SPA0471	hypotheticalprotein	1	-0.3219	1	-0.628	1	-0.4695
vacJ	SPA0472	VacJlipopro tein	0.3861	-0.4237	0.7492	-0.1872	0.902	-0.2991
fadL	SPA0473	long-chainf attyacidtransportprotein	1	-1.585	0.2691	-1.1299	3E-06	-1.509
yfcZ	SPA0474	hypotheticalprotein	0.373	0.62307	0.0082	1.37932	0.1475	0.94363
yfcY	SPA0475	3-ketoacyl-CoAthi olase	2E-17	1.99048	0.0193	1.47307	1	1.18442
yfcX	SPA0476	fattyaci doxidationcomplexsubunitalpha	0.0926	0.9783	0.422	1.00934	0.9005	0.6612
sixA	SPA0477	phosphohistidinephosphatase	1	0.25573	0.4055	0.94062	1	0.21701
yfcN	SPA0478	hypotheticalprotein	0.8153	-0.2583	1	0.07943	1	-0.0444
yfcB	SPA0479	hypotheticalprotein	0.2199	-0.4339	0.0077	-0.8722	0.0156	-0.8797
aroC	SPA0480	chorismatesynthase	1	-0.077	0.2175	-0.4991	1	0
mepA	SPA0481	penicillin-insensitivemureinendopeptidase	0.6989	-0.1699	0.2551	-0.4709	1	-0.0911
yfcA	SPA0482	hypotheticalprotein	1	0.0614	1	-0.2295	1	0.38333
yfcM	SPA0483	hypotheticalprotein	0.8912	-0.2313	1	0.026	0.7096	0.69188
yfcL	SPA0484	hypotheticalprotein	0.1874	-0.3479	1	0.13327	1	0.40599
-	SPA0485	hypotheticalprotein	1	0.76553	1	0.5656	1	0.70044
fabB	SPA0486	3-oxoacyl-ACPs ynthase	1	0.41038	1	0.53895	0.9462	0.55459
-	SPA0487	hypotheticalprotein	1	0	1	0	1	1
-	SPA0488	lipoprotein	1	1	1	#DIV/0!	1	#DIV/0!
-	SPA0489	hypotheticalprotein	1	1.58496	1	#DIV/0!	1	#DIV/0!
-	SPA0490	DNA-bindingp rotein	1	#DIV/0!	1	#DIV/0!	1	#DIV/0!
-	SPA0491	bacteriophageprotein	1	0	1	0	1	-1
-	SPA0492	transmembranetransporter	1	-0.387	1	-0.3755	1	-0.2713
div	SPA0493	Divpro tein	1	0	1	-0.834	1	-0.9005
pdxB	SPA0494	erythronate-4-phosphate dehydrogenase	0.844	-0.2972	0.2849	-0.4016	1	-0.157
usg	SPA0495	semialdehydedehydrogenase	0.8318	-0.2141	0.3946	-0.3653	1	-0.027
truA	SPA0496	tRNAps eudouridinesynthaseA	1	-0.415	1	-0.4044	1	-0.2065
dedA	SPA0497	DedApro tein(dsg -1protein)	0.024	-0.6374	0.1186	-0.5719	1	-0.0759

accD	SPA0498	acetyl-CoAc arboxylasesubunitbeta	0.272	-0.5146	0.6338	-0.5811	0.589	-0.5187
folC	SPA0499	folylpolyglutamatesynthase	1	-0.1905	1	0.01511	0.9336	-0.2313
dedD	SPA0500	DedDprotei n	0.7318	-0.235	1	0.12338	1	-0.1326
cvpA	SPA0501	colicinVproductionprotein(DedEprotein)	0.2657	-0.4031	2E-16	-1.8745	0.0002	-1.0561
purF	SPA0502	amidophosphoribosyltransferase	0.4314	-0.4034	9E-22	-2.3391	9E-05	-1.3489
-	SPA0503	transcriptionalregulator	1	0.55114	0.008	1.37126	1	0.1375
-	SPA0504	aminoaci ddecarboxylase	1	0.16993	1	-0.585	1	-1.3219
-	SPA0505	aminoaci dtransporter	1	-0.3626	1	-0.737	1	-1
-	SPA0506	hypotheticalprotein	1	-0.1203	1	-0.7776	1	-1
-	SPA0507	aminoaci dpermease	1	-0.2479	1	-0.341	1	-0.2224
ubiX	SPA0508	decarboxylase	0.8912	-0.152	0.433	-0.3334	1	-0.0525
argT	SPA0509	lysine-arginine-ornithine-bindingpe riplasmicprotein	1	-0.585	1E-07	-1.48	1	0.5025
hisJ	SPA0510	histidine-bindingpe riplasmicprotein	0.1733	-0.55	0.6951	-0.4987	1	-0.1427
hisQ	SPA0511	histidinetransportsystempermease	1	-0.737	0.0012	-1.0753	1	-0.3959
hisM	SPA0512	histidinetransportsystempermease	1	-0.585	1	-1.0841	1	-0.2016
hisP	SPA0513	histidinetransportATP -binding protein	1	-0.3626	0.0092	-0.8382	1	-0.3219
yfcH	SPA0514	hypotheticalprotein	0.4344	-0.2721	0.8142	-0.2095	1	-0.1956
yfcG	SPA0515	glutathione-Stransfe rase	1	0	1	-1.5305	1	-0.737
yfcF	SPA0516	glutathione-Stransfe rase	0.3508	-0.3785	1	-0.0849	1	-0.1333
yfcE	SPA0517	hypotheticalprotein	0.323	-0.335	0.1082	-0.5168	0.2474	-0.4657
-	SPA0518	hypotheticalprotein	1	-0.0911	0.5275	-0.3436	1	-0.3193
-	SPA0519	transcriptionalregulator	1	0.09622	0.213	1.01707	1	0.48187
-	SPA0520	sugarpho sphotransferasecomponentIIA	1	0	1	0.70044	1	-1
-	SPA0521	sugarpho sphotransferasecomponentIIB	0.0397	-0.496	1	0.41504	1	-0.8745
-	SPA0522	hypotheticalprotein	1	-0.3515	1	0.34577	1	-0.7655
-	SPA0523	transketolase	1	0.0973	1	0.43929	1	-0.372
-	SPA0524	transketolase	1	-0.0946	1	0.14439	1	-0.4948
yfcC	SPA0525	hypotheticalprotein	1	-0.415	1	0.22239	1	0
pta	SPA0526	phosphate acetyltransferase	1	0.50209	1	-0.4905	1	-0.0418
ackA	SPA0527	acetatek inase	1	0.16914	0.9968	-0.3834	1	-0.3539
-	SPA0528	hypotheticalprotein	0.8571	-0.1047	0.8014	-0.1343	1	-0.2717
yfbU	SPA0529	hypotheticalprotein	1	-0.0085	1	0.36821	1	0.22932
yfbT	SPA0530	phosphatase	1	0.07192	1	0.21033	1	0.13053
yfbS	SPA0531	sodium/sulfatetransporter	1	-0.0525	1	0.50696	1	0.65896
-	SPA0532	oxetanocinAbiosyntheticprotein	1	-0.3785	1	0.03103	1	-0.0841
yfbQ	SPA0533	aminotransferase	0.2398	-0.3959	0.095	-0.6971	1	0.09311
lrhA	SPA0534	NADH dehydrogenaseoperontranscriptionalregulator	6E-20	-1.7289	0.1014	-0.5493	1	0
-	SPA0535	hypotheticalprotein	1	-1	1	-1	1	1
nuoA	SPA0536	NADH dehydrogenaseIsubunitA	1	0.20545	1	-0.0472	1	-0.1003
nuoB	SPA0537	NADH dehydrogenaseIsubunitB	1	0.31657	1	-0.0967	1	-0.1679
nuoC	SPA0538	NADH dehydrogenaseIsubunitCD	1	0.12151	1	-0.4194	1	-0.1979
nuoE	SPA0539	NADH dehydrogenaseIsubunitE	0.871	-0.2674	1	-0.2989	0.908	-0.3699
nuoF	SPA0540	NADH dehydrogenaseIsubunitF	1	-0.2683	1	-0.1609	1	-0.3765
nuoG	SPA0541	NADH dehydrogenaseIsubunitG	1	-0.304	1	-0.1068	1	-0.3653
nuoH	SPA0542	NADH dehydrogenaseIsubunitH	0.844	-0.451	1	-0.1707	1	-0.3866
nuoI	SPA0543	NADH dehydrogenaseIsubunitI	0.8441	-0.3855	1	-0.0821	1	-0.2465
nuoJ	SPA0544	NADH dehydrogenaseIsubunitJ	0.8659	-0.3668	1	-0.1327	1	-0.228
nuoK	SPA0545	NADH dehydrogenaseIsubunitK	0.4386	-0.3886	1	-0.0998	1	-0.227

nuoL	SPA0546	NADH dehydrogenaseIsubunitL	1	-0.354	1	-0.126	1	-0.1531
nuoM	SPA0547	NADH dehydrogenaseIsubunitM	1	-0.2224	1	-0.0538	1	-0.0957
nuoN	SPA0548	NADH dehydrogenaseIsubunitN	0.7474	-0.3162	1	-0.2705	1	-0.0548
-	SPA0549	receptor/regulatorprotein	0.0005	1.54057	0.3081	1.26474	1	0.21824
elaC	SPA0550	hydrolase	1	0.41504	1	0.41504	1	0.38466
elaA	SPA0551	hypotheticalprotein	1	0	1	0.26303	1	0.19265
elaB	SPA0552	hypotheticalprotein	1	0.10497	0.0481	-0.968	1	-0.2662
menF	SPA0553	isochorismatesynthase	1	-0.1926	1	-0.2563	1	-0.0577
menD	SPA0554	menaquinonebiosynthesisprotein	1	0.39472	0.159	1.24345	0.6772	0.71669
yfbB	SPA0555	hypotheticalprotein	1	0	0.523	0.89691	0.0008	1.29546
menB	SPA0556	naphthoate synthase	1	-0.1273	1	0.42365	0.3489	0.90847
menC	SPA0557	O-succinylbenzoate-CoAs ynthase	0.7904	-0.22	1	0.42321	0.167	0.93707
menE	SPA0558	O-succinylbenzoicacid --CoAl igase	1	-0.1754	1	0.33842	0.4041	0.83188
pmrD	SPA0559	polymyxinB resistanceprotein	0.3115	-0.3822	1	0.42951	1	0.31729
-	SPA0560	hypotheticalprotein	1	0.29546	1	1.27009	1	0.26303
-	SPA0561	hypotheticalprotein	1	0.01465	0.0244	1.26534	1	0.50815
pqaB	SPA0562	melittinresistanceproteinPqaB	1	-0.1884	0.3042	0.97924	1	0.52083
-	SPA0563	hypotheticalprotein	0.4636	-0.3763	0.26	1.10019	1	0.57886
yfbG	SPA0564	lipopolysaccharidemodificationprotein	0.9741	-0.2944	0.7381	1.01898	0.3291	0.92541
pmrF	SPA0565	lipopolysaccharidemodificationprotein	0.1609	-0.5461	0.0868	0.80145	0.0122	1.23266
yfbE	SPA0566	lipopolysaccharidebiosynthesisprotein	0.2854	-0.4397	0.1602	1.19068	0.002	1.34239
ais	SPA0567	Aispro tein	1	-0.6781	0.2878	1	1	0.45568
yfaO	SPA0568	hypotheticalprotein	0.1092	-0.5208	0.4092	0.848	1	0.28951
yfaZ	SPA0569	hypotheticalprotein	1	-0.4594	1	-0.263	1	-0.263
-	SPA0570	hypotheticalprotein	1	-0.0825	1	-0.0361	1	0.365
yfaX	SPA0571	transcriptionalregulator	1	0.91754	1	2	1	1.34792
yfaW	SPA0572	MR-MLE-familyprotein	1	0.86876	0.0434	1.22239	1	0.7885
yfaV	SPA0573	transporter	1	0.51457	1	0.48543	1	0.48543
-	SPA0574	2,4-dihydroxyhept-2-ene-1,7-dioic acidaldolase	1	0.34104	1	0.21681	1	0.16227
-	SPA0575	hypotheticalprotein	1	0	1	-0.2224	1	0.09311
-	SPA0576	hypotheticalprotein	1	0.76553	1	#DIV/0!	1	0.58496
-	SPA0577	hypotheticalprotein	1	0.43063	1	#DIV/0!	1	2.58496
glpC	SPA0578	anaerobicglycerol -3-phosphate dehydrogenasesubunitC	1	0.04053	0	6.1375	0	6.45533
glpB	SPA0579	anaerobic glycerol-3-phosphate dehydrogenasesubunitB	1	-0.0077	0	6.77917	0	6.15843
glpA	SPA0580	anaerobicglycerol -3-phosphate dehydrogenasesubunitA	1	-0.2009	0	8.25424	0	6.35504
glpT	SPA0581	glycerol-3-phosphatetransporter	1	-0.2511	6E-92	3.90804	1E-172	3.82838
glpQ	SPA0582	glycerophosphoryldiesterphosphodiesteraseperiplasmicprecursor	1	-0.0983	4E-82	3.85495	3E-109	3.60688
-	SPA0583	transcriptionalregulator	1	0.41504	1	1.43296	1	1.51457
-	SPA0584	transmembranetransportprotein	1	0	1	0	1	1
yfaE	SPA0585	ferredoxin	0.0005	-0.7625	1	0.19114	1	0.1452
nrdB	SPA0586	ribonucleoside-diphosphatereductase1subunitbeta	0.2247	-0.5296	1	0.06054	1	0.04939
nrdA	SPA0587	ribonucleoside-diphosphatereductase1subunitalpha	0.8484	-0.1993	0.9693	-0.4055	1	-0.02
ubiG	SPA0588	3-demethylubiquinone-93 -methyltransferase	0.4784	-0.3251	1	-0.152	0.3181	-0.5467
-	SPA0589	hypotheticalprotein	1	0	1	0.41504	1	0.26303
-	SPA0590	hypotheticalprotein	1	#DIV/0!	1	#DIV/0!	1	#DIV/0!
-	SPA0591	MR-MLE-familyprotein	1	0	1	0.58496	1	-0.415
gyrA	SPA0592	DNAg yrasesubunitA	1	-0.1834	0.6098	-0.7791	0.6708	-0.5243
rcsC	SPA0593	sensor proteinRcsC	1	-0.3301	1	-0.8074	1	-0.372

rcsB	SPA0594	regulatorofcapsulesynthesisBcomponent	1	-0.0667	1	-0.0916	1	0.21645
yojN	SPA0595	two-componentsystemsensorkinase	1	-0.3626	1	-0.5454	1	-0.174
-	SPA0596	-	1	1	1	#DIV/0!	1	#DIV/0!
ompC	SPA0597	outerme mbraneproteinC	1	-0.5583	0.8069	-0.8777	0.1851	-1.1562
yojL	SPA0598	thiamine biosynthesisprotein	1	-0.848	1	-0.8194	1	-0.415
ada	SPA0599	ADAre gulatoryprotein	1	-0.0375	1	0.01577	1	-0.2153
alkB	SPA0600	AlkB protein	1	0	1	0.18057	0.5931	-0.387
yojI	SPA0601	ABCtra nsporterATP -bindingp rotein	1	0.26303	1	-0.585	1	-0.6374
eco	SPA0602	ecotin precursor	1	0.20257	0.0868	1.24427	0.9601	0.53051
napF	SPA0603	ferredoxin-typeprote inNapF	1	-0.585	0.0364	1.56179	0.2084	0.91943
yojF	SPA0604	napABas semblyprotein	1	-0.5146	0.0042	1.42852	0.1162	0.97312
napA	SPA0605	nitrate reductase	1	-0.0995	0.8995	1.20259	0.1527	1.557
napG	SPA0606	ferredoxin-typeprote inNapG	1	0.32193	0.4172	1.01495	2E-10	2.00605
napH	SPA0607	ferredoxin-typeprote inNapH	1	0.41504	0.5891	0.79391	2E-12	2.06457
napB	SPA0608	cytochromec -type proteinN apBprecursor	1	0.16993	0.2389	1.092	3E-09	1.88779
napC	SPA0609	cytochromec -typeprote inNapC	1	0.32193	0.0782	1.18709	1E-13	2.08387
ccmA	SPA0610	hemee xporterproteinA1	1	-0.1979	0.3959	0.93318	5E-08	1.80539
ccmB	SPA0611	heme exporter proteinB1	1	-0.2451	0.6472	0.83615	1E-08	1.82873
ccmC	SPA0612	hemee xporterproteinC1	0.466	-0.3081	0.5108	0.96592	0.0023	1.47725
ccmD	SPA0613	hemee xporterproteinD1	0.7932	-0.1349	0.156	1.03598	2E-07	1.62916
ccmE	SPA0614	cytochromec -typebio genesisproteinE1	1	-0.0614	0.3322	1.00539	3E-05	1.5776
ccmF	SPA0615	cytochromec -typebio genesisproteinF1	1	-0.2955	0.6144	0.8965	0.0017	1.53051
dsbE	SPA0616	thiol:disulfideinterchangeprotein	1	0	0.107	1.05795	2E-06	1.55141
ccmH	SPA0617	cytochromec -typebio genesisproteinH1	1	0	0.1921	1.21645	0.0458	1.12883
narP	SPA0618	nitrate/nitriteresponseregulatorproteinNarP	0.2347	-0.4306	1	0.1822	1	-0.1959
-	SPA0619	hypotheticalprotein	1	#DIV/0!	1	#DIV/0!	1	#DIV/0!
-	SPA0620	virulenceproteinMsgA	1	#DIV/0!	1	#DIV/0!	1	#NUM!
-	SPA0621	XaatRN A	1	-0.628	1	-0.6781	1	-0.3219
yejM	SPA0622	sulfatase	0.4424	-0.3286	1	-0.6374	1	-0.4671
yejL	SPA0623	hypotheticalprotein	0.0466	-0.5965	0.3642	-0.4001	0.0458	-0.6581
yejK	SPA0624	nucleoid-asociatedprotein	1	0.04372	1	-0.3755	1	-0.174
-	SPA0625	hypotheticalprotein	1	-0.1926	1	-0.152	1	0.16993
rplY	SPA0626	50Sribos omalproteinL25	0.3948	-0.4194	0.9501	-0.1187	1	0.33104
yejH	SPA0627	helicase	1	0.39232	1	0.60572	1	0.5502
yejD	SPA0628	ribosomalsmallsubunitpseudouridinesynthase	1	-0.0291	0.1728	-0.4389	0.0413	-0.715
bcr	SPA0629	bicyclomycinresistanceprotein	1	-0.2996	1	-1	1	-0.8365
-	SPA0630	hypotheticalprotein	1	-0.2224	1	-1.1699	1	-0.585
yejG	SPA0631	hypotheticalprotein	0.5397	0.57089	1	0.4899	1	0.19931
yejF	SPA0632	ABCtra nsporterATP -bindingp rotein	1	-0.0401	1	0.01612	1	-0.1031
yejE	SPA0633	binding-protein-dependenttra nsporter	1	-0.2141	1	-0.2095	1	-0.1864
yejB	SPA0634	binding-protein-dependenttra nsporter	1	-0.273	1	-0.3744	1	-0.3326
yejA	SPA0635	transport systemperiplasmicbindingprotein	1	-0.2756	1	-0.5261	1	-0.4005
rtn	SPA0636	rtnprotein	1	-0.0962	1	-0.0506	1	0
spr	SPA0637	lipoprotein	0.3379	-0.4702	0.156	-0.6264	0.8236	-0.3293
yeiU	SPA0638	hypotheticalprotein	0.9676	-0.1031	1	0.15754	1	0.40599
yeiR	SPA0639	hypotheticalprotein	0.3406	0.67319	1	0.66676	0.8973	0.63435
yeiP	SPA0640	elongationfactor	0.0325	-0.6197	0.0437	-0.6215	1	-0.7843
-	SPA0641	hypotheticalprotein	1	0	1	1	1	0

-	SPA0642	hypotheticalprotein	1	0	1	#DIV/0!	1	#DIV/0!
-	SPA0643	hypotheticalprotein	1	0	1	#DIV/0!	1	#DIV/0!
yeiO	SPA0644	sugare ffluxtransporter	1	0	1	0	1	0
fruB	SPA0645	PTSsys tem fructose-specifictransportersubunitIIA/FPR	1	0.41504	1	0.58496	1	-0.585
fruK	SPA0646	1-phosphofructokinase	1	0.32193	1	0	1	-0.585
fruA	SPA0647	PTSsys temfructose -specifictransportersubunitIIBC	1	-0.2224	1	-0.415	1	-0.6521
nfo	SPA0648	endonucleaseIV	1	-0.0161	1	0.12553	1	0.21681
yeiH	SPA0649	hypotheticalprotein	1	1.74723	1	2.22239	1	1.35364
yeiE	SPA0650	transcriptionalregulator	1	0.12738	1	0.1375	1	-0.2895
lysP	SPA0651	lysine-specificpermease	1	-0.0641	1	-0.2996	1	-0.1806
cirA	SPA0652	colicinIreceptor	1	-1	1	0.58496	1	-0.585
-	SPA0653	hypotheticalprotein	1	0	1	0	1	-1
-	SPA0654	hydrolase	1	-1	1	2	1	0.58496
-	SPA0656	DNA-bindingp rotein	1	0.71989	1	0.20163	1	0.43296
yeiG	SPA0657	esterase	0.3482	-0.5674	1	0.13422	1	0.39476
folE	SPA0658	GTPc yclohydrolaseI	1	0.10604	0.702	-0.1426	0.6212	-0.352
yeiB	SPA0659	hypotheticalprotein	1	0.09311	1	-0.4406	1	-0.1605
galS	SPA0660	mglre pressorandgalactoseultrainductionfactor	1	-0.6781	1	0.83007	1	-0.8931
mglB	SPA0661	D-galactose-bindingpe riplasmicprotein	5E-10	-1.6552	1	0.41063	0.0021	-1.0614
mglC	SPA0663	galactosidetransportsystempermeaseproteinMglC	1	-1.415	1	-0.0444	1	-1
yeiA	SPA0664	dihydropyrimidinedehydrogenase	1E-21	1.90689	0.0314	1.27723	7E-06	1.65486
-	SPA0665	oxidoreductase	3E-13	1.86162	0.0001	1.71621	2E-13	2.07039
-	SPA0666	hypotheticalprotein	1	-0.4764	0.353	0.71049	1	0.16046
sanA	SPA0667	vancomycinresistanceprotein	0.1053	-0.5334	1	0.61891	1	0.04307
cdd	SPA0668	cytidinedeaminase	0.0421	0.91561	0.3837	0.90689	0.0256	1.13598
yohK	SPA0669	hypotheticalprotein	1	-0.1293	1	-0.4854	1	-0.7279
yohJ	SPA0670	hypotheticalprotein	1	-0.074	1	-0.585	1	-0.6674
-	SPA0671	transcriptionalregulator	1	0.19265	1	-0.1375	1	0.26303
-	SPA0672	n-hydroxybenzoatetransporter	1	1	1	0.32193	1	0
-	SPA0673	gentisate1,2 -dioxygenase	1	0.63743	1	0.71049	1	-0.152
-	SPA0674	FAA-hydrolase-familyprotein	1	0.46949	1	0.12553	1	0.05658
-	SPA0675	glutathione-S-transferase-familyprotein	1	0.44057	1	0.07039	1	0
-	SPA0676	n-hydroxybenzoatehydroxylase	1	0.33442	1	0	1	-0.0614
yohI	SPA0677	hypotheticalprotein	1	0	1	-0.6781	1	-0.848
-	SPA0678	hypotheticalprotein	1	#NUM!	1	-1	1	-0.3219
yohG	SPA0679	lipoprotein	1	1.32193	1	1.32193	1	0.73697
yohF	SPA0680	oxidoreductase	1	0	1	-1.3219	1	-0.2224
yohD	SPA0681	hypotheticalprotein	1	0.22239	1	0	1	0.28951
yohC	SPA0682	hypotheticalprotein	1	#DIV/0!	1	-2	1	-2.1155
pbpG	SPA0683	penicillin-bindingpro tein7	1	-0.152	0.2889	-0.4406	0.9993	-0.2578
dld	SPA0684	D-lactatede hydrogenase	1	-0.0893	0.2198	-0.859	1	-0.174
bglX	SPA0685	periplasmicbeta -glucosidase	1	-0.3923	1	-0.8074	1	-0.263
yehZ	SPA0686	hypotheticalprotein	1	-0.1926	5E-06	-1.2701	0.9488	-0.3684
yehY	SPA0687	permease	1	0.26303	3E-05	-1.189	1	-0.25
yehX	SPA0688	ABCtra nsporterATP -bindingp rotein	1	0	0.0005	-1.0506	1	-0.2224
yehW	SPA0689	permease	1	0	1	-0.8845	1	-0.3219
-	SPA0690	hypotheticalprotein	1	0.3265	1	0.4021	1	-0.3551
yehV	SPA0691	transcriptionalregulator	1	-0.8074	1	-1.2115	4E-06	-1.1806

yehU	SPA0692	two-componentsystemsensorkinase	1	-0.3344	1	-0.0458	1	-0.2895
yehT	SPA0693	two-componentsystemresponseregulator	0.4046	-0.2869	1	0.07039	0.1581	-0.5329
yehS	SPA0694	hypotheticalprotein	0.0015	-0.8112	1	-0.2572	0.0088	-0.75
-	SPA0695	lipoprotein	1	-0.585	1	#NUM!	1	#NUM!
yehR	SPA0696	lipoprotein	1	-1	1	-1	1	0
metG	SPA0697	methionyl-tRNAs ynthetase	1	-0.0666	0.4822	-0.656	0.2228	-0.6477
mrp	SPA0698	hypotheticalprotein	1	-0.1624	1	-0.0153	1	0.18528
yehE	SPA0699	hypotheticalprotein	1	-0.415	1	-0.1926	1	-0.6521
stcA	SPA0700	fimbrialsubunitprotein	1	#DIV/0!	1	1.65208	1	1.8365
stcB	SPA0701	fimbrialchaperone protein	1	#DIV/0!	1	#DIV/0!	1	#DIV/0!
stcC	SPA0702	outerme mbraneusherprotein	1	#DIV/0!	1	0	1	#DIV/0!
stcD	SPA0703	hypotheticalprotein	1	#DIV/0!	1	#DIV/0!	1	#DIV/0!
yohN	SPA0704	hypotheticalprotein	0.4528	-0.2955	1	-0.0361	1	0.47393
thiM	SPA0705	hydroxyethylthiazolekinase	1	0.28011	1	0.38702	1	0.80735
thiD	SPA0706	phosphomethylpyrimidinekinase	1	0.1375	1	0.24793	1	0.39232
yegW	SPA0707	GntRfam ilytranscriptionalregulator	1	0.06054	1	0.60881	1	0.16439
yegV	SPA0708	sugark inase	1	-0.7105	1	-0.4546	1	-0.6521
yegU	SPA0709	hydrolase	1	-0.5639	1	-0.3785	1	-0.6781
yegT	SPA0710	nucleosidepermease	1	-1.585	1	-0.7004	1	-1.0995
fbaB	SPA0711	fructose-bisphosphatealdolase	1	0.16993	0.0849	-1.3895	1	-0.1753
yegS	SPA0712	diacylglycerolkinasecatalyticdomain	1	-0.263	0.0072	-0.8329	0.0528	-0.7162
-	SPA0713	hypotheticalprotein	1	-1.3219	1	-1.585	1	-2.4594
-	SPA0714	hypotheticalprotein	1	-1.585	1	#NUM!	1	#NUM!
-	SPA0715	hypotheticalprotein	1	#DIV/0!	1	#DIV/0!	1	#DIV/0!
yegQ	SPA0716	protease	1	0.16993	1	0	1	-0.737
-	SPA0717	hypotheticalprotein	1	#NUM!	1	#DIV/0!	1	#DIV/0!
-	SPA0718	hypotheticalprotein	1	#DIV/0!	1	#DIV/0!	1	#DIV/0!
-	SPA0719	hypotheticalprotein	1	#DIV/0!	1	#DIV/0!	1	#DIV/0!
-	SPA0720	hypotheticalprotein	1	#DIV/0!	1	#DIV/0!	1	#DIV/0!
-	SPA0721	hypotheticalprotein	1	#DIV/0!	1	#DIV/0!	1	#DIV/0!
-	SPA0722	hypotheticalprotein	1	#DIV/0!	1	0	1	0
-	SPA0723	hypotheticalprotein	1	#DIV/0!	1	#DIV/0!	1	#DIV/0!
-	SPA0724	hypotheticalprotein	1	#DIV/0!	1	#DIV/0!	1	#DIV/0!
-	SPA0725	hypotheticalprotein	1	#DIV/0!	1	#DIV/0!	1	#DIV/0!
-	SPA0726	hypotheticalprotein	1	#DIV/0!	1	#DIV/0!	1	#DIV/0!
-	SPA0727	hypotheticalprotein	1	#DIV/0!	1	#DIV/0!	1	#DIV/0!
-	SPA0728	hypotheticalprotein	1	#DIV/0!	1	#DIV/0!	1	#DIV/0!
-	SPA0729	hypotheticalprotein	1	#DIV/0!	1	#DIV/0!	1	#DIV/0!
-	SPA0730	hypotheticalprotein	1	-1	1	1	1	-0.585
-	SPA0731	hypotheticalprotein	1	-0.585	1	0	1	-0.585
-	SPA0732	hypotheticalprotein	1	#DIV/0!	1	-1	1	-1
-	SPA0733	hypotheticalprotein	1	#DIV/0!	1	-1	1	-1.585
baeR	SPA0734	two-componentsystemresponseregulator	1	0.12553	1	0.09954	1	0.05153
baeS	SPA0735	two-componentsystemsensorkinase	1	0.69188	1	0.36257	1	1.07039
yegB	SPA0736	transporterprotein	1	1.05889	1	1.22239	1	1.58496
yegO	SPA0737	RND-familytransporterprotein	1	-0.2224	1	0.73697	1	1
yegN	SPA0738	RND-familytransporterprotein	1	-0.585	1	0	1	0
-	SPA0740	-	6E-16	-1.6714	1	0	1	-0.6781

yegD	SPA0741	hypotheticalprotein	1	-0.415	1	0	1	-0.3626
alkA	SPA0742	DNA-3-methyladenineglycosidaseII	1	0	1	0	1	-0.3626
yegE	SPA0743	hypotheticalprotein	1	0	1	-0.415	1	-0.1203
udk	SPA0744	uridinek inase	1	-0.0231	0.3057	-0.3692	0.0893	-0.6027
dcd	SPA0745	deoxycytidinetriphosphatedeaminase	0.2043	-0.4446	0.0968	-0.6521	0.2474	-0.5922
asmA	SPA0746	outerme mbraneassemblyprotein	0.0315	-0.6245	0.0203	-0.9303	1	-0.6732
yegH	SPA0747	hypotheticalprotein	1	0.44746	1	-0.0297	1	0.09311
wza	SPA0748	polysaccharideexportprotein	1	#DIV/0!	1	#DIV/0!	1	#DIV/0!
wzb	SPA0749	protein-tyrosinephosphatase	1	#DIV/0!	1	#DIV/0!	1	#DIV/0!
wzc	SPA0750	tyrosine-proteink inase	1	#DIV/0!	1	-0.415	1	-0.8931
wcaA	SPA0751	hypotheticalprotein	1	0	1	-0.6781	1	-1
wcaB	SPA0752	acetyltransferase	1	#DIV/0!	1	-1	1	-0.415
wcaC	SPA0753	glycosyltransferase	1	0	1	-0.6781	1	-0.585
wcaD	SPA0754	colanicacidpolymerase	1	#DIV/0!	1	-1	1	-1.585
wcaE	SPA0755	glycosyltransferase	1	#DIV/0!	1	0	1	-1
wcaF	SPA0756	acetyltransferase	1	#DIV/0!	1	0	1	#NUM!
gmd	SPA0757	GDP-mannose4,6 -dehydratase	1	0	1	-0.4854	1	-1
fcl	SPA0758	GDP-fucosesynthetase	1	0	1	-0.737	1	-0.585
wcaH	SPA0759	O-antigen biosynthesisprotein	1	0	1	-1.585	1	-1.585
wcaI	SPA0760	glycosyltransferase	1	#NUM!	1	-1.585	1	0
manC	SPA0761	mannose-1-phosphate guanylyltransferase	1	0	1	-0.585	1	-0.585
manB	SPA0762	phosphomannomutase	1	#DIV/0!	1	#DIV/0!	1	#DIV/0!
wzxC	SPA0764	transmembranetransportprotein	1	#NUM!	1	-1.8074	1	-1
wcaL	SPA0766	glycosyltransferasefamilyprotein	1	#DIV/0!	1	-1.3219	1	-1.3219
wcaM	SPA0767	hypotheticalprotein	1	#DIV/0!	1	-0.415	1	-1.3219
rfbB	SPA0769	dTDP-glucose4,6 -dehydratase	0.5554	-0.2801	0.2173	-0.5549	0.467	-0.505
rfbD	SPA0770	dTDP-4-dehydrorhamnosereductase	1	-0.1346	0.0852	-0.8556	0.4701	-0.5045
rfbA	SPA0771	TDP-glucosepyrophosphorylase	0.9512	-0.1641	0.0368	-0.9518	0.342	-0.4975
rfbC	SPA0772	dTDP-4-dehydrorhamnose3,5 -epimerase	0.5706	-0.251	0.0333	-0.8385	0.2494	-0.585
rfbI	SPA0773	reductaseRfbI	0.8912	-0.1905	0.1606	-0.721	0.3344	-0.5018
rfbF	SPA0774	glucose-1-phosphate cytidylyltransferase	0.974	-0.2459	1	-0.2089	1	-0.2603
rfbG	SPA0775	CDP-glucose4,6 -dehydratase	0.85	-0.2207	1	-0.2278	1	-0.1856
rfbH	SPA0776	dehydrataseRfbH	0.8912	-0.3856	1	-0.2732	1	-0.289
rfbS	SPA0777	paratosesynthase	1	-0.0151	1	0.01715	1	-0.013
rfbE	SPA0778	CDP-tyvelose-2-epimerase	1	0.14598	1	0.11632	1	-0.0477
rfbX	SPA0779	O-antigen transporter	1	0.16227	1	0.21539	1	0.21412
rfbV	SPA0780	glycosyltransferasefamilyprotein	1	0.21573	1	0.18508	1	0.09526
rfbU	SPA0781	glycosyltransferase	1	0.16993	1	0.12553	1	-0.0232
rfbV	SPA0782	glycosyltransferasefamilyprotein	1	0.21864	1	0.18649	1	0.10931
rfbU	SPA0783	glycosyltransferase	1	0.21759	1	0.1343	1	0.01038
rfbV	SPA0784	glycosyltransferasefamilyprotein	1	0.21864	1	0.18649	1	0.10931
rfbU	SPA0785	glycosyltransferase	1	0.19855	1	0.0581	1	-0.19
rfbN	SPA0786	rhamnosyltransferase	1	0.06366	1	0.04008	1	-0.2457
rfbM	SPA0787	mannose-1-phosphate guanylyltransferase	1	0.12234	1	-0.0595	1	-0.2418
rfbK	SPA0788	phosphomannomutase	1	0.16993	1	0.21245	1	-0.0241
rfbP	SPA0789	undecaprenyl-phosphate galactosephosphotransferase	1	0.20945	1	0.25154	1	-0.1209
gnd	SPA0790	6-phosphogluconatedehydrogenase,decarboxylating	1	0.06373	0.8341	-0.5116	0.6468	-0.4417
ugd	SPA0791	UDP-glucose6 -dehydrogenase	1	0	0.2097	1.06012	0.1316	0.96347

cld	SPA0792	polysaccharidechainlengthregulator	0.7266	-0.2048	0.0062	-1.152	0.0068	-0.9546
hisI	SPA0793	phosphoribosyl-AMPcy clohydrolase/phosphoribosyl -ATPp yrophosphohydrolase	0.0611	-0.5742	0.0598	-0.6805	0.2196	-0.585
hisF	SPA0794	cyclaseHisF	0.1184	-0.4975	0.0147	-0.7802	0.266	-0.4764
hisA	SPA0795	phosphoribosylformimino-5-aminoimidazolecarboxamideribotideisomerase	0.1208	-0.4806	0.0139	-0.7574	1	-0.6828
hisH	SPA0796	amidotransferase	0.2455	-0.4021	0.0472	-0.6582	0.1359	-0.5771
hisB	SPA0797	imidazoleglycerol-phosphate dehydratase; histidinolphosphatase	0.313	-0.3847	0.3139	-0.372	0.5448	-0.4294
hisC	SPA0798	histidinol-phosphate aminotransferase(imidazole)	0.08	-0.5463	0.1613	-0.5784	0.4806	-0.5436
hisD	SPA0799	histidinoldehydrogenase	0.0966	-0.5146	0.5523	-0.3219	1	-0.2268
hisG	SPA0800	ATPpho sphoribosyltransferase	0.0026	-0.7705	1	-0.0849	1	0.29546
yeeZ	SPA0801	hypotheticalprotein	1	0.08453	0.3293	-0.3744	0.986	-0.241
yeeY	SPA0802	transcriptionalregulator	1	-0.0849	1	-0.5343	1	-0.5712
yeeF	SPA0803	amino acidtranspo rterprotein	0.0422	-0.7343	5E-19	-2.0124	1	-1.263
sbcB	SPA0804	exodeoxyribonucleaseI	1	0	0.3994	-0.326	0.619	-0.3602
phsB	SPA0807	thiosulfatereductaseelectrontransportproteinPhsB	0.0325	-0.8036	1	1	1	-0.6464
phsC	SPA0808	thiosulfatereductasecytochromebsubunit	0.0054	-1.0591	1	0.80735	1	-0.4475
sbmC	SPA0810	DNAg yraseinhibitoryprotein	0.313	-0.602	0.2481	-0.3967	0.0003	-1.0227
yeeA	SPA0811	hypotheticalprotein	0.4774	-0.3593	1	-0.3744	1	-0.4021
yeeX	SPA0812	hypotheticalprotein	1	-0.1358	1	0.27199	0.9993	-0.183
pduX	SPA0813	hypotheticalprotein	1	-0.5525	1	0.342	1	-0.1758
pduW	SPA0814	propionatekinase	1	0	1	0	1	-0.263
pduV	SPA0815	propanediolutilizationproteinPduV	1	#DIV/0!	1	0	1	-0.3219
-	SPA0816	propanediolutilizationproteinPduU	1	#DIV/0!	1	0	1	-0.263
pduT	SPA0817	propanediolutilizationproteinPduT	1	#DIV/0!	1	0.32193	1	-1
pduS	SPA0818	ferredoxin	1	#DIV/0!	1	0	1	-0.415
pduQ	SPA0819	propanol dehydrogenase	1	0	1	0	1	-0.3219
pduP	SPA0820	CoA-dependentpro prionaldehydedehydrogenase	1	0	1	0.26303	1	-0.263
pduO	SPA0821	hypotheticalprotein	1	0.58496	1	0	1	-0.3219
pduN	SPA0822	Propanediolutilization:polyhedralbodies	1	0.58496	1	0	1	-0.848
pduM	SPA0823	hypotheticalprotein	1	0.32193	1	0.19265	1	-0.8745
pduL	SPA0824	hypotheticalprotein	1	0.22239	1	0.1375	1	-1.0875
pduK	SPA0825	propanediolutilizationproteinPduK	1	0.152	1	0.22239	1	-1.1844
pduJ	SPA0826	propanediolutilizationproteinPduJ	1	0.152	1	0.09954	1	-1.5025
pduH	SPA0827	PduHprote in	1	0.58496	1	0	1	-1.8074
pduG	SPA0828	PduGpro tein	1	0	1	0	1	-1.8074
pduE	SPA0829	diolde hydratasesmallsubunit	1	1	1	0	1	-4.6439
pduD	SPA0830	diolde hydratasemediumsubunit	1	1	1	0	1	-4.9542
pduC	SPA0831	glycerol dehydrataselargesubunit	1	0	1	0	1	-5
pduB	SPA0832	propanediolutilizationproteinPduB	1	0	1	0	1	#NUM!
pduA	SPA0833	propanediolutilizationproteinPduA	1	#DIV/0!	1	#DIV/0!	1	#NUM!
pocR	SPA0835	pdu/cob regulatoryproteinPocR	4E-08	-1.2288	1	0.63743	0.0091	-0.9005
cbiB	SPA0837	CbiBpro tein	1	0	1	0.54432	1	0.21299
cbiC	SPA0838	synthesisofvitaminB12adenosylcobalamide	1	0.41504	1	0.62619	1	0.30203
cbiD	SPA0839	CbiDpro tein	1	0.41504	1	0.54749	1	0.07215
cbiE	SPA0840	precorrin-6YC5, 15-methyltransferase	1	0.32193	1	0.57116	1	-0.0893
cbiT	SPA0841	precorrin-8Wdecar boxylase	1	0.67807	1	0.66985	1	-0.0242
cbiF	SPA0842	precorrin-4C(11) -methyltransferase	1	0.16993	1	0.66985	1	-0.0458
cbiG	SPA0843	CbiGpro tein	1	0.078	1	0.31797	1	-0.1502
cbiH	SPA0844	precorrin-3C17 -methyltransferase	1	0.27302	1	0.34692	1	-0.0251

cbiJ	SPA0845	synthesisofvitaminB12adenosylcobalamide	1	0.55254	1	0.26882	1	-0.1769
cbiK	SPA0846	synthesisofvitaminB12adenosyl cobalamide	1	0.26303	1	0.47337	1	-0.0101
cbiL	SPA0847	precorrin-2C(20) -methyltransferase	1	0.16993	1	0.28951	1	-0.0966
cbiM	SPA0848	synthesisofvitaminB12adenosylcobalamide	1	0	1	0	0.7607	-0.4431
cbiN	SPA0849	cobalt transportproteinCbiN	1	0	1	0.04947	0.144	-0.5305
cbiQ	SPA0850	cobalt transportproteinCbiQ	1	0.19265	1	0.10561	1	-0.3185
cbiO	SPA0851	cobalt transportATP -bindingp roteinCbiO	1	0.20645	1	0.14359	1	-0.263
cbiP	SPA0852	cobyricacidsynthase	1	0.078	1	0.2007	1	-0.0531
cobU	SPA0853	cobinamidekinaseandguanylyltransferase	1	0.152	1	0.09954	1	-0.0931
cobS	SPA0854	cobalamin(5' -phosphate) synthase	1	0	1	-0.1203	1	-0.2479
cobT	SPA0855	nicotinate-nucleotide--dimethylbenzimidazolephosphoribosyltransferase	1	0	1	0.0458	1	-0.1375
erfK	SPA0856	hypotheticalprotein	1	-0.0875	0.6468	-0.2591	1	-0.309
-	SPA0857	hypotheticalprotein	1	-0.2224	1	0	1	-0.507
-	SPA0858	AsntRN A	1	-1.3219	1	-0.585	1	-1
-	SPA0860	AsntRN A	1	-0.3219	1	-0.4854	1	-0.415
-	SPA0861	hypotheticalprotein	0.5729	-0.2398	1	0.79355	1	0.09464
-	SPA0862	hypotheticalprotein	1	-0.1825	1	0.11366	0.9601	-0.2274
-	SPA0863	hypotheticalprotein	1	#DIV/0!	1	#DIV/0!	1	#DIV/0!
amn	SPA0864	AMPnuc leosidase	1	0.16146	1	-0.0167	1	0.08049
-	SPA0865	AsntRN A	1	#DIV/0!	1	0.58496	1	-1
-	SPA0866	hypotheticalprotein	1	0	1	0	1	-0.415
-	SPA0867	hypotheticalprotein	1	-0.585	1	-0.3626	1	-0.6374
asnT	SPA0868	AsntRN A	1	-0.6951	1	1	1	0.19265
yeeI	SPA0869	hypotheticalprotein	1	-0.1593	0.3088	1.05174	1	0.02405
serU	SPA0870	SertRNA	1	-0.8074	1	0	1	-0.4854
-	SPA0871	hypotheticalprotein	1	0	1	-0.1699	1	-0.1069
umuD	SPA0872	UmuDprotei n	1	-0.074	1	-0.4288	1	-0.2115
umuC	SPA0873	UmuCpro tein	1	-0.387	1	-0.1699	1	-0.2801
cspB	SPA0874	cold shock protein	1	0.20992	0.9723	0.62244	0.5957	0.60334
ompS	SPA0875	outerme mbraneproteinS1	1	-1.1375	1	-1	1	-0.415
yedJ	SPA0877	hypotheticalprotein	1	-0.1312	1	0.13124	1	-0.2141
dcm	SPA0878	DNA-cytosinemethyltransferase	1	-0.15	1	0.18345	1	-0.0199
vsr	SPA0879	patchrepa irprotein	1	-0.2775	1	0.19931	1	-0.0444
yedA	SPA0880	hypotheticalprotein	1	0.62803	1	0.36257	1	0.67807
yedI	SPA0881	innerme mbraneprotein	1	-0.2115	1	-0.415	1	-0.3049
-	SPA0882	hypotheticalprotein	1	-0.3536	0.1425	-0.5729	0.01	-0.7527
-	SPA0883	hypotheticalprotein	1	0	1	-1	1	-0.585
yedP	SPA0884	hypotheticalprotein	1	0	1	-1.1375	1	-0.6101
-	SPA0885	-	1	0	1	-0.4594	1	-0.6881
yodD	SPA0886	hypotheticalprotein	1	-0.415	1	-0.7105	1	-0.5052
dsrB	SPA0887	DsrBp rotein	1	-0.2168	1	0.12553	1	-0.4721
rcsA	SPA0888	colanicacidcapsullarbiosynthesisactivationproteinA	1	#DIV/0!	1	0	1	0.58496
fliR	SPA0889	flagellarbiosyntheticproteinFliR	1	0.152	1	0.58496	1	-0.3219
fliQ	SPA0890	flagellar biosyntheticproteinFliQ	1	1.14439	1	0.81444	0.9671	-0.1476
fliP	SPA0891	flagellarbiosyntheticproteinFliP	0.0028	1.08406	0.9356	0.67377	1	-0.1283
fliO	SPA0892	flagellarproteinFliO	0.0004	1.13516	0.5517	0.79414	1	-0.1819
fliN	SPA0893	flagellarmotorswitchproteinFliN	0.0128	1.0145	0.2953	0.93627	1	-0.0815
fliM	SPA0894	flagellarmotorswitchproteinFliM	0.0003	1.15634	0.5529	0.92114	1	-0.0319

fliL	SPA0895	FliLpro tein	0.0317	0.94212	0.6997	0.82073	1	-0.2674
fliK	SPA0896	flagellarhook -lengthc ontrolprotein	0.0018	1.17348	0.657	0.83975	0.8159	-0.3729
fliJ	SPA0897	flagellarFliJprotein	0.0003	1.15295	0.7357	0.78351	0.8515	-0.3626
fliI	SPA0898	flagellum-specificATPsynthase	0.0009	1.14684	1	0.62344	1	-0.1751
fliH	SPA0899	flagellarassemblyproteinFliH	0.0042	1.07895	1	0.60386	1	-0.3079
fliG	SPA0900	flagellarmotorswitchproteinFliG	0.0008	1.10069	1	0.51785	0.7947	-0.4133
fliF	SPA0901	flagellarbasal -bodyM -ringpro tein	0.0111	1	1	0.16046	0.3576	-0.6613
fliE	SPA0902	flagellarhook -basalbo dycomplexproteinFliE	1	0.62149	1	0.2863	4E-05	-1.0418
-	SPA0903	hypotheticalprotein	1	0	1	1.16993	1	-0.3479
yedF	SPA0904	hypotheticalprotein	1	-1.1155	1	0.848	1	0.41504
yedE	SPA0905	hypotheticalprotein	1	-1	1	0.73697	1	0
yedD	SPA0906	lipoprotein	1	1	0.9206	-0.122	0.619	-0.3177
amyA	SPA0907	alpha-amylase	1	0.76553	3E-13	-1.7843	1	-0.5683
fliT	SPA0908	flagellarproteinFliT	3E-05	1.29876	1	0.5283	1	0.00733
fliS	SPA0909	flagellarproteinFliS	9E-05	1.23147	1	0.59589	1	-0.0337
fliD	SPA0910	flagellarhookassociatedprotein2	0.1283	1.38171	1	0.77787	1	0.00518
fliC	SPA0911	flagellin	0.4123	1.4768	0.7004	1.1767	1	-0.0462
fliA	SPA0913	RNApo lymerasesigmatranscriptionfactorforflagellar operon	2E-05	1.30189	0.0814	1.30986	1	0.36438
fliZ	SPA0914	FliZpro tein	8E-06	1.33598	0.215	1.08179	1	0.34469
fliY	SPA0915	cystine-bindingpe riplasmicproteinprecursor	0.87	0.39759	0.6818	-0.2102	1	-0.0307
yedO	SPA0916	deaminase	1	0.3112	0.7296	-0.2775	1	-0.172
yecS	SPA0917	ABCtra nsportermembraneprotein	1	0.24998	0.178	-0.5004	1	-0.2388
yecC	SPA0918	ABCtra nsporterATP -bindingp rotein	1	0.35908	0.285	-0.3561	1	-0.0693
sdiA	SPA0919	cell-divisionregulatoryprotein	7E-07	1.44908	0.2859	1.01012	0.9601	-0.3243
yecF	SPA0920	hypotheticalprotein	0.0035	-0.6845	1	-0.585	1E-06	-1.3744
-	SPA0921	hypotheticalprotein	1	-0.8074	1	-0.4854	1	-1
sirA	SPA0922	invasionresponse -regulator	1	-0.0766	0.523	-0.5655	0.1851	-0.8243
uvrC	SPA0923	excinucleaseABCsubunitC	1	0.19931	0.6154	-0.5374	0.3833	-0.6262
pgsA	SPA0924	phosphotidylglycerophosphatesynthetase	0.3048	-0.3943	1	0.21759	1	-0.2943
glyW	SPA0925	GlytR NA	0.0007	-0.7574	1	0.3267	0.0994	-0.5724
cysT	SPA0926	CystR NA	6E-05	-0.8737	1	0.1707	0.0583	-0.6171
leuZ	SPA0927	LeutRN A	1E-06	-1.0492	0.7339	-0.185	0.0762	-0.7094
-	SPA0928	innerme mbraneprotein	1	-2	1	#NUM!	1	-1
-	SPA0929	hypotheticalprotein	1	-0.6881	1	-0.263	1	-1
-	SPA0930	glucose-6-phosphate dehydrogenase	1	-1.337	1	-1.263	1	-1.585
yecA	SPA0931	hypotheticalprotein	1	-0.0317	0.2431	1.13871	1	0.53287
tyrP	SPA0932	tyrosine-specifictransportprotein	1	0.41504	1	0.58496	1	0
yecH	SPA0933	hypotheticalprotein	0.3147	-0.3803	1	1.28011	1	-0.1699
ftnA	SPA0934	ferritin	0.0582	-0.7655	1	-0.1271	0.2101	-0.6691
-	SPA0935	lipoprotein	0.0106	0.96153	0.8995	0.71543	0.6058	-0.509
yecI	SPA0936	ferritin-like protein	3E-05	-1	0.0346	-0.7225	1	0.31464
araH	SPA0937	intracellular protease/amidase	1	-0.3219	1	0.45943	1	0.26303
-	SPA0938	hypotheticalprotein	1	#DIV/0!	1	#DIV/0!	1	0
otsB	SPA0939	trehalosephosphatase	1	0.73697	0.0017	-1	1	0.45372
otsA	SPA0940	trehalose-6-phosphate synthase	1	0.58496	0.0017	-1.0506	1	0.19555
yecG	SPA0941	hypotheticalprotein	1	-0.0555	0.1575	1.1882	1	0.52484
-	SPA0942	hypotheticalprotein	1	0.152	1	0.95109	1	0.4361
flhD	SPA0943	flagellartranscriptionalactivatorFlhD	0.0841	0.83419	0.7698	0.7152	0.6431	-0.3593

flhC	SPA0944	flagellartranscriptionalactivator	0.0907	0.87591	1	0.49803	0.2868	-0.5425
motA	SPA0945	motilityproteinA	2E-16	1.81762	0.2218	1.08139	1	0.02666
motB	SPA0946	motilityproteinB	1E-09	1.63346	0.4926	0.86207	1	0.22897
cheA	SPA0947	chemotaxis proteinC heA	0.0014	1.47999	1	0.53218	1	0.07204
cheW	SPA0948	purinebindi ngchemotaxisprotein	0.0028	1.09387	0.8214	0.65032	1	-0.1839
cheR	SPA0950	chemotaxisproteinmethyltransferase	1E-14	1.88408	0.1743	1.05504	1	0.19704
cheB	SPA0951	protein-glutamatemethylesterase	7E-11	1.66297	0.4968	0.8657	1	0.45305
cheY	SPA0952	chemotaxisproteinCheY	0.0014	1.14938	1	0.57442	1	0.05367
cheZ	SPA0953	chemotaxisproteinCheZ	0.024	0.90357	1	0.31994	1	0.07573
flhB	SPA0954	flagellar biosyntheticproteinFlhB	1	0.58496	1	0.08746	1	-0.7105
flhA	SPA0955	flagellarbiosynthesisproteinFlhA	1	0.53051	1	0.07215	0.1413	-0.7085
flhE	SPA0956	flagellarproteinFlhE	1	0.67807	1	0.37197	0.018	-0.6823
tnpA	SPA0957	transposasefor insertionsequenceelementIS200	1	-0.152	1	-0.3219	1	-0.8074
-	SPA0958	hypotheticalprotein	1	0.51457	1	-0.8074	1	-0.585
-	SPA0959	hypotheticalprotein	1	0.32193	1	0.41504	1	0.41504
argS	SPA0960	arginyl-tRNAs ynthetase	1	-0.0798	0.0842	-0.9755	0.0006	-1.1783
yecM	SPA0961	hypotheticalprotein	1	-0.4695	1	-0.4361	1	-0.3219
cutC	SPA0962	copperho meostasisprotein	1	0	1	0.57374	1	0.16601
yecP	SPA0963	hypotheticalprotein	0.5554	-0.2838	0.0172	-0.8112	0.2868	-0.6394
yecO	SPA0964	hypotheticalprotein	0.4506	-0.3278	0.0199	-0.7993	0.3643	-0.6335
yecN	SPA0965	hypotheticalprotein	0.0305	-0.5614	0.1953	-0.5122	0.2755	-0.4639
yecE	SPA0966	hypotheticalprotein	1	0.20645	1	-0.074	1	0.63227
yecD	SPA0967	hydrolase	1	0	1	0.21997	0.5114	0.70526
aspS	SPA0968	aspartyl-tRNAs ynthetase	1	0.00468	1	-0.2331	1	0.06542
ntpA	SPA0969	dATPp yrophosphohydrolase	0.8751	-0.2016	0.8274	-0.1685	1	0.14886
yebC	SPA0970	hypotheticalprotein	0.1412	-0.4802	0.9245	-0.213	1	-0.2256
ruvC	SPA0971	crossoverjunctionendodeoxyribonuclease	0.0117	-0.7088	0.5533	-0.2106	0.511	-0.3626
yebB	SPA0972	hypotheticalprotein	1	-0.3219	1	-0.737	1	-0.415
-	SPA0973	hypotheticalprotein	1	#DIV/0!	1	#DIV/0!	1	#DIV/0!
ruvA	SPA0974	Holliday junction DNAhelicase	0.9346	-0.1038	1	0.07595	1	-0.0687
ruvB	SPA0975	HollidayjunctionDNAhelicase	0.6806	-0.2303	1	-0.2345	1	0.04439
yebI	SPA0976	high-affinityzincuptakesystemmembraneprotein	1	0.11548	1	-0.2756	1	-0.628
znuC	SPA0977	high-affinityzincuptakesystemATP -bindingpro tein	1	0	1	0	0.0071	-0.8301
yebL	SPA0978	high-affinityzincuptakesystemperiplasmicbindingprotein	1	0.09163	1	0.26793	1	0.19265
yebA	SPA0979	hypotheticalprotein	1	0.30189	0.628	-0.2767	1	0.23901
msbB	SPA0980	lipidA acyltransferase	1	-0.0651	1	-0.0973	1	-0.213
pykA	SPA0981	pyruvate kinaseA	1	0.60266	0.6965	1.15978	0.8455	0.77215
hexR	SPA0982	hex-regulon repressor	1	0.09516	1	1.27563	1	0.41504
zwf	SPA0983	glucose6 -phosphate dehydrogenase	1	0.09163	1	-0.2044	1	0.03847
edd	SPA0984	6-phosphogluconatedehydratase	1	0.30812	1	0.37197	1	0.79355
eda	SPA0985	hypotheticalprotein	1	0.23447	1	0.21198	1	0.47478
purT	SPA0986	phosphoribosylglycinamideformyltransferase2	1	-0.1255	1	-2.1293	1	-1.585
yebF	SPA0988	hypotheticalprotein	0.4372	-0.2944	6E-05	-1.1979	0.1706	-0.6653
yebE	SPA0989	hypotheticalprotein	0.2383	-0.4191	0.0064	-0.848	1	-0.1538
opdB	SPA0990	oligopeptidase	1	0.20353	0.0327	-0.8625	0.6028	-0.415
exoX	SPA0991	exodeoxyribonucleaseX	0.907	-0.1806	1	0.31836	1	0.26006
-	SPA0992	hypotheticalprotein	1	0.37851	1	0.20645	1	0.58496
holE	SPA0993	DNApo lymeraseIII,thetasubunit	1	-0.1926	1	-0.5025	1	-1.1255

yobA	SPA0994	cation resistanceprotein	0.9282	-0.2298	1	0.06369	1	0.07332
-	SPA0995	cation transporter	1	-0.1059	1	-0.0134	1	0.24393
-	SPA0996	hypotheticalprotein	0.9869	-0.1681	1	-0.0392	1	0.10128
-	SPA0997	hypotheticalprotein	1	0	1	0.41504	1	-0.6781
-	SPA0999	hypotheticalprotein	1	#DIV/0!	1	1	1	0
-	SPA1000	hypotheticalprotein	1	#DIV/0!	1	#NUM!	1	#NUM!
-	SPA1001	hypotheticalprotein	1	#DIV/0!	1	2	1	-0.3219
-	SPA1002	phagei ntegraseprotein	1	#DIV/0!	1	#DIV/0!	1	#DIV/0!
-	SPA1003	hypotheticalprotein	1	#DIV/0!	1	#DIV/0!	1	#DIV/0!
-	SPA1004	hypotheticalprotein	1	-1	1	#NUM!	1	#NUM!
-	SPA1005	hypotheticalprotein	1	-0.415	1	-1	1	-1
yjcS	SPA1006	hydrolase	1	-0.0995	1E-18	-2.257	0.0677	-0.8312
-	SPA1007	hypotheticalprotein	1	-1.0995	1	-1	1	-1
-	SPA1008	hypotheticalprotein	1	-1	1	#NUM!	1	#NUM!
-	SPA1009	hypotheticalprotein	1	-2	1	#NUM!	1	-1
pagO	SPA1010	hypotheticalprotein	1	-1.8745	1	-2.3219	1	-1.585
-	SPA1011	hypotheticalprotein	1	#DIV/0!	1	#DIV/0!	1	#DIV/0!
-	SPA1013	hypotheticalprotein	1	-0.8074	1	-0.9386	1	-1.1699
-	SPA1014	hypotheticalprotein	1	0	1	-1	1	-1.585
-	SPA1015	acetyltransferase	1	-0.6374	1	-1.6439	1	-0.6521
-	SPA1016	hypotheticalprotein	1E-10	-1.2345	1	-0.0875	1	-0.7549
-	SPA1017	hypotheticalprotein	1	-1	1	-0.1926	1	0.19265
sopE2	SPA1018	TypeI II-secretedproteineffector:invasion -associatedprotein	1	0.20163	0.8005	0.72348	0.0731	-0.759
-	SPA1019	hypotheticalprotein	1	-2	1	-1.3785	1	-1.737
pphA	SPA1020	serine/threonineproteinphosphatase1	1	-0.3219	1	-1	1	-1.585
yebW	SPA1021	hypotheticalprotein	1	-0.3626	1	-0.6781	6E-05	-1.1898
-	SPA1022	hypotheticalprotein	1	0.72437	0.354	-0.3276	0.9336	-0.3936
yebU	SPA1023	hypotheticalprotein	1	0.04307	1	-0.5502	1	-0.6374
-	SPA1024	hypotheticalprotein	1	0	0.0508	-0.9551	0.9154	-0.3049
yebS	SPA1025	hypotheticalprotein	1	0.39855	1	-0.0614	1	0.23133
yebR	SPA1026	hypotheticalprotein	0.4957	-0.3732	1	0.19325	1	0.50626
prc	SPA1028	tail-specificprotease	1	-0.1181	0.3587	-0.6612	0.9422	-0.3334
htpX	SPA1029	heatsho ckprotein	0.0422	-0.7421	0.0034	-1.1261	0.1306	-0.6666
-	SPA1030	transporter	1	0	1	-0.5025	1	-0.1069
kdgR	SPA1031	transcriptionalregulatorKdgR	0.1874	-0.4903	1	0.03505	0.506	-0.415
-	SPA1032	hypotheticalprotein	1	0	0.0302	1.078	1	-0.0875
yobG	SPA1033	hypotheticalprotein	0.6865	-0.2141	1	1.11548	1	0.19931
-	SPA1034	hypotheticalprotein	1	-0.1926	1	0.70627	1	-0.4854
yobF	SPA1035	hypotheticalprotein	0.1727	-0.8396	0.9033	-0.4582	1	-0.0237
cspC	SPA1036	colds hock-like proteinC spC	0.474	-0.849	1	-0.552	1	-0.1161
ftsI	SPA1037	penicillin-bindingpro tein	1	0.22239	1	0.25526	1	0.08246
rrmA	SPA1038	rRNAg uanine-N1-methyltransferase	1	-0.0704	1	0.15754	1	-0.3561
yebN	SPA1039	hypotheticalprotein	0.0355	-0.6101	1	-0.4381	1	-0.737
-	SPA1040	hypotheticalprotein	1	0.36257	1	0.80735	1	-0.3785
manZ	SPA1041	phosphotransferaseenzymeII,Dcomponent	1	0.40684	1	0.24949	1	-0.0815
manY	SPA1042	phosphotransferaseenzymeII,Ccomponent	1	0.3318	1	0.39114	1	-0.1489
manX	SPA1043	PTSsys temmannose -specifictransportersubunitIIAB	1	0.47175	0.9939	0.72864	1	0.06926
-	SPA1044	hypotheticalprotein	1	-0.341	1	-0.2801	1	-0.415

yoaE	SPA1045	hypotheticalprotein	1	-0.1605	1	-0.372	1	-0.4406
-	SPA1046	hypotheticalprotein	1	0	1	-1.5025	1	-1.078
sdaA	SPA1047	L-serine deaminase1	0.063	-0.6947	0.1689	-1.1901	0.0036	-1.3083
yeaB	SPA1048	hypotheticalprotein	1	-0.2854	0.007	-0.9198	1	-0.4671
pabB	SPA1049	para-aminobenzoatesynthasecomponentI	1	-0.0375	0.0036	-0.9462	1	-0.4072
yoaH	SPA1050	hypotheticalprotein	0.0357	-0.4953	1	0.29546	0.0156	-0.6612
yoaB	SPA1051	hypotheticalprotein	0.4071	-0.2904	1	0.35364	1	0.23661
yoaA	SPA1052	ATP-dependent helicase	1	0.05247	1	-0.6041	1	-0.263
yeaZ	SPA1053	hypotheticalprotein	1	0.05445	0.523	-0.2388	0.2474	-0.4815
slp	SPA1054	lipoprotein	1	0.07496	1	0	0.349	-0.4268
fadD	SPA1055	long-chain-fatty-acid--CoAl igase	1	0.27009	0.1619	-0.5585	1	-0.3923
rnd	SPA1056	ribonucleaseD	1	-0.0995	1	-1.1699	1	-0.241
minE	SPA1057	cell divisiontopologicalspecificityfactor	1	-0.2145	0.6431	-0.2228	0.6197	-0.3528
minD	SPA1058	septum sitedeterminingprotein	0.9887	-0.2007	1	-0.3219	1	-0.3118
minC	SPA1059	septum sitedeterminingprotein	1	-0.117	0.7519	-0.1886	1	-0.0825
ycgL	SPA1060	hypotheticalprotein	0.546	-0.2908	0.3081	-0.4337	0.6926	-0.3527
ycgM	SPA1061	hydrolase	1	-0.1788	0.2255	-0.5121	0.349	-0.5146
ycgN	SPA1062	hypotheticalprotein	0.246	-0.3859	1	-0.3668	1	-0.5683
-	SPA1063	hypotheticalprotein	1	-0.2996	3E-25	-2.1226	5E-11	-1.4622
-	SPA1064	hypotheticalprotein	0.1602	-0.3926	1	0.32989	1	-0.1668
-	SPA1065	hypotheticalprotein	1	0.48543	1	0.11548	1	0
dsbB	SPA1066	disulfidebondformationproteinB	0.1383	-0.4361	0.1861	-0.5198	0.9737	-0.2568
nhaB	SPA1067	regulatorofintracellularpH;Na+/H+antiporter	1	-0.3388	1	-0.0291	1	0.47917
fadR	SPA1068	fattyaci d-fatty acylresponsiveDNA -bindingpro tein	0.5554	-0.3643	1	0.35386	0.7607	-0.4164
ycgB	SPA1069	hypotheticalprotein	0.7319	0.57191	0.7582	-0.1783	0.6708	-0.4241
dadA	SPA1070	D-aminoaci ddehydrogenase	0.1483	-0.5694	1	0.67807	1	0.27009
dadX	SPA1071	alanine racemase	0.0001	-0.9456	0.4691	0.82491	1	0.14439
ycgO	SPA1072	Na+/H+ exchanger	0.871	0.39366	1	0.0651	1	-0.2089
ycgQ	SPA1073	hypotheticalprotein	1	0.05772	1	-0.1255	1	-0.189
mltE	SPA1074	membrane-boundly ticmureintransglycosylaseE	1	-0.1069	1	-0.7105	1	-0.387
ymgE	SPA1076	hypotheticalprotein	1	-0.415	1	-0.9542	1	-0.7567
treA	SPA1077	trehalase,periplasmic	1	0	0.4529	-0.3529	0.3705	-0.534
-	SPA1078	glutamatedehydrogenase	1	-0.1872	1	-0.6093	1	-0.4235
-	SPA1079	hypotheticalprotein	1	0.58496	1	1.32193	1	0.58496
appB	SPA1080	cytochromeoxidase subunitII	1	0.58496	1	1	1	0.58496
appC	SPA1081	thirdcyto chromeoxidase,subunitI	1	1	1	1	1	1
hyaF	SPA1082	hydrogenase-1operonpro teinHyaF	1	#DIV/0!	1	1	1	#DIV/0!
hyaE	SPA1083	hydrogenase-1operonpro teinHyaE	1	0	1	2	1	#DIV/0!
hyaD	SPA1084	hydrogenase-1operonpro teinHyaD	1	0	1	1.32193	1	#DIV/0!
hyaC	SPA1085	Ni/Fe-hydrogenase1b -typecy tochromesubunit	1	#DIV/0!	1	#DIV/0!	1	#DIV/0!
hyaB	SPA1086	hydrogenase-1largesu bunit	1	1	1	2	1	#DIV/0!
-	SPA1088	hypotheticalprotein	1	-0.3049	1	0.47393	1	0.21412
ychF	SPA1089	ATP/GTP-bindingpro tein	0.0072	-0.7279	0.0008	-1.2778	0.0007	-1.1559
pth	SPA1090	peptidyl-tRNAh ydrolase	1	-0.2895	1	-0.2928	0.0314	-0.7235
ychH	SPA1091	hypotheticalprotein	1	0.02018	0.7744	0.77761	0.9336	-0.2313
ychM	SPA1092	sulfatetransporter	1	-0.1699	1	-0.8875	1	-0.415
prsA	SPA1093	ribose-phosphatepyrophosphokinase	0.8984	-0.366	1	-0.4397	1	-0.3178
ipk	SPA1094	isopentenylmonophosphatekinase	1	-0.0525	0.8862	-0.1091	1	-0.0753

hemM	SPA1095	outer membranelipoprotein	1	0.20482	1	0.19265	1	0.19669
hemA	SPA1096	glutamyl-tRNAre ductase	0.9314	-0.1916	1	0.16909	1	-0.2744
prfA	SPA1097	peptidec hainreleasefactor1(RF -1)	1	-0.0931	0.477	-0.4945	1	0
hemK	SPA1098	protoporphyrinogenoxidaseHemK	1	-0.0412	0.0832	-0.7225	1	-0.0344
sirC	SPA1099	regulator	1	-0.0506	1	-0.4005	1	0.33442
ychA	SPA1100	regulator	1	0.0581	0.2128	-0.4764	1	0.26303
kdsA	SPA1101	2-dehydro-3-deoxyphosphooctonatealdolase	0.3414	-0.4708	1	-0.237	1	-0.1339
chaA	SPA1102	calcium/protonantiporter	1	-1.3985	1	-1.585	1	-1
ychN	SPA1104	hypotheticalprotein	1	-0.507	1	0.66297	1	-0.152
ychP	SPA1105	invasin	1	0.28951	1	0.34792	1	0.16993
narL	SPA1106	nitrate/nitriteresponseregulatorproteinNarL	1	0.02137	0.8559	-0.1098	1	0.11136
narX	SPA1107	nitrate/nitritesensorproteinNarX	1	-0.078	0.4971	-0.2583	1	0.2303
narK	SPA1108	nitritee xtrusionprotein(nitritefacilitator)	1	0	1	#DIV/0!	1	#DIV/0!
narG	SPA1109	respiratorynitratereductase1subunitalpha	1	0.46949	1	1	1	1.16993
narH	SPA1110	respiratorynitratereductase1subunitbeta	1	0.43296	1	0.58496	1	1.16993
narJ	SPA1111	respiratorynitratereductase1subunitdelta	1	0.29956	1	0.54057	1	0.91754
narI	SPA1112	respiratorynitratereductase1 subunitg amma	1	-0.0931	1	0	1	0.36257
-	SPA1113	hypotheticalprotein	1	-0.1375	1	0.28011	1	0
-	SPA1114	-	1	-0.3049	1	#DIV/0!	1	#DIV/0!
-	SPA1115	-	1	-0.1312	1	1	1	0
-	SPA1116	-	1	-0.1699	1	0.58496	1	0.58496
-	SPA1117	-	1	-0.0995	1	0	1	0.41504
-	SPA1118	-	1	-0.1699	1	0.19265	1	0.41504
tyrT	SPA1119	TyrtRN A	1	-0.1409	1	0.07973	0.9337	-0.2895
tyrT	SPA1120	TyrtRN A	1	-0.1587	0.9385	-0.0755	0.816	-0.3061
-	SPA1121	hypotheticalprotein	1	-0.3219	1	0.58496	1	-0.152
purU	SPA1122	formyltetrahydrofolatedeformylase	1	-0.0614	1	-0.0566	0.775	-0.3692
ychJ	SPA1123	hypotheticalprotein	0.3551	-0.3785	1	-0.1155	1	-0.273
ychK	SPA1124	hypotheticalprotein	1	-0.1155	0.8274	-0.1613	1	-0.1182
hnr	SPA1125	regulatoryprotein	1	-0.0555	0.588	-0.3219	1	-0.0682
galU	SPA1126	glucose-1-phosphate uridylyltransferase	1	-0.0882	0.8953	-0.329	1	0.24576
hns	SPA1127	DNA-bindingp rotein(histone -like proteinHlp -II)	1	-0.5904	1	-0.0811	1	-0.5
tdk	SPA1128	thymidinekinase	1	-0.0931	0.9646	-0.078	0.0576	-0.6262
adh	SPA1129	alcoholdehydrogenase	1	0.82177	1	0.44535	1	0.45998
ychE	SPA1130	hypotheticalprotein	1	-0.585	1	-0.5305	1	-0.5305
oppA	SPA1131	periplasmicoligopeptide -bindingpro tein	0.1295	-0.6804	0.6902	-0.9016	0.725	-0.4883
oppB	SPA1132	oligopeptidetransportsystempermeaseproteinOppB	5E-05	-1.0247	0.0061	-1.0641	0.012	-0.8657
oppC	SPA1133	oligopeptideABCtransportermembraneprotein	0.0009	-0.8863	0.0325	-0.8793	1	-0.6688
oppD	SPA1134	oligopeptidetransport ATP-binding proteinOppD	1	-0.567	0.2557	-0.6769	0.144	-0.6919
oppF	SPA1135	oligopeptidetransportATP -binding proteinOppF	1	-0.509	0.0938	-0.7521	0.2616	-0.6294
-	SPA1136	membranetransportprotein	1	-0.7004	1	-0.5361	1	-0.6674
yciU	SPA1137	hypotheticalprotein	1	-0.2283	1	0.09954	1	-0.3785
cls	SPA1138	cardiolipinsynthetase	1	-0.2801	1	-0.1926	1	-0.152
yciI	SPA1139	hypotheticalprotein	0.0339	-0.6057	0.0155	0.97654	1	0.23266
tonB	SPA1140	TonBpro tein	1	0.8365	2E-15	-1.7965	1	-1.5361
yciA	SPA1141	acyl-coAh ydrolase	1	-0.2345	1	-0.585	1	-0.433
ispZ	SPA1142	intracellularseptationprotein	0.1448	-0.449	0.0004	-1.0235	0.4124	-0.3923
yciC	SPA1143	hypotheticalprotein	0.0339	-0.613	0.0041	-1.1388	0.1907	-0.7258

-	SPA1144	hypotheticalprotein	0.0033	-0.759	2E-10	-1.663	6E-05	-1
ompW	SPA1145	outerme mbraneprotein	1	0.37294	0.1907	1.66021	0.8707	0.7877
-	SPA1146	hypotheticalprotein	1	-1	1	0.45943	7E-45	2.67807
yciE	SPA1147	hypotheticalprotein	1	#DIV/0!	1	0.87447	1	3.29278
yciF	SPA1148	hypotheticalprotein	1	#DIV/0!	0.2698	0.95109	6E-89	3.04731
yciG	SPA1149	hypotheticalprotein	1	-1	0.3541	0.85798	9E-11	1.8625
trpA	SPA1150	tryptophan synthasesubunitalpha	1	0.08573	0.657	-0.2763	1	-0.0275
trpB	SPA1151	tryptophan synthasesubunitbeta	1	0.10128	0.6418	-0.2196	1	0.19704
trpC	SPA1152	indole-3-glycerolphosphatesynthase	1	0	1	-0.0704	1	0.67807
trpD	SPA1153	anthranilatesynthasecomponentII;anthranilatephosphoribosyltransferase	1	-0.3219	1	-0.6374	1	0
trpE	SPA1154	anthranilatesynthasecomponentI	1	-0.3219	1	-0.6781	1	0.32193
trpH	SPA1155	hypotheticalprotein	1	0.03519	1	0.16046	1	0.08881
yciO	SPA1156	hypotheticalprotein	1	0.30023	1	0.16711	1	0.2071
yciL	SPA1157	pseudouridinesynthase	1	0.03684	1	-0.0242	1	-0.318
btuR	SPA1158	COB(I) alaminadenosyltransferase	0.155	-0.4458	1	0.03171	1	-0.3418
yciK	SPA1159	hypotheticaloxidoreductase	0.2893	-0.3847	1	-0.0871	0.53	-0.4036
sohB	SPA1160	protease	0.4824	-0.263	1	-0.0857	1	-0.0687
yciN	SPA1161	hypotheticalprotein	0.0786	-0.4938	1	0.62678	0.6211	-0.3339
topA	SPA1162	DNAto poisomeraseI,omegaproteinI	1	0.02076	0.1283	-0.737	1	-0.1822
cysB	SPA1163	cysre gulontranscriptionalactivator	1	-0.1024	0.1046	-0.8249	0.0156	-0.8858
acnA	SPA1164	aconitatehy dratase1	1	0.39899	1	0.23199	0.5691	0.8436
ribA	SPA1165	GTPc yclohydrolaseII	1	-0.0571	1	0.61626	1	-0.0359
pgpB	SPA1166	phosphatidylglycerophosphataseB	1	0	1	-0.2224	1	-0.1069
yciS	SPA1167	hypotheticalprotein	0.3406	-0.2932	1	0.05795	0.8002	-0.3064
yciM	SPA1168	hypotheticalprotein	1	-0.0753	1	0.11321	1	-0.237
pyrF	SPA1169	orotidine-5'-Pdeca rboxylase	1	0.04307	1	-0.7105	1	-0.9411
yciH	SPA1170	translationinitiaitonfactor	1	-0.1699	1	-0.9069	1	-0.9175
osmB	SPA1171	osmoticallyinduciblelipoproteinB	1	0.21573	0.0003	-1.114	0.467	-0.3915
yciT	SPA1172	regulatoryprotein	0.5865	-0.2568	0.4793	-0.3388	0.8351	-0.3312
-	SPA1173	hypotheticalprotein	0.0004	-0.7744	0.5381	-0.2937	0.9337	-0.1462
yciR	SPA1174	hypotheticalprotein	1	-0.3479	1	-0.8625	1	-0.737
rnb	SPA1175	exoribonucleaseII	1	0.03653	0.0103	-1.3001	0.4973	-0.477
yciW	SPA1176	hypotheticalprotein	1	0.26303	0	-4.2479	1	-3
fabI	SPA1177	enoyl-ACP reductase	0.1724	-0.6521	0.2351	-0.7168	0.3488	-0.5543
-	SPA1179	hypotheticalprotein	1	-0.4854	1	2.52356	1	1.37851
sapF	SPA1180	peptidetra nsportsystemATP -bindingp roteinSapF	0.8878	-0.1155	0.0026	-0.9368	1	-0.3388
sapD	SPA1181	peptide transports ystemATP -bindingp roteinSapD	1	0.05063	0.0409	-0.7244	1	-0.1013
sapC	SPA1182	peptidetra nsportsystempermeaseSapC	1	0.15754	1	-0.5146	1	-0.1444
-	SPA1183	integrase	1	#DIV/0!	1	0	1	-1.585
-	SPA1186	hypotheticalprotein	1	#DIV/0!	1	-1	1	-1.585
-	SPA1187	hypotheticalprotein	1	#DIV/0!	1	#DIV/0!	1	#DIV/0!
-	SPA1188	hypotheticalperiplasmicprotein	1	-1	1	#NUM!	1	#NUM!
-	SPA1190	hypotheticalprotein	1	0	1	0	1	0
sapB	SPA1191	peptidetra nsportsystempermeaseSapB	1	-0.0671	1	-0.613	1	0.06413
sapA	SPA1192	peptidetra nsportperiplasmicproteinSapA	1	0.14086	1	-0.0375	1	-0.0291
pspF	SPA1193	pspoperon transcriptionalactivatorPspF	1	-0.4361	1	-0.1468	1	0.35364
pspA	SPA1194	phages hockproteinA	0.4344	-0.3281	0.001	-1.0247	1E-06	-1.3496
pspB	SPA1195	phages hockproteinB	1	-0.3103	4E-05	-0.9792	7E-07	-1.3038

pspC	SPA1196	phages hockproteinC	1	-0.2035	0.0007	-0.9419	5E-06	-1.1605
pspD	SPA1197	phages hockproteinD	1	-0.241	1	-0.8541	1	-1.1375
pspE	SPA1198	phages hock proteinE	0.0282	-0.571	0.0028	1.49068	0.6176	0.70109
ycjX	SPA1199	ATP-bindingpro tein	1	0	1	0.18641	1	-0.2775
ycjF	SPA1200	hypotheticalprotein	1	-0.2479	1	-0.2295	1	-0.1031
tyrR	SPA1201	transcriptionalregulatoryproteinTyrR	1	0.18948	1	0.10069	1	-0.179
tpx	SPA1202	thiolpe roxidase	1	-0.4001	1	-0.1629	0.831	0.69384
ycjG	SPA1203	mandelateracemase	0.8279	-0.143	1	-0.3626	0.6655	-0.3923
ycjI	SPA1204	hypotheticalprotein	1	-0.4854	1	0	1	-0.4739
mppA	SPA1205	periplasmicmurein peptide-bindingpro teinMppA	1	-0.0864	1	0.22659	1	0.08573
-	SPA1207	transcriptionalregulator	1	0.1375	1	0.19265	1	-0.2224
-	SPA1208	oxidoreductase	0.1356	0.79751	0.1445	-0.5045	1	-0.0297
yjgI	SPA1209	oxidoreductase	1	-0.3785	1	-1	1	-1
-	SPA1210	transcriptionalregulator	1	0.10692	1	0	1	-0.3785
-	SPA1211	lipoprotein	1E-06	1.33342	1	1.61471	1	1.16227
-	SPA1213	transcriptionalregulator	1	#DIV/0!	1	#DIV/0!	1	#DIV/0!
-	SPA1214	lipoprotein	1	#DIV/0!	1	#DIV/0!	1	#DIV/0!
-	SPA1216	hypotheticalprotein	1	0	1	#NUM!	1	0
-	SPA1217	thiolpe roxidase	1	-0.737	1	0	1	-0.585
-	SPA1218	hypotheticalprotein	1	-0.1926	1	0	1	0
-	SPA1219	hypotheticalprotein	1	-0.152	1	0	1	0
-	SPA1220	DNA-bindingp rotein	1	-0.415	1	-0.263	1	-0.737
ynaI	SPA1221	hypotheticalprotein	0.094	-0.48	1	-0.2224	1	-0.7997
ynaJ	SPA1222	hypotheticalprotein	0.3495	-0.44	1	-0.0417	0.9101	-0.432
ydaA	SPA1223	hypotheticalprotein	1	0.1977	1	0.69727	1	0.44688
fnr	SPA1224	fumarate andnitratereduction regulatoryprotein	0.5373	-0.4142	0.6346	-0.5342	0.0195	-1.1159
ogt	SPA1225	O6-methylguanine-DNA-alkyltransferase	0.4081	-0.2685	1	0.28798	1	0.04182
ydaL	SPA1226	hypotheticalprotein	1	-0.2283	0.0113	-0.9956	8E-06	-1.4353
-	SPA1228	membrane transportpro tein	1	0.16601	1	-0.3293	1	-0.1829
-	SPA1229	-	1	0	2E-10	-1.6503	0.0315	-0.8931
dbpA	SPA1230	ATP-dependent RNAhelicase,stimulatedby23SrRNA	1	-0.3219	1	-1.4525	1	-0.8413
ydaO	SPA1231	hypotheticalprotein	0.9314	-0.1069	0.4115	-0.3344	0.1642	-0.6439
-	SPA1232	hypotheticalprotein	1	#NUM!	1	#DIV/0!	1	#DIV/0!
-	SPA1233	multidrug transporter	1	-0.7885	1	-0.5475	1	-0.3219
ynaF	SPA1234	hypotheticalprotein	1	-0.2733	1	0.7764	1	0.60733
-	SPA1235	-	1	#DIV/0!	1	#DIV/0!	1	#DIV/0!
nifJ	SPA1236	pyruvate-flavodoxinoxidoreductase	1	0.58496	1	-0.1497	1	-0.0194
-	SPA1237	hypotheticalprotein	0.57	-0.2943	0.6439	-0.2147	0.0009	-0.8931
hslJ	SPA1238	heatsho ckprotein	2E-07	1.35364	0.0054	1.36257	0.767	0.59904
ldhA	SPA1239	D-lactatede hydrogenase	1	0	0.0215	-0.7843	0.0143	-1
ydbH	SPA1240	hypotheticalprotein	1	-0.0931	1	-0.5406	1	-0.4695
ynbE	SPA1241	lipoprotein	1	-0.3561	1	-0.4436	1	-0.2295
ydbL	SPA1242	hypotheticalprotein	1	0	1	-0.6027	1	-0.5377
-	SPA1243	hypotheticalprotein	1	-0.1255	1	-0.663	1	-0.6057
acpD	SPA1244	acylca rrierproteinphosphodiesterase	1	-0.3626	1	0.51457	1	0.38702
hrpA	SPA1245	ATP-dependent helicaseHrpA	1	0.30256	0.7739	-0.2433	1	-0.0995
ydcF	SPA1246	innerme mbrane protein	1	0	1	0.05445	1	-0.4389
ydcG	SPA1247	hypotheticalprotein	0.0926	-0.5443	0.0467	-0.8171	0.2032	-0.6428

-	SPA1248	hypotheticalprotein	1	#DIV/0!	1	#NUM!	1	#DIV/0!
-	SPA1249	glycolateoxidase	1	#NUM!	1	#NUM!	1	#DIV/0!
aac	SPA1250	aminoglycoside6' -N-acetyltransferase	1	0.09954	1	0.05063	1	-0.0473
sgcR	SPA1251	regulatoryprotein	1	-0.1155	1	0.13327	1	0.16993
-	SPA1252	ribulose-5-phosphate3 -epimerase	1	0.18057	1	0.08746	1	0
sgcA	SPA1253	phosphotransferaseenzyme	1	0.09622	1	0.1375	1	-0.1553
sgcQ	SPA1254	hypotheticalprotein	1	0.09311	1	0.73697	1	-0.2065
sgcC	SPA1255	phosphotransferaseenzyme	1	-0.0931	1	0.58496	1	-0.585
-	SPA1256	phosphotransferaseenzyme	1	-0.2345	1	0.60039	1	-0.5146
-	SPA1257	hypotheticalprotein	1	-0.507	1	0.36257	1	-0.5594
rimL	SPA1258	ribosomal-protein-serine acetyltransferase	0.1099	0.77961	1	0.22077	1	-0.0483
ydcK	SPA1259	transferase	1	-0.152	1	-0.737	1	-0.6781
tehA	SPA1260	telluriteresistanceproteinTehA	1	0.03653	1	-0.6521	1	-0.3785
tehB	SPA1261	telluriteresistanceproteinTehB	0.7463	-0.2272	0.2535	-0.4352	0.0743	-0.6428
-	SPA1262	lipoprotein	0.4284	-0.404	0.4802	-0.6538	1	-0.263
ydcP	SPA1264	peptidase	1	-0.2016	1	-1.2224	1	-1.263
yncJ	SPA1265	hypotheticalprotein	1	#NUM!	1	0	1	-1.585
ugtL	SPA1267	hypotheticalprotein	1	#DIV/0!	1	#DIV/0!	1	#DIV/0!
-	SPA1268	hypotheticalprotein	1	#DIV/0!	1	#DIV/0!	1	#DIV/0!
pcgL	SPA1269	D-alanyl-D-alanine dipeptidase	1	-0.1069	1	-1	1	-0.9386
ydcR	SPA1270	regulatoryprotein	1	-0.0544	1	-0.7705	1	-0.6781
ydcW	SPA1271	aldehyde dehydrogenase	1	0	1	-0.9652	1	-0.926
ydcX	SPA1272	innerme mbraneprotein	1	-0.1174	0.5913	0.67377	1	-0.1092
srfC	SPA1273	virulenceeffectorprotein	2E-05	1.34239	0.5065	0.91312	1	-0.2021
srfB	SPA1274	virulenceeffectorprotein	0.0044	1.02237	1	0.5961	1	-0.3004
srfA	SPA1275	virulenceeffectorprotein	1	0.85561	1	0.52763	1	-0.0444
ydcY	SPA1276	hypotheticalprotein	0.5981	-0.1375	1	0.82312	1	-0.1699
ydcZ	SPA1277	hypotheticalprotein	1	-0.0931	1	0.68589	1	0.35614
yncA	SPA1278	acetyltransferase	0.7843	-0.139	1	0.57619	1	0.42269
yncB	SPA1279	NADP-dependento xidoreductase	1	0.18641	0.0116	-0.872	0.3319	-0.5497
yncC	SPA1280	regulatoryprotein	1	0.58496	3E-23	-1.8898	1	-0.1375
yncD	SPA1281	TonB-dependentre ceptor	1	0	3E-09	-1.6323	1	-0.7004
-	SPA1282	ATP-bindingpro tein	1	-0.1255	1	-0.4263	1	-0.6464
-	SPA1283	lipoprotein	1	0	1	0.58496	1	0
ansP	SPA1284	L-asparagine permease	1	-0.6374	1	-0.737	1	-0.3626
-	SPA1285	hypotheticalprotein	0.6124	-0.3138	1	0.36528	1	0.1822
nhoA	SPA1286	N-hydroxyarylamineO -acetyltransferase	1	0	1	-0.0506	1	-0.3219
yddE	SPA1287	hypotheticalprotein	0.7166	-0.2078	1	-0.0995	1	0
narV	SPA1288	nitratere ductase2subunitgamma	1	#DIV/0!	1	-1.8074	1	-1.7655
narY	SPA1290	respiratorynitratereductase2subunitbeta	1	0	1	-2	7E-22	-2
narZ	SPA1291	respiratorynitratereductase2subunitalpha	1	0.36257	1	-2.237	1	-1.9668
narU	SPA1292	nitritee xtrusionprotein	1	0	1	-3.8074	1	-2
-	SPA1293	regulatoryprotein	1	-0.9005	1	-0.7521	1	-1.1605
smvA	SPA1294	methyl viologenresistanceproteinSmvA	1	-1.2224	1	-1.8745	1	-1.585
-	SPA1295	hypotheticalprotein	1	#DIV/0!	1	0.48063	1	-0.5607
nmpC	SPA1296	outerme mbraneprotein	1	#DIV/0!	1	0.21415	1	-0.5473
yddG	SPA1297	permease	1	#DIV/0!	1	-1	1	-1.585
fdnG	SPA1298	molybdopterinoxidoreductase	1	#DIV/0!	1	1.16227	1	0.40054

fdnH	SPA1299	formatedehydrogenase -N,Fe -Ssubunit beta	1	#DIV/0!	0.137	1.03953	1	0.60266
fdnI	SPA1300	formatedehydrogenase -N,cy tochromeB556(Fdn)subunitgamma	1	#DIV/0!	0.8119	0.69302	1	0.152
adhP	SPA1301	alcoholdehydrogenase	8E-07	1.43792	1	-0.2728	1	-0.4617
sfcA	SPA1302	NAD-linked malicenzyme;malateoxidoreductase	1	-0.1709	0.523	-0.6366	1	-0.0882
rpsV	SPA1303	30Sribos omalproteinS22	1	0.07678	1	0.13663	0.6225	-0.4117
yddX	SPA1304	hypotheticalprotein	1	0	1	-0.9329	1	0.77052
osmC	SPA1305	osmoticallyinducibleproteinC	1	0.32193	0.0162	-0.9837	0.1073	-0.7623
hlyE	SPA1306	hemolysinHlyE	1	-0.1375	1	-0.8365	1	-0.4764
-	SPA1308	hypotheticalprotein	2E-42	2.36484	1E-82	3.10434	0.0006	1.29123
-	SPA1309	hypotheticalprotein	1	0	1	-1.9475	1	-0.3219
-	SPA1310	hydrolase	1	0.41504	1	-1.1155	1	0.49957
-	SPA1311	hydrolase	1	0	0.008	-1.0265	1	0.56828
-	SPA1312	glycogendebranchingprotein	1	0.11548	0.156	-0.6114	1	0.42968
-	SPA1313	aminotransferase	1	-0.387	1	0	1	-0.6781
-	SPA1315	hypotheticalprotein	1	0	1	#DIV/0!	1	#DIV/0!
-	SPA1316	regulatoryprotein	1	-0.8745	1	0	1	0.58496
hyaA2	SPA1317	uptakehy drogenasesmallsubunit	0.0618	-0.5619	0.3339	0.89616	1	1
hyaB2	SPA1318	hydrogenase-1largesu bunit	1	-0.585	0.663	0.76553	1	0.85982
hyaC2	SPA1319	Ni/Fe-hydrogenase1b -typecy tochromesubunitHyaC2	1	-0.152	1	0.61005	1	0.44057
hyaD2	SPA1320	hydrogenase1maturationprotease	1	0.18286	0.4802	0.82491	1	0.45686
hyaE2	SPA1322	hydrogenase-1operonpro teinHyaE2	1	0.20945	0.4968	0.87685	0.9414	0.59516
hyaF2	SPA1323	hydrogenase-1operonpro teinHyaF2	1	0.08746	0.7003	0.79564	0.349	0.7885
-	SPA1324	ATP/GTP-bindingpro tein	1	0.1375	1	0.73697	1	0.82597
-	SPA1325	hydrogenase	1	#DIV/0!	1	0.80735	1	0.7885
-	SPA1326	outerme mbraneprotein	1	3.54432	0	4.09592	1	4.05889
-	SPA1327	hypotheticalprotein	0.0019	1.10309	1	1.24793	1	1.05063
-	SPA1328	hypotheticalprotein	1	0.67807	1	-0.8931	1	-0.2895
yneG	SPA1329	hypotheticalprotein	1	-0.142	1	0.26303	1	-0.5185
yneH	SPA1330	hypotheticalprotein	1	0	1	0.35364	1	0.09954
yneI	SPA1331	aldehyde-dehydrogenase	1	0.848	0.1745	1.08489	0.2755	0.88753
yneJ	SPA1332	regulatoryprotein	1	-0.1699	1	0	1	-0.1699
ydeA	SPA1333	membranetransportprotein	1	0.36257	1	-0.848	1	-0.3219
marC	SPA1334	hypotheticalprotein	0.2225	0.67807	1	0.46566	1	0.28379
marR	SPA1335	multipleantibioticresistanceproteinMarR	5E-07	1.34792	4E-15	2.20716	4E-14	2.04532
marA	SPA1336	multipleantibioticresistanceproteinMarA	2E-10	1.59694	3E-06	1.83206	2E-09	1.86894
marB	SPA1337	multipleantibiotic resistanceproteinMarB	1	1.48543	9E-10	1.78427	9E-12	1.91289
ydeE	SPA1338	hypotheticalprotein	1	0.22239	2E-10	1.76553	2E-14	2.01886
-	SPA1339	hypotheticalprotein	1	-0.9175	1	-0.3985	1	-0.4948
ydeI	SPA1340	hypotheticalprotein	1	0.152	0.0006	-1.0952	0.3833	-0.4266
ydeJ	SPA1341	hypotheticalprotein	1	-0.585	1	-1.585	1	-0.2224
-	SPA1342	hypotheticalprotein	1	0	1	0.6256	3E-13	2.01057
dcp	SPA1343	dipeptidylcarboxypeptidaseII	1	-0.1096	1	-0.1561	1	0.0902
ydfG	SPA1344	oxidoreductase	1	0.36257	1	0.43108	0.4806	0.74454
ydfH	SPA1345	regulatoryprotein	1	0.1375	1	0.46778	1	0.15417
ydfZ	SPA1346	hypotheticalprotein	0.254	0.64599	4E-12	2.20336	0.0026	1.24537
ydfI	SPA1347	mannitoldehydrogenase	1	-0.3049	1	-0.585	1	-0.7776
ydfJ	SPA1348	membranetransportprotein	1	-1.1926	1	-1	1	#NUM!
rspB	SPA1349	dehydrogenase	1	-0.4594	1	-1	1	-1

rspA	SPA1350	starvationsensingproteinRspA	1	-0.8074	1	-0.415	1	-1.3219
ynfA	SPA1351	hypotheticalprotein	1	0	1	-1	1	-1
ynfB	SPA1352	hypotheticalprotein	1	-0.1258	1	0.32193	1	0.07263
speG	SPA1353	spermidineN1 -acetyltransferase	1	-0.0181	1	0.43531	1	0.34792
ynfC	SPA1354	hypotheticalprotein	1	-0.415	1	0	1	-0.3219
ynfD	SPA1355	outerme mbraneprotein	1	-0.0732	1	-0.0165	1	-0.2213
-	SPA1356	putativeanaerobicdimethylsulfoxidereductasesubunitA	0.6784	0.80509	0.0493	1.5536	0.0685	1.2735
dmsB	SPA1357	anaerobicdimethylsulfoxidereductasesubunitB	2E-05	1.29278	0.0067	1.40988	6E-08	1.65992
-	SPA1358	dimethyl sulfoxidereductasesubunit	0.227	0.76296	0.3119	0.89308	0.0007	1.41504
ynfI	SPA1359	hypotheticalprotein	1	0.44859	1	0.48543	0.2381	0.89812
-	SPA1360	ABCtra nsportermembraneprotein	1	0	1	-1.3785	1	1
-	SPA1361	ABCtra nsporter substrate-bindingpro tein	1	1	1	-1	1	0.93289
-	SPA1362	ABCtra nsportermembraneprotein	1	1	1	-0.9386	1	0.77761
-	SPA1363	ABCtra nsporterATP -bindingp rotein	1	0.73697	0.0548	-0.7036	1	0.39855
ynfK	SPA1365	dethiobiotinsynthetase	0.0032	-0.7737	1	0.55639	1	-0.3626
mlc	SPA1366	regulatoryprotein	1	-0.2996	1	0.43296	1	-0.1333
ynfL	SPA1367	regulatoryprotein	1	0.16993	1	0	1	-0.152
ynfM	SPA1368	membranetransportprotein	3E-166	3.07529	2E-15	2.34958	3E-32	2.48543
asr	SPA1369	stress response protein	1	-0.4475	1	0.32193	1	0.32193
-	SPA1370	hypotheticalprotein	1	-0.273	1	-0.4021	1	-0.6919
ydgF	SPA1372	hypotheticalprotein	0.0018	1.10362	1E-09	-1.3103	1	-0.6974
-	SPA1373	hypotheticalprotein	0.8318	0.50619	0.0012	-1.0525	0.0049	-0.9786
-	SPA1374	hypotheticalprotein	1	-0.152	1	-0.848	1	-0.263
pntB	SPA1375	pyridine nucleotidetranshydrogenasesubunit -beta	0.0765	-0.6764	0.031	-0.8528	0.7319	-0.3446
pntA	SPA1376	pyridine nucleotidetranshydrogenasesubunit -alpha	0.6371	-0.468	0.6659	-0.5634	1	-0.1719
ydgH	SPA1377	hypotheticalprotein	0.7744	-0.3204	1	-0.194	1	-0.2828
ydgI	SPA1378	aminoaci dpermease	1	-1.3219	1	-0.415	1	-1.8074
ydgC	SPA1379	hypotheticalprotein	1	0	1	-0.737	1	-0.415
rstA	SPA1380	two-componentresponse regulator	2E-06	-1.1113	0.0397	-0.628	0.0001	-1.1293
ompN	SPA1382	outerme mbraneprotein	1	-0.5025	1	-0.1155	1	0.48543
-	SPA1383	hypotheticalprotein	1	-0.6781	1	-1.3219	1	-2
rstB	SPA1384	twocom ponentsensorkinase	1	-0.3219	1	-0.8745	1	-0.848
tus	SPA1385	DNAre plicationterminussite -bindingp rotein;DNAsequence -specificcontrahelicase	1	-0.9005	1	-1.0704	1	-0.415
fumC	SPA1386	fumarate hydrataseclassII	1	0.43328	1	0.40009	1	0.17796
fumA	SPA1387	Fumarateh ydrataseclassI,aerobic	1	0.38529	1	0.47364	1	0.52284
manA	SPA1388	mannose-6-phosphate isomerase	0.4314	-0.3388	0.4609	-0.3677	1	-0.1054
ydgA	SPA1389	hypotheticalprotein	0.7474	-0.263	0.2926	-0.7004	1	-0.275
ydgJ	SPA1391	oxidoreductase	1	-0.1799	0.3741	-0.5031	0.902	-0.2735
ydgT	SPA1392	hypotheticalprotein	0.0093	-0.6702	0.0237	-0.6781	0.0788	-0.532
ydgK	SPA1393	hypotheticalprotein	0.0994	-0.5305	0.3293	-0.4281	0.0399	-0.6719
-	SPA1394	hypotheticalprotein	0.4863	-0.3344	0.0006	-1.0931	0.0146	-0.7442
ydgM	SPA1395	ferredoxin-like protein,cytoplasmicmembrane	1	-0.2157	1	-0.9511	1	-0.3785
-	SPA1396	NADH reducingdehydrogenase	1	-0.1481	1E-06	-1.4475	1	-0.628
ydgO	SPA1397	hypotheticalprotein	1	-0.7045	1	-1.2955	1	-0.848
ydgP	SPA1398	hypotheticalprotein	1E-05	-1.0473	0.0168	-0.7618	1	-0.6027
ydgQ	SPA1399	hypotheticalprotein	5E-05	-0.9827	0.0319	-0.663	1	-0.6215
nth	SPA1400	endonucleaseIII	0.0004	-0.866	1	0	1	-0.166
ydgR	SPA1401	proton/oligopeptidesymporter	0.2485	-0.5434	6E-06	-1.5981	0.1242	-0.727

gst	SPA1402	glutathioneS -transferase	1	0.28453	0.1836	1.22239	1	0.39098
pdxY	SPA1403	pyridoxaminekinase	1	0.35147	0.1266	-0.6308	1	-0.152
tyrS	SPA1404	tyrosyl-tRNAs ynthetase	1	-0.1359	0.7953	-0.5807	1	-0.1513
pdxH	SPA1405	pyridoxamine5' -phosphate oxidase	1	0.19052	1	0.3505	1	0.2783
ydhA	SPA1406	lipoprotein	1	0.22827	1	0.51847	1	0.3523
ydhH	SPA1407	hypotheticalprotein	1	0	1	-0.3985	1	-0.0589
slyB	SPA1408	outerme mbranelipoproteinSlyB	0.0902	-0.5085	0.5298	-0.3108	0.2755	-0.5377
slyA	SPA1409	transcriptionalregulator	1	-0.0171	1	0.27694	0.4986	-0.423
ydhI	SPA1410	hypotheticalprotein	1	-0.6521	1	-0.263	1	-0.2065
ydhJ	SPA1411	HlyD-familyprotein	1	-0.3626	1	-0.7885	1	-0.6919
-	SPA1412	hypotheticalprotein	1	-0.1926	1	-1.3219	1	-0.263
sodC	SPA1413	copper-zincs uperoxidedismutase	1	0.02237	0.0024	-1.0372	0.0397	-0.7766
ydhF	SPA1414	oxidoreductase	1	-0.0465	0.406	0.95025	1	0.20163
ydhL	SPA1415	hypotheticalprotein	1	-0.585	1	-1.0995	1	-0.8625
ydhM	SPA1416	TetR-familytranscriptionalregulator	0.0308	0.87447	1	0.56704	1	0.14585
nemA	SPA1417	N-ethylmaleimidereductase	0.3948	0.80468	1	0.24311	1	-0.0926
gloA	SPA1418	lactoylglutathionelyase	1	0.10026	1	0.15886	1	-0.0149
rnt	SPA1419	ribonucleaseT	0.9889	-0.0946	0.4549	-0.3591	0.054	-0.8343
ydhD	SPA1420	hypotheticalprotein	0.4123	-0.4072	0.4028	-0.8932	0.0938	-0.8451
ydhO	SPA1421	hypotheticalprotein	1	0.26919	0.0139	-0.737	1	-0.4623
sodB	SPA1422	superoxide dismutase	1	0.05793	0.606	0.88897	1	0.56483
purR	SPA1423	purinenucl eotidesynthesisrepressor	0.0574	-0.5525	1	-1.826	1	-1
ydhB	SPA1424	transcriptionalregulator	1	-0.3626	1	0	1	-0.263
ydhC	SPA1425	integral membranetransportprotein	1	0.54749	1	-0.4475	1	-0.2283
cfa	SPA1426	cyclopropane-fatty-acyl-phospholipidsynthase	7E-06	1.38391	1	0.03324	1	0.50589
ribE	SPA1427	riboflavinsynthasesubunitalpha	1	-0.2382	1	-0.3219	1	-0.4525
ydhE	SPA1428	hypotheticalprotein	0.0003	-0.889	6E-21	-2.0919	8E-14	-1.7105
-	SPA1429	ValtRN A	1	-1.0875	1	-1.4594	1	-2
-	SPA1430	ValtRN A	1	-0.7885	1	-0.263	1	-1.415
ssaU	SPA1431	typeIII secretionprotein	1	#NUM!	1	#NUM!	1	#NUM!
ssaT	SPA1432	typeIII secretionprotein	1	#DIV/0!	1	#DIV/0!	1	#NUM!
ssaS	SPA1433	typeIII secretionprotein	1	#NUM!	1	#NUM!	1	#NUM!
yscR	SPA1434	typeIII secretionprotein	1	-1.585	1	-1	1	-3.3219
ssaQ	SPA1435	typeIII secretionprotein	1	-0.415	1	-1.3219	1	-2
ssaP	SPA1436	typeIII secretionprotein	1	-0.737	1	-1.585	1	-3
ssaO	SPA1437	typeIII secretionprotein	1	-1.2224	1	-1.415	1	-2.7004
ssaN	SPA1438	typeIII secretionATPsynthase	1	-0.8074	1	-1.8074	1	-2.2479
ssaV	SPA1439	Secretionsystemapparatus	1	-1	1	-2.585	1	-2.3219
ssaM	SPA1440	pathogenicityislandprotein	1	-1	1	#NUM!	1	#NUM!
ssaL	SPA1441	secretionsystemprotein	1	-1.415	1	-1.585	1	-2.585
ssaK	SPA1442	pathogenicityislandprotein	1	-2	1	#DIV/0!	1	#NUM!
-	SPA1443	pathogenicityislandprotein	1	-2.585	1	#DIV/0!	1	#NUM!
ssaJ	SPA1444	pathogenicityislandlipoprotein	1	-3	1	#DIV/0!	1	#NUM!
ssaI	SPA1445	pathogenicityislandprotein	1	-2.7004	1	#NUM!	1	-4.7004
ssaH	SPA1446	pathogenicityislandprotein	1	-3.1699	1	#NUM!	1	-4.3923
ssaG	SPA1447	pathogenicityisland protein	1	-3	1	#DIV/0!	1	#NUM!
sseG	SPA1448	pathogenicityislandeffectorprotein	1	-0.8074	1	-1.585	1	-1.585
sseF	SPA1449	pathogenicityislandeffectorprotein	1	-0.7776	1	-1	1	-2

sscB	SPA1450	pathogenicityislandprotein	0.0004	-0.7952	1	-2.585	1	-3
sseE	SPA1451	pathogenicityislandeffectorprotein	0.0696	-0.5305	1	-2	1	-2.8074
sseD	SPA1452	pathogenicityislandeffectorprotein	1	-0.6781	1	#NUM!	1	#NUM!
sseC	SPA1453	pathogenicityislandeffectorprotein	1	-1.3219	1	-1.585	1	#NUM!
sscA	SPA1454	TypeI IIsecretionsystemchaperoneprotein	1	-1.3785	1	-1.585	1	-3.585
-	SPA1455	pathogenicityislandeffectoreffectorprotein	1	-1.9069	1	-2.3219	1	-3.7004
-	SPA1456	pathogenicityislandprotein	1	-1.585	1	-1.585	1	#NUM!
ssaE	SPA1457	secretionsystemprotein	1	-1	1	#NUM!	1	#NUM!
ssaD	SPA1458	pathogenicityislandprotein	1	0	1	#NUM!	1	#NUM!
spiA	SPA1459	outerme mbranesecretoryprotein	1	#NUM!	1	#DIV/0!	1	#NUM!
spiC	SPA1460	pathogenicityislandsecretedeffectorprotein	1	#DIV/0!	1	#DIV/0!	1	#NUM!
ssrA	SPA1461	two-componentsensorkinase	1	-1	1	-1.3219	1	-1.8074
ssrB	SPA1462	two-componentresponseregulator	1	-0.7776	1	-0.5146	1	-1.7225
-	SPA1463	transcriptionalregulator	1	-0.3219	1	-0.4854	1	-1.1444
-	SPA1464	pathogenicityislandprotein	1	0.83007	0.8341	-0.152	1	0.31748
ydhZ	SPA1465	hypotheticalprotein	0.0019	-0.6933	1	0.66051	1	-0.0304
ttrR	SPA1466	two-componentresponseregulator	0.0232	-0.6781	0.0267	1.24793	1	0.7885
ttrS	SPA1467	hypotheticalprotein	4E-05	-1.2692	0.2821	1.08406	0.7252	0.63077
ttrC	SPA1469	tetrathionatereductasesubunitC(membraneprotein)	0	8.20212	1	1	1	1.58496
ttrA	SPA1470	tetrathionatereductasesubunitA	0	8.33613	1	0.26303	1	-0.1926
-	SPA1472	hypotheticalprotein	1	1.76553	1	#DIV/0!	1	#NUM!
-	SPA1473	hydrolase/acyltransferase	1	#DIV/0!	1	#DIV/0!	1	#NUM!
-	SPA1474	aminoaci dpermease	1	1	1	-1	1	-1.585
pykF	SPA1475	pyruvate kinase	1	0.38512	0.1146	-1.0862	1	-0.2182
lppA	SPA1476	major outerme mbranelipoprotein	1	-0.425	1	0.17455	1	-0.4441
lppB	SPA1477	majoro utermembranelipoprotein	1	0	1	0.34211	1	0.32193
lppB	SPA1478	majoro utermembranelipoprotein	1	0	1	1	1	0.89308
ynhG	SPA1479	LysMdom ain-containingprotein	1	0.28951	0.0246	-0.9209	0.3587	-0.5507
ynhA	SPA1480	hypotheticalprotein	1	0	1	0.10692	1	-0.2801
sufC	SPA1483	ABCtra nsporterATP -bindingp rotein	1	0.48543	1	-1.585	1	-0.7105
sufB	SPA1484	hypotheticalprotein	1	0.32193	1	-1	1	-0.585
sufA	SPA1485	hypotheticalprotein	1	0	1	-2	1	-1
-	SPA1486	transporter	1	-0.3049	1	0.18057	1	0.51457
-	SPA1487	-	1	0.37851	1	0.58496	1	-0.1926
ydiH	SPA1488	hypotheticalprotein	1	0.09404	1	0.24826	1	-0.0223
-	SPA1489	hypotheticalprotein	1	0	1	-0.4406	1	-0.3833
ydiJ	SPA1490	FAD-bindingpro tein	1	-0.0601	0.4018	-0.9569	1	0.03477
ydiK	SPA1491	hypotheticalprotein	1	-0.2224	1	-0.5377	1	-0.3479
-	SPA1492	-	1	0	1	0.58496	1	-0.585
aroD	SPA1493	3-dehydroquinatedehydratase	1	-0.4546	1	-0.1096	1	-0.2224
ppsA	SPA1494	phosphoenolpyruvatesynthase	1	-0.2561	1	-0.7889	1	-0.5404
ydiA	SPA1495	hypotheticalprotein	0.882	-0.15	1	0.1481	1	0.03847
aroH	SPA1496	3-deoxy-D-arabinoheptulosonate-7-phosphate synthase	1	-0.0217	1	-0.2462	1	0
ydiE	SPA1497	hypotheticalprotein	1	2.70044	1	#NUM!	1	-1.585
ydiU	SPA1498	hypotheticalprotein	1	0	3E-07	-1.389	1	-1
ydiV	SPA1499	hypotheticalprotein	1	-1	1	-1.4594	1	-1.263
nlpC	SPA1500	lipoprotein	9E-28	-1.7687	0.0008	-0.9749	1	-0.759
btuD	SPA1501	vitaminB12ABCtransportATP -bindingpro tein	1	0.32193	1	-0.143	1	0

btuE	SPA1502	glutathioneperoxidase/vitaminB12transportperiplasmicproteinBtuE	1	0.16993	0.7437	-0.2065	1	-0.0713
btuC	SPA1503	vitaminB12transportsystempermease	1	-0.3985	1	-0.344	1	-0.263
himA	SPA1504	integrationhostfactorsubunitalpha	0.5655	-0.3691	0.6024	-0.4584	1	-0.236
pheT	SPA1505	phenylalanyl-tRNAs ynthetasesubunitbeta	0.1976	-0.5907	0.557	-0.6621	0.9598	-0.3588
pheS	SPA1506	phenylalanyl-tRNA synthetasesubunitalpha	0.9915	-0.1397	0.1578	-0.5639	0.775	-0.4666
rplT	SPA1507	50Sribos omalproteinL20	1	-0.4608	1	-0.937	1	-0.2291
rpmI	SPA1508	50Sribos omalsubunitproteinL35	1	-0.4227	1	-0.9102	1	-0.2122
infC	SPA1510	translation initiationfactorIF -3	1	-0.2101	1	-0.5525	1	-0.241
thrS	SPA1511	threonyl-tRNAs ynthetase	1	0.15707	1	0.72379	1	0.47718
rfc	SPA1512	O-antigen polymerase	1	0	1	-0.1031	1	-0.5986
-	SPA1513	hypotheticalprotein	1	#NUM!	1	#DIV/0!	1	#DIV/0!
-	SPA1514	DNA/RNAnon -specificendonuclease	1	-1.8074	1	-1.585	1	-3
-	SPA1515	hypotheticalprotein	1	#NUM!	1	#DIV/0!	1	#NUM!
-	SPA1516	outerme mbraneprotein	1	-1	2E-48	-2.4594	0	-3.6756
ydiY	SPA1517	outerme mbraneprotein	1	0.0902	1	-0.6781	1	-1
pfkB	SPA1518	6-phosphofructokinase	1	0.41504	1	-0.3565	1	0.06413
ydiZ	SPA1519	hypotheticalprotein	1	0.36565	1	-0.0146	1	-0.0453
-	SPA1520	hypotheticalprotein	1	0.59653	0.1465	1.75512	1	0.57454
yniB	SPA1521	hypotheticalprotein	1	-0.5594	1	-0.7225	1	-0.75
yniC	SPA1522	hydrolase	1	0	1	-0.4448	1	-0.6674
ydjM	SPA1523	hypotheticalprotein	1	0	1	-0.415	1	-0.3219
ydjN	SPA1524	sodium:dicarboxylatesymporter	1	-0.1444	3E-45	-3.0343	6E-31	-2.4932
cedA	SPA1525	cell divisionactivatorCedA	1	0.13124	0.2209	0.76296	0.3291	-0.341
katE	SPA1526	catalaseHPII	1	0.37851	0.0479	-1.0802	1	-0.1323
celG	SPA1527	hypotheticalprotein	0.1279	-0.4806	1	-1.3536	1	-1.263
celF	SPA1528	phospho-beta-glucosidaseB	1	-0.585	1	-1.1699	1	-1.1375
celD	SPA1529	cel operonre pressor	1	-0.387	1	-0.5406	1	-1.0473
celC	SPA1530	phosphoenolpyruvatedependentphosphotransferaseenzymeIII -cellobiose	1	-0.433	1	-0.6041	9E-05	-1.0682
celB	SPA1531	PTSsys temcellobiose -specifictransportersubunitIIC	1	-0.585	1	-0.3219	1	-1.263
celA	SPA1532	PTSsys temcellobiose -specifictransportersubunitIIB	0.0417	-0.5714	1	0.34359	0.2499	-0.6104
osmE	SPA1533	osmoticallyinduciblelipoproteinEprecursor	1	-0.0125	0.4246	-0.5611	1	-0.274
nadE	SPA1534	NH3-dependentN ADsynthetase	1	0.2019	1	-0.0578	1	0.28281
-	SPA1535	hypotheticalprotein	1	0.16993	1	0.2115	1	-0.4475
spy	SPA1536	hypotheticalprotein	0.1137	-0.4354	0.0003	-1.263	1	0.18807
astE	SPA1537	succinylglutamatedesuccinylase	1	#DIV/0!	1	-2.3219	1	-1.585
astB	SPA1538	succinylargininedihydrolase	1	0	1	-2.8074	1	-2
astD	SPA1539	succinylglutamicsemialdehydedehydrogenase	1	-0.585	5E-90	-2.9696	1	-1.9386
astA	SPA1540	arginines uccinyltransferase	1	0	0	-3.415	1	-1.7004
astC	SPA1541	succinylornithinetransaminase	1	-0.585	0	-3.5699	1	-1.1699
xthA	SPA1542	exodeoxyribonucleaseIII	0.5947	-0.25	1	-0.0995	0.9163	-0.4039
-	SPA1543	MutT-familyprotein	1	-0.3985	1	-0.0875	1	-0.585
-	SPA1544	hypotheticalprotein	0.0005	1.16075	0.1964	1.06753	1	-0.1486
gdhA	SPA1545	NADP-specificglutamatedehydrogenase	1	0.14018	0.354	-0.4546	1	0.44626
topB	SPA1546	DNAto poisomeraseIII	1	0.23816	1	0.25081	1	0.34104
selD	SPA1547	selenophosphatesynthase	1	0.16227	1	0.34373	1	0.27053
ydjA	SPA1548	nitroreductase	1	0.07306	1	0.17403	1	0.06559
sppA	SPA1549	protease IV	0.1138	-0.4903	0.0139	-0.8863	1	-0.415
ansA	SPA1550	L-AsparaginaseI	1	-0.2016	0.0043	-0.8787	1	-0.3626

pncA	SPA1551	pyrazinamidase/nicotinamidase	1	-0.3451	1	-0.7462	1	-0.2538
yeaC	SPA1552	hypotheticalprotein	1	-0.0717	1	-0.0864	0.9245	-0.2766
yeaA	SPA1553	hypotheticalprotein	1	-0.0479	1	-0.0984	1	-0.3015
gapA	SPA1554	glyceraldehyde3 -phosphatedehydrogenaseA	1	0.15693	1	0.52931	0.902	0.80384
yeaD	SPA1555	aldose 1-epimerase	1	0.83007	0.4031	0.94062	0.0019	1.35267
-	SPA1556	oxidoreductase	1	-0.0473	1	0.47644	1	0.77052
-	SPA1557	arylsulfataseregulator	1	0	1	0.22239	1	1
mipA	SPA1558	outerme mbraneprotein	0.4607	-0.4253	1	-0.0241	0.8685	-0.3597
yeaH	SPA1560	hypotheticalprotein	1	-0.1278	0.2557	-0.7585	0.1773	-0.8525
yeaJ	SPA1561	methyl-acceptingchemotaxisprotein	1	-0.3219	1	-0.6919	1	-1
yeaK	SPA1562	hypotheticalprotein	0.3894	0.60486	0.1729	-0.5164	0.0276	-0.7726
-	SPA1563	inner membraneprotein	1	0	1	0.77761	1	0.11548
yeaL	SPA1564	hypotheticalprotein	1	0.1375	1	-0.4021	1	-0.0525
yeaM	SPA1565	transcriptionalregulator	1	0.02915	1	0.22239	1	-0.1806
yeaN	SPA1566	hypotheticalprotein	1	0	1	0	1	-0.585
yeaO	SPA1567	bacteriophageprotein	0.5501	-0.2224	0.9255	-0.1699	0.0017	-0.8541
-	SPA1568	hypotheticalprotein	0.4549	-0.3231	1	0.29797	1	-0.2224
yaoF	SPA1569	hypotheticalprotein	0.3147	-0.3663	0.9741	0.59368	1	0.26679
yeaQ	SPA1570	hypotheticalprotein	1	0.11103	2E-05	-1.0875	1	-0.1007
-	SPA1571	hypotheticalprotein	1	1.67807	1	-0.415	1	0
-	SPA1572	-	1	#DIV/0!	1	#DIV/0!	1	#NUM!
-	SPA1573	hypotheticalprotein	1	1.87447	1	0.73697	1	0.73697
yoaG	SPA1574	hypotheticalprotein	1	0.06711	1	0	1	0
yeaR	SPA1575	hypotheticalprotein	1	0.45943	1	-0.2756	1	0.41504
yeaS	SPA1576	membranetransportprotein	0.4123	-0.3523	1	-0.3561	1	-0.2538
aroQ	SPA1577	chorismatemutase	1	-2	1	-2.8074	1	-1.585
-	SPA1578	hypotheticalprotein	1	#NUM!	1	#NUM!	1	#NUM!
-	SPA1579	hypotheticalprotein	1	-1	5E-157	-2.978	2E-05	-1.0589
-	SPA1580	transcriptionalregulator	1	-0.2801	1	0.09516	1	-0.0498
-	SPA1581	regulatoryprotein	1	#DIV/0!	1	-1.3219	1	-1.3479
aadA	SPA1582	aminoglycoside-resistanceprotein	1	-1.0589	1	-1	1	-1.1783
-	SPA1583	hypotheticalprotein	1	-0.737	1	-0.585	1	-0.8074
-	SPA1584	ArgtRN A	1	0	1	-0.4739	1	0.43296
-	SPA1585	hypotheticalprotein	1	-0.1031	0.1655	-0.5115	0.8335	0.63941
-	SPA1586	hypotheticalprotein	1	0	1	-1.1699	1	-1.1375
-	SPA1587	ABCtra nsporterATP -bindingp rotein	1	-0.1699	1	-0.9069	1	-1
-	SPA1588	ABCtra nsporterATP -bindingp rotein	1	-0.0247	1	-0.7655	1	-0.5305
-	SPA1589	innerme mbranetransportprotein	1	-0.2955	1	-1.2224	1	-0.415
-	SPA1590	innerme mbrane transportpro tein	0.006	-0.703	1	-1.3219	1	-0.8074
-	SPA1591	substrate-bindingtra nsportprotein	0.1165	-0.6821	1	-0.9542	1	-1.1926
-	SPA1592	lipoprotein	0.0149	-0.7105	1	0.25064	1	0.5271
-	SPA1593	cytochrome	1	-0.1255	1	0.48187	1	-0.1666
-	SPA1594	hypotheticalprotein	1	-0.4854	1	-0.1605	1	-1.263
-	SPA1596	hypotheticalprotein	7E-10	-1.3026	1	0.37485	0.0333	-0.6433
-	SPA1597	ArgtRN A	1	1	1	2	1	-0.263
pagC	SPA1599	outerme mbraneinvasionprotein	1	-2.4594	1	-2.585	1	-4.1699
-	SPA1600	hypotheticalprotein	1	#NUM!	1	#DIV/0!	1	#NUM!
-	SPA1601	hypotheticalprotein	1	#DIV/0!	1	#DIV/0!	1	#DIV/0!

pagD	SPA1602	outerme mbranevirulenceprotein	1	#NUM!	1	#NUM!	1	#NUM!
cspH	SPA1603	colds hockprotein	1	0.65208	1	-0.737	1	-0.6521
envE	SPA1604	lipoprotein	1	-1.1155	1	-2.9542	1	-2.1293
msgA	SPA1605	virulenceprotein	5E-08	-1.0217	0.0823	-0.6256	3E-08	-1.3347
cdtB	SPA1606	toxin-like protein	1	-1.415	1	-1.4594	1	-1.263
-	SPA1607	hypotheticalprotein	1	-1	1	0	1	-1
-	SPA1608	hypotheticalprotein	1	-0.4406	1	0	1	-0.585
-	SPA1609	pertussis-like toxinsubunit	1	-0.3479	1	0.32193	1	-0.3479
-	SPA1610	pertussis-like toxinsubunit	1	-0.1699	1	0.19265	1	-0.2895
-	SPA1611	bacteriophageprotein	1	0.45066	1	0.05063	1	-1.0275
icdA	SPA1612	isocitratedehydrogenase	1	-0.4105	1	-0.368	1	0.37334
rluB	SPA1613	ribosomallargesubunitpseudouridinesynthaseB	1	0.16993	1	-0.0759	0.2767	-0.4493
-	SPA1614	hypotheticalprotein	1	0.24101	1	-0.2439	0.0462	-0.5648
ymfB	SPA1615	MutT-familyprotein	1	0.1343	1	-0.2345	1	-0.6215
trmU	SPA1616	tRNA(5 -methylaminomethyl -2-thiouridylate)-methyltransferase	1	0.05324	0.1353	-0.5792	0.0356	-0.8838
ycfC	SPA1617	hypotheticalprotein	0.7016	-0.2265	0.0067	-0.8365	0.0135	-0.7705
purB	SPA1618	adenylosuccinatelyase	0.9828	-0.1822	1E-07	-1.7345	0.0033	-1.1587
phoP	SPA1619	transcriptionalregulatoryproteinPhoP,regulatorofvirulencedeterminants	0.7369	-0.6297	1	0.34594	1	0.03108
phoQ	SPA1620	sensor proteinPhoQ,regulatorof virulencedeterminants	0.4314	-0.4594	1	0.40663	1	0.26546
ycfD	SPA1621	hypotheticalprotein	0.9346	-0.2259	0.3756	-0.4288	0.1624	-0.6245
-	SPA1622	hypotheticalprotein	1	0.152	1	1.16993	1	0.73697
pepT	SPA1623	aminotripeptidase	1	-0.0393	0.1263	1.08746	1	0.25418
potA	SPA1624	spermidine/putrescineABCtransporterATP -bindingpro teinPotA	1	0.1964	1	-0.1926	1	-0.6077
potB	SPA1625	spermidine/putrescinetransportsystempermeasePotB	1	-0.1806	1	-0.4854	1	-0.4854
sifA	SPA1626	virulence determinant	1	-0.0623	1	#DIV/0!	1	#NUM!
potC	SPA1627	spermidine/putrescinetransportsystempermeaseproteinPotC	0.4957	-0.2801	1	-0.2895	1	-0.3626
potD	SPA1628	spermidine/putrescine-bindingpe riplasmicproteinprecursor	0.0045	-0.7515	0.0118	-0.7814	1	-0.6845
cobB	SPA1629	regulatoryprotein	0.8676	-0.2224	1	0.10639	1	-0.0942
ycfX	SPA1630	ROK-familyprotein	0.9923	-0.1581	1	0.16506	1	0.15806
ycfW	SPA1631	ABCtra nsporter	1	-0.174	1	-0.2937	1	-0.0525
ycfV	SPA1632	ABCtra nsporter ATP-bindingp rotein	0.9803	-0.1013	0.0226	-0.7299	1	-0.3973
ycfU	SPA1633	ABCtra nsporter	1	-0.263	1	-0.5683	1	-0.3899
mfd	SPA1634	transcription-repairc ouplingfactor(TrcF)	1	0.02203	0.5799	-0.5421	1	-0.0728
ycfS	SPA1635	hypotheticalprotein	1	-0.9175	1	-2.3219	1	-1.078
tnpA	SPA1636	transposaseforinsertionsequenceelementIS200	1	-0.0489	1	-0.737	1	-0.8074
ycfR	SPA1637	hypotheticalprotein	2E-15	1.81943	1	0.58496	1	0.87447
ycfQ	SPA1638	TetR-familyregulatoryprotein	1	0.08424	1	-0.0878	0.0036	-1.0172
ycfJ	SPA1639	hypotheticalprotein	1	#DIV/0!	1	0	1	0.73697
ndh	SPA1640	NADH dehydrogenase	1	0.24793	1	0.56828	1	-0.142
ycfP	SPA1641	hypotheticalprotein	1	0.34217	0.7239	0.71865	1	0.36893
ycfO	SPA1642	glycosylhydrolase	1	0.28688	1	-0.0224	1	0.14018
ycfN	SPA1643	hypotheticalprotein	1	0.28011	1	-0.3356	1	-0.0704
ycfM	SPA1644	lipoprotein	1	-0.0406	0.1001	-0.6872	1	-0.2464
ycfL	SPA1645	lipoprotein	1	0	0.4802	-0.3598	1	0
ycfF	SPA1646	proteink inaseCinhibitor	0.5944	-0.2254	0.523	-0.3274	1	-0.0556
ptsG	SPA1648	PTSsys temglucose -specifictransportersubunitIIBC	1	-0.0873	1	-0.7708	1	-1.0561
ycfH	SPA1649	hypotheticalprotein	1	0	0.11	-0.5564	0.167	-0.6119
holB	SPA1650	DNApo lymeraseIII,delta'subunit	0.8318	-0.1489	0.3615	-0.4227	1	-0.4903

tmk	SPA1651	thymidylatekinase	1	-0.0453	0.6105	-0.2771	0.9187	-0.4317
yceG	SPA1652	hypotheticalprotein	1	-0.2713	1	-0.3326	1	-0.1993
pabC	SPA1653	4-amino-4-deoxychorismatelyase	1	-0.1699	1	-0.2224	1	-0.273
fabF	SPA1654	3-oxoacyl-ACPs ynthase	0.9037	-0.3454	0.618	-0.7663	1	-0.363
acpP	SPA1655	acylca rrierprotein	0.5944	-0.7484	0.9394	-0.3971	0.8236	-0.4214
fabG	SPA1656	3-oxoacyl-ACPre ductase	0.4607	-0.6734	0.8197	-0.5292	1	-0.0763
fabD	SPA1657	malonyl CoA-acylc arrierproteintransacylase	0.6459	-0.3158	0.8274	-0.5227	1	0.03191
fabH	SPA1658	3-oxoacyl-ACPs ynthase	1	-0.1587	0.4793	-0.3819	1	0.12899
plsX	SPA1659	fattyaci d/phospholipidsynthesisproteinPlsX	0.916	-0.221	1	0.11632	1	0.078
rpmF	SPA1660	50Sribos omalproteinL32	0.6595	-0.681	0.9747	-0.3553	0.39	-0.5935
yceD	SPA1661	hypotheticalprotein	0.5706	-0.7505	0.7144	-0.6628	0.7607	-0.4744
-	SPA1662	-	0.0003	-0.798	8E-07	-1.1102	0.4159	-0.4349
yceF	SPA1663	hypotheticalprotein	0.1098	-0.4611	0.5808	-0.2157	0.5239	-0.3382
rluC	SPA1664	ribosomallargesubunitpseudouridinesynthaseC	1	-0.341	1	-0.858	1	-1.2701
-	SPA1665	hypotheticalprotein	1	#DIV/0!	1	#DIV/0!	1	#DIV/0!
rne	SPA1666	ribonucleaseE	0.974	-0.306	0.8005	-0.9053	1	0.07215
flgL	SPA1667	flagellarhook -associatedprotein3	0.0132	1.35828	0.704	0.75737	1	0.06811
flgK	SPA1668	flagellarhook -associatedprotein1	0.0053	1.56957	0.7261	0.79712	1	-0.0862
flgJ	SPA1669	flagellarproteinFlgJ	0.0195	1.01527	1	0.66676	1	-0.0646
flgI	SPA1670	flagellarP -ringprote in	0.026	0.96253	1	0.57901	1	-0.1685
flgH	SPA1671	flagellarL -ringprote in	0.0695	0.88944	1	0.68557	1	-0.1123
flgG	SPA1672	flagellarbasal -bodyrod proteinFlgG(distalrodprotein)	0.1999	0.90781	0.9511	0.55342	1	-0.0802
flgF	SPA1673	flagellarbasal -bodyrod proteinFlgF	0.2649	0.81522	1	0.51165	1	-0.1127
flgE	SPA1674	flagellarhookproteinFlgE	0.3675	0.84508	1	0.59525	1	-0.201
flgD	SPA1675	flagellarhookformationproteinFlgD	0.2599	0.65085	1	0.40982	1	-0.2129
flgC	SPA1676	flagellarbasal -bodyrod proteinFlgC	0.5887	0.62619	1	0.27633	0.9376	-0.3541
flgB	SPA1677	flagellarbasal -bodyrod proteinFlgB	0.5062	0.6389	1	0.24371	0.6211	-0.46
flgA	SPA1678	flagellarbasalbody P-ringprote inFlgAprecursor	0.0926	0.89308	1	0.21681	0.2101	-0.6394
flgM	SPA1679	negativeregulatorofflagellinsynthesis(anti -sigma factor)	3E-08	1.57488	0.1322	1.22181	1	-0.1064
flgN	SPA1680	flagellasynthesisproteinFlgN	1E-11	1.72991	0.0788	1.24757	1	0.0342
mviN	SPA1681	virulencefactorMviN	1	-0.0875	1	-0.5146	1	0
mviM	SPA1682	virulencefactorMviM	1	0.1302	0.3873	0.94647	1	0.36984
yceH	SPA1683	hypotheticalprotein	1	0.11768	0.6224	0.85878	1	0.33109
rimJ	SPA1684	ribosomal-protein-alanine acetyltransferase	1	0.04394	0.526	0.88523	1	0.52319
yceL	SPA1685	membranetransporter	1	0	1	-0.3677	1	0.04731
grxB	SPA1686	glutaredoxin	0.6503	0.7083	1	0.03044	1	0.37966
pyrC	SPA1688	dihydroorotase	0.7723	-0.1985	7E-13	-1.8618	0.6289	-0.4678
dinI	SPA1689	damage-inducibleprotein	1	-0.613	1	-1.1375	1	-0.1926
yceP	SPA1690	hypotheticalprotein	1	0.30929	1	-0.0363	1	-0.0406
solA	SPA1691	sarcosineoxidase	1	0	1	-0.0332	1	-0.297
yceO	SPA1692	hypotheticalprotein	1	0	1	0.41504	1	-0.3219
yceJ	SPA1693	cytochrome	1	0	1	-1.585	1	-1
yceI	SPA1694	hypotheticalprotein	1	0.152	1	-0.9386	1	-0.8931
yceA	SPA1695	hypotheticalprotein	1	-0.2224	1	-1.237	1	-1.0641
htrB	SPA1696	lipidA biosynthesislauroyl acyltransferase(heatshockprotein)	1	0.06926	1	0.11103	1	-0.2466
yceE	SPA1697	membranetransportprotein	1	1.94753	1	1.37851	0.2366	0.84327
msyB	SPA1698	acidicpro teinMsyB;multicopysuppressorofSecY	1	0.42531	0.0024	-0.9497	0.1332	-0.6766
yceK	SPA1699	lipoprotein	1	-0.585	1	-0.3785	1	-1.1155

mdoH	SPA1700	periplasmicglucansbiosynthesisproteinMdoH	0.4208	-0.4245	0.2739	-1.0321	0.1696	-0.6951
mdoG	SPA1701	periplasmicglucansbiosynthesisproteinMdoGprecursor	1	-0.2399	0.7492	-0.6473	0.2125	-0.7713
mdoC	SPA1702	glucansbiosynthesisprotein	1	0.36257	1	-0.263	1	0.24793
ymdC	SPA1703	hypotheticalprotein	0.882	0.38995	1	0.43522	0.7947	-0.393
-	SPA1704	hypotheticalprotein	0.5073	0.50628	1	0.61086	1	-0.323
ymdA	SPA1705	hypotheticalprotein	0.0039	1	0.3106	0.94584	1	-0.3028
csgC	SPA1706	hypotheticalprotein	1	0.28951	1	0.80735	1	-0.4406
csgA	SPA1707	majorc urlinsubunitprecursor	1	-1.3219	1	-2	1	-2.3219
csgB	SPA1708	curlinm onomernucleationprotein	1	#DIV/0!	1	#DIV/0!	1	#NUM!
csgD	SPA1709	regulatoryprotein	1	#NUM!	1	#NUM!	1	#NUM!
csgE	SPA1710	assembly/transportcomponentincurliproduction	1	#NUM!	1	#NUM!	1	#NUM!
csgG	SPA1712	assembly/transportcomponentincurliproduction	1	-1	1	-1.585	1	-1
ycdZ	SPA1713	hypotheticalprotein	1	0.35147	1	0.09622	1	0.49957
ycdY	SPA1714	hypotheticalprotein	0.563	-0.2538	1	-0.063	1	-0.0225
ycdX	SPA1715	hypotheticalprotein	0.7284	-0.2352	1	0.10362	1	-0.0265
ycdW	SPA1716	2-hydroxyaciddehydrogenase	0.175	-0.4731	1	-0.241	1	-0.3626
serX	SPA1717	SertRNA	1	#DIV/0!	1	#NUM!	1	#NUM!
yjhC	SPA1718	oxidoreductase	1E-11	1.60881	1	-1.3626	1	-1.2016
-	SPA1719	transporter	1	2	1	-2.3219	1	#NUM!
-	SPA1720	hypotheticalprotein	1	1.1375	1	-1.8074	1	#NUM!
-	SPA1722	hypotheticalprotein	1	2.18442	0.1133	-0.574	1	-0.585
-	SPA1723	sodium/glucosecotransporter	1	0.93289	0.0437	-0.7873	1	-1.0544
-	SPA1724	transcriptionalregulator	1	-0.0982	0.5795	-0.337	0.2647	-0.585
phoH	SPA1725	PhoHpro tein (phosphatestarvation -inducibleproteinPsiH)	0.0008	1.17284	0.8334	-0.4197	0.3426	-0.6667
putP	SPA1726	sodium/prolinesymporter(prolinepermease)	1	1.06413	7E-06	-1.4463	1	-1.585
putA	SPA1727	proline dehydrogenase(prolineoxidase)	1E-72	3.6051	1	-0.8639	0.056	-1.2877
-	SPA1728	hypotheticalprotein	4E-44	2.52585	0.6254	-0.2577	0.0027	-1.1503
ycdC	SPA1729	transcriptionalregulator	1	-0.9386	1	-0.5475	1	-0.273
ymdF	SPA1730	hypotheticalprotein	0.4569	0.54174	1	0.0517	1	-0.1883
wrbA	SPA1731	trp repressorbindingprotein	0.0398	0.84435	1	0.13884	0.3884	1.07438
yccJ	SPA1732	hypotheticalprotein	0.2452	0.66928	1	0.02153	0.1905	0.91938
agp	SPA1733	glucose-1-phosphataseprecursor(G1Pase),secreted	1	0.57379	0.3642	1.20789	0.1568	1.0624
scsD	SPA1734	secretedprotein,suppressorforcopper -sensitivityD	1	0.29956	1	-0.263	1	-0.415
scsC	SPA1735	secretedprotein,suppressorforcopper -sensitivityCprecursor	1	0.41504	1	0	1	0
scsA	SPA1737	membraneprotein,suppressorfor copper-sensitivityA	1	0.04439	1	-0.628	1	-0.3515
cbpA	SPA1738	curvedD NA-bindingpro tein	1	0.48396	0.618	0.8594	0.8351	0.66789
yccD	SPA1739	hypotheticalprotein	0.9152	0.39079	0.8463	0.69883	0.7658	0.67005
-	SPA1740	hypotheticalprotein	1	0	1	-0.1699	1	1
-	SPA1741	hypotheticalprotein	1	-0.4854	1	-0.7776	1	-0.6521
hpaA	SPA1742	4-hydroxyphenylacetate3 -monooxygenaseoperonregulatoryprotein	1	0	1	-0.585	1	-0.585
hpaX	SPA1743	4-hydroxyphenylacetatepermease	1	-0.415	1	-0.3479	1	-0.5146
hpcH	SPA1744	2,4-dihydroxyhept-2-ene-1,7-dioic acidaldolase	1	0.73697	0.0535	-0.6234	1	-0.4739
hpcG	SPA1745	2-oxo-hepta-3-ene-1,7-dioic acidhydratase	1	0.41504	1	-0.4739	1	-0.5305
hpcD	SPA1746	5-carboxymethyl-2-hydroxymuconatedelta -isomerase	1	0.58496	1	-0.1979	1	-0.507
hpcB	SPA1747	3,4-dihydroxyphenylacetate2,3 -dioxygenase	1	0	1	-0.237	1	-0.6167
hpaE	SPA1748	4-hydroxyphenylacetatecatabolism	1	0.32193	1	-0.0759	1	-0.585
hpcR	SPA1750	homoprotocatechuatedegradativeoperonrepressor	1	-0.263	1	0.35364	1	-0.263
hpaB	SPA1751	4-hydroxyphenylacetate3 -monooxygenase	1	1	1	-0.1926	1	0.73697

hpaC	SPA1752	4-hydroxyphenylacetate3 -monooxygenasecouplingprotein	1	-0.263	1	-0.1155	1	-0.1926
-	SPA1753	hypotheticalprotein	0.2161	-0.4395	1	-0.415	1	-0.9027
copR	SPA1754	responseregulator	1	-0.2553	1	-0.078	1	-0.2016
copS	SPA1755	histidinekinase	1	-0.263	1	0	1	0
-	SPA1757	hypotheticalprotein	1	0.04307	1	0.1375	1	-0.415
-	SPA1758	hypotheticalprotein	1E-07	-1.1079	1	0.06075	8E-19	-1.848
sigD	SPA1759	cell invasionprotein	1	0.46803	1	0.34362	0.1905	-1.089
sigE	SPA1760	cell invasionprotein	1	0.50317	1	0.53171	0.0024	-1.2207
-	SPA1761	innerme mbraneprotein	1	#DIV/0!	1	#DIV/0!	1	#DIV/0!
pipB	SPA1762	hypotheticalprotein	1	0.83399	1	1	1	-1
pipA	SPA1763	hypotheticalprotein	1	0.09954	1	0.10692	1	-0.2996
serT	SPA1764	SertRNA	1	#DIV/0!	1	0.11548	1	-0.3479
yccA	SPA1765	hypotheticalprotein	0.558	-0.6552	0.1809	-1.1322	0.8277	-0.4021
yccK	SPA1766	hypotheticalprotein	1	-0.0995	0.3814	-0.3785	0.0635	-0.6004
yccX	SPA1767	acylphosphatase	1	-0.1293	1	0.18556	1	-0.1013
-	SPA1768	bacterialregulatoryprotein,AraCfamily	1	-0.0671	1	0.078	1	0.23133
yccW	SPA1770	hypotheticalprotein	0.413	-0.3149	1	-0.5502	1	-0.8651
yccV	SPA1771	hypotheticalprotein	0.0978	-0.4854	1	-0.0387	0.3084	-0.5406
-	SPA1772	hypotheticalprotein	0.9761	-0.1069	0.3642	-0.3998	0.3023	-0.6157
yccT	SPA1773	hypotheticalprotein	1	-1	1	-1	1	-2.1699
mgsA	SPA1774	methylglyoxalsynthase	0.5414	-0.401	0.5666	0.8686	1	0.21501
helD	SPA1775	helicaseIV(75kDhelicase)	1	0.05889	1	-0.2044	1	-0.1043
yccF	SPA1776	hypotheticalprotein	1	-0.4695	1	-0.2801	1	-0.4975
yccS	SPA1777	hypotheticalprotein	1	-0.3479	1	-0.7885	1	-0.3479
yccR	SPA1778	hypotheticalprotein	1	-0.4034	1	0.58496	1	0.08746
sulA	SPA1779	cell divisioninhibitor	0.1383	-0.4389	1	0.16273	1	0.22628
ompA	SPA1780	outerme mbraneproteinA	1	0.26601	1	-0.5158	0.8236	-0.6028
ycbG	SPA1781	hypotheticalprotein	0.8318	-0.2377	1	0.48063	1	0.16175
lonH	SPA1782	hypotheticalprotein	1	-0.2224	1	-0.585	1	-0.6374
fabA	SPA1783	D-3-hydroxydecanoyl-(acyl carrier-protein)	0.293	-0.3785	0.2218	-0.4878	1	-0.3547
rmf	SPA1784	ribosomemodulationfactor(proteinE)	0.0243	-0.6346	0.2557	-0.4403	3E-07	-1.653
ymbA	SPA1785	lipoprotein	0.4343	-0.2771	1	-0.1325	0.1242	-0.5771
pqiB	SPA1786	hypotheticalprotein	0.145	-0.4938	1	-0.0581	1	-0.4475
pqiA	SPA1787	inner membraneprotein	1	-0.6215	1	-0.3819	1	-0.1844
uup	SPA1788	ABCtra nsporterATP -bindingp rotein	0.0039	-0.8033	0.0367	-0.878	1	-0.4263
ycbY	SPA1789	hypotheticalprotein	1	-0.2224	1	-0.6374	1	-0.8395
-	SPA1790	hypotheticalprotein	1	-0.7162	1	-0.6674	1	-0.4854
ycbW	SPA1791	hypotheticalprotein	0.2447	-0.3363	0.0017	-1.0203	3E-13	-1.6865
pyrD	SPA1792	dihydroorotatedehydrogenase	1	0.13124	1	-0.737	1	-0.8931
pepN	SPA1793	aminopeptidaseN	1	0.26984	1	-0.2394	1	0.05703
pncB	SPA1794	nicotinatephosphoribosyltransferase	9E-05	1.33121	1	0.34901	1	0.50007
-	SPA1795	ion:aminoacidsymporter	1	#DIV/0!	1	#DIV/0!	1	#DIV/0!
-	SPA1796	putatiavediaminopropionateammonialyase	1	0	1	-1	1	-1
-	SPA1797	transcriptionalregulator	1	-0.9542	1	0.37851	1	-0.6374
asnS	SPA1798	asparaginyl-tRNAs ynthetase	0.5948	-0.3831	0.0673	-1.5264	0.2347	-0.7514
ompF	SPA1799	outerme mbraneproteinF	0	-4.6402	0	-6.3309	0	-5.534
aspC	SPA1800	aspartate aminotransferase	0.2951	-0.6547	0.6021	-0.8116	1	-0.2315
ycbL	SPA1801	hypotheticalprotein	1	0.07155	0.1242	-0.6004	0.8249	-0.3429

ycbK	SPA1802	hypotheticalprotein	1	-0.0153	0.1141	-0.7579	0.2945	-0.5377
ycbB	SPA1803	hypotheticalprotein	1	0.12553	1	0.10561	1	-0.0503
mukB	SPA1804	cell divisionprotein	1	-0.2295	1	-0.1735	1	-0.3384
mukE	SPA1805	KicA protein	1	-0.1036	0.618	-0.3158	1	-0.0797
mukF	SPA1806	killingfactorKicB	1	-0.1876	0.5961	-0.3103	1	-0.2003
smtA	SPA1807	SmtAprote in	1	-0.1651	1	-0.0375	1	-0.0395
ycbC	SPA1808	hypotheticalprotein	1	-0.7776	1	-0.2895	1	-0.7004
-	SPA1809	hypotheticalprotein	1	0.48543	0.002	1.51728	0.4062	0.87092
kdsB	SPA1810	3-deoxy-manno-octulosonatecytidylyltransferase	1	0	1	-0.0378	0.5821	-0.4809
ycaR	SPA1811	hypotheticalprotein	0.7711	-0.0956	1	0.04439	0.2888	-0.4594
ycaQ	SPA1812	hypotheticalprotein	1	-0.4854	1	-0.1255	1	-0.1444
lpxK	SPA1813	tetraacyldisaccharide4' -kinase	0.2493	-0.3523	0.1514	-0.5747	0.7105	-0.4222
msbA	SPA1814	transport ATP-binding proteinMsbA	0.5292	-0.2818	0.0968	-0.6498	0.0301	-0.848
himD	SPA1816	integrationhostfactorbeta -subunit(IH F-beta)	0.056	-0.6622	0.2787	-0.8861	0.0004	-1.1605
rpsA	SPA1817	30Sribos omalproteinS1	1	-0.6423	1	-1.0015	1	-0.7448
cmk	SPA1818	cytidylatekinase	1	-0.0653	0.1205	-0.5542	1	-0.2736
ycaL	SPA1819	lipoprotein	1	-0.3219	1	-0.1375	1	-0.5305
aroA	SPA1820	3-phosphoshikimate1 -carboxyvinyltransferase	0.1967	-0.4498	1	-0.9107	1	-0.2895
serC	SPA1821	phosphoserineaminotransferase	0.3378	-0.4496	0.1425	-1.0084	1	-0.1497
ycaP	SPA1822	hypotheticalprotein	1	-0.585	1	-1.737	1	-1
ycaO	SPA1823	hypotheticalprotein	1	-0.263	1	-1	1	-0.8231
focA	SPA1824	formatetransporter	1	-0.0187	0.1046	-0.8667	0.3713	-0.7036
pflB	SPA1825	formate acetyltransferase1	1	0.42719	1	-0.3928	1	-0.3219
-	SPA1827	hypotheticalprotein	1	-0.6781	1	0.26303	1	-0.415
pflA	SPA1828	pyruvate formate-lyase1activatingenzyme	0.6998	-0.2327	1	-0.0242	1	-0.337
ycaM	SPA1829	transport protein	1	-1.0995	1	-1.1699	1	-1.2224
ycaD	SPA1830	transport protein	1	0.26303	1	-1.3026	1	-0.5564
-	SPA1831	hypotheticalprotein	2E-13	1.46566	6E-08	1.66742	3E-12	1.90378
dmsC	SPA1832	dimethylsulfoxidereductasesubunitC	2E-05	1.24998	0.0005	1.60446	7E-06	1.64386
dmsB	SPA1833	anaerobicdimethylsulfoxidereductasesubunitB	0.0021	1.1316	0.0832	1.49173	0.0841	1.4039
dmsA	SPA1834	anaerobicdimethylsulfoxidereductasesubunitA	1	0.82753	0.3111	1.46395	0.6836	0.96435
serS	SPA1835	seryl-tRNAs ynthetase	1	0.27846	1	0.37974	1	0.35206
ycaJ	SPA1836	hypotheticalprotein	1	0.33805	1	0.39523	1	-0.2941
lolA	SPA1837	outerme mbranelipoproteincarrierprotein	1	0.17998	1	0.25992	1	-0.2717
ftsK	SPA1838	cell divisionprotein,requiredforcelldivisionand chromosomepartitioning	1	-0.1468	0.8476	-0.647	0.7235	-0.5025
lrp	SPA1839	leucine-responsiveregulatoryprotein	0.8591	-0.2345	0.4092	-0.38	1	-0.1705
trxB	SPA1840	thioredoxinreductase	0.85	-0.2422	0.3955	-0.6696	1	-0.2955
cydD	SPA1841	transport ATP-binding proteinCydD	0.1502	-0.4938	0.0917	-0.6919	0.0082	-1.0531
cydC	SPA1842	transport ATP-binding proteinCydC	0.0385	-0.659	0.0673	-0.7428	0.0425	-0.8643
aat	SPA1843	leucyl/phenylalanyl-tRNA-proteintra nsferase	1	-0.5305	0.4738	-0.2679	1	-0.7447
-	SPA1844	innerme mbraneprotein	0.7447	-0.2012	0.4609	-0.3486	0.8351	-0.4637
infA	SPA1845	initiationfactorIF -1	0.6042	-0.2741	0.24	-0.4375	0.2789	-0.5597
-	SPA1846	transcriptionalactivator	1	0.32193	1	0.16993	1	0
-	SPA1847	pirin-related protein	1	0	1	-1.2016	1	-1
-	SPA1848	hypotheticalprotein	1	0.04891	0.0535	-0.8811	0.0017	-1.2337
-	SPA1849	SertRNA	1	-1.1699	1	-0.8745	1	-1.1312
-	SPA1850	hypotheticalprotein	1	-1.585	1	-0.6781	1	-0.6521
-	SPA1851	integrase remnant	1	1	1	0	1	#NUM!

-	SPA1852	hypotheticalprotein	1	3	2E-307	3.79647	1E-48	2.68054
clpA	SPA1854	ATP-dependent ClpproteaseATP -bindings ubunitClpA	1	0.56878	1	0.4011	1	0.30166
yljA	SPA1855	hypotheticalprotein	1	0.37909	0.9899	0.65124	0.9126	0.54189
cspD	SPA1856	colds hock-like proteinCspD	0.0005	-1.1528	0.042	-0.6958	0.533	-0.4738
ybjZ	SPA1857	ABCtra nsporter	0.4945	-0.3395	1	-1.4288	1	-0.5475
ybjY	SPA1858	hypotheticalprotein	0.3186	-0.3814	1	-1.0931	1	-0.4854
ybjX	SPA1859	virK protein	1	0.29209	0.7043	-0.4863	1	-0.065
ybjD	SPA1860	hypotheticalprotein	1	0.09686	0.7381	0.76081	1	-0.0304
ybjE	SPA1861	hypotheticalprotein	1	-0.3219	1	-0.585	1	-0.2016
hcp	SPA1862	prismane-like protein	1	2.20945	1	0.54749	1	1.22239
hcr	SPA1863	NADH oxidoreductaseHcr	1	1.8365	1	0.26303	1	1.07039
poxB	SPA1864	pyruvate dehydrogenase	1	1.58496	1	-1.2044	1	0.03953
ybjU	SPA1865	L-allo-threonine aldolase	0.8253	-0.2106	1	0.16812	1	0.42011
ybjT	SPA1866	hypotheticalprotein	1	-0.1876	1	0.14018	1	0.53766
-	SPA1867	oxidoreductase	1	-0.4274	1	-0.0995	1	-0.6057
ybjR	SPA1868	N-acetylmuramoyl-L-alanine amidase	1	-0.0151	1	0.08616	1	-0.3536
-	SPA1869	hypotheticalprotein	0.7613	-0.1325	1	0	1	-0.628
ybjP	SPA1870	lipoprotein	1	0.27185	1	0.02893	1	-0.1949
artP	SPA1871	argininetra nsportATP -bindingpro teinArtP	0.2515	-0.415	0.3959	-0.3971	0.0036	-1.1185
artI	SPA1872	arginine/ornithineABCtransportersubstrate -bindingpro tein	0.5935	-0.3081	1	-0.2312	0.5141	-0.5602
artQ	SPA1873	argininetra nsportsystempermeaseproteinArtQ	0.1971	-0.4445	0.4341	-0.3671	1	-0.3334
artM	SPA1874	argininetra nsportsystempermeaseproteinArtM	0.3019	-0.3728	0.166	-0.5181	1	-0.1392
artJ	SPA1875	arginine-bindingpe riplasmicprotein	1	0.05247	1	0.51457	6E-09	-1.4361
-	SPA1876	sulfatase	1	-0.3626	1	-0.585	1	-0.3219
-	SPA1877	PTSsys temtransportersubunitIIB	1	-0.415	1	-0.737	1	-1
-	SPA1878	transport protein	1	#DIV/0!	1	#DIV/0!	1	#DIV/0!
-	SPA1879	hypotheticalprotein	1	#DIV/0!	1	#DIV/0!	1	#DIV/0!
ybjF	SPA1880	RNAm ethyltransferase	1	0	1	-0.6167	1	-0.6439
ybjO	SPA1881	hypotheticalprotein	1	-0.1375	1	0	1	-0.5146
potI	SPA1882	putrescinetransportsystempermeasePotI	1	-1	1	-0.8074	1	-1.3219
potH	SPA1883	putrescine transports ystempermeasePotH	1	-1.585	1	-2.585	1	#NUM!
potG	SPA1884	putrescinetransportATP -bindingpro teinPotG	1	-1	1	-1.8745	1	-1.1699
potF	SPA1885	putrescine-bindingpe riplasmicprotein	1	-0.737	1	-2.0356	1	-1.1699
ybjN	SPA1886	hypotheticalprotein	1	0.04731	1	0.53051	1	-0.1375
rimK	SPA1887	ribosomalproteinS6modificationprotein	1	0.27563	1	0	1	0
nfsA	SPA1888	oxygen-insensitiveNADPHnitroreductase	1	0.81943	1	0.71823	1	0.62344
ybjC	SPA1889	hypotheticalprotein	1	1	1	0.848	1	0.64046
grxA	SPA1890	glutaredoxin	1	-0.1396	0.6623	0.74507	0.816	0.56009
ybjM	SPA1891	hypotheticalprotein	1	-0.415	1	1.58496	1	0.28951
-	SPA1892	hypotheticalprotein	1	-0.2553	1	-1.3081	1E-06	-1.3785
-	SPA1893	putativetetR -family transcriptionalregulator	1	-0.3219	1	0.41504	1	0
-	SPA1894	hypotheticalprotein	1	0	1	0.34104	1	0.54749
-	SPA1895	hypotheticalprotein	1	0.14086	1	0.57258	1	0.55459
mdfA	SPA1896	multidrug translocaseMdfA	1	-0.3219	1	-0.585	1	-0.737
ybjG	SPA1897	permease	0.1385	-0.415	0.4601	0.85415	0.6358	0.59309
deoR	SPA1898	deoxyriboseoperonrepressor	0.6653	-0.2268	1	0.13006	1	-0.0291
dacC	SPA1899	D-alanyl-D-alanine carboxypeptidase(penicillin -bindingpro tein6precursor)	0.1396	-0.4716	0.3106	-0.4266	0.3503	-0.4968
yliJ	SPA1900	glutathiones -transferasefamilyprotein	1	0.14549	1	0.59474	0.7818	0.57032

yliI	SPA1901	oxidoreductase	1	0.12553	1	-0.6781	1	-0.6004
yliH	SPA1902	hypotheticalprotein	1	0.05434	1	0.19265	0.7789	-0.4073
yliG	SPA1903	hypotheticalprotein	0.6584	-0.2361	1	-1.031	1	-1.1031
yliD	SPA1904	ABCtra nsporterpermease	1	0.12029	0.0004	-1.1132	0.0003	-1.0623
yliC	SPA1905	ABCtra nsporterpermease	1	0	1E-07	-1.5146	3E-07	-1.352
yliB	SPA1906	ABC transporter substrate-bindingpro tein	1	0.1587	0.0068	-1.207	0.0004	-1.2721
yliA	SPA1907	ABCtra nsporterATP -bindingp rotein	1	0.04731	0.0003	-1.3276	0.0023	-1.1751
ybiK	SPA1908	L-asparaginase	1	0.05063	0.0016	-1.218	0.0005	-1.2295
moeA	SPA1909	molybdopterinbiosynthesisMoeAprotein	0.8902	-0.1769	0.2734	-0.4787	1	-0.3326
moeB	SPA1910	molybdopterinbiosynthesisproteinMoeB	0.447	-0.3219	0.0887	-0.5279	1	-0.1699
ybiY	SPA1911	pyruvate formate-lyase3activatingprotein	1	1.45943	1	1.58496	1	0.58496
ybiW	SPA1912	formateacetyltransferase3	2E-05	1.36257	1	0.32193	1	0.67807
ybiV(1)	SPA1913	HADs uperfamilyhydrolase	0.1981	0.67807	0.1199	-0.535	1	0.03653
ybiU	SPA1914	hypotheticalprotein	1	-0.2224	1	-1.1699	1	-0.737
ybiT	SPA1915	ABCtra nsporterATP -bindingp rotein	1	0.18442	1	-0.3561	1	-0.237
ybiS	SPA1916	hypotheticalprotein	1	0.06228	0.0367	-0.7492	0.1346	-0.7287
ybiR	SPA1917	hypotheticalprotein	1	-0.6521	1	-0.4475	1	-0.263
-	SPA1918	irondepe ndentrepressor familytranscriptionalregulator	1	-0.241	1	-0.3959	1	-0.415
ybiP	SPA1919	hypotheticalprotein	1	1	1	-0.8745	1	-0.737
ompX	SPA1920	outerme mbraneproteinxprecursor	1	0.29315	1	-0.3777	1	0.0016
dps	SPA1922	DNApro tectionduringstarvation protein	0.7264	0.58563	1	-0.1017	1	-0.023
glnH	SPA1923	glutamine-bindingpe riplasmicprotein	1	0.20732	0.022	1.6458	0.0021	1.54417
glnP	SPA1924	glutaminetransportsystempermeaseproteinGlnP	1	-0.0498	0.0852	1.14839	1E-05	1.59282
glnQ	SPA1925	glutaminetransportATP -bindingpro teinGlnQ	0.466	-0.3103	1	0.60039	0.0004	1.44171
ybiO	SPA1926	hypotheticalprotein	1	0	1	-1.585	1	-0.3626
ybiN	SPA1927	SAM-dependentm ethyltransferase	1	-0.0614	1	0.03477	1	-0.1203
ybiI	SPA1928	Zinc-finger containingprotein	1	-0.152	1	-0.2016	1	-0.7655
-	SPA1929	hypotheticalprotein	1	1.1375	1	0.91754	1	0.69188
ybiJ	SPA1930	hypotheticalprotein	9E-38	2.23522	0.004	1.16146	2E-06	1.51658
ybiB	SPA1931	transferase	1	0.40054	1	0.2003	1	0.33703
dinG	SPA1932	LexA regulated(SOS)repairenzyme	1	-0.0721	1	0.52607	1	0.30256
rhlE	SPA1933	ATP-dependent RNAhelicaserhlE	1	0.64636	1	-0.2065	1	0.30485
ybiH	SPA1934	hypotheticaltetR -familytranscriptionalregulator	1	1.06413	1	0.50901	1	0.45066
-	SPA1935	HlyD-familysecretionprotein	0.185	0.7885	0.9979	-0.1871	1	0.19745
ybhF	SPA1936	ABCtra nsporterATP -bindingp rotein	1	0.76553	1	-0.4475	1	0.46297
ybhS	SPA1937	innerme mbraneprotein	1	0.24101	1	-0.7705	1	0.11548
ybhR	SPA1938	inner membraneprotein	1	0.12553	1	-0.9125	1	-0.2157
ybhQ	SPA1939	hypotheticalprotein	0.6123	-0.2722	0.3111	0.9968	1	0.13058
ybhP	SPA1940	hypotheticalprotein	1	0	1	-1.585	1	-0.1375
ybhO	SPA1941	phospholipase	1	0	1	-2.2479	1	-0.5146
ybhN	SPA1942	hypotheticalprotein	1	-0.415	1	-1	1	-0.5146
-	SPA1943	hypotheticalprotein	1	#DIV/0!	1	#DIV/0!	1	#DIV/0!
ybhM	SPA1944	hypotheticalprotein	1	#DIV/0!	1	#DIV/0!	1	#DIV/0!
ybhL	SPA1945	permease	1	0.06413	0.4989	-0.4211	1	-0.1675
moaE	SPA1946	molybdopterinconvertingfactor,subunit2	1	0.32757	0.0003	-1.0768	0.0288	-0.7105
moaD	SPA1947	molybdopterinconvertingfactor,subunit1	1	0.31146	0.0004	-1.1155	0.0241	-0.7028
moaC	SPA1948	molybdenumcofactorbiosynthesisproteinC	1	0.45003	0.0025	-1.0959	0.1568	-0.6933
moaB	SPA1949	molybdenumcofactorbiosynthesisproteinB	1	0.36167	0.0119	-1.0106	0.0192	-0.8958

moaA	SPA1950	molybdenumcofactorbiosynthesisproteinA	1	0.1635	0.0378	-0.8365	0.0885	-0.7776
ybhK	SPA1951	hypotheticalprotein	0.0695	-0.52	1	0.30117	1	-0.0238
-	SPA1953	hypotheticalprotein	1	#NUM!	1	#DIV/0!	1	#DIV/0!
uvrB	SPA1954	excisionnucleaseABCsubunitB	1	0.20436	1	0.20945	1	-0.2996
bioD	SPA1955	dethiobiotinsynthetase	1	#NUM!	1	0	1	0
bioC	SPA1956	biotins ynthesisproteinBioC	1	#DIV/0!	1	#NUM!	1	#DIV/0!
bioF	SPA1957	8-amino-7-oxononanoatesynthase	1	#DIV/0!	1	#DIV/0!	1	#DIV/0!
bioB	SPA1958	biotins ynthetase	1	#NUM!	1	#DIV/0!	1	#DIV/0!
bioA	SPA1959	adenosylmethionine-8-amino-7-oxononanoateaminotransferase	1	-0.585	1	-1	1	-1
ybhB	SPA1960	hypotheticalprotein	1	0.26303	0.2698	-0.4884	1	0.11991
hutH	SPA1961	histidineammonia -lyase	0.4212	-0.3599	0.282	-0.7075	0.0275	-0.9289
hutC	SPA1963	histidineutilizationrepressor	1	-0.0566	1	0.28798	1	-0.1769
hutG	SPA1964	formiminoglutamase	1	0.22239	1	0.19094	1	0.0217
hutI	SPA1965	imidazolonepropionase	1	0.06413	1	0.18521	1	0.17195
ybhC	SPA1966	pectinesterase	2E-05	-1.0513	0.1129	-0.6812	0.1584	-0.7432
ybhE	SPA1967	hypotheticalprotein	1	0.47584	1	-0.1755	1	-0.0924
ybhA	SPA1968	hypotheticalprotein	1	-0.026	1	0.1822	1	0.22239
modC	SPA1969	molybdenumtransportATP -binding proteinModC	0.3683	0.70044	1	0.30812	1	0.10962
modB	SPA1970	molybdenumtransportsystempermeaseproteinModB	0.1024	0.73697	1	0.40526	1	0.11247
modA	SPA1971	molybdate-bindingpe riplasmicprotein	0.1978	0.67271	1	0.55339	1	0.17655
ybhT	SPA1972	hypotheticalprotein	1	-0.0862	0.5412	0.63346	0.4861	-0.3466
modE	SPA1973	molybdenumtransportproteinModE	0.3151	-0.4489	0.36	-0.3318	0.0736	-0.8093
modF	SPA1974	molybdenumtransportATP -binding proteinModF	1	-0.3785	1	-0.3132	1	-0.6477
-	SPA1975	hypotheticalprotein	1	0	1	#NUM!	1	#DIV/0!
galE	SPA1976	UDP-glucose4 -epimerase	1	0.10997	1	0.64816	1	0.22556
galT	SPA1977	galactose-1-phosphate uridylyltransferase	1	0.34514	0.5368	0.8178	1	0.5009
galK	SPA1978	galactokinase	1	0.42509	1	0.5765	1	0.47883
galM	SPA1979	aldose 1-epimerase (mutarotase)	1	0.20387	1	0.47953	0.7799	0.61844
gpmA	SPA1980	phosphoglyceratemutase	1	0.20407	1	-0.1302	1	-0.1015
-	SPA1981	ABCtra nsporterATP -bindingp rotein	1	0.58496	1	0.58496	1	1
-	SPA1982	FecCD familyABCtransporterpermease	1	0.36257	1	0.41504	1	0
aroG	SPA1983	phospho-2-dehydro-3-deoxyheptonatealdolase(DAHPsynthetase)phenylalaninerepressible	1	0.01792	0.1964	-0.6192	0.6889	-0.4251
ybgS	SPA1984	secretedprotein	1	-1	0.005	-0.8854	0.4599	-0.4406
ybgR	SPA1985	cation transportpro tein	1	-0.3132	1	0.25526	1	-0.142
pnuC	SPA1986	pnuCprote in	1	-0.737	1	-0.9329	1	-0.8745
nadA	SPA1987	quinolinatesynthetaseAprotein	1	-1	1	-0.585	1	0
-	SPA1988	LystR NA	0.1329	-0.3697	0.5521	-0.2048	0.1434	-0.5896
-	SPA1989	LystR NA	0.0865	-0.4132	0.9723	-0.1	0.065	-0.5793
-	SPA1990	LystR NA	0.2479	-0.4594	1	-0.029	0.2755	-0.3649
-	SPA1991	ValtRN A	0.2161	-0.5329	1	-0.0135	0.1546	-0.4748
-	SPA1992	LystR NA	0.2555	-0.4854	0.914	-0.0939	0.1925	-0.5104
ybgF	SPA1993	hypotheticalprotein	0.6503	-0.3771	0.6965	-0.6247	0.8236	-0.37
pal	SPA1994	peptidoglycan-associatedlipoproteinprecursor	0.5597	-0.8014	0.7572	-0.8357	0.614	-0.5548
tolB	SPA1995	tolBpro teinprecursor	0.1727	-0.7603	0.3955	-1.0322	0.2191	-0.7889
tolA	SPA1996	tolApro tein	1	-0.663	1	-1.1312	1	-0.7004
tolR	SPA1997	tolRpro tein	0.2657	-0.4201	2E-07	-1.4317	0.0029	-0.8405
tolQ	SPA1998	TolQ protein	0.1656	-0.4406	3E-06	-1.2882	0.0004	-1.0426
ybgC	SPA1999	hypotheticalprotein	0.2828	-0.4091	0.0199	-0.7127	0.0173	-0.6919

ybgE	SPA2000	hypotheticalprotein	1	0.35073	0.0038	1.4284	1	0.06518
ybgT	SPA2001	hypotheticalprotein	1	0.31711	0.472	0.88268	1	-0.1688
cydB	SPA2002	cytochromedubiquinoloxidasesubunitII	1	0.28606	1	0.87241	1	-0.151
cydA	SPA2003	cytochromedubiquinoloxidasesubunitI	1	-0.0527	1	0.80416	1	-0.3774
sucD	SPA2004	succinyl-CoAs ynthetasesubunitalpha	1	-0.0889	0.8909	-0.623	1	0.08595
sucC	SPA2005	succinyl-CoAs ynthetasesubunitbeta	1	-0.1072	1	-0.5523	1	0.02311
sucB	SPA2006	dihydrolipoamidesuccinyltransferasecomponent(E2)	1	-0.0987	1	-0.3466	1	0.11001
sucA	SPA2007	2-oxoglutaratedehydrogenaseE1component	1	-0.142	1	-0.2334	1	-0.2525
sdhB	SPA2008	succinatedehydrogenaseiron -sulfurpr otein	0.6503	-0.7758	1	-0.1655	1	-0.4562
sdhA	SPA2009	succinatedehydrogenaseflavoproteinsubunit	0.8318	-0.45	1	-0.0573	0.8735	-0.3658
sdhD	SPA2010	succinatedehydrogenasehydrophobicmembraneanchorprotein	0.3948	-0.4218	0.8341	-0.5311	0.1142	-0.6881
sdhC	SPA2011	succinatedehydrogenasecytochromeb -556subunit	1	-0.2415	1	-0.3803	0.3812	-0.6389
-	SPA2012	hypotheticalprotein	1	#DIV/0!	1	#DIV/0!	1	#DIV/0!
gltA	SPA2013	citrate synthase	1	-0.2483	1	-0.671	1	-0.2932
abrB	SPA2014	hypotheticalprotein	1	0	1	-0.1031	1	0.05063
nei	SPA2015	endonucleaseVIII,DNAN -glycosylasewithanAPlyaseactivity	1	0.07276	1	0.08246	1	-0.3626
-	SPA2016	hypotheticalprotein	1	-0.241	1	0	1	-0.3626
-	SPA2017	glycosyltransferasefamily protein	1	-0.737	1	#NUM!	1	0
-	SPA2018	hypotheticalprotein	1	-0.585	1	#NUM!	1	#NUM!
-	SPA2019	cell wallbiogenesisglycosyltransferase	1	-1	1	#DIV/0!	1	#DIV/0!
-	SPA2020	polysaccharideexportABCtransporterATP -bindingpro tein	1	-1.585	1	#DIV/0!	1	#DIV/0!
-	SPA2021	galactosyltransferase	1	-0.585	1	#DIV/0!	1	#DIV/0!
-	SPA2022	UDP-galactopyranosemutase	1	0	1	#DIV/0!	1	#DIV/0!
-	SPA2023	hypotheticalprotein	1	-0.0825	1	0	1	-1
-	SPA2025	DNAre combinase	1	0.14585	1	0.152	1	-0.415
-	SPA2026	hypotheticalprotein	1	-0.4854	1	0	1	0
ybgL	SPA2027	hypotheticalprotein	1	-0.0515	0.1146	-0.5489	1	-0.6781
ybgK	SPA2028	hypotheticalprotein	1	-0.038	0.1016	-0.674	0.5552	-0.5525
ybgJ	SPA2029	hypotheticalprotein	0.9562	-0.1758	0.074	-0.7443	0.4947	-0.5348
ybgI	SPA2030	hypotheticalprotein	1	-0.1532	0.1729	-0.5802	0.5266	-0.4792
ybgH	SPA2031	PTR2-familytransportprotein	1	-0.1699	1	0	1	-0.6521
phrB	SPA2032	deoxyribodipyrimidinephotolyase	1	1.70044	1	-0.585	1	-0.3785
ybfA	SPA2033	hypotheticalprotein	4E-51	2.40125	2E-08	2.02419	0.7789	0.76156
-	SPA2034	hypotheticalprotein	1	#DIV/0!	1	#DIV/0!	1	#DIV/0!
kdpA	SPA2035	potassium-transportingATPasesubunitA	1	#DIV/0!	1	#NUM!	1	#NUM!
kdpB	SPA2036	P-typeAT Pase, high-affinitypotassiumtransportsystemsubunitB	1	0	1	-0.415	1	0
kdpC	SPA2037	potassium-transportingATPasesubunitC	1	0	1	-0.6521	1	-0.1699
kdpD	SPA2038	sensor proteinKdpD	1	-0.1155	1	-0.341	1	-0.2801
kdpE	SPA2039	KDPo peron transcriptionalregulatoryprotein	1	-0.1926	1	-0.2838	1	-0.4005
speF	SPA2040	ornithine decarboxylaseisozyme,inducible	0.1053	1.29931	0.0771	1.64297	6E-16	2.91816
potE	SPA2041	putrescine-ornithine antiporter	1	1.58496	0.8531	0.66964	0.0283	1.61162
-	SPA2042	5-nitroimidazoleantibioticresistance	1	0.23133	0.0134	1.33703	2E-16	2.23491
pgm	SPA2043	phosphoglucomutase	1	-0.1065	1	-0.1312	1	0.27328
seqA	SPA2044	seqApro tein	1	-0.0414	1	0.54749	1	0.07917
ybfF	SPA2045	esterase/lipaseYbfF	1	-0.1312	1	0	1	-0.2937
ybfE	SPA2046	hypotheticalprotein	1	-0.0406	1	0.14202	1	-0.3219
fldA	SPA2047	flavodoxin1	0.882	-0.1959	1	0.37672	1	-0.0317
fur	SPA2048	ferric uptakeregulationprotein	0.8431	-0.2783	1	0.08593	1	-0.1582

-	SPA2049	lysR-familytranscriptionalregulator	1	0.0458	1	-0.3819	1	-0.3561
-	SPA2050	hypotheticalprotein	1	0.32193	1	-0.3049	1	-0.4854
-	SPA2051	citB-like protein	1	0	1	-0.8301	1	-1.415
citA	SPA2052	citrate-protonsy mporter	1	-0.848	1	-0.6215	1	-1.3219
ybfN	SPA2053	lipoprotein	1	-0.585	1	0	1	-0.9386
ybfM	SPA2054	outerme mbraneprotein	1	-1.4507	1	-0.4854	1	-1.7162
glnS	SPA2055	glutaminyl-tRNAs ynthetase	0.8861	-0.3034	0.8995	-0.4955	0.8031	-0.3727
nagE	SPA2056	PTSsys tem N-acetylglucosamine-specifictransportersubunitIIABC	0.868	-0.37	1	0.18728	1	-0.24
nagB	SPA2057	glucosamine-6-phosphate isomerase	1	0	0.2516	-0.4413	0.5448	-0.3897
nagA	SPA2058	N-acetylglucosamine-6-phosphate deacetylase	1	-0.0774	0.7543	-0.1319	1	-0.1436
nagC	SPA2059	N-acetylglucosaminerepressor	1	-0.1699	0.958	-0.1895	0.8387	-0.3841
nagD	SPA2060	NagDpro tein	0.1036	-0.4458	0.0589	-0.6049	0.1901	-0.5389
metU	SPA2062	MettRNA	0.3425	-0.3536	0.4609	-0.2697	0.7252	-0.3077
leuW	SPA2063	Leu tRNA	0.3508	-0.3168	0.5924	-0.2398	0.222	-0.4788
glnW	SPA2064	GlntRN A	0.2957	-0.3434	0.2754	-0.378	0.0362	-0.6817
glnW	SPA2065	GlntRN A	0.3115	-0.3891	0.236	-0.458	0.0142	-0.7303
metU	SPA2066	MettRNA	0.1045	-0.3968	0.1747	-0.4958	0.0143	-0.6872
glnX	SPA2067	GlntRN A	1	-0.2996	0.0185	-0.6444	0.2196	-0.585
glnX	SPA2068	GlntRN A	1	-0.1926	1	-0.7655	1	-0.493
yleB	SPA2069	monooxygenase	1	0.25815	1	0.60234	1	0.23794
miaB	SPA2070	tRNA-thiotransferaseMiaB	1	0.02647	0.36	-0.4063	0.4469	-0.4739
ybeZ	SPA2071	PhoH-like ATP-bindingpro tein	1	-0.0896	0.7698	-0.1961	1	-0.1236
ybeY	SPA2072	hypotheticalprotein	0.9803	-0.1718	0.4409	-0.3171	1	-0.1747
ybeX	SPA2073	hemolysin-like protein	0.8264	-0.2746	0.5885	-0.3143	0.9162	-0.3611
lnt	SPA2074	apolipoproteinN -acyltransferase	1	-0.1884	0.0307	-0.737	1	-0.3761
ybeJ	SPA2075	ABCtra nsportersubstrate -bindingpro tein	1	-0.1299	0.3529	-1.0734	1	0.17932
gltJ	SPA2076	glutamate/aspartatetransportsystempermeaseGltJ	1	-0.6439	0.0006	-1.2319	1	0
gltK	SPA2077	glutamate/aspartatetransportsystempermeaseGltK	1	-1	2E-05	-1.1763	1	#DIV/0!
gltL	SPA2078	glutamate/aspartatetransportATP -binding proteinGltL	0.0004	-0.8991	0.1208	-0.6145	1	0
ybeK	SPA2079	nucleosidehydrolase	1	0.11548	0.8995	0.75169	0.0192	1.15381
-	SPA2080	hypotheticalprotein	1	0.11784	0.2431	1	0.0007	1.32971
ybeL	SPA2081	hypotheticalprotein	1	0.08005	0.6349	0.7719	1	-0.1176
-	SPA2082	sigma-54dependent transcriptionalregulator	1	-0.1454	1	0.39993	1	0.30895
-	SPA2083	permease	1	-0.3219	1	0.58496	1	1.41504
-	SPA2084	hydrolaseC -terminus	1	-0.585	1	3.08746	1	4.70044
-	SPA2085	hydrolaseN -terminus	1	0	1	4.24793	1	5.58496
leuS	SPA2086	leucyl-tRNAs ynthetase	1	-0.1936	0.7591	-0.7639	0.7282	-0.585
rlpB	SPA2087	rarelipo proteinB	0.1189	-0.5062	0.0375	-0.8913	0.1162	-0.7294
holA	SPA2088	DNApo lymeraseIIIsubunitdelta	0.3151	-0.3999	0.11	-0.6215	0.3365	-0.5394
ybeN	SPA2089	hypotheticalprotein	1	-0.3785	0.2351	-0.4594	1	-0.6015
cobD	SPA2090	aminotransferaseCobD	1	0.04244	1	1.23266	1	0.27009
cobC	SPA2091	alpha-ribazole-5'-phosphate phosphatase	0.7751	-0.1567	1	0.64534	1	-0.1278
ybeB	SPA2092	hypotheticalprotein	0.5476	-0.2695	1	-0.0724	0.3947	-0.4496
ybeA	SPA2093	hypothetical protein	0.7087	-0.2174	0.7838	-0.157	0.4548	-0.4381
pbpA	SPA2094	penicillin-bindingpro tein2	1	-0.1844	1	-0.6167	1	-0.415
mrdB	SPA2095	rodshape -determiningproteinRodA	1	-0.507	1	-0.6215	1	-0.3785
rlpA	SPA2096	rarelipo proteinAprecursor	0.4177	-0.4039	0.6712	-0.2582	0.3478	-0.5086
dacA	SPA2097	D-alanine carboxypeptidase	1	-0.1616	0.3814	-0.391	0.9993	-0.2102

ybeD	SPA2098	hypotheticalprotein	0.0071	-0.7237	0.5834	-0.2801	0.0053	-0.7984
lipB	SPA2099	lipoate-proteinl igaseB (lipoatebiosynthesisproteinB)	1	-0.0324	1	0.1635	1	-0.3479
ybeF	SPA2100	lysR-familytranscriptionalregulator	1	-0.3626	1	-1.4854	1	-0.858
lipA	SPA2101	lipoicacidsynthetase	1	0.17236	1	-0.1237	0.3685	-0.6781
tatE	SPA2102	sec-independent proteintranslocaseproteinTatE	1	0.14684	0.7744	-0.2053	1	-0.03
ybeM	SPA2103	hydrolase	1	1	1	0	1	0
crcB	SPA2104	hypotheticalprotein	1	0	1	0.5025	1	0.20645
cspE	SPA2105	colds hock-like proteincspE	0.7083	-0.626	1	-0.295	1	-0.4816
pagP	SPA2106	antimicrobialpeptideresistanceandlipidAacylationprotein	5E-06	-1.0395	1	-0.848	2E-05	-1.0943
dcuC	SPA2107	C4-dicarboxylateanaerobiccarrier	1	-1.5146	1	-0.737	1	-1.1255
dpiA	SPA2108	transcriptionalregulatoryprotein DpiA	1	-0.737	1	-0.585	1	-1
citC	SPA2110	[citrate(pro -3S)-lyase]ligase	1	#DIV/0!	1	#DIV/0!	1	#DIV/0!
citD	SPA2111	citrate lyaseacylcarrierprotein	1	#DIV/0!	1	#DIV/0!	1	#DIV/0!
citE	SPA2112	citrate lyasesubunitbeta	1	#DIV/0!	1	#DIV/0!	1	#DIV/0!
citF	SPA2113	citrate lyasesubunitalpha	1	#DIV/0!	1	#DIV/0!	1	#DIV/0!
citX	SPA2114	hypotheticalprotein	1	#DIV/0!	1	#DIV/0!	1	#DIV/0!
citG	SPA2115	CitGprotei n	1	#DIV/0!	1	#DIV/0!	1	#DIV/0!
citT	SPA2116	citrate carrier	1	-1.585	1	-0.585	1	-1
rna	SPA2117	ribonucleaseIprecursor	1	-0.1378	1	0.06738	1	0.20436
rnk	SPA2118	regulatorofnucleosidediphosphatekinase	0.0215	-0.6651	0.0977	-0.6296	0.148	-0.4854
ybdQ	SPA2120	hypotheticalprotein	1	-0.3245	1	0.66148	1	0.12357
-	SPA2121	molybdopterin-containingoxidoreductasemembraneanchorsubunit	1	-0.4739	1	-0.585	1	-0.341
-	SPA2122	molybdopterin-containingoxidoreductaseiron -sulfurs ubunit	1	-1.585	1	-0.585	1	-1
-	SPA2123	molybdopterin-containingoxidoreductasecatalytic subunit	1	0	1	0	1	0
-	SPA2124	hypotheticalprotein	1	#DIV/0!	1	#DIV/0!	1	#DIV/0!
ahpF	SPA2125	alkyl hydroperoxidereductaseF52Aprotein(subunitF)	1	0.16993	1	0.45138	1	0.41504
ahpC	SPA2126	alkyl hydroperoxidereductasec22protein	1	0.24252	1	0.57437	1	0.0941
dsbG	SPA2127	thiol:disulfideinterchangeproteinDsbGprecursor	1	-0.263	0.6431	-0.2996	1	0.2713
ybdO	SPA2128	putativelysR -familytranscriptionalregulator	1	0	1	0.32193	1	-0.0875
ybdN	SPA2129	hypotheticalprotein	1	0	1	-1	1	-0.737
ybdM	SPA2130	hypotheticalprotein	1	-0.2065	1	-0.4739	1	-0.7965
ybdL	SPA2131	aminotransferase	0.8378	0.54749	1	2.21299	4E-271	3.80735
ybdH	SPA2132	oxidoreductase	0.1098	0.82491	1	2.70044	7E-280	3.94486
ybdD	SPA2133	hypotheticalprotein	0.0764	-0.4238	1	0.33487	0.0634	-0.5334
cstA	SPA2134	carbons tarvationproteinA	1	-0.4475	1	-0.0339	1	-0.613
ybdB	SPA2135	hypotheticalprotein	1	0	1	-0.3219	1	-0.4854
entA	SPA2136	2,3-dihydro-2,3-dihydroxybenzoatedehydrogenase	1	0	1	-0.585	1	0
entB	SPA2137	isochorismatase	1	0	1	-0.415	1	-0.585
entE	SPA2138	2,3-dihydroxybenzoate-AMPl igase	1	-1	1	-1.585	1	-1
entC	SPA2139	isochorismatesynthaseEntC	1	0.58496	1	-0.585	1	-1
fepB	SPA2140	ferrienterobactin-bindingpe riplasmicprotein precursor	1	1.80735	1	-1.8745	1	-1.585
ybdA	SPA2141	membraneproteinp43	1	0	1	0	1	#NUM!
fepD	SPA2142	ferric enterobactintransportproteinFepD	1	#DIV/0!	1	#NUM!	1	#NUM!
fepG	SPA2143	ferric enterobactintransportproteinFepG	1	-1	1	-2.3219	1	-1
fepC	SPA2144	ferric enterobactintransportATP -bindingpro teinFepC	1	0	1	#NUM!	1	#NUM!
fepE	SPA2145	ferric enterobactin(enterochelin)transporter	1	-0.585	0.1342	-0.5594	0.1087	-0.7225
entF	SPA2146	enterobactin synthetasecomponentF	1	-1	1	-1.3219	1	-0.585
ybdZ	SPA2147	hypotheticalprotein	1	#DIV/0!	1	#NUM!	1	#NUM!

fes	SPA2148	enterochelinesterase	1	1	1	-1	1	-1
fepA	SPA2149	ferrienterobactinreceptor	1	0	1	0	1	-0.3219
entD	SPA2150	enterobactin synthetasecomponentD	1	#DIV/0!	1	0	1	0
ybdK	SPA2151	hypotheticalprotein	1	0	1	-1.5406	1	-1.1375
ybdJ	SPA2152	hypotheticalprotein	1	-0.585	1	-0.7004	1	-0.585
ramA	SPA2153	transcriptionalactivatorRamA	2E-05	1.38971	1	0.46357	1	0.25873
-	SPA2154	putativetetR -family transcriptionalregulator	0.0008	1.26912	0.3955	0.90613	0.3788	0.82597
ybdF	SPA2155	hypotheticalprotein	5E-05	1.2916	0.2842	0.93161	0.2163	0.8693
nfnB	SPA2156	oxygen-insensitiveNAD(P)Hnitroreductase	0.1347	1.20014	1	0.59579	0.775	0.63009
apeE	SPA2157	outerme mbraneesterase	1	-0.4525	1	-1.415	1	-0.8074
ybdG	SPA2158	hypotheticalprotein	0.0143	-0.6521	1	-1	1	-0.7549
pheP	SPA2159	phenylalanine-specificpermease	1	-0.263	1	-0.737	1	-1
-	SPA2160	ATPase	1	-0.3985	1	0	1	-0.7997
ykgB	SPA2161	hypotheticalprotein	1	-1	1	-1.3219	1	-1.585
-	SPA2162	hypotheticalsecretedprotein	1	#DIV/0!	1	#NUM!	1	#NUM!
ykgC	SPA2163	pyridine nucleotide-disulfideoxidoreductase	1	-1	1	-0.415	1	-0.3219
ykgD	SPA2164	hypotheticalaraC -family transcriptionalregulator	0.0697	-0.5645	0.4671	-0.5305	0.2647	-0.5575
silA	SPA2165	innerme mbraneproton/cationantiporter	1	-0.2996	1	-0.848	1	-1
-	SPA2166	copper-bindingp rotein	1	#NUM!	1	#NUM!	1	#NUM!
gtrA	SPA2167	bactoprenol-linked glucosetranslocase	1	-0.1979	1	-0.5146	1	-0.5343
gtrB	SPA2168	bactoprenolglucosyltransferase	1	-0.0525	1	-0.5475	1	-0.6439
-	SPA2170	transposase	1	-0.3219	1	0	1	-1.1699
-	SPA2172	ArgtRN A	1	-2	1	#NUM!	1	#NUM!
fimW	SPA2173	fimbriaewprotein	1	-0.585	1	-0.585	1	-1
-	SPA2174	hypotheticalprotein	1	-0.415	1	0	1	-0.585
fimY	SPA2175	fimbriaeYprotein	1	-1	1	#DIV/0!	1	#NUM!
fimZ	SPA2176	transcriptionalregulator)	1	0	1	0	1	-0.152
fimF	SPA2177	fimbria-like proteinFimF precursor	1	-0.2479	1	-0.2224	1	-0.415
fimH	SPA2178	FimHpro tein	1	-0.2115	1	-0.585	1	-0.585
fimD	SPA2179	outerme mbraneusherproteinFimD	1	-0.1155	1	0	1	-0.585
fimC	SPA2180	fimbrialchaperoneprotein	1	-0.3049	1	#DIV/0!	1	#NUM!
fimI	SPA2181	hypotheticalprotein	1	-0.2168	1	#DIV/0!	1	#NUM!
fimA	SPA2182	type-1fimbrial proteinsubunitA	1	-0.1079	1	-1	1	-4.1699
folD	SPA2183	bifunctionalmethylenetetrahydrofolatedehydrogenase/methenyltetrahydrofolatecyclohydrolase	0.7711	-0.2201	0.7207	-0.2115	0.4885	-0.4361
ybcJ	SPA2184	hypotheticalprotein	0.2416	-0.3058	0.3955	-0.372	0.1947	-0.455
ybcI	SPA2185	hypotheticalprotein	1	-0.4854	1	0	1	0
cysS	SPA2186	cysteinyl-tRNAs ynthetase	0.6406	-0.307	0.1339	-0.5976	0.3362	-0.5036
ppiB	SPA2187	peptidyl-prolyl cis-transi someraseB	0.5671	-0.4039	1	-0.0794	1	-0.4004
ybbF	SPA2188	hypotheticalprotein	0.9024	-0.1394	0.2594	-0.415	0.2701	-0.5485
purE	SPA2189	phosphoribosylaminoimidazolecarboxylasecatalyticsubunit	1	-0.0931	1E-13	-1.6262	5E-06	-1.1155
purK	SPA2190	phosphoribosylaminoimidazolecarboxylaseATPasesubunit	1	-0.1174	8E-14	-1.8413	1	-1.1758
arcC	SPA2191	carbamatekinase	1	#NUM!	1	0	1	0
ylbF	SPA2192	hypotheticalprotein	1	#DIV/0!	1	0	1	0
ylbE	SPA2193	hypotheticalprotein	1	#DIV/0!	1	0	1	#NUM!
allD	SPA2195	ureidoglycolatedehydrogenase	1	-0.3219	1	0.73697	1	-0.585
allC	SPA2196	allantoateamidohydrolase	1	-0.3479	1	-0.1699	1	-0.263
ylbA	SPA2197	hypotheticalprotein	1	-0.1444	1	-0.3847	1	-0.5361
glxK	SPA2198	glyceratekinase	1	0	1	-0.3219	1	-1

ybbY	SPA2199	permease	1	#NUM!	1	-0.415	1	-0.585
allB	SPA2200	allantoinase	1	-2.2224	1	-1	1	-2.585
-	SPA2202	metabolitetransportprotein	1	#NUM!	1	#NUM!	1	#NUM!
-	SPA2203	2-hydroxy-3-oxopropionatereductase	1	-1.8074	1	-1.585	0	-5.9542
hyi	SPA2204	hydroxypyruvateisomerase	1	-1.5146	1	-1.585	1	-5.858
gcl	SPA2205	glyoxylatecarboligase	1	-1.1699	1	-0.737	1	-4.4594
allR	SPA2206	negativeregulatorofallantoinand glyoxylateutilizationoperons	0.4638	-0.2937	1	-0.031	1	-0.2955
allA	SPA2207	ureidoglycolatehydrolase	1	-0.5639	1	0.44746	1	-1.0589
ybbS	SPA2208	hypotheticallysR -familytranscriptionalregulator	1	0.20163	1	1.37851	1	0
ybbB	SPA2209	hypotheticalprotein	1	0.34792	0.8128	0.74507	1	0.442
sfbC	SPA2210	ABCtra nsporter	1	0	1	-1	1	-0.241
sfbB	SPA2211	ABCtra nsporterATP -bindingp rotein	1	0.26303	1	-0.415	1	0.08246
sfbA	SPA2212	lipoprotein	1	0.19265	1	-0.2451	1	0.14086
-	SPA2213	outerme mbraneprotein	1	0.34465	3E-13	2.28379	1	2.05889
ybbP	SPA2214	hypotheticalprotein	1	-0.663	1	-1	1	-0.4594
ybbA	SPA2215	ABCtra nsporterATP -bindingp rotein	1	-0.4263	1	-0.613	1	-0.4361
tesA	SPA2216	acyl-coAthi oesteraseI	1	-0.3943	1	-0.2775	1	0.07595
ybbO	SPA2217	hypotheticaloxidoreductase	1	-0.0214	0.7873	-0.179	1	0.1193
ybbN	SPA2218	thioredoxin-like protein	1	-0.1409	0.9206	-0.1268	1	0.07555
ybbM	SPA2219	hypotheticalprotein	1	-0.0458	1	-0.4854	1	-0.241
ybbL	SPA2220	ABC transporter ATP-bindingp rotein	1	0.12553	1	-0.3219	1	-0.1699
ybbJ	SPA2222	hypotheticalprotein	0.5554	-0.2895	1	-0.1699	1	-1.0995
cueR	SPA2223	coppere ffluxregulator	1	0.05311	1	0.3278	1	0.11277
ybaR	SPA2224	copper-transportingATPase	4E-09	2.17169	0.0717	1.83131	0.0004	2.17612
-	SPA2225	secretedprotein	1	0	1	0.87447	1	1.16993
ybaP	SPA2226	hypotheticalprotein	0.0472	-0.5539	1	-0.2937	1	-0.493
ybaK	SPA2227	hypotheticalprotein	1	0.07039	1	-0.0458	0.9386	-0.237
ushA	SPA2228	UDP-sugarhy drolase5' -nucleotidase	0.6488	-0.353	1	0.13124	1	0.35716
fsr	SPA2229	fosmidomycinresistanceprotein	1	0.3744	0.001	-1.0559	1	-0.1481
ybaL	SPA2230	transporter	1	-0.6415	1	-0.478	1	-0.6374
gsk	SPA2231	inosine-guanosinekinase	1	0.1375	1	-0.5146	1	-0.7776
aes	SPA2232	acetyle sterase	1	0	1	1.58496	1	1.1375
hemH	SPA2233	ferrochelatase	0.1466	-0.4245	1	-0.433	1	-0.6057
adk	SPA2234	adenylatekinase	1	-0.1233	0.4636	-0.3479	1	-0.1737
htpG	SPA2235	heatsho ckproteinHtpG	1	-0.0106	1	0.23195	1	0.46234
recR	SPA2236	recombinationproteinRecR	0.4952	-0.3785	0.4609	-0.3249	0.6891	-0.337
ybaB	SPA2237	hypotheticalprotein	0.558	-0.3516	0.3369	-0.3944	0.4913	-0.4173
dnaX	SPA2238	DNApo lymeraseIIIsubunitsgammaandtau	1	-0.0492	1	-0.1558	1	-0.0862
apt	SPA2239	adenine phosphoribosyltransferase	1	0	1	0.04182	1	0.2115
ybaN	SPA2240	hypotheticalprotein	1	0	1	-0.737	1	-0.3219
priC	SPA2241	primosomalreplicationproteinN	1	-0.0721	1	-0.1993	1	-0.3219
ybaM	SPA2242	hypotheticalprotein	1	-0.1444	1	-0.2479	1	-0.433
-	SPA2243	hypotheticalprotein	0.4386	-0.3175	1	0.40599	1	-0.1019
aefA	SPA2244	integral membraneproteinAefA	1	-0.415	1	-1.4044	1	-0.737
acrR	SPA2245	acrABope ronrepressor	0.009	0.94342	1E-05	1.70526	2E-06	1.5639
acrA	SPA2246	acriflavinresistanceproteinA	0.3674	0.83081	1	0.20622	1	0.46
acrB	SPA2247	acriflavinresistanceproteinB	1	0.35921	1	-0.4039	1	0.25076
ybaJ	SPA2248	hypotheticalprotein	1	0.17932	0.0039	-1.0044	0.098	-0.7516

hha	SPA2249	hemolysinexpressionmodulatingprotein	1	0.12832	0.0009	-1.0554	0.0134	-0.9694
maA	SPA2250	maltoseO -acetyltransferase	1	0	0.0056	-0.8745	0.0005	-0.9868
ylaC	SPA2251	hypotheticalprotein	1	-0.1299	1	0.60113	1	0.48705
rpmJ2	SPA2252	50S ribosomalproteinL36	1	0.16993	1	-0.2224	1	-0.7776
rpmE2	SPA2253	50Sribos omalproteinL31	1	0	1	0	1	-0.6781
ylaB	SPA2254	hypotheticalprotein	1	-0.263	1	-0.1926	1	-0.1806
-	SPA2255	-	1	-1	1	0	1	0
ybaZ	SPA2256	methylated-DNA methyltransferase	1	-0.0468	1	0.49881	1	-0.1054
ybaY	SPA2257	hypotheticalprotein	1	0.45457	1	-0.1699	1	0.32722
tesB	SPA2258	acyl-CoAthi oesteraseII	1	0.20436	1	#DIV/0!	1	-0.3847
amtB	SPA2259	ammoniumtransporter	1	0.32193	1	1	1	1.22239
glnK	SPA2260	nitrogen regulatoryproteinP -II	1	1	1	#DIV/0!	1	2.58496
mdlB	SPA2261	ABCtra nsporterATP -bindingp rotein	1	-0.415	1	-0.415	1	-0.4594
mdlA	SPA2262	ABCtra nsporterATP -bindingp rotein	1	-0.1155	1	-0.3923	1	-0.5525
ybaO	SPA2263	hypotheticaltranscriptionalregulator	1	-0.5619	1	-0.1751	1	-0.6656
-	SPA2264	lyase	1	-0.585	1	0	1	0
cof	SPA2265	hypotheticalprotein	1	-1.4854	1	0.14439	1	-0.7004
ybaE	SPA2266	solute-bindingpro tein	1	0	1	1.71049	1	0.80735
ybaX	SPA2267	hypotheticalprotein	1	-0.1699	1	0.22239	1	0.11548
ybaW	SPA2268	hypotheticalprotein	1	1.73697	0.0011	1.24793	1	0.92057
ybaV	SPA2269	hypotheticalprotein	1	0	1	0	1	0
ppiD	SPA2270	peptidyl-prolyl cis-transi someraseD	1	-0.172	0.4423	-0.3312	1	-0.1454
hupB	SPA2271	DNA-bindingp roteinHU -beta	0.3186	-0.6215	1	0.03553	1	-0.2667
lon	SPA2272	Lonprote ase	1	-0.1425	1	-0.1757	1	0.25656
clpX	SPA2273	ATP-dependent clpproteaseATP -bindings ubunitClpX	1	0.07369	1	-0.3979	1	-0.0312
clpP	SPA2274	ATP-dependent clpproteaseproteolyticsubunit	0.85	-0.2128	1	0.09818	1	-0.152
tig	SPA2275	trigger factor	0.4806	-0.8781	0.7357	-0.8408	0.8469	-0.5164
bolA	SPA2276	BolA protein	0.0059	-0.7334	0.0009	-1.057	0.0399	-0.8996
yajG	SPA2277	lipoprotein	3E-06	-1.0834	1E-05	-1.1993	0.0005	-1.012
ampG	SPA2278	AmpGprotei n	1	-0.7885	1	-1.2895	1	-0.7199
cyoA	SPA2279	cytochromeoubiquinoloxidasesubunitII	8E-05	-1.39	0.5879	-1.1765	5E-12	-1.8201
cyoB	SPA2280	cytochromeoubiquinol oxidasesubunitI	4E-05	-1.9012	1	-0.8486	0.0044	-1.4067
cyoC	SPA2281	cytochromeoubiquinoloxidasesubunitIII	1E-16	-2.1048	0.9979	-0.7135	6E-05	-1.291
cyoD	SPA2282	cytochromeoubiquinoloxidaseCsubunit	4E-16	-1.8826	0.6994	-0.6715	0.0043	-1.103
cyoE	SPA2283	cytochromeoubiquinoloxidaseCsubunit	2E-08	-1.7126	0.7838	-0.6781	0.0299	-0.8737
-	SPA2284	hypotheticalprotein	1	0	1	0	1	0
-	SPA2285	hypotheticalprotein	1	#NUM!	1	-1.585	1	0
-	SPA2286	transposase	1	#DIV/0!	1	#NUM!	1	#NUM!
yajR	SPA2287	hypotheticalmajorfacilitatorfamilytransportprotein	1	0	1	-0.613	1	-0.4361
yajQ	SPA2288	hypotheticalprotein	0.7447	-0.2889	1	-0.1647	0.7818	-0.4764
apbA	SPA2289	ApbAprote in	0.006	1.0199	0.027	1.31228	0.0074	1.26894
thiJ	SPA2290	4-methyl-5(b-hydroxyethyl)-thiazole monophosphatebiosynthesisproteinThiJ	0.823	0.65208	0.275	0.94705	0.225	0.91177
phnX	SPA2291	phosphonoacetaldehydephosphonohydrolase	1	0	1	0	1	0
phnW	SPA2292	2-aminoethylphosphonate--pyruvatetransaminase	1	-0.585	1	0	1	1
phnR	SPA2293	regulatorof2 -aminoethylphosphonateuptakeandmetabolismoperon	1	-0.3219	1	0	1	-0.5443
phnS	SPA2294	2-aminoethylphosphonatetransportersubstrate -binding protein	1	0	1	1	1	0.58496
phnT	SPA2295	2-aminoethylphosphonatetransporterATP -bindingpro tein	1	0.32193	1	1.32193	1	0.26303
phnU	SPA2296	2-aminoethylphosphonatetransportermembraneprotein	1	#DIV/0!	1	0	1	0

phnV	SPA2297	2-aminoethylphosphonatetransporter membraneprotein	1	0	1	0.58496	1	0
thiI	SPA2298	thiamine biosynthesisproteinThiI	1	0.34792	1	-0.2854	1	-0.3081
xseB	SPA2299	exodeoxyribonucleasesmallsubunit	0.5683	-0.2661	1	0.54253	1	0.06926
ispA	SPA2300	geranyltranstransferase	1	0	1	0.40505	1	0.07215
dxs	SPA2301	1-deoxy-D-xylulose-5-phosphate synthase	1	-0.1056	1	-0.0802	1	0.20645
yajO	SPA2302	oxidoreductase	0.7326	0.58496	0.7381	0.75798	1	0.31207
pgpA	SPA2303	phosphatidylglycerophosphataseA	1	-0.1926	1	-0.074	1	-0.1733
thiL	SPA2304	thiamine-monophosphatekinase	1	0.09622	1	-0.0857	1	-0.263
nusB	SPA2305	Nutili zationsubstanceproteinB	1	0.0234	1	0.04675	1	-0.0359
ribH	SPA2306	6,7-dimethyl-8-ribityllumazinesynthase	1	-0.0113	1	0.03308	1	-0.0497
ribD	SPA2307	riboflavinbiosynthesisproteinRibD	1	0.03355	1	-0.0503	1	0.00872
ybaD	SPA2308	hypotheticalprotein	1	-0.078	1	0.06522	1	-0.1831
yajI	SPA2309	lipoprotein	1	-1	1	0.41504	1	0.45943
tsx	SPA2310	nucleoside-specificchannel -formingproteintsx	1	0.10373	1	0.22487	1	0.60726
-	SPA2311	hypotheticalprotein	0.781	-0.2081	1	1	1	0.67807
yajD	SPA2312	hypotheticalprotein	0.0966	-0.5097	1	0.65208	1	0.18587
-	SPA2313	deoR-familytranscriptionalregulator	1	-0.3219	1	0.26303	1	-0.1444
-	SPA2314	hypotheticalprotein	1	-0.1255	1	0.42884	1	-0.1304
secF	SPA2315	protein-exportm embraneproteinSecF	0.0415	-0.5329	0.1722	-0.5171	1	0.0902
secD	SPA2316	protein-exportm embraneproteinSecD	0.0817	-0.737	0.4669	-0.7885	1	-0.1635
yajC	SPA2317	hypotheticalprotein	0.0144	-0.8954	0.4242	-0.3404	1	0.10982
tgt	SPA2318	queuinetR NA-ribosyltransferase;tRNA -guanine transglycosylase	0.046	-0.6328	0.1396	-0.585	1	-0.031
queA	SPA2319	S-adenosylmethionine--tRNAri bosyltransferase-isomerase	1	0.20645	1	-0.1255	1	-0.3344
yajB	SPA2320	hypotheticalprotein	0.9555	0.47307	1	0.2115	1	0.07189
-	SPA2321	peroxidase	1	0.44746	1	0.4975	1	0.03327
malZ	SPA2322	maltodextringlucosidase	1	0	1	-0.737	1	0
proY	SPA2323	proline-specificpermeaseProY	1	-0.241	1	-0.7162	1	-0.1605
brnQ	SPA2324	branchedc hainaminoacidtransportsystemIIcarrierprotein	1	-0.415	1	0	1	0
phoR	SPA2325	phosphate regulonsensor proteinP hoR	1	-0.3049	1	-0.6167	1	0
phoB	SPA2326	phosphate regulontranscriptionalregulatoryproteinPhoB	0.5554	-0.2818	1	-0.433	1	-0.2224
sbcD	SPA2327	exonucleaseSbcD	1	0.16993	1	-0.3985	1	-0.3985
sbcC	SPA2328	exonucleaseSbcC	1	-0.1575	1	-0.3923	1	-0.2955
araJ	SPA2329	MFSfamil y,arabinosepolymertransporter	1	-0.2224	1	0.36257	1	-0.415
yajF	SPA2330	hypotheticalROK -familyprotein	1	0.10692	1	0.1375	1	0.23447
rdgC	SPA2331	recombinationassociatedproteinRdgC	1	0.01937	1	-0.5185	1	-0.5619
yaiE	SPA2332	hypotheticalprotein	0.0271	-0.5747	1	0.17354	1	-0.114
aroM	SPA2333	proteino farooperon,regulatedbyaroR	1	-0.0995	1	-0.7182	0.0005	-1
yaiA	SPA2334	hypotheticalprotein	1	-0.0258	1	-0.1106	1	-0.1751
aroL	SPA2335	shikimatekinase	1	0	1	0.34792	1	0.11704
yaiI	SPA2336	hypotheticalprotein	1	0	1	-0.0641	0.3649	-0.4339
proC	SPA2337	pyrroline-5-carboxylatereductase	1	0.14147	1	0.03457	1	-0.0333
adrA	SPA2338	adrAprote in	1	-1	1	-1.3785	1	-0.8845
psiF	SPA2339	phosphate starvation-inducibleproteinPsiF	1	-0.7655	2E-11	-1.7162	0.0513	-0.8634
yaiB	SPA2340	hypotheticalprotein	1E-08	-1.2473	0.2444	-0.4715	0.2541	-0.5443
-	SPA2341	effluxpump	1	1.58496	1	0.67807	1	0.73697
-	SPA2342	hypotheticalprotein	1	-0.415	1	-0.585	1	-0.387
yaiZ	SPA2344	hypotheticalprotein	0.5588	-0.2795	0.8559	0.72528	0.3964	-0.419
yaiY	SPA2345	hypotheticalprotein	1	0.22239	1	-0.7225	1	0.08017

yaiW	SPA2346	lipoprotein	1	0.22239	0.2561	-0.4753	1	0.50901
sbmA	SPA2347	ABC-transporter innermembraneproteinSbmA	1	0.24101	1	-0.372	1	-0.078
ampH	SPA2348	penicillin-bindingpro teinAmpH	1	-0.3923	1	-0.074	1	-0.078
yaiV	SPA2349	hypotheticalprotein	1	-1	1	0.32193	1	-0.263
yaiU	SPA2350	flagellinstructuralprotein	1	-0.858	1	-1	1	-0.5475
hemB	SPA2351	delta-aminolevulinicaciddehydratase	1	0.51987	0.5834	0.92243	1	0.54394
prpE	SPA2352	PrpEpro tein	1	-0.8074	1	-0.1293	0.0103	-1.0167
prpD	SPA2353	PrpDpro tein	1	-0.8074	1	0.10497	0.1162	-0.75
prpC	SPA2354	methylcitratesynthase	1	-0.3219	1	0.20082	0.081	-0.7717
prpB	SPA2355	carboxyvinyl-carboxyphosphonatephosphorylmutase	1	-0.3219	1	0.05842	0.0211	-0.9511
prpR	SPA2356	propionatecatabolismoperonregulatoryprotein	1	-0.2895	1	1.05445	1	0
yahO	SPA2357	secretedprotein	1	-1.6374	5E-110	-2.8309	5E-20	-1.8679
yahN	SPA2358	RhtC-like transporter	1	0.06485	0.1073	1.13124	1	0.47393
foxA	SPA2359	ferrioxamineBreceptor	1	0	1	-0.415	1	-0.585
-	SPA2360	AraCfam ilytranscriptionalregulator	1	0.51457	1	-0.7105	1	-0.3479
-	SPA2362	terminaloxidasesubunitII	1	-0.1926	1E-25	-2.0753	1	-0.613
-	SPA2363	terminaloxidasesubunitI	1	-1	1	-2.9206	1	-0.9329
-	SPA2364	hypotheticalprotein	1	0	1	-2.4919	1	-0.2756
res	SPA2365	DNA restriction(DNAhelicase	1	-0.2345	1	-0.0911	1	-0.241
mod	SPA2366	typeIII restriction-modificationsystemStyLTIenzymemod	1	-0.2141	1	-0.2016	1	-0.2224
-	SPA2367	metabolitetransportprotein	0.4344	0.65605	0.523	0.85532	1	1.96683
-	SPA2369	hypotheticalprotein	1	0.152	1	-0.737	1	-1
-	SPA2370	lipoprotein	1	0	1	-0.585	1	-0.585
-	SPA2371	secretedprotein	1	#DIV/0!	1	#DIV/0!	1	#DIV/0!
-	SPA2372	transcriptionlregulator	1	#DIV/0!	1	#DIV/0!	1	#DIV/0!
-	SPA2373	outerme mbraneprotein	1	#DIV/0!	1	#DIV/0!	1	#DIV/0!
-	SPA2375	transmembraneregulator	1	-0.585	1	-0.8931	1	-1
-	SPA2376	rtnprotein	1	-0.3049	1	-1	1	-1
-	SPA2377	hypotheticalprotein	1	0	1	0	1	0
-	SPA2378	transmembraneregulator	1	0.26303	1	0.45943	1	0.1375
stbA	SPA2379	fimbrialprotein	1	#DIV/0!	1	#DIV/0!	1	#DIV/0!
stbB	SPA2380	fimbrialchaperoneprotein	1	#DIV/0!	1	#DIV/0!	1	#DIV/0!
stbC	SPA2381	outerme mbranefimbrialusherprotein	1	0	1	0	1	-0.585
stbD	SPA2382	fimbrialprotein	1	0	1	-0.585	1	-0.585
stbE	SPA2383	fimbrialchaperoneprotein	1	0	1	-1.585	1	-0.585
-	SPA2384	secretedprotein	1	0.26303	1	#DIV/0!	1	#DIV/0!
-	SPA2385	O-antigen conversion:glucosyltransferase	1	-0.1203	1	-0.5146	1	-0.4854
-	SPA2386	O-antigen conversion: bactoprenyltransferase	1	0.22239	1	-0.5475	1	-0.585
-	SPA2387	O-antigen conversion:translocase	1	#DIV/0!	1	-1	1	-0.4854
gp9	SPA2388	tailspike	1	#DIV/0!	1	-0.4594	1	-0.4594
mnt	SPA2389	regulatory	1	#DIV/0!	1	-0.3103	1	-0.2801
gp16	SPA2390	DNA transferprotein	1	#DIV/0!	1	-0.2996	1	-0.1155
gp20	SPA2391	DNAtra nsferprotein	1	#DIV/0!	1	-1.8074	1	0
gp7	SPA2392	DNAtra nsferprotein	1	#DIV/0!	1	-2.4594	1	-1
gp14	SPA2393	hypotheticalprotein	1	#DIV/0!	1	-2.585	1	#NUM!
gp1	SPA2394	portal protein	1	#DIV/0!	1	-1.8745	1	-1
-	SPA2395	hypotheticalprotein	1	#DIV/0!	1	-2.3219	1	-3
-	SPA2396	hypotheticalprotein	1	#DIV/0!	1	-2.1699	1	-1

gp19	SPA2397	lysozyme	1	#DIV/0!	1	-2.1699	1	-1
gp13	SPA2398	lysis(holin)	1	#DIV/0!	1	-3	1	-1.585
gp23	SPA2399	antitermination	1	#DIV/0!	1	-2.3219	1	#NUM!
ninH	SPA2400	hypotheticalprotein	1	#DIV/0!	1	-3	1	-2
rus	SPA2401	hypotheticalprotein	1	#DIV/0!	1	-2.585	1	-2.585
-	SPA2402	hypotheticalprotein	1	#DIV/0!	1	-2.585	1	-2.3219
ninF	SPA2403	hypotheticalprotein	1	#DIV/0!	1	-3	1	#NUM!
ninX	SPA2404	hypotheticalprotein	1	#DIV/0!	1	#NUM!	1	#NUM!
ninE	SPA2405	hypotheticalprotein	1	#DIV/0!	1	#NUM!	1	#NUM!
ninD	SPA2406	hypotheticalprotein	1	#DIV/0!	1	#NUM!	1	#NUM!
ninB	SPA2407	hypotheticalprotein	1	#DIV/0!	1	-2.585	1	#NUM!
-	SPA2408	hypotheticalprotein	1	#DIV/0!	1	-3	1	#NUM!
-	SPA2409	hypotheticalprotein	1	#DIV/0!	1	-2.8074	1	-2
gp12	SPA2410	DNAre plication(helicase)	1	#DIV/0!	1	-1.2801	1	-1.3219
gp18	SPA2411	DNA replication	1	#DIV/0!	1	-1.263	1	-1.263
-	SPA2412	hypotheticalprotein	1	#DIV/0!	1	-1.8074	1	-1.737
gpC1	SPA2413	transcriptionalactivator -regulatoryprotein	1	#DIV/0!	1	#NUM!	1	-2.8074
gpC1	SPA2414	transcriptional activator-regulatoryprotein	1	#DIV/0!	1	-0.0106	1	0.23907
gp24	SPA2415	hypotheticalprotein	1	#DIV/0!	1	-1.585	1	-2.415
sieB	SPA2416	superinfectionexclusion	1	#DIV/0!	1	-0.415	0.0736	-0.6262
-	SPA2417	hypotheticalprotein	1	#DIV/0!	1	-2	1	-2.1155
ral	SPA2418	antirestrictionprotein	1	#DIV/0!	1	-1.8074	1	-2
-	SPA2419	hypotheticalprotein	1	#DIV/0!	1	-0.8074	1	-1
gpC3	SPA2420	hypotheticalprotein	1	#DIV/0!	1	#NUM!	1	-3.3219
kil	SPA2421	hypotheticalprotein	1	#DIV/0!	1	-2.585	1	-3.7004
-	SPA2422	hypotheticalprotein	1	#DIV/0!	1	-2.585	1	-3.4594
-	SPA2423	hypotheticalprotein	1	#DIV/0!	1	-3.1699	1	-3.9069
abc1	SPA2424	hypotheticalprotein	1	#DIV/0!	1	-3.4594	1	-3.3219
abc2	SPA2425	hypotheticalprotein	1	#DIV/0!	1	-3.3219	1	-3.1699
-	SPA2426	hypotheticalprotein	1	#DIV/0!	1	-2.8074	1	-2.8745
-	SPA2427	hypotheticalprotein	1	#DIV/0!	1	-3	1	-3
eaa1	SPA2428	hypotheticalprotein	1	0	1	-1.585	1	-1.9069
-	SPA2429	hypotheticalprotein	1	#DIV/0!	1	-1.8074	1	-2
xis	SPA2430	excisionase	1	#DIV/0!	1	-0.3785	1	-0.585
int	SPA2431	integrase	1	#DIV/0!	1	0.1375	1	0
-	SPA2432	ThrtRNA	1	-1.585	1	0.90689	1	0.37851
proA	SPA2433	gamma-glutamylphosphatereductase	0.293	-0.387	0.046	-0.7678	1	0.18709
proB	SPA2434	glutamate5 -kinase	0.716	-0.2102	0.5171	-0.3388	1	0.47865
phoE	SPA2435	outerme mbraneporeproteinE	1	-1.585	1	0	1	-1
crl	SPA2436	curling enestranscriptionalactivator	0.6805	-0.2549	1	-0.0759	1	-0.1195
yafA	SPA2437	hypotheticalprotein	1	-0.0618	1	-0.0083	0.9232	-0.3427
gpt	SPA2438	xanthine-guanine phosphoribosyltransferase	0.9828	-0.153	0.1126	-0.6337	4E-07	-1.5221
pepD	SPA2439	aminoacyl-histidinedipeptidaseprecursor	1	-0.1368	1	-0.2013	1	0.29445
prfH	SPA2440	peptidec hain releasefactor	1	-0.4475	1	-1.8074	1	-1.3785
-	SPA2441	hypotheticalprotein	1	-0.2345	1	-1.5025	1	-1.4406
dinP	SPA2442	hypotheticalprotein	1	-0.659	1	-0.0671	1	-0.2479
yafK	SPA2443	hypotheticalprotein	1	-0.5703	0.0006	-1.0849	1	-0.9038
yafJ	SPA2444	hypotheticalprotein	0.1636	-0.4684	1	-0.3017	1	-0.3785

gmhA	SPA2445	phosphoheptoseisomerase	0.0902	-0.6259	0.4999	-0.3219	0.6465	-0.5034
yafH	SPA2446	acyl-CoAde hydrogenase	2E-15	1.90949	2E-07	2.4133	1	1.28011
yafV	SPA2447	hydrolase	1	-0.0328	1	0.21254	1	0.22588
-	SPA2448	secretedprotein	1	-0.0649	1	0.31034	0.2511	0.8679
-	SPA2449	outerme mbraneadhesin	0.0006	-0.8532	1	-1.0506	1	-0.5564
tinR	SPA2451	transcriptionalregulator	1	0.58496	1	-0.585	1	-1.1699
tcfD	SPA2452	fimbrailprotein	0.0003	-0.8606	1	-0.2996	0.0025	-0.9569
tcfC	SPA2453	outermembranefimbrialusherprotein	1	0	1	-0.737	1	-0.585
tcfB	SPA2454	fimbrialsubunit	1	-0.4854	1	-1.8074	1	-1.585
tcfA	SPA2455	fimbrialprotein	1	#NUM!	1	#DIV/0!	1	#NUM!
-	SPA2456	hypotheticalprotein	1	#DIV/0!	1	#DIV/0!	1	#DIV/0!
-	SPA2457	hypotheticalprotein	1	-1	1	#NUM!	1	0
-	SPA2458	hypotheticalprotein	1	-1	1	#NUM!	1	-1
sinR	SPA2459	LysR-familytranscriptionalregulatorSinR	1	-0.8074	1	-0.3219	1	-1.1699
-	SPA2460	ybeJ-like protein	1	-0.585	1	-0.585	1	-1
safC	SPA2462	outer-membranefimbrialusherprotein	1	0	1	-0.585	1	-0.415
safB	SPA2463	periplasmicfimbrialchaperoneprotein	1	0	1	-2	1	-1
safA	SPA2464	lipoprotein	1	-1	1	-1	1	0
-	SPA2465	hypotheticalprotein	1	#DIV/0!	1	#DIV/0!	1	#DIV/0!
-	SPA2466	hypotheticalprotein	1	#NUM!	1	#DIV/0!	1	#DIV/0!
-	SPA2467	hypotheticalprotein	1	#DIV/0!	1	#DIV/0!	1	#DIV/0!
-	SPA2469	hypotheticalprotein	1	#DIV/0!	1	-0.8074	1	-0.6781
-	SPA2470	Rhs-familyprotein	1	#DIV/0!	1	0	1	-0.585
-	SPA2471	hypotheticalprotein	1	#DIV/0!	1	-0.737	1	-0.737
-	SPA2472	hypotheticalprotein	1	#DIV/0!	1	0	1	#NUM!
-	SPA2473	hypotheticalprotein	1	#DIV/0!	1	#NUM!	1	#NUM!
-	SPA2474	secretedprotein	1	#DIV/0!	1	#DIV/0!	1	#NUM!
-	SPA2475	hypotheticalprotein	1	#DIV/0!	1	0	1	0
-	SPA2476	secretedprotein	1	#DIV/0!	1	#NUM!	1	#NUM!
-	SPA2478	hypotheticalprotein	1	0	1	-1	1	-1.585
-	SPA2479	innerme mbraneprotein	1	-0.585	1	-0.848	1	-1
-	SPA2480	shiga-like toxinAsubunit	1	#DIV/0!	1	#NUM!	1	0
-	SPA2481	hypotheticalprotein	1	0	1	-1	1	-1.585
-	SPA2482	hypotheticalprotein	1	-0.585	1	-1	1	-2
-	SPA2483	hypotheticalprotein	1	-1	1	-0.585	1	-1
-	SPA2484	lipoprotein	1	#DIV/0!	1	#NUM!	1	#NUM!
-	SPA2485	hypotheticalprotein	1	#NUM!	1	-1.585	1	-1.585
-	SPA2486	hypotheticalprotein	1	#DIV/0!	1	0	1	0
-	SPA2487	hypotheticalprotein	1	#DIV/0!	1	-1	1	0
-	SPA2488	hypotheticalprotein	1	#DIV/0!	1	#NUM!	1	#NUM!
-	SPA2489	hypotheticalprotein	1	#DIV/0!	1	-1.1844	1	-1.7004
-	SPA2490	hypotheticalprotein	1	#DIV/0!	1	-0.737	1	-1.3219
-	SPA2491	hypotheticalprotein	1	#DIV/0!	1	-0.585	1	-0.737
-	SPA2492	hypotheticalprotein	1	0	1	0	1	-0.4594
-	SPA2493	hypotheticalprotein	1	0.26303	1	-0.1806	1	-0.4854
-	SPA2494	hypotheticalprotein	1	0	1	-0.585	1	-0.263
-	SPA2495	hypotheticalprotein	1	-0.415	1	-1	1	-0.8074
-	SPA2496	ClpB-like protein	1	0	1	-1.3219	1	-0.585

-	SPA2497	hypotheticalprotein	1	0	1	#NUM!	1	0
-	SPA2499	hypotheticalprotein	1	0.16993	1	-0.2895	1	-0.3219
-	SPA2500	hypotheticalprotein	1	0.26303	1	-0.737	1	0
-	SPA2501	hypotheticalprotein	1	0.58496	1	-0.737	1	0
-	SPA2502	hypotheticalprotein	1	0.58496	1	-0.6781	1	0
-	SPA2503	hypotheticalprotein	1	0.41504	1	-0.4475	1	-0.1375
-	SPA2504	AsptRN A	1	-0.663	1	-0.3785	1	-0.4854
dnaQ	SPA2505	DNApo lymeraseIIIsubunitepsilon	0.2893	-0.3012	1	-0.2003	0.4346	-0.4081
rnhA	SPA2506	ribonucleaseH	1	-0.263	1	-0.0614	1	-0.0931
yafS	SPA2507	hypotheticalprotein	1	-0.1926	1	-0.0489	1	0.0458
gloB	SPA2508	hydroxyacylglutathionehydrolase	1	0.1375	1	0.60407	1	-0.1043
mltD	SPA2509	membrane-boundly ticmureintransglycosylasedprecursor	0.0864	-0.8153	0.0034	-1.1612	0.005	-1.1115
yafE	SPA2510	methyltransferase	1	0.3505	1	0.848	1	0.52356
yafD	SPA2511	hypotheticalprotein	1	0.21604	0.663	0.76139	0.7799	0.68634
-	SPA2512	drugeff luxprotein	1	0	1	-0.4854	1	-0.263
yafC	SPA2513	hypotheticaltranscriptionalregulator	1	0.05658	1	0.2091	1	0.17585
yafB	SPA2514	hypotheticaloxidoreductase	1	-0.3219	1	0	1	-1
-	SPA2515	AsptRN A	1	#DIV/0!	1	1	1	#NUM!
rrfG	SPA2516	5Sribosom alRNA	1	0	1	0	1	-1
rrlG	SPA2517	23Sribos omalRNA	1	0.03317	1	0.6059	0.9993	-0.5664
-	SPA2518	hypotheticalprotein	1	-0.1699	1	1	1	0
-	SPA2519	GlutRN A	1	-0.3219	1	0.75899	1	-0.4475
rrsG	SPA2520	16Sribos omalRNA	1	0.01759	0.9	0.60466	0.2032	-0.7885
clpB	SPA2521	ClpBpro tein(heatshockproteinf84.1)	1	-0.1123	1	-0.013	1	0.31421
yfiH	SPA2522	hypotheticalprotein	0.994	-0.1592	0.9672	-0.2031	1	-0.0122
sfhB	SPA2523	ftsHs uppressorproteinSfhB	0.4612	-0.4083	0.8995	-0.0866	1	-0.0831
yfiO	SPA2524	lipoprotein	0.8342	-0.2458	1	0.08078	1	0.06782
yfiA	SPA2525	sigma(54)modulation protein	1	0.15787	1	0.88234	1	0.36144
pheA	SPA2526	chorismatemutase -P/prephenatedehydratase	0.0981	-0.585	1	-0.1806	1	0.11704
-	SPA2527	hypotheticalprotein	1	0	1	-1.0589	1	-0.6674
tyrA	SPA2528	chorismatemutase/prephenatedehydrogenase	1	0	1	0	1	0.12553
aroF	SPA2529	phospho-2-dehydro-3-deoxyheptonatealdolase,tyr -sensitive	1	0.27563	1	-0.1255	1	0.39232
yfiR	SPA2530	hypotheticalprotein	1	-0.2996	1	-0.585	1	-0.737
yfiN	SPA2531	hypotheticalprotein	1	-0.4475	1	-0.585	1	-0.6521
rplS	SPA2532	50Sribos omalproteinL19	0.4386	-0.9073	1	-0.1669	1	0.22853
trmD	SPA2533	tRNA(guanine-N1)methyltransferase	0.6806	-0.8777	1	-0.3579	1	0.04866
yfjA	SPA2534	16SrRNA processingprotein	0.847	-0.7184	1	-0.4166	1	-0.1899
rpsP	SPA2535	30S ribosomalproteinS16	0.4762	-0.7641	0.7611	-0.4202	1	-0.304
ffh	SPA2536	signalrecognitionparticleprotein	1	0.334	1	0.22517	1	0.11884
corE	SPA2537	hypotheticalprotein	1	-0.4005	1	-0.7105	1	-0.5639
corB	SPA2538	hypotheticalprotein	1	-0.0802	1	-0.5619	1	-0.2065
-	SPA2539	hypotheticalprotein	1	#DIV/0!	1	0.58496	1	0.51457
grpE	SPA2540	heatsho ckproteinGrpE(heatshockproteinb25.3)(hsp24)	0.8868	-0.2592	1	0.48745	1	-0.1024
-	SPA2541	hypotheticalprotein	1	-0.1069	1	0.58496	1	0
yfjB	SPA2542	inorganicpolyphosphate/ATP -NADk inase	0.8378	-0.1806	1	0.21412	1	-0.0451
recN	SPA2543	DNAre pairprotein	0.0504	-0.5747	1	-0.433	1	-0.0825
smpA	SPA2544	small proteinA	0.1488	-0.4671	1	0.32989	1	-0.1914
yfjF	SPA2545	hypotheticalprotein	1	-0.0508	1	0.35982	1	-0.22

yfjG	SPA2546	hypotheticalprotein	1	-0.1413	1	0.2722	1	-0.1168
smpB	SPA2547	SsrA(tm RNA)-bindingpro tein	0.3565	-0.3615	1	0.05571	0.4986	-0.4509
-	SPA2548	hypotheticalprotein	1	0	2E-278	-3.8278	1	-2.3985
-	SPA2549	typel secretionprotein	1	1.58496	1	-2.6323	1	-1.6699
-	SPA2550	typelse cretionprotein,ATP -binding protein	1	-0.263	1	-2.7004	1	-1.263
-	SPA2551	typelse cretionprotein	1	0	1	-1.8074	1	-1
-	SPA2552	-	1	-0.3247	0.2981	0.38994	1	-0.3976
-	SPA2554	hypotheticalprotein	1	-0.2801	1	-0.1033	0.6562	-0.4263
-	SPA2555	positiveregulatoroflategenetranscription	1	-0.7885	1	-0.415	1	-0.5305
-	SPA2556	regulatoroflategeneexpression	1	0	1	-0.263	1	-0.4854
-	SPA2557	phageta ilprotein	1	0.12553	1	-0.152	1	-0.4594
-	SPA2558	hypotheticalprotein	1	-0.1926	1	-0.585	1	0
-	SPA2559	hypotheticalprotein	1	-0.415	1	0	1	0
-	SPA2560	phageta ilprotein	1	-0.1926	1	-0.585	1	0
-	SPA2561	majorta iltubeprotein	1	-0.415	1	0	1	0
-	SPA2562	majorta il sheathpro tein	1	-0.4594	1	0	1	0
pin	SPA2563	inversionofadjacentDNA;atlocusofe14element	1	#DIV/0!	1	#DIV/0!	1	#DIV/0!
sopE	SPA2564	invasion-associatedsecretedprotein	0.742	0.83595	0.5713	1.04901	0.5284	-0.7902
-	SPA2565	phageta ilfiber protein	1	-0.2224	1	-0.7655	1	-0.2224
-	SPA2566	phageta ilfiberprotein	1	-0.3219	1	-1	1	-1
-	SPA2567	phageta ilprotein	1	#DIV/0!	1	#NUM!	1	#NUM!
-	SPA2568	phageba seplateassemblyprotein	1	#DIV/0!	1	0	1	0
-	SPA2569	phageba seplateassembly protein	1	0	1	#DIV/0!	1	#NUM!
-	SPA2570	phageba seplateassemblyprotein	1	#DIV/0!	1	#DIV/0!	1	#DIV/0!
-	SPA2571	phageta ilcompletionprotein	1	-1	1	#DIV/0!	1	#NUM!
-	SPA2572	phageta ilprotein	1	-0.415	1	#DIV/0!	1	#NUM!
-	SPA2573	regulatory protein	1	0	1	#NUM!	1	#NUM!
-	SPA2574	hypotheticalprotein	1	0	1	#DIV/0!	1	#DIV/0!
nucD	SPA2575	lysozyme	1	1	1	#DIV/0!	1	#DIV/0!
nucE	SPA2576	secretionprotein	1	#DIV/0!	1	#DIV/0!	1	#DIV/0!
-	SPA2577	phageta ilprotein	1	#NUM!	1	#DIV/0!	1	#DIV/0!
-	SPA2578	capsid completionprotein	1	0	1	#DIV/0!	1	#DIV/0!
-	SPA2579	phagete rminase	1	0	1	#DIV/0!	1	#DIV/0!
-	SPA2580	majorc apsidprotein	1	-0.1699	1	#DIV/0!	1	#DIV/0!
-	SPA2581	capsid protein	1	-0.3626	1	#DIV/0!	1	#DIV/0!
-	SPA2582	terminasesubunit	1	#DIV/0!	1	#DIV/0!	1	#DIV/0!
-	SPA2583	capsid portalprotein	1	#DIV/0!	1	#DIV/0!	1	#DIV/0!
-	SPA2584	hypotheticalprotein	1	0.30151	0.007	1.39232	0.128	0.99048
-	SPA2585	hypotheticalprotein	1	0.21931	0.0149	1.33092	0.3505	0.85914
-	SPA2586	hypotheticalprotein	0.904	-0.1754	0.1141	1.17585	0.9598	0.70261
-	SPA2587	hypotheticalprotein	1	-0.585	1	1	1	1
-	SPA2588	hypotheticalprotein	1	-0.8074	1	0	1	0.67807
-	SPA2589	hypotheticalprotein	1	-0.737	1	0.19265	1	1.22239
-	SPA2590	hypotheticalprotein	1	-1	1	#DIV/0!	1	#DIV/0!
-	SPA2591	DNAad eninemethylase	1	-1.1069	1	#DIV/0!	1	#DIV/0!
-	SPA2592	exonuclease	1	-1.2115	1	#NUM!	1	#DIV/0!
-	SPA2593	hypotheticalprotein	8E-13	-1.2801	1	#DIV/0!	1	#DIV/0!
-	SPA2594	hypotheticalprotein	1E-10	-1.2496	1	#NUM!	1	#NUM!

-	SPA2595	hypotheticalprotein	1	-1.8745	1	#DIV/0!	1	#DIV/0!
-	SPA2596	hypotheticalprotein	1	-1.4406	1	#DIV/0!	1	#DIV/0!
cII	SPA2597	phagere gulatoryprotein	1	-1.628	1	#NUM!	1	0
apl	SPA2598	phagere gulatoryprotein	1	-1.2854	1	0	1	0
cI	SPA2599	phagere pressorproteincI	1	-0.1769	1	-0.7162	1	0.16046
-	SPA2600	phagei ntegrase	1	-0.1069	1	-0.8745	1	0.16993
-	SPA2601	bacteriophageintegrase	1	#DIV/0!	1	-0.585	1	-1.585
-	SPA2602	hypotheticalprotein	1	#DIV/0!	1	-1	1	-0.585
-	SPA2603	hypotheticalprotein	1	#DIV/0!	1	-1	1	-1
-	SPA2604	hypotheticalprotein	1	#DIV/0!	1	-1.1375	1	-1.1699
-	SPA2605	hypotheticalprotein	1	#DIV/0!	1	-0.6781	1	-1
-	SPA2607	hypotheticalprotein	1	#DIV/0!	1	#DIV/0!	1	#DIV/0!
-	SPA2608	hypotheticalprotein	1	#DIV/0!	1	#NUM!	1	#DIV/0!
-	SPA2609	hypotheticalprotein	1	#DIV/0!	1	#DIV/0!	1	#NUM!
-	SPA2610	hypotheticalprotein	1	#DIV/0!	1	#NUM!	1	#DIV/0!
-	SPA2611	hypotheticalprotein	1	#DIV/0!	1	0	1	#NUM!
-	SPA2612	hypotheticalprotein	1	#DIV/0!	1	#DIV/0!	1	#DIV/0!
-	SPA2613	hypotheticalprotein	1	#DIV/0!	1	0	1	-1
-	SPA2614	hypotheticalprotein	1	#DIV/0!	1	0	1	0
-	SPA2615	hypotheticalprotein	1	#DIV/0!	1	#NUM!	1	#DIV/0!
-	SPA2616	hypotheticalprotein	1	#DIV/0!	1	#DIV/0!	1	#DIV/0!
-	SPA2617	hypotheticalprotein	1	#DIV/0!	1	#DIV/0!	1	#DIV/0!
-	SPA2618	hypotheticalprotein	1	#DIV/0!	1	#DIV/0!	1	#DIV/0!
-	SPA2619	hypotheticalprotein	1	#DIV/0!	1	#DIV/0!	1	#DIV/0!
-	SPA2620	hypotheticalprotein	1	#DIV/0!	1	#DIV/0!	1	#DIV/0!
-	SPA2621	hypotheticalprotein	1	#DIV/0!	1	0	1	-0.585
-	SPA2622	hypotheticalprotein	1	#DIV/0!	1	-0.1699	1	-0.848
-	SPA2623	hypotheticalprotein	1	#DIV/0!	1	0	1	0
-	SPA2624	hypotheticalprotein	1	#DIV/0!	1	-1	1	0
-	SPA2625	hypotheticalprotein	1	#DIV/0!	1	#NUM!	1	#DIV/0!
fljA	SPA2626	Flagellar synthesis:repressoroffliC	1	#DIV/0!	1	#DIV/0!	1	#DIV/0!
fljB	SPA2627	Flagellar synthesis:phase2flagellin(filamentstructuralprotein)	0.0735	1.59991	0.236	1.04975	1	-0.3139
iroB	SPA2629	glycosyltransferase	1	0	1	0.58496	1	0
iroC	SPA2630	ABCtra nsporter	1	0	1	0	1	0.41504
iroD	SPA2631	ferric enterochelinesterase	1	0	1	-0.415	1	0
iroE	SPA2632	hypotheticalprotein	1	0	1	-0.415	1	0
iroN	SPA2633	TonB-dependento utermembranesiderophorereceptorprotein	1	0.58496	1	-1.415	1	-1.1699
-	SPA2635	innerme mbraneprotein	1	-1.3026	1	-2.4021	1	-1.8845
-	SPA2636	hypotheticalprotein	1	-1.1699	1	-1.4854	1	-1.3219
virK	SPA2637	virulence protein	0.0003	-1.1082	1	-1.2756	1	-0.5502
mig-14	SPA2638	transcriptionalregulator	6E-23	-1.7972	8E-42	-2.2538	1	-1.6088
nxiA	SPA2639	nickeltransporter	1	0	1	0.26303	1	-0.585
tctE	SPA2640	two-componentsystemsensorkinase	1	-0.1605	1	0.1635	1	-0.4975
tctD	SPA2641	transcriptionalregulator	1	-0.0825	1	-0.0217	1	-0.5525
-	SPA2642	hypotheticalprotein	1	0	0	3.90689	1	2.16993
-	SPA2643	hypotheticalprotein	1	-1	0	4.33498	1	2.32193
-	SPA2644	hypotheticalprotein	1	-1	0	4.60204	1	4.08746
-	SPA2645	hypotheticalprotein	1	-0.585	3E-176	3.82782	1	1.848

-	SPA2646	Gabprote in	1	-0.415	2E-134	-3.2548	1	-1.585
ygaF	SPA2647	GABD TPgeneclusterrepressor	1	-1.3219	9E-146	-3.2327	1	-1.7776
gabD	SPA2648	succinate-semialdehyde dehydrogenase	1	-0.7776	6E-46	-2.7948	5E-22	-2.0275
gabT	SPA2649	4-aminobutyrateaminotransferase	1	-0.7655	3E-46	-2.7993	9E-19	-2.1728
gabP	SPA2650	GabApe rmease(4 -aminob utyratetransportcarrier)	1	-1	6E-53	-2.6356	1	-2.6374
ygaE	SPA2651	transcriptionalregulator	1	0.26303	1	-2.2016	1	-2
ygaU	SPA2652	LysMdom ain-containingprotein	1	0	0.0005	-1.1074	1	0.23374
yqaE	SPA2653	hypotheticalprotein	1	0	1	-0.926	1	-0.3959
-	SPA2654	transcriptionalregulator	8E-17	1.76296	0	4.60486	0	4.86752
ygaP	SPA2655	hypotheticalprotein	1E-05	1.37022	0	4.31482	0	4.51517
-	SPA2656	hypotheticalprotein	0.031	0.8436	9E-210	3.52112	0	3.96203
stpA	SPA2657	DNA-bindingp roteinStpA	0.6296	-0.2643	0.0168	-0.8515	0.0263	-0.6742
-	SPA2658	hypotheticalprotein	0.0086	-1.0075	1	-0.585	1	-2.4594
ygaC	SPA2659	hypotheticalprotein	1	0.80735	1	0	1	0.42321
-	SPA2660	hypotheticalprotein	1	-0.0489	1	-0.3479	1	-0.1155
-	SPA2661	hypotheticalprotein	1	-0.1806	1	0	1	0.11548
-	SPA2662	hypotheticalprotein	1	-0.3626	1	0.28951	1	0
nrdH	SPA2663	glutaredoxin	1	#DIV/0!	1	#NUM!	1	#NUM!
nrdI	SPA2664	NrdIprotei n	1	#DIV/0!	1	#NUM!	1	#NUM!
nrdE	SPA2665	ribonucleoside-diphosphatereductase2subunitalpha	1	#DIV/0!	1	-1.585	1	-1
proV	SPA2667	glycine/betaine/prolineABCtransporterATP -bindingp rotein	1	1.28011	1	0.32193	1	0.58496
proW	SPA2668	glycinebetaine/L -proline transportsystempermeaseproteinP	1	1	1	0.152	1	0.16993
proX	SPA2669	glycinebetaine -bindingpe riplasmic protein	1	1.22239	1	0.69515	1	0.65208
-	SPA2670	transmembranetransportprotein	1	0.5025	1	-0.2345	1	-0.1375
emrR	SPA2671	transcriptionalregulator	0.0001	1.23644	0.0256	1.26748	0.0611	1.02714
emrA	SPA2672	multidrug resistanceproteinA	0.0181	0.93963	0.857	0.7137	0.3022	0.87662
emrB	SPA2673	multidrug resistanceproteinB	1	0.70627	1	0.41504	1	1
luxS	SPA2675	autoinducer-2productio nproteinLuxS	1	0.08881	1	-0.2639	0.5795	-0.5129
-	SPA2676	-	1	#NUM!	1	#DIV/0!	1	#DIV/0!
gshA	SPA2677	gamma-glutamylcysteinesynthetase	1	0.0458	0.702	-0.4813	1	0.11103
yqaA	SPA2678	hypotheticalprotein	0.8581	-0.1699	1	0.06954	1	0.0902
yqaB	SPA2679	hypotheticalprotein	0.9701	-0.2101	1	0.07189	1	-0.091
-	SPA2680	ArgtRN A	1	-0.0679	1	0.44057	0.1356	-0.6374
-	SPA2681	ArgtRN A	0.7699	-0.1465	1	0.09478	0.0003	-0.9723
-	SPA2682	ArgtRN A	0.6375	-0.2297	1	0.06046	4E-05	-1.0224
-	SPA2683	SertRNA	0.4784	-0.296	1	0.07765	4E-05	-1.0341
csrA	SPA2684	carbons torageregulator	0.0057	-0.7328	0.143	-0.6185	0.848	-0.3785
alaS	SPA2685	alanyl-tRNAs ynthetase	0.6037	-0.3735	0.6951	-0.6815	1	-0.2388
oraA	SPA2686	regulatoryproteinRecX	1	-0.1605	1	-0.1699	1	-0.3479
recA	SPA2687	recombinaseA	0.4219	-0.4039	0.9787	-0.0414	1	-0.1751
ygaD	SPA2688	hypotheticalprotein	1	-0.0577	0.5041	-0.2996	1	-0.1592
mltB	SPA2689	membrane-boundly tictransglycosylaseBprecursor	1	0	1	-1.2479	1	-0.826
srlA	SPA2690	PTSsys temglucitol/sorbitol -specifictransportersubunitIIBC	1	0.22239	1	0.41504	1	-2.7004
srlE	SPA2691	PTSsys temglucitol/sorbitol -specifictransportersubunitIIBC	1	0.848	1	0.45943	1	-1.7655
srlB	SPA2692	PTSsys temglucitol/sorbitol -specifictransportersubunitIIA	1	0.77761	1	0.22239	1	-1.263
srlD	SPA2693	sorbitol-6-phosphate2 -dehydrogenase(glucitol -6-phosphate dehydrogenase)	1	0.69661	1	0	1	-1.1806
srlM	SPA2694	glucitoloperonactivatorprotein	1	0.37851	1	0.32193	1	-1
srlR	SPA2695	glucitoloperonrepressor	1	0.02487	1	0.62385	1	-0.23

gutQ	SPA2696	phosphosugarbindingprotein	1	0.11247	1	0.61891	1	-0.0995
ygaA	SPA2697	sigma-54-dependenttra nsriptionalregulator	1	0.19265	1	0.31247	1	0.24793
-	SPA2698	flavoprotein	1	1	1	-0.1926	1	0
ygbD	SPA2699	rubredoxin reductase	1	0	1	-0.152	1	-0.152
hypf	SPA2700	hydrogenasematurationprotein	1	0	1	-0.7199	1	-0.2756
hydN	SPA2701	electrontransportprotein	1	0	1	1.32193	1	1.58496
-	SPA2702	hypotheticalprotein	1	0	1	0.41504	1	0.22239
hycI	SPA2703	hydrogenase3maturationprotease	1	0	1	0.32193	1	0.51457
hycH	SPA2704	formatehydrogenlyasematurationprotein	1	-0.263	1	0.45943	1	0.65208
hycG	SPA2705	formatehydrogenlyasesubunit7	1	-0.3219	1	0.58496	1	0.36257
hycF	SPA2706	formatehydrogenlyasesubunit6	1	0	1	0.32193	1	1.22239
hycE	SPA2707	formatehydrogenlyasesubunit5	1	0	1	0.41504	1	1.32193
hycD	SPA2708	formatehydrogenlyasesubunit4	1	#DIV/0!	1	0	1	#DIV/0!
hycC	SPA2709	formatehydrogenlyasesubunit3	1	0	1	0	1	1.58496
hycB	SPA2710	formatehydrogenlyasesubunit2	1	#DIV/0!	1	#DIV/0!	1	2
hycA	SPA2711	formatehydrogenlyaseregulatoryprotein	1	#DIV/0!	1	#DIV/0!	1	2.58496
hypA	SPA2712	HypApro tein	0.1563	0.69661	1E-12	1.97575	2E-07	1.65208
hypB	SPA2713	hydrogenaseisoenzymesformationproteinHypB	0.2854	0.96691	0.0065	1.92098	0.008	1.70011
hypC	SPA2714	hydrogenaseisoenzymesformationproteinHypC	0.0062	1.00269	4E-07	1.87759	7E-09	1.87013
hypD	SPA2715	hydrogenaseexpression/formationproteinHypD	0.1374	0.9893	0.0467	1.5225	6E-07	1.88187
hypE	SPA2716	hydrogenaseisoenzymesformationproteinHypE	0.0361	0.9573	0.0608	1.22973	2E-05	1.79984
fhlA	SPA2717	transcriptionalactivatoroftheformatehydrogenlyasesystem	0.0012	1.14684	1	0.45568	0.0027	1.35509
ygbA	SPA2718	hypotheticalprotein	1	0.90689	1	0.28951	1	0
sitA	SPA2719	Irontranspo rtprotein,periplasmic -binding protein	1	0	1	-3.273	1	-1.7004
sitB	SPA2720	Irontranspo rtprotein,ATP -binding component	1	0	1	-2.1699	1	-1
sitC	SPA2721	Irontranspo rtprotein,innermembrane component	1	0	1	-1.8074	1	-1
sitD	SPA2722	Irontranspo rtprotein,innermembranecomponent	1	-0.585	1	-1.585	1	-1.585
-	SPA2723	hypotheticalprotein	1	#NUM!	1	#NUM!	1	#NUM!
sprB	SPA2724	AraC-familytranscriptionalregulator	0.0181	0.93074	7E-07	1.94132	1	0.43539
sprA	SPA2725	AraC-familytranscriptionalregulator	0.0013	1.12146	2E-05	1.75854	1	0.42114
-	SPA2726	hypotheticalproteinfoundwithinS.typhipathogenicityisland1	0.8048	0.43195	0.322	0.91222	0.4806	-0.434
orgB	SPA2727	oxygen-regulatedinvasionprotein	0.7074	0.68033	0.3991	0.93707	1	-0.2135
orgA	SPA2728	oxygen-regulatedinvasionprotein	0.3758	0.81184	0.4878	1.03616	1	-0.1804
prgK	SPA2729	pathogenicity1islandeffectorprotein	0.7998	0.82111	1	0.96577	1	-0.2383
prgJ	SPA2730	pathogenicity1islandeffectorprotein	0.4806	0.89446	0.7314	1.07263	1	-0.3685
prgI	SPA2731	pathogenicity1islandeffectorprotein	0.3884	0.90447	0.57	1.07113	0.9737	-0.3802
prgH	SPA2732	pathogenicity1islandeffector protein	0.3414	0.85899	0.4636	1.09226	0.7812	-0.4054
hilD	SPA2733	AraCfam ilytranscriptionalregulator	1	0.52402	0.2296	1.34676	0.9163	0.58014
iagA	SPA2734	invasionproteinregulator	0.1006	0.75489	1	0.57916	0.0545	-0.8677
iagB	SPA2735	cell invasionprotein	0.313	0.63077	0.6902	0.77642	0.0021	-1.1327
-	SPA2736	stpA-like protein	1	0.71049	1	0.94342	1	-1
sicP	SPA2737	chaperone(associatedwithvirulence)	1	0.80735	1	1.10692	1	-1.0911
-	SPA2738	hypotheticalprotein	0.2837	0.68182	1E-05	1.45457	0.0004	-0.9133
sipF	SPA2739	acylca rrierprotein	0.4943	0.57116	2E-06	1.53605	0.0016	-0.8667
sipA	SPA2740	pathogenicityisland1effectorprotein	0.7462	0.65896	0.0467	1.29123	0.006	-0.9769
sipD	SPA2741	pathogenicityisland1effector protein	0.2813	0.69188	0.0554	1.22239	0.1663	-0.6571
sipC	SPA2742	pathogenicityisland1effectorprotein	0.7202	0.82923	1	0.94694	0.4055	-1.0704
sipB	SPA2743	pathogenicityisland1effectorprotein	0.994	0.62967	1	0.79864	0.2207	-0.973

spaT	SPA2744	hypotheticalprotein	0.7721	0.66933	0.4486	0.87087	0.1733	-0.6569
spaS	SPA2745	secretoryprotein(associatedwithvirulence)	1	0.42884	1	0.55639	1	-0.3923
spaR	SPA2746	secretoryprotein(associatedwithvirulence)	1	0.33121	1	0.58496	1	-0.5146
spaQ	SPA2747	secretoryprotein(associatedwithvirulence)	1	0.4039	0.7836	0.70402	0.0389	-0.6077
spaP	SPA2748	secretoryprotein(associatedwithvirulence)	1	0.4441	0.8341	0.71409	0.5931	-0.5222
spaO	SPA2749	surfacep resentationof antigensprotein(associatedwithtypeIIIsecretionandvirulence)	0.2649	0.64111	0.1836	1.06343	0.3576	-0.5065
spaN	SPA2750	antigen presentationproteinSpaN	0.6026	0.71137	0.1964	1.22934	0.3865	-0.5406
spaM	SPA2751	virulence-associatedsecretoryprotein	0.7462	0.53434	0.2	0.96438	0.5374	-0.3908
spaI	SPA2752	virulence-associatedsecretoryapparatusATPsynthase	0.5758	0.7084	0.6139	0.88009	0.7235	-0.4631
spak	SPA2753	virulence-associatedsecretoryprotein	1	0.24442	0.354	0.95217	0.0601	-0.6314
invA	SPA2754	secretoryprotein	1	0.44171	1	0.60823	0.264	-0.6067
invE	SPA2755	cell invasionprotein	0.4666	0.61498	0.4669	0.87447	1	-0.2224
invG	SPA2756	secretoryprotein(associatedwithvirulence)	0.5946	0.7137	0.4805	1.0066	1	-0.2582
invF	SPA2757	AraC-familyregulatoryprotein	0.1671	0.82916	0.0661	1.37426	0.9337	-0.3642
invH	SPA2758	cell adherance/invasionprotein	0.0079	0.97162	0.0084	1.33744	1	0.078
-	SPA2759	hypotheticalprotein	1	0	1	#DIV/0!	1	#DIV/0!
-	SPA2760	hypotheticalprotein	0.2452	-0.4259	0.24	-0.478	0.0017	-0.8797
-	SPA2761	hypotheticalprotein	0.4325	-0.309	0.1789	-0.4206	0.0075	-0.848
-	SPA2764	hypotheticalprotein	1	-1.3219	1	-1.585	1	0
-	SPA2765	hypotheticalprotein	1	#NUM!	1	#DIV/0!	1	#DIV/0!
mutS	SPA2766	DNAm ismatchrepairprotein	1	-0.2313	1	-0.2176	1	0.21681
-	SPA2767	hypotheticalprotein	1	0.41504	1	0.1375	1	-0.1375
-	SPA2768	membranetransportprotein	1	-1	1	0	1	0.26303
-	SPA2769	LysR-familytranscriptionalregulator	1	-0.3626	1	0.41504	1	0.19265
-	SPA2770	permease	1	-0.1926	1	0	1	-0.415
-	SPA2771	hypotheticalprotein	1	-0.415	1	0.36257	1	-0.8625
-	SPA2772	hydroxypyruvateisomerase	1	0.41504	1	0.44746	1	-0.5146
ygbL	SPA2773	sugaral dolase	1	0.32193	1	0.23266	1	-0.5443
-	SPA2774	hypotheticalprotein	1	0	1	0.10434	1	-0.7485
ygbJ	SPA2775	3-hydroxyisobutyratedehydrogenase	1	-0.2224	1	-0.0825	1	-1.078
ygbI	SPA2776	DeoR familytranscriptionalregulator	1	-0.509	1	-0.1769	1	-0.4406
-	SPA2777	slyA-like protein	1	0.17177	0.3152	1	1	0.47393
-	SPA2778	hypotheticalprotein	1	1.37851	1	0.41504	1	0.73697
-	SPA2779	hypotheticalprotein	1	1.08746	1	0.41504	1	0
rpoS	SPA2780	RNApo lymerasesigmasubunitRpoS (sigma-38)	1	-0.2042	1	-0.6799	1	-0.1499
nlpD	SPA2781	lipoproteinNlpD	1	-0.3119	1	-0.3929	1	-0.0581
pcm	SPA2782	L-isoaspartylproteincarboxylmethyltransferasetypeII	1	-0.0729	1	0.37615	1	0.4769
surE	SPA2783	stationary-phases urvivalprotein	1	0	1	0.0614	1	0.34008
ygbO	SPA2784	hypotheticalprotein	1	0	0.7519	-0.1816	1	0.27009
ygbB	SPA2785	2C-methyl-D-erythritol2,4 -cyclodiphosphatesynthase	1	0.10309	0.3767	-0.3356	1	0.14439
ygbP	SPA2786	2-C-methyl-D-erythritol4 -phosphate cytidylyltransferase	1	0.2575	1	-0.1478	1	0.48033
ygbQ	SPA2787	hypotheticalprotein	1	0.08688	1	-0.0601	1	0.31464
ygbE	SPA2788	hypotheticalprotein	1	0.29546	1E-14	-1.5171	3E-06	-1.215
cysC	SPA2789	adenosine5 -phosphosulfatekinase	1	0.37851	0	-4.0404	0	-4.2705
cysN	SPA2790	ATPs ulfurylase(ATP:sulfateadenyltransferase)subunit	1	0.16046	0	-4.3157	0	-3.8955
cysD	SPA2791	ATPs ulfurylase	1	-0.1255	0	-4.4229	0	-3.9414
ygbF	SPA2793	hypotheticalprotein	1	0.32193	1	0.41504	1	0
-	SPA2794	hypotheticalprotein	1	0.24793	1	0.19265	1	0

-	SPA2795	hypotheticalprotein	1	0.07039	1	-0.1926	1	0
-	SPA2796	hypotheticalprotein	1	0	1	-0.152	1	0.16993
-	SPA2797	hypotheticalprotein	1	0.05445	1	-0.152	1	0.16993
-	SPA2798	hypotheticalprotein	1	0.09311	1	-0.1255	1	0
sopD	SPA2801	hypotheticalprotein	1	0.33258	0.0414	1.25716	0.0517	-0.8289
cysH	SPA2802	3'-phosphoadenosine5' -phosphosulfatesulfotransferase	1	1.69188	2E-183	-3.4181	0	-4.4086
cysI	SPA2803	sulfitereductase(NADPH) hemoproteinsubunitalpha	1	1.078	9E-177	-3.6237	0	-3.9109
cysJ	SPA2804	sulfitereductase(NADPH)flavoproteinsubunitbeta	1	0.80735	4E-169	-3.4717	5E-245	-3.5443
ptpS	SPA2805	6-pyruvoyltetrahydrobiopterinsynthase	1	-0.2937	1	-1.3626	1	-1.7162
ygcF	SPA2807	hypotheticalprotein	1	-0.0931	0.7902	-0.1255	0.1441	-0.6226
-	SPA2808	-	0.2599	-0.2934	0.0241	-0.5282	1	-0.0732
eno	SPA2809	enolase	1	-0.2587	1	-0.5123	1	-0.0062
pyrG	SPA2810	CTPs ynthetase	1	0.13217	0.8014	-0.5995	1	0.05389
mazG	SPA2811	hypotheticalprotein	0.4344	-0.3219	0.8995	-0.1234	1	-0.1999
steA	SPA2812	fimbrialsubunit	1	#NUM!	1	-0.585	1	0
steB	SPA2813	outerme mbraneusherprotein	1	#DIV/0!	1	#DIV/0!	1	#DIV/0!
steC	SPA2814	periplasmicfimbrialchaperone	1	#DIV/0!	1	#DIV/0!	1	#DIV/0!
steD	SPA2815	fimbrialsubunit	1	#DIV/0!	1	#NUM!	1	#DIV/0!
steE	SPA2816	fimbrialsubunit	1	0	1	#DIV/0!	1	#DIV/0!
steF	SPA2817	fimbrialsubunit	1	#DIV/0!	1	#DIV/0!	1	#DIV/0!
-	SPA2818	hypotheticalprotein	1	#DIV/0!	1	#DIV/0!	1	#DIV/0!
-	SPA2819	hypotheticalprotein	1	#DIV/0!	1	#DIV/0!	1	#NUM!
-	SPA2820	hypotheticalprotein	0.3674	-0.3735	1	0.14086	1	-0.2102
relA	SPA2821	GTPp yrophosphokinase	1	0.12653	1	0.24793	1	0.24903
ygcA	SPA2822	RNAm ethyltransferase	1	-0.0169	1	0.54314	1	0.42824
barA	SPA2823	sensor protein	1	0	1	0.24793	1	0.32193
-	SPA2824	hypotheticalprotein	1	1.44746	1	0.28951	1	0.22239
ygcX	SPA2825	glucaratedehydratase	4E-16	1.86994	1	0	1	0.26303
-	SPA2827	hypotheticalprotein	0.1396	-0.4511	1	-0.111	1	-0.1019
yqcB	SPA2828	RNAps eudouridylatesynthase	1	-0.4557	1	-0.5305	1	-0.3785
yqcC	SPA2829	hypotheticalprotein	0.1355	-0.3505	1	-0.2955	1	-0.263
-	SPA2830	-	1	-0.1926	1	0	1	-0.0995
syd	SPA2831	sydprot ein	0.7199	-0.2505	1	0.38466	1	0.05445
yqcD	SPA2832	hypotheticalprotein	0.3406	-0.3515	0.7381	-0.1993	1	-0.1618
ygdH	SPA2833	hypotheticalprotein	1	0.1911	1	0.75583	0.6358	0.9003
sdaC	SPA2834	serine transporter	0.0453	-1.2278	0.6662	-1.3272	0.0732	-1.2374
sdaB	SPA2835	L-serine dehydratase2(L -serine deaminase2)	0.0007	-1.3477	1	-0.6887	0.2755	-0.9043
exo	SPA2836	5'-3'exonuc lease	0.4806	-0.2783	1	-0.387	1	-0.174
fucO	SPA2837	1,2-propanedioloxidoreductase(lactaldehydereductase)	1	0	1	0.58496	1	0.58496
fucA	SPA2838	fuculose-1-phosphate aldolase	1	-0.1699	1	0.41504	1	0.48543
fucP	SPA2839	L-fucosepermease	1	0	1	1.09954	1	0.26303
fucI	SPA2840	L-fuculoseisomerase	1	0.19265	1	1.14684	1	-0.0614
fucK	SPA2841	L-fuculosekinase	1	0	1	0.89308	1	0
fucU	SPA2842	fuscoseoperonfucUprotein	1	0.04307	1	0.76553	1	-0.1203
fucR	SPA2843	l-fucoseoperonactivator	1	-0.3847	1	-0.166	1	-0.5525
ygdE	SPA2844	hypotheticalprotein	0.9416	-0.172	0.1474	-0.5493	1	-0.2141
ygdD	SPA2845	hypotheticalprotein	1	-0.0978	1	-0.7045	1	-0.2563
gcvA	SPA2846	regulatoryproteinforglycinecleavagepathway	1	0	1	-0.7618	1	0.10309

-	SPA2847	-	1	0.541	0.6659	0.81101	1	-0.1425
ygdI	SPA2848	lipoprotein	1	0.14585	0.0958	-0.6871	0.612	0.74206
csdA	SPA2849	aminotransferase	1	0.02203	1	-0.1278	1	0.11018
ygdK	SPA2850	hypotheticalprotein	1	-0.0973	1	-0.2937	1	-0.0375
-	SPA2851	hypotheticalprotein	1	0.36257	1	1.09954	1	0.35364
ygdL	SPA2852	hypotheticalprotein	1	-0.241	1	0	1	-0.3626
mltA	SPA2853	membrane-boundly ticmureintransglycosylaseA	0.1699	-0.4389	0.0026	-0.9038	1	-0.5146
metZ	SPA2854	MettRNA	1	0.34104	1	1.45943	1	-0.3626
metZ	SPA2855	MettRNA	1	0.34104	1	1.11548	1	-0.415
amiC	SPA2856	N-acetylmuramoyl-L-alanine amidase	1	-0.2095	1	-0.6101	1	-0.2224
argA	SPA2857	N-acetylglutamatesynthase	1	0	1	0.58496	1	-0.3344
recD	SPA2858	exonucleaseValpha -subunit	1	0.14086	1	0.09311	1	-0.241
recB	SPA2859	exonucleaseVsubunit	1	0.152	1	-0.0365	1	-0.0902
ptr	SPA2860	protease III	1	-0.1993	1	-0.5656	1	-0.241
recC	SPA2861	exonucleaseVsubunit	1	-0.263	1	-0.5656	1	-0.2016
ppdC	SPA2862	prepilin peptidasedependentproteinCprecursor	1	-0.2224	1	-0.3219	1	0
ygdB	SPA2863	hypotheticalprotein	1	-0.585	1	-0.585	1	0
ppdB	SPA2864	prepilin peptidasedependentproteinBprecursor	1	-0.415	1	-0.585	1	-0.585
ppdA	SPA2865	prepilin peptidasedependentproteinAprecursor	1	-0.415	1	0	1	0
thyA	SPA2866	thymidylate synthetase	1	0.15101	0.5674	-0.2386	0.7855	-0.3237
lgt	SPA2867	prolipoproteindiacylglyceryltransferase	1	0.07039	0.9774	-0.1722	0.8406	-0.3881
ptsP	SPA2868	phosphoenolpyruvate-proteinpho sphotransferase	1	0.11736	1	0.18111	1	-0.07
ygdP	SPA2869	hypotheticalprotein	0.7199	-0.2677	1	0.21881	1	-0.0032
mutH	SPA2870	DNAm ismatchrepairprotein	0.5107	-0.3219	1	0.08746	1	-0.2295
ygdQ	SPA2871	hypotheticalprotein	1	0.03747	1	0.14684	1	0.25526
ygdR	SPA2872	lipoprotein	1	-0.0764	1	0.61429	1	0.13124
tas	SPA2873	oxidoreductase	1	0.05842	1	-0.0885	1	0.09686
ygeD	SPA2874	hypotheticalprotein	1	-0.263	1	-0.6167	1	-0.1069
aas	SPA2875	2-acylglycerophosphoethanolamineacyltransferase	1	-0.3536	1	-0.8171	1	0
-	SPA2876	-	1	#DIV/0!	1	0	1	1
-	SPA2877	-	1	#DIV/0!	1	0	1	1
galR	SPA2878	galactoseoperonrepressor	1	-0.1255	1	0.47063	1	0.32558
-	SPA2879	regulatoryprotein	0.5706	-0.2801	1	0.44746	1	0.14086
lysA	SPA2880	diaminopimelatedecarboxylase	1	0	1	-1.1699	1	-0.3219
lysR	SPA2881	transcriptionalactivatorproteinLysR	1	-0.3219	1	0	1	0
ygeA	SPA2882	hypotheticalprotein	1	-0.1806	1	0.2134	1	0.29373
araE	SPA2883	L-arabinoseisomerase	1	-0.1926	1	0.41504	1	0
kduD	SPA2884	2-keto-3-deoxygluconateoxidoreductase	1	-0.2224	1	0.58496	1	0.53051
kduI	SPA2885	5-keto-4-deoxyuronateisomerase	1	-0.1926	1	0.89308	1	0.848
yqeF	SPA2886	acetyl-CoAace tyltransferase	0.3149	-0.3811	0.0228	-0.926	1	-0.7935
-	SPA2887	regulatoryprotein	1	-0.2801	1	-0.1255	1	0
-	SPA2888	hypotheticalprotein	1	-0.585	0.0518	-0.791	0.2993	-0.7102
-	SPA2889	aminoaci dtransportprotein	1	-0.152	1	-0.5146	1	-0.5236
yohL	SPA2890	hypotheticalprotein	1	-0.628	1	0.20811	0.0688	-0.5287
yohM	SPA2891	innerme mbraneprotein	1	-1	1	1	1	-0.1926
-	SPA2892	hypotheticalprotein	1	-0.415	1	-0.1333	1E-08	-1.4034
-	SPA2893	hypotheticalprotein	1	-0.848	0.4803	-0.3219	6E-10	-1.5007
-	SPA2894	hypotheticalprotein	1	-1	1	-0.1575	6E-05	-1.1193

stdC	SPA2895	fimbrialchaperoneprotein	1	-0.3626	1	-0.2115	2E-05	-1.1538
stdB	SPA2896	outerme mbranefimbrialusherprotein	1	-0.415	0.8909	-0.5112	0.0677	-1.0921
stdA	SPA2897	fimbrialprotein	1E-19	-1.6189	1	-0.612	0.2993	-1.8492
-	SPA2898	hypotheticalprotein	1	-0.5025	1	-0.4854	1	0.19265
tnpA	SPA2900	transposaseforinsertionsequenceelementIS200	0.5615	-0.1926	1	-0.6374	1	-1.241
-	SPA2901	hypotheticalprotein(assiciatedwithvirulence)	0.0095	-0.6495	0.7013	-0.2317	1	0.17148
-	SPA2902	hypotheticalprotein (assiciatedwithvirulence)	0.0114	-0.6948	0.523	-0.2862	1	0.18903
-	SPA2903	endonucleasefragment	1	#DIV/0!	1	1	1	0.36257
-	SPA2904	hypotheticalprotein	1	0.0902	1	1.53051	1	1.36257
glyU	SPA2905	GlytR NA	1	-0.4854	1	1.05445	1	0.25376
-	SPA2906	lipoprotein	1	0.09818	1	0.35466	1	0.10692
idi	SPA2907	isomerase	0.4959	0.66985	0.0104	1.36146	0.0655	1.078
lysS	SPA2908	lysyltRNAsynthetase(LysRS)	1	0.01114	1	-0.2968	1	-0.0476
prfB	SPA2909	peptidec hainreleasefactor2	1	-0.0853	0.1782	-0.534	0.4529	-0.4607
recJ	SPA2910	single-stranded DNA-specificexonuclease	1	0.10309	0.9669	-0.1644	1	0.37485
dsbC	SPA2911	thiol:disulfideinterchangeprotein	1	0.05302	1	-0.0393	0.8998	0.64442
xerD	SPA2912	site-specific integrase/recombinase	1	0	1	0.09954	1	0.58496
fldB	SPA2913	flavodoxinII	0.9889	-0.0956	1	0.41504	1	0.04182
ygfX	SPA2914	hypotheticalprotein	1	-0.1558	1	0.58092	1	0.32558
ygfY	SPA2915	hypotheticalprotein	0.3847	-0.3578	1	0.50462	1	0.19953
ygfZ	SPA2916	hypotheticalprotein	1	-0.0912	1	0.31797	1	0.1587
yqfA	SPA2917	hypotheticalprotein	0.0334	0.88026	0.8142	0.70811	0.5886	0.76641
yqfB	SPA2918	hypotheticalprotein	0.1981	-0.4103	1	0.39855	1	0
bglA	SPA2919	6-phospho-beta-glucosidase	1	-0.0332	1	0.34792	1	0.51937
-	SPA2920	hypotheticalprotein	1	-0.3626	1	0.41504	1	-0.585
gcvP	SPA2921	glycinedehydrogenase(decarboxylating)	1	-0.1312	1	-0.7431	1	-0.5941
gcvH	SPA2922	glycinecleavagesystemHprotein	1	-0.3815	1	-0.6217	1	-0.7023
gcvT	SPA2923	aminomethyltransferase	1	-0.4772	1	-0.6039	1	-0.5485
visC	SPA2924	monooxygenase	1	0.37037	0.7848	-0.1229	1	0.0555
visB	SPA2925	2-octaprenyl-6-methoxyphenolhydroxylase	1	0.10343	1	0.11548	1	0.17354
pepP	SPA2926	proline aminopeptidaseII	1	0.04993	1	0.17132	1	0.1608
ygfB	SPA2927	hypotheticalprotein	1	0.00629	1	0.3147	1	0.26303
ygfE	SPA2928	hypotheticalprotein	1	0.20261	1	0.41134	0.7683	0.6143
-	SPA2930	-	1	0.08886	1	0.32625	1	-0.0292
ygfA	SPA2931	hypotheticalprotein	1	0.41107	0.6658	0.77471	1	0.27053
-	SPA2932	-	1	-0.6323	1	0.36257	1	0.20645
serA	SPA2933	D-3-phosphoglyceratedehydrogenase	1	-0.5208	0.0006	-1.3081	1	0.14938
rpiA	SPA2934	ribose 5-phosphate isomerase	0.2657	-0.4914	1	0.08319	1	-0.3008
iciA	SPA2935	chromosomeintitiationinhibitor	1	-0.585	1	-0.4594	1	-0.337
yggE	SPA2936	hypotheticalprotein	0.3738	0.59864	0.0002	-1.1424	1	-0.2996
yggA	SPA2937	membranetransportprotein	1	1	1	0	1	-0.415
yggB	SPA2938	hypotheticalprotein	1	-0.4507	8E-09	-1.5377	1	-0.4507
fba	SPA2939	fructose1,6 -bisphosphatealdolase	1	0.33518	1	0.21624	1	0.38592
pgk	SPA2940	phosphoglyceratekinase	1	0.2402	1	0.50675	1	0.38885
epd	SPA2941	D-erythrose 4-phosphate dehydrogenase	1	0.18442	0.4997	0.89175	1	0.55748
-	SPA2942	hypotheticalprotein	1	-0.585	1	-0.0825	1	-1
-	SPA2943	hypotheticalprotein	1	-0.6374	1	-0.152	1	-0.585
-	SPA2944	hypotheticalprotein	1	-0.1806	1	0.152	1	0.41504

-	SPA2945	ABC-transporter ATP-bindingp rotein	1	-0.1844	1	0.08489	1	0.32193
-	SPA2946	ABC-transporter ATP-bindingp rotein	1	0	1	-0.1699	1	0.45943
tktA	SPA2947	transketolase	1	-0.4832	1	-0.0911	1	-0.0383
yggG	SPA2948	hypotheticalprotein	0.6242	-0.3328	1	0.2363	1	0
speB	SPA2949	agmatineure ohydrolase	0.2596	-0.5247	0.3991	-0.6332	0.8041	-0.3706
speA	SPA2950	biosyntheticargininedecarboxylase	0.7721	-0.3317	0.4747	-0.9448	1	-0.136
yqgB	SPA2951	hypotheticalprotein	0.0325	-0.5095	0.1605	-0.476	1	0.16665
yqgD	SPA2952	hypotheticalprotein	1	0	1	#DIV/0!	1	#DIV/0!
metK	SPA2953	S-adenosylmethioninesynthetase	1	0.47851	5E-12	2.26628	1E-34	2.64245
galP	SPA2954	galactose-protonsy mport(galactosetransporter)	1	-0.0995	1	0.19526	0.144	1
sprT	SPA2955	hypotheticalprotein	1	0.1375	1	-0.2224	1	-0.585
endA	SPA2956	endonucleaseI	1	-0.0995	1	-0.5146	1	-0.8074
yggJ	SPA2957	hypotheticalprotein	1	0.08881	1	0.30117	0.6015	0.59436
gshB	SPA2958	glutathionesynthetase	1	0.21371	1	0.39993	0.767	0.76478
yqgE	SPA2959	hypotheticalprotein	1	-0.0566	1	0.12553	1	0.38187
yqgF	SPA2960	hypotheticalprotein	1	0.18057	1	0.17218	1	0.41923
-	SPA2961	globalregulatoryprotein	1	-0.585	1	-0.263	1	-0.3219
pilT	SPA2962	TypeI Isecretion, ATP-binding, protein	1	0	1	0	1	0
yggS	SPA2963	hypotheticalprotein	0.8912	-0.1255	0.5851	-0.2102	1	-0.2095
yggT	SPA2964	hypotheticalprotein	0.8318	-0.2081	0.257	-0.4297	1	-0.0841
yggU	SPA2965	hypotheticalprotein	0.9723	-0.1583	0.1328	-0.4854	1	0.02647
yggV	SPA2966	hypotheticalprotein	0.9815	-0.1019	0.0462	-0.6641	1	-0.1561
yggW	SPA2967	oxygen-independentcoproporphyrinogenIIIoxidase	1	-0.1069	0.027	-0.75	1	-0.0687
yggM	SPA2968	hypotheticalprotein	1	0	1	2	1	1.71621
ansB	SPA2969	L-asparaginase	1	-0.0791	0.0004	2.2207	0.0731	1.4075
yggN	SPA2970	hypotheticalprotein	1	0.07039	0.8186	0.7891	1	0.40828
yggL	SPA2971	hypotheticalprotein	0.4574	-0.3392	0.6021	-0.2829	1	0.11864
yggH	SPA2972	hypotheticalprotein	0.4274	-0.2922	1	-0.585	1	-0.2313
mutY	SPA2973	A/G-specificadenineglycosylase	1	-0.0671	1	0.0902	1	0
yggX	SPA2974	hypotheticalprotein	0.4372	0.63322	1	0.31194	1	0
mltC	SPA2975	membrane-boundly ticmureintransglycosylaseC	1	0.20353	1	-0.3755	1	-0.263
nupG	SPA2976	nucleosidepermease	0.5562	-0.6746	1	0.30766	1	-0.058
speC	SPA2977	ornithine decarboxylaseisozyme	1	-0.3219	1	-1.1069	1	-0.2065
yqgA	SPA2978	hypotheticalprotein	1	1.926	1	1.73697	1	1.64386
pheV	SPA2979	PhetRN A	1	-1	1	0	1	-0.1699
-	SPA2980	hypotheticalprotein	1	1	1	#DIV/0!	1	#DIV/0!
-	SPA2981	hypotheticalprotein	1	#DIV/0!	1	#DIV/0!	1	#DIV/0!
-	SPA2982	hypotheticalprotein	1	#DIV/0!	1	#DIV/0!	1	#DIV/0!
-	SPA2983	bacteriocinimmunityprotein	1	1	1	0	1	0
-	SPA2984	bacteriocinimmunityprotein	1	-0.415	1	-0.737	1	1
-	SPA2985	hypotheticalprotein	1	#DIV/0!	1	#DIV/0!	1	0
-	SPA2986	hypotheticalprotein	1	#NUM!	1	#DIV/0!	1	#DIV/0!
-	SPA2987	hypotheticalprotein	1	#DIV/0!	1	#DIV/0!	1	#DIV/0!
-	SPA2988	hypotheticalprotein	1	0	1	#DIV/0!	1	#DIV/0!
-	SPA2989	hypotheticalprotein	1	#DIV/0!	1	#DIV/0!	1	#DIV/0!
-	SPA2990	membraneprotein	1	#DIV/0!	1	#DIV/0!	1	#DIV/0!
-	SPA2991	hypotheticalprotein	1	#DIV/0!	1	#DIV/0!	1	#DIV/0!
-	SPA2992	LysR family transcriptionalregulator	1	-1.3785	1	-1.3219	1	-1

-	SPA2993	hypotheticalprotein	1	-0.585	1	-0.585	1	-1
-	SPA2994	aminoaci dtransportprotein	1	-0.737	1	-0.737	1	-1
-	SPA2995	hypotheticalprotein	1	-0.6374	1	-0.337	1	-0.4406
ordL	SPA2996	oxidoreductase	1	-0.585	1	-0.585	1	0
-	SPA2997	aldehyde dehydrogenase	1	-0.1926	1	0.32193	1	0.152
-	SPA2998	hypotheticalprotein	0.2161	-0.4443	5E-08	1.60666	8E-12	1.91146
-	SPA2999	hypotheticalprotein	0.3147	-0.3821	0.0016	1.50635	1E-08	1.74723
-	SPA3000	hypotheticalprotein	1	0	1	0	1	0.16993
-	SPA3001	hydrolase	1	#DIV/0!	1	0.58496	1	0
exuT	SPA3002	hexuronatetransporter	1	0.41387	0.4075	1.356	1	0.60208
uxuA	SPA3003	D-mannonatehydrolase	1	1.09655	0.107	1.74748	0.1242	1.54881
uxuB	SPA3004	D-mannonateoxidoreductase	0.2521	1.33417	0.2059	1.62673	0.0452	1.64166
uxaC	SPA3005	uronatei somerase(glucuronateisomerase)	0.3948	1.2118	0.9646	0.92332	0.2268	1.33667
-	SPA3006	hypotheticalprotein	1	0.38466	0.3448	1.15579	1	-0.263
gsp	SPA3007	glutathionylspermidinesynthase	1	0.26679	1	0.37304	0.7002	0.78351
yghU	SPA3008	transferase	1	0.29255	1	-0.0671	1	0.01658
-	SPA3009	hypotheticalprotein	1	0	1	0	1	0
hybG	SPA3011	hydrogenase-2componentpro tein	0.1609	0.70966	2E-13	1.9098	6E-05	1.39232
hybF	SPA3012	hydrogenase-2componentpro tein	0.7388	0.58823	3E-07	1.84645	3E-05	1.45943
hybE	SPA3013	hydrogenase-2componentpro tein	0.5747	0.52698	2E-05	1.7439	0.0003	1.46211
hybD	SPA3014	hydrogenase-2componentpro tein	1	0.46031	0.0007	1.56924	0.0001	1.51032
hybC	SPA3015	hydrogenase-2largesu bunit	1	0.54557	0.0835	1.64853	0.0054	1.64311
hybB	SPA3016	hydrogenase-2cytochro mebsubunit	0.9562	0.40691	7E-08	1.97199	7E-10	1.89812
hybA	SPA3017	hydrogenase-2smalls ubunit	1	0.44801	5E-14	2.31159	4E-07	1.72732
hyb0	SPA3018	hydrogenase-2smalls ubunit	1	0.25258	0.0123	1.9357	0.2605	1.15829
yghW	SPA3019	hypotheticalprotein	0.4075	0.64909	1	0.24101	1	-0.387
-	SPA3020	hypotheticalprotein	1	0.58496	1	-0.2224	0.0731	-0.7171
yqhA	SPA3021	hypotheticalprotein	1	-0.3081	0.2829	-0.4537	0.1377	-0.5406
-	SPA3022	ATP-dependent RNAhelicase -like protein	1	0.08746	0.1321	-0.585	0.0027	-0.895
-	SPA3023	hypotheticalprotein	0.0902	0.79355	1	-0.0931	1	-0.2742
-	SPA3024	hypotheticalprotein	0.1959	0.75743	1	-0.263	0.013	-0.7188
yghA	SPA3025	oxidoreductase	1	0.55639	0.414	-0.874	0.9671	-0.3405
exbD	SPA3026	biopolymertransportExbDprotein	1	0.60266	1	-1.1783	1	-0.737
exbB	SPA3027	biopolymertransportExbB protein	0.8676	0.52242	0.002	-0.9594	0.0641	-0.7045
-	SPA3028	hypotheticalprotein	1	0.16993	1	0.28951	1	0.32193
metC	SPA3029	beta-cystathionase	1	0.41504	0.0125	1.34104	7E-11	1.9386
yghB	SPA3030	DedA-familyintegralmembraneprotein	1	-0.0356	1	0.41773	1	-0.122
yqhC	SPA3031	AraC-familytrancriptionalregulatoryprotein	1	-0.074	1	0.12553	1	-0.1069
yqhD	SPA3032	alcoholdehydrogenase	0.0695	1.31832	0.1818	1.19719	0.0675	1.16559
yqhE	SPA3033	2,5-diketo-D-gluconatereductaseA	2E-06	1.39158	0.7004	-0.2442	1	0.22913
-	SPA3034	membranetransportprotein	1	#DIV/0!	1	0	1	0
-	SPA3035	hypotheticalprotein	1	0.08746	1	0.20532	0.6261	0.62263
ygiR	SPA3036	hypotheticalprotein	1	-0.263	1	-1.2224	1	-1
-	SPA3037	hypotheticalprotein	1	-0.3219	1	-0.1926	1	0
-	SPA3038	hypotheticalprotein	1	-0.737	1	-0.3219	1	0
-	SPA3039	hypotheticalprotein	1	#DIV/0!	1	#NUM!	1	#DIV/0!
sufI	SPA3041	SufIprotei n	0.2027	-0.4546	0.2336	-0.4594	1	-0.2895
plsC	SPA3042	1-acylglycerol-3-phosphate O-acyltransferase	0.2807	-0.3959	1	-0.4764	1	-0.1069

parC	SPA3043	topoisomeraseIVsubunitA	1	-0.1462	0.1108	-0.6167	1	0.08406
-	SPA3044	AraC-familytranscriptionalregulator	1	0.45943	1	0.01792	1	-0.2436
ygiW	SPA3045	hypotheticalprotein	1	0.24984	1	-0.0317	1	-0.141
ygiX	SPA3046	two-componentsystemresponseregulator	1	-0.387	1	0.16046	1	0.4361
ygiY	SPA3047	two-componentsystemsensorhistidinekinase	1	-0.1699	1	0	1	0.41504
mdaB	SPA3048	NADPHspecific quinoneo xidoreductase(drugmodulator)	1	-0.1125	0.663	0.78943	0.9846	0.56902
ygiN	SPA3049	hypotheticalprotein	1	0.17255	0.5529	0.85432	1	0.4234
parE	SPA3050	topoisomeraseIVsubunitB	1	0.35252	1	-0.0831	1	0.25697
yqiA	SPA3051	hypotheticalprotein	1	0	1	0.5642	1	0.12234
icc	SPA3052	hypotheticalprotein	1	-0.088	1	0.51637	1	0.06748
yqiB	SPA3053	hypotheticalprotein	1	-0.0837	1	0.53964	1	0.32193
yqiE	SPA3054	hypotheticalprotein	1	0.13124	1	0.25716	1	0.48981
tolC	SPA3055	outerme mbraneproteinTolCprecursor	1	0.00406	1	0.11029	1	0.20959
ygiB	SPA3056	lipoprotein	1	-0.1935	1	0.11151	1	0.38282
ygiC	SPA3057	hypotheticalprotein	0.9887	-0.2505	1	0.15879	1	0.55117
ygiD	SPA3058	hypotheticalprotein	1	0.87447	1	1	1	0.34792
ygiE	SPA3059	hypotheticalprotein	0.6293	-0.241	1	-0.1699	1	0.1375
assT	SPA3060	arylsulfatesulfotransferase	1	0.2115	0.7513	0.80523	0.0068	1.75409
-	SPA3061	dsbA-like protein	1	0	1	0.36654	0.0017	1.53552
-	SPA3062	dsbB-like protein	1	-0.0931	1	0.03148	0.0084	1.23799
ribB	SPA3063	3,4-dihydroxy-2-butanone 4-phosphate synthase	0.0896	-0.5177	0.0587	-0.7309	0.8854	-0.263
yqiC	SPA3064	hypotheticalprotein	0.0007	-0.8127	0.9761	-0.1169	0.9572	-0.4127
glgS	SPA3065	glycogen synthesisproteinGlgS	3E-09	1.61969	2E-08	1.96963	0.0023	1.33096
-	SPA3066	hypotheticalprotein	1	-1.3219	1	-2	1	-0.415
yqiK	SPA3067	hypotheticalprotein	1	-0.6781	1	-0.4594	1	-0.152
rfaE	SPA3068	ADP-heptose synthase	1	0.02466	0.5647	-0.3219	1	-0.2675
glnE	SPA3069	adenyl-transferase	1	0	1	-0.415	1	0.12553
ygiF	SPA3070	hypotheticalprotein	0.9416	-0.2016	0.0823	-0.737	1	0.37615
ygiM	SPA3071	hypotheticalprotein	0.4952	0.64853	0.0256	1.32558	1	0.5502
cca	SPA3072	tRNA nucleotidyltransferase	1	0.33342	1	0.42833	1	-0.1007
bacA	SPA3073	bacitracinresistanceprotein	1	-0.4594	1	-0.3479	1	-0.6374
folB	SPA3074	dihydroneopterinaldolase	1	0.152	1	0	1	-0.2224
ygiH	SPA3075	hypotheticalprotein	1	0	1	0.38529	1	0.37851
gcp	SPA3076	glycoprotease	0.9887	-0.1193	1	-0.1844	1	-0.1031
rpsU	SPA3077	30Sribos omalproteinS21	0.2685	-0.4851	0.1602	-0.5755	0.0399	-0.883
dnaG	SPA3078	DNApri mase	0.4549	-0.4374	0.9747	-0.1007	0.7022	-0.3509
rpoD	SPA3079	RNApo lymerase sigma-70factor	0.8048	-0.5096	0.9511	-0.5988	1	-0.1942
mug	SPA3080	G/Um ismatch-specificDNAglycosylase	1	-0.1926	1	0.12553	1	-0.1926
ileX	SPA3081	MettRNA	1	#DIV/0!	1	#DIV/0!	1	#DIV/0!
yqjH	SPA3082	hypotheticalprotein	1	1	1	-2.3219	1	-1.2224
yqjI	SPA3083	hypotheticalprotein	1	0.19265	1	-0.3626	1	-1.0489
cheM	SPA3084	methyl-acceptingchemotaxisproteinII	0.0203	0.92724	0.6254	0.87854	1	-0.115
air	SPA3085	aerotaxisreceptorprotein	3E-11	1.62619	1	1.32193	0.6346	-0.4454
oat	SPA3086	aminotransferase	1	0.41504	5E-95	-2.9635	1	-1.5025
fadH	SPA3087	2,4-dieonyl-coaredu ctase	7E-41	2.41954	1	-0.0485	1	0.04036
ygjO	SPA3088	hypotheticalprotein	1	-0.0324	1	-0.1155	1	-0.5052
ygjP	SPA3089	hypotheticalprotein	1	-0.152	1	0.29698	1	-0.2313
ygjQ	SPA3090	hypotheticalprotein	1	0	1	1	1	0.73697

ygjR	SPA3091	oxidoreductase	1	0.06711	0.3096	1.17932	1	0.29235
-	SPA3092	-	1	0	1	1.58496	1	0.58496
ygjT	SPA3093	drugeff luxprotein	1	-1.3479	1	-1	1	0
ygjU	SPA3094	membranetransport protein	2E-05	-1	0.0001	-1.4091	4E-05	-1.1592
yqjA	SPA3095	hypotheticalprotein	0.0004	-0.848	0.0149	-0.7922	0.1073	-0.602
yqjB	SPA3096	hypotheticalprotein	0.0006	-0.8425	0.0002	-0.9511	0.4325	-0.3334
yqjC	SPA3097	hypotheticalprotein	1	-0.1344	0.2525	-0.5398	1	0.02034
yqjD	SPA3098	hypotheticalprotein	0.2599	-0.5061	0.1235	-0.7046	1	-0.3277
yqjE	SPA3099	hypotheticalprotein	0.1874	-0.542	0.0964	-0.6915	1	-0.2247
yqjK	SPA3100	hypotheticalprotein	0.1114	-0.517	0.0308	-0.6781	1	-0.3033
yqjF	SPA3101	hypotheticalprotein	1	0	1	-1	1	0.58496
yqjG	SPA3102	hypotheticalprotein	1	-0.1069	5E-13	-1.7127	0.0088	-0.8606
yhaH	SPA3103	hypotheticalprotein	0.0582	-0.5217	0.0751	-0.585	1	-0.1849
yhaJ	SPA3104	LysR-family transcriptionalregulator	1	-0.2801	1	-0.3049	1	0
yhaK	SPA3105	hypotheticalprotein	1	0.73697	1	1.51457	1	1.22239
yhaN	SPA3107	hypotheticalprotein	1	0	1	0	1	0.55639
tdcG	SPA3109	L-serine dehydratase	1	0.41504	3E-15	2.44626	6E-11	2.20163
tdcE	SPA3110	formateacetyltransferase	1	1.19265	3E-28	3.07215	1E-28	2.79989
tdcD	SPA3111	propionatekinase	1	2.41504	6E-86	3.49691	3E-36	2.88753
tdcC	SPA3112	HAAAPfamily,L -threonine/L -serine permease,anaerobicallyinducible	2E-08	1.53916	6E-21	3.00628	3E-08	2.44123
tdcB	SPA3113	catabolicthreoninedehydratase	5E-05	1.67549	3E-105	3.69898	2E-08	2.53188
tdcA	SPA3114	TDCo perontranscriptionalactivator	0.7668	0.64412	2E-64	3.3373	0.0011	1.84374
-	SPA3115	-	1	0.30023	1	0.61753	0.3833	0.67991
garK	SPA3116	hypotheticalprotein	4E-88	2.75489	1	0.58496	1	0
garR	SPA3117	2-hydroxy-3-oxopropionatereductase	5E-27	2.36613	1	-0.3479	1	-0.4475
garL	SPA3118	5-keto-4-deoxy-D-glucaratealdolase	2E-56	2.6396	1	-0.1699	1	-0.152
-	SPA3120	carbohydratekinase	0.0244	-0.6101	1	-0.2701	1	-0.585
agaR	SPA3121	hypotheticalprotein	1	-0.5525	1	-0.0544	1	-0.2451
gatY	SPA3122	tagatose-bisphosphatealdolase	1	0	1	1.58496	1	-0.737
-	SPA3123	carbohydratekinase	1	#DIV/0!	1	#DIV/0!	1	-1
-	SPA3124	PTSsys temsugarphosphotransferasetransportersubunitIIBC	1	#DIV/0!	1	#DIV/0!	1	-1
-	SPA3125	PTS-transportf amilyphosphoryltransferprotein	1	#DIV/0!	1	#DIV/0!	1	-1
gatZ	SPA3126	tagatose6 -phosphatekinase1	1	0	1	#DIV/0!	1	0
gatA	SPA3127	PTSsys temgalactitol -specifictransportersubunitIIA	1	#DIV/0!	1	1	1	-0.263
gatB	SPA3128	PTSsys temgalactitol -specifictransportersubunitIIB	1	0	1	0.26303	1	-0.4594
gatC	SPA3129	PTSsys temgalactitol -specifictransportersubunitIIC	1	0	1	0.41504	1	-0.263
gatD	SPA3130	galactitol-1-phosphate dehydrogenase	1	1	1	0	1	-0.415
gatR	SPA3131	galactitolutilizationoperonrepressor	0.8897	-0.1736	0.285	0.926	1	0.25154
yraL	SPA3132	hypotheticalprotein	1	0	1	-0.0825	1	-0.3451
yraM	SPA3133	hypotheticalprotein	0.8318	-0.2421	0.4803	-0.4829	1	0.08659
yraN	SPA3134	hypotheticalprotein	0.323	-0.3567	0.2926	-0.3572	1	0.2007
yraO	SPA3135	phosphoheptoseisomerase	0.4846	-0.3141	0.4549	-0.4361	1	0.26065
yraP	SPA3136	lipoprotein	0.8902	-0.2239	1	-0.321	1	-0.0285
yraR	SPA3137	hypotheticalprotein	1	0.24101	1	-0.759	1	-0.433
yhbO	SPA3138	hypotheticalprotein	1	0	1E-05	-1.2854	1	-0.0077
yhbP	SPA3139	hypotheticalprotein	0.1451	0.72747	0.0068	1.20645	0.0118	1.13465
yhbQ	SPA3140	hypotheticalprotein	1	-0.7618	1	-0.2801	1	-0.9475
yhbS	SPA3141	acetyltransferase	1	0.39557	0.0761	1.23085	0.3582	0.87662

yhbT	SPA3142	hypotheticalprotein	1	0.24437	0.1689	1.25272	0.3702	0.83922
yhbU	SPA3143	protease	1	-0.0995	1	1.26303	1	0.29546
yhbV	SPA3144	hypotheticalprotein	1	0.02346	1	1.4021	1	0.6477
mtr	SPA3146	aminoaci dpermease	1	0.26303	1	-0.3219	1	-1
deaD	SPA3147	ATP-dependent RNAhelicase	1	0.39486	0.2648	-1.0065	1	0.12439
nlpI	SPA3148	hypotheticalprotein	1	-0.2814	1	0.21954	1	-0.2333
pnp	SPA3149	polynucleotidephosphorylase	1	-0.6083	1	-0.4691	1	0.20763
-	SPA3150	-	1	#DIV/0!	1	#DIV/0!	1	#DIV/0!
rpsO	SPA3151	30Sribos omalproteinS15	0.0095	-0.9974	1	-0.0808	1	0.19943
truB	SPA3152	tRNAps eudouridine55 synthase(psi55synthase)(p35protein)	0.3482	-0.4762	1	0.05504	1	0.49553
rbfA	SPA3153	ribosome-bindingf actorA(P15Bprotein)	0.3494	-0.4232	1	0.02635	1	0.40795
infB	SPA3154	proteinc haininitiationfactor2	0.974	-0.5613	1	-0.3698	1	0.17779
nusA	SPA3155	Lfactor	0.9253	-0.3014	0.8064	-0.5706	1	0.05389
yhbC	SPA3156	hypotheticalprotein	1	-0.0625	0.3182	-0.4475	1	0.05063
-	SPA3157	MettRNA	0.0006	-0.9735	1	0.28011	1	-0.4792
argG	SPA3158	argininosuccinatesynthetase	1	-0.0489	1	0	0.0752	-0.8349
leuU	SPA3159	LeutRN A	0.0014	-0.7152	0.236	-0.5305	0.0803	-0.7991
secG	SPA3160	protein-exportm embraneprotein	0.0361	-0.7512	0.2101	-0.4957	0.1581	-0.6743
mrsA	SPA3161	PGM/PMM-familyprotein	1	-0.0551	1	0.20811	1	0.39927
folP	SPA3162	dihydropteroatesynthase	1	0.19794	1	0.27753	1	0.22239
ftsH	SPA3163	cell divisionprotein	0.9887	-0.492	0.6468	-0.9564	1	-0.0108
ftsJ	SPA3164	cell divisionprotein	0.6118	-0.2966	1	0	1	0.30792
yhbY	SPA3165	hypotheticalprotein	0.0524	-0.585	0.2351	-0.4389	0.7825	-0.279
greA	SPA3166	transcriptionelongationfactor	1	-0.042	0.843	-0.182	1	-0.1287
dacB	SPA3167	penicillin-bindingpro tein	1	-0.2157	1	-0.415	1	0
yhbZ	SPA3168	GTP-bindingpro tein	0.51	-0.3326	0.0452	-0.7004	0.8453	-0.4569
yhbE	SPA3169	hypotheticalprotein	1	-0.3312	1	-0.415	1	-0.2895
rpmA	SPA3170	50Sribos omalproteinL27	0.1207	-0.6074	0.4609	-0.3789	0.8691	-0.3817
rplU	SPA3171	50Sribos omalproteinL21	0.272	-0.5845	0.5443	-0.3087	1	-0.3059
ispB	SPA3172	octaprenyl-diphosphatesynthase	1	-0.1954	0.8881	-0.1263	1	-0.1231
nlp	SPA3173	Ner-like regulatoryprotein	1	-0.415	1	0.58496	1	0.58496
murA	SPA3174	UDP-N-acetylglucosamine1 -carboxyvinyltransferase	1	-0.1536	0.1186	-0.6175	1	0.21573
yrbA	SPA3175	hypotheticalprotein	0.185	-0.3505	1	-0.1255	1	0.24793
yrbB	SPA3176	anti-sigma factorantagonist	0.6279	-0.2125	1	-0.0504	1	0.33902
yrbC	SPA3177	hypotheticalprotein	1	-0.098	1	0.05426	1	0.27024
yrbD	SPA3178	hypotheticalprotein	1	-0.1203	0.8108	-0.1278	1	0.26849
yrbE	SPA3179	hypotheticalprotein	1	0.08246	1	-0.1699	1	0.29956
yrbF	SPA3180	ABC-transporter ATP-bindingp rotein	1	0.17509	1	0.08881	1	0.23919
yrbG	SPA3181	hypotheticalprotein	0.2222	-0.3286	1	-0.1926	1	0.3744
yrbH	SPA3182	hypotheticalprotein	0.8961	-0.2442	0.5515	-0.3219	1	0
yrbI	SPA3183	hypotheticalprotein	0.7648	-0.1998	0.2028	-0.5181	1	0.0614
yrbK	SPA3184	hypotheticalprotein	0.7864	-0.2207	0.0959	-0.6181	1	0.11346
yhbN	SPA3185	hypotheticalprotein	1	-0.0644	0.2059	-0.4831	1	0.07199
yhbG	SPA3186	ABC-transporter ATP-bindingp rotein	1	-0.1859	0.2175	-0.4764	1	0.00965
rpoN	SPA3187	RNApo lymerasesigma -54factor(si gma-N)	0.6974	-0.4074	1	-0.343	0.3906	-0.611
yhbH	SPA3188	sigma(54)modulationprotein	0.7116	-0.4764	0.9723	-0.2866	0.0316	-1.1422
ptsN	SPA3189	nitrogen regulatoryIIAprotein	0.8571	-0.2305	1	-0.1962	0.6815	-0.4141
yhbJ	SPA3190	hypotheticalprotein	1	-0.1371	1	-0.1188	0.8318	-0.4178

ptsO	SPA3191	phosphocarrierprotein(nitrogen related hpr)	0.0871	-0.5244	1	0.02487	1	-0.1571
yrbL	SPA3192	hypotheticalprotein	1	0.09818	1	-0.507	1	0.03395
mtgA	SPA3193	monofunctionalbiosyntheticpeptidoglycantransglycosylase	1	0.03953	1	0.11247	1	-0.415
yhbL	SPA3194	hypotheticalprotein	1	0.07375	1	0.17437	0.5393	-0.4797
-	SPA3195	-	1	-1	1	0.19265	1	-0.5146
arcB	SPA3196	aerobic respirationcontrolsensorprotein	1	-0.1666	1	-0.028	1	0
yhcC	SPA3197	hypotheticalprotein	1	-0.415	1	0.41504	1	-0.3479
gltB	SPA3198	glutamatesynthase [NADPH]largesubunit	1	0.24101	0.4803	-0.6781	1	0.26303
gltD	SPA3199	glutamatesynthase(NADPH)smallsubunit	1	0	0.3642	-0.3653	1	-0.2701
yhcG	SPA3200	hypotheticalprotein	1	-1	1	0	1	0
codB	SPA3201	cytosinepermease	1	-0.1155	1	-2.1293	1	-0.585
codA	SPA3202	cytosinedeaminase	1	-0.2345	1E-13	-1.7625	1	-0.5208
yhcH	SPA3203	hypotheticalprotein	1	-0.0199	1	0.24793	1	0.21273
nanK	SPA3204	kinase	1	0.90689	1	0.59664	0.2494	0.76553
nanE	SPA3205	ManNAc-6Pepi merase	0.0518	0.7866	0.4262	0.90122	0.1413	0.91754
nanT	SPA3206	sialicacidtransporter	1	0.41504	1	0.35755	1	0.51457
nanA	SPA3207	N-acetylneuraminatelyase	1	1.39855	1	0.90689	1	-0.1699
yhcK	SPA3208	GntRfam ilytranscriptionalregulator	0.5943	-0.2981	1	0.37707	1	0.16827
sspB	SPA3209	stringent starvationproteinB	1	-0.0943	1	0.23704	1	0.32957
sspA	SPA3210	stringent starvationproteinA	1	-0.025	1	0.43713	1	0.26979
rpsI	SPA3211	30Sribos omalproteinS9	0.3482	-0.6988	0.6302	-0.4858	0.4312	-0.5631
rplM	SPA3212	50S ribosomalproteinL13	0.6426	-0.7041	0.9672	-0.401	0.3267	-0.656
yhcM	SPA3213	ATP/GTP-bindingpro tein	1	0.08489	1	0.4361	1	0.64046
yhcB	SPA3214	hypotheticalprotein	0.0691	-0.6374	1	0.09882	1	0.21354
degQ	SPA3215	serine protease	1	-0.1409	0.6474	-0.2286	1	0.03194
degS	SPA3216	serine protease	1	-0.0952	1	-0.3141	1	-0.0809
-	SPA3217	innerme mbraneprotein	1	-0.415	1	-1	1	-1
oadB	SPA3218	oxaloacetatedecarboxylasesubunitbeta	1	-1	1	-1.585	1	0
oadA	SPA3219	oxaloacetatedecarboxylase subunital pha	1	-0.585	1	-1	1	-1
oadG	SPA3220	oxaloacetatedecarboxylasesubunitgamma	1	0	1	#NUM!	1	#NUM!
ttdB	SPA3221	tartratede hydratase	1	-0.737	1	#NUM!	1	0
ttdA	SPA3222	tartratede hydratase	1	-0.585	1	#DIV/0!	1	#DIV/0!
-	SPA3224	transcriptionalregulator	1	-0.2224	1	0	1	0
-	SPA3225	GntRfam ilytranscriptionalregulator	1	0.06711	1	-0.0365	1	-0.2345
mdh	SPA3226	malate dehydrogenase	1	-0.0889	1	-0.2881	1	0.38072
argR	SPA3227	argininere pressor	0.0857	-0.5369	1	0.04307	0.9993	-0.3753
yhcN	SPA3228	hypotheticalprotein	0	4.02106	8E-27	2.42321	1E-53	2.79941
-	SPA3229	hypotheticalprotein	2E-165	3.09592	2E-16	2.08092	7E-31	2.45003
yhcO	SPA3230	hypotheticalprotein	1	-0.415	1	-0.5146	1	-0.273
yhcP	SPA3231	hypotheticalprotein	1	0	1	0	1	0.41504
yhcQ	SPA3232	hypotheticalprotein	1	1	1	-0.152	1	0.20645
yhcR	SPA3233	hypotheticalprotein	1	0.58496	1	0.58496	1	1
yhcS	SPA3234	LysR familytranscriptionalregulator	1	0.19265	1	-0.1844	1	0.35364
tldD	SPA3235	TldDprotei n	1	-0.05	1	0.28951	1	0.16046
yhdP	SPA3236	hypotheticalprotein	1	-0.4546	1	-0.152	1	-0.0473
rnG	SPA3237	ribonucleaseG	1	-0.1102	0.6377	-0.1699	1	0.38247
yhdE	SPA3238	hypotheticalprotein	0.4784	-0.2283	1	-0.0663	1	0.31034
mreD	SPA3239	rodshape -determiningprotein	1	-0.1651	1	-0.4695	1	0.06711

mreC	SPA3240	rodshape -determiningprotein	0.5739	-0.2479	0.0108	-0.8769	1	-0.3061
mreB	SPA3241	rodshape -determiningprotein	1	-0.0152	0.55	-0.4888	1	-0.2902
yhdA	SPA3242	lipoprotein	1	0	1	0.23607	1	0.5115
yhdH	SPA3243	oxidoreductase	1	-0.1045	0.6727	0.77118	1	0.55733
-	SPA3244	hypotheticalprotein	0.4806	-0.4373	1	-0.6475	1	-0.039
-	SPA3245	hypotheticalprotein	0.0667	-0.5539	0.4926	-0.7748	1	-0.0192
accB	SPA3246	biotinc arboxylcarrierprotein	0.1686	-0.6011	0.7004	-0.668	1	-0.2245
accC	SPA3247	biotinc arboxylase	0.6124	-0.5364	0.4262	-1.1799	1	-0.1777
yhdT	SPA3248	hypotheticalprotein	1	-0.585	1	-0.585	1	-0.585
panF	SPA3249	sodium/pantothenatesymporter(pantothenatepermease)	1	-0.4695	1	-0.737	1	0
prmA	SPA3250	ribosomalproteinL11methyltransferase	0.0045	-0.7176	0.0479	-0.6101	1	0.12199
yhdG	SPA3251	hypotheticalprotein	0.8279	-0.2962	0.0921	-0.6122	0.1642	-0.6663
fis	SPA3252	FisDN A-bindingpro tein	0.5775	-0.2547	0.0216	-0.7935	0.7698	-0.291
yhdU	SPA3254	hypotheticalprotein	1	-1.0704	1	-0.585	1	-0.8074
-	SPA3255	diguanylatecyclase/phosphodiesterasedomain -containingprotein	1	-1	1	-2.1155	1	-1.4854
envR	SPA3256	transcriptionalrepressorforenvCD(acrEF)(TetR/AcrRfamily)	1	#DIV/0!	1	#DIV/0!	1	#DIV/0!
acrE	SPA3257	transmembraneprotein	1	#DIV/0!	1	0	1	0
acrF	SPA3258	RNDf amily,multidrugtransportprotein,acriflavinresistance proteinF	1	0	1	-0.415	1	-0.3219
yhdV	SPA3259	lipoprotein	1	0.26303	1	0.62149	1	1.16993
rrfF	SPA3260	5Sribosom alRNA	1	1	1	1	1	-1.2224
-	SPA3261	ThrtRNA	1	0	1	0	1	-1
rrfD	SPA3262	5Sribosom alRNA	1	#DIV/0!	1	#DIV/0!	1	-1.585
rrlD	SPA3263	23S ribosomalRNA	1	0.04915	1	0.60424	0.9926	-0.5543
-	SPA3264	GlutRN A	1	-0.1699	1	0.66297	1	-0.4288
rrsD	SPA3265	16Sribos omalRNA	1	0	0.9304	0.60894	0.2066	-0.7912
yrdA	SPA3266	transferase	1	0.04731	0.095	1.11704	0.6456	0.72348
yrdB	SPA3267	hypotheticalprotein	1	0.10434	1	-0.4525	1	-0.1193
aroE	SPA3268	shikimatedehydrogenase	1	0.26919	0.3955	-0.3894	1	0.01465
yrdC	SPA3269	hypotheticalprotein	1	0.38333	1	0.02944	1	0.34034
yrdD	SPA3270	hypotheticalprotein	1	0.29956	1	0.1901	1	0.10935
smg	SPA3271	hypotheticalprotein	1	0.11281	1	0.22356	1	-0.0252
smf	SPA3272	hypotheticalprotein	1	0.01649	1	0.19265	1	0
fms	SPA3273	polypeptidedeformylase	0.3959	-0.4137	0.7836	-0.152	0.5817	-0.4322
fmt	SPA3274	methionyl-tRNA formyltransferase	1	-0.1657	0.4968	-0.3291	0.2774	-0.5954
sun	SPA3275	sunprotei n	1	0.15403	0.0931	-0.6088	0.8685	-0.415
trkA	SPA3276	potassiumtransportprotein	1	0.0973	0.0051	-0.9069	1	-0.3505
mscL	SPA3277	largeco nductance mechanosensitivechannelprotein	0.0181	-0.6202	2E-08	-1.5502	0.0035	-0.8724
zntR	SPA3278	Zn(II)-responsiveregulator	0.0006	-0.8231	1	-0.3219	0.1675	-0.4898
yhdN	SPA3279	hypotheticalprotein	0.0013	-0.7454	1	-0.2479	1	-0.4053
rplQ	SPA3280	50S ribosomalproteinL17	0.2599	-1.1353	0.9206	-0.5929	1	0.03769
rpoA	SPA3281	DNA-directed RNApolymerasesubunitalpha	1	-1.0412	1	-0.6531	1	-0.1269
rpsD	SPA3282	30Sribos omalproteinS4	0.6712	-0.9657	1	-0.6011	1	-0.1365
rpsK	SPA3283	30S ribosomalproteinS11	0.2542	-0.9052	0.8559	-0.5015	1	-0.1644
rpsM	SPA3284	30Sribos omalproteinS13	0.5292	-0.7954	1	-0.3403	1	-0.0806
rpmJ	SPA3285	50Sribos omalproteinL36	0.0842	-0.7873	1	-0.0743	1	0.31854
prlA	SPA3286	preprotein translocasesubunit	1	-1.1787	1	-0.2457	1	0.20209
rplO	SPA3287	50Sribos omalproteinL15	0.1035	-1.352	1	-0.2398	1	0.03673
rpmD	SPA3288	50Sribos omalproteinL30	0.1329	-1.2136	1	-0.2996	1	-0.0281

rpsE	SPA3289	30Sribos omalproteinS5	0.3738	-1.2305	1	-0.3673	1	-0.0558
rplR	SPA3290	50Sribos omalproteinL18	0.3093	-1.1338	1	-0.4376	1	-0.0426
rplF	SPA3291	50Sribos omalproteinL6	1	-1.0472	1	-0.5101	1	-0.0794
rpsH	SPA3292	30Sribos omalproteinS8	0.5276	-1.0184	1	-0.5501	1	-0.1163
rpsN	SPA3293	30Sribos omalproteinS14	0.7166	-0.9371	1	-0.629	1	-0.2438
rplE	SPA3294	50Sribos omalproteinL5	1	-0.8425	1	-0.6468	1	-0.3454
rplX	SPA3295	50Sribos omalproteinL24	0.7029	-0.9038	1	-0.6005	1	-0.3334
rplN	SPA3296	50Sribos omalproteinL14	0.7074	-0.8999	1	-0.5843	1	-0.4005
rpsQ	SPA3297	30Sribos omalproteinS17	0.0283	-1.6098	1	-0.0834	1	0.28793
rpmC	SPA3298	50Sribos omalproteinL29	0.0135	-1.6574	1	-0.0808	1	0.33883
rplP	SPA3299	50Sribos omalproteinL16	0.076	-1.6197	1	-0.074	1	0.41893
rpsC	SPA3300	30Sribos omalproteinS3	0.4015	-1.6747	1	-0.1639	1	0.31726
rplV	SPA3301	50Sribos omalproteinL22	0.0334	-1.595	1	-0.3507	1	0.16654
rpsS	SPA3302	30Sribos omalproteinS19	0.0283	-1.5609	1	-0.3678	1	0.13132
rplB	SPA3303	50S ribosomalproteinL2	0.6198	-1.4717	1	-0.519	1	0.00494
rplW	SPA3304	50Sribos omalproteinL23	0.1045	-1.3604	0.9469	-0.6201	1	-0.107
rplD	SPA3305	50Sribos omalproteinL4	0.388	-1.2084	1	-0.6115	1	-0.1766
rplC	SPA3306	50Sribos omalproteinL3	1	-1.0227	1	-0.5759	1	-0.3012
rpsJ	SPA3307	30Sribos omalproteinS10	0.3024	-1.0721	0.7687	-0.5891	0.9585	-0.3455
hopD	SPA3308	TypeI Illeaderpeptidase	1	0	1	#DIV/0!	1	#DIV/0!
bfr	SPA3309	bacterioferritin	1	0	0.0001	-1.363	0.209	-0.7528
yheA	SPA3310	bacterioferritin-associatedferredoxin	1	1	1	-2.9386	1	-2.6781
tufA	SPA3311	elongationfactorTu	1	-0.7655	1	-0.1069	1	0.20017
fusA	SPA3312	elongationfactorG	0.7613	-1.1296	1	-0.6124	1	-0.1658
rpsG	SPA3313	30Sribos omalproteinS7	0.3482	-1.0005	0.6831	-0.6959	0.9337	-0.3906
rpsL	SPA3314	30Sribos omalproteinS12	0.3861	-0.9857	0.7698	-0.6326	0.5393	-0.4928
yheL	SPA3315	hypotheticalprotein	1	-0.2572	1	0.09622	1	0.12928
yheM	SPA3316	hypotheticalprotein	0.1325	-0.415	1	0.24998	1	0.16601
yheN	SPA3317	hypotheticalprotein	0.7116	-0.2508	1	0.14756	1	0.21254
yheO	SPA3318	hypotheticalprotein	0.8431	-0.2073	1	0.31853	1	0.26303
fkpA	SPA3319	FKBP-typepepti dyl-prolyl isomerase	0.9437	-0.2745	1	0.53937	0.8854	0.6009
slyX	SPA3320	hypotheticalprotein	1	-0.415	1	-0.031	1	-0.1229
slyD	SPA3321	FKBP-typepepti dyl-prolyl cis-transi somerase	0.9856	-0.2613	1	0.17433	1	0.13518
yheV	SPA3322	hypotheticalprotein	0.994	-0.105	0.8862	-0.1485	1	0.12553
kefB	SPA3323	glutathione-regulatedpotassium -effluxsystemprotein(K(+)/H(+)antiporter)	1	-0.0825	1	-0.3626	1	0.39232
yheR	SPA3324	oxidoreductase	1	-0.0825	1	-0.4996	1	-0.263
yheS	SPA3325	ABC-transporter ATP-bindingp rotein	1	0.17333	1	-0.3451	1	0.21681
-	SPA3327	hypotheticalprotein	1	-0.078	0.1139	1.11894	1	0.49154
yheT	SPA3328	hydrolase	1	0.28293	0.5587	0.86836	0.6015	0.80296
yheU	SPA3329	hypotheticalprotein	1	0.10893	1	0.67211	0.7789	0.67243
prkB	SPA3330	phosphoribulokinase	1	0	1	0.45418	1	0.52295
yhfA	SPA3331	hypotheticalprotein	1	-0.038	0.0454	1.2541	1	0.62015
crp	SPA3332	cyclicAMPreceptorprotein,catabolitegeneactivator	0.7961	-0.5119	0.9975	-0.3312	1	-0.1799
yhfK	SPA3333	innerme mbraneprotein	1	-0.1375	1	-0.3985	1	0.05445
argD	SPA3334	acetylornithineaminotransferase	1	-0.1561	1	0.11548	0.614	-0.509
pabA	SPA3335	para-aminobenzoatesynthase,glutamineamidotransferasecomponentII	0.5027	-0.3149	1	-0.3755	1	-0.2313
fic	SPA3336	cell filamentationproteinFic	1	0.54749	1	-0.75	1	-0.3536
yhfG	SPA3337	hypotheticalprotein	1	0.33703	0.0398	-0.659	0.614	-0.3399

ppiA	SPA3338	peptidyl-prolyl cis-transi somerase	1	0.0973	0.5079	-0.3446	1	0
yhfC	SPA3339	hypotheticalprotein	1	0.93289	1	-0.6781	1	0.41504
nirB	SPA3340	nitritere ductaselargesubunit	1	0.26303	1	1.22239	1	0.50524
nirD	SPA3341	nitritere ductase(NAD(P)H)smallsubunit	1	0.58496	1	1.28011	1	1.078
nirC	SPA3342	nitritetra nsporter	1	-0.415	1	0	1	0.80735
cysG	SPA3343	sirohemesynthase	0.2111	-0.4537	1	0	0.9486	-0.3169
bigA	SPA3344	surface-exposedvirulenceprotein	1	0.32193	1	0.32193	1	0
trpS	SPA3346	tryptophanyl-tRNAs ynthetase	0.4015	-0.387	0.6965	-0.2119	1	0.10518
gph	SPA3347	phosphoglycolatephosphatase	0.4762	-0.3759	1	-0.0429	1	0.16646
rpe	SPA3348	ribulose-phosphate 3-epimerase	0.7607	-0.3219	1	-0.0196	1	-0.0065
dam	SPA3349	DNAad eninemethylase	0.1981	-0.4436	1	-0.1699	1	0
damX	SPA3350	DamXpr otein	0.293	-0.5461	0.5101	-0.7434	0.9123	-0.3847
aroB	SPA3351	3-dehydroquinatesynthase	0.4702	-0.371	0.0947	-0.7081	1	-0.2154
aroK	SPA3352	shikimatekinaseI	0.6042	-0.3408	0.2306	-0.5113	0.9337	-0.3241
hofQ	SPA3353	typeII secretionsystemprotein	1	0.36257	1	0.22239	1	0
yrfA	SPA3354	hypotheticalprotein	1	1	1	0	1	0
yrfB	SPA3355	hypotheticalprotein	1	0.41504	1	#DIV/0!	1	0
yrfC	SPA3356	hypotheticalprotein	1	0.32193	1	1.58496	1	0.41504
mrcA	SPA3358	penicillin-bindingpro tein1A	1	-0.3847	1	-1.2756	1	-0.4594
yrfE	SPA3359	NUDIXhydrolase	1	0.25154	0.5808	-0.1895	1	0.44746
yrfF	SPA3360	hypotheticalprotein	1	-0.2168	1	-0.2895	1	0.11247
yrfG	SPA3361	hydrolase	1	0.12029	1	-0.2863	1	-0.1644
hslR	SPA3362	heatsho ckprotein	1	0.18903	1	-0.415	1	-0.1089
yrfI	SPA3363	heatsho ckprotein	1	-0.0418	1	-0.4034	1	0.07215
yhgE	SPA3364	hypotheticalprotein	1	-0.152	1	0	1	0.48543
pckA	SPA3365	phosphoenolpyruvatecarboxykinase	1	-0.1375	0.7855	0.98348	0.9026	0.71841
envZ	SPA3366	two-componentsensorkinaseEnvZ	1	0.09192	1	0.14296	1	0.47131
ompR	SPA3367	two-componentresponseregulatorOmpR	1	0.16908	1	0.32406	1	0.26303
greB	SPA3368	transcriptionelongationfactorGreB	1	-0.3219	1	0	1	-0.1699
yhgF	SPA3369	transcriptionaccessoryprotein	1	-0.0794	0.0015	-1.2319	1	-0.074
feoA	SPA3370	ferrous irontransportprotein	0.1159	0.77761	0.1669	-0.5624	0.0995	-0.5774
feoB	SPA3371	ferrous irontransportproteinB	1	0.46713	0.3061	-1.0073	0.4079	-0.581
yhgG	SPA3372	hypotheticalprotein	1	0.10236	0.0015	-1.0271	0.6982	-0.2682
-	SPA3373	hypotheticalprotein	1	-0.3049	1	0.52356	1	0
bioH	SPA3374	biotinbi osynthesisprotein	1	-0.1255	1	0.32193	1	0.36257
yhgH	SPA3375	competenceprotein	1	-0.6919	1	0	1	0.41504
yhgI	SPA3376	hypotheticalprotein	0.3675	-0.4431	0.4763	-0.2768	1	0.404
gntT	SPA3377	high-affinitygluconatetransporter	1	-0.585	0.175	-0.5663	0.1517	-0.7655
malQ	SPA3378	4-alpha-glucanotransferase	1	0.41504	1	0.18442	1	0.47644
malP	SPA3379	maltodextrinphosphorylase	1	0.5639	1	1	1	1.05445
malT	SPA3380	MalTreg ulatory protein	1	0.23112	1	0.81455	1	0.45264
glpR	SPA3381	glycerol-3-phosphateregulonrepressor	1	-0.1699	1	-0.2955	1	-0.152
glpG	SPA3382	hypotheticalprotein	1	-0.0458	1	0.10309	1	0.11103
glpE	SPA3383	hypotheticalprotein	1	-0.2928	1	0.34289	1	0.04439
glpD	SPA3384	aerobic glycerol-3-phosphate dehydrogenase	2E-79	2.67243	5E-106	3.87178	1E-121	3.30875
glgP	SPA3385	glycogenphosphorylase	1	0.2822	1	0.07288	1	0.3101
glgA	SPA3386	glycogensynthase	1	0.27085	1	0.42071	1	0.53287
glgC	SPA3387	glucose-1-phosphate adenylyltransferase	1	0.12649	1	0.56965	1	0.53368

glgX	SPA3388	hypotheticalprotein	1	0.04103	0.8034	-0.5572	1	0.50492
glgB	SPA3389	1,4-alpha-glucanbranchingenzyme	1	-0.0544	0.2829	-1.0452	1	0.42884
asd	SPA3390	aspartate-semialdehydedehydrogenase	0.4474	-0.4867	0.7671	-0.5982	1	0.46467
tnpA	SPA3391	transposaseforinsertionsequenceelementIS200	0.5768	-0.1926	1	-0.415	1	-1.1255
gntU	SPA3392	low-affinitygluconatetransporter	1	-0.263	1	0	1	0
gntK	SPA3393	gluconokinase	1	0	1	1	1	0
gntR	SPA3394	gluconateutilizationoperonrepressor	1	-0.0297	1	0.35267	1	-0.1983
yhhW	SPA3395	hypotheticalprotein	1	0.19265	1	0.36257	1	0.51457
-	SPA3397	-	1	#DIV/0!	1	#DIV/0!	1	#DIV/0!
yhhY	SPA3398	acetyltransferase	1	-0.6167	1	0.12029	1	0.26303
-	SPA3399	ribokinase	1	2.16993	1	2.41504	1	3
-	SPA3400	hypotheticalprotein	1	0.87447	1	1.51457	1	2.2854
-	SPA3401	hypotheticalprotein	1	0	1	0.58496	1	1.16993
-	SPA3402	phophotriesterase	1	0	1	0.09954	1	0.88452
ggt	SPA3403	gamma-glutamyltranspeptidase	1	-0.2224	9E-63	-2.663	0.003	-1.1497
yhhA	SPA3404	hypotheticalprotein	1	0.3927	0.3106	-0.4009	0.9516	-0.3477
ugpQ	SPA3405	glycerophosphoryldiesterphosphodiesterase	1	0.36257	1	-0.4854	1	-0.4475
ugpC	SPA3406	sn-Glycerol-3-phosphate transportATP -bindingpro tein	1	0	1	-1.1375	1	-0.2224
ugpE	SPA3407	sn-Glycerol-3-phosphate transportsystempermeaseprotein	1	0	1	-1.8074	1	-0.5406
ugpA	SPA3408	glycerol-3-phosphatetransportsystem permeaseprotein	1	-0.3219	1	-1.7004	1	-0.7105
ugpB	SPA3409	glycerol-3-phosphate-bindingpe riplasmicprotein	1	-0.2065	0.0007	-1.3004	0.1257	-0.707
-	SPA3410	hypotheticalprotein	0.6825	-0.241	1	-0.2086	0.3344	-0.3462
livF	SPA3411	high-affinitybranched -chainam inoacidtransporterATP -binding protein	1	-0.1375	1	-1.078	1	-0.7105
livG	SPA3412	high-affinitybranched -chainam inoacidtransporterATP -binding protein	1	-0.263	1	-1.3219	1	-0.5406
livM	SPA3413	high-affinity branched-chainam inoacidtransportsystempermease	1	-0.415	1	-1.263	1	-0.4854
livH	SPA3414	high-affinitybranched -chainam inoacidtransportsystempermease	1	-0.585	1	-1.585	1	-0.848
livK	SPA3415	leucine-specificbindingprotein	1	-0.8931	1	-1	1	-0.7776
yhhK	SPA3416	hypotheticalprotein	1	0	0.3949	0.88452	0.3702	0.80735
-	SPA3417	hypotheticalprotein	1	-0.0931	1	0.80735	1	0.71049
livJ	SPA3418	high-affinitybranched -chainam inoacidtransporterATP -binding protein	1	0.32193	1	0	1	0.73697
rpoH	SPA3419	RNApo lymerasesigma -32factor	1	0.13972	1	0.27376	1	0.22691
ftsX	SPA3420	cell divisionprotein	1	-0.1644	0.4669	-0.372	1	0.19555
ftsE	SPA3421	cell divisionATP -bindingpro teinFtsE	0.6405	-0.2589	0.6021	-0.3036	1	0.14938
ftsY	SPA3422	cell divisionprotein	0.844	-0.2765	0.8559	-0.1155	1	-0.1293
yhhF	SPA3423	hypotheticalprotein	1	0	1	0.1587	1	0.16711
yhhL	SPA3424	hypotheticalprotein	1	-0.1926	1	0.18556	1	0.20945
yhhM	SPA3425	hypotheticalprotein	1	-0.2996	1	0	1	-0.3219
yhhN	SPA3426	hypotheticalprotein	1	0.08246	1	0.14439	1	0.47603
zntA	SPA3427	heavym etal-transportingATPase	0.0003	-0.9296	1	-0.4406	1	0.12029
tcp	SPA3428	methyl-acceptingchemotaxiscitratetransducer	0.0851	1.12956	0.5086	1.01027	1	0.11149
yhhP	SPA3429	hypotheticalprotein	0.3151	-0.3561	0.4968	0.61143	0.7551	-0.2051
yhhQ	SPA3430	hypotheticalprotein	1	0.16993	1	-0.4854	1	0.09954
-	SPA3431	lipoprotein	1	-0.0258	1	0.55141	1	0.17509
yhhS	SPA3432	hypotheticalprotein	1	-0.152	1	0.63743	1	0.53051
yhhT	SPA3433	hypotheticalprotein	1	0	1	-1.0704	1	-0.6167
yhhU	SPA3434	hypotheticalprotein	0.1399	-0.4695	1	-0.3293	0.5727	-0.3382
nikR	SPA3435	nickelresponsiveregulator	1	-0.1926	1	-0.1587	0.5036	-0.3219
yhhJ	SPA3436	ABC-transporter ATP-bindingp rotein	1	0.40846	1	1.05063	1	0.76184

yhiH	SPA3437	ABCtra nsporterATP -bindingp rotein	1	0.34049	0.0654	1.22948	0.3582	0.90182
yhiI	SPA3438	HlyD-familysecretionprotein	1	0.13268	0.1133	1.09311	0.2755	0.88634
-	SPA3439	hypotheticalprotein	1	-0.5475	1	0.77761	1	0.52356
-	SPA3440	aminotransferase	1	-0.2996	1	0.87971	1	0.91754
-	SPA3441	regulatoryprotein	0.0057	-0.6903	1	0.16601	1	0.41504
-	SPA3442	DNA-bindingp rotein	1	-0.4361	1	-0.1155	1	-0.3626
-	SPA3443	hypotheticalprotein	1	-1	1	0	1	0.41504
-	SPA3444	hypotheticalprotein	1	-2	1	0	1	0
yhiN	SPA3445	hypotheticalprotein	0.3884	-0.3155	1	-0.0995	1	-0.6215
pitA	SPA3446	low-affinityinorganicphosphatetransporter	0.1213	-0.6179	0.0007	-1.2613	0.816	-0.3119
uspB	SPA3447	universalstressproteinB	1	0.03989	0.2926	-0.4468	0.2525	-0.585
uspA	SPA3448	universalstressproteinA	1	0.03199	1	0.548	1	0.6296
yhiP	SPA3449	PTR2fam ilytransportprotein	1	0.53312	0.0008	2.19768	0.0617	1.46982
yhiQ	SPA3450	hypotheticalprotein	0.6503	-0.2003	0.4589	-0.2818	1	0
prlC	SPA3451	oligopeptidaseA	0.5944	-0.3242	1	0.07973	1	0.38272
-	SPA3452	lipoprotein	1	-1	1	0	1	0
-	SPA3453	hypotheticalprotein	1	-1.585	1	0	1	0
yhiR	SPA3454	hypotheticalprotein	1	0.12199	1	0.17688	1	0.04223
gor	SPA3455	glutathionereductase	1	-0.1038	1	-0.0731	1	0.20859
-	SPA3456	hypotheticalprotein	0.0357	-0.6125	0.004	-0.9094	0.1774	-0.4488
-	SPA3457	phosphosugar-bindingpr otein	0.1497	-0.5594	0.0598	-0.8373	0.1219	-0.7176
-	SPA3458	gntRfam ilyregulatoryprotein	1	0	1	0.77259	1	0.44746
treF	SPA3459	cytoplasmictrehalase	1	-0.0641	0.0589	-0.7442	1	0.07943
-	SPA3460	hypotheticalprotein	1	0.42946	0.4472	1.06871	1	0.43376
-	SPA3461	phage-like lysozyme	1	#NUM!	1	#DIV/0!	1	#DIV/0!
yhjB	SPA3462	hypotheticalluxR -familytranscriptionalregulator	1	-0.3049	1	-0.585	1	-0.3219
yhjD	SPA3464	hypotheticalprotein	1	-0.415	1	-0.8231	1	-0.737
yhjE	SPA3465	metabolitetransportprotein	1	-0.737	1	-1.8074	1	-0.585
yhjH	SPA3467	hypotheticalprotein	2E-23	1.98089	0.14	1.13516	1	0.24385
kdgK	SPA3468	2-dehydro-3-deoxygluconokinase	1	0.2863	1	1.58496	0.0003	1.33015
yhjJ	SPA3469	zinc-proteaseprecursor	1	-0.1414	1	0.38565	1	0.37037
dctA	SPA3470	C4-dicarboxylatetransportprotein	0.0074	-0.7225	1	0.68966	1	-1.2955
yhjK	SPA3471	hypotheticalprotein	1	-0.2479	1	-0.6167	1	-0.2224
yhjL	SPA3472	hypotheticalprotein	1	-0.1293	1	-1	1	-0.6781
yhjM	SPA3473	endoglucanase	0.4015	-0.3499	1	-1.7105	1	-0.9386
yhjN	SPA3474	polysaccharidebiosynthesisproteinsubunitB	1	-0.4381	1	-2.3219	1	-1.3785
yhjQ	SPA3476	hypotheticalprotein	1	-0.0601	9E-22	-2.0171	1E-06	-1.1926
yhjR	SPA3477	hypotheticalprotein	1	-0.1229	2E-16	-1.826	1	-1.0473
yhjS	SPA3478	hypotheticalprotein	1	-0.078	0.0074	-0.9419	0.242	-0.6301
yhjT	SPA3479	hypotheticalprotein	0.2238	-0.3219	2E-05	-1.2065	1	-0.6781
yhjU	SPA3480	hypotheticalprotein	1	-0.2801	7E-10	-1.585	1	-0.7472
-	SPA3481	hypotheticalprotein	0.0033	-0.7776	1	0	0.005	-0.7955
yhjV	SPA3482	aminoaci dpermease	1	-0.1926	1	0	1	-0.585
dppF	SPA3483	dipeptide transportATP -binding proteinDppF	1	-0.5475	0.0887	-1.4757	1	-0.5639
dppD	SPA3484	dipeptide transportATP -binding proteinDppD	1	-0.2756	0.0971	-1.4727	1	-0.297
dppC	SPA3485	dipeptide transportsystempermeaseproteinDppC	1	-0.387	0.0005	-1.8178	1	-0.3219
dppB	SPA3486	dipeptide transportsystempermeaseproteinDppB	1	-0.4695	0.0056	-1.7239	1	-0.5361
dppA	SPA3487	periplasmicdipeptidetransportprotein	0.5865	-0.3593	1	-0.7499	0.4079	-0.628

-	SPA3488	xanthine permease	1	-1	1	-3	1	-1.8074
-	SPA3489	hypotheticalprotein	1	-0.3785	1	-2.0875	1	-1.5236
-	SPA3490	lacI-familytranscriptionalregulator	1	-0.2065	1	-1.5025	1	-1.3626
proK	SPA3491	ProtRNA	1	-1	1	-0.585	1	-0.263
yhjY	SPA3493	hypotheticalprotein	1	-1	1	-1.3219	1	-1.3985
tag	SPA3494	3-methyladenineDNAglycosylaseI,constitutive	0.6234	-0.3332	1	0.12928	1	-0.0805
yiaC	SPA3495	acetyltransferase	1	-0.1862	1	0.22239	1	-0.1829
bisC	SPA3496	biotins ulfoxidereductase	1	-0.1844	1	-0.7045	1	-0.1031
yiaD	SPA3497	outerme mbraneprotein	1	0.33258	1	0.35428	0.6708	0.58496
yiaE	SPA3498	2-hydroxyaciddehydrogenase	1	-0.0937	1	0.38286	1	0.24558
yiaF	SPA3499	hypotheticalprotein	0.6831	-0.2566	0.2566	-0.4258	1	0.27096
cspA	SPA3501	colds hockprotein	1	0.475	0.1578	1.26047	0.0073	1.47376
-	SPA3502	hypotheticalprotein	0.2843	1.01594	0.0722	1.45038	7E-16	2.42836
-	SPA3503	acetyltransferase	0.3257	-0.3421	1	0.29639	1	-0.1769
-	SPA3504	hypotheticalprotein	0.0725	-0.5146	1	0.11396	1	-0.3479
yafP	SPA3505	acetyltransferase	1	-1.2224	1	-0.585	1	-0.585
glyS	SPA3506	glycine-tRNAs ynthetasesubunitbeta	1	-0.6674	0.2097	-0.9344	1	-0.2115
glyQ	SPA3507	glycine-tRNAs ynthetasesubunitalpha	0.1978	-0.5368	0.1729	-0.5792	0.6358	-0.403
-	SPA3508	lipoprotein	1	-0.241	1	-0.5475	1	-0.2895
yiaH	SPA3509	innerme mbraneprotein	1	-0.415	1	-0.4854	1	-0.2224
yiaB	SPA3510	hypotheticalprotein	1	-2	1	#DIV/0!	1	#DIV/0!
xylB	SPA3511	xylulosekinase	1	-0.2065	1	-0.2224	1	0
xylA	SPA3512	D-xyloseisomerase	1	-0.1155	1	0.44746	1	0
xylR	SPA3513	xyloseoperonregulatoryprotein	1	-0.2313	1	-0.0962	1	-0.2224
bax	SPA3514	exported amidase	0.0011	-0.8663	0.002	-1	0.0057	-1.0884
malS	SPA3515	alpha-amylase	1	0.58496	1	0.41504	1	0.48543
avtA	SPA3516	valine--pyruvate aminotransferase	1	-0.1699	1	0	1	0.45943
ysaA	SPA3517	electron-transportpro tein	1	-0.1181	1	0.37851	1	0.05344
yiaJ	SPA3518	transcriptionalregulator	1	-0.3219	1	-0.7521	1	-0.3479
yiaK	SPA3519	carboxylicaciddehydrogenase	1	-0.585	1	#DIV/0!	1	#NUM!
yiaL	SPA3520	hypotheticalprotein	1	0	1	#DIV/0!	1	#DIV/0!
yiaM	SPA3522	hypothetical protein	1	#DIV/0!	1	#DIV/0!	1	#DIV/0!
yiaN	SPA3523	hypotheticalprotein	1	#DIV/0!	1	#DIV/0!	1	#DIV/0!
yiaO	SPA3524	dicarboxylate-binding periplasmicprotein	1	-1.585	1	#NUM!	1	#NUM!
lyxK	SPA3525	L-xylulosekinase	1	#NUM!	1	#NUM!	1	#DIV/0!
yiaQ	SPA3526	hexulose-6-phosphatesynthase	1	0	1	0	1	-1
yiaR	SPA3527	sugar-phosphateisomerase	1	0	1	0	1	-1
yiaS	SPA3528	sugari somerase	1	0	1	1	1	-0.585
-	SPA3529	transcriptionalregulator	1	-0.237	1	0.55943	1	0
-	SPA3530	hypotheticalprotein	1	-0.3219	1	0.1375	1	-0.1926
aldB	SPA3531	aldehyde dehydrogenaseB	1	-0.3943	0.1092	-0.6818	0.012	-0.9175
-	SPA3532	sugark inase	1	-0.1069	1E-10	-1.7004	1	-0.0704
selB	SPA3533	selenocysteine-specificelongationfactor	1	0.42489	0.7511	0.7137	0.405	0.77887
selA	SPA3534	L-seryl-tRNA(Ser) seleniumtransferase	1	0.30986	0.606	0.85561	1	0.43472
yibF	SPA3535	glutathionetransferase	0.3675	-0.431	0.1213	-0.6071	0.2868	-0.5616
mtlA	SPA3536	mannitol-specificenzymeIIof phosphotransferasesystem	0.4566	-0.3737	0.1173	-0.6049	0.327	-0.5208
mtlD	SPA3538	mannitol-1-phosphate dehydrogenase	1	0.2363	1	0.10497	1	-0.1778
-	SPA3540	hypotheticalprotein	4E-14	1.76053	0.0031	1.44746	1	0.63615

yibL	SPA3541	hypotheticalprotein	0.1017	-0.5052	1	0.20859	1	0.03006
-	SPA3542	lipoprotein	1	#DIV/0!	1	#DIV/0!	1	#DIV/0!
lldP	SPA3544	L-lactatepe rmease	1	#NUM!	0.4968	-0.9101	1	-0.763
lctR	SPA3545	L-lactatede hydrogenaseoperonregulator	1	-1.585	1	0.07933	1	-0.2025
lctD	SPA3546	L-lactatede hydrogenase	1	-0.5146	1	0.63927	1	0.40034
yibK	SPA3547	RNA-methyltransferase	1	0.12553	0.0467	1.23241	1	0.19931
-	SPA3548	lacIfam ilytranscriptionalregulatorregulator	1	-0.387	1	-0.0825	1	-0.2955
-	SPA3549	racemase	1	0	1	0	1	-0.415
-	SPA3550	hypotheticalprotein	1	-0.415	1	0	1	0
cysE	SPA3551	serine acetyltransferase	0.8279	-0.241	0.9255	-0.2084	1	-0.0529
gpsA	SPA3552	glycerol-3-phosphatedehydrogenase	0.901	-0.2204	1	0.07001	1	0.40734
secB	SPA3553	protein-exportpro teinSecB	0.5763	-0.4007	1	0.07975	1	0.50455
grxC	SPA3554	glutaredoxin3	0.213	-0.4377	0.1956	-0.4924	1	0.09106
yibN	SPA3555	hypotheticalprotein	0.058	-0.5747	0.0631	-0.7328	1	0.03491
pmgI	SPA3556	2,3-bisphosphoglycerate-independent phosphoglyceratemutase	0.5191	0.59664	0.3293	0.97863	0.9737	0.65838
yibP	SPA3557	hypotheticalprotein	1	-0.0888	1	-0.0458	1	0.1394
yigQ	SPA3558	hypotheticalprotein	1	0.078	0.5065	-0.2838	1	-0.2186
yibD	SPA3559	glycosyltransferasefamilyprotein	1	-0.415	1	1	1	1.32193
tdh	SPA3560	threonine 3-dehydrogenase	0.882	-0.3796	1	-0.3481	0.4534	-0.6228
kbl	SPA3561	2-amino-3-ketobutyratecoenzymeAligase	0.6193	-0.4537	1	-0.1117	0.558	-0.5114
rfaD	SPA3562	ADP-L-glycero-D-manno-heptose-6-epimerase	1	0.08233	1	0.51581	1	0.21175
waaF	SPA3563	ADP-heptose--LPS-heptosyltransferaseII	1	0.09916	1	0.37018	1	0.36421
waaC	SPA3564	lipopolysaccharideheptosyltransferase -1	1	-0.0194	1	0.11818	1	0.37197
waaL	SPA3565	O-antigen ligase	0.5284	-0.2922	1	-0.6966	1	0.16227
waaK	SPA3566	lipopolysaccharide1,2 -N-acetylglucosaminetransferase	0.4314	-0.3337	1	-0.241	1	0.07943
waaZ	SPA3567	lipopolysaccharidecorebiosynthesisproteinRfaZ	0.6503	-0.2256	1	0.59436	0.5016	0.72698
waaY	SPA3568	lipopolysaccharidecorebiosynthesisprotein	0.266	-0.3656	1	0.13327	1	0.41504
waaJ	SPA3569	lipopolysaccharide1,2 -glucosyltransferase	0.0789	-0.5525	1	-0.0946	1	0.02554
waaI	SPA3570	lipopolysaccharide1,3 -galactosyltransferase	0.4502	-0.3258	1	-0.121	1	0.04064
waaB	SPA3571	lipopolysaccharide1,6 -galactosyltransferase	0.546	-0.2801	0.7744	-0.2263	1	-0.2679
wabA	SPA3572	hypotheticalprotein	1	#DIV/0!	1	-0.1343	1	-0.1125
waaP	SPA3573	lipopolysaccharidecorebiosynthesisprotein	0.032	-0.5956	0.0173	-0.7294	1	-0.263
waaG	SPA3574	lipopolysaccharidecorebiosynthesisprotein	0.1069	-0.52	0.0072	-0.9069	0.9941	-0.3923
waaQ	SPA3575	lipopolysaccharidecorebiosynthesis protein	0.0434	-0.5928	0.2981	-0.4475	0.8679	-0.4361
kdtA	SPA3576	3-deoxy-D-manno-octulosonic-acidtra nsferase	0.4428	-0.3382	1	-0.3219	1	-0.4903
coaD	SPA3577	phosphopantetheineadenylyltransferase	0.0422	-0.5228	0.4056	-0.2765	0.2404	-0.4764
mutM	SPA3578	formamidopyrimidine-DNAg lycosylase	1	-0.2801	1	0.73697	1	-0.2224
rpmG	SPA3579	50Sribos omalproteinL33	0.0239	-0.6482	0.4168	-0.3639	1	-0.3549
rpmB	SPA3580	50Sribos omalproteinL28	0.2852	-0.593	1	-0.2316	1	-0.318
radC	SPA3581	DNA repairpro tein	0.0063	-0.7678	1	0.29956	1	-0.0902
dfp	SPA3582	hypotheticalprotein	0.4081	-0.4083	1	-0.0424	0.6176	-0.3833
dut	SPA3583	deoxyuridine5' -triphosphatenucleotidohydrolase	0.0889	-0.5364	1	-0.078	0.9478	-0.2548
ttk	SPA3584	TetR-familytranscriptionalregulator	0.2833	-0.3547	1	-0.387	1	0.03395
pyrE	SPA3585	orotate phosphoribosyltransferase	1	0.34104	1	-0.6323	1	-1.1444
rph	SPA3586	RNase PH	1	0.11548	1	-0.4594	1	-1.2479
yicC	SPA3587	hypotheticalprotein	0.52	-0.3492	1	0.32496	1	0.14958
-	SPA3588	regulatoryprotein	1	-0.3536	1	0.16046	1	0.34104
-	SPA3589	beta-lactamase	1	-0.1926	1	0	1	-0.415

yicG	SPA3590	hypotheticalprotein	1	-0.834	1	-0.848	1	-0.4546
yicF	SPA3591	DNAl igase	1	-0.585	1	0.58496	1	0
gmk	SPA3592	5'guanylatekinase	1	0.08246	1	0.25118	1	0.31637
rpoZ	SPA3593	DNA-directed RNApolymerasesubunitomega	0.5671	-0.3314	1	0	1	0.00769
spoT	SPA3594	guanosine-3',5'-bis(diphosphate)3' -pyrophosphohydrolase;CGSiteNo.156	1	-0.2582	0.8873	-0.1587	1	0.18903
trmH	SPA3595	tRNA(g uanosine-2'-O)-methyltransferase	0.2586	-0.3555	0.462	-0.2675	1	0.02137
recG	SPA3596	ATP-dependent DNAhelicase	0.6163	-0.3103	1	-0.237	1	0.09311
gltS	SPA3597	glutamatepermease	0.0027	-0.7898	0.0336	-0.7442	1	-0.1402
yicE	SPA3598	purineperm ease	1	-0.7776	1	-2.9069	1	-1.1699
yicH	SPA3599	hypotheticalprotein	0.0007	-0.8745	0.8069	-0.1054	1	0.40663
yicJ	SPA3601	sodium:galactosidefamilysymporter	1	-0.585	1	#DIV/0!	1	#DIV/0!
selC	SPA3602	SectRN A	1	-1.585	1	0.58496	1	-1
-	SPA3603	hypotheticalprotein	1	#NUM!	1	#DIV/0!	1	#DIV/0!
-	SPA3604	hypotheticalprotein	1	#NUM!	1	#DIV/0!	1	#DIV/0!
rhuM	SPA3606	DNA-bindingp rotein	0.2377	-0.4005	1	0.26303	1	-0.0721
rmbA	SPA3607	hypotheticalprotein	1	#DIV/0!	1	#DIV/0!	1	#DIV/0!
misL	SPA3608	autotransportedprotein	1	-0.415	1	0	1	-0.415
fidL	SPA3609	hypotheticalprotein	1	0.58496	1	-1.1155	1	-0.7885
marT	SPA3610	transcriptionalregulator	1	-0.263	1	-1	1	-0.8931
slsA	SPA3611	hypothetical protein	0.0038	1.07529	2E-07	2.15938	0	3.86295
cigR	SPA3612	innerme mbraneprotein	0.0022	-0.7437	0.0233	-0.6859	0.0008	-0.9776
mgtB	SPA3613	MagnesiumtransportATPase,P -type2	1	-1.3692	1	-1	1	-1
mgtC	SPA3614	hypotheticalprotein	1	-1.2095	1	#DIV/0!	1	#DIV/0!
yicL	SPA3615	hypotheticalprotein	1	-0.4475	1	-0.415	1	0.18057
-	SPA3616	hypotheticalprotein	1	-0.3626	1	0.26303	1	0
-	SPA3617	hypotheticalprotein	1	0.11548	1	0.19794	1	0.20163
-	SPA3618	transferase	1	0	1	0.14684	1	0
-	SPA3619	PTSsys temtransporterprotein	1	0.41504	1	0.30485	1	0.26303
-	SPA3620	PTSsys temtransporterprotein	1	0	1	-0.0704	1	-0.1375
-	SPA3621	PTSsys temtransporterprotein	1	#NUM!	1	0.41504	1	0.19265
-	SPA3622	PTSsys temtransporterprotein	1	#DIV/0!	1	0.30812	1	0.11548
-	SPA3623	NtrCf amilytranscriptionalregulatorATPasedomain -containingprotein	1	-0.263	0.3943	0.95818	1	0.67377
-	SPA3624	hypotheticalprotein	1	1	1	-0.9434	1	-0.1155
-	SPA3625	glycosylhydrolase	1	0.32193	1	-0.4854	1	0
yicM	SPA3626	innerme mbranetransportprotein	1	0	1	-0.585	1	0
-	SPA3628	DNA-bindingp rotein	1	-0.6521	1	-0.507	1	-0.9542
-	SPA3629	PTSsys temphosphocarrierprotein	1	0	1	-0.7776	1	0.22239
-	SPA3630	hypotheticalprotein	1	0	1	-0.415	1	0
-	SPA3631	carbohydratekinase	1	-0.0931	1	0.58496	1	-0.1255
-	SPA3632	PTSsys temtransportersubunitIIC	1	0	1	0.65711	1	-0.4948
-	SPA3633	PTSsys temtransportersubunitIIB	1	0.28824	0.0002	1.46263	1	0.29474
-	SPA3634	hypotheticalprotein	1	0.36427	0.001	1.5518	1	0.24998
-	SPA3635	GntRfam ilytranscriptionalregulator	1	0.21299	0.0033	1.48712	1	0.18763
yicN	SPA3636	hypotheticalprotein	1	-0.8365	1	-0.2016	1	-0.4306
uhpA	SPA3640	two-componentsystemresponseregulatorprotein	1	-0.2016	1	-0.1255	1	0.12553
-	SPA3641	hypotheticalprotein	1	0.05063	1	0.58496	1	-0.2016
-	SPA3642	permease	1	-0.1926	1	0.80735	1	-0.4406
-	SPA3643	carbohydratekinase	1	0	1	1.02975	1	0.14296

-	SPA3644	DeoR familytranscriptionalregulator	1	-0.1806	1	1.44057	1	0.41504
ilvN	SPA3645	acetohydroxyacidsynthaseI,smallsubunit	1	-0.297	0.4641	-0.3268	1	0.04509
ilvB	SPA3646	acetohydroxyacidsynthaseI,smallsubunit	1	-0.337	0.935	-0.1255	1	0.35614
ivbL	SPA3647	ilvBNoperon attenuator peptide	0.0582	-0.4582	1	0.01288	1	-0.1024
-	SPA3648	hypotheticalprotein	1	-0.4475	1	0	1	0.41504
emrD	SPA3649	multidrug resistanceproteinD	1	-0.1312	2E-11	-1.7726	0.0049	-0.9419
-	SPA3650	hypotheticalprotein	1	-0.4005	1	0.14684	1	0
dsdC	SPA3651	D-serine deaminaseactivator	1	-0.5146	1	0	1	-0.6374
dsdX	SPA3652	DsdX permease	1	-2.1155	1	-0.585	1	-0.585
dsdA	SPA3653	D-serine dehydratase	1	-0.858	1	-0.0875	1	-0.3219
yidF	SPA3654	hypotheticalprotein	1	0.1592	0.18	1.04495	0.1655	0.91847
yidG	SPA3655	hypotheticalprotein	1	0	1	0.1822	0.5562	0.61738
yidH	SPA3656	innerme mbraneprotein	1	-0.4053	1	0.10912	1	0.45943
yidE	SPA3657	hypotheticalprotein	1	0.41504	2E-08	2.07039	0.028	1.24511
hslS	SPA3658	heatsho ckproteinB	0.0008	-0.846	1	-0.0753	1	0.22013
hslT	SPA3659	heatsho ckproteinA	0.0742	-0.6718	1	0.38014	0.9536	-0.2024
yidQ	SPA3660	lipoprotein	0.1488	-0.3479	1	0.16993	1	-0.0911
yidR	SPA3661	ATP/GTP-bindingpro tein	1	-0.0544	1	0.17688	1	0.25376
ccmG	SPA3663	hemel yase/disulfideoxidoreductase,cytochromec -typebi ogenesis	1	0	0.1063	1.05795	2E-06	1.55141
ccmF	SPA3664	cytochromec -typebio genesisproteinF1	1	-0.2955	0.6144	0.8965	0.0017	1.53051
ccmE	SPA3665	cytochromec -typebio genesis proteinE 1	1	-0.0614	0.3322	1.00539	3E-05	1.5776
ccmD	SPA3666	hemee xporterproteinD1	0.7932	-0.1349	0.156	1.03598	2E-07	1.62916
ccmC	SPA3667	hemee xporterproteinC1	0.466	-0.3081	0.5108	0.96592	0.0023	1.47725
ccmB	SPA3668	hemee xporterproteinB1	1	-0.2451	0.644	0.83615	1E-08	1.82873
ccmA	SPA3669	hemee xporterproteinA1	1	-0.2479	0.4707	0.8861	2E-07	1.76755
yhjA	SPA3670	cytochromecperoxidase	0.6002	-0.2721	1	0.23266	1	0.52356
torD	SPA3671	TorDp rotein	1	0	1	1	1	0
torA	SPA3672	trimethylamine-N-oxide reductaseprecursor	1	0	1	0.41504	1	0.41504
torC	SPA3673	hypotheticalprotein	1	0	1	0	1	1
torR	SPA3674	responseregulatorinmulti -componentregualtorysystemwtihTorS(sensorykinase)andTorT(periplasmicsensor), regulatestoroperon(TorRfamily)	0.5763	-0.5169	1	0.64307	1	0.05658
torT	SPA3675	Solutebindi ngreceptorprotein	1	0.08489	1	1.24101	1	1.20645
torS	SPA3676	two-componentsensorproteinhistidineproteinkinase	1	0.41504	1	0.80735	1	0.77761
dgoT	SPA3677	MFSfamil y,D -galactonatetransportprotein	1	#DIV/0!	1	#NUM!	1	#NUM!
dgoA	SPA3678	galactonatedehydratase	1	#DIV/0!	1	0	1	-0.585
-	SPA05605	2-dehydro-3-deoxy-6-phosphogalactonatealdolase	1	#DIV/0!	1	0	1	0
gyrB	SPA3679	DNAg yrasesubunitB	0.9676	-0.2668	1	-0.2996	0.775	-0.476
recF	SPA3680	recFprote in	1	-0.2824	1	-0.6571	1	-0.0671
dnaN	SPA3681	DNApo lymeraseIIIbeta -subunit	1	-0.1407	0.0398	-0.8176	1	-0.1793
dnaA	SPA3682	chromosomalreplicationinitiatorprotein	1	-0.0073	0.3513	-0.3827	1	-0.21
rpmH	SPA3683	50sribos omalproteinl34	0.4343	-0.3671	0.8665	-0.1422	0.3442	-0.6302
rnpA	SPA3684	RNase P,proteincomponent	1	-0.1216	0.4928	-0.3255	0.1102	-0.7328
-	SPA3685	innerme mbraneprotein	0.9253	-0.1285	0.1956	-0.5203	0.0635	-0.6405
yidC	SPA3686	hypotheticalprotein	0.462	-0.5398	0.2698	-1.0112	0.1905	-0.816
thdF	SPA3687	thiophene andfuranoxidationprotein	1	-0.4034	0.0007	-1.0931	1	-0.1375
yidY	SPA3688	membranetransportprotein	1	-0.3219	0.1483	-0.5542	1	-0.0173
yidZ	SPA3689	LysR-familytranscriptionalregulator	1	-0.241	1	-0.241	1	0.28798
yieE	SPA3690	hypotheticalprotein	1	-0.0339	0.4707	0.86434	0.1206	0.87072

yieF	SPA3691	hypotheticalprotein	1	-0.0548	1	0.38488	1	0.26559
yieG	SPA3692	membranetransportprotein	1	-0.3081	1	-1.9635	1	-1.3219
yieH	SPA3693	hydrolase	0.1868	-0.4753	1	-0.8745	1	-0.6215
phoU	SPA3694	phosphate transportsystemregulatoryprotein	0.0013	-0.8171	0.0537	-0.6781	1	-0.4623
pstB	SPA3695	phosphate transportA TP-bindingpro tein	0.0902	-0.4948	0.0254	-0.6868	1	-0.152
pstA	SPA3696	phosphate transportsystempermease	1	-0.663	1	-1.3219	1	-0.263
pstC	SPA3697	phosphate transportsystempermease	1	-0.3785	1	-1.1699	1	0
pstS	SPA3698	phosphate-binding protein	0.1403	-0.4811	0.0002	-1.0962	1	0.13327
-	SPA3699	hypotheticalprotein	1	-0.7885	1	0.58496	1	0.51457
glmS	SPA3700	glucosamine--fructose-6-phosphate aminotransferase	0.907	-0.3839	0.9154	-0.6151	1	-0.0706
glmU	SPA3701	UDP-N-acetylglucosaminepyrophosphorylase	1	-0.2979	1	-0.1503	1	0.04509
-	SPA3702	hypotheticalprotein	1	-0.8745	1	0.73697	1	0.73697
atpC	SPA3703	ATPs ynthasesubunitepsilon	0.5562	-0.9292	1	-0.4003	1	-0.248
atpD	SPA3704	ATPs ynthasesubunitbeta	1	-0.9218	1	-0.3995	1	-0.1697
atpG	SPA3705	ATPs ynthasesubunitgamma	0.3378	-1.1954	1	-0.6332	1	0.00256
atpA	SPA3706	ATPs ynthasesubunitalpha	1	-1.0915	1	-0.5814	1	-0.0168
atpH	SPA3707	ATPs ynthasesubunitdelta	0.184	-1.2151	0.8476	-0.4962	1	-0.0588
atpF	SPA3708	ATPs ynthasesubunitB	0.1451	-1.2777	0.8463	-0.499	1	-0.0903
atpE	SPA3709	ATPs ynthasesubunitC	0.0579	-1.2456	0.7357	-0.4866	1	-0.2452
atpB	SPA3710	ATPs ynthasesubunitA	0.0361	-1.004	0.1092	-0.9236	0.282	-0.5963
atpI	SPA3711	ATPs ynthaseproteinI	0.0016	-0.8191	0.0339	-0.6537	0.5447	-0.3536
gidB	SPA3712	glucoseinhibiteddivisionprotein	1	-0.372	1	-0.5025	1	-0.3626
gidA	SPA3713	glucoseinhibiteddivisionprotein	1	-0.1375	1	-0.926	1	-0.6374
mioC	SPA3714	MioC protein	0.2685	-0.3935	0.4147	-0.3219	0.0187	-0.9439
asnC	SPA3715	regulatoryprotein	1	-0.585	1	0.25154	1	-0.5406
asnA	SPA3716	asparaginesynthetaseA	1	0.08092	0.5091	1.00258	0.816	-0.4468
yieM	SPA3717	hypotheticalprotein	1	0.13327	1	0.36257	1	0.83289
yieN	SPA3718	hypotheticalprotein	1	0.11818	1	0.34211	1	0.54862
kup	SPA3719	membranetransportprotein	1	-0.241	1	-0.337	1	-0.1806
rbsD	SPA3720	highaff inityribosetransportproteinRbsD	2E-07	1.49476	1	0.23062	1	0.58496
rbsA	SPA3721	high affinityribosetransportprotein	1	1.72247	1	0.20876	1	0.41504
rbsB	SPA3723	D-ribose-bindingpe riplasmicprotein	1	-0.0595	1	0.18514	1	0.09828
rbsK	SPA3724	ribokinase	1	0.01974	1	0.12017	1	0.26141
yieO	SPA3726	MFSfamil ytranportprotein	1	0	1	0.35364	1	0.48543
yieP	SPA3727	hypotheticalprotein	1	0.05344	0.3625	0.95818	1	0.64853
rrsC	SPA3728	16Sribos omalRNA	1	0.01759	0.9001	0.60212	0.2032	-0.7885
-	SPA3729	GlutRN A	1	-0.1699	1	0.66297	1	-0.4288
rrlC	SPA3730	23Sribos omalRNA	1	0.02748	1	0.60609	0.9946	-0.5621
rrfC	SPA3732	5Sribosom alRNA	1	#DIV/0!	1	1	1	-2
aspT	SPA3733	AsptRN A	1	-1.0825	0.8064	0.75207	1	0.48543
trpT	SPA3734	TrptRNA	1	-1.1293	0.702	0.75489	1	0.51019
yifA	SPA3735	LysR familytranscriptional regulatoryprotein	0.1964	0.72991	0.4056	0.87447	0.8173	0.63743
yifE	SPA3736	hypotheticalprotein	0.0004	-0.8948	0.0022	-0.9856	3E-11	-1.6668
tnpA	SPA3737	transposaseforinsertionsequenceelementIS200	1	-0.263	1	0	1	0.58496
yifB	SPA3738	magnesiumchelatasesubunitChlI	1	0.26303	1	0.41504	1	0.58496
ilvL	SPA3739	ilvGMEDAoperonattenuatorpeptide	1	-0.1255	1	1.06413	1	1.05445
ilvG	SPA3740	acetolactatesynthaselargesubunit	1	-0.5146	1	0	1	1.26303
ilvM	SPA3741	acetohydroxyacid synthaseII,smallsubunit	1	-0.3668	1	0	1	0.97491

ilvE	SPA3742	branched-chainam ino-acidamino transferase	1	0.02046	1	0.2123	0.3245	0.80296
ilvD	SPA3743	dihydroxyaciddehydratase	1	0.1745	1	-0.1197	1	0.49185
ilvA	SPA3744	threonine deaminase	1	0.078	0.4779	-0.2756	1	0.47393
-	SPA3745	hypotheticalprotein	1	-0.926	1	-0.5025	1	-0.737
-	SPA3746	hypotheticalprotein	1	-0.507	1	-0.6101	1	-0.585
ilvY	SPA3747	LysR-familyregulatoryproteinforilvCexpression	1	-0.5102	1	0.34104	1	0.04307
ilvC	SPA3748	ketol-acidreduct oisomerase	1	0.05377	1	1.05889	1	0.63227
ppiC	SPA3749	peptidyl-prolyl cis-transi someraseC	0.0009	-0.7472	0.3533	-0.3912	0.39	-0.3265
-	SPA3750	hypotheticalprotein	1	-0.3479	1	0.32193	1	0.1375
-	SPA3751	uridine phosphorylase	1	-0.1926	1	0.48543	1	0.48543
-	SPA3752	membranetransportprotein	1	-0.5305	1	0.41504	1	1
rep	SPA3753	ATP-dependent DNAhelicase	1	0.0458	1	-0.3479	1	-0.4475
gppA	SPA3754	guanosine-5'-triphosphate,3'-diphosphatepyrophosphatase(guanosinepentaphosphatase)	1	-0.1137	1	0.34792	1	0.29639
trxA	SPA3756	thioredoxin	0.8048	-0.3267	1	0.18057	1	-0.1169
rho	SPA3757	transcriptionterminationfactor	1	0.29378	1	-0.2173	1	-0.144
rfe	SPA3758	undecaprenyl-phosphate alpha-N-acetylglucosaminyltransferase	0.6956	-0.2303	1	-0.143	1	0.02801
wzzE	SPA3759	lipopolysaccharidebiosynthesisprotein	0.3192	-0.3819	0.4876	-0.3555	1	-0.25
wecB	SPA3760	UDP-N-acetyl-D-glucosamine2 -epimerase	1	0.10053	0.6839	-0.1837	1	-0.0809
rffD	SPA3761	UDP-ManNAcdeh ydrogenase	1	0.02576	0.1747	-0.6374	1	-0.0759
rffG	SPA3762	UDP-N-acetylglucosamineepimerase(UDP -GlcNAc-2-epimerase)	1	-0.0764	0.2034	-0.585	1	-0.0291
rffH	SPA3763	glucose-1-phosphate thymidylyltransferase	0.8843	-0.2174	0.7511	-0.2255	1	-0.1509
rffC	SPA3764	lipopolysaccharidebiosynthesisprotein	1	-0.0802	1	-0.0418	1	-0.0375
rffA	SPA3765	lipopolysaccharidebiosynthesisprotein	1	-0.1795	1	-0.0646	1	-0.1135
wzxE	SPA3766	lipopolysaccharidebiosynthesisprotein	1	-0.2224	0.3293	-0.3908	1	0.10188
-	SPA3767	hypotheticalprotein	1	-0.2141	1	-0.4381	1	0.08746
rffT	SPA3768	4-alpha-L-fucosyltransferase	1	-0.415	1	-0.3677	1	0.0614
rffM	SPA3769	UDP-N-acetyl-D-mannosaminuronicacidtransferase	0.0471	-0.6101	0.7494	-0.1898	1	-0.1312
yifK	SPA3770	aminoaci dpermease	1	-0.4525	1	-0.834	1	-0.3049
argX	SPA3771	ArgtRN A	1	-0.0745	1	0.05209	1	-0.1281
hisR	SPA3772	HistR NA	1	0.01728	1	0.10118	1	-0.1275
leuT	SPA3773	LeutRN A	1	0.06477	1	0.11967	0.9596	-0.1348
proM	SPA3774	ProtRNA	1	0.10692	1	0.18442	1	-0.3833
-	SPA3775	-	0.1981	-0.4456	2E-09	-1.4962	6E-06	-1.3065
hemY	SPA3776	Porphyrinbiosyntheticprotein	1	0	0.463	-0.3454	1	0.57116
hemX	SPA3777	uroporphyrinogenIIImethylase	1	0.13493	1	0.18641	1	0.4717
hemD	SPA3778	uroporphyrinogenIIIsynthase	1	0.07617	1	0.49442	1	0.63537
hemC	SPA3779	porphobilinogendeaminase	1	0.22853	1	0.58496	1	0.53297
cyaA	SPA3780	adenylatecyclase	1	0.47075	1	0.1635	0.9486	0.60466
-	SPA3781	hypotheticalprotein	1	0	1	1	1	0.58496
-	SPA3782	hypotheticalprotein	1	0	1	#DIV/0!	1	#DIV/0!
-	SPA3783	hypotheticalprotein	1	-0.585	1	#NUM!	1	0
cyaY	SPA3784	CyaY protein	1	-0.628	1	0.51457	1	-0.6521
-	SPA3785	hypotheticalprotein	1	#NUM!	1	#DIV/0!	1	#DIV/0!
yifL	SPA3787	lipoprotein	0.3813	-0.2901	1	0.1452	1	0.19878
dapF	SPA3788	diaminopimelateepimerase	1	-0.0634	1	0.1479	1	0.15528
yigA	SPA3789	hypotheticalprotein	1	0.05193	1	0.08366	1	0.01065
xerC	SPA3790	integrase/recombinase	1	0.12553	1	0.27652	1	0.20401
yigB	SPA3791	hypotheticalprotein	1	0.19855	1	0.17333	1	0.08746

uvrD	SPA3792	DNAhe licaseII	1	0.06075	1	0.11736	1	0.38414
corA	SPA3793	magnesiumand cobalt transportprotein	1	-0.628	1	-0.9329	1	-0.628
-	SPA3794	hypotheticalprotein	1	#DIV/0!	1	#DIV/0!	1	#DIV/0!
-	SPA3795	hypotheticalprotein	1	#DIV/0!	1	#DIV/0!	1	#DIV/0!
rarD	SPA3796	chloramphenicol-sensitiveproteinRarD	1	-0.5406	1	-1	1	-0.2224
yigI	SPA3797	hypotheticalprotein	1	-0.415	1	-1.0911	1	-0.263
pldA	SPA3798	detergent-resistantphospholipaseA	0.9856	-0.2022	1	0.12553	0.9376	-0.2653
recQ	SPA3799	ATP-dependent DNAhelicase	1	-0.1884	1	-0.585	1	-0.2685
rhtC	SPA3800	threonine effluxprotein	1	0.26303	1	0.54057	1	0.41504
rhtB	SPA3801	homoserine/homoserinelactoneeffluxprotein	1	-0.415	1	0.32193	1	-0.0825
pldB	SPA3802	lysophospholipaseL2	1	-0.2141	1	-0.0589	1	0.11103
yigL	SPA3803	hypotheticalprotein	1	0	1	-0.263	1	-0.0431
yigM	SPA3804	hypotheticalprotein	1	-0.263	1	0	1	0
metR	SPA3805	trans-activatorofmetEandmetH	1	0.43296	1	2.11548	1	3.66297
metE	SPA3806	5-methyltetrahydropteroyltriglutamate/homocysteineS -methyltransferase	1	1.51937	1	1.11548	1	1
-	SPA3807	regulatoryprotein	1	1.73697	1	0.58496	1	1.22239
ysgA	SPA3808	hydrolase	1	-0.1826	0.0798	-0.743	1	-0.1078
udp	SPA3809	uridine phosphorylase	1	0.81379	0.4472	1.0752	0.0332	1.38161
yigN	SPA3810	hypotheticalprotein	1	0.1375	1	0.85798	1	0.90046
ubiE	SPA3811	ubiquinone/menaquinonebiosynthesismethyltransferaseUbiE	1	-0.1069	1	0.51987	1	0.42183
yigP	SPA3812	hypotheticalprotein	1	0.01057	1	0.20163	1	0.45568
aarF	SPA3813	ubiquinone biosynthesisprotein	1	-0.0414	1	0.05889	1	0.51074
tatA	SPA3814	sec-independent proteintranslocaseprotein	0.2813	-0.4747	1	0.00744	1	-0.0428
tatB	SPA3815	sec-independent proteintranslocaseprotein	0.4549	-0.3864	0.9185	-0.0977	1	-0.2415
tatC	SPA3816	sec-independent proteintranslocaseprotein	0.781	-0.2224	0.8533	-0.1926	1	-0.0148
tatD	SPA3817	deoxyribonuclease	1	0.152	1	-0.2824	0.0853	-0.6521
rfaH	SPA3818	transcriptionalactivator	1	-0.0317	1	-0.0275	0.816	-0.2895
yigC	SPA3819	hypotheticalprotein	1	-0.0471	1	0.08813	1	-0.0111
ubiB	SPA3820	flavin reductase	0.313	-0.3686	0.7537	-0.2578	1	-0.241
fadA	SPA3822	small (beta)subunitofthefatty acid-oxidizingmultienzymecomplex	1E-06	-1.7255	1	0.07973	1	0
fadB	SPA3823	large(al pha)subunitofthefattyacid -oxidizingmultienzymecomplex	0.1466	-0.9029	1	0.02915	1	0.27563
pepQ	SPA3824	proline dipeptidase	0.6124	-0.3295	1	-0.0899	1	0.32473
yigZ	SPA3825	hypotheticalprotein	0.2837	-0.387	0.4779	-0.2538	1	0.25154
trkH	SPA3826	trksys tempotassiumuptakeprotein	1	-0.3626	1	-0.4406	1	0
hemG	SPA3827	protoporphyrinogenoxidase	1	-0.0931	1	-0.2044	1	-0.0601
rrsA	SPA3828	16S ribosomalRNA	1	0.01759	0.9001	0.60212	0.2032	-0.7885
ileT	SPA3829	IletRN A	5E-06	-0.8962	1	0.07039	0.1162	-0.4745
alaT	SPA3830	AlatRN A	5E-07	-1.0228	1	-0.0377	0.3022	-0.463
rrlA	SPA3831	23Sribos omalRNA	1	0.04307	1	0.6087	0.9941	-0.5587
rrfA	SPA3833	5Sribosom alRNA	1	#DIV/0!	1	#DIV/0!	1	-1.585
mobB	SPA3834	molybdopterin-guanine dinucleotidebiosynthesisproteinB	1	0.19265	1	0.65896	1	0.75002
mobA	SPA3835	molybdopterin-guanine dinucleotidebiosynthesisproteinMobA	1	0.18903	1	0.70627	0.2364	0.82782
yihD	SPA3836	hypotheticalprotein	1	-0.1027	0.0847	1.18539	0.6597	0.79328
yihE	SPA3837	hypotheticalprotein	1	0.17616	0.9979	0.73135	0.7262	0.71049
dsbA	SPA3838	thiol:disulfideinterchangeprotein	0.4209	-0.4003	0.2255	-0.5122	1	-0.0721
yihG	SPA3839	acyltransferase	1	-0.2224	1	-0.3219	1	0.58496
polA	SPA3840	DNApo lymeraseI	1	-0.0605	1	0.57032	1	0.43741
-	SPA3841	-	1	-1.3219	1	-0.737	1	-1.737

yihA	SPA3842	ATP/GTP-bindingpro tein	0.2131	-0.4387	1	-0.0159	0.7818	-0.4053
-	SPA3843	hypotheticalprotein	1	-0.0839	1	-0.1407	1	-0.7748
yihI	SPA3844	hypotheticalprotein	0.0075	-0.6735	0.2064	-0.5099	0.3366	-0.6245
hemN	SPA3845	oxygen-independentcoproporphyrinogenIIIoxidase	1	-0.2003	0.8274	-0.1716	1	0.17148
glnG	SPA3846	two-componentsystem,responseregulator	1	0.4975	1	0.74723	0.0515	1.08017
glnL	SPA3847	two-componentsystemsensoryhistidinekinase	0.0725	0.82103	1	1.12928	1	1.18903
glnA	SPA3848	glutaminesynthetase	0.6029	1.01468	0.0185	1.86365	0.6913	1.02699
-	SPA3849	hypotheticalprotein	0.0697	0.77052	1E-21	2.13124	0.0057	1.11704
typA	SPA3850	GTP-bindingpro tein	0.8676	-0.41	0.3362	-1.0875	1	-0.2689
-	SPA3851	hypotheticalprotein	1	-0.737	1	-0.585	1	-1
-	SPA3852	hypotheticalprotein	1	#DIV/0!	1	#NUM!	1	#NUM!
-	SPA3853	hypotheticalprotein	1	#DIV/0!	1	#NUM!	1	0
-	SPA3854	hypotheticalprotein	1	#NUM!	1	-1	1	0
-	SPA3855	hypotheticalprotein	1	#DIV/0!	1	#DIV/0!	1	#DIV/0!
-	SPA3856	hypotheticalprotein	1	-1	1	-1	1	0
yshA	SPA3857	hypotheticalprotein	1	#DIV/0!	1	#DIV/0!	1	#DIV/0!
yihO	SPA3858	membranepermease	1	-0.585	1	-0.585	1	0.32193
yihP	SPA3859	membranepermease	1	-0.5146	1	0.1375	1	0.16993
yihQ	SPA3860	glycosylhydrolase	1	0.26303	1	0.37197	1	0.09311
yihR	SPA3861	hypotheticalprotein	1	0.22239	1	0.7885	1	0.58496
yihS	SPA3862	isomerase	1	0.11548	1	0.77052	1	0.58496
yihT	SPA3863	aldolase	1	0.11548	1	0.8365	1	0.58496
yihU	SPA3864	oxidoreductase	1	-0.415	1	0.87447	1	0.58496
yihV	SPA3865	sugark inase	1	-0.0995	1	0.36257	1	0
yihW	SPA3866	DeoR familytranscriptionalregulator	0.918	-0.219	1	0.64111	1	0.1964
yihX	SPA3867	haloacid dehalogenase-like hydrolase	0.0168	-0.6741	1	0.07696	0.5546	-0.3943
yihZ	SPA3869	hypotheticalprotein	1	-0.1354	1	0.30256	1	0.43812
yiiD	SPA3870	acetyltransferase	1	-0.0589	1	0.26303	1	0.17834
ygjM	SPA3871	hypotheticalprotein	0.0005	-0.8515	0.1883	-0.5305	1	-0.4854
ygjN	SPA3872	hypotheticalprotein	8E-07	-1.0194	0.3361	-0.4339	1	-0.2382
-	SPA3873	lipase	1	-0.2295	1	1.11548	1	1.32193
yiiF	SPA3874	CopG-familyDNA -binding protein	1	-0.663	0.523	0.77961	1	0.10579
-	SPA3875	hypotheticalprotein	0.0304	-0.5305	0.8541	0.70526	1	0.00959
fdhE	SPA3876	FdhEprotei n	1	0.152	1	0.29698	1	0.23704
fdoI	SPA3877	formatedehydrogenase -Osubuni tgamma	1	0.4435	1	0.49033	1	0.38333
fdoH	SPA3878	formatedehydrogenase -Osubuni tbeta	0.974	0.53975	1	0.58496	1	0.29639
fdhD	SPA3880	FdhDprotein	1	-0.1587	1	0.70044	1	0.14086
-	SPA3881	lipoprotein	1	-0.415	1	0	1	0
yiiG	SPA3882	lipoprotein	1	#NUM!	1	#DIV/0!	1	#DIV/0!
-	SPA3883	innerme mbraneprotein	0.6124	-0.2942	1	1	1	1.70044
-	SPA3884	hypotheticalprotein	1	-0.0334	1	1.26303	1	1.76553
-	SPA3885	DNA-bindingp rotein	1	0.11321	0.1322	1.11864	0.097	0.87971
yiiL	SPA3886	hypotheticalprotein	1	0.21587	0.0256	1.27417	6E-05	1.38745
-	SPA3887	alcoholdehydrogenase	1	0.34635	0.0075	1.69032	0.0027	1.42206
rhaD	SPA3888	rhamnulose-1-phosphate aldolase	1	0.16993	1	1.58496	1	1.26303
rhaA	SPA3889	L-rhamnose isomerase	1	0	1	0	1	0
rhaB	SPA3890	rhamnulokinase	1	#DIV/0!	1	#DIV/0!	1	#DIV/0!
rhaS	SPA3891	L-rhamnoseoperonregulatoryprotein	1	-0.858	1	0	1	-0.4854

rhaR	SPA3892	L-rhamnoseoperontranscriptionalactivator	1	-0.6919	1	1.41504	1	-0.263
rhaT	SPA3893	Lrhamno se-protonsy mporter	1	-1	1	0	1	0
-	SPA3894	hypotheticalprotein	1	#NUM!	1	#DIV/0!	1	#DIV/0!
-	SPA3895	integral membranetransportprotein	1	-1	1	-1	1	-1
-	SPA3896	membranetransportprotein	1	#DIV/0!	1	#NUM!	1	#NUM!
-	SPA3897	dicarboxylate-binding periplasmicprotein	1	#DIV/0!	1	#DIV/0!	1	#NUM!
sodA	SPA3898	manganesesuperoxidedismutase	1	0.07416	2E-15	-2.2903	2E-08	-1.8413
yiiM	SPA3899	hypotheticalprotein	0.4534	-0.2429	1	0.0217	1	0.30666
-	SPA3900	hypotheticalprotein	1	-0.1083	1	0.09464	1	0.62344
cpxA	SPA3901	two-componentsensorkinaseprotein	0.466	-0.3811	0.0309	-0.8953	1	-0.074
cpxR	SPA3902	two-componentresponseregulatoryprotein	0.9047	-0.227	0.2653	-0.4644	1	-0.0172
cpxP	SPA3903	extracytoplasmicstressproteinforprotein -mediatedtoxicities	1	0.25502	0.0959	-0.6141	1	0.48543
yiiP	SPA3904	transmembraneeffluxprotein	0.3698	-0.2685	1	-0.0849	1	-0.0704
pfkA	SPA3905	6-phosphofructokinase	1	0.20645	1	0	1	-0.0339
sbp	SPA3906	periplasmicsulfatebindingprotein	1	-1.3219	0	-5.3443	0	-4.4725
cdh	SPA3907	CDP-diglyceridehydrolase	2E-08	-1.2436	0.0265	-0.737	1	-0.389
-	SPA3909	carbohydratekinase	1	0	1	-1	1	-1
-	SPA3910	hypotheticalprotein	1	-0.2224	1	-0.337	1	-0.6439
-	SPA3911	GntRfam ilytranscriptionalregulator	1	-0.4854	1	-0.415	1	-0.5052
-	SPA3912	hypotheticalprotein	1	0	1	-1.3219	1	-1.3219
-	SPA3913	CDP-diacylglycerolphosphotidylhydrolase	1	-1	1	-0.585	1	-1
-	SPA3914	hypotheticalprotein	0.8958	0.54057	0.5819	0.65208	1	0.12029
ydeV	SPA3915	sugark inase	1	0.28129	1	0.69515	1	0.1375
ydeW	SPA3916	regulatoryprotein	1	0.22928	1	0.48543	1	0.23934
ego	SPA3917	ABCtra nsporterATP -bindingp rotein	1	-0.1751	1	0.72583	1	-0.1926
ydeY	SPA3918	ABC transporter permease	1	0.08539	1	0.79647	1	0.1481
ydeZ	SPA3919	ABC-transporter membraneprotein	1	0.30075	1	0.58496	1	0.1822
yneA	SPA3920	ABCtra nsportersubstrate -bindingpro tein	0.6933	0.5979	1	0.29105	1	-0.0449
yneB	SPA3921	aldolase	0.3913	0.69969	1	0.03242	1	0.28011
yneC	SPA3922	hypotheticalprotein	0.2807	0.67088	1	-0.074	1	0.0156
-	SPA3923	ribulose-phosphate 3-epimerase	0.4772	0.63254	0.8665	-0.1213	1	-0.0463
tpiA	SPA3924	triosephosphateisomerase	1	-0.1634	1	-0.1958	1	0.21527
yiiQ	SPA3925	hypotheticalprotein	1	-0.2996	1	-0.3536	1	-0.0566
fpr	SPA3927	ferredoxin--NADP reductase	1	0.03242	0.9723	0.73448	1	0.59234
glpX	SPA3928	glycerolmetabolicprotein	0.2096	0.78319	1	1.41504	1	0.27753
glpK	SPA3929	glycerolkinase	9E-06	2.35067	1E-19	3.18737	0.0863	1.40587
glpF	SPA3930	glyceroluptakefacilitatorprotein	6E-15	2.19984	1E-63	3.31418	0.0004	1.44383
yiiU	SPA3931	hypotheticalprotein	1	-0.0827	1	0.50763	1	0.24016
menG	SPA3932	menaquinonebiosynthesisprotein	1	0.00407	1	0.48799	1	0.22032
menA	SPA3933	menaquinonebiosyntheticprotein	1	-0.3049	1	-0.4975	1	-0.2479
hslU	SPA3934	heatsho ckprotein	1	-0.1426	0.648	-0.213	1	0.46522
hslV	SPA3935	heatsho ckprotein	1	0.05123	1	-0.1402	1	0.26607
ftsN	SPA3936	cell divisionprotein	0.7751	-0.2306	1	-0.1583	1	0.07215
cytR	SPA3937	transcriptionalrepressor	0.6503	-0.3434	1	0.16993	1	0.36059
priA	SPA3938	primosomalproteinreplicationfactor	1	0.24616	1	-0.1876	1	-0.1926
rpmE	SPA3939	50Sribos omalproteinL31	0.0132	-0.9416	0.5368	-0.2285	0.9993	-0.2206
-	SPA3940	hypotheticalprotein	1	0	1	0.32193	1	0.48543
-	SPA3941	hypotheticalprotein	1	-0.3626	1	0.41504	1	0.58496

metJ	SPA3942	repressorofthemethionineregulon	0.189	-0.4024	1	0.58496	1	0.16398
metB	SPA3943	cystathioninegamma -synthase	1	-0.387	1	-0.3785	1	0.8365
metL	SPA3944	bifunctionalaspartokinaseII/homoserinedehydrogenase	1	-0.387	1	-0.585	1	0.16993
-	SPA3945	innerme mbraneprotein	1	#DIV/0!	1	#NUM!	1	#NUM!
-	SPA3946	hypotheticalprotein	1	-0.1769	1	0.926	1	0.08746
-	SPA3947	hypotheticalprotein	1	-0.2895	1	0.41504	1	0.67807
-	SPA3949	alanine racemase	1	-1	1	0	1	0
-	SPA3950	GntRfam ilytranscriptionalregulator	1	0.0614	1	1.24793	1	1.078
metF	SPA3951	5,10 methylenetetrahydrofolatereductase	1	0.79141	1	3.58496	0	4.89077
katG	SPA3952	catalase(hydroperoxidaseI)	0.85	0.7287	0.0282	1.83484	0.0031	1.79375
gldA	SPA3953	glyceroldehydrogenase	1	0.50386	0.2577	1.32193	0.1422	1.39908
talC	SPA3954	transaldolase	1	0.24005	0.3717	0.9098	0.7799	0.58496
yijO	SPA3955	AraCfam ilytranscriptionalregulator	1	-0.5305	1	-0.1155	1	-0.2224
yijP	SPA3956	hypotheticalprotein	2E-06	-1.1085	1	-0.3959	1	0.17509
ppc	SPA3957	phosphoenolpyruvate carboxylase	1	-0.1069	0.7107	-0.2322	1	0.24793
argE	SPA3958	acetylornithinedeacetylase	1	0.11103	1	0.3152	1	0.56704
argC	SPA3959	N-acetyl-gamma-glutamyl-phosphate reductase	1	0.05889	1	-0.152	1	-1.2854
argB	SPA3960	acetylglutamatekinase	1	0	1	-0.585	1	-0.6781
argH	SPA3961	argininosuccinatelyase	1	0.13327	1	-0.7004	1	-0.1699
-	SPA3962	-	1	#DIV/0!	1	#DIV/0!	1	#DIV/0!
oxyR	SPA3963	hydrogen peroxide-inducibleregulonactivator	1	-0.0406	0.8895	-0.2395	1	0.26006
udhA	SPA3964	pyridine nucleotide-disulfideoxidoreductase	1	0.35665	1	0.16681	1	-0.012
yijC	SPA3965	TetRf amilytrancriptionalregulatoryprotein	1	-0.0081	1	0.47615	0.3951	0.82716
yijD	SPA3966	hypotheticalprotein	0.7235	-0.2138	0.5799	0.77323	1	0.48543
trmA	SPA3967	tRNA(ura cil-5)-methyltransferase	1	0.09954	1	-0.1926	1	-0.1699
btuB	SPA3968	vitaminB12receptorprotein	0.2059	-0.5381	0.3904	-0.4415	0.9915	-0.1926
murI	SPA3969	glutamateracemase	1	0.15587	1	0.48543	1	0.28141
rrsB	SPA3970	16Sribos omalRNA	1	-0.02	0.9774	0.60742	0.1843	-0.8331
ileU	SPA3971	IletRN A	5E-06	-0.8962	1	0.07039	0.1162	-0.4745
alaU	SPA3972	AlatRN A	5E-07	-1.0228	1	-0.0377	0.3022	-0.463
rrlB	SPA3973	23Sribos omalRNA	1	0.02748	1	0.60609	0.9946	-0.5621
rrfB	SPA3975	5S ribosomalRNA	1	#DIV/0!	1	#DIV/0!	1	-2
murB	SPA3976	UDP-N-acetylenolpyruvoylglucosaminereductase	0.871	-0.1402	1	0.54314	1	0.15472
birA	SPA3977	bifunctionalbiotinoperonrepressor/biotin -[acetyl-CoAc arboxylase]synthetase	0.4076	-0.2515	1	0.15612	1	0.18286
coaA	SPA3978	pantothenatekinase	1	-0.3103	1	-0.3536	1	-0.3626
-	SPA3979	hypotheticalprotein	1	#DIV/0!	1	#DIV/0!	1	#DIV/0!
thrU	SPA3980	ThrtRNA	0.0379	-0.5105	0.6519	-0.2473	0.0251	-0.6795
tyrU	SPA3981	TyrtRN A	0.1106	-0.439	0.6563	-0.2492	0.178	-0.7099
glyT	SPA3982	GlytR NA	1	-0.0844	0.3529	-0.3445	0.1581	-0.5209
thrT	SPA3983	ThrtRNA	1	-0.0317	0.2674	-0.4264	0.6111	-0.319
tufB	SPA3984	elongationfactorTu	1	-0.673	1	-0.1693	1	-0.0783
secE	SPA3985	preprotein translocaseSecEsubunit	0.185	-0.5512	0.2375	-0.5146	1	-0.1844
nusG	SPA3986	transcriptionantiterminationprotein	0.3482	-0.4697	0.3694	-0.3442	0.9337	-0.2184
rplK	SPA3987	50Sribos omalproteinL11	0.6691	-0.7423	1	-0.3391	1	-0.1593
rplA	SPA3988	50S ribosomalproteinL1	0.871	-0.797	1	-0.3248	1	-0.0655
rplJ	SPA3989	50Sribos omalproteinL10	0.9915	-0.7986	1	0.24702	1	0.4902
rplL	SPA3990	50Sribos omalproteinL7/L12	0.6754	-0.809	1	0.21019	0.9993	0.51017
rpoB	SPA3991	DNA-directed RNA polymerase,beta -subunit	1	-0.8595	1	-0.4864	1	-0.4273

rpoC	SPA3992	DNA-directed RNApolymerase,beta' -subunit	1	-0.5737	1	0.02084	1	-0.2769
-	SPA3993	innerme mbraneprotein	1	-1.585	1	0.26303	1	-0.3219
-	SPA3994	hypotheticalprotein	1	#DIV/0!	1	#DIV/0!	1	#DIV/0!
-	SPA3995	hypotheticalprotein	1	-1	1	-0.585	1	-0.415
thiH	SPA3996	thiamine biosynthesisprotein	1	0	1	-0.585	1	0.152
thiG	SPA3997	thiamine biosynthesisprotein	1	-0.415	1	-0.5406	1	-0.152
thiS	SPA3998	thiamine biosynthesisprotein	1	#NUM!	1	-0.9069	1	0.36257
thiF	SPA3999	thiamine biosynthesisprotein	1	-0.3219	1	-0.7004	1	0
thiE	SPA4000	thiamine-phosphate pyrophosphorylase	1	0	1	-0.926	1	-0.1699
thiC	SPA4001	thiamine biosynthesisprotein	1	0	1	-0.5406	1	0.16993
rsD	SPA4002	regulatoryprotein	0.1115	-0.511	4E-06	-1.241	0.0004	-0.9434
yjaD	SPA4003	hypotheticalprotein	1	0	1	-0.2224	1	0.62149
hemE	SPA4004	uroporphyrinogendecarboxylase	1	0.05063	1	0.08746	1	0.26694
nfi	SPA4005	endonuclease	1	0.19265	1	0.06274	1	0.28011
yjaG	SPA4006	hypotheticalprotein	1	-0.1129	1	0.02801	1	-0.0661
hupA	SPA4007	histone likeDNA -bindingpro teinHU -alpha(NS2)(HU-2)	1	-0.4806	1	0.05697	1	0.00378
yjaH	SPA4008	hypotheticalprotein	1	-0.015	1	-0.0984	1	0.38995
zraP	SPA4009	hypotheticalprotein	1	0	1	0.28043	1	-0.4057
hydH	SPA4010	two-componentsystemsensorprotein	1	0.41504	1	0.3388	1	-0.4623
hydG	SPA4011	transcriptionalregulator	0.3813	0.57706	1	0.57619	1	-0.0978
purD	SPA4012	phosphoribosylglycineamidesynthetase	1	-0.263	2E-18	-2.2867	7E-14	-1.7472
purH	SPA4013	bifunctionalphosphoribosylaminoimidazolecarboxamideformyltransferase/IMPcyclohydrolase	1	0.14439	2E-45	-2.5025	1	-1.3668
rrsE	SPA4014	16Sribos omalRNA	1	0.01759	0.9006	0.59724	0.2024	-0.7885
-	SPA4015	GlutRN A	1	-0.1699	1	0.66297	1	-0.4288
rrlE	SPA4016	23Sribos omalRNA	1	0.03363	1	0.60808	0.9902	-0.5641
rrfE	SPA4018	5Sribosom alRNA	1	#DIV/0!	1	#DIV/0!	1	-2
yjaB	SPA4019	acetyltransferase	1	0.19526	1	0.2123	1	0.26303
metA	SPA4020	homoserineO -succinyltransferase	1	-0.1926	1	1.28011	1	0.91754
aceB	SPA4021	malate synthaseA	4E-10	1.7211	1E-09	-2.4827	4E-150	-3.1293
aceA	SPA4022	isocitratelyase	0.3747	0.81794	8E-06	-2.3128	0	-4.2399
-	SPA4024	hypotheticalprotein	1	#DIV/0!	3E-17	-1.7944	1	-1.4903
iclR	SPA4025	acetateo peronrepressor	1	0.22239	1E-13	-1.8789	1E-09	-1.5128
metH	SPA4026	B12-dependent homocysteine-N5-methyltetrahydrofolatetransmethylase	1	-0.2515	1	-0.6004	1	0.33442
yjbB	SPA4027	hypotheticalprotein	1	0.18442	1	-0.2295	1	0.40336
pepE	SPA4028	peptidaseE	0.4372	0.73558	0.0074	1.39626	0.0752	1.07582
-	SPA4029	hypothetical protein	1	-0.737	1	1.32193	1	1
-	SPA4030	hypotheticalprotein	0.1097	-0.5081	1	-0.0555	0.8387	-0.2671
yjbC	SPA4031	pseudouridinesynthase	0.1053	-0.4773	0.2191	-0.4514	0.7619	-0.3886
yjbD	SPA4032	hypotheticalprotein	0.6009	-0.2333	1	0.51987	1	-0.0391
-	SPA4033	deoRf amilyregulatoryprotein	1	-0.3119	1	-0.2895	1	-0.491
-	SPA4034	hypotheticalprotein	1	0	1	0	1	0
-	SPA4035	hypotheticalprotein	1	0	1	0.41504	1	0.58496
-	SPA4036	hypotheticalprotein	1	-0.3219	1	1	1	1
lysC	SPA4037	lysine-sensitiveaspartokinaseIII	0.0695	-0.5917	1	0.12832	1	0.62149
pgi	SPA4038	glucose-6-phosphate isomerase	1	0.35466	1	0.12428	0.7116	0.68954
yjbE	SPA4039	hypotheticalprotein	1	-0.1926	1	1.1375	1	1.1375
yjbF	SPA4040	lipoprotein	1	#DIV/0!	1	#DIV/0!	1	#DIV/0!
yjbG	SPA4041	hypotheticalprotein	1	#DIV/0!	1	#DIV/0!	1	#DIV/0!

yjbH	SPA4042	lipoprotein	1	-0.2224	1	0.32193	1	0.32193
yjbA	SPA4043	hypotheticalprotein	1	-0.4594	1	0	1	0.58496
malG	SPA4044	maltosetransportinnermembrane protein	1	0.58496	1	1.94753	1	1
malF	SPA4045	maltosetransportinnermembraneprotein	1	1.32193	1	2.35755	1	1.71049
malE	SPA4046	periplasmicmaltose -bindingpr otein	1	1.32193	6E-09	2.12858	0.0211	1.43348
malK	SPA4047	maltose/maltodextrintransportATP -bindingpro tein	1	#DIV/0!	1	3.05889	4E-06	1.52356
lamB	SPA4048	maltoporin	1	0.80735	2E-31	2.72247	0.0061	1.30066
malM	SPA4049	maltoseoperonperiplasmicprotein	1	0.09954	2E-13	2.30933	0.0332	1.16729
ubiC	SPA4050	chorismatelyase	1	0.4397	1	0.36018	1	0.32484
ubiA	SPA4051	4-hydroxybenzoateoctaprenyltransferase	1	0.4344	1	0.12711	1	0.21412
plsB	SPA4052	glycerol-3-phosphateacyltransferase	1	0.06751	1	-0.2359	1	0.04826
dgkA	SPA4053	diacylglycerolkinase	0.0877	-0.4475	1	-0.0704	1	-0.1733
lexA	SPA4054	LexA repressor	0.8659	-0.237	1	0.56096	1	0.15451
dinF	SPA4055	DNA-damage-induciblemembraneprotein	1	-0.2313	1	0.45943	1	0.22239
-	SPA4056	hypotheticalprotein	1	-0.297	0.5761	-0.2996	1	0.19265
yjbJ	SPA4057	hypotheticalprotein	0.1207	-0.3973	0.323	-0.4233	1	0.21105
zur	SPA4058	zincupta keregulationprotein	0.2813	-0.3969	1	0.29698	1	-0.2265
-	SPA4059	hypotheticalprotein	1	0.1375	1	-0.585	1	0.43063
yjbN	SPA4060	hypotheticalprotein	1	-0.0931	1	-0.1635	1	-0.1651
yjbO	SPA4061	hypotheticalprotein	1	-2.585	1	-1	1	-1.585
qor	SPA4062	quinoneo xidoreductase	1	0.17509	0.7963	-0.1132	1	0.01197
dnaB	SPA4063	replicativeDNAhelicase	0.901	-0.1895	0.657	-0.2922	1	-0.142
alr	SPA4064	alanine racemase	1	0.05889	1	-0.415	1	-0.0525
tyrB	SPA4065	aromatic-amino-acidamino transferase	0.3716	-0.3561	1	0.45066	1	0.73697
aphA	SPA4066	class Bacidphosphataseprecursor	0.8897	-0.391	1	0.24491	0.6208	0.78022
yjbQ	SPA4067	hypotheticalprotein	1	-0.075	1	0.2735	1	0.12445
yjbR	SPA4068	hypotheticalprotein	1	-0.0259	1	0.35184	1	-0.1185
-	SPA4069	hypotheticalprotein	1	#NUM!	1	0	1	0
-	SPA4070	lipoprotein	1	#DIV/0!	1	#DIV/0!	1	#DIV/0!
uvrA	SPA4071	excision nucleasesubunitA	0.9814	-0.1629	0.4055	-0.6374	1	0.11247
ssb	SPA4072	single-strandD NA-bindingpro tein	0.4081	-0.4176	0.5674	-0.2786	0.4207	-0.4968
-	SPA4073	hypotheticalprotein	1	#DIV/0!	1	-1.8745	1	-4
-	SPA4074	hypotheticalprotein	1	#DIV/0!	1	-1.585	1	-3.4594
-	SPA4075	type-Isecreti onprotein	1	#DIV/0!	1	-1.3219	1	-4.1699
-	SPA4076	type-Isecreti onprotein	1	#DIV/0!	1	-1	1	-3.6439
-	SPA4077	innerme mbraneprotein	1	-0.263	1	-0.341	2E-17	-2.3424
-	SPA4078	type-1secretio nprotein	1	#NUM!	1	-0.737	1	-3
yjcB	SPA4079	hypotheticalprotein	1	-0.1375	1	0.26303	1	0.22239
yjcC	SPA4080	hypotheticalprotein	1	-0.585	1	-2.4594	1	-2.1699
soxS	SPA4081	regulatoryproteinSoxS	1	1.71049	1	0.67807	1	0.93289
soxR	SPA4082	SoxRprote in	1	-0.3219	1	0	1	0
-	SPA4083	-	1	#DIV/0!	1	-1.585	1	-1
-	SPA4084	glutathione-S-transferase	1	-0.4406	3E-05	-1.2451	0.0006	-0.9835
yjcD	SPA4085	xanthine/uracilpermeasesfamilyprotein	1	-0.585	6E-133	-2.9307	1	-1.3626
yjcE	SPA4086	sodium/hydrogenexchangerfamilyprotein	1	0	0.1954	1.05063	0.1212	1.02046
-	SPA4087	lysR familyregulatoryprotein	1	-0.166	1	0.04064	1	-0.241
-	SPA4088	hypotheticalprotein	1	0	1	0.58496	1	0
-	SPA4089	hypotheticalprotein	1	0	1	0	1	0

yjcG	SPA4090	Sodium:solutesymporterfamilyprotein	1	-1.585	1	-1.585	1	-1.2224
acs	SPA4092	acetyl-coenzymeAsynthetase	0.0005	-0.9048	0.0757	-1.4478	1	-0.4792
-	SPA4093	hypotheticalprotein	1	-0.8074	1	0.24101	1	-0.1926
nrfA	SPA4094	cytochromec552 precursor	1	0.42809	0.1141	1.57393	2E-05	2.01639
nrfB	SPA4095	cytochromec -typeprote inNrfBprecursor	0.1971	0.69188	2E-06	1.83432	5E-33	2.52453
nrfC	SPA4096	cytochromec -typebio genesisprotein	0.0405	0.848	2E-05	1.75974	2E-35	2.56022
nrfD	SPA4097	cytochromec -typebio genesisprotein	1	0.91754	1	1	6E-61	2.79008
nrfE	SPA4098	cytochromec -typebio genesisprotein	1	1	1	1	1	2.70044
-	SPA4099	cytochromec -typebio genesisprotein	1	0.73697	1	1.078	1	2.53605
nrfG	SPA4100	NrfGp rotein	1	0.73697	1	1.08746	1	2.22239
gltP	SPA4101	protongl utamatesymportprotein	1	-0.4854	1	-0.6919	1	-0.0875
yjcO	SPA4102	hypotheticalprotein	0.0234	-0.6521	1	-0.613	1	-0.5146
fdhF	SPA4103	formatedehydrogenaseH	1	0.21022	1	0.78241	0.0808	1.05311
lpxO	SPA4104	membrane-boundbeta -hydroxylase	1	0	1	0.03477	1	0.50696
phnO	SPA4105	acetyltransferase	1	-0.5361	1	0.20645	1	0.26303
phnB	SPA4106	hypotheticalprotein	1	0	9E-07	-1.2505	0.2475	-0.478
phnA	SPA4107	hypotheticalprotein	0.4355	-0.3349	1	-0.415	1	-0.3959
proP	SPA4108	ProP	1	0.152	1	-0.8969	1	0.39734
pmrB	SPA4109	two-componentsensorkinase	0.0015	-0.8007	1	0.52442	1	0.10128
pmrA	SPA4110	two-componentresponseregulator	0.0422	-0.7147	1	0.42294	1	0.08552
yjdB	SPA4111	hypotheticalprotein	1	-0.6167	1	0.13124	1	0.32193
yjdE	SPA4112	aminoaci dpermease	1	1.44057	1	1.11548	1	0.46949
adiY	SPA4113	AraCfam ilyregulatoryprotein	0.0003	1.1193	1	-0.9709	1	-1.3985
adi	SPA4114	argininede carboxylase	1	2	1	2	1	1.1375
melR	SPA4115	melibioseoperonregulatoryprotein	1	0.32193	0.137	1.08439	1	-0.1806
melA	SPA4116	alpha-galactosidase	1E-55	-2.3053	1	0.73697	1	-1.737
melB	SPA4117	melibiosecarrierprotein	8E-91	-2.433	1	1	1	-1.8074
fumB	SPA4118	fumarate hydrataseclassI	1	0.44057	1	0.848	2E-05	-1.3708
dcuB	SPA4119	anaerobicC4 -dicarboxylatetransporter	1	0.16993	1	1.71621	1	-2.3219
-	SPA4120	hypotheticalprotein	1	#DIV/0!	1	#DIV/0!	1	#NUM!
dcuR	SPA4121	two-componentresponseregulator	1	-0.2224	1	0.44057	1	-0.4594
dmsB	SPA4124	anaerobicdimethylsulfoxidereductasesubunitB	1	0	1	0.41504	1	0.152
dmsC	SPA4125	anaerobicdimethylsulfoxidereductasesubunitC	1	0	1	0	1	-0.737
-	SPA4126	hypotheticalprotein	1	-0.3219	1	-0.737	1	-0.152
-	SPA4127	hypotheticalprotein	1	-1	1	0	1	-1
-	SPA4128	hypotheticalprotein	1	-0.415	1	-1.415	1	-2.1699
-	SPA4129	hypotheticalprotein	1	0.73697	1	0	1	0
-	SPA4130	hypotheticalprotein	1	0.70044	1	1.22239	1	-0.7776
-	SPA4131	GerEf amilyregulatoryprotein	1	0.73697	1	0.80735	1	-0.4975
-	SPA4132	araCfam ilyregulatoryprotein	1	0.48938	1	0.56828	0.0007	-1.0764
-	SPA4133	hypotheticalprotein	1	#DIV/0!	1	#DIV/0!	1	#DIV/0!
-	SPA4134	hypotheticalprotein	0.4848	-0.2869	0.4341	-0.3515	0.0037	-0.8519
-	SPA4135	acetyltransferase	0.7453	-0.2193	0.4383	-0.3119	0.0062	-0.8285
phoN	SPA4136	nonspecificacidphosphatase	0.4081	-0.2955	1	-0.3312	1	-0.6015
-	SPA4137	PhetRN A	1	0	1	-1.585	1	0
yjdC	SPA4138	transcriptionalregulator	1	0.13972	0.0458	-0.7063	0.6176	-0.3276
dsbD	SPA4139	thiol:disulfideinterchangeproteinDsbD	1	0.11864	1	-0.2451	1	0.49957
cutA	SPA4140	periplasmicdivalentcationtoleranceproteinCutA	0.705	-0.2182	1	0.10852	1	0.34933

dcuA	SPA4141	anaerobic C4-dicarboxylatetransporter	1	0.22417	0.3541	1.29123	0.6708	1.0131
aspA	SPA4142	aspartate ammonia-lyase	1	0.47629	0.702	1.62334	0.4466	1.22001
-	SPA4143	hypotheticalprotein	1	0.38485	0.008	1.69402	0.0114	1.27298
fxsA	SPA4144	FxsApro tein	1	-0.3744	1	-0.2928	1	-0.3356
yjeH	SPA4145	permease	1	-0.737	1	0	1	0.32193
groES	SPA4146	GroESprote in	0.1874	-0.6043	0.6398	-0.3238	1	0.24689
groEL	SPA4147	GroELpro tein	1	-0.3056	1	-0.2468	1	0.43226
yjeI	SPA4148	hypotheticalprotein	0.2672	-0.5264	1	0.57898	1	0.28134
yjeJ	SPA4149	hypotheticalprotein	1	-0.8745	1	-1.3219	1	-1.3219
yjeK	SPA4150	hypotheticalprotein	1	0.11103	1	-0.3899	1	-0.5719
efp	SPA4151	elongationfactorP	0.0283	-0.781	0.3184	-0.4927	0.2013	-0.589
ecnA	SPA4152	entericidinAprecursor	1	-0.6015	1	-0.585	1	-0.6881
ecnB	SPA4153	entericidinB	1	-0.1699	7E-05	-0.8845	0.8701	-0.2565
ecnR	SPA4154	transcriptionalregulator	1	0.16993	1	-0.585	1	-0.9668
sugE	SPA4155	SugEprote in	1	-1.0641	1	-0.5406	1	-0.628
blc	SPA4156	lipoprotein	1	1	0.0002	-1.1089	0.1901	-0.7168
frdD	SPA4157	fumarate reductasecomplexsubunitD;membraneanchorpolypeptide	1	0.45709	0.5757	0.86012	0.081	1.06547
frdC	SPA4158	fumarate reductasecomplexsubunitC;membraneanchor polypeptide	1	0.49741	0.6418	0.83512	0.0296	1.16439
frdB	SPA4159	fumarate reductase,iron -sulfurpro tein	1	0.58436	0.4549	1.08338	0.2101	1.20016
frdA	SPA4160	fumarate reductase,flavoproteinsubunit	1	0.41504	0.3949	1.40273	0.771	0.95392
yjeA	SPA4161	lysyl-tRNAs ynthetase	1	0.27563	1	0.32193	1	0.12553
yjeM	SPA4162	aminoaci dpermease	1	-0.1926	1	-0.415	1	0.26303
yjeN	SPA4163	hypotheticalprotein	1	-0.4854	1	-0.4854	1	0.32193
psd	SPA4165	phosphatidylserinedecarboxylaseproenzyme	0.7598	-0.2081	1	0.16601	1	0.26303
yjeQ	SPA4166	hypotheticalprotein	1	0.07595	1	0.37587	1	0.15078
orn	SPA4167	oligoribonuclease	0.4032	-0.2876	1	-0.0857	1	0.02915
artJ	SPA4168	arginine-bindingpe riplasmicprotein	1	0.45943	0.8186	0.74108	0.0001	1.41504
-	SPA4169	GlytR NA	0.0003	-0.8018	1	0.21632	0.2897	-0.4513
glyW	SPA4170	GlytR NA	0.0039	-0.6656	1	0.10253	0.0329	-0.6852
glyW	SPA4171	GlytR NA	0.0024	-0.721	1	0.23563	0.0662	-0.8011
yjeS	SPA4172	4Fe-4Sbindingp rotein	1	0.22239	1	0.53051	1	0
yjeF	SPA4173	hypotheticalprotein	1	0	1	-0.567	1	0.18057
yjeE	SPA4174	hypotheticalprotein	1	-0.1031	1	-0.6167	1	-0.0759
amiB	SPA4175	N-acetylmuramoyl-L-alanine amidase	0.7932	-0.2086	0.1376	-0.6314	1	0.02346
mutL	SPA4176	DNAm ismatchrepairprotein	1	-0.0191	0.5656	-0.3049	1	0.07886
miaA	SPA4177	tRNAde lta-2-isopentenylpyrophosphate(IPP)transferase	0.85	-0.2024	1	-0.1033	1	0.22039
hfQ	SPA4178	hostfacto r-Iprotein	1	-0.2081	1	0	1	0.18179
hflX	SPA4179	HflX protein,putativeGTP -binding protein	1	-0.0059	1	-0.2563	1	0.05636
hflK	SPA4180	HflK protein	0.7166	-0.2521	0.215	-1.1098	1	-0.2756
hflC	SPA4181	HflC protein	0.0842	-0.7232	0.0705	-1.4352	0.8972	-0.3671
yjeT	SPA4182	hypotheticalprotein	1	-0.3785	1	-0.5305	1	-0.9329
purA	SPA4183	adenylosuccinatesynthetase	0.5123	-0.8948	0.648	-0.7485	0.3702	-0.7909
yjeB	SPA4184	hypotheticalprotein	1	0.07529	1	0.40939	0.9601	0.59756
rnr	SPA4185	ribonucleaseR	1	0.22683	1	-0.013	1	0.36306
yjfH	SPA4186	tRNA/rRNA methyltransferase	1	0.25198	0.3642	-0.3558	1	0.00851
yjfI	SPA4187	hypotheticalprotein	1	0	1	#DIV/0!	1	#DIV/0!
yjfJ	SPA4188	phages hockproteinA	1	-0.585	1	0	1	0
-	SPA4189	hypotheticalprotein	1	-1.3219	1	0	1	0

yjfK	SPA4190	hypotheticalprotein	1	-1.585	1	#NUM!	1	#DIV/0!
yjfL	SPA4191	hypotheticalprotein	1	-0.585	1	#NUM!	1	0
yjfM	SPA4192	hypotheticalprotein	1	-0.585	1	-0.585	1	-0.415
yjfC	SPA4193	hypotheticalprotein	1	-0.585	1	0.41504	1	0
aidB	SPA4194	acylCo -Adehydro genase	1	0.28379	1	0.23266	1	0.03477
yjfN	SPA4195	hypotheticalprotein	1	-0.1436	0.0314	1.49521	1	0.26443
yjfO	SPA4196	hypotheticalprotein	1	-0.1894	0.1422	1.2986	1	0.44203
yjfP	SPA4197	hypotheticalprotein	0.4657	-0.2451	0.974	-0.1816	1	0.08246
yjfQ	SPA4198	transcriptionalregulator	0.4345	-0.3009	1	0.19265	1	-0.0716
yjfR	SPA4199	hypotheticalprotein	1	0	1	0.73697	1	1.32193
sgaT	SPA4200	transport proteinSgaT	1	0	8E-09	2.06088	2E-06	1.68118
sgaB	SPA4201	PTSsys temtransportersubunitIisga	1	0.46949	3E-22	2.37156	3E-18	2.07358
sgaA	SPA4202	sugarpho sphotransferase	1	0.53051	9E-19	2.39046	3E-26	2.36923
sgaH	SPA4203	hexulose-6-phosphatesynthase	1	0.41504	1E-13	2.19931	2E-27	2.35755
sgaU	SPA4204	hypotheticalprotein	1	0.41504	5E-06	1.85086	6E-21	2.22239
sgaE	SPA4205	class IIaldolase	1	0.36257	4E-05	1.60666	2E-23	2.27684
yjfY	SPA4206	hypotheticalprotein	1	-0.152	1	-0.3219	1	-0.6781
-	SPA4207	hypotheticalprotein	5E-06	-1.0265	1	-0.241	1	0.09311
rpsF	SPA4208	30sribos omalproteinS6	0.3494	-1.0264	1	-0.2462	1	-0.0995
priB	SPA4209	primosomalreplicationproteinN	0.3331	-1.0507	1	-0.2062	1	0.13556
rpsR	SPA4210	30sribos omalsubunitproteinS18	0.2854	-1.0946	1	-0.1853	1	0.16237
rplI	SPA4211	50sribos omalsubunitproteinL9	0.2407	-1.1377	1	-0.1777	1	0.19382
yifZ	SPA4212	hypotheticalprotein	1	0	1	-1.585	1	0
ytfB	SPA4213	hypotheticalprotein	1	-0.0085	1	0.33214	1	0.18778
fklB	SPA4214	FkbP-typepepti dyl-prolyl cis-transi somerase	1	-0.2838	1	-0.1312	1	-0.2756
cycA	SPA4215	D-serine/D-alanine/glycinetransporter	1	-0.0687	0.0108	-1.0251	1	0.11548
-	SPA4216	hypotheticalprotein	1	#NUM!	1	0	1	#NUM!
ytfE	SPA4218	hypotheticalprotein	1	-0.263	1	0.58496	1	1
ytfF	SPA4219	hypotheticalprotein	1	-0.1375	1	-0.8625	1	-0.1926
ytfG	SPA4220	hypotheticalprotein	1	0.87447	1	0.77761	1	1
ytfH	SPA4221	hypotheticalprotein	1	-0.3219	1	0	1	0
cpdB	SPA4222	2',3'-cyclic-nucleotide2' -phosphodiesterase	1	0.23644	0.3632	0.97797	1	0.56598
cysQ	SPA4223	cysQ protein	1	0.09311	1	0.38702	1	0.21632
ytfJ	SPA4224	hypotheticalprotein	1	0.47032	1	0.61411	1	0.0955
ytfK	SPA4225	hypotheticalprotein	0.1053	0.74347	0.1497	1.23778	0.4861	0.74046
tnpA	SPA4226	transposaseforinsertionsequenceelementIS200	0.5522	-0.2451	1	-1	1	-1
ytfL	SPA4227	hypotheticalprotein	1	-0.3536	1	-0.5261	0.0315	-0.8707
msrA	SPA4228	peptidem ethioninesulfoxidereductase	1	-0.1431	0.7163	-0.205	1	0.1006
ytfM	SPA4229	hypotheticalprotein	1	-0.0581	0.9686	-0.0661	1	0.02203
ytfN	SPA4230	hypotheticalprotein	1	-0.0671	0.5108	-0.585	1	-0.0265
ytfP	SPA4231	hypotheticalprotein	0.9045	-0.1536	1	0.0217	1	0.12611
-	SPA4232	sugartra nsporter	1	-0.585	1	#NUM!	1	#DIV/0!
-	SPA4233	hypotheticalprotein	1	1	1	#NUM!	1	0
ppa	SPA4234	inorganicpyrophosphatase	0.3553	-0.5188	1	-0.2731	1	-0.2296
fbp	SPA4235	fructose-1,6-bisphosphatase	0.8751	-0.3649	1	-0.1747	1	-0.0239
yjga	SPA4237	hypotheticalprotein	1	-0.1494	1	-0.25	1	-0.4232
pmbA	SPA4238	PmbApro tein	0.9813	-0.1961	1	0.03882	1	0.11346
cybC	SPA4239	solublecytochromeb562	0.0582	-0.7021	0.1494	-0.691	1	-0.1492

-	SPA4240	hypotheticalprotein	1	0	1	0	1	0
-	SPA4241	hypotheticalprotein	1	0	1	0	1	-0.1699
-	SPA4242	hypotheticalprotein	1	0.19265	1	-0.585	1	-0.3219
-	SPA4243	hypotheticalprotein	1	0	1	-0.737	1	-0.415
-	SPA4244	hypotheticalprotein	1	0.41504	1	-0.737	1	-0.585
-	SPA4245	hypotheticalprotein	1	0.32193	1	-0.4854	1	0
-	SPA4246	hypotheticalprotein	1	0.26303	1	-0.737	1	-0.415
-	SPA4247	hypotheticalprotein	1	0.22239	1	-0.6521	1	-0.1926
-	SPA4248	BglB-familytranscriptionalantiterminator	1	0.09954	1	0	1	0.09311
relB	SPA4249	RelB protein	0.0303	-0.5251	1	0.19265	1	-0.1312
relE	SPA4250	hypotheticalprotein	0.0756	-0.4425	1	0.36773	1	-0.166
nrdG	SPA4251	anaerobicribonucleoside -triphosphatereductaseactivatingprotein	1	-0.2224	1	2.27302	1	1.22239
nrdD	SPA4252	anaerobicribonucleoside -triphosphatereductase	1	0	8E-05	1.88858	0.1851	0.91146
-	SPA4253	hypotheticalprotein	1	#DIV/0!	1	#DIV/0!	1	#DIV/0!
treC	SPA4254	trehalose-6-phosphate hydrolase	0.0004	-1.1405	1	-0.972	1	-0.3943
treB	SPA4255	PTSsys temtrehalose -specifictransportersubunitIIBC	2E-09	-1.5594	1	-0.8425	1	-0.8625
treR	SPA4256	trehaloseoperonrepressor	1	1.1375	1	1.12928	1	0.922
-	SPA4258	hypotheticalprotein	0.2657	-0.4339	1	0.54432	1	0.11321
yjgF	SPA4259	hypotheticalprotein	0.8776	-0.3802	1	0.17817	1	-0.1271
pyrI	SPA4260	aspartate carbamoyltransferaseregulatory subunit	0.8567	0.52223	1	-0.0406	0.3365	-0.585
pyrB	SPA4261	aspartate carbamoyltransferasecatalyticsubunit	1	0.42884	0.4805	-0.24	0.01	-1.0282
pyrL	SPA4262	pyrBloperon leaderpeptide	0.0283	-0.561	1	-0.415	1	-0.9511
-	SPA4263	transcriptionalregulator	0.4081	-0.5116	0.1964	-0.4546	0.031	-0.7929
-	SPA4264	hypotheticalprotein	0.8571	-0.5484	0.4926	-0.3668	0.0056	-1.0356
-	SPA4265	ornithine carbamoyltransferase	1	-0.2697	1	-0.0515	0.2266	-0.776
-	SPA4266	carbamatekinase	1	-0.2148	1	-0.0911	0.0952	-0.8972
-	SPA4267	argininede iminase	1	-0.318	1	-0.2883	0.0512	-1.0979
yjgK	SPA4268	hypotheticalprotein	0.4274	-0.3219	1	0.54253	0.3788	0.6849
argI	SPA4269	ornithine carbamoyltransferase	1	-0.0614	1	-0.1699	1	-2.0704
yjgD	SPA4270	hypotheticalprotein	0.4965	-0.2589	1	0.12338	0.9441	-0.4123
miaE	SPA4271	tRNAhy droxylase	1	-0.1751	1	-0.0332	0.0641	-0.6612
-	SPA4272	hypotheticalprotein	1	0	1	#DIV/0!	1	#DIV/0!
ytgA	SPA4273	hypotheticalprotein	1	-1.3219	1	#DIV/0!	1	#NUM!
yjgM	SPA4274	acetyltransferase	1	-0.5208	1	0.2115	1	0.33703
yjgN	SPA4275	innerme mbraneprotein	1	0	1	0	1	0.58496
valS	SPA4276	valyl-tRNAs ynthetase	0.8981	-0.3536	0.6254	-0.7905	0.8598	-0.3508
holC	SPA4277	DNApo lymeraseIII,chisubunit	0.026	-0.6581	0.0437	-0.636	0.5295	-0.3509
pepA	SPA4278	cytosolaminopeptidase	0.2234	-0.6289	0.3533	-0.7897	0.8733	-0.3536
yjgP	SPA4279	innerme mbraneprotein	0.4218	-0.3219	1	-0.4021	1	-0.1605
yjgQ	SPA4280	innerme mbraneprotein	1	-0.1699	1	-0.5208	1	-0.2451
idnR	SPA4281	regulatoryprotein	1	0.60145	1	1.22239	1	0.29546
idnT	SPA4282	GntPf amily,L -idonate transportprotein	1	0.32193	1	1.20645	1	0.61298
idnO	SPA4283	5-keto-D-gluconate-5-reductase	1	#DIV/0!	1	0.77761	1	0.51457
idnD	SPA4284	L-idonate 5-dehydrogenase	1	#DIV/0!	1	1.32193	1	0.58496
idnK	SPA4285	D-gluconatekinase,thermosensitive	1	#DIV/0!	1	0.48543	1	0.078
yjgB	SPA4286	alcoholdehydrogenase	1	#NUM!	2E-19	-1.978	0.619	-0.5389
leuX	SPA4287	LeutRN A	1	-0.8745	1	-0.1926	1	-0.1699
int	SPA4288	integrase	1	-1	1	-0.3785	1	-0.3219

hsdM	SPA4289	DNAm ethyltransferaseSptAIM;protectsDNAagainstPvuIIendonuclease	1	#DIV/0!	0.1138	-0.6057	1	-0.1085
hsdS	SPA4290	subunitSo ftypeI restriction-modificationsystem	1	#DIV/0!	1	0.30485	1	0.55254
hsdR	SPA4291	subunitR oftypeIrestriction -modificationsystem	1	#DIV/0!	1	0.22422	1	0.57236
-	SPA4292	hypotheticalprotein	1	#DIV/0!	1	1	1	-0.585
-	SPA4293	hypotheticalprotein	1	#DIV/0!	1	1	1	0
cI	SPA4296	phagei mmunityrepressorprotein	1	#DIV/0!	1	0.41504	1	-0.585
-	SPA4297	hypotheticalprotein	1	#DIV/0!	1	0.58496	1	0
-	SPA4298	hypotheticalP4phageprotein	1	#DIV/0!	1	-0.585	1	-1
-	SPA4299	hypotheticalprotein	1	#DIV/0!	1	0	1	0
-	SPA4300	hypotheticalprotein	1	#DIV/0!	1	#DIV/0!	1	#DIV/0!
-	SPA4301	hypotheticalprotein	1	-0.5694	1	0.58496	1	0.60572
sefA	SPA4304	fimbrialstructuralprotein	1	-0.737	0.1888	-0.5038	0.0589	-0.7919
sefB	SPA4305	fimbrial chaperoneprotein	1	#DIV/0!	1	#DIV/0!	1	#DIV/0!
sefC	SPA4306	outerme mbranefimbrialusherprotein	1	#DIV/0!	1	#DIV/0!	1	#DIV/0!
sefR	SPA4307	fimbrialregulator	1	#DIV/0!	1	#DIV/0!	1	#DIV/0!
-	SPA4309	GerE-familyregulatoryprotein	1	-1	1	-0.737	1	-0.585
-	SPA4310	hypotheticalprotein	1	#NUM!	1	#DIV/0!	1	#NUM!
-	SPA4311	outerme mbraneprotein	1	#DIV/0!	1	#DIV/0!	1	#DIV/0!
-	SPA4312	hypotheticalprotein	1	-0.263	1	-0.3626	1	-0.4594
-	SPA4313	hypotheticalprotein	1	0	1	-0.3219	1	-0.3219
yjiU	SPA4314	hypotheticalprotein	1	0.41504	1	0.56704	1	0.46949
-	SPA4315	hypotheticalprotein	1	0.3388	1	0.848	1	0.52356
-	SPA4316	hypotheticalprotein	1	#DIV/0!	1	#DIV/0!	1	#DIV/0!
-	SPA4317	hypotheticalprotein	1	-0.585	1	#DIV/0!	1	0
yeeN	SPA4319	hypotheticalprotein	1	-0.055	1	0.46395	1	0.49533
yjhP	SPA4320	hypotheticalprotein	0.3559	-0.493	1	0.1964	0.2573	-0.5952
-	SPA4321	hypotheticalprotein	0.0002	-0.8625	1	0.34514	1	-0.5607
-	SPA4322	hypotheticalprotein	1	-0.415	1	0.80735	1	0.48543
-	SPA4323	hypotheticalprotein	1	0.41504	1	1	1	0
-	SPA4324	hypotheticalprotein	1	-0.263	1	0	1	-0.2065
-	SPA4325	hypotheticalprotein	1	-0.4594	1	-0.7199	1	-0.8194
uxuR	SPA4326	uxuoperon transcriptionalregulator	0.5123	-0.3022	1	0.02032	1	-0.1926
-	SPA4327	trpS-like protein	1	-0.7618	1	0.32193	1	-0.074
-	SPA4328	hypotheticalprotein	1	0	1	#DIV/0!	1	#DIV/0!
-	SPA4329	hypotheticalprotein	0.0601	-0.5727	0.0139	-0.8205	1	-0.6347
-	SPA4330	aspartate racemase	3E-34	-2.0704	0.036	-0.6707	1	0.20945
yjiE	SPA4331	transcriptionalactivator	1	-0.2224	1	0.16993	0.1162	0.9542
iadA	SPA4332	isoaspartyldipeptidase	0.1925	-0.5944	0.8995	-0.1301	1	0.58129
yjiG	SPA4333	hypotheticalprotein	2E-05	-1.0411	1	-0.0581	0.996	0.63941
yjiH	SPA4334	hypotheticalprotein	2E-08	-1.2055	1	0.08746	0.8685	0.68001
-	SPA4335	hypotheticalprotein	1	#DIV/0!	1	#NUM!	1	#DIV/0!
yjiJ	SPA4336	hypotheticalprotein	1	0.16993	1E-09	-1.5639	1	0.09954
yjiN	SPA4337	hypotheticalprotein	1	-0.263	1	-0.4854	1	-0.585
-	SPA4339	hypotheticalprotein	1	-0.263	1	0.32193	1	0
-	SPA4340	hypotheticalprotein	1	0.28951	0.0718	-0.7761	1	-0.0337
-	SPA4341	hypotheticalprotein	1	#DIV/0!	1	#DIV/0!	1	#DIV/0!
yjiS	SPA4342	hypotheticalprotein	1	0	1	#DIV/0!	1	#DIV/0!
-	SPA4343	hypotheticalprotein	1	0	1	0	1	0

yjiW	SPA4344	hypotheticalprotein	1	-0.5146	1	0.11548	1	0.22239
hsdS	SPA4345	subunitSo ftypeIrestriction -modificationsystem	1	-0.1069	1	-0.0589	1	0.65896
hsdM	SPA4346	DNAm ethylaseM,host modification	1	0.25376	1	0.19265	1	0.37851
hsdR	SPA4347	subunitR oftypeIrestriction -modificationsystem	1	0.11832	0.4865	0.9027	0.2596	0.89308
mrr	SPA4348	mrrrestri ctionsystemprotein	1	-0.152	1	0.19265	1	0.32193
-	SPA4349	hypothetical protein	1	0	1	0.57511	1	0.24101
-	SPA4350	hypotheticalprotein	1	-0.061	1	0.45768	1	0.17557
yjiA	SPA4351	hypotheticalprotein	0.0697	1.25184	1	0.47393	1	-0.0108
yjiX	SPA4352	hypotheticalprotein	0.0006	1.19967	0.2584	0.75384	1	0.21527
cstA	SPA4353	carbons tarvationproteinA	1	0.91898	1	0.44009	0.8335	-0.671
tsr	SPA4354	methyl-acceptingchemotaxisproteinI,serinesensorreceptor	5E-08	1.52793	1	0.27253	1	-0.2101
mdoB	SPA4355	phosphoglyceroltransferase	2E-07	-1.2035	1	-0.7521	1	-0.6859
yjjA	SPA4356	hypotheticalprotein	0.4986	-0.2421	1	-0.0356	1	-0.0725
dnaC	SPA4357	DNAre plicationprotein	1	0.04639	1	-0.1416	1	-0.1375
dnaT	SPA4358	primosomalproteinI	1	0.01057	1	0.08836	1	0.05938
yjjB	SPA4359	hypotheticalprotein	0.5987	-0.2854	1	-0.415	1	-0.2996
yjjP	SPA4360	hypotheticalprotein	1	-0.1783	1	-0.4854	1	-0.2224
yjjQ	SPA4361	regulatoryprotein	1	#DIV/0!	1	#DIV/0!	1	#DIV/0!
bglJ	SPA4362	regulatoryprotein	1	#DIV/0!	1	#DIV/0!	1	#DIV/0!
-	SPA4363	hypotheticalprotein	0.0485	-0.5639	0.0061	-0.8373	0.1162	-0.5784
fhuF	SPA4364	ferric ironreductaseprotein	1	1	1	-1.9069	1	-1.3626
-	SPA4365	hypotheticalprotein	1	0	1	-0.2345	1	-0.2141
-	SPA4366	hypotheticalprotein	1	2	1	0	1	0
leuT	SPA4367	Leu tRNA	0.004	-0.6498	1	-0.166	1	-0.5236
leuT	SPA4368	LeutRN A	0.024	-0.6218	1	-0.1333	1	-0.3458
leuT	SPA4369	LeutRN A	0.0018	-0.7118	1	-0.1806	1	-0.3833
rsmC	SPA4370	hypotheticalprotein	1	-0.0962	1	-0.7965	1	-0.9069
holD	SPA4371	DNApo lymeraseIII, psis ubunit	0.974	-0.1605	1	-0.337	0.0399	-0.6398
rimI	SPA4372	ribosomal-protein-alanine acetyltransferase	1	-0.1069	1	-0.4021	1	-0.4792
yjjG	SPA4373	hypotheticalprotein	1	-0.0566	1	-0.3479	1	-0.3811
prfC	SPA4374	peptidec hainreleasefactor3	1	0.04975	0.0706	-0.659	1	-0.1666
osmY	SPA4375	hypotheticalprotein	1	0.10893	0.5683	-0.8322	1	0.51567
-	SPA4376	hypotheticalprotein	1	0.10434	0.0071	-0.8039	1	0.37691
yjjU	SPA4377	hypotheticalprotein	1	0	0.4409	-0.3626	0.9601	-0.3841
yjjV	SPA4378	hypotheticalprotein	1	0	1	-0.433	1	-0.5045
yjjW	SPA4379	hypotheticalprotein	0.4936	0.62963	1	2	1	1.40599
yjjI	SPA4380	hypotheticalprotein	1	0.33208	0.0014	1.54889	0.3582	0.8696
deoC	SPA4381	deoxyribose-phosphate aldolase	0.8897	0.60287	1	0.35954	0.293	0.85745
deoA	SPA4382	thymidinephosphorylase	0.363	0.85057	1	0.1375	0.6937	0.64534
deoB	SPA4383	phosphopentomutase	0.6002	0.85059	1	-0.0342	1	0.21753
deoD	SPA4384	purinenucl eosidephosphorylase	0.1923	0.71049	1	-0.0237	1	0.32022
yafM	SPA4385	hypotheticalprotein	1	0.58496	1	0	1	0.41504
lplA	SPA4386	lipoate-proteinl igaseA	1	-0.1186	1	0.02509	1	0.05247
smp	SPA4387	hypotheticalprotein	1	-0.5475	1	-0.2801	1	-0.387
serB	SPA4388	phosphoserinephosphatase	1	-0.3312	1	-0.415	1	-0.2065
radA	SPA4389	DNAre pairprotein	0.2526	-0.415	0.0977	-0.6374	1	-0.2016
nadR	SPA4390	transcriptionalregulator	1	-0.0406	0.7032	-0.1953	1	0.01862
yjjK	SPA4391	ABCtra nsporter	0.2234	-0.5622	0.0468	-1.4434	0.4534	-0.5182

slt	SPA4392	lytic mureintra nsglycosylase	1	0.15673	1	-0.2361	1	0.32193
trpR	SPA4393	trpoperon repressor	0.7413	-0.263	1	0.23919	0.589	-0.2706
yjjX	SPA4394	hypotheticalprotein	0.4021	-0.3312	1	-0.1444	1	-0.3959
gpmB	SPA4395	phosphoglyceratemutase	1	-0.035	1	-0.0988	1	-0.2455
rob	SPA4396	rightori gin-bindingpr otein	0.0403	-0.8488	0.133	-0.7464	0.0655	-0.765
creA	SPA4397	hypotheticalprotein	0.0038	-0.7521	0.0433	-0.6907	0.1966	-0.4822
creB	SPA4398	two-componentresponseregulator	0.1385	-0.4903	0.3293	-0.4253	0.5717	-0.4258
creC	SPA4399	two-componentsensorkinase	1	-0.4406	1	-0.387	1	-0.1926
creD	SPA4400	innerme mbraneproteinCreD	1	-0.1699	1	-0.152	1	-0.2895
sthE	SPA4401	majorf imbrialsubunit	1	-1	1	-0.737	1	-0.3219
sthD	SPA4402	fimbrialsubunit	1	0	1	#NUM!	1	-1
sthC	SPA4403	fimbrialusherprotein	1	0	1	#NUM!	1	#NUM!
sthB	SPA4404	fimbrialchaperoneprotein	1	#NUM!	1	#NUM!	1	#NUM!
sthA	SPA4405	fimbrialprotein	1	-1.585	1	#NUM!	1	-1
-	SPA4406	transcriptionalregulator	1	-0.5475	1	-1.078	1	-1.0589
arcA	SPA4408	globalresponseregulator	1	-0.2766	1	-0.3167	1	-0.1648
yjjY	SPA4409	hypotheticalprotein	1	0	1	0.41504	1	0
lasT	SPA4410	RNAm ethyltransferase	1	0.12553	1	-0.1155	1	0